PROCEEDINGS

ENVIRA 2019

5th International Conference on Environmental Radioactivity ENVIRA 2019: Variations of Environmental Radionuclides

8 – 13 September 2019, Praha, Czech Republic

Organized by

Nuclear Physics Institute of the Czech Academy of Sciences

in cooperation with

Faculty of Nuclear Sciences and Physical Engineering, Czech Technical University in Prague
Comenius University in Bratislava
Journal of Environmental Radioactivity
International Union of Radioecology

ENVIRA 2019 PROCEEDINGS

Published by	Czech technical university in Prague
Prepared by	Faculty of Nuclear Sciences and Physical Engineering of CTU in Prague, Department of Nuclear Chemistry
	Nuclear Physics Institute CAS, Department of Radiation Dosimetry
Contact address	Kateřina Pachnerová Brabcová
	Na Truhlářce 39/64, 180 00 Praha
Editors	Ivo Světlík, Pavel P. Povinec, Kateřina Pachnerová Brabcová
Edition	first
Number of pages	345
ISBN	978-80-01-06692-8 (electronic version)
	978-80-01-06691-1 (printed version)
DOI	https://doi.org/10.14311/ENVIRA.2019

ENVIRA 2019

Local Organizing Committee

I. Světlík (Chair), Nuclear Physics Institute of the CAS, Prague
M. Němec, (Vice-Chair) Czech Technical University in Prague
M. Molnár, ATOMKI, Debrecen
T. Němcová, Czech Technical University in Prague
K. Pachnerová Brabcová, Nuclear Physics Institute of the CAS, Prague
Z. A. Ovšonková, Nuclear Physics Institute of the CAS, Prague
M. Petrová, Nuclear Physics Institute of the CAS, Prague
N. Megisová, Nuclear Physics Institute of the CAS, Prague
V. Suchý, Nuclear Physics Institute of the CAS, Prague
R. Garba, Nuclear Physics Institute of the CAS, Prague
J. Šneberger, Nuclear Physics Institute of the CAS, Prague

International Organizing Committee

P.P. Povinec (Chair), Comenius University, Bratislava
I. Světlík (Co-Chair), Nuclear Physics Institute of the CAS
F. Bréchignac, International Union of Radioecology, Paris
M. Garcia León, University of Sevilla
A. Ioannidou, Aristotle University, Thessaloniki
G. Lujaniene, Center for Physical Sciences and Technology, Vilnius
S.C. Sheppard, Chief Editor, Journal of Environmental Radioactivity

International Advisory Board

P.P. Povinec (Chair), Comenius University, Bratislava
I. Světlík (Co-Chair), Nuclear Physics Institute of the CAS
L. Benedik, Josef Stefan Institute, Ljubljana
E. Boaretto, Weizmann Institute of Science, Rehovot
A.E. Cherkinsky, University of Georgia, Athens
R. Garcia-Tenorio, University of Sevilla
M. Hult, EC, Joint Research Centre - Institute for Reference Materials and Measurements, Geel
S. Jerome, IAEA-EL, Monaco
J. John, Czech Technical University in Prague
A.J.T. Jull, University of Arizona, Tucson
W.E. Kieser, University of Ottawa
T. Kovacs, Pannonia University
J. Kučera, Nuclear Physics Institute of the CAS
O. Masson, Institut de Sureté Nucléaire, Saint-Paul-lez-Durance
M. Molnár, ATOMKI, Debrecen
M. Němec, Czech Technical University in Prague
S. Pan, University of Nanjing
A. Rakowski, SUT, Gliwice
P. Steier, University of Vienna
G. Steinhauser, University of Hannover
E. Steinnes, Norwegian University of Science and Technology, Trondheim
F. Terrasi, CIRCE, Caserta
C. Tsabaris, Hellenic Centre for Marine Research, Anavyssos
P. Vojtyla, CERN, Geneva
G. Wallner, University of Vienna
G. Wallova, WRI, Bratislava

Ionplus

Scientific Instruments for Radiocarbon Dating
and Accelerator Mass Spectrometry

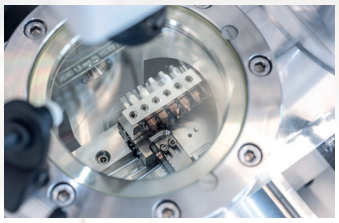

MICADAS *Mini Carbon Dating System*

The most compact ^{14}C-AMS system in the world.

Highest precision and lowest backgrounds – get the best performance with the world's most compact radiocarbon AMS system and our versatile sample preparation instruments.

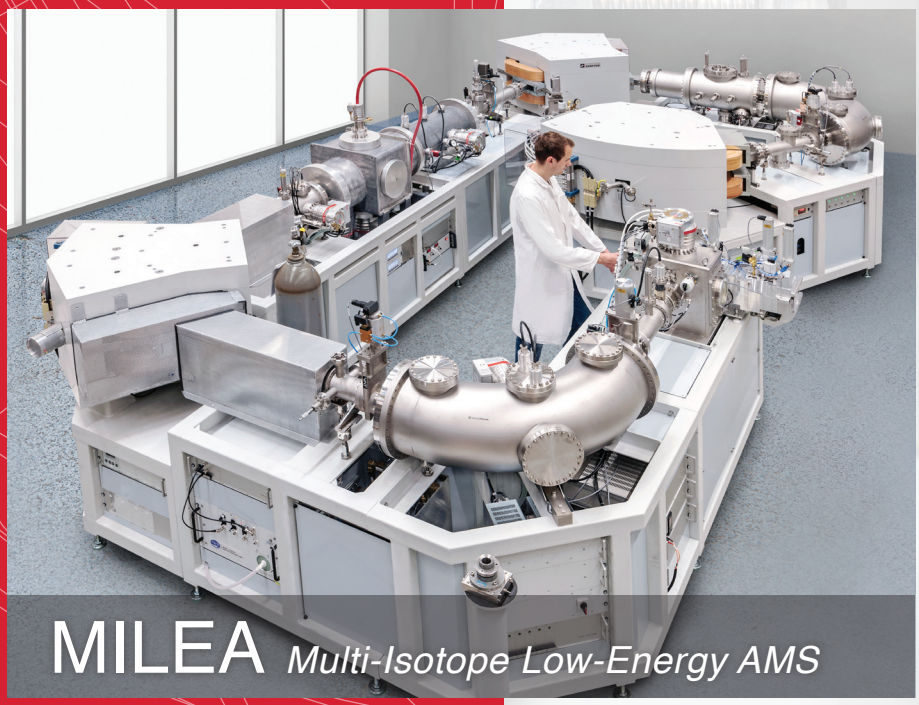

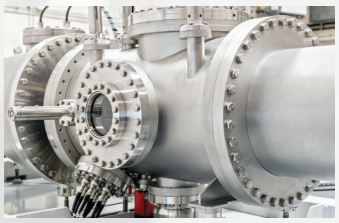

MILEA *Multi-Isotope Low-Energy AMS*

The world's most innovative multi-isotope AMS system.

From ^{10}Be to actinides – our newly designed MILEA system provides outstanding measurement capabilities for ^{10}Be, ^{14}C, ^{26}Al, ^{41}Ca, ^{129}I, U, Pu and other actinides at lowest energies.
Contact us to learn more about the exciting possibilities with MILEA.

Dedicated to excellence.

www.ionplus.ch . info@ionplus.ch . T +41 43 322 31 60

List of content

The contributions are listed alphabetically.

Foreword

This Book of Proceedings contains papers as well as selected abstracts of invited lectures, oral presentations and posters presented at the 5th International Conference on Environmental Radioactivity ENVIRA 2019: Variations of Environmental Radionuclides organized by Nuclear Physics Institute of the Czech Academy of Sciences in Praha from 8 to 14 September 2019, in cooperation with Faculty of Nuclear Sciences and Physicsl Engineering, Czech Technical University in Prague, Comenius University in Bratislava, Journal of Environmental Radioactivity, and International Union of Radioecology.

Following traditions of previous ENVIRA conferences – Monaco (2004), Rome (2010) , Thessaloniki (2015), Vilnius (2017) – the ENVIRA 2019 included invited talks on the relevant environmental radioactivity and radioanalytical topics, given by prominent representatives of the field, as well as oral and poster contributions on various environmental radioactivity aspects on the application of natural and anthropogenic radionuclides and isotopes in tracer studies in the terrestrial (atmosphere, hydrosphere, biosphere, pedosphere, etc.) and marine (seawater, marine biota, sediments, etc.) environments.

The participants (291) from all over the world presented 149 lectures, including 25 keynote plenary lectures, in two parallel sessions, and 135 posters. The keynote speakers covered a wide range of recent developments, including radiocarbon research and AMS applications (Prof. I. Levin, Dr. M. Molnár, Prof. T.M. Nakanishi, Dr. P. Steier and Prof. H.-A. Synal), evaluating environmental impacts of the Fukushima accident (Prof. M. Aoyama, Prof. K. Hirose, Prof. Y. Kumamoto, Dr. S-H. Lee and Prof. N. Yasuda), new trends in nuclear technologies (Prof. M. Clemenza, Prof. J. Kučera and Dr. Laubenstein), estimating effects of NPPs on the environment (Dr. O. Masson, Prof. B. Salbu, Dr. G. Steinhauser and Dr. V. Wagner) applying of radionuclides as tracers to study environmental processes (Dr. G. Lujaniene), new trends in radioecology (Dr. F. Brechignac, Prof. X. Hou, Prof. A.J.T. Jull, Dr. J-W. Mietelski and Prof. S. Nisi).

The oral presentations and posters covered variety of the environmental radioactivity topics – developments in analytical techniques (accelerator mass spectrometry, low energy mass spectrometry (ICPMS, TIMS), underground gamma-spectrometry, radioanalytical techniques, neutron activation analysis), the estimation of effects of both natural and anthropogenic radionuclides in the environment, transport and redistribution of radionuclides in ecosystems, NORMS, radioecology studies for the protection of humans, fauna and flora, and the application of radionuclides as tracers to study various processes in the biosphere, atmosphere, geosphere and hydrosphere.

The Proceedings contains 25 full papers presented during the ENVIRA 2019 Conference which passed the reviewing process. Moreover, the book comprises abstracts of invited lectures as well as the selected abstracts of oral presentations and posters covering the latest technological innovations in low-level radioactivity detection techniques and the recent developments on applications of nuclear technologies in environment protection (including waste management and remediation actions on contaminated territories), in tracing environmental processes, assessing the Chernobyl and Fukushima impacts, as well as in radioecology.

The Editors would like to thank all the authors and reviewers as well as members of the Organizing Committees and ENVIRA 2019 team for their effort during organization of the conference and preparation of the Proceedings. We greatly appreciate your time and expertise because without you it would be impossible to manage an efficient peer review process and publication of the Proceedings.

We hope that you had great time in Praha during the ENVIRA 2019 Conference, meeting colleagues, making new friends, discussing, considering and thus contributing to the development of the research in the field of the environmental radioactivity and applications of radionuclides to trace environmental processes.

Ivo Světlík and Kateřina Pachnerová Brabcová
Department of Radiation Dosimetry,
Nuclear Physics Institute of the Czech Academy of Sciences
Praha, Czech Republic

Pavel P. Povinec
Department of Nuclear Physics and Biophysics,
Faculty of Mathematics, Physics and Informatics,
Comenius University, Bratislava, Slovakia

Simulation of the influence of the Radium concentration in soil and Radon concentration in air on the response of a NaI detector aboard of a drone

N. Alegría[1], F. Legarda[1]

[1]Department of Nuclear Engineering and Fluid Mechanics, University of Basque Country, Bilbao, 48013, Spain
Keywords: scintillators, simulations, efficiencies.
Presenting author, e-mail: natalia.alegria@ehu.eus

When a nuclear incident or accident occurs, it is necessary to know quickly and exactly the surface contamination in order to assess the population dose. In Preparedness project, unmanned aerial vehicles with detectors should go to the contamination area, get spectra and calculate the contamination and dose. However, it is necessary to analyse the influence of soil and air natural radionuclides.

Introduction

Within the framework of the European Association of National Metrology Institutes (EURAMET) & European Commission Horizon 2020 Program (H2020), Preparedness project (2017) is being carried out to develop technology that will be used to deal with radiological emergency situations.

Among the goals of the project "New measurement techniques and new traceable calibration methods will be developed for the determination of ground surface activity concentrations using data collected by unmanned aerial vehicles, and for radioactivity in air measurement using transportable air-sampling systems. Novel calibration procedures will be developed, which are based on the application of Monte Carlo calculations and measurements using standard sources and validated traceable reference materials."

In this regard, the detector which will be used have to be characterized in order to obtain contamination from spectra and the influence of other radionuclides, for example, radium concentration in the soil and radon concentration in air has to be assessed. In this paper a NaI detector has been considered.

Materials and Methods

When a radiological incident occurs, the ground will become a surface contaminated with radionuclides, so using Monte Carlo techniques (MCNP) an analysis of the photon flux and the associated dose distribution can be done.

The study of the 2 x 2 inches Sodium Iodide (NaI) detector has consisted of the following analyses:

The first step has been the experimental analysis. Calibration in energy and resolution and collection of spectra derived from a point-like source of ^{137}Cs. The angular influence has to be analyzed, so the measurements have been made at 0º, 45º and 90º.

The second step has been simulation. Using the Monte Carlo MCNP code, the laboratory where the experimental part (with source positioner and collimator) will be carried out, the detector geometry and the radioactive sources have been simulated.

The plot of figure 1 shows the 661.7 keV peak from ^{137}Cs obtained experimentally and through simulation.

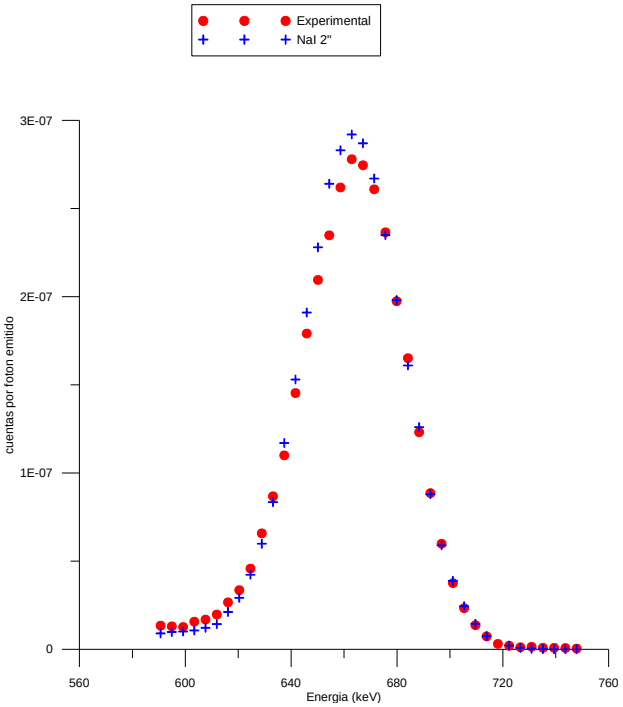

Figure 1. experimental and simulated peak.

It is observed that experimental and simulated results are in good agreement, with differences smaller than 5%.

Radium and its decay chain is very commonly present in soils at different concentrations (UNSCEAR radium concentration), the influence of the radium concentration on the spectrum and dose has to be evaluated.

For radium decay chain, considering only photons with an emission probability higher than 1%, the energy ranges chosen for photons binning are: < 500 keV, between 500 – 1500 keV and finally 1500 – 2500 keV and frequencies obtained are shown in Figure 2.

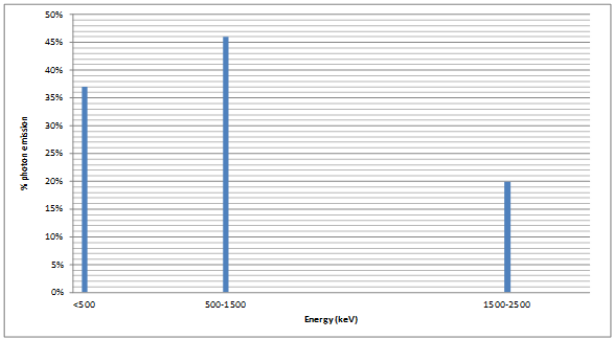

Figure 2. Photon binning for radium and radon decay chains.

These radionuclides are hosted in a typical silty soil with a density of 1.625 g/cm^3 and the following volume composition: 30% water, 20% air and 50% solid materials

and by weight: 57% nitrogen , 7% oxygen, 27.1% silicon, 5% aluminum, 4.1% calcium, 2.1% hydrogen, 1.6% carbon, 1.3% potassium and 1.1% of iron.
The soil has been simulated as a cylinder and in this study the cylinder is 1 m deep, with radius of 10 m, 20 m etc. up to 150 m. A second cylinder has been considered, this time for a layer from 1 to 2 m depth.
The source representations are shown in Figures 3 and 4.

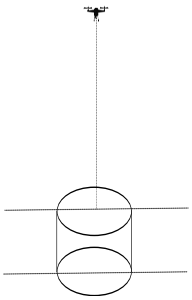

Figure 3. For 0 to1 m depth simulation.

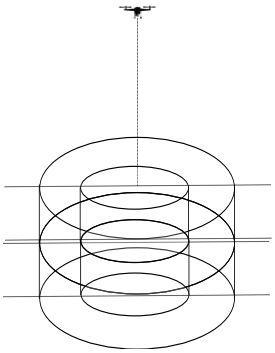

Figure 4. For 1 to 2 m depth simulation.

In the atmosphere there is airbone radon with its daughters. The usual value considered in the bibliography, for example in UNSCEAR, is 10 Bq/m^3. Considering only photons with an emission probability higher than 1%, the same criteria than for radium and its decay chain, the energy ranges chosen for photon binning are: < 500 keV, between 500 – 1500 keV and finally 1500 – 2500 keV, and frequencies obtained are shown in Figure 2.
Flying at a height of 20 m, two different situations have been analysed: the first one for height of 20 m, below detector, and radius of 100 m, 200 m, up to 600 m, and the second one for height of 20 m above the detector, and radius of 100 m, 200 m, up to 600 m.
The simulation representations are shown in Figures 5 and 6.

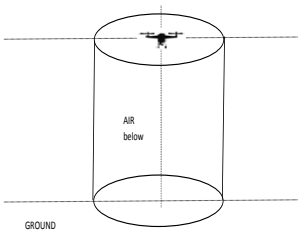

Figure 5. For 0 to1 m depth simulation.

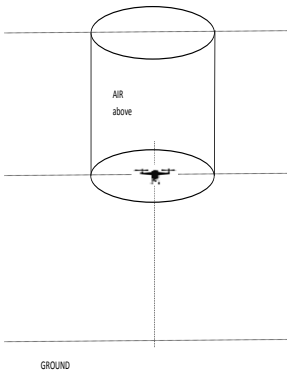

Figure 6. For 1 to 2 m depth simulation.

Results
The obtained values in counts per emitted photon per unit mass of soil for the influence of radium in soil for the different radius considered are shown in Table 1.

Table 1. Obtained values in count per emitted photon per mass unit

Radius (m)	100 keV	1000 keV	2000 keV
10	23.18	82.70	103.63
20	68.61	251.14	314.47
30	102.46	395.13	487.03
60	179.37	632.21	786.59
100	207.78	821.92	1060.00
150	218.24	903.98	1139.46

These results are due to radium in the first metre as the results of the second metre are several orders of magnitude lower than those for the first metre, so it is not necessary to consider this influence.
In the bibliography a usual value of radium in soil is 50 Bq/kg, and that means 0.05 photon/g·s and that value will be used for the comparison
The influence of radon and its daughters has been simulated in two separated situations, one for air below the detector and another for air above the detector. The response of the detector has been obtained in counts per photon emitted per unit volume for cylinders with the radii shown in table 2.

Table 2. Contribution to counting rate (cps)

Radius (m)	100 keV	1000 keV (below/above)	2000 keV
100	1.0/0.9	1.1/1.0	1.1/1.0
200	1.2/1.0	1.4/1.4	1.3/1.4
300	1.2/1.1	1.4/1.6	1.5/1.5
400	1.1/1.2	1.6/1.5	1.5/1.6
500	1.2/1.1	1.7/1.7	1.5/1.7
600	1.3/1.1	1.7/1.6	1.6/1.7

With a typical value of radon of 10 Bq/m^3 and 50 Bq/kg of radium the comparison of the influence of radium and radon with the contaminated surface is shown in Table 3
In an accident situation with a relatively small release of radionuclides into the atmosphere, count rates ranging between ~800 cps and 200 cps (table 3) as a function of energy are expected.
It is clear that such radium as radon influences are not very relevant.

Table 3. Contribution to counting rate from source (cps)

Energy (keV)	Deposition	Radium	Radon (below/above)
100	781	10.3	0.5/0.4
1000	280	57.5	0.8/0.7
2000	180	30.5	0.3/0.3

Conclusions
It can be concluded that the influence of radium and radon is very low as compared to that due to deposition. In the case of radon in the worst scenario the percentage is around 0.5%. The radium influence in the worst scenario is around 17 %, but this influence refers to the lowest contribution in terms of percentage of emitted photons.

PREPAREDNESS. Metrology for mobile detection os ionizing radiation following a nuclear or radiological incident http://www.preparedness-empir.eu/

Los Alamos National Laboratory, 2005. MCNP. Monte-Carlo N-Particle Transport Code System, versión 5. New México. USA.

UNSCEAR 2000 REPORT Vol. I SOURCES AND EFFECTS OF IONIZING RADIATION United Nations Scientific Committee on the Effects of Atomic Radiation. UNSCEAR 2000 Report to the General Assembly, with scientific annexes.

An improvised method for Carbon-14 measurement in gaseous effluents

Bharath[1], R.S. D'Souza[1], S.R. Nayak[1], Dileep B. N.[2], S.S. Manganvi[3], Ravi P. M.[1,4], Karunakara N.[1*]

[1]Centre for Advanced Research in Environmental Radioactivity (CARER), Mangalore University, Mangalagangothri –574199, India
[2]Environmental Survey Laboratory, Kaiga Generating Station, Kaiga-581 400, India
[3]Health Physics Unit, KGS 3&4, Kaiga Generating Station, Kaiga-581 400, India
[4]Formerly with Health Physics Division, Bhabha Atomic Research Centre, Trombay, Mumbai – 400 085, India
Keywords: Radiocarbon, LSS
Presenting author: Bharath, corresponding author e-mail id: drkarunakara@gmail.com

Introduction

Carbon-14 (^{14}C) is a pure beta emitter ($T_{1/2}$= 5730 y and E_{max}=156 keV) and occurs naturally in the environment due to cosmic ray induced production in the atmosphere, mainly through ^{14}N (n, p) ^{14}C reaction (Libby, 1945). Due to many atmospheric weapon testing in 1950's, the ^{14}C concentration in air rose sharply to a maximum level and has decreased gradually after that (Mazeika et al., 2007). A small amount of ^{14}C may also get released (mainly in the form of $^{14}CO_2$) during the routine operation of nuclear facilities also. The released $^{14}CO_2$ may be assimilated by the plants and enter the food chain (IAEA, 2004; Mazeika et al., 2008; Saxén and Hanste, 2009). Knowledge on the extent of ^{14}C release is important for the public dose assessments. Environmental impact assessments programs around the facilities often favour quick and direct methods for the determination of radionuclide concentrations in effluents and environmental biota samples. The method often employed for $^{14}CO_2$ determination in gaseous effluents is the absorption of this gas in NaOH, taken in a series of bubblers (Joshi et, al., 1987). This method is time-consuming in view of the complex chemical procedure involved, such as precipitation of absorbed CO_2 species as $BaCO_3$, regeneration of CO_2 and collection in an amine solution and liquid scintillation spectrometer (LSS). In this paper, an improvised method for the determination of ^{14}C activity in gaseous effluents is presented.

Materials and method

A set of two 125 mL bubblers containing 50 mL of 1M ultra-pure NaOH solution was used for sampling $^{14}CO_2$ from gaseous effluents from the common stack of two units of PHWR (each of 220 MWe) at Kaiga, south India. Before passing through the NaOH solution the gaseous effluent sample was bubbled through 0.1M HNO_3in order to remove ^{3}H. The flow rate was maintained at 1 L $min^{-1}$and sampling duration was 24 h. An aliquot (3 mL) of CO_2 dissolved NaOH was mixed with Hionic-Fluor scintillator (PerkinElmer, Inc.m USA) in a glass vial and analyzed for ^{14}C activity in a LSS (Quantulus1220, PerkinElmer, Inc.m USA) following standard method.

Results

Optimization of sample- scintillator ratio

Sample –scintillator ratio was optimised by mixing different combinations ((1 ml+19 ml, 2 ml+18 ml, 3ml+17 ml etc,) of sample (NaoH) and scintillator (Hionic-Fluor) by keeping the total volume fixed (20ml). The miscibility of the sample + scintillator combination was checked. It was observed that a maximum 3 ml of sample is miscible with 17 ml of scintillator without any phase separation and turbidity formation. Hence, 3ml of sample with 17 ml of scintillator was used for all experiments.

Generation of quench curve

The quench curve was generated by preparing a set of ^{14}C standards in which the activity (DPM) per vial was constant but quench level varied by addition of external quench agent nitromethane. These quench standards were counted in LSS for 30 min. and the spectral quench indicating parameter SQP(E) and corresponding counting efficiency were determined. The SQP(E) against the counting efficiency was plotted and the best fit for the plot was found to be a second order polynomial function as given by the following equation:

$$\text{Efficiency\%} = a \times SQP(E)^2 + b \times SQP(E) + c \quad (1)$$

Where a, b and c are the coefficient of the SQP(E) value. The above expression is used to determine the counting efficiency of the samples individual being analyzed for ^{14}C activity.

The minimum detectable activity (MDA)

The minimum detectable activity for ^{14}C in the method described here was computed as under:

$$MDA = \frac{4.65 * \sqrt{B}}{60 * E * Vs * T * Va * Et}$$

Where B (=3.48 cpm) is the background count for the combination of 3 ml of NaOH and 17 ml Hionic Flour mixture, E is the fractional counting efficiency, V_s (=0.06) is the ratio of volume of NaOH taken for bubbling to that taken for counting, V_a (=1.44 m^3) is the volume of air sampled, Et (=62%) is the trapping efficiency, and T (=500 min) is the counting time. For the observed counting efficiency of 50.57%, the MDA was determined to be 0.0115 Bqm^{-3} of air at 95% confidence level.

^{14}C in gaseous effluents

Upon standardization of the method, its suitability was tested for stack monitoring program of the nuclear power plant at Kaiga, south India. Although the stack used for the sampling program incorporates the gaseous effluents from 2 units of 220 MWe PHWR's, at the time sampling only one unit was operating. A total of 10 samples were collected and analyzed for the ^{14}C activity and the results are presented in Table 1.

From the results presented in Table 1, it is evident that the method can be conveniently adopted for the stack monitoring program of NPP. The advantages of the

method standardized in this work is that CO_2 sampled NaOH can be directly taken for ^{14}C counting in LSC without subjecting it any chemical processing.

The authors would like to thank the Board of Research in Nuclear Science (BRNS), DAE, Govt. Of India, for funding the research program. The authors would like to thank the officials of members of ESL, Kaiga and NPCIL, Kaiga for their support during sampling.

Libby, W.F., 1945. Atmospheric helium three and radiocarbon from cosmic radiation. *Phys. Rev.* 69, 671–672.

Mazeika, J., Petrosius, R., Pukiene, R., 2007. Carbon-14 in tree rings in the vicinity of ignalina nuclear power plant, Lithuania. *Geochronometria* 28, 31–37.

IAEA -2004. Management of waste containing tritium and C-14. Report IAEA 421, Vienna.

Mazeika, J., Petrosius, R., Pukiene, R., 2008. Carbon-14 in tree rings and other terrestrial samples in the vicinity of Ignalina Nuclear Power Plant, Lithuania. *J. Environ. Radioact.* 99, 238–247.

Saxén, R., Hanste, U-M., 2009. An oxidizer/lsc method for the determination of samples. *Adv. Liq. Scintill. Spectrom.* 279–285.

M.L Joshi, B. Ramamritham, S.D. Soman, 1987. Measurement of ^{14}C emission rates from a pressurized heavy water reactor, *Health physics*.

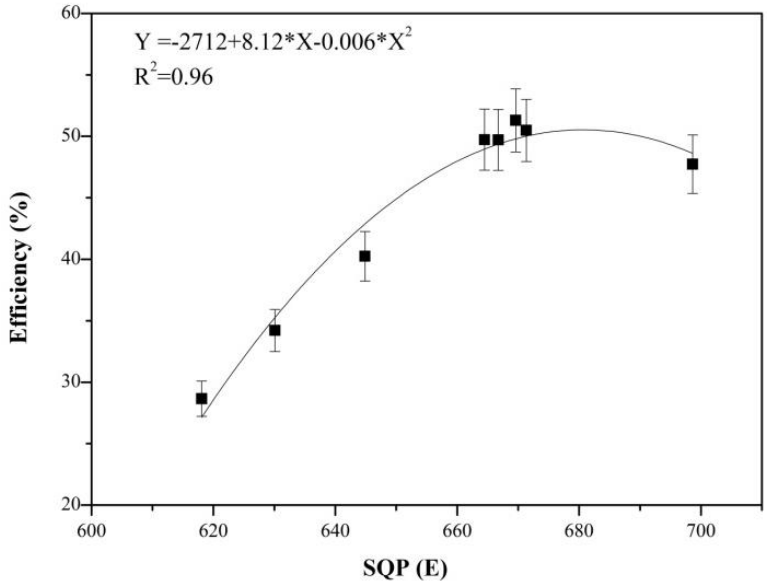

Figure 1. Quench curve for Hionic-Fluor and NaOH combination.

Table 1. ^{14}C activity in stack effluents

Sample ID	Activity ±SD (Bq m^{-3})	Sample ID	Activity ±SD (Bq m^{-3})
SM-1	0.41 ± 0.09	SM-6	4.34 ± 0.15
SM-2	2.6 ± 0.11	SM-7	4.75 ± 0.12
SM-3	0.35 ± 0.10	SM-8	3.93 ± 0.11
SM-4	1.91 ± 0.21	SM-9	6.40 ± 0.15
SM-5	2.04 ± 0.10	SM-10	3.32 ± 0.1

Mathematical modelling of the impacts of Chernobyl nuclear power plant accident on Turkey

E. Bilgiç[1], O. Gunduz[2]

[1]The Graduate School of Natural and Applied Sciences City, Dokuz Eylul University, 35390, Turkey
[2]Department of Environmental Engineering, Dokuz Eylul University, 35390, Turkey
Keywords: Chernobyl accident, Atmospheric fate and transport modeling, Dose estimation, Risk assessment, Turkey
Presenting author, e-mail: efem.bilgic@deu.edu.tr

During 1950s, nuclear fission began to be used in the generation of electricity, and it became one of the most significant energy production alternatives after the oil crisis of 1970s. However, the Chernobyl Nuclear Power Plant (NPP) accident that occurred on April 26, 1986 and the Fukushima NPP accident that occurred on March 11, 2011 have created a radical change in the overall understanding of nuclear power plants and caused intense debates about the security of nuclear energy. The impacts of the Chernobyl NPP accident that influenced highly populated regions of Turkey and Europe have not yet been completely understood. Despite the 33 years passed and all technological and scientific developments made in due time, the total amount and characteristics of radionuclides released from the accident has not been determined exactly. It is also generally accepted that the assessments made on human and environmental health effects of the accident are also highly controversial. In addition to all these, impacts of the accident on Turkey could not be discussed adequately in scientific terms and the number of research conducted on this subject has been limited because of the conditions of the period. Considering these deficiencies in scientific literature, this study focuses on the atmospheric dispersion and ground level deposition of the radionuclides released from Chernobyl NPP accident. Simulations were carried out to predict the likely effects of the accident on Turkish territory and the results were compared with data from previous studies. To achieve this objective, simulations of atmospheric dispersion and total deposition of radionuclides were carried out with a mathematical model, FLEXPART. The data required for the source term was obtained from three different studies in the literature (Brandt et al., 2002; Talerko, 2005; Evangeliou et al., 2017). The meteorological data requirements of the model were supplied from ECMWF and GFS datasets obtained from global circulation models. For the simulations conducted in the present study, three different re-analysis data sets (NCEP / NCAR, ERA-INTERIM, ERA-40) were used. In total, nine simulations were conducted considering each source term and meteorology set; and the results were compared with the ground level measurements performed after Chernobyl NPP accident. The combination having the highest correlation with measurement results were assumed as the most successful simulation and the impacts of the accident on Turkey were investigated by using these results. Impact analysis was made by calculating short-term and long-term radiation dose values through model outputs and different exposure pathways. The results obtained were visualized with a geographic information system software. The results were further analysed statistically and spatially by comparison with the calculations made based on previous real time ground level measurements of the Turkish Atomic Energy Agency.

Introduction

One of the worst anthropogenic catastrophes in the history of humanity has happened in Chernobyl Nuclear Power Plant (NPP) in 1986. Approximately 14 EBq (14×10^{18} Bq) of radioactivity was released to the environment as a result of the accident. Various measurements and estimations were conducted after the accident mostly in Europe and former Soviet Union region. These studies predominantly focused on the total release amounts of various radionuclides from the accident site as well as their atmospheric and ground level depositions (Abagyan et al., 1986; IAEA, 1992; Devell et al., 1995; De Cort et al. 1998; Brandt et al., 2002; Talerko, 2005a, 2005b; Davoine and Bocquet, 2007; Evangeliou et al., 2016; Evangeliou et al., 2017).

On the other hand, the majority of research conducted in Turkey for analyzing the potential effects of Chernobyl NPP accident focused on radionuclide accumulation in soil and plants (Akçay and Ardisson, 1988; Köse et al., 1994; Varinlioğlu et al., 1994, Varinlioğlu and Köse, 1996; Varinlioğlu and Köse, 2005; Celik et al., 2009). In 2006, Turkish Atomic Energy Agency (TAEK) published a series of books on Chernobyl accident and one of these books included a compilation of Chernobyl related studies on Turkish territory. This compilation included all available research conducted in Turkey and presented some dose estimations for Cs-137, Cs-134 and I-131. However, the dose values estimated in this study was not enough to be generalized for entire Turkish territory due to lack of data.

In addition to limited ground level deposition data, there is also extremely limited number of studies that simulate the atmospheric dispersion of Chernobyl related radionuclides and their effects on Anatolian Peninsula. Apart from the study conducted by Simsek et al. (2014), there are no published research on mathematical modeling of the dispersion and deposition patterns of radionuclides on Turkish territory.

Based on these premises, this study aims to conduct mathematical modeling of the atmospheric dispersion and ground level deposition of radionuclides emitted from Chernobyl NPP accident, and further intends to assess the potential consequences of the accident on Turkey by developing exposure and dose conditions.

Methodology

Atmospheric Dispersion Model

A Lagrangian particle dispersion model (FLEXPART v9.0.3) was used in this study to simulate the atmospheric dispersion and deposition of radionuclides. The

FLEXPART model is commonly used model in nuclear risk studies for simulating the dispersion and deposition of particles emitted from NPP accidents.
FLEXPART uses two major inputs: (i) source-related data, (ii) meteorological data. There are a number of studies that focus on the source term of Chernobyl accident and three of them (Brandt et al., 2002; Talerko, 2005a and 2005b; Evangeliou et al., 2017) were used in this study. Furthermore, the model uses 3-D meteorological fields in grib format to estimate atmospheric transport and depositions. Three different meteorological datasets from NOAA and ECMWF were used in this study: (i) NCAR/NCEP (NOAA), (ii) ERA-40, and (iii) ERA-INTERIM. Among these, NCAR/NCEP and ERA-40 have 6-hourly temporal and 0.5x0.5 degree horizontal resolution while ERA INTERIM has 3-hourly temporal and 0.75x0.75 degree horizontal resolution.
The simulations conducted in this study were performed for a domain that covered an area of about 60° by 40°, which included the Chernobyl NPP site (roughly at the center of the domain) and the territories of the countries of Ukraine, Romania, Bulgaria, Greece, Turkey, Georgia as well as some parts of Russia, Belarus, Poland, Slovakia, Hungary and Serbia. The model used a grid resolution of 0.1° by 0.1°, which corresponded to 240000 grid cells within the simulation domain.
Nine different simulations for three most common radionuclides (Cs-137, Cs-134 and I-131) were conducted using 3 different source terms and 3 different meteorological data-sets. Starting with the time of the accident, all simulations were run for 20 days with a total of 10 days release from the source.

Dose Estimations

There are four major exposure pathways for dose estimations in nuclear risk studies: (i) cloud-shine, (ii) ground-shine, (iii) inhalation and (iv) ingestion. In this study ingestion exposure was neglected as mostly in literature because it requires complicated approaches and very detailed data sets are typically not available.
Total effective dose equivalents (TEDE) caused by I-131, Cs-137 and Cs-134 were estimated for adults using the simulation results that gave the best output when compared to the real measurements. The simulation with highest correlation between measured vs. simulated was assumed to be the most satisfactory case and all further analysis of dose calculations were performed with the simulation results of this case. TEDE for each radionuclide were estimated by multiplying related model output with dose conversion factors for the corresponding pathway. Dose conversion factors were obtained from Health Canada (1999). Moreover, some dose reduction factors were also applied in this study. Considering shielding effect of buildings and time spent outside, a reduction factor was defined. In this study, shielding factor of 0.36 was used similar to the one used in TAEK (2006). The dose values calculated from the best run of this study were later compared with the dose values calculated by TAEK (2006).

$$\text{TEDE} = \sum_{t=0}^{t_n}\left[\left(\sum_{p=1}^{2} f_p^l f_p^d C_t\right) + f_{p=3}^l f_{p=3}^d f_{p=3}^r Dep_t\right] \quad (1)$$

where C_t represents concentration in the air and Dep_t represents deposition in the ground at time step t, f^l represents location factor (shielding), f^d represents dose conversion factor and f^r represents dose reduction factor due to radioactive decay for the related pathway (p=1 for inhalation, p=2 for cloud-shine and p=3 for ground-shine).

Results and Discussions

Selection of Best Model Scenario and Deposition Results

In this study, atmospheric dispersion and ground level deposition of I-131, Cs-134 and Cs-137 released from Chernobyl NPP accident were simulated using three different source terms and three different meteorological fields under nine cases. The results of all simulations were then compared with the Cs-137 measurements depicted in De Cort et al. (1998) and Evangeliou et al. (2016). The comparisons were only limited to Cs-137 as there were no extensive dataset available for other radionuclides. The scenario case that gave best correlation with the measured Cs-137 data was also assumed to be the best for other radionuclides simulated in this study too. The simulation case conducted with the source term data of Evangeliou et al. (2017) together with ERA 40 meteorological data set gave the most satisfactory results (Figure 1). From this point on, all calculations were conducted with the results of this particular run.

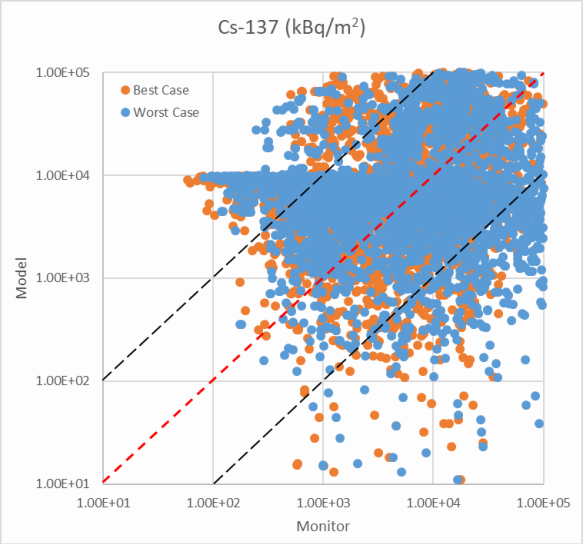

Figure 1. Comparison of model results and measurements for Cs-137 deposition (Best case is the simulation case conducted with the source term data of Evangeliou et al. (2017) together with ERA-40)

The deposition of Cs-134 was mainly simulated to be higher in the vicinity of the accident site. Three mainstream depositions were observed to be transported in southern, northwestern and southeastern directions, which had total deposition values exceeding 100 kBq/m^2. These depositions mainly influenced Ukraine, Moldova, Romania and Belarus. The depositions of Cs-134 in Turkey was not significant and the majority of deposition in Turkish soil was detected to be lower than 10 kBq/m^2 except Black Sea region.
The results revealed that the spatial distribution of Cs-137 depositions were found to be similar behavior to Cs-134

because of total release amount of Cesium isotopes are close each other in Evangeliou et al. (2017). A more dispersed pattern is quite evident with values reaching as high as 1000 kBq/m^2 in remote territories such as the Scandinavian region, Siberia and the Caucasus region (Figure 2). While the three mainstream plume-like depositions were also evident for Cs-137 with values exceeding 100 kBq/m^2, the results showed that the total depositions of Cs-137 was very close that of Cs-134. The situation in Turkey was also quite similar to Cs-134. Significant depositions that was in the order of 10^2 kBq/m^2 was simulated for the coastline of eastern Black Sea in Turkish and the Georgian territories. Within Turkey, highest depositions were found in the Eastern Black Sea region associated with the precipitation event in these locales. (Figure 2).

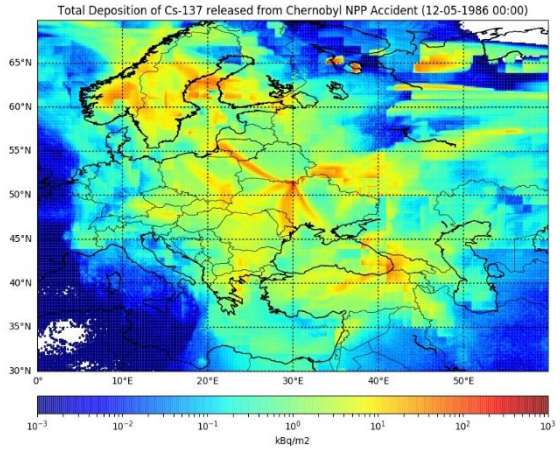

Figure 2. Total ground level deposition of Cs-137

Dose Estimations

Simulated depositions and air column concentrations of the radionuclides were taken from the best case. The dose values were calculated by using these values and later compared with the dose values reported by TAEK (2006) for the receptor points. TAEK (2006) divided Turkey into 4 different regions and estimated average 1-year dose values for each region: Eastern Black Sea, Western and Middle Black Sea, Marmara and Others. Regional averages were calculated by using the values calculated for each receptor point reported by TAEK (2006). The simulation results for these receptor points were used to calculate the simulated doses, which are later averaged to obtain the simulated regional averages.

The regionally averaged TEDE values are presented in Table 1. It is clearly seen that regional averages were highest in the eastern Black Sea region in both measurements and simulations. This was followed by western and central Black Sea regions. The values in eastern Black Sea demonstrated an acceptable fit between the measurements and the best simulation results. A similar pattern is also true for the western and central Black Sea regions. It is also noteworthy to mention that in the entire Black Sea regions, simulation results were higher than the measurements but demonstrate a close fit. On the contrary, measurements were found to be above the simulated results in Marmara region and Other regions of Turkey. In these territories, simulations were significantly lower than the measurements. One reason for these differences might be related to relatively shorter simulation period of 20 days, which did not allow radionuclides to disperse to these areas sufficiently. Another potential reason for these deficiencies might be related to poor simulation of meteorological conditions in the datasets. (Table 1).

Table 1. Comparison of Regionally Averaged TEDE results for 1 year (mSv)

	TAEK (2006)	**This study**
Eastern Black Sea	0.5045	0.5456
Western-Central Black Sea	0.1895	0.2251
Marmara	0.1695	0.0665
Other Regions	0.1787	0.0389

When spatial distribution of TEDE of Cs-134 were analyzed, relatively higher values were observed extensively in Turkish territories. Highest TEDE of Cs-134 was observed in Black Sea regions as expected (Figure 3). Similarly, highest TEDE of Cs-137 was also observed in Black Sea regions, particularly in eastern Black Sea region (Figure 4). TEDE of Cs-137 were simulated to be lower than Cs-134 due to the dose conversion factors. On the other hand, TEDE distribution map of I-131 demonstrated that highest values were observed in central and eastern Black Sea regions due to atmospheric transport of I-131. (Figure 5).

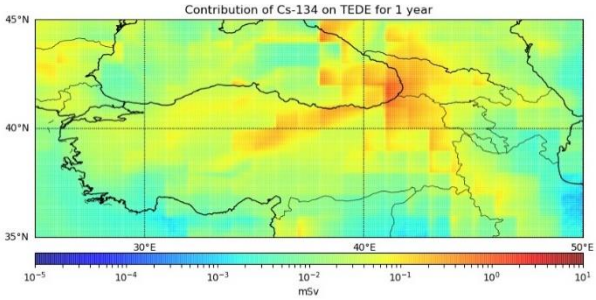

Figure 3. Spatial distribution total effective dose equivalent of Cs-134 for 1 year

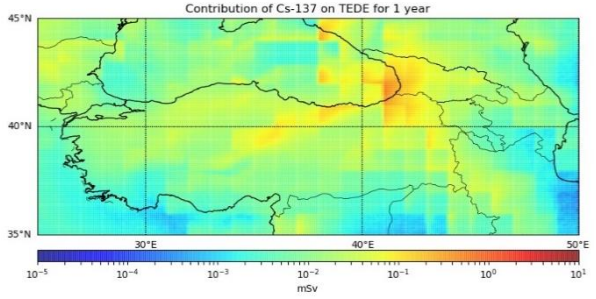

Figure 4. Spatial distribution total effective dose equivalent of Cs-137 for 1 year

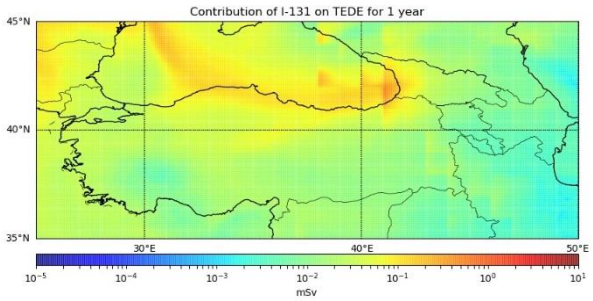

Figure 5. Spatial distribution total effective dose equivalent of I-131 for 1 year

Conclusions and Recommendations

Environmental and health effects of Chernobyl NPP accident on Turkey were investigated in present study based on mathematical modeling of dispersion and deposition of radionuclides. Total effective dose equivalents were estimated for each region and later compared for each pathway with measurements made from Turkish territories. Spatial distribution patterns of depositions and 1 year TEDE for each radionuclides were plotted for Turkey. The TEDE results obtained in this study were found to be close in Black Sea region but were mostly lower in other regions of the country when compared to the measurements complied by TAEK (2006). These differences were mostly associated with relatively dynamic pathways such as inhalation and cloud-shine, which were strongly dependent on air concentration measurements that are quite variable.

This study is one of the earliest of the cases where the effect of Chernobyl accident was mathematically simulated to represent conditions in Turkish territory. It is also the first study that uses verification data obtained from Turkey. The results revealed that Chernobyl source terms can be reformulated by using the measured data from Turkey in addition to the currently available measurement data from Europe and western territories of former Soviet Union. Nevertheless, additional measurement from different parts of the country are still needed to better calibrate and verify the model.

Abagyan, A. A., Ilyin, L. A., Izrael, Y. A., Legasov, V. A., and Petrov, V. E., 1986. The information on the Chernobyl accident and its consequences prepared for IAEA. *Sov. At. Energy.* 61: 301–320.

Akcay, H. and Ardisson, A., 1988. Radioactive pollution of Turkish biota one year after Chernobyl accident, J. Radioanal. *Nucl. Chem. Letter* 128(4): 273–281.

Brandt, J., Christensen, H. and Frohn, L. M., 2002. Modelling transport and deposition of cesium and iodine from the Chernobyl accident using the DREAM model. *Atmos. Chem. Phys.* 2: 397–417.

Celik, N., Cevik, U., Celik, A. and Koz, B. 2009. Natural and artificial radioactivity measurements in Eastern Black Sea region of Turkey. *J. Hazard. Mater.* 162(1): 146-153.

Davoine, X. and Bocquet, M., 2007. Inverse modelling-based reconstruction of the Chernobyl source term available for long-range transport. *Atmos. Chem. Phys.* 7: 1549–1564.

De Cort, M., Dubois, G., Fridman, S. D., Germenchuk, M. G., Izrael, Y. A., Janssens, A., Jones, A., Kelly, G. N., Knaviskova, E., Matveenko, I. I., Nazarov, I. M., Pokumeiko, Y. M., Sitak, V. A., Stukin, E. D., Tabachny, L.Y and Tsaturov, Y. S., 1998. Atlas of Cesium 137 Deposition on Europe after the Chernobyl Accident. Office for Official Publications of the European Communities. ISBN: 92-828-3140-X.

Devell, L., Guntay, S., and Powers, D. A., 1995. The Chernobyl reactor accident source term, Organization for Economic Cooperation and Development, Nuclear Energy Agency, Paris.

Evangeliou, N., Hamburger, T., Talerko, N., Zibtsev, S., Bondar, Y., Stohl, A., Balkanski, Y., Mousseau, T. A., and Møller, A.P., 2016, Reconstructing the Chernobyl Nuclear Power Plant (CNPP) accident 30 years after. A unique database of air concentration and deposition measurements over Europe. *Environ. Pollut.* 216: 408–418.

Evangeliou, N, Hamburger, T., Cozic, A, Balkanski, Y., and Stohl, A., 2017. Inverse modeling of the Chernobyl source term using atmospheric concentration and deposition measurements. *Atmos. Chem. Phys.* 17: 8805-8824.

Health Canada, 1999. Recommendations on dose coefficients for assessing doses from accidental radionuclide releases to the environment. Prepared by a Joint Working Group of Radiation Protection Bureau, Health Canada, Atomic Energy Control Board, Atomic Energy of Canada Limited.

IAEA, 1992. The Chernobyl accident: Updating of INSAG-1. A report by the International Nuclear Safety Advisory Group, Safety Series No. 75-INSAG-7, International Atomic Energy Agency (IAEA), Vienna.

Köse, A., Topcuoğlu, S., Varinlioğlu, A., Kopya, A. I., Azar, A., Uzun, O., and Karal, H., 1994. The levels of cesium radionuclides in lichens in the eastern Black Sea area of Turkey, *Toxicol. Environ. Chem.* 45: 221–224,

Simsek, V., Pozzoli, L., Unal, A., Kindap, T. and Karaca, M. (2014). Simulation of 137-Cs transport and deposition after the Chernobyl Nuclear Power Plant accident and radiological doses over the Anatolian Peninsula. *Science of the Total Environment* 499: 74–88.

Stohl, A., Forster, C., Frank, A., Seibert, P., and Wotawa, G., 2005. Technical note: The Lagrangian particle dispersion model FLEXPART version 6.2. *Atmos. Chem. Phys. 5*: 2461-2474.

TAEK, 2006. 20. Yılında Çernobil Serisi - Türkiye için Doz Değerlendirmeleri, Türkiye Atom Enerjisi Kurumu. ISBN 975-8898-19-1. (Original in Turkish)

Talerko, N., 2005a. Mesoscale modelling of radioactive contamination formation in Ukraine caused by the Chernobyl accident. *J. Environ. Radioactivity* 78: 311-329.

Talerko, N., 2005b. Reconstruction of 131-I radioactive contamination in Ukraine caused by the Chernobyl

accident using atmospheric transport modelling. *J. Environ. Radioactivity* 84: 343–362.

Varinlioğlu, A., Topcuoğlu, S., Köse, A., Kopya, A. I., Uzun, O., Azar, A., and Karal, H., 1994. Levels of cesium radionuclides in mosses in the eastern Black Sea area of Turkey, *J. Radioanal. Nucl. Ch.* 187: 435–440.

Varinlioğlu, A. and Köse, A., 2005. Determination of natural and artifical radıonuclide levels in soils of western and southern coastal area of Turkey, *Water, Air, and Soil Pollution* 164: 401–407.

Varinlioğlu, A. and Köse, A., 1996. Deposition of the radiocesium in soil at Black Sea coastal area in Turkey after Chernobyl accident. Proceedings of the International Conference One Decade After Chernobyl Vienna, Austria 8–12 April.

Study of radioactivity in arctic marine seaweed from Kongsfjorden (Svalbard)

E. Gordo[1], C. Íñiguez[2], S. Cañete[1], C. Jiménez[3], F.J.L. Gordillo[3], R. Carmona[3], F.J. Santos[4], J.M. López-Gutiérrez[4] and R. García-Tenorio[4]

[1]SCAI, Central Research Facilities, University of Malaga, Spain
[2]Research Group on Plant Biology under Mediterranean Conditions, Universitat de les Illes Balears–INAGEA, Spain
[3]Department of Ecology, Faculty of Sciences, University of Malaga, Spain
[4]Centro Nacional de Aceleradores (CNA), University of Sevilla-Junta Andalucía-CSIC, Spain
Keywords: Arctic, radionuclides, seaweed
Presenting author, e-mail: elisagp@uma.es

In this work, levels of natural and anthropogenic radionuclides have been determined in seven brown and red seaweed species from Arctic coasts (Kongsfjorden, Spitsbergen, Svalbard Islands) in order to characterise the radioactivity in this ecosystem.
Samples were collected in Hansneset in September 2014, August 2017 and July 2019. Levels of ^{7}Be, ^{40}K, ^{210}Pb, ^{226}Ra and ^{228}Ra were measured by high-resolution gamma spectrometry using high-purity germanium. While anthropogenic radionuclides such as ^{14}C and ^{129}I have been additionally determined by low-energy accelerator mass spectrometry (LEAMS).
The high concentration of ^{7}Be in the brown macroalga *Fucus distichus* revealed the influence of cosmogenic radionuclides in the intertidal zone. ^{40}K were detected in all species, instead ^{210}Pb has been observed only in the red species.
The levels of ^{129}I found in the arctic samples present more variability than the ^{14}C results and are two orders of magnitude higher than those found in algae collected in other latitudes, suggesting the influence of the Sellafield discharges in the arctic coast.

Introduction

The West Spitsbergen Current has a strong Atlantic character and brings relatively warm and nutrient-rich waters to Kongsfjorden (0 to 6°C) (Hanelt et al., 2004). The influx of Atlantic water and glacier's melting in this region has been linked to climate change (Svendsen et al., 2002) and thus algal communities of Kongsfjorden act as climate indicators at a local scale (Gordillo et al., 2006).
Seaweeds are useful as environmental bioindicators since they bioaccumulate radioisotopes at very low concentrations.
Comparison of the concentrations of various radionuclides including ^{7}Be, U- and Th-series radionuclides and ^{40}K having different origins and different chemical properties, may provide some important information on the enrichment mechanisms of the nuclides in various marine (Ishikawa et al., 2104).
^{129}I is a long-lived radionuclide ($T_{1/2} = 15.7 \times 10^{6}$ years) with a strongly increasing presence in the environment since the beginning of the nuclear era. Most of the anthropogenic radionuclide ^{129}I released to the marine environment from the nuclear fuel reprocessing plants at Sellafield (England) and La Hague (France) is transported to the Arctic Ocean via the North Atlantic Current and the Norwegian Coastal Current (Vivo-Vilches et al, 2018).
The radiological importance of ^{14}C derives from its long half-life, mobility in the environment and propensity for entering the food chain. A large percentage of the ^{14}C content of aqueous discharges from Sellafield is released in the form of carbonate/bicarbonate, and so is immediately incorporated into the dissolved inorganic carbon that is used by seaweeds, as primary producers, during photosynthesis (Keogh et al 2011).

Materials and methods

Seven species of macroalgae were collected from the Kongsfjord (see Figure. 1) at Spitsbergen, Norwegian Arctic (78º 55‘ N, 11º 56’ E) during September 2014, August 2017 and July 2019 at depths of 2–6 m; five brown: *Chorda filum*, *Saccharina latissima*, *Fucus distichus*, *Desmarestia aculeata* and *Alaria esculenta* and two red: *Phycodrys rubens* and *Ptilota gunneri.*

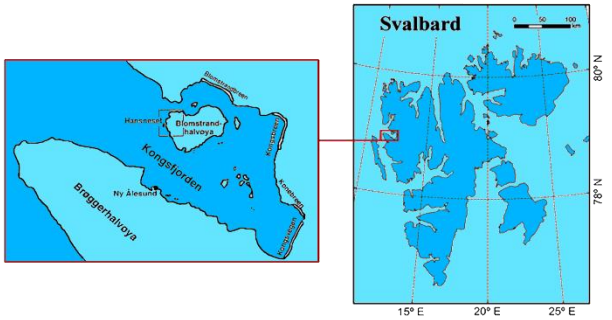

Figure 1. Map of sampling point.

Young thalli, free from macroscopic epibiota, were lyophilized, powdered and confined in a standard geometry before gamma spectrometry measurements. Two different detector systems have been used to carry out the gamma analysis: The first one consists of a Canberra type-n Ge detector (BeGe). The second detector system is composed by a Canberra type-p Ge detector XtRa. Both detectors were calibrated using a traceable multi gamma standard source and were verified using the reference standard IAEA 446, corresponding to a Baltic Sea Seaweed: *Fucus vesiculosus*. Besides, the Canberra ISOCS/LabSOCS, used for gamma spectrometry analyses allows efficiency calibration for a wide range of both measuring geometries and sample materials including marine biota (Tejera et al., 2019).
^{226}Ra was determined from the weighted average between ^{214}Pb (using the 351.9 keV) and ^{214}Bi (609 keV emission line) when they are in equilibrium. ^{210}Pb ^{40}K and ^{7}Be were directly determined using the 46.5 keV, 1460.8 keV and 477.6 keV emission lines, respectively. ^{228}Ra was

determined from ^{228}Ac (911.2 keV). The counting time for each sample was around 172,800 s.
Measurements of ^{129}I and ^{14}C were carried out at the 1 MV AMS facility at the Centro Nacional de Aceleradores in Sevilla (CNA, Spain). The measurement method has been previously described in detail (Gómez-Guzmán et al., 2012).

Results
Table 1 shows the results of the gamma analysis referred to dry weight and are decay corrected to the date of sampling and their uncertainties. The ^{228}Ra/^{226}Ra ratio has also been studied due to it is considered a particularly important indicator of circulation of coastal water (Inoue et al., 2005). These values are similar to the reported for a previous study (Inoue et al., 2005). In this studio, the ^{228}Ra/^{226}Ra ratio clearly showed a seasonal variation. We will study this behaviour in the future by similar measurements in seaweeds sampled in different seasons.

Table 1. Concentrations and their uncertainties (1σ) of gamma-emitting radionuclides in seaweeds referred to dry weight and the ratio ^{228}Ra/^{226}Ra

	^{7}Be	^{40}K	^{228}Ra/^{226}Ra	^{210}Pb
	Bq Kg^{-1}	Bq Kg^{-1}		Bq Kg^{-1}
Chorda filum	<37	2410 ± 38	<5	<19
Saccharina latissima	<7	1280 ± 21	<4	<12
Fucus distichus	26 ± 8	759 ± 15	1.5 ± 0.1	<17
Desmarestia aculeata	<3	1260 ± 25	0.45 ± 0.01	<8
Phycodrys rubens	<22	635 ± 15	2.3 ± 0.2	130 ± 10
Ptilota gunneri	20 ± 4	1530 ± 127	1.5 ± 0.1	110 ± 22
Alaria esculenta	10 ± 4	1080 ± 92	3 ± 0.1	<12

^{7}Be is detected only in three species and the higher concentration correspond to *Fucus distichus*, the only analysed species inhabiting the intertidal.
High concentrations of ^{40}K were observed in all species, as this is one of the essential elements in biota. Remarkably is the high content of ^{210}Pb in the red seaweeds, suggesting that these species might possess a higher capacity for heavy metals bioaccumulation than the analysed brown seaweeds.
Table 2 shows the results of the LEAMS analysis. ^{129}I presents more variability than the ^{14}C results indicating their different affinity to this element depending on the species.

Table 2. Concentrations and their uncertainties (1σ) of anthropogenic radionuclides in seaweeds referred to dry weight

	^{14}C	^{129}I
	mBq gC^{-1}	mBq Kg^{-1}
Saccharina latissima	237 ± 2	(170 ± 0.1)·10^{-1}
Phycodrys rubens	231 ± 2	(8.9 ± 0.3)·10^{-2}
Ptilota gunneri	237 ± 2	(3.7 ± 0.1)·10^{-1}
Alaria esculenta	242 ± 2	(3.3 ± 0.1)·10^{-2}

Figure 2. Schematic flow from the sources of ^{129}I.

The concentrations of ^{14}C are very similar in all species analyzed and they must be related with the ^{14}C content of the dissolved inorganic carbon source in their medium together with the ^{14}C isotopic discrimination of the main fixing enzyme in photosynthetic organisms, the Ribulose biphosphate carboxylase-oxygenase (Rubisco). This is a highly conserved enzyme through evolution, although significant changes in the Rubisco discrimination between ^{13}C and ^{12}C have been observed between different autotrophic organisms (Boller et al. 2015), suggesting that discrimination between ^{14}C and ^{12}C might differ between species ^{14}C values might be slightly higher than those observed in algae collected in other parts of the northern hemisphere, which might reflect an anthropogenic impact of the Sellafield nuclear complex (UK) radioactive discharges. These radioactive discharges might be transported to the Arctic through marine currents (Karcher et al., 2012) as it is shown in the Figure 2.

However, this assumption might be validated in the future by similar measurements in seaweeds from other locations not influenced by radioactive discharges.
Conversely, the influence of the Sellafield discharges is evident in the ^{129}I determinations performed. The levels of this radionuclide found are two orders of magnitude higher than those found in algae collected, for example, on the Spanish Mediterranean Coast, but lower than the found ones in algae collected on the North Sea. This result is similar to the obtained by Vivo-Vilches et al (2018) in samples of seawater.

Conclusions

The results revealed the influence of cosmogenic radionuclide (^{7}Be) in the intertidal zone. ^{40}K was detected in all the species but ^{210}Pb only in the red seaweeds analysed.
The levels of ^{129}I found were higher than those found in algae collected in Spanish Coast; that reveals the influence of the Sellafield discharges.
A more complete study will be carried out to determine the seasonal variation of the ^{228}Ra/^{226}Ra ratio, as well as a comparison of the measures of ^{14}C in algae taken at different latitudes to study the contribution of Sellafield discharges.

This study was financed by the project CGL2015-67014R from the Spanish Ministry for Science and Innovation. Authors thank the Alfred Wegener Institute (AWI)-diving team for sample collection.

Boller, A.J., Thomas, P.J., Cavanaugh, C. M. and Scott, K. M. 2015. Isotopic discrimination and kinetic parameters of RubisCO from the marine bloom-forming diatom, Skeletonema costatum. *Geobiology* 13:33-43.

Gordillo, J. L., Aguilera, J., Jiménez, C. The response of nutrient assimilation and biochemical composition of Arctic seaweeds to a nutrient input in summer. 2006. *J. Exp. Bot.* 57(11):2661-71.

Gómez-Guzmán, J. M., López-Gutiérrez, J.M., Pinto-Gómez, A.R. and Holm, E. 2012. ^{129}I measurements on the 1 MV AMS facility at the Centro Nacional de Aceleradores (CNA, Spain). *Appl. Radiat. Isot.* 70 263–268.

Hanelt, D., Tüg, H., Bischof, K., Groß, C., Lippert, H., Sawall, T., Wiencke, C. 2001. Light regime in an Arctic fjord: a study related to stratospheric ozone depletion as a basis for determination of UV effects on algal growth. *Marine Biology* 138(3):649-58.

Inoue, M., Kofuji, H., Yamamoto, M. and Komura, K. 2005. Seasonal variation of ^{228}Ra/^{226}Ra ratio in seaweed: implications for water circulation patterns in coastal areas of the Noto Peninsula, Japan. *J. Environ. Radioactiv.* 80. 341–355.

Ishikawa, Y., Kagaya, H. and Saga, K. 2004. Biomagnification of ^{7}Be, ^{234}Th, and ^{228}Ra in marine organisms near the northern Pacific coast of Japan *J. Environ. Radioactiv.* 76. 103–112.

Karcher, M.J., Smith, J., Kauker, R., Gerdes, R. and Smethie, W. M. 2012. Recent changes in Arctic Ocean circulation revealed by iodine-129 observations and modeling. *J. Geo. Res. Atmos.* 117 (C8):8007.

Keogh, S. M., Cournane, S., León Vintró, L., McGee, E. J. and Mitchell, P.I. 2011. Modelling the biological half-life and seasonality of ^{14}C in Fucus vesiculosus from the east coast of Ireland: Implications for the estimation of future trends. *Marine Pollution Bulletin* 62 696–700.

Tejera, A., Pérez-Sánchez, L., Guerra, G., Arriola-Velásquez, A.C., Alonso, H., Arnedo, M.A., Rubiano, G. and Martel, P. 2019. Natural radioactivity in algae arrivals on the Canary coast and dosimetry assessment. *Sci. Total Environ.* 658. 122–131.

Vivo-Vilches, C., López-Gutiérrez, J. M., Periáñez, R., Marcinkod, C., Le Moignee, F., McGinnityf, P., Peruchena, J.I and Villa-Alfageme, M. 2018. Recent evolution of ^{129}I levels in the Nordic Seas and the North Atlantic Ocean. *Sci. Total Environ.* 621 376–386.

Natural radioactivity and its associated radiological hazards at seila area south eastern desert, Egypt

Hanfi M. Y[1,2]. Mostafa. Y. A. Mostafa[1,3]

[1]Ural Federal University, Mira Street 19, 620002, Ekaterinburg, Russia
[2]Nuclear Materials Authority, 520, Maadi, Cairo, Egypt
[3] Physics Department – Faculty of Science, Minia University, Minia, Egypt
Keywords: Natural radioactivity; Exposure; Spectrometer; Radiological hazard; Organs.
Presenting author, e-mail: m.nuc2012@gmail.com

Natural radioactivity in two sites at seila area, south eastern desert of Egypt is measured. Nearly Fifty locations distributed on the two sites were chosen to determine the natural radioactivity content in the stream sediments at these locations with a portable RS-230 Gamma-Ray Spectrometer (1,024 channels). This study presents Specific activities (A) of ^{238}U, ^{232}Th and ^{40}K radionuclides, Radium equivalent activities (Ra_{eq}), external and internal hazard indices (H_{ext}, H_{int}), external and internal level indices (I_γ, I_α), activity utilization index (I), exposure rate (ER) and other important parameters. Finally, the effective dose rate delivered to the particular organs (Lungs, Ovaries, Bone marrow, Testes and Whole body) from air dose indoor and outdoor are estimated.

Introduction

During the whole life, humans are exposed to various risks from environmental contaminants. Natural and anthropogenic sources are part of these risks. Permanent and unavoidable risk is associated with natural (terrestrial and cosmic) radiation. Terrestrial radiation consist the primordial radionuclides present in the Earth's crust (^{238}U and ^{232}Th, and ^{40}K) and cosmic radiation produces cosmogenic radionuclides (^{3}H, ^{14}C, ^{7}Be and ^{22}Na) in interactions with nuclei in Earth's atmosphere (Hanfi, 2019a; UNSCEAR, 2008).

The present study was carried out to determine the activity concentrations of ^{238}U, ^{232}Th and ^{40}K in surface of stream sediments at seila area, south eastern desert of Egypt, and are used to assess the potential radiological hazards associated with these sediments.

Materials and methods

Fifty-one locations were distributed in the studied area at Seila area (Figure 1). The site has an area of 1.75 × 1.25 km^2. These locations were chosen to measure terrestrial radionuclides content in the stream sediments.

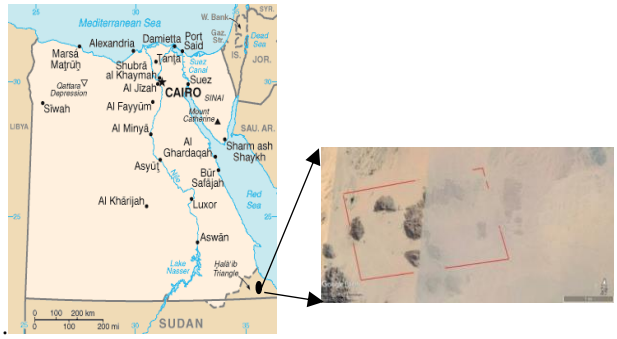

Figure 1. Geological map of Seila area, Southeastern desert, Egypt, showing the studied area.

A RS-230 BGO spectrometer (1024 channels) was used to measure the wide range of potential radiation concentrations during the uranium exploration process.

Calculations of activities, hazard indices and dose parameters

Radium equivalent activities (Ra_{eq})

Radium equivalent (Ra_{eq}) index in Bq kg^{-1} is an exceedingly used radiological hazard index. It was calculated as follows.

$$Ra_{eq}=C_U+1.43\,C_{Th}+0.077C_k \quad (1)$$

Where C_U, C_{Th} and C_k are the activity concentrations of ^{238}U, ^{232}Th and ^{40}K in Bq kg^{-1}, respectively.

Absorbed gamma dose rate (D_R)

The natural radionuclides contribution to the absorbed dose rate in air (D) Bqkg^{-1} at 1 m above the ground can be calculated (UNSCEAR, 2000)..

$$D_R\,(nGyh^{-1}) = 0.462C_U+0.604C_{Th}+0.0417C_K \quad (2)$$

Where C_U, C_{Th} and C_k are the activity concentrations of ^{238}U, ^{232}Th and ^{40}K in Bq kg^{-1}, respectively.

Internal radiation hazard (H_{in})

The using of internal hazard index (H_{in}) to control the internal exposure to ^{222}Rn and its progeny(Tabar et al., 2017).

$$H_{in}=C_U/185+C_{Th}/259+C_K/4810) <1 \quad (3)$$

Where C_U, C_K and C_{Th} are the activity concentrations of ^{238}U, ^{40}K and ^{232}Th in Bq kg^{-1}, respectively.

External radiation hazard (H_{ex})

The external hazard index (H_{ex}) represents the external radiation exposure associated with gamma irradiation from radionuclides of concern. The external hazard index (H_{ex}) is defined by equation (Janković et al., 2008):

$$H_{ex}=(C_U/370+C_{Th}/259+C_K/4810) \leq 1 \quad (4)$$

Where C_U, C_K and C_{Th} are the concentration in (Bq kg^{-1}) of radium, potassium and thorium respectively.

External (γ-radioactivity) gamma index (I_γ)

The representative level *gamma* index (I_γ) is used to assessment the level of γ-radiation hazard associated with the natural radionuclides in specific study samples. The **γ**-radiation hazard level of the samples associated with natural radionuclides was calculated by using the following equation, which was based on the radiation hazard index I_γ. (Beretka and Mathew, 1985):

$$I_\gamma=(C_U/300+C_{Th}/200+C_K/3000) \quad (5)$$

Where C_{Ra}, C_K and C_{Th} are the specific activities (Bq kg^{-1}) of ^{238}U, ^{40}K and ^{232}Th, respectively. The OECD group of experts suggested some criteria for a definition of

different levels of to be (representative, first enhanced, second enhanced). $I_\gamma = 1$ as an upper limit, $I_\gamma \leq 1$ corresponds to 0.3 mSv y^{-1}, $I_\gamma \leq 3$ corresponds to 1 mSv y^{-1}.

Internal (α-radioactivity) level index I_α

The excess alpha radiation due to radon inhalation originating from building materials is estimated using the relation below

$$I_\alpha = C_U/200 \leq 1 \quad (6)$$

I_α should be lower than the maximum permissible value of $I_\alpha = 1$, which corresponds to 200 Bq kg^{-1}.

Activity Utilization Index I

Activity utilization index defines the dose rate in air due to different combinations of ^{238}U, ^{232}Th and ^{40}K in the tailing enriched soil samples. AUI was calculated from the relation

$$I = \frac{C_U}{50} f_u + \frac{C_{Th}}{50} f_{Th} + \frac{C_K}{500} f_K \quad (7)$$

Where the fractional contributions, f_U, f_{Th} and f_K to the total gamma radiation dose rate in the air from the activity concentrations of ^{238}U, ^{232}Th and ^{40}K, respectively.

Annual effective dose (mSv.y^{-1})

The annual effective dose (AED) outdoors in units of ($mSvy^{-1}$), resulting from natural radionuclides of ^{238U}, ^{40}K and ^{232}Th. was calculated by the following formula (UNSCEAR, 2000)

$$AED\ (mSv.y^{-1}) = D_R \times T \times O \times F \times 10^{-6} \quad (8)$$

Where, D_R is absorbed dose rate in (nGy h^{-1}), , T is the full occupancy time in year (8760 h), F is the conversion coefficient 0.7 Sv/Gy, (0.2) is the outdoor occupancy factor and (0.8) is the indoor occupancy factor (Kalaitzis et al., 2019). The recommended total annual effective dose due to external exposure to natural terrestrial sources is 0.48 mSv y^{-1} and the criterion of the total annual effective dose should be less than 1 mSv y^{-1} (UNSCEAR, 2000).

Effective dose rate (D_{organ}) to different body organs and tissues

The effective dose rate delivered to a particular organ can be calculated using the following relation (O'Brien and Sanna, 1976):

$$D_{organ} = AED * F \quad (9)$$

Where f is the conversion factor of organ dose from air dose. The energies of interest in the present work, is 0.2 – 3 MeV f is almost independent of energy. The average values of F for various organs and tissues are given in Table 1. Using these f values, D_{organ} was calculated by applying Eq. (8) (Darwish et al., 2015; El-Gamal et al., 2007)

Table 1: Average value of F factor for different organs or tissues(Darwish et al., 2015; El-Gamal et al., 2007).

Organ or tissue	F
Lungs	0.64
Ovaries	0.58
Bone marrow	0.69
Testes	0.82
Whole body	0.68

The annual gonadal dose (AGD) for a resident of a house

The gonads, the active bone marrow and the bone surface cells are considered to be the organs of importance. The annual gonadal equivalent dose (AGED) due to the specific activities of ^{238}U, ^{232}Th and ^{40}K was calculated using the following relation (Arafa, 2004).

$$AGED\left(\mu\frac{Sv}{y}\right) = 3.09\ C_U + 418\ C_{Th} + 0.0317 C_K \quad (10)$$

The world averages of AGED of a house containing activity concentrations of ^{238}U, ^{232}Th and ^{40}K are 35, 35 and 370 mSv y^{-1}, respectively. The standard UNSCEAR value for AGED is 300 mSv y^{-1}.

Excess lifetime cancer risk (ELCR) in mSv yr^{-1}

This gives the probability of developing cancer over a lifetime at a given exposure level. The ELCR has been calculated using the following equation:

$$ELCR = AED\ x\ DL\ x\ RF \quad (11)$$

Where DL is the duration of life (70 years average) and RF is the risk factor (Sv^{-1}) i.e. fatal cancer risk per Sievert. For stochastic effects, the ICRP 106 used a value of RF = 0.05 for the public.

Clark value $^{232}Th/^{238}U$ concentration ratio

This ratio will give an indication that the samples collected from a certain region have either higher or lower uranium concentration to be economic for uranium mining and extraction (UNSCEAR, 2000).

Results and discussions

The average values of the ^{238}U, ^{232}Th and ^{40}K activity concentrations in the stream sediments were 39±11 (15-66), 33±9 (18-68) and 657±109 (470-1100) Bq kg^{-1} respectively. These values are higher than the worldwide average of ^{238}U and ^{40}K, 33 and 412 Bq kg^{-1}, and less than for ^{232}Th 45 Bq kg^{-1} according to UNSCEAR (UNSCEAR, 2008). This is due to relatively abundant of potassium, high concentration of uranium and thorium is attributed to presence of accessory minerals such as zircon, monazite, iron oxides, fluorite and other radioactive related minerals. A negative correlation exists between the activity of ^{232}Th and ^{238}U in the two sites with fitting equation $^{232}\mathbf{Th} = \mathbf{-0.156}\ ^{238}\mathbf{U} + \mathbf{39.2}$ and standard error (± 0.11) as shown in Figure 3.While a clear positive correlation exists between the activity of ^{232}Th and ^{40}K in the two sites with fitting equation $^{232}\mathbf{Th} = \mathbf{0.046}\ ^{40}\mathbf{K} + \mathbf{3.05}$ and standard error (± 0.009) as shown in Figure 3. Finally, independent correlation between ^{238}U and ^{40}K as shown in Figure 2.

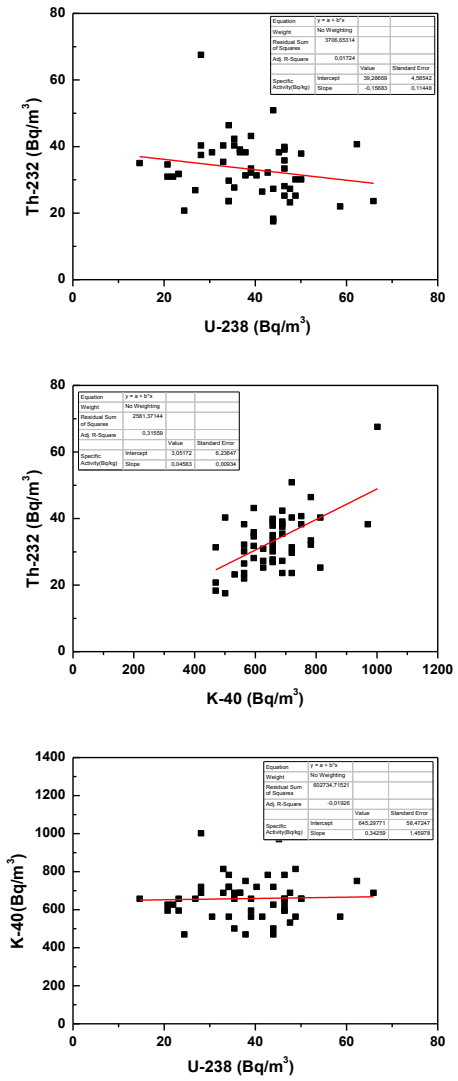

Figure 2. Correlation between natural radionuclides in all measured sites.

The ratio of ^{232}Th /^{238}U is represented in Fig 3. The red line represents the world average value. The ^{232}Th/^{238}U ratio was ranged from 1.07–7.22 with a mean value of 2.86, which is lower than the world average Th/U ratio in sediment (3.94) (Baba-ahmed et al., 2018). The difference is due to the geochemical variation of stream sediment, solubility differences between ^{238}U and ^{232}Th and may have the effects of weathering. In addition, the radionuclides exploration activities were done near to the studied area. In the studied area, the ^{232}Th/ ^{238}U ratio for 81% from the stations is lower than the world average value. This is due to high uranium contents in the studied area are derived from the surrounding granitic rocks which have elevated uranium content (Abdel-Razek et al., 2015). The highest value of the ratio was observed in 19% from all stations, confirming the presence of thorium due to the stream sediments are contain on the biotite, zircon, and muscovite are the characteristic minerals of the studied granites.

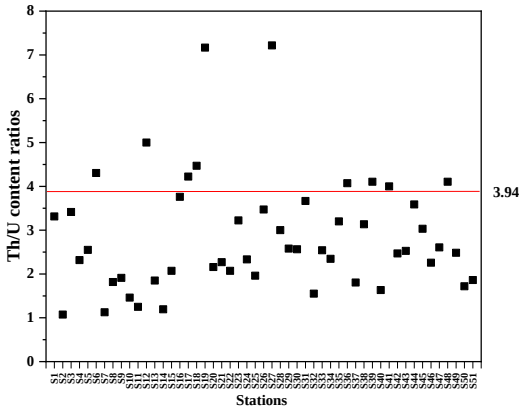

Figure 3. ^{232}Th/^{238}U content ratios from stream sediments of 51 stations in Seila area. Comparison with the world average (3.94) (Baba-ahmed et al., 2018).

Table 2. Radiological hazard parameters.

	Ra_{eq} Bqkg^{-1}	D nGy h^{-1}	H_{ex}	H_{in}	(I_γ)	(I_α)	(I)	AED_{out}	AED_{in}	AED mSv y^{-1}
AVG	137	65	0.4	2.8	0.5	0.2	1.0	0.08	0.3	0.41
MIN	90	8	0.2	1.9	0.3	0.1	0.7	0.01	0.1	0.27
MAX	202	100	0.5	4.3	0.8	0.3	1.6	0.12	0.5	0.45
STD	21	13	0.1	0.5	0.1	0.1	0.2	0.02	0.1	0.06
MID	135	65	0.4	2.7	0.5	0.2	0.9	0.08	0.3	0.41

Average radiological hazard parameters for the measured area are listed in Table 2 as Radium equivalent (Ra_{eq}), the dose rate (D), hazard indices (H_{ex} and H_{in}), Gamma and Alpha indexes (I_γ , I_α), radiation index I, annual effective dose (AED) outdoor and indoor.

Internal hazard indices (H_{in}) were ranged between 1.9 and 4.3, with mean value 2.8, radium equivalent activity (Ra_{eq}) were ranged between 90 to 202 with average mean 137 Bq/kg, activity concentration indices (I) were 0.7 – 1.6 with 1 average value, and alpha index (I_α) were 0.1 to 0.3 with mean average 0.2. These results show that there is over-exposure, for example, internal hazard indices (H_{in}) in all measured points are found to be more than unity then it exceeds the upper limit of exposure. While activity concentration indices (I) slightly exceed the permissible limits which met 0.3 mSv y^{-1} (Mubarak et al., 2017).

The calculated value for the absorbed dose rate ranged from 8 to 100 nGyh^{-1} with an average mean of 65 ± 13 nGyh^{-1}. which is relatively higher than the world wide mean of 58 nGyh^{-1} (UNSCEAR, 2008). The frequency distribution (in percent) of the total absorbed dose rates of the 51 measured locations is plotted in Figure 4.

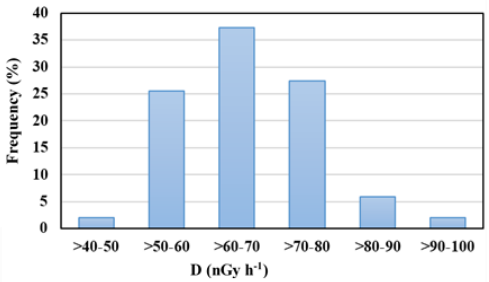

Figure 4. Frequency distribution of the absorbed dose rates of the measured stations in Seila area.

The indoor annual effective dose rate (AED_{in}) as presented in Table 2 for the selected quarry sites in this study varies from 0.1 to 0.5 mSv y^{-1} with the arithmetic mean value of 0.3 $mSvy^{-1}$ when compared with the worldwide effective dose of 0.41mSv y^{-1} (UNSCEAR, 2008) the results in this work are higher. For AED_{out} varies from 0.01 to 0.12 $mSv.y^{-1}$ with mean value 0.08 $mSv.y^{-1}$ which also higher compared with the worldwide effective dose of 0.07 mSv y^{-1}. The acceptable annual effective dose rate recommended for members of the public without constraint is 1 mSv. for safety purposes (Valentin, 2007). The frequency normal distribution of Ra_{eq} for all samples under investigation are shown in Figure 5. These results indicate all values of Ra_{eq} are less than the recommended limit 370 $Bqkg^{-1}$ (Beretka and Mathew, 1985) that keep the external dose below 1.5 mSv y^{-1} as reported by UNSCEAR. Figure 6 illustrates the relation between Ra_{eq} and ^{238}U activity with the fitted straight line. There is a positive and a good correlation between uranium concentration and radium equivalent activity level in area of interest.

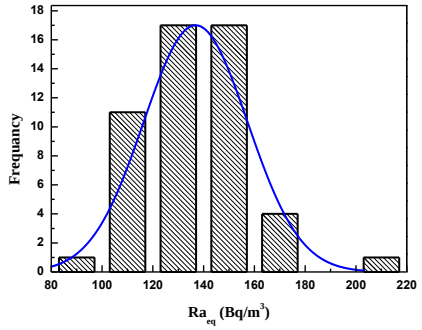

Figure 5. Frequency normal distribution of Ra_{eq} for all samples under investigation.

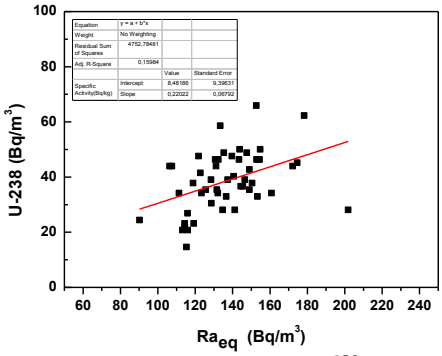

Figure 6. Correlation between ^{238}U and Ra_{eq} in all measured sites.

Excess lifetime cancer risk (ELCR) and annual gonadal dose (AGED) distributions are presented in Figure 7. Total Excessive Lifetime Cancer Risk (ELCR) is found to be ranged between 0.95 - 2.14 with an average of 1.44 which is close to the world average limits 1.45 (Qureshi et al., 2014).

The obtained values of annual gonadal dose varied from 7 to 18 mSv y^{-1} with mean value and standard deviation of 14±4 mSv y^{-1}. The mean values of soil samples were 0.44 mSv y^{-1} for Nigeria , 2.4 mSv y^{-1} for Egypt, and 0.18 mSv $y^{-1}$for Saudi Arabia (Al-kaabi and Al-shimary, 1996). This mean that the obtained results are high.

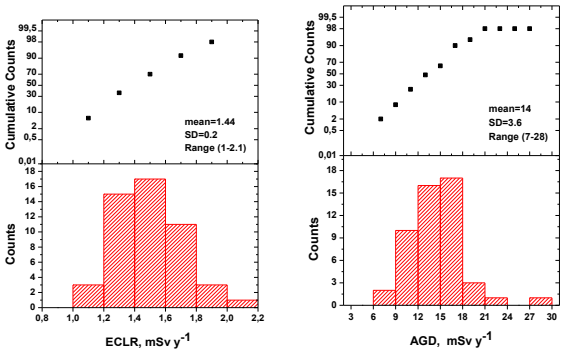

Figure 7. Excess lifetime cancer risk (ELCR) and the annual gonadal dose (AGED) distributions.

The effective dose rate delivered to the particular organs (Lungs, Ovaries, Bone marrow, Testes and Whole body) from air dose indoor and outdoor are shown in Figure 8. D_{org} values are less than the set limit but always indoors is higher than outdoors as expected. Also, we can conclude that, the testes have a highest radiation sensitivity while ovaries have a lowest radiation sensitivity. There for males more affected than females with radiation.

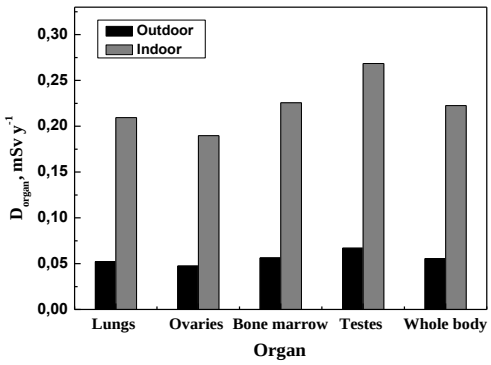

Figure 8. The effective dose rate delivered to the particular organs (Lungs, Ovaries, Bone marrow. Testes and Whole body) from air dose indoor and outdoor.

Risk assessment

In the studied areas, the radiological risk is very low according to the data which showed that the exposure time for public due to natural radioactive over 1 m from the ground. The obtained results were clarified that the average annual effective dose in the studied areas (0.08 mSv) is lower than the reference level 0.3 – 1 mSv (UNSCEAR, 2010). So, it is safe for the shepherds and camels around this area., population living and can be

used as a building raw materials or other human activities without any radiological risk.

Conclusions

From the experimental and computational work on natural radioactivity of selia area, Egyptian south eastern desert, we can conclude the following:

The seila area, south eastern desert, Egypt contain ^{238}Uand 40K radionuclides with activity concentrations higher and comparable than the set world limits.

The ^{232}Th activity concentration is lower than the set world limits

The radium equivalent activity is less than the world limit.

In general, the hazard indices, not all the level indices and the activity utilization indices are less than the world set criteria.

Internal hazard indices (H_{in}) in all measured points are found to be more than unity then it exceeds the upper limit of exposure.

Males more affected than females with radiation during the testes have a highest radiation sensitivity while ovaries have a lowest radiation sensitivity

Abdel-Razek, Y.A., Masoud, M.S., Hanafi, M.Y., El-Nagdy, M.S., 2015. Study of the parameters affecting radon gas flux from the stream sediments at Seila area Southeastern desert, *Egypt. Environ. Earth Sci.* 73, 8035–8044.

Al-kaabi, M.A., Al-shimary, A., 1996. Study of the radiological doses and hazard indices in soil samples from Karbala city , *Iraq Abstract* : 1–9.

Arafa, W., 2004. Specific activity and hazards of granite samples collected from the Eastern Desert of Egypt. *J. Environ. Radioact.* 75, 315–327.

Baba-ahmed, L., Benamar, M.E.A., Belamri, M., Azbouche, A., 2018. Natural radioactivity levels in sediments in Algiers Bay using instrumental neutron activation analysis 1–10.

Beretka, J., Mathew, P.J., 1985. Natural radioactivity of australian building materials, industrial wastes and by-products. *Health Phys.* 48, 87–95.

Darwish, D.A.E., Abul-Nasr, K.T.M., El-Khayatt, A.M., 2015. The assessment of natural radioactivity and its associated radiological hazards and dose parameters in granite samples from South Sinai, Egypt. *J. Radiat. Res. Appl. Sci.* 8, 17–25.

El-Gamal, A., Nasr, S., El-Taher, A., 2007. Study of the spatial distribution of natural radioactivity in the upper Egypt Nile River sediments. *Radiat. Meas.* 42, 457–465.

Hanfi, M.Y.M., 2019. Radiological assessment of gamma and radon dose rates at former uranium mining tunnels in Egypt. *Environ. Earth Sci.* 78, 0.

Janković, M., Todorović, D., Savanović, M., 2008. Radioactivity measurements in soil samples collected in the Republic of Srpska. *Radiat. Meas.* 48, 1448–1452.

Kalaitzis, A., Stoulos, S., Melfos, V., Kantiranis, N., Filippidis, A., 2019. Application of zeolitic rocks in the environment: assessment of radiation due to natural radioactivity. *J. Radioanal. Nucl. Chem.* 319, 975–985.

Mubarak, F., Fayez-Hassan, M., Mansour, N.A., Salah Ahmed, T., Ali, A., 2017. Radiological Investigation of High Background Radiation Areas. *Sci. Rep.* 7, 1–12.

O'Brien, K., Sanna, R., 1976. The Distribution of Absorbed Dose-rates in Humans from Exposure to Environmental Gamma Rays. *Health Phys.* 30, 71–78.

Qureshi, A.A., Tariq, S., Din, K.U., Manzoor, S., Calligaris, C., Waheed, A., 2014. Evaluation of excessive lifetime cancer risk due to natural radioactivity in the rivers sediments of Northern Pakistan. *J. Radiat. Res. Appl. Sci.* 7, 438–447.

Tabar, E., İçhedef, M., Kuş, A., Saç, M.M., Taşköprü, C., Yakut, H., 2017. Natural radioactivity levels and related risk assessment in soil samples from Sakarya, Turkey. *J. Radioanal. Nucl. Chem.* 313, 249–259.

UNSCEAR, 2008. Sources, Effects and Risks of Ionizing Radiation, Radiation Research. New York,. https://doi.org/10.2307/3577647

UNSCEAR, 2000a. 2000-Sources and Effects of Ionizing Radiation: Volume I. https://doi.org/10.1097/00004032-199907000-00007

UNSCEAR, 2000b. Sources and effects of ionizing radiation: United Nations Scientific Committee on the Effects of Atomic Radiation. UNSCEAR 2000 Rep. to Gen. Assem. 1–10.

Valentin, J., 2007. Annals of the ICRP PUBLICATION 103 The 2007 Recommendations of the International Commission on Radiological Protection.

Contribution of environmental radionuclides to radiological hazard effects due to surface soils collected from Amman Governorate, Jordan.

Mefleh S. Hamideen

Department of Physics and Basic Sciences, Faculty of Engineering Technology, Al-Balqa Applied University, Amman, 11134, Jordan

Keywords: Environmental radionuclides; Gamma ray spectroscopy; Hazard indices

E-mail: mhamideen@bau.edu.jo

The environmental radioisotopes concentrations of some specimens of surface soil from Amman Governorate, Jordan have been analyzed using an HPGe- detector to check the contributions of environmental radioisotopes to the radiation hazard effects. The activity concentrations were estimated for ^{226}Ra (range from 12.9 ± 1.0 to 58.9 ± 4.6 Bq/kg), ^{232}Th (range from 8.2 ± 1.0 to 68.9 ± 5.6 Bq/kg), and ^{40}K (range from 142.9 ± 15.2 to 347.4 ± 31.5 Bq/kg). Average values of radium equivalent activities (Ra_{eq}), absorbed dose rate (D_R), the annual effective dose rate (H_R), the internal hazard index (H_{in}), and external hazard index (H_{ex}) were calculated to be 102.02 Bq/kg, 46.54 nGy/h, 0.056 mSv/y, 0.352 and 0.275 respectively**.** It was noticed that all values of Ra_{eq} are among the permissible value (370 Bq/kg). The radiological implication in working site has shown that most of the soil samples have a dose rate less than the world recommended value except soil samples from two locations (S9 and S11). From the results, one can see that total annual effective dose, that a person can absorb from soils located in his place for all sample locations is below the accepted value (1.0 mSv/y).The H_{in} and H_{ex} values were within the standard values. From the analysis carried out in this study, ^{232}Th-radionuclides was found to be the main contributor to the environmental radionuclides for most discussed radiological hazard effects.

Introduction

Most of the environmental radioisotopes are alpha producers, so when a person inhale or ingest them, those radioisotopes contribute strongly to the radiation dose that a person may take (Colmnero Sujeo et al., 2004). Readers should note that soils contain radioisotopes which in turn produce outdoor radiations with its related doses. Additionally, natural radioactivity data are of considerable limits as baseline when standard and regular actions on radiological aspects are issued (UNSCEAR, 2000). Because the levels determined by terrestrial radiation are related to the kinds of rocks from it originate, natural environmental radiation depends mainly on geological and geographic conditions (Florou and Kritidis, 1992). The inhalation dose comes from the presence of dust particles in the air, including radionuclides from uranium and thorium progenies. Concentrations of radioactivity in the soil provide data on both natural and anthropogenic sites that are important in radiological checking point of view and determining doses received by people (Hammood and Al-Khalifa, 2011).The natural radioactive material that occurs when processed, the concentration of radionuclides is higher in waste, so radionuclides have a very long half-life when it comes to public safety (Hassan et al., 2013). The first aim of this work is to estimate the concentration of radioisotopes in soil from some selected places in Amman Governorate, Jordan. The second one is to check the contribution of environmental radioisotopes to some selected radiation hazard effects due to surface soils.

Materials and Methods

A total of twelve surface soils specimens were gathered from different locations distributed throughout Amman Governorate, Jordan. The samples were classified upon the source from which they were collected. An oven (100°C) was utilized to dry the samples to get fixed weight and a suitable sieve was used to get rid of strange particles. The diameter of the released particle is 0.2 mm and the weight of each sample was around 1kg. Radionuclide concentration was determined using (HPGe)-detector. The detector is a 3.5-kV detector, with a range from 3 keV-10 MeV.

Uranium (radium) existence in the samples was assessed by their progeny isotopes which gives radiations, which were mainly determined from the 609keV-line.By keeping them in a store to thirty days in order get a balance among the parents and daughters nuclei, thorium existence was determined from the 239 keV-line and ^{40}K from 1460 keV-line.

Data and Data analysis

Table 1 gives the activity concentrations (in Bq/kg) of the tested radioisotopes. The results show that the activity concentrations varies for ^{226}Ra (ranges from 12.9 ± 1.0 to 58.9 ± 4.6 Bq/kg), ^{232}Th (ranges from 8.2 ± 1.0 to 68.9 ± 5.6 Bq/kg), and ^{40}K (ranges from 142.9 ± 15.2 to 347.4 ± 31.5 Bq/kg). The average values were 28.31 Bq/kg, 38.26 Bq/kg, and 246.83 Bq/kg for ^{226}Ra, ^{232}Th, and ^{40}K, respectively.

In order to find the risk of radiation contained in soil specimens, different radiation hazards were determined relative to the standards. Ra_{eq} is very wide using factor, that we can determine its value using the activity concentrations of radioisotopes. Its value can be determined by a formula given by Beretka and his colleague Mathew in 1985 (Beretka and Mathew, 1985):

$$Ra_{eq}(Bq/Kg) = A_{Ra} + 1.43A_{Th} + 0.077A_{K} \quad (1)$$

where A_{Ra}**,** A_{Th} and A_K are the activities of ^{226}Ra, ^{232}Th and ^{40}K respectively in units of Bq/kg. The calculated values of Ra_{eq} for soils are shown in Table 2. Its values range from 42.35 (S1) to 155.68 (S11) in Bq/kg where the average value is 102.02 Bq/kg. The calculated results for all values of Ra_{eq} were within the permissible limit (370 Bq/kg) (NEA-OECD, 1979).

Table 1. Radioisotopes concentration in some soil specimens

Sample code	^{226}Ra (Bq/kg)	^{232}Th (Bq/kg)	^{40}K (Bq/kg)
S1	17.5±1.5	8.2±1.0	170.5±20.1
S2	58.9±4.6	30.0±3.1	175.6±20.2
S3	29.6±2.8	43.6±4.2	185.6±16.2
S4	25.7±2.5	33.3±3.5	142.9±15.2
S5	26.1±2.5	30.1±3.0	371.1±35.5
S6	29.1±2.8	47.6±3.9	201.1±20.4
S7	17.7±1.8	26.2±2.0	282.6±30.2
S8	30.2±3.0	40.5±3.5	278.0±28.4
S9	33.7±3.8	49.3±5.0	321.8±32.1
S10	27.9±2.8	42.0±4.1	236.5±24.5
S11	30.4±3.5	68.9±5.6	347.4±31.5
S12	12.9±1.0	39.4±3.5	248.9±25.0
Mean values	28.31	38.26	246.83

Figure 1 contains the environmental radionuclides contribution of radioisotopes to Ra_{eq} in each soil sample. It can be obviously seen that ^{232}Th-radionuclides are the main contributor to the environmental radionuclides for radium equivalent activity.

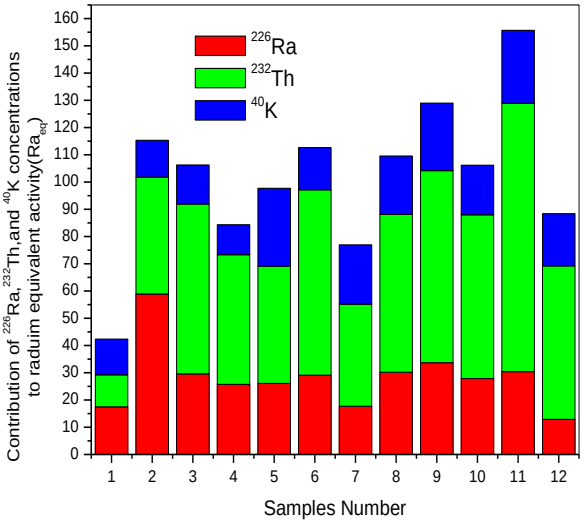

Figure 1. The contributions of environmental isotopes in Ra_{eq} in each soil specimen.

The D_R values in nGy/h was determined by an expression given by UNSCEAR in 2000 (UNSCEAR, 2000).

$$D_R(nGy/h) = 0.427A_{Ra} + 0.623A_{Th} + 0.043A_K \quad (2)$$

The determined values of D_R is shown in Table 2. Their values range from 19.91 (S1) to 70.84 (S11). Its mean value is 46.54nGy/h where it is relatively less than the permissible limit which is 59 nGy/h (ICRP, 1993).

Figure 2 contains the environmental radionuclides contribution of ^{226}Ra, ^{232}Th and ^{40}K to D_R in each soil sample. It can be obviously seen that ^{232}Th-radionuclides are the main contributor to the environmental radionuclides for absorbed dose rate. The last mentioned reports suggest a value of (0.7) Sv/Gy to use it as a conversion coefficient from the air-absorbed dose to the effective dose taken by persons and 0.2 as an external occupant person. The H_R is calculated by the next equation (Hamideen et al., 2019):

$$H_R(mSv/y) = D_R(nGy/h) \times 1.23x10^{-3} \quad (3)$$

The H_R values in soil specimens are shown in Table 2. Their values range from 0.025mSv/y (S1) to 0.087mSv/y (S11). The average value of annual outdoor effective dose rate is 0.056mSv/y (The permissible limit is 0.07mSv/y) (UNSCEAR, 2000). H_{ex} is a new factor that was utilized to determine the hazard by applying the following expression (Taskin et al., 2009):

$$H_{ex} = \frac{A_{Ra}}{370} + \frac{A_{Th}}{259} + \frac{A_K}{4810} \quad (4)$$

From Table 2, one can notice that the H_{ex} values ranges from 0.114 (S1) to 0.420 (S11) a mean value of 0.275 is seen which is less than unity (UNSCEAR, 2000). H_{in} can be evaluated by applying the following expression (Taskin et al., 2009):

$$H_{in} = \frac{A_{Ra}}{185} + \frac{A_{Th}}{259} + \frac{A_K}{4810} \quad (5)$$

Table 2. Calculated set of values of D_R, Ra_{eq}, H_R, H_{in} and H_{ex} in some soil specimens

Specimen Code	Ra_{eq} Bq/kg	D_R nGy/h	H_R mSv/y	H_{in}	H_{ex}
S1	42.35	19.91	0.025	0.162	0.114
S2	115.32	51.39	0.063	0.471	0.311
S3	106.24	47.78	0.058	0.367	0.286
S4	84.32	37.87	0.046	0.297	0.228
S5	97.72	45.85	0.056	0.334	0.263
S6	112.65	50.73	0.062	0.383	0.304
S7	76.93	36.03	0.044	0.255	0.208
S8	109.52	50.08	0.062	0.377	0.295
S9	128.97	58.94	0.072	0.439	0.348
S10	106.17	48.25	0.059	0.362	0.287
S11	155.68	70.84	0.087	0.503	0.420
S12	88.41	40.75	0.050	0.274	0.238
Mean values	102.02	46.54	0.056	0.352	0.275

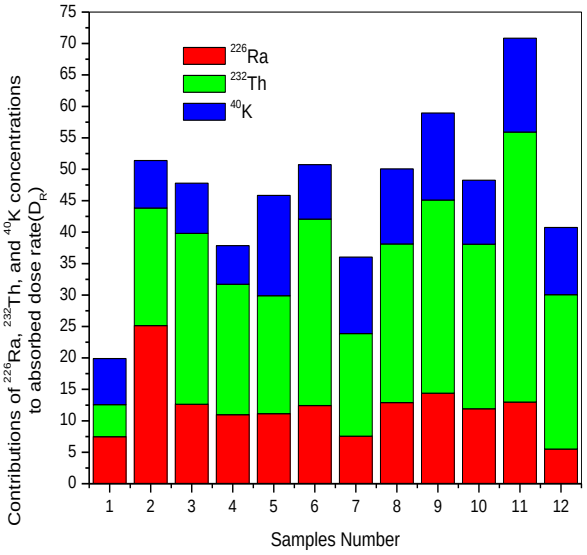

Figure 2. The contributions of environmental isotopes in D_R in each soil specimen.

Values of H_{in} has to be less than one to get a minimum radiological impact (UNSCEAR, 2000). The calculated values show that the minimum value is 0.162 (S1) and the maximum one is 0.503 (S11) with an average value of 0.352.

Conclusion

Radioactivity of some soil sites in Amman governorate were tested using an (HPGe)-detector. The estimated levels were found to be low compared to standard levels. The mean value of the D_R is 46.54nGy/h (the global mean value is of 59 nGy/h). The values of Ra_{eq} of tested specimens were lower than the accepted value (370 Bq/kg). The results for internal and external risk indicator is less than one. Effective annual dose is below the standard level of ICRP. We can come to a conclusion that:
(1) Data come out from this study are among the permissible limits.
(2) ^{232}Th-radionuclides are the main contributor to the environmental radionuclides for most discussed radiological hazard effects.

The author would like to thank some of his students for gathering the samples.

Beretka, J., Mathew, P.J. 1985. Natural Radioactivity of Australian Building Materials, Industrial Wastes and By-Products. *Health Phys.* 48, 87-95.

Colmenero Sujo, L., Montero Cabera, M. E., Villalba, L., Renteria Villalobos, M., Torres Moye, E., Garcia Leon, M., Garcia-Tenorio, R., Mireles Garcia, F., Herrera Peraza, E. F., Sanchez Aroche, D. 2004. Uranium-238 and thorium-232 series concentrations in soil, radon-222 indoor and drinking water concentrations and dose assessment in the city of Aldama, Chihuahua, Mexico. *J. Environ. Radioac.*77, 205.

Florou, H., Kritidis, P. 1992. Gamma radiation measurements and dose rate in the coastal areas of a volcanic island ocean Sea, Greece. *Radiat. Prot. Dosim.* 45, 277.

Hammood, H.A., Al-Khalifa I.J.M. 2011. Radon Concentration Measurement in Water of Dhi-Qar Governorate (in Iraq) Using Manometer. *J. Basrah Res. (Sciences)* 37, 22

Hassan, N.M., Mansour, N.A., Hassan, M.F. 2013. Evaluation of radionuclide concentrations and associated radiological hazard indexes in building materials used in Egypt. *Radiat. Protec. Dos.* 157, 214-220.

Hamideen, M.S., Chandrasekaran, A., Elimat, Z.M. 2019. Statistical assessment of radiological data of tiles collected from Jordan. *J. Env. An. Ch.* 99, 1325–1339.

ICRP. 1993. Reports, International Commission on Radiological Protection Statement on Radon.

NEA-OECD.1979. Reports, exposure to radiation from the natural radioactivity in building materials, reported by an NEA group of experts.

Taskin H., Karavus, M., Ay, P., Topuzoglu, A., Hidiroglu, S., Karahan, G. 2009. Radionuclide concentrations in soil and lifetime cancer risk due to gamma radioactivity in Kirklareli, Turkey. *J. Environ. Radioact.* 100, 49.

UNSCEAR (2000) United Nations Scientific Committee on the Effects of Atomic Radiation.

The change in characteristics of soil and Cs elution by heat treatment

M. Ikegami[1], K. Kuroki[2], S. Fukutani[1], Y. Shimada[2], M. Yoneda[2]

[1]Institute for Radiation and Nuclear Science, Kyoto University, Osaka, 590-0494, Japan
[2]Department of Environmental Engineering, Kyoto University, Kyoto, 615-8540, Japan
Keywords: Soil, Heat treatment, Cs, Elution, CEC.
M. Ikegami, e-mail: ikegami@rri.kyoto-u.ac.jp

Introduction

After the accident of Fukushima Daiichi nuclear power plant in 2011, decontamination work has been carried out. Radioactively contaminated soil is present in the decontamination waste. It is necessary to understand the behavior of radioactive materials in soil in case of incineration of the waste. It is known from previous research that the elution rate of Cs in heated soil decreased with increasing heat treatment temperature in the range of 100 – 500°C (Ikegami et al., 2014).

Cs is adsorbed on the negatively charged sites on clay minerals and organic matter in soil and there are different types of sites: (1) the selectivity of Cs over other cations is low (e.g. organic matter), (2) the selectivity of Cs is high, but the adsorption is reversible (e.g. the interlayer of 2:1 clay minerals), (3) the selectivity of Cs over other cations is high and Cs is strongly fixed (e.g. frayed edge sites) (Yamaguchi, 2014).

Cs is strongly adsorbed on clay minerals. The selectivity of Cs is higher for 2:1 clay minerals such as montmorillonite and vermiculite than 1:1 clay minerals such as kaolinite. Clay minerals may change under the influence of heat treatment as follows: loss of adsorbed water and interlayer water of clay minerals at the temperature lower than 300°C, loss of constitution water at 500 – 750°C, and decomposition and recrystallization of clay minerals at 850 - 1000°C (Kato, 1989).

Cs is weakly adsorbed on soil organic matter. Soil organic matter plays a role in the physical, chemical, and biological properties of the soil. However, organic matter in soil plays a minor role in binding Cs (Lofts, 2002) and decreases the adsorption of Cs on clay minerals (Staunton, 2002). Organic matter in soil is reduced due to heat treatment and starts at 200 – 250°C (Giovannini et al., 1988).

Therefore, in this study, it was confirmed how heat treatment influenced on the characteristics of soil and Cs elution.

Materials and methods

Soils were collected in Takizawa experimental forest of Iwate University, which is located in Iwate prefecture, Japan. The weather and soil properties of this area are similar to those of Fukushima area. There were two kinds of collected soils: soil under coniferous trees (named Soil A, B) and soil under broad-leaved trees (named Soil C, D) The collected soils were dried at 45°C and sieved to 2mm. To observe the characteristics of the soil by heating, the soils (Soil A, B, C and D) were heated at different temperatures (100, 200, 300, 400, 500, 600, 700, 800, 900 and 1000°C) for an hour and left to cool to room temperature. The change of the weight, CEC and pH (H_2O) of the heated soil was investigated in this study.

CEC (Cation Exchange Capacity) is the total capacity of soil to hold exchangeable cations and a measure of negatively charged sites on the surface. Soil with a higher clay and organic matter contents tends to have a higher CEC. Cs adsorption on soil cannot be explained with only CEC, however, it is important to understand the properties of soil changed by heat treatment. CEC was measured by the method proposed by Muramoto et al. (1992).

To investigate the change of the elution of Cs in the heated soil, the elution experiment was conducted using the heated soil containing Cs as follows. 5 ml of 1 ppm stable Cs solution was added to 5 g of the dried and sieved soil. The soil containing Cs was dried at 45°C for 24 hours. After dried, the soil was heated at temperatures every 100°C in the range of 100 – 1000°C for an hour. The elution method with water was used to elute Cs from the heated soil. This procedure is based on the leaching technique adopted in Japan's soil contamination countermeasures law for evaluating the dissolution of heavy metals in soil. Water was added to the heated soil with a solid-liquid ratio of 1:10, shaken at 200 rpm for 6 hours at 25°C, and centrifuged at 3000 rpm for 20 min. The supernatant solution was filtered through a 0.45 μm filter, and the filtrate was diluted and measured by ICP-MS.

Results and discussion

The weight of the heated soil is shown in Figure 1. The weight of all the soils was decreasing rapidly at 200°C and gradually from 200 to 1000°C. Soil contains organic matter. The organic materials in soil are reduced by heat treatment and start decreasing at 200 - 250°C. Most of organic matter in the soil is combusted at 450°C (Araya et.al., 2017). It cannot be said that all of the decrease of the weight is due to loss of organic matter, but most of the weight decrease is loss of organic matter. The loss on ignition method is used for estimating the organic matter content of soils. In this study, this estimation was based on JIS (JIS A1226, 2009) and the fraction of organic matter was estimated using the weight of heated soils at 100°C and 700°C. The percentages of organic matter in Soil A, B, C and D were 36.4%, 41.1%, 31.2% and 26.0% respectively. Therefore, the collected soils contained a lot of organic matter.

Figure 2. shows the CEC of the heated soil. CEC reached a peak at non-heated or 100°C, decreased rapidly until 400°C and declined gradually from 400 to 1000°C. CEC changed in almost the same way as the weight of soil. Organic matter has a high CEC ranging from 100 to 200 cmol/kg, whereas clay minerals also have a high CEC, but range from close to 0 cmol/kg to about 150 cmol/kg (Sato, 2001). These soils had much organic matter content

and therefore, it is possible that a decrease of CEC was attributed to loss of organic matter.

Figure 3. shows the elution rate of Cs in the heated soil. The elution rate of Cs was smaller in the range of 400 to 500°C with the same results as previous research. Soil organic matter which decreases the adsorption of Cs on clay minerals is combusted at 450°C. Because of loss of organic matter, Cs was adsorbed on clay minerals and the Cs elution decreased at the temperature lower than 500°C. Cs elution rate went up at 600 - 800°C and went down at 800 - 1000°C. pH (H_2O) of the soil at non-heated, 500°C, 800°C, and 1000°C was measured (Table 1.). The values of pH increased by heat treatment. However, pH was smaller at 800°C than 500°C and 1000°C in an opposite way of the change in the elution rate.

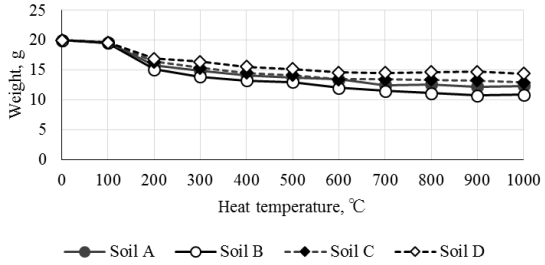

Figure 1. Weight of the heated soil.

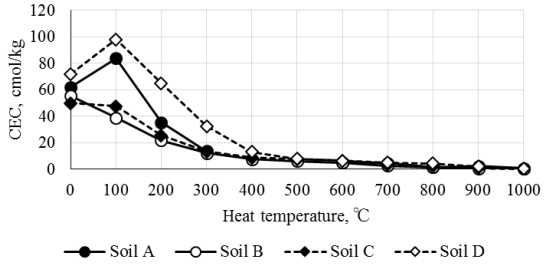

Figure 2. CEC of the heated soil.

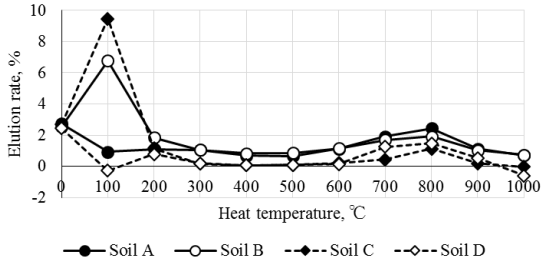

Figure 3. Elution rate of Cs in the heated soil.

Table 1. pH of the soil

	non-heated	500℃	800℃	1000℃
Soil A	4.97	10.00	8.77	9.46
Soil B	4.46	9.59	8.17	9.42
Soil C	4.70	8.15	7.24	8.66
Soil D	4.97	10.62	9.94	9.66

In Figure 2., CEC tended to decrease at a higher heat temperature. Different from CEC, the elution rate of Cs peaked at 800°C. These results indicated that a decline in the Cs elution rate at a temperature lower than 500°C was related to a decrease of organic matter and that a change of Cs elution rate at a temperature higher than 600°C was not related to cation exchange but likely to structure of clay minerals which adsorb Cs.

This research was supported by the Environment Research and Technology Development Fund (1-1702) of the Environmental Restoration and Conservation Agency of Japan.

Araya, A. N., Fogel, M. L., Berhe, A. A. 2017. Thermal alteration of soil organic matter properties: a systematic study to infer response of Sierra Nevada climosequence soils to forest fires. *J. of soil*, 3, 31-44.

Giovannini, G., Lucchesi, S., Giachetti, M. 1988. Effect of heating on some physical and chemical parameters related to soil aggregation and erodibility. *J. of Soil Sci.* 146, 255-261.

Ikegami, M., Takase, Y., Konetani, T., Yoneda, M., Shimada, Y., Matsui, Y., Fukutani, S. 2014. Elution Characteristics of Cs and Sr in heat-treated soil. *J. of JSCE.* 70 (7), III_203-III_208.

Japanese Industrial Standards Committee. 2009. JIS A 1226.

Kato, C. 1989. Condition of adsorbed water, interlayer water and constitution water of clay minerals. *J. of the Clay Science Society of Japan*. 29 (3), 118-128.

Lofts, S., Tipping, E. W., Sanchez, A. L., Dodd, B.A. Modelling the role of humic acid in radiocaesium distribution in a British upland peat soil. 2002. *J Environ. Radioactiv.* 61, 133-147.

Muramoto, J., Goto, I., Ninaki, M. 1992. Rapid analysis of exchangeable cations and cation exchange capacity (CEC) of soils by a shaking extraction method. *Jpn. J. of Soil Sci. Plant Nutr*. 63 (2), 210-215.

Sato, T. 2001.Characteristics and applications of clays. *J. of the Clay Science Society of Japan*. 41 (1), 26-33.

Staunton, S., Dumat, C., Zsolnay, A. 2002. Possible role of organic matter in radiocaesium adsorption in soils. *J Environ. Radioactiv.* 58, 163-173.

Yamaguchi, N. 2014. Adsorption mechanism of radiocesium on soil. *J. of Jpn. Soc. Soil Phys*. 126, 11-21.

Analysis of increased radiocaesium activity derived from Fukushima Dai-ichi Nuclear Power Plant accident until 2017

Yayoi Inomata[1], Michio Aoyama[2], Yasunori Hamajima[1], and Masatoshi Yamada[3]

[1]Institute of Nature and Environmental Technology, Kanazawa University, Kanazawa, 920-1192, Japan
[2]Faculty of Life and Environmental Sciences, Univ. of Tsukuba, 305-8577, Japan
[3]Institute of Radiation Emergency Medicine, Hirosaki University, 036-8564, Japan
Keywords: Radiocaesium, Fukushima Dai-ichi Nuclear Power Plant accident, Sea of Japan, East China Sea
Keywords; FNPP1, ^{137}Cs, ^{134}Cs, Re-circulation, SOJ, global fallout
Presenting author, e-mail: yinomata@se.kanazawa-u.ac.jp

This study investigated the spatiotemporal variations of activity concentrations of ^{137}Cs in the Sea of Japan (SOJ) and these transport process from the North Pacific Ocean to the SOJ through the East China Sea (ECS) during 2012–2017. The ^{137}Cs activity concentrations in the SOJ have been increasing since 2012–2013 and reached a maximum in 2015–2016 of approximately 3.4 Bq m^{-3}, which is more than twice the pre–Fukushima accident ^{137}Cs activity concentration of ~1.5 Bq m^{-3}. The integrated amount of Fukushima Nuclear Power Plant (FNPP)1-derived ^{137}Cs that entered the SOJ until 2017 was estimated to be 0.27 ± 0.02 PBq, which consist 6.4 % of the estimated total amount of FNPP1-derived ^{137}Cs in the SubTropical Mode Water (STMW). The integrated amount of FNPP1-derived ^{137}Cs that returned to the North Pacific Ocean through the Tsugaru Strait was estimated to be 0.11 ± 0.01 Bq, 42 % of the total amount of FNPP1-derived ^{137}Cs transported to the SOJ and 2.7 % of the estimated total amount of FNPP1-derived ^{137}Cs in the STMW.

Introduction

The Fukushima Daiichi Nuclear Power Plant (FNPP1) accident in March 2011 released radiocaesium (^{137}Cs, half-life 30.07 yr, and ^{134}Cs, half-life 2.06 yr) directly to the air and discharged contaminated water into the ocean in March and April 2011. Eighty per cent of the radiocaesium released to the atmosphere was deposited on the surface of the ocean (Aoyama et al., 2016; Tsumune et al., 2013).

Several years after the FNPP1 accident, we found that ^{137}Cs activity concentrations were gradually increased in the Sea of Japan (SOJ) (Aoyama et al., 2017; Inomata et al, 2018). The ^{137}Cs activity concentrations in the SOJ have been increasing since 2012–2013 and reached a maximum in 2015–2016 of approximately 3.4 Bq m^{-3}, more than twice the pre–Fukushima accident ^{137}Cs activity concentration of ~1.5 Bq m^{-3}. The ^{134}Cs/^{137}Cs activity ratios ranged from 0.36 to 0.51 in 2016. These ^{134}Cs/^{137}Cs activity ratios were evidence that the Fukushima accident caused the increase of the ^{137}Cs activity concentrations. In the North Pacific south of Japan (NPSJ), the highest ^{137}Cs activities were observed in 2012–2013 with a depth of 300 m, which the potential density anomaly (σ_θ) corresponded to subtropical mode water (STMW). In the ECS, a clear increase of the ^{137}Cs activity concentration started at a depth of 140 m in April 2013 and propagated to the surface layers at depths of roughly 0–50 m, reached a maximum in 2015, and decreased in subsequent years. The FNPP1-^{137}Cs activity concentrations in the SOJ reached a maximum in 2015 – 2016. The propagation of FNPP1-^{137}Cs and ^{134}Cs in the surface seawater from the ECS into the SOJ therefore required approximately one year. These temporal changes in ^{137}Cs activity concentrations and ^{134}Cs/^{137}Cs activity ratios indicated that part of the ^{137}Cs and ^{134}Cs derived from the FNPP1 was transported within several years to the ECS and then to the SOJ via STMW from the NPSJ. The integrated amount of FNPP1-derived ^{137}Cs that entered the SOJ before 2016 was estimated to be 0.21 ± 0.01 PBq, 5.0 % of the estimated total amount of FNPP1-derived ^{137}Cs in the STMW. The integrated amount of FNPP1-derived ^{137}Cs that returned to the North Pacific Ocean through the Tsugaru Strait was estimated to be 0.09 ± 0.01 Bq, 43 % of the total amount of FNPP1-derived ^{137}Cs transported to the SOJ and 2.1 % of the estimated total amount of FNPP1-derived ^{137}Cs in the STMW.

In this study, we further investigated the temporal variations of ^{137}Cs activity concentrations and estimated the inflow amount of FNPP1-^{137}Cs in the SOJ until 2017. We also discussed the long-term variation of ^{137}Cs activity concentrations after the 1960s in the SOJ (Figure 1).

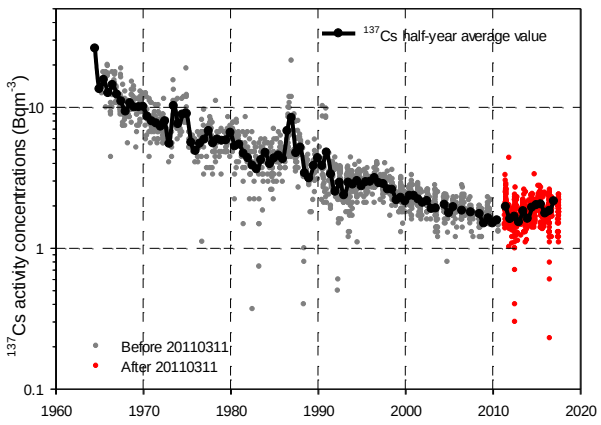

Figure 1. Temporal variations of ^{137}Cs concentrations in the SOJ. Red circle is measured after FNPP1 accident.

Materials and methods

We compiled all available data from the literature and reported studies to investigate the temporal variation of ^{137}Cs in the SOJ. Most of the data before the FNPP1 accident are included in the database "Historical Artificial Radionuclides in the Pacific Ocean and its Marginal Seas (HAM database)" (Aoyama and Hirose, 2004 and their updated version). The term "surface seawater" as used in

this study refers to a sample collected at a depth of less than 10 m.

In this study, we focused on the Japanese government's monitoring data collected at Tomari (42.98–43.17°N, 140.21–140.30°E), Aomori (41.13–41.22°N, 141.50–141.67°E), Niigata (37.62–38.10°N, 138.38–138.84°E), Ishikawa (36.87–37.29°N, 136.43–136.47°E), Fukui (35.75–36.09°N, 135.50–135.83°E), Shimane (35.67–35.80°N, 132.87–133.2°E), Saga (33.57–33.62°N, 129.73–129.98°E), and Kagoshima (31.58–31.93°N, 130.02–130.15°E) (Marine Ecology Research Institute, 2011, 2012, 2013, 2014, 2015, 2016, 2017). These measurements were taken once a year. Near the Aomori sites, offshore monitoring was also conducted twice a year at the Rokkasho Reprocessing Plant (39.5–41.4°N, 141.5–142.3°E). Monitoring data from the Korean government (304–01(33.0°N, 127.7°E): and 105–11 (37.3°N, 131.3°E) were also used in this analysis (Korea Institute of Nuclear Safety, 2011, 2012, 2013, 2014, 2015, 2016).

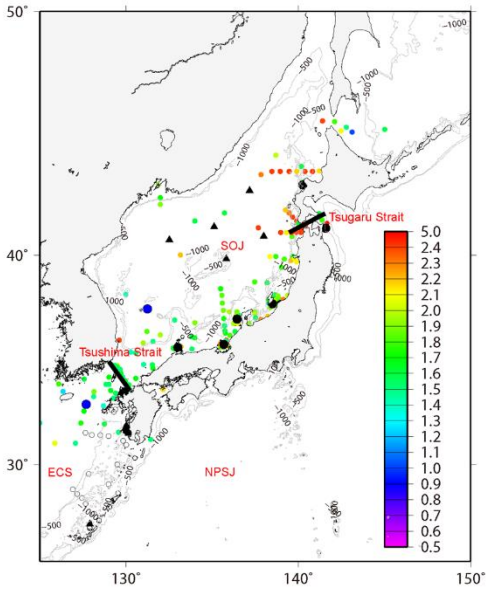

Figure 2. Location of the sampling points after the FNPP1 accident. Large black circles are sites monitored by the Japanese government. Blue circles are sites monitored by the Korean government. Black triangles are sites with measured vertical profiles. Circle colours correspond to the ^{137}Cs activity concentrations measured in 2011. The area around Japan was divided into 3 regions: the SOJ, ECS, and NPSJ (<141.5°E).

In this study, FNPP1 derived ^{137}Cs are defined as follows;

$$\text{FNPP1-}^{137}\text{Cs}=[^{137}\text{Cs}]_{\text{measurement}}-[^{137}\text{Cs}]_{\text{global fallout}} \quad (1)$$

$[^{137}\text{Cs}]_{\text{global fallout}}$ was estimated by extracting the measured ^{137}Cs activity concentration data in the SOJ from 2000 to 2010.

Results and discussion

Propagation of FNPP1-^{137}Cs from ECS to SOJ

Figure 3 shows temporal variations of FNPP1-^{137}Cs activity concentrations in the SOJ and ECS. The increase of ^{137}Cs activity concentrations in the surface seawater were firstly founded in the ECS, and reached a maximum in 2014–2015, following then the FNPP1-^{137}Cs activity concentrations tend to decrease after 2016. Whereas the concentration in the SOJ reached a maximum in 2015–2016, and in 2017, decrease of FNPP1-^{137}Cs activity concentrations were also found in the monitoring stations in the SOJ.

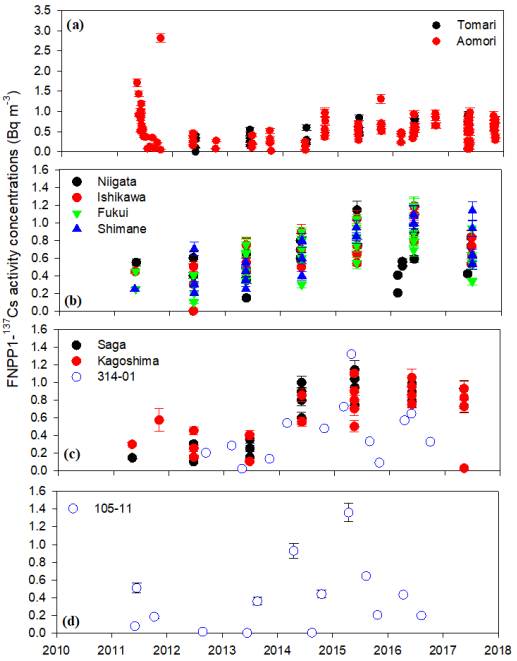

Figure 3. Temporal variations of FNPP1-^{137}Cs activity concentrations in the SOJ.

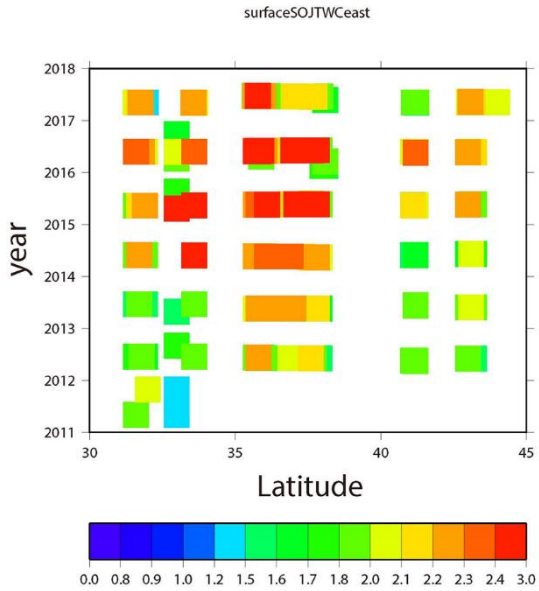

Figure 4. Hovmöller diagram of the ^{137}Cs activity concentrations at a potential density along with an eastern Tsushima Warm Current at a potential density of 25.2 ±0.5 kg m^{-3}. In the SOJ, a time lag of the propagation of FNPP1-radiocaesium of approximately one year was observed.

Figure 4 shows the Hovmöller diagram of ^{137}Cs activity concentrations along with an eastern Tsushima Warm Current at σ_θ 25.2 ±0.5 kg m^{-3}. The surfaces on σ_θ were

selected to show the maximum ^{137}Cs activity concentrations in the ECS. In the ECS, the ^{137}Cs activity concentrations gradually increased and attained maxima during 2014–2015. The ^{137}Cs activity concentrations in the ECS tended to decrease in 2016. In the south-western part of the SOJ (Shimane, Fukui, Ishikawa, and Niigata), the ^{137}Cs activity concentrations gradually increased beginning in 2012 and reached a maximum of 2.5 Bq m^{-3} during 2015–2016. In the north-western SOJ (Aomori and Tomari), the ^{137}Cs activity concentrations increased slightly and exceeded 2 Bq m^{-3} in 2016. These results indicate that the propagation of FNPP1-derived ^{137}Cs from the ECS to the SOJ along the TWC occurred within one year. The ^{134}Cs/^{137}Cs activity ratios ranged from 0.36 to 0.51 in 2016. After taking into account radioactive decay and ocean mixing, we concluded that these ^{134}Cs/^{137}Cs activity ratios were evidence that the Fukushima accident caused the increase of the ^{137}Cs activity concentrations.

Table 1 shows the maximum FNPP1-^{137}Cs activity concentrations and these measured years. The maximum FNPP1-^{137}Cs activity concentration at each monitoring station was 0.9-1.4 Bqm^{-3}, which contribute to about 40-49% increase against those to the ^{137}Cs activity concentration derived from the global fallout. The temporal changes of ^{137}Cs activity concentrations and ^{134}Cs/^{137}Cs activity ratios indicated that part of the FNPP1-derived ^{137}Cs and ^{134}Cs was transported within 4-5 years timescale to the ECS and then to the SOJ via STMW from the NPSJ.

Table 1. Maximum FNPP1-^{137}Cs activity concentrations at each monitoring station.

		Max year	FNPP1-^{137}Cs Activity Concs (Bqm^{-3})	FNPP1-^{137}Cs Activity_SD (Bqm^{-3})	Increase rate (%)
Shizuoka	NPSJ	2015	1.6	0.14	55
Kagoshima	ECS	2015	1.1	0.13	45
Saga	ECS	2015	1.1	0.11	46
Korea(ECS)	ECS	2015	1.4	0.10	49
Korea(SOJ)	SOJ	2015	1.3	0.09	48
Shimane	SOJ	2016	1.1	0.10	46
Fukui	SOJ	2016	1.2	0.10	48
Niigata	SOJ	2016	1.2	0.11	48
Ishikawa	SOJ	2016	1.2	0.10	48
Tsugaru	SOJ	2016	1.3	0.12	49
Tomari	SOJ	2016	0.9	0.08	41

Estimation of FNPP1-^{137}Cs inflow flux into the SOJ during 2012 and 2017

We estimated the amounts of FNPP1-derived ^{137}Cs transported in each region during 2012–2017 as following equation.

Transport amount = $\sum_{i=2012}^{n}$(FNPP1 − derived 137Cs activity concentration in year i) × (annual average seawater transport volume in year i)

where n = 2017.

We used the annual average FNPP1–derived ^{137}Cs activity concentrations at stations Saga and 304-11 for the ECS, station Shimane for the eastern TWC, and station 105-01 for the western TWC. The annual average volume of seawater transported through the TWC was estimated from the data of Fukudome et al. (2010) and Han et al. (2016).

The most reliable estimates of the amount of FNPP1-derived ^{137}Cs deposited in the North Pacific Ocean via atmospheric release and direct release to the Ocean are 11.7–14.8 PBq (Aoyama et al., 2016b; Tsubono et al., 2016) and 3.5 ± 0.7 PBq (Tsumune et al., 2013), respectively. The FNPP1–derived ^{137}Cs inventory in the North Pacific Ocean has been estimated to be 15.2–18.3 PBq by comparing the observed inventory with model simulation results (Aoyama et al., 2016), 15.3 ± 2.6 PBq by optimum interpolation analysis (Inomata et al., 2016), and 16.1 ± 1.4 PBq by model simulation (Tsubono et al., 2016). According to the estimation by Kaeriyama et al. (2014), the amount of ^{134}Cs in the STMW was approximately 4.2 ± 1.1 PBq in 2012. The estimation by Kaeriyama et al. (2014) implies that the FNPP1-derived ^{137}Cs transported into the SOJ from 2012 to 2016 accounted for 5.0 % of the FNPP1-derived ^{137}Cs inventory in the STMW.

In Inomata et al. (2018), we already estimated the integrated amount of FNPP1-derived ^{137}Cs that entered the SOJ until 2016, which was estimated to 0.21± 0.02 PBq (5% of the estimated total amount of FNPP1-derived ^{137}Cs in the STMW). The integrated amount of FNPP1-derived ^{137}Cs that entered the SOJ until 2017 increased and estimated to be 0.27 ± 0.02 PBq, which is 6.4 % of the estimated total amount of FNPP1-derived ^{137}Cs in the STMW. The integrated amount of FNPP1-derived ^{137}Cs that returned to the North Pacific Ocean through the Tsugaru Strait was estimated to be 0.11 ± 0.01 Bq, 42 % of the total amount of FNPP1-derived ^{137}Cs transported to the SOJ and 2.7 % of the estimated total amount of FNPP1-derived ^{137}Cs in the STMW.

Conclusion

Re-circulation of FNPP1-^{137}Cs entered into the SOJ until 2017, which was deposited in the STMW formation region caused by the FNPP1 accident, were estimated in this study. FNPP1-^{137}Cs propagated to SOJ via Tsushima Straight from ECS and returned to the North Pacific Ocean via Tsugaru straight. Maximum FNPP1-^{137}Cs activity concentration was observed in 2015 in the ECS, and 2016, one–year later, in the SOJ. Main body of FNPP1-^{137}Cs might have passed through the surface seawater in the SOJ until 2017. The integrated amount of FNPP1-derived ^{137}Cs that entered the SOJ until 2017 increased and estimated to be 0.27 ± 0.02 PBq, which is 6.4 % of the estimated total amount of FNPP1-derived ^{137}Cs in the STMW. The integrated amount of FNPP1-derived ^{137}Cs that returned to the North Pacific Ocean through the Tsugaru Strait was estimated to be 0.11 ± 0.01 Bq, which is 2.7 % of the estimated total amount of FNPP1-derived ^{137}Cs in the STMW.

This research was financially supported by Grant-in-Aid for Scientific Research on Innovative Areas, “Interdisciplinary study on environmental transfer of radionuclides from the Fukushima Dai-ichi NPP Accident” (Project No. 25110511) of the Japanese Ministry of Education, Culture, Sports, Science and Technology

(MEXT). This research was also supported by the cooperation program by Institute of Radiation Emergency Medicine, Hirosaki University (JFY2016, 2017) and Kanazawa University (JFY2016, 2017).

Aoyama, M., Kajino, M., Tanaka, T.Y., Sekiyama, T.T., Tsumune, D., Tsubono, T., Hamajima, Y., Inomata, Y., Gamo. 2016. ^{134}Cs and ^{137}Cs in the North Pacific Ocean derived from the March 2011 TEPCO Fukushima Dai-ichi Nuclear Power Plant accident, Japan. Part two: estimation of ^{134}Cs and ^{137}Cs inventories in the North Pacific Ocean, *J. Oceanogr.*, 72, 67–76.

Aoyama, M., Hamajima, Y., Inomata, Y., Oka, E. 2017. Recirculation of FNPP1-derived radiocaesium observed in winter 2015/2016 in coastal regions of Japan, *App. Rad. Isotopes.*, 126, 83–87.

Fukudome, K., Yoon, J-H., Ostrovskii, A., Takikawa, T., Han. I-S. 2010. Seasonal volume transport variation in the Tsushima warm current through the Tsushima Straits from 10 Years of ADCP Observations, *J. Oceanogr.*, 66, 539–551.

Han, S., Hirose, N., Usui, N., Miyazawa, Y. 2016. Multi-model ensemble estimation of volume transport through the straits of the East/Japan Sea, *Ocean Dynamic.*, 66, 59–76.

Inomata, Y., Aoyama, M., Tsubono, T., Tsumune, D., Hirose, K. 2016. Spatial and temporal distributions of ^{134}Cs and ^{137}Cs derived from the TEPCO Fukushima Daiichi Nuclear Power Plant accident in the North Pacific Ocean by using optimal interpolation analysis, *Environ. Sci.: Processes Impacts*, 18, 126–136.

Inomata, Y., Aoyama, M., Hamajima, Y., Yamada, M. 2018. Transport of FNPP1-derived radiocaesium from subtropical mode water in the western North Pacific Ocean to the Sea of Japan. *Ocean Sci.*, 14, 813-826.

Kaeriyama, H., Shimizu, Y., Ambe, D., Masujima, M., Shigenobu, Y., Fujimoto, K., Ono, T., Nishiuchi, K., Taneda, T., Kurogi, H. 2014. Southwest intrusion of ^{134}Cs and ^{137}Cs derived from the Fukushima Dai-ichi Nuclear Power Plant accident in the Western North Pacific, *Environ. Sci. Technol.*, 48, 3120–3127.

Korea Institute of Nuclear Safety: Marine Environmental Radioactivity Survey, 2011-2016.

Marine Ecology Research Institute: Radiation level survey in marine organizations and their environment, 2011-2017.

Tsubono, T., Misumi, K., Tsumune, D., Bryan, F.O., Hirose, K., Aoyama, M. 2016. Evaluation of radioactive cesium impact from atmospheric deposition and direct release fluxes into the North Pacific from the Fukushima Daiichi nuclear power plant, *Deep Sea Res, Part I*, 115, 10–21.

Tsumune, D., Tsubono, T., Aoyama, M., Uematsu, M., Misumi, K., Maeda, Y., Yoshida, Y., Hayami, H. 2013. One-year, regional-scale simulation of ^{137}Cs radioactivity in the ocean following the Fukushima Daiichi Nuclear Power Plant accident, *Biogeosci.*, 10, 5601–5617.

Evaluation of the consequences after potential accidents with the Russian nuclear submarine K-27 in the Arctic marine environment

Mikhail Iosjpe[1], Ingar Amundsen[1], Justin Brown[1], Mark Dowdall[1], Ali Hosseini[1]

[1]Department of Nuclear Safety and Environmental Protection, Norwegian Radiation and Nuclear Safety Authority, Østerås, 1361, Norway
Keywords: nuclear submarine, radioecological assessment, Arctic marine region
Presenting author, Mikhail Iosjpe, e-mail: mikhail.iosjpe@dsa.no

Introduction

The Arctic is a vulnerable region with regards to radioactive contamination. The present paper has considered potential accidents related to the Russian nuclear submarine K-27 (NS K-27) as a consequence of the action plan concerning the safe and secure management and disposal of sunken radioactive objects in the Arctic.

We believe the present study can provide additional information to the previous results of (Hosseini et al., 2015, 2016; Brown & Hosseini, 2019), because: (i) additional assumptions for the release scenarios for nuclear submarines K-27, (ii) the inclusion of water-sediment interactions into the process of distribution of radionuclides in the marine environment and (iii) the inclusion of a wider set of radionuclides in the radioecological assessment of the potential release scenarios in comparison with the previous studies.

Description of the ARCTICMAR model (the NRPA box modelling approach)

The ARCTICMAR model is based on a modified compartment modelling approach that includes terms describing radionuclide dispersion in the marine environment with non-instantaneous mixing (Iosjpe et al., 2002, 2009, 2016). The model includes the processes of advection of radioactivity between compartments, sedimentation, diffusion of radioactivity through sediment pore water, remobilization, bioturbation, particle mixing, pore water mixing, radionuclide burial processes to deep sediment layers and radioactive decay. The structure of the surface compartment for the ARCTICMAR model is shown in Figure 1. The model has 345 water and sediment compartments.

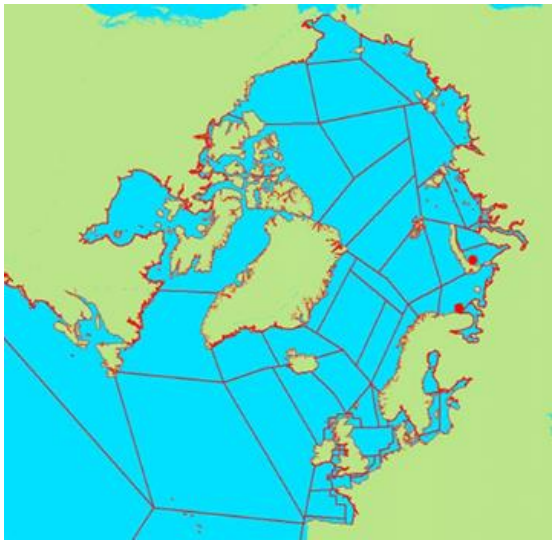

Figure 1. The structure of the surface water boxes for the ARCTICMAR compartment model. The red points correspond to the locations of the potential accidents with NC K-27.

The accumulation of radioactive activtity in biota is further calculated from radionuclide concentrations in filtered seawater in different water regions. Doses to humans are calculated on the basis of given seafood consumptions, based on available data for seafood catches and assumptions about human diet in the respective areas. Dose rates to biota are developed on the basis of calculated radionuclide concentrations in marine organisms, water and sediment, using dose conversion factors.

Concentrations of the radionuclides in marine organisms can be calculated from radionuclide concentrations in filtered seawater and the concentrations factors, but more detailed information concerning the bioaccumulation processes in biota can be provided by using a kinetic modelling approach (Brown et al., 2004; Heling et al., 2002; Iosjpe et al., 2016; Maderich et al., 2013; Thomann, 1981; Vives i Batlle et al., 2008). A kinetic sub-model for bioaccumulation processes has been used in the present study.

Inventory and release scenarios for NS K-27

Based on the previous reports (Hosseini et al., 2015, 2016; Brown & Hosseini, 2019), we have chosen the following locations as the most likely sites for a potential accident with the NC K-27: (i) the Stepovogo Bay in the southern part of the Kara Sea and (ii) in the southern part of the Barents Sea. Both locations are shown in Figure 1.

The present study is based on the radionuclide inventories and assumptions about radionuclide releases presented by Hosseini et al. (2015) with two additional scenarios for Cs-137 from Brown & Hosseini (2019).

The following radionuclides were under consideration in the present study, chosen in part due to their potential for bioaccumulation: Am-241, Am-242m, Co-60, Cs-137, Eu-152, Eu-155, Fe-55, I-129, Nb-93m, Ni-59, Ni-63, Np-237, Pm-147, Pu-238, Pu-239, Pu-240, Pu-241, Se-79, Sm-151, Sn-121m, Sn-126, Sr-90, U-234, U-236, Zr-93.

For the worst-case scenario, a release pattern, divided into two fractions, was assumed: (i) an instantaneous release of radionuclides (instant release fraction) and (ii) a slow long-term release similar to the model of the dissolution of the uranium oxide matrix. Instant releases of considered radionuclides and are shown in Figure 2.

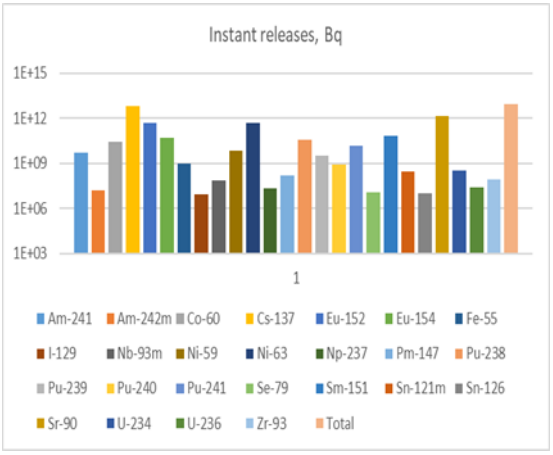

Figure 2. Instant releases of radionuclides.

Radioecological assessment after potential accidents with the nuclear submarines K-27

Figures 3 and 4 show the doses to the group of humans with high consumption of sea food after radionuclide releases into the Stepovogo Bay (the Kara Sea). Figure 3 shows the distribution of the total dose due ten years of exposure and the impact of selected radionuclides. Figure 4 shows the most significant impacts of radionuclides to the maximum annual dose. Both figures demonstrate that Cs-137 dominates the doses to the human group for this release scenario. It is necessary to note that the maximum annual dose exceeds the annual dose for humans from natural sources with a factor of 2-3.

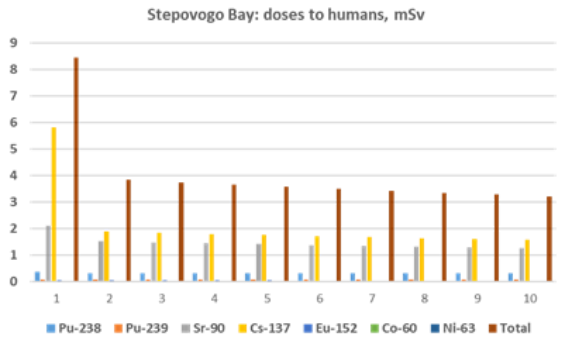

Figure 3. Distribution of the total dose.

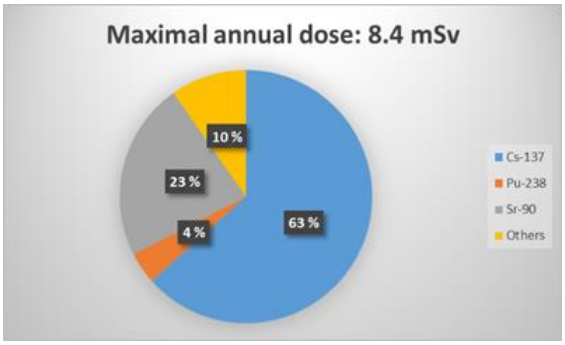

Figure 4. Impact of different radionuclides to the maximum annual dose.

The maximum dose rates for biota are shown in Figures 5 – 9. Cs-137 dominate dose rates to fish, sea mammals and sea birds, while dose rates to crustaceans and mollusks are dominated by Sr-90 and Pu-238. Results of the simulation shows that only the maximum dose rate to mollusks exceed the screening dose rate for biota (10 µGy/h).

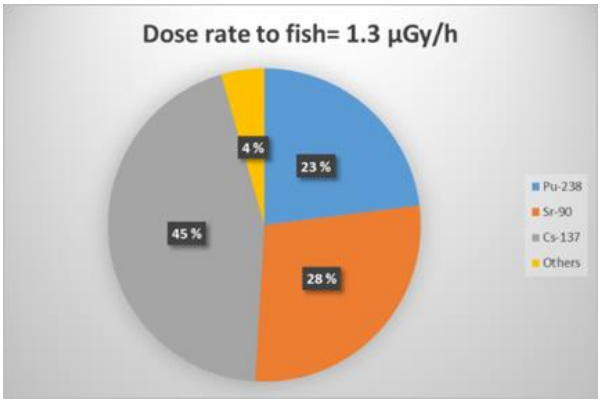

Figure 5. Maximum dose rate to fish.

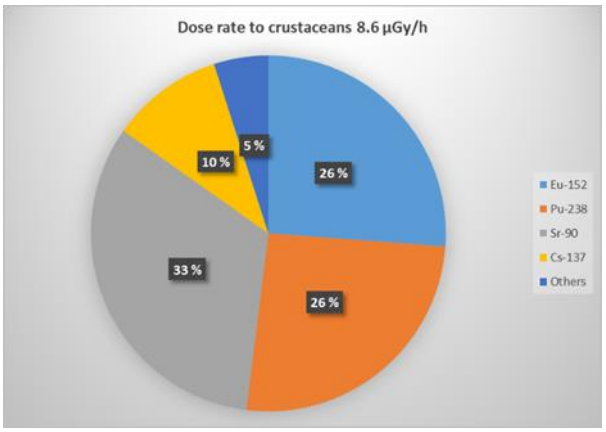

Figure 6. Maximum dose rate to crustaceans.

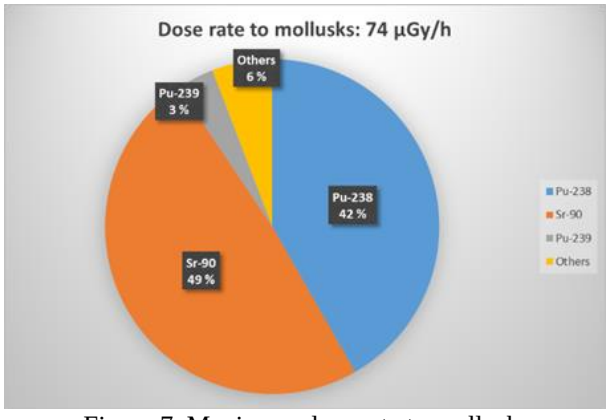

Figure 7. Maximum dose rate to mollusk.

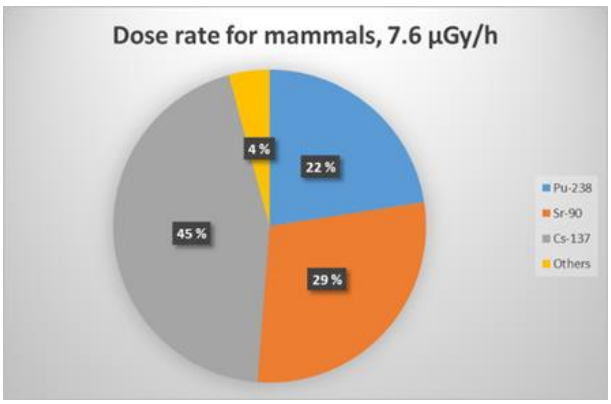

Figure 8. Maximum dose rate to sea mammals.

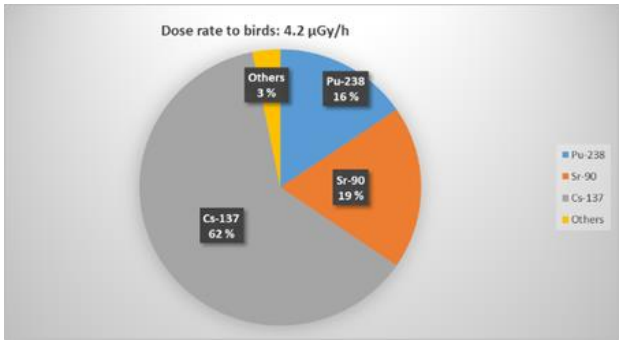

Figure 9. Maximum dose rate to sea birds.

Figures 10 and 11 show doses to humans from Cs-137 for the same release scenario in the Stepovogo Bay and in the southern part of the Barents Bay. Doses differ up to six orders of magnitude because of the fast dilution of activity in the Barents Sea. It is also interesting that the shape of the dose distribution is different for the different marine environments.

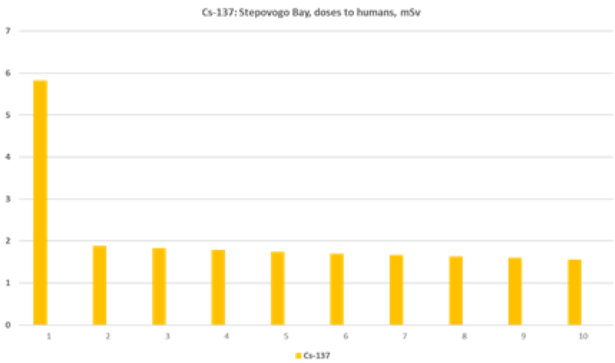

Figure 10. Dose from Cs-137 after releases into the Stepovogo Bay.

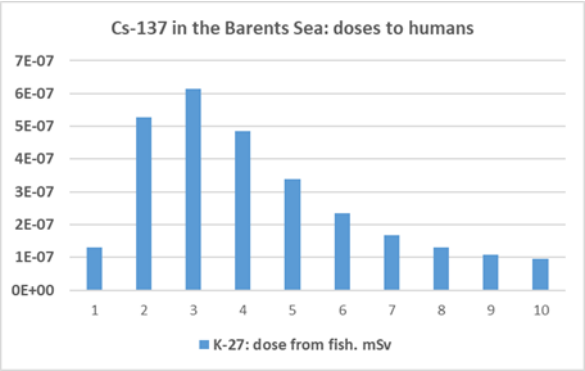

Figure 11. Dose from Cs-137 after releases into the Barents Sea.

Conclusions

The present simulations demonstrate that Cs-137 alone cannot correctly describe the consequences to humans and biota after the release of radionuclides in a potential accident involving a nuclear submarine. Radionuclides such as Pu-238, Sr-90, Eu-152 and others can provide significant and even dominate the impacts to the end points of radioecological analysis.

It is demonstrated that for the present release scenarios, doses to humans and biota, as well as concentrations in biota, can exceed the guidance level of radionuclide concentrations in seafood, the doses from natural sources for humans and the screening doses for biota.

It is shown that the sensitivity of the marine environment is a significant factor for the dose assessment.

The work has been partial funded by the EC project FEASIBILITY (Contract NSI 2014 / 354026).

Brown, J.E. & Hosseini, A. (2019). 'Task 3.3 - Prioritization based on radiological hazards'

Feasibility study INSC/2013/ MC.04/13 Report for Feasibility Study and Preparation for the Implementation of an Action Plan Concerning the Safe and Secure Management/Disposal of Sunken Radioactive Objects in the Arctic Sea; Report to: Directorate General for International Cooperation and Development – Europeaid.

Brown J., Børretzen P., Dowdall M., Sazykina T., and Kryshev I., 2004. The derivation of transfer parameters in the assessment of radiological impacts on Arctic marine biota. *Arctic* 57, 279–289.

Hosseini, A., Amundsen, I., Bartnicki, J., Brown, J.E., Dowdall, M., Dyve, J.E., Karcher, M., Kauker, F., Klein, H., Lind, O.C., Salbu, B., Schnur, R., Standring, W., (2016). Environmental Modelling and Radiological Impact Assessment Associated with Hypothetical Accident Scenarios for the Nuclear Submarine K-27. StrålevernRapport 2016:8. Statens strålevern, Østerås, Norway.

Heling R., Koziy I., Bulgakov V., 2002. On the dynamic uptake model developed for the uptake of radionuclides in marine organisms for the POSEIDON-R model system. *Radioprotection* 37 (C1), 833–838.

Hosseini, A., Amundsen, I., Brown, J.E., Dowdall, M., Standring W. (2015). Inventory and source term evaluation on the dumped nuclear submarine K-27. StrålevernRapport 2015:06. Østerås: Statens strålevern, 2015.

Iosjpe M., Brown J. & Strand P. 2002. Modified Approach for Box Modelling of Radiological Consequences from Releases into Marine Environment, *J. Environ. Radioactiv.* 91–103.

Iosjpe M., Isaksson M., Joensen H.P., Jonsson G., Logemann K., Roos P., Suolanen V., Thomas R., 2016. Effects of dynamic behaviour of Nordic marine environment to radioecological assessments, 15 Febr 2016, ISBN: ISBN 978-87-7893-442-0, http://www.nks.org/en/nks_reports/view_document.htm?id=111010213400466

Iosjpe M., M. Karcher, J. Gwynn, I. Harms, R. Gerdes and F. Kauker, 2009. Improvement of the dose assessment tools on the basis of dispersion of the 99Tc in the Nordic Seas and the Arctic Ocean. *Radioprotection* 44, 531–536.

Maderch V., Bezhenar R., Heling R., G. de With, Jung K.T., Myoung J.G., Cho Y.-K., Qiao F., Robertson L., 2013. Regional long-term model of radioactivity dispersion and fate in the Fukushima Dai-ichi accident. *J. Environ. Radioactiv.* 2013, www.elsevier.com/locate/jenvrad

Thomann R.V., 1981. Equilibrium model of fate of microcontaminants in diverse aquatic food-chains. *Can. J. Fish. Aquat. Sci.* 38:280–296.

Vives i Batlle J., Wilson R.C., Watts S.J., Jones S.R., McDonald P., Vives-Lynch S., 2008. Dynamic model for assessment of radiological exposure to marine biota. *J. Environ. Radioactiv.* 99, 1711–1730.

Evaluation of the activity of the high activity particles in the intertidal beach region near the Sellafield nuclear facilities after long-term exposure

Mikhail Iosjpe[1], Justin Brown[1], Juan Carlos Mora Cañadas[2], Justin Smith[3]

[1]Department of Nuclear Safety and Environmental Protection, Norwegian Radiation and Nuclear Safety Authority, Østerås, 1361, Norway
[2]Centro de Investigaciones Energéticas, Medioambientales y Tecnológicas, Madrid, 28040, Spain
[3]Radiation Assessments Department, Public Health England, Chilton, OX11 0RQ, United Kingdom
Keywords: modelling, high activity particles, intertidal beach region
Presenting author, Mikhail Iosjpe, e-mail: mikhail.iosjpe@dsa.no

Introduction

The beach areas near the Sellafield nuclear reprocessing facility, UK, have been exposed to radionuclides released over many decades. Information about liquid releases of different radionuclides into the Irish Sea and results of the monitoring programs in this region are relatively well documented (BNFL, 1976-2016; RIFE, 1995-2014; MARINA II, 2003).

Additionally, since 2007, a special monitoring program for the intertidal beach regions has been conducted to detect particles with high activity (Sellafield Ltd, 2011; 2013-2017), but, unlike the liquid discharges, release scenarios for high activity particles are unknown.

The present study is an attempt to describe the activity of high activity particles in the intertidal beach region near the Sellafield nuclear facilities after a long-term exposure.

Modelling approach

The present study is based on a modified compartment modelling approach that includes terms describing radionuclide dispersion in the marine environment with non-instantaneous mixing (Iosjpe et al., 2002, 2009, 2016). The model includes the processes of advection of radioactivity between compartments, sedimentation, diffusion of radioactivity through sediment pore water, remobilization, bioturbation, particle mixing, pore water mixing, radionuclide burial processes to deep sediment layers and radioactive decay. The structure of the surface compartment for the constructed model is shown in Figure 1, where the intertidal beach region near the Sellafield nuclear facilities is included within the Cumbrian water compartment.

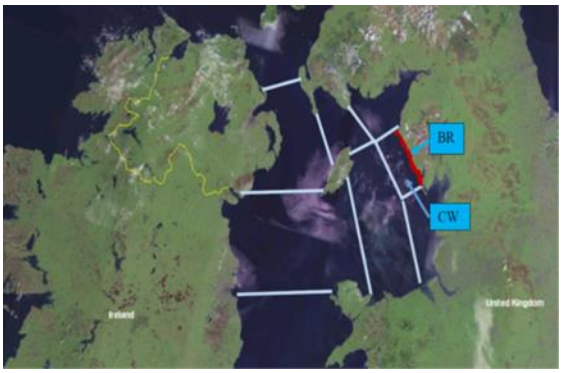

Figure 1. The structure of the model: CW and BR correspond to the Cumbrian water compartment and the intertidal beach region, respectively.

The choice of the environmental parameters

The corroboration and the potential improvement of environmental model parameters has been provided based on the comparison of results from model simulations with experimental data for liquid discharges of Cs-137, Pu-239 and Am-241 into Cumbrian waters.

There are three main reasons for the selection of these radionuclides: (i) relatively good information about releases of these radionuclides into the Cumbrian waters from the Sellafield nuclear facilities, (ii) availability of monitoring data for these radionuclides in the Cumbrian waters and (iii) the selected radionuclides have strong connection with sediment particles, while the sediment distribution coefficient (k_d) values for Cs-137, Pu-239 and Am- 241 differ by orders of magnitude.

Selection of the values for model parameters is based on a satisfactory comparison with monitoring data for all three radionuclides simultaneously.

Additionally, the results from the kinetic sub-models for the exchange of radionuclides between water and sediment phases is used to construct "apparent" k_d during numerical simulations (Periáñez et al., 2018).

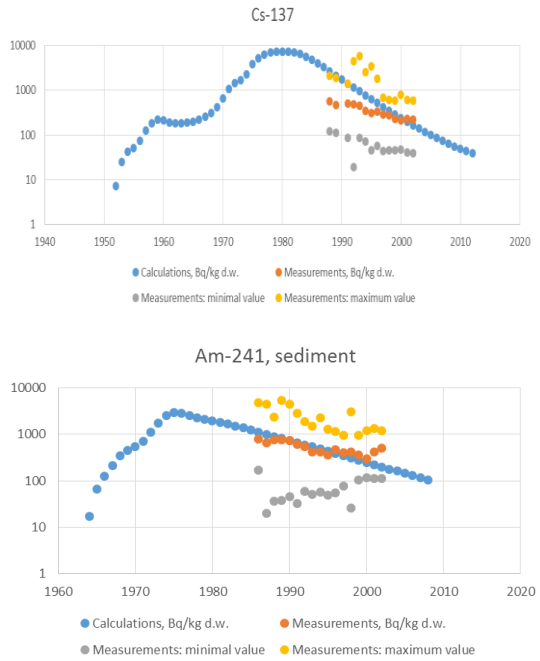

Figure 2. Comparison results of the model simulations with monitoring data for the Cumbrian waters for the liquid releases of Cs-137 (top) and Am-241 (bottom) for the sediment, Bq/kg d.w.

Assumptions for the release scenarios for the high activity particles.

Contrary to the relatively well-known authorized liquid discharges of radioactivity, discharges of high activity particles from the Sellafield nuclear facilities are not well characterized. According to a recently published Sellafield Ltd report (2018), the non-numerical sources for the particle discharges can be described as (i) discharges via pipeline (for alpha and beta rich particles up to 1983 and 1985, respectively) and (ii) due to debris from the Sealine Recovery Project 1990s and 2003-2006 (for all types of particles).

The present study simulates radionuclides Cs-137 and Am-241, as examples of beta and alpha rich particles. For each of these radionuclides, six release scenarios are considered: (i) one scenario proportional to the liquid discharges of the specified radionuclide, (ii) three scenarios proportional to the uniform releases of one unit of activity during the abovementioned time of potential releases and (iii) two release scenarios constructed using Monte-Carlo simulations based on the aforementioned scenarios described in (i) and (ii).

Furthermore, the present modelling approach implements a non-instantaneous mixing of radioactivity in model compartments. According to the algorithm of the simulations, high activity particles, released into the initial box (the Cumbrian Waters) via the pipeline, can reach the box boundaries within approximately 500 hours if they remain in suspension. However, a rough estimate of the time taken for high activity particles to settle to the seabed even for "very fine sand" (Krumbein & Aberdeen, 1937) will be 7 – 27 min, approximately. As such, the assumption of particles releasing directly into the sediment is used here as the release scenario for the high activity particles.

Results and discussion

The comparison of the results of the simulations with monitoring data for high activity particles demonstrates that the present modelling approach can be used to quantify the possible release scenarios and the long-term fate of high activity particles in the intertidal beach region. Figure 3 shows comparison between results of the model simulations and monitoring data for Am-241 in the intertidal beach region for three of the selected scenarios.

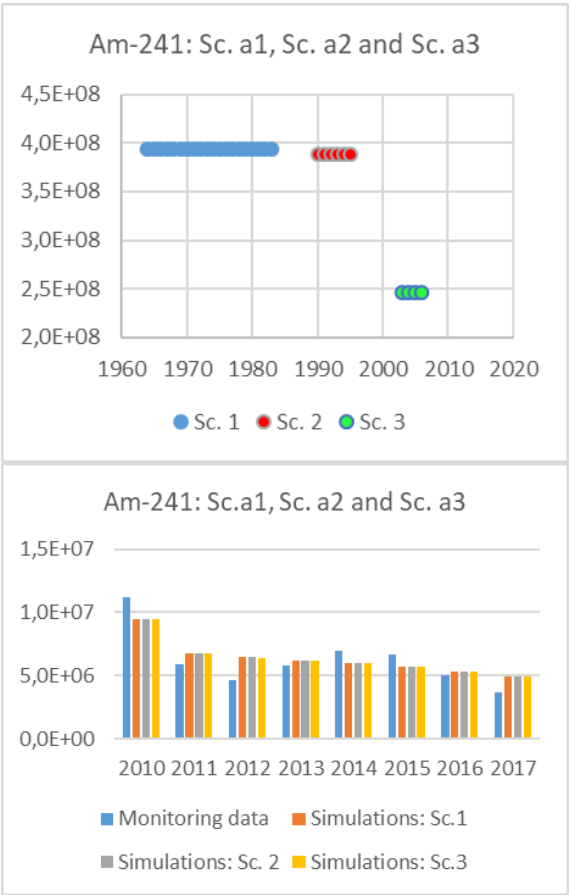

Figure 3. Comparison of the three assumed different release scenarios for high activity particles from the Sellafield nuclear facilities (top) with the total activities for high activity particles selected from the monitoring data in the intertidal beach region near the Sellafield nuclear facilities (bottom). Releases of Am-241 as well as data from monitoring and simulations are presented in Bq.

It is important to note that according to the Sellafield Ltd (2017) report, at the end of 2009 the monitoring process of the high activity particles was improved, in part with regards to the detection of particles containing Am-241. Figure 4 shows comparisons between prediction and monitoring data for Am-241 for the entire period of monitoring and for the monitoring data after 2009. Figure 4 indicates a better agreement between the calculations and the experimental data after the improvement in the monitoring methodology.

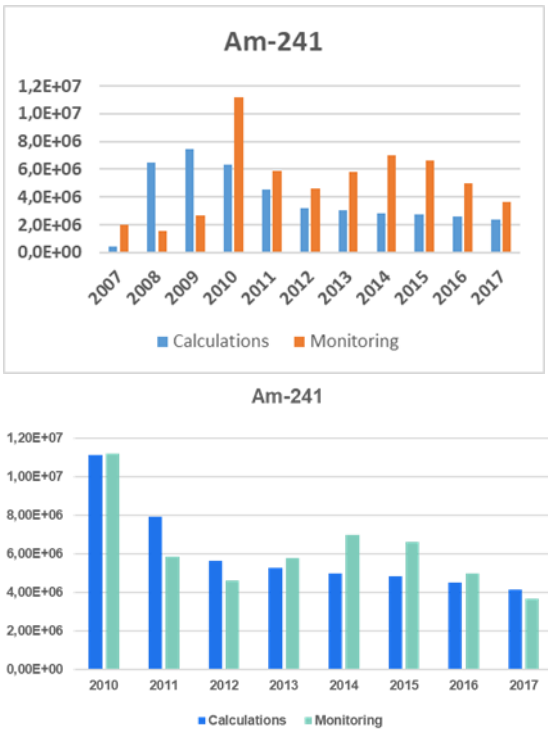

Figure 4 Comparison of the result for the whole time for monitoring (top) and for time after improvement monitoring methodology (bottom) for the selected scenario. Data for Am-241 from monitoring and simulations are presented in Bq.

The best results for the comparison between simulations and monitoring data, for the selected scenarios, are shown in Figure 5. Simulations in Figure 5 show that "old" high activity particles (released 1953-1985) strongly dominate (99-100%) among the particles found under the monitoring program. The total released activity for Cs-137 is of $1.6 \cdot 10^{10}$ Bq with a range provided by uncertainty analysis of $6.9 \cdot 10^{8}$ - $7.6 \cdot 10^{10}$ Bq. Similarly, the total released activity for Am-241 is equal to $8.3 \cdot 10^{9}$ Bq with a range of $9.8 \cdot 10^{8}$ - $4.4 \cdot 10^{10}$ Bq.

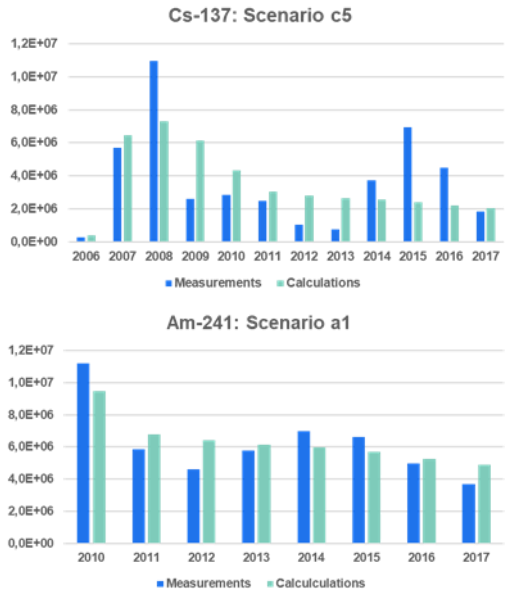

Figure 5. Comparison of the finally selected scenarios with monitoring data.

Conclusions

A specific regional model for the Cumbrian Waters has been constructed to investigate the fate of radionuclides in the intertidal beach region near the Sellafield nuclear facilities. Corroboration of the model has been provided based on liquid discharges of Cs-137, Pu-239 and Am-241 into the Cumbrian waters. Comparison of the results of calculations with monitoring data shows that the majority of results do not differ by more than a factor of two and are within the range between minimum and maximum values.

The release scenarios for Cs-137 and Am-241 associated with high activity particles, based on reasonable assumptions, have been prepared.

Comparison of the results of calculations with monitoring data for high activity particles demonstrates that the present modelling approach can be used to quantify the consequences of long-term exposure for the intertidal beach region.

The simulations show that "old" high activity particles (released 1953-1985) strongly dominate (99-100%) among the particles found under the monitoring program.

The work has been funded by the project TERRITORIES (CONCERT) under the Euratom research and training programme 2014-2018 (grant agreement No 662287).

BNFL, 1976 – 2016. Discharges and Environmental Monitoring Annual Reports.

Iosjpe M., Brown J. & Strand P., 2002. Modified Approach for Box Modelling of Radiological Consequences from Releases into Marine

Environment, *J. of Environ. Radioactiv*. 60, No 1-2, 91–103.

Iosjpe M., Isaksson M., Joensen H.P., Jonsson G., Logemann K., Roos P., Suolanen V., Thomas R. Effects of dynamic behavior of Nordic marine environment to radioecological assessments, 2016. *ISBN: ISBN 978-87-7893-442-0, http://www.nks.org/en/nks_reports/view_document.htm?id=111010213400466*

Iosjpe M., M. Karcher, J. Gwynn, I. Harms, R. Gerdes and F. Kauker, 2009. Improvement of the dose assessment tools on the basis of dispersion of the 99Tc in the Nordic Seas and the Arctic Ocean. *Radioprotection* 44, no. 5, 531–536.

Krumbein W. C., Esther Aberdeen, 1937. The Sediments of Barataria Bay, *J. of Sedimentary Petrology* 7, 3–17.

MARINA II, 2003. Update of the MARINA Project on the radiological exposure of the European Community from radioactivity in North European marine waters. *RP-132*.

Periáñez, R., Brovchenko, I., Jung, K. T., Kim, K. O., Maderich, V. 2018. The marine kd and water/sediment interaction problem. *J. of Environ. Radioactiv*. 192, 635–647.

RIFE, 1995-2014. RIFE reports: liquid and gaseous discharges from nuclear sites in England and Wales from 1995 to 2014.

Sellafield Ltd, 2011. Particles in the Environment. Annual Report for 2010/2011 and Forward Programme, Whitehaven: Nuclear Decommission Authority.

Sellafield Ltd, 2014. Particles in the Environment. Annual Report for 2013/2014 and Forward Programme, Whitehaven: Nuclear Decommission Authority.

Sellafield Ltd, 2015. Particles in the Environment. Annual Report for 2014/2015 and Forward Programme, Whitehaven: Nuclear Decommission Authority.

Sellafield Ltd, 2016. Particles in the Environment. Annual Report for 2015/2016 and Forward Programme, Whitehaven: Nuclear Decommission Authority.

Sellafield Ltd, 2017. Particles in the Environment. Annual Report for 2016/2017 and Forward Programme, Whitehaven: Nuclear Decommission Authority.

Sellafield Ltd, 2018. Particles in the Environment. Annual Report for 2017 and Forward Programme, Whitehaven: Nuclear Decommission Authority

Natural radiation exposure in geothermal power plant in the Philippines

K. Iwaoka[1], L.J.H. Palad[2], C.O. Mendoza[2], E.B. Enriquez[2], R.J. Aniago[2], T.Y. Garcia[2], M. Hosoda[3], S. Tokonami[3], C.P. Feliciano[2], R. Kanda[1]

[1]National Institutes for Quantum and Radiological Sciences and Technology, 4-9-1 Anagawa, Inage, Chiba, 263-8555, Japan.
[2]Health Physics Research Section, Atomic Research Division, Department of Science and Technology – Philippine Nuclear Research Institute (DOST-PNRI), Commonwealth Avenue, Diliman, Quezon City, 1101, the Philippines.
[3]Hirosaki University,66-1 Honcho, Hirosaki, Aomori 036-8564 Japan.
Keywords: Natural radiation, NORM, fossil fuel
Kazuki Iwaoka, e-mail: iwaoka.kazuki@qst.go.jp

In recent years, a growing number of geothermal power plants has been operating in the world as one of the energy generating industries. In the Philippine, although there are relatively many geothermal power plants compared with other countries, radiological information in these plants is scarce. In this study, measurements of activity concentration of scale and soil and ambient dose equivalent rate in a geothermal power plant in the Philippines were performed. The ambient equivalent dose rates in all work sites ranged from 0.038 to 0.051 μSv h^{-1}, which were less than average value of those in the Philippines. The activity concentrations of the ^{238}U series, ^{232}Th series and ^{40}K in the samples were lower than the relevant values (10 Bq g^{-1} for ^{40}K and 1 Bq g^{-1} for all other radionuclides of natural origin) in the IAEA Safety Standards.

Introduction

Natural radioactive nuclides such as ^{226}Ra are widely distributed in the earth's crust. A material containing significant amounts of natural radioactive nuclides is referred to as a naturally occurring radioactive material (NORM). The relevant values for the safe handling of NORM of 10 Bq g^{-1} for ^{40}K and 1 Bq g^{-1} for all other radionuclides of natural origin were given in the International Atomic Energy Agency (IAEA) Safety Guide (IAEA, 2004). Radiation exposure to NORM is recognized as a matter of international concern for health risk.

In recent years, a growing number of geothermal power plants has been operating in the world as one of the energy generating industries (Bertani, 2015; ESMAP 2012). The geothermal power plant generates electrical power by using geothermal fluid which consists of steam and heated water from the earth's crust. The compounds in the fluid are dissolved in water under conditions of high temperature and pressure and can cause the deposition of scale on the facilities such as pipes (Brown, 2013). In the Philippine, there are relatively many geothermal power plants compared with other countries (Bertani, 2015; Ogena et al., 2010), radiological information in these plants is scarce. If the scale in the plant includes natural radioactive nuclides with high concentration, the workers in the plant can be exposed at high level.

In this study, measurements of activity concentration of scale and soil and ambient dose equivalent rate in a geothermal power plant in the Philippines were performed.

Materials and methods

A geothermal power plant in Bicol Region, Philippines was chosen for this study. The measurements the ambient dose equivalent rate and sample collection for pipe scale (Figure 1) and soil were performed in work sites in the plant and public areas around the plant (background, BG). A CsI (TI) scintillation detector (PDR-101, ALOKA) was used for measuring the ambient dose equivalent rates in each work site. Each measurement was performed at a height of 1 m from the floor or surface of the ground. The average ambient dose equivalent rate was determined by averaging six measurements for 10 seconds each. The activity concentrations of ^{226}Ra, ^{228}Ra and ^{40}K in samples were determined by gamma-ray spectrum analyses. Collected samples were dried in a convection oven at a temperature of 105°C for 24 to 48 hours. The dried samples were crushed, homogenized, and sieved. About 200 g of each sample was placed in a 250 ml container and was tightly sealed. The sealed containers were allowed to stand for 30 days to reach secular equilibrium between ^{226}Ra and its decay products. A High Purity Germanium Detector (HPGe) (CPVCS 30-20190, ORTEC) coupled to multichannel analyzer (MCA) with MAESTRO software for gamma-ray spectrum analysis was used for obtaining data on gamma-ray spectrum. The activity concentration of the ^{226}Ra (^{238}U series) was determined from the energy peak of ^{214}Bi (609.31 keV) by assuming equilibrium between ^{226}Ra and ^{214}Bi. The activity concentration of ^{228}Ra (^{232}Th series) was determined from the energy peak of ^{228}Ac (911.2 keV) by assuming equilibrium between ^{228}Ra and ^{228}Ac. The activity concentration of ^{40}K was determined from the energy peak at 1460.75 keV.


Figure 1. Photo of the pipe scale in the geothermal plant.

Results and discussion

The results of ambient equivalent dose rate in the work sites and BG are shown in Table 1. The value of the ambient equivalent dose rate in the meeting room was higher than that of other work sites. This might be attributed to natural radioactive nuclides included in in construction materials such as rock (Iwaoka et al., 2013) because there were no samples related to geothermal power generations in the room. The ambient equivalent dose rates in all work sites were in good agreement with those in BG and were less than an average value of those in the Philippines (0.052 μGy h^{-1}) (Nazarea et al., 2004) based on the assumption that ambient dose equivalent (μSv)/absorbed dose in air (μGy) is 1.2 (ICRP, 1996; Bossew et al., 2017). The results of activity concentrations in the samples in Table 2. The activity concentrations of the ^{238}U series, ^{232}Th series and ^{40}K in the scale and soils were lower than the relevant values (i.e., 10 Bq g^{-1} for ^{40}K and 1 Bq g^{-1} for all other radionuclides of natural origin) in the IAEA Safety Standards (IAEA, 2014). These results might indicate that radiation impacts of workers on geothermal power plants are relatively small.

Table 1. Ambient equivalent dose rate in the plant.

Type	Place	Ambient dose equivalent rate[a] (μSv h^{-1})
Work site	Meeting room	0.051 ± 0.007
Work site	Gate	0.038 ± 0.002
Work site	Stack yard	0.040 ± 0.005
Work site	Well site	0.039 ± 0.005
BG	Cararayan, Tiwi	0.036 ± 0.003
BG	Naga, Tiwi	0.036 ± 0.004
BG	Poblacion, Tiwi	0.035 ± 0.004
BG	Malinao, Albay	0.031 ± 0.003

a: The uncertainty means the relative standard deviation (1 sigma) based on six measurements.

Table 2. Activity concentration of the samples.

Type	Place	sample	Activity concentration (Bq g^{-1})[a]		
			^{238}U series	^{232}Th series	^{40}K
			^{226}Ra	^{228}Ra	
Work site	Gate	soil	0.016 ± 0.001	0.017 ± 0.002	0.53 ± 0.01
Work site	Stack yard	Pipe scale	0.0031 ± 0.0005	ND[b]	0.14 ± 0.01
Work site	Well site	soil	0.021 ± 0.001	0.026 ± 0.002	0.56 ± 0.01

a: The uncertainty means the relative standard deviation (1 sigma) based on counting statistics.
b: ND (not determined): The activity concentration was less than one standard deviation (1 sigma).

Conclusion

Activity concentration of samples, and ambient dose equivalent rate in a geothermal power plant in the Philippines was performed. The ambient equivalent dose rates in all work sites were average value of those in the Philippines. The activity concentrations of the ^{238}U series, ^{232}Th series and ^{40}K in the samples were lower than the relevant values in the IAEA Safety Standards. These results might indicate that radiation impacts of workers on geothermal power plants are relatively small. On the other hand, it is reported that radon concentrations of samples related to production process in industries utilizing underground resorces (e.g., oil production) are relatively high (Hamlat et al., 2003). Because the geothermal power generation is also one of the industries utilizing underground resorces, accumulating data with radon is expected in the future.

The authors declare that they have no conflicts of interest.

Bertani, R. 2015. Geothermal power generation in the world-2010–2014 update report. *Proceedings World Geothermal Congress 2015*. Melbourne, Australia.

Bossew, P., Cinelli, G., Hernández-Ceballos, M., Cernohlawek, N., Gruber, V., Dehandschutter, B., Menneson, F., Bleher, M., Stöhlker, U., Hellmann, I., Weiler, F., Tollefsen, T., Tognoli, P.V., de Cort, M. 2017. Estimating the terrestrial gamma dose rate by decomposition of the ambient dose equivalent rate. *J Environ. Radioact.* 166, 296-308.

Brown, K. 2013. Mineral scaling in geothermal power production. *UNU-GTP Technical Report.* 39.

ESMAP (Energy Sector Management Assistance Program), Geothermal Handbook: Planning and Financing Power Generation. *Technical Report.* 002/12.

Hamlat, M.S., Kadi, H., Djeffal, S., Brahimi, H. 2003. Radon concentrations in Algerian oil and gas industry. *Appl. Radiat. Isot.* 58, 125-130.

IAEA (International Atomic Energy Agency). 2014. Radiation protection and safety of radiation sources: international basic safety standards. *General Safety Requirements Part 3*.

ICRP (International Commission on Radiological Protection). 1996. Conversion Coefficients for use in Radiological Protection against External Radiation. *ICRP Publication* 74.

Iwaoka, K., Hosoda, M., Tabe, H., Ishikawa, T., Tokonami, S. and Yonehara, H. 2013. Activity concentration of natural radionuclides and radon and thoron exhalation rates in rocks used as decorative wall coverings in Japan. *Health Phys*. 104, 41–50.

Nazarea, T.Y., Nato, A.Q., Enriquez, E.B., Palad, L.J.H., Dela Cruz, F.M., Garcia, T.Y., Asada, A.A., Cobor, M.L.C. 2004. Radiological surveillance of the former U.S. Base: Poro Point, San Fernando City, La Union. *Philippine Nuclear Journal* 14, 40-47.

Ogena, M.S., Maria, R.B.Sta., Stark, M.A., Oca, R.A.V., Reyes, A.N., Fronda, A.D., Bayon, F.E.B. 2010. Philippine country update: 2005-2010 geothermal energy development. *Proceedings World Geothermal Congress 2010*. Bali, Indonesia.

Comparative analysis of active and passive dosimetry systems used in environmental gamma radiation monitoring

D. Jakab[1], I. Apáthy [1], A. Csőke [1], S. Deme [1], G. Endrődi [2], L. Tósaki [2], T. Pázmándi [1]

[1]Radiation Protection Department, Centre for Energy Research, Budapest, 1121, Hungary
[2]Environmental Protection Service, Centre for Energy Research, Budapest, 1121, Hungary
Keywords: environmental gamma radiation monitoring, thermoluminescence dosimetry, free-field measurements, experimental characterization
Corresponding author, e-mail: Dorottya Jakab, jakab.dora@energia.mta.hu

A series of field measurements were performed to compare the elements of typical active and passive dosimetry systems used in environmental gamma radiation monitoring. Based on the database (containing two winter and two summer semesters) effects of environmental parameters on the accuracy of the measurements were evaluated. In order to identify the potential causes of differences between the systems and to characterize dosimeters responses due to influence quantities, a supplementary series of laboratory experiments were performed, during which the dosimeters were subjected to variant irradiations in controlled gamma radiation fields. Based on the results of field and laboratory measurement series, proposals for a correction procedure as well as for technological improvements were developed. The work aims to improve the measurement accuracy of the dosimetry systems used for environmental radiation monitoring purposes.

Introduction

As part of the environmental radiation monitoring network, a gamma radiation monitoring system operates at the KFKI Campus (located in Budapest; 47°29'20.89"N, 18°57'13.44"E), where two primary (Budapest Research Reactor – BRR, A-level isotope laboratory of Institute of Isotopes Co. Ltd. – IZOTOP) and several minor nuclear and radiological facilities are located. The gamma radiation monitoring network consists of on-line connected dose rate meters to provide real time gamma dose rates and thermoluminescent dosimeters (TLDs) to provide control and supplementary dose data. For passive dose measurements two different TLD systems are simultaneously applied.

Within the framework of this study, a comparative analysis of these routinely used active and passive dosimetry systems was carried out on the basis of continuous field measurements and a series of experimental characterization performed under laboratory conditions. The work aimed to enable the comparability of the dosimetry systems as well as of their response to environmental gamma radiation, to determine whether the passive systems could provide accurate dose data in case of the data loss from the real-time active dosimetry systems (i.e. in case of a failure). The work allows to interpret the doses measured with different dosimetry systems using both active and passive detectors as well as to increase the reliability of dose measurements applied for environmental radiation monitoring purposes.

Materials and methods

Detector characteristics

For the real-time gamma dose rate monitoring, dose rate meters equipped with a high-sensitive type of ZP1220 and a low sensitive type of ZP1301 Centronic manufactured Geiger-Müller (GM) tubes are used at the site. The acquisition period of the data logger of the dose rate meters is 2 seconds, averaged values of external environmental gamma dose rates are computed over 1- and 10-minute-long periods. As the objective of the monitoring system is to give an indication that levels from nuclear facilities are acceptable within the specified dose constraint, the calibration factor was programmed by software to convert the measured air kerma rate to ambient dose equivalent rate.

The passive dosimetry network is based on portable TLD systems, the Pille and the PorTL systems, both systems developed and manufactured by the former MTA KFKI AEKI for commercial use. The Pille system was developed primarily for space dosimetry purposes, whereas the PorTL system is delicately used for environmental dosimetry on the ground. With TLDs only average gamma dose rates can be determined on the basis of the integration of the measured absorbed dose over the given field exposure time. Initially the Pille dosimeters provide air kerma as measured quantity, however the dosimeters were recalibrated to convert the air kerma reading to ambient dose equivalent after irradiation in a ^{137}Cs photon field, for which a conversion factor of 1.2 $Sv \cdot Gy^{-1}$ (for monoenergetic photon radiation at energy level of 660 keV according to Thompson et al. (1999)) were used. Thereby all the measured data were provided in terms of ambient dose equivalent rate (H*(10)) in unit of $nSv \cdot h^{-1}$.

The main characteristics of the used active and passive detectors are summarized in Table 1.

Table 1. Specification of the used dosimetry systems

Dosimetry system	Passive		Active
	Pille	PorTL	Centroni
Detector type	TLD	TLD	GM count
Dosimeter configuration	Bulb	Cell	Tube
TL material	$CaSO_4$:Dy	Al_2O_3:C	-
Measuring range	3 µGy-10 Gy (air kerma)	10 µSv-100 mSv (ambient dose equiv.)	20 nGy·h 1 Gy·h^{-1} (air kerm rate)
Meas. uncert.	< 5%	< 5%	15%

Field measurements

The location of the field measurement points (see in Figure 1) was primarily determined by the fixed location of the active gamma dose rate system, whose detectors are installed at 16 measuring points of the site with critical function in relation to the monitoring of environmental radiation (distributed near the primary nuclear facilities), next to the main routes and also distant from the potential local release points (for monitoring of the background radiation level). At 9 measuring points simultaneous active dose rate and passive dose measurements (both with Pille and PorTL systems) were carried out. At 4 additional critical locations (predominantly near to radioactive material storages), where the installation of active dose rate meters – which would require in situ electronics and power supply – was impracticable, only TL dosimeters were placed.

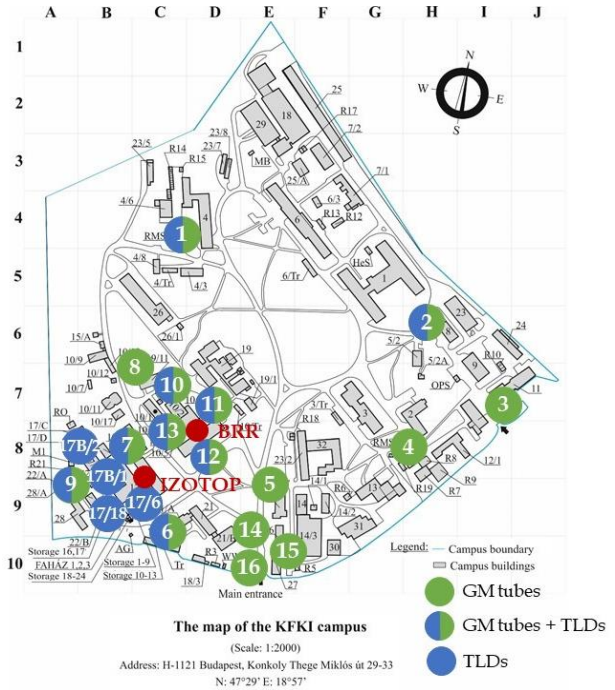

Figure 1. Measuring point locations at the site.

At the same measuring points, the different types of detectors are typically placed at a standard height of 1 m above the ground, next to each other. The placement of the dosimeters was performed with special attention paid to avoid potential self-shielding, on the other hand, the closeness of the dosimeters precluded the deviations of the terrestrial background radiation (due to geological variations, i.e. differences between the local soil compositions and surface coverage under the detectors) at the same measuring points. The influence of the cosmic radiation on the dose rate was taken to be identical for each measuring points.

The passive dosimeters were exposed to environmental radiation regularly for an exposure time of about one month. The laboratory, where the subsequent readouts of the TLDs after field exposure were performed, is located in the field measurement area, therefore monitoring and consideration of additional dose contribution of transit doses during the evaluation was not necessary. To estimate the intrinsic background contributions to the dosimetric signal – caused predominantly by the holder material's self-dose and the uncompleted annealed contribution of past exposures (residual dose) –, a separate reading was performed individually on each TLDs after every readouts of field exposure. By subtracting the second reading (intrinsic background signal) from the first readout's (total) signal, the net signal could be computed. Typical values for intrinsic background doses were 5.9 and 4.4 μSv for Pille and PorTL dosimeters, respectively.

Experimental characterization

Functional relationship between the following influence quantities and dosimeter responses were determined under laboratory conditions:

- dose dependence and response linearity,
- photon energy dependence and its relation to the spectral distribution of the environmental radiation fields,
- angular dependence,
- and TL material properties, such as the thermal and athermal fading.

The responses (ratio of the corresponding indicated value to the reference value of the quantity) were determined through a series of irradiations using a collimated reference gamma radiation field from a certified ^{137}Cs source (gamma photon energy: 661.7 keV (Bé et al., 2016). For the GM tubes parameters of the manufacturing specification were used. To supplement the measurements of dosimetric properties, testing of repeatability was also performed, for which a min. of 4 dosimeters were irradiated for each influence quantity to estimate the standard deviation of the measured values from the nominal value. The determined coefficient of variation (ratio of standard deviation to the arithmetic mean of a set of measurements) for measurement series of each dosimetric properties was 1.0% in the case of Pille and 2.0% for the PorTL.

The obtained levels of the natural radiation dose rate at the site is in the range of 100 nSv·h^{-1}, however passive detectors must be capable to measure doses of more order of magnitude higher, in places where elevated radiation levels are observed. To consider how the response varies with doses, the dose dependence was tested with irradiations at different dose levels over the range from 60 μSv up to 12 mSv covering the expected dose range of interest. The dose response (R_{dose}) was determined as the ratio of the measured dose to the irradiation dose.

The energy dependence was determined according to McKeever et al. (1995). For photon irradiation this is defined in terms of the mass energy absorption coefficient (μ_{en}/ρ), and the photon energy response ($S_E(E)$) is determined as:

$$S_E(E) = (\mu_{en}/\rho)_{TL} \cdot [(\mu_{en}/\rho)_{ref}]^{-1}$$

where the subscripts refer to the TL and the reference material (air). The μ_{en}/ρ values regarding the TL materials was taken from the NIST X-ray Attenuation database (Hubbell and Seltzer, 2004), for compositions they were calculated as the weighted summation of coefficients for elemental media. The photon energy response has been normalized to unity for a ^{137}Cs source, thus the Relative Energy Response (R_{energy}):

$$R_{energy} = S_E(E) \cdot [S_E(661.7\ keV)]^{-1}.$$

To evaluate the variation of the response with angle of incidence (R_{ang}), irradiations were performed with a fixed dose by rotating the dosimeters by 45° 1) around their longitudinal axis at vertical orientation, and 2) perpendicular to their longitudinal axis, when they were oriented horizontally. The reference orientation (0°), to which the measured doses at given angles were referred 1) coincided with the dosimeters' longitudinal axis, or 2) was perpendicular to the dosimeters' longitudinal axis. For the angular dependence correction an average value of the response due to angle of incidence can be used with the assumption of isotropic field.

The effect of thermal fading (R_{fading}) was defined as the ratio of the background-corrected doses after post-irradiation storage of fading control detectors to the nominal irradiation dose. The fading control dosimeters were irradiated at the beginning of the field exposure period. As the fading rate, which results in the reduction of the readout, might be not constant in time and depends strongly on the ambient temperature, fading effect was investigated not only in controlled room temperature, but at open air reference locations in field temperature. Thereby the effects of short-term changes in temperature on the TL signal loss could have been also quantified. In order to determine reliable fading correction factors, several reference locations of variant but representative climatic conditions (i.e. sunny and shadowed locations) were selected.

Correction

The model function to determine the value of measurand (D, absorbed dose) is:

$$D = M \cdot N^{-1} \cdot \prod R_i^{-1}$$

where M is the indicated value of the dosimetry system (net readout), N is the calibration coefficient, R_i is the relative responses due to the given influence quantity.

The responses were determined as the arithmetic mean ($\hat{R}_i$) of n observations for the relative response due to given influence quantity, obtained under the same conditions. The uncertainty of the relative responses was determined as the half-width of confidence interval for the mean ($\hat{R}_i - U_{\hat{R}i}$, $\hat{R}_i + U_{\hat{R}i}$) with the approximation of:

$$U_{\hat{R}i} = t_{n-1} \cdot n^{-1/2} \cdot s(R_i) =$$
$$= t_{n-1} \cdot n^{-1/2} \cdot [1 \cdot (n-1)^{-1} \cdot \Sigma(R_i - \hat{R}_i)^2]^{1/2}$$

where $s(R_i)$ is the standard deviation for the response due to the given influence quantity and t_{n-1} is the Student's t coverage factor for 95% confidence level.

Results and discussion

Field measurements

A database of about one and a half year obtained as the outcome of the simultaneous field measurements was evaluated. Uncorrected variations in equivalent gamma dose rates (for GM counters values averaged over the exposure cycle) for the three types of detectors over the complete monitoring period are shown in Figure 2. Significant difference exists between passive systems, on the other hand a systematic underestimation was determined of passive dosimetry systems (-15% and -26% for Pille and PorTL, respectively) compared to the active system. The overestimation of the active dosimetry system is presumably due to the used GM counter's sensitive detector response to the cosmic radiation.

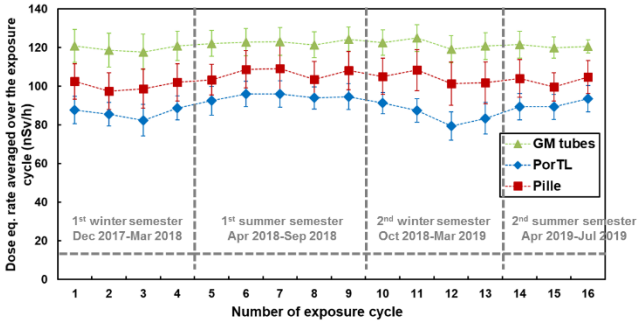

Figure 2. Uncorrected variations in gamma dose rates over the monitoring periods.

Experimental characterization

The functional dependence of the intensity of the measured TL signal upon the absorbed dose is linear over a wide dose range for both of the TLDs. In spite of the linear characteristic, each passive system shows over-response (≥ 5%) in the low-dose range (< 300 µSv) when the measured and the nominal irradiation doses are compared (see in Figure 3).

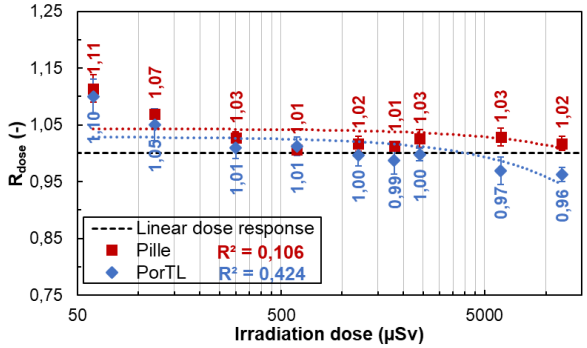

Figure 3. Dose response (R_{dose}) of Pille and PorTL systems per unit dose over the range of 60 µSv - 12 mSv.

The effective atomic number is Z_{eff} = 15.3 and Z_{eff} = 10.2 for $CaSO_4$:Dy (Pille) and Al_2O_3:C (PorTL) TL materials, respectively. These effective atomic numbers are relatively high compared to the soft tissue atomic composition (Z_{eff} = 8.2 (Thompson et al., 1999)) with regards of photons, which results in a significant over-response by a maximum factor of 10.3 and 3.6 at low photon energies without energy compensation for $CaSO_4$:Dy and Al_2O_3:C TL materials, respectively (see in Figure 4). To overcome the over-response of GM counters at low photon energies, energy compensating filter is fitted to the counter, which results in an average response of unity, however absorbs the low energy photons so the counter' response falls off rapidly below energies of approx. 100 keV for high sensitive type of GM tube. However, it is important to note that the low energy photon components' (<100 keV) contribution to the absorbed dose in air (6%) is significantly lower than the contribution of higher energy components of a typical environmental spectrum, for which the mean photon energy of exposure rate is 1.2 MeV (Thompson et al., 1999).

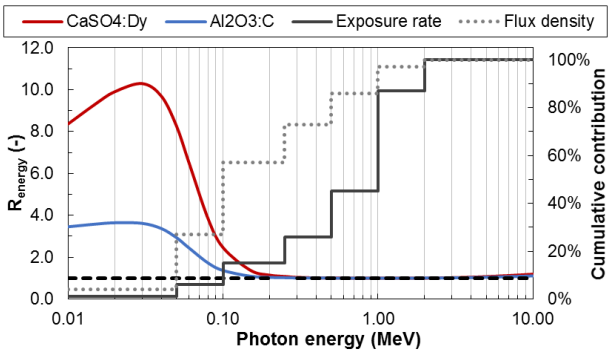

Figure 4. Photon energy response (R_{energy}) of TL materials ($CaSO_4$:Dy – Pille; Al_2O_3:C - PorTL) and the environmental radiation exposure rate and flux distribution as a function of energy (NCRP, 1976).

According to Figure 5, the longitudinal direction dependence is significantly higher for each system, consistently with the expected angular dependence due to the holders design and construction (thickness and atomic numbers as well as the shielding effect of materials surrounding the detectors).

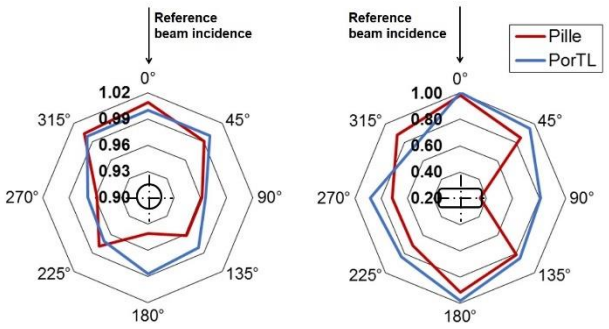

Figure 5. Dependence of the passive systems' response with angle of incidence (R_{ang}).

The fading of PorTL considered to be negligible (<1%) for about a month-long exposure. The Pille is more affected by the ambient temperature, following a month-long environmental exposure period the thermally induced loss of the TL signal was about 3% (regardless of permanent or variable temperature). However, for Pille the application of fading correction should be considered for long term environmental monitoring, as the loss of TL signal increases to more than 10% after six months exposures (see in Figure 6).

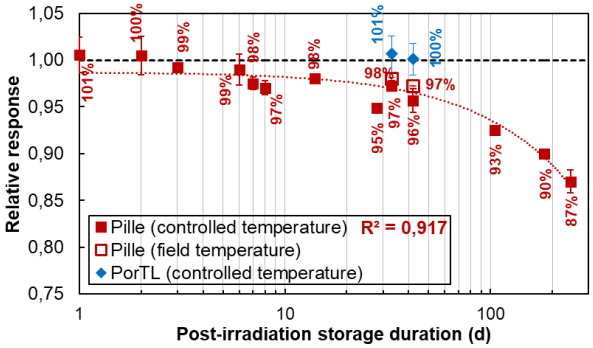

Figure 6. The relative response variation due to fading effect (R_{fading}) as a function of the post-irradiation storage duration.

Correction

The determined correction factors related to the influence dosimetric quantities correspond to the requirements stated in the standard of IEC 62387:2012 (see in Table 2). As a consequence of the corrections, the difference between the dosimetry systems could be reduced significantly (see in Figure 7).

Table 2. Requirements and correction factors related to the detector characteristics

Response	Requirement $(\hat{R}_i \pm U_{\hat{R}i}) \in [\ldots]$	Determined value $\hat{R}_i \pm U_{\hat{R}i}$	
		Pille	PorTL
R_{dose}	$\in$ [0.91 … 1.11]	1.04 ± 0.03	1.01 ± 0.03
R_{energy}	$\in$ [0.71 … 1.67]	1.35 ± 0.11	1.10 ± 0.12
R_{ang}	$\in$ [0.71 … 1.67]	0.88 ± 0.09	0.95 ± 0.04
R_{fading}	$\in$ [0.91 … 1.11]	0.97 ± 0.03	0.99 ± 0.02

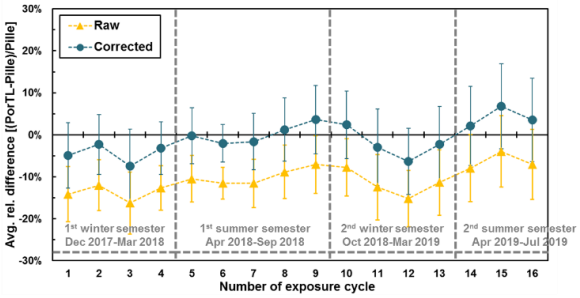

Figure 7. Relative differences between passive systems for uncorrected (raw) and corrected gamma dose rates.

Conclusions

Comparison of uncorrected gamma dose rates, obtained from a field measurements database, showed considerable differences between the dosimetry systems. Correction of the measurements for the influence quantities by accurately determined detector responses resulted in significant improvements in dose estimations.

Bé, M.-M. et al. 2016. *Monographie BIPM-5 - Table of Radionuclides (Vol. 8)*. Bureau International des Poids et Mesures, Sèvres. ISBN: 978-92-822-2264-5.

Hubbell, J.H., Seltzer, S.M. 2004. X-Ray Mass Attenuation Coefficients. *NIST Standard Reference Database 126*. https://dx.doi.org/10.18434/T4D01F.

IEC 62387:2012, Radiation protection instrumentation - Passive integrating dosimetry systems for personal and environmental monitoring of photon and beta radiation

McKeever, S.W.S. et al. 1995. *Thermoluminescence dosimetry materials: properties and uses*. Nuclear Technology Publishing, Ashford. ISBN: 1 870965 19 1.

NCRP. 1976. Environmental Radiation Measurements *Report No. 50*, National Council on Radiation Protection and Measurements, Washington, ISBN: 0-913392-32-4

Thompson, I.M.G. et al. (Eds.). 1999. Technical Recommendations on Measurements of External Environmental Gamma Radiation Doses. *Radiation Protection series 106*. European Commission, Luxembourg. ISBN: 92-828-7811-2.

Atom counting of long-lived radionuclides using neutron activation analysis

J. Kučera[1], J. Kameník[1], P. P. Povinec[2], I. Krausová[1], I. Světlík[1], M. Fikrle[1]

[1]Nuclear Physics Institute of CAS, Husinec-Řež, 25068, Czech Republic
[2]Centre for Nuclear and Accelerator Technologies (CENTA), Faculty of Mathematics, Physics and Informatics, Comenius University, Bratislava, 84248, Slovakia
Keywords: Long-lived radionuclides, Decay counting, Atom counting, Neutron activation analysis
J. Kučera, e-mail: kucera@ujf.cas.cz

Introduction

It is obvious from equation (1) that measurement of long-lived radionuclides can be carried out by both decay counting (radiometric method) and atom counting

$$A = \lambda N \qquad (1)$$

where A is the activity, N is the number of atoms, and λ is the decay constant related to the half-life $T_{1/2}$ by equation $\lambda = \ln 2/T_{1/2}$. Despite the advances in radiometric technologies, atom counting has recently received much more attention for measurement of long-lived radionuclides. Recently, mass spectrometry techniques, namely ICP-MS and AMS, proved to be superior for determination of long-lived radionuclides, when compared to radiometric counting (Povinec et al., 2018). Another possibility is neutron activation analysis (NAA) provided that a long-lived radionuclide has favorable nuclear characteristics, i.e., the nuclide has a large neutron capture cross section for formation of a product nuclide (or its daughter) with good measurement properties, such as a short half-life and suitable gamma-ray spectrometric characteristics (Byrne and Benedik, 1999). The activity, A, after the irradiation time, t_i, decay time, t_d, and counting time, t_c, is given by equation (2)

$$A = N\left(\Phi_{th}\sigma_{th} + \Phi_{epi}I_0\right)SDC \qquad (2)$$

where N is the number of atoms, Φ_{th} is the thermal neutron fluence rate, Φ_{epi} is the epithermal neutron fluence rate, σ_{th} is the thermal neutron cross section, I_0 is the resonance integral cross section, S is the saturation factor ($S = \left(1 - e^{-\lambda t_i}\right)$), D is the decay factor ($D = e^{-\lambda t_d}$), and C is the counting factor ($C = (1 - e^{\lambda t_c})/\lambda t_c$).

The above authors calculated advantage factors (AFs) of long-lived alpha-emitters as a ratio of signals obtained in NAA and decay counting, whereas AFs for other long-lived radionuclides were calculated by another author for different NAA and radiometric conditions (Hou, 2008). Table 1 shows differences in both sets of values. It should be pointed out here that the AFs only indicate a potential for NAA relative to radiometry. Important factors to consider in practice are the counting efficiency and background of both measurement modes.

Since we have favorable conditions for NAA using a LVR-15 reactor at Řež, we explored the determination of ^{99}Tc, ^{129}I, ^{232}Th, ^{238}U in environmental and other samples by NAA as reported in this work.

Table 1. AFs for NAA of some long-lived radionuclides

Nuclide pair	$T_{1/2}$ of target (y)	AF[a]	AF[b]
^{99}Tc/^{100}Tc	2.1 x 10^5	-	2.1 x 10^4
^{129}I/^{130}I	1.57 x 10^7	-	1.3 x 10^6
^{135}Cs/^{136}Cs	2.06 x 10^6	-	3.86 x 10^3
^{230}Th/^{231}Th	7.54 x 10^4	27	8.6 x 10^3
^{232}Th/^{233}Pa	1.40 x 10^{10}	4.0 x 10^5	2.5 x 10^6
^{231}Pa/^{232}Pa	8.27 x 10^4	106	1.2 x 10^4
^{238}U/^{239}U	4.46 x 10^9	7.0 x 10^6	3.4 x 10^8
^{238}U/^{239}Np	4.46 x 10^9	8.0 x 10^5	3.4 x 10^8
^{237}Np/^{238}Np	2.14 x 10^6	640	3.6 x 10^5
^{242}Pu/^{243}Pu	3.75 x 10^5	-	3.6 x 10^4

[a] – Byrne and Benedik 1999, [b] – Hou 2008

Technetium–99 ($T_{1/2}$ = 2.1 x 10^5 y)

The ^{99}Tc determination by NAA is based on parameters given in Table 2.

Table 2. Nuclear parameters for ^{99}Tc determination

Nuclear reaction	σ (barn)	I_0 (barn)	$T_{1/2}$ of product	Main γ-line (keV); int. (%)
^{99}Tc(n, γ)^{100}Tc	20	30	15.8 s	539.5; 6.6

We employed both instrumental NAA (INAA) and epithermal NAA (ENAA) with irradiation and counting parameters given in Table 3 together with the resulting limits of detection (LOD).

Table 3. Irradiation and counting parameters

INAA	ENAA
Φ_{th}=3 x 10^{13} cm^{-2} s^{-1}	Φ_{epi}=1 x 10^{13} cm^{-2} s^{-1}
t_i=15 s	t_i=20 s
t_d=12–17 s	t_d=16-21 s
t_c=30 s	t_c=30 s
LOD=200 mBq	LOD=50–70 mBq

Irradiations were carried out using a pneumatic transfer system with a transport time of 3.5 s, however, due to manual repacking and sample transfer to a coaxial HPGe detector with relative efficiency of 21 % and FWHM resolution of 1.75 keV (both for the 1332.5 keV photons of ^{60}Co) the decay time, t_d, was somewhat longer compared to the transport time. In ENAA, thermal neutrons were shielded off with the aid of a Cd box with wall thickness of 1 mm. The LODs achieved in both NAA modes were insufficient for the Tc determination in environmental samples, such as algae Fucus serratus from the vicinity of La Hague reprocessing plant and Novo-Shepelyci soil from the vicinity of the crashed Chernobyl nuclear power plant (NPP). In these samples, the Tc

concentration was determined by liquid scintillation counting (LSC) after pre-separation with TOGDA-PAN resin and extraction using methyl ethyl ketone (Fikrle, 2011, cf. Table 4). The accuracy of the ^{99}Tc determination by LSC measurement was proved by analysis of NIST SRM 4359 Seaweed Radionuclide Standard. Our values agree with the NIST noncertified value (median 38 mBq g^{-1}, range 17–48 mBq g^{-1}).

Table 4. Concentrations of ^{99}Tc determined by LSC

Sample	Tc (mBq g^{-1})
Fucus serratus 1	26.8 ± 5.4
Fucus serratus 2	22.7 ± 5.1
Soil Novo-Shepelyci	14.1 ± 2.6
NIST SRM 4359 Seaweed	20.2 ± 7.6; 29.6 ± 7.4

Although pre-irradiation separation may improve LOD of ^{99}Tc determination by NAA (Hou, 2008), there are other methods, namely resonance ionization mass spectrometry (RIMS), thermal ionization mass spectrometry (TIMS), ICP-MS and accelerator mass spectrometry (AMS), which provide much more favourable LOD of ^{99}Tc (Hou and Roos, 2008).

Iodine–129 ($T_{1/2}$ = 1.57×10^7 y)

The ^{129}I determination by NAA is based on parameters given in Table 5.

Table 5. Nuclear parameters for ^{129}I determination

Nuclear reaction	σ (barn)	I_0 (barn)	$T_{1/2}$ of product	Main γ-line (keV); int. (%)
^{129}Tc(n, γ)^{130}I	27±3	36±4	12.36 h	536.1; 15.7

There are several nuclear interferences in the ^{129}I determination by NAA, which should be accounted for (Hou, 2008).

We employed NAA with both pre-irradiation and post-irradiation separation, so-called radiochemical NAA (RNAA) with irradiation and counting parameters as follows: Φ_{th} = 4 x 10^{13} cm^{-2} s^{-1}, t_i = 4–10 h, t_d = 10–15 h, t_c = 2–4 h. First we used the NAA procedures for large-scale studies of ^{129}I concentration and the ^{129}I/^{127}I ratio in samples from the Baltic Sea (Hou et al. 2002), thyroid and urine samples from Ukraine and Denmark (Hou et al., 2003a), and in Chernobyl contaminated soil (Hou et al., 2003b). In these studies, we employed NAA with both pre-irradiation and post-irradiation separation (RNAA) described in the above publications. Later we measured both ^{129}I and the ^{129}I/^{127}I ratio in biomonitors from the vicinity of Temelín NPP. The samples comprised thyroids of cattle grazing in the NPP vicinity, moss Pleurozium Schreberi and three river sediments collected in the catchment of the NPP, upstream and downstream of the NPP water outlets. The thyroid samples, highly sensitive biomonitors of radio-iodine pollution, were collected prior to the start of NPP operation and after several years of its functioning to investigate whether releases of ^{129}I occur into the environment during normal operation of the NPP. In this work, we developed pre-irradiation separation based on sample combustion followed by trapping of the released iodine in a LiOH solution and RNAA procedure consisting of extraction of elementary iodine in $CHCl_3$. LOD of ^{129}I of our procedure was in the range of 8 – 10 mBq kg^{-1} (Krausová et al., 2013).

Results for the ^{129}I/^{127}I ratio in the bovine thyroids are schematically depicted in Figure 1 and compared with world-wide values of animal thyroids.

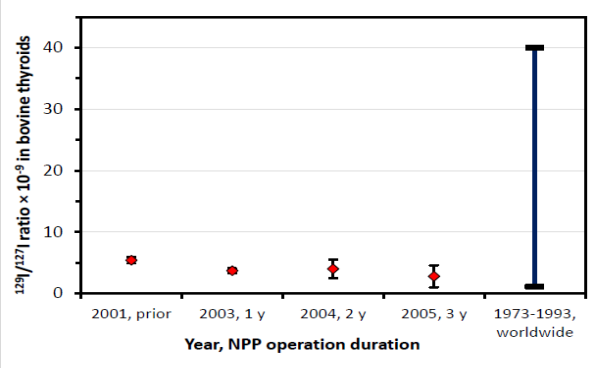

Figure 1. ^{129}I/^{127}I ratios in bovine thyroids from the vicinity of Temelín NPP and their comparison with world-wide values.

Figure 1 shows no local contamination with ^{129}I due to the Temelín NPP releases. A similar conclusion can be derived from results of the ^{129}I and ^{129}I/^{127}I ratio determination in moss and sediment samples, other biomonitors of ^{129}I pollution (cf. Table 6).

Table 6. ^{129}I levels and ^{129}I/^{127}I ratio in biomonitors

Sample	Year of sampling (N)	^{129}I (mBq kg^{-1})	^{129}I/^{127}I x 10^{-9}
Moss P. Schreberi	2004 (5)	23 ± 16	2.3 ± 1.9
Sediment upstream NPP	2004 (4)	< 10	-
Sediment NPP catchment area	2004 (7)	< 8	-
Sediment downstream NPP	2004 (4)	< 10	-

Quality control of the study was pursued by analysis of reference algae sample F. Serratus, and good agreement was obtained with published results (Krausová et al., 2013). Our LOD values for the ^{129}I/^{127}I ratio were better than those of other methods, except for AMS (cf. Table 7). However, ICP-MS and AMS techniques recently further improved their LOD values for ^{129}I (and other long-lived radionuclides), as was reported at this symposium.

Table 7. LOD for ^{129}I achieved by different methods (Rosenberg, 1993)

Method	Number of atoms	^{129}I/^{127}I ratio
LSC	3.5 x 10^{13}	> 10^{-6}
γ-spectrometry	10^{13}	> 10^{-6}
ICP-MS	3 x 10^{11}	> 10^{-8}
TIMS	10^7	-
NAA	10^7	10^{-12} – 10^{-13}
AMS	2 x 10^6	10^{-13}

Thorium–232 ($T_{1/2}$ = 1.40×10^{10} y)

The ^{232}Th determination by NAA is based on parameters given in Table 8.

Table 8. Nuclear parameters for ^{232}Th determination

Nuclear reaction	σ (barn)	I_0 (barn)	$T_{1/2}$ of product	Main γ-line (keV); int. (%)
^{232}Th(n, γ)^{233}Th →^{233}Pa	7.3±0.1	84 ± 4	27.0 d	311.9; 38.5

In underground nuclear physics experiments focused on investigations of rare nuclear processes and decays, radiopurity of construction parts of the detectors and all materials used is crucial for background reduction. For SuperNEMO experiment, which aims at detection of neutrinoless double beta decay of ^{82}Se (Arnold et al., 2010), we measured levels of ^{232}Th in the ^{82}Se source material (with ~ 80 % enrichment) and in Cu, a part of the detection system, by RNAA using the following irradiation and counting conditions: Φ_{th} = 4 x 10^{13} cm^{-2} s^{-1}, t_i = 20 h, t_d = 10–15 d, t_c = 4–8 h. Counting was carried out with a coaxial HPGe detector (rel. efficiency 77 %, FWHM resolution 1.85 keV, both for the 1332.5 keV photons of ^{60}Co). Two types of RNAA procedures were employed. First (denoted A in Figure 2) was based on ^{233}Pa extraction with 5% TOPO in toluene from 7 M HNO_3 according to Byrne and Benedik (1999). It turned out that one of the enriched ^{82}Se samples was contaminated with Te, which produced ^{131}I upon neutron irradiation by the reaction ^{130}Te(n,γ)^{131}Te ($T_{1/2}$ = 1.26 d) → ^{131}I ($T_{1/2}$ = 8.04 d) and significantly increased background in the measured γ-ray spectra (cf. Figure 2) Therefore, second RNAA procedure (denoted B) was designed, which was based on ^{233}Pa separation from 7 M HNO_3 with Triskem TRU resin (Kučera et al., 2017). Using RNAA-B procedure, LODs for ^{232}Th in Cu and ^{82}Se of 0.08 μBq and 1 μBq, respectively, were achieved (Kučera et al. 2017). It can be seen from a comparison of LODs for the ^{233}Pa determination in Cu with different methods in Table 9 that RNAA provided the third lowest LOD, after AMS and ICP-MS.

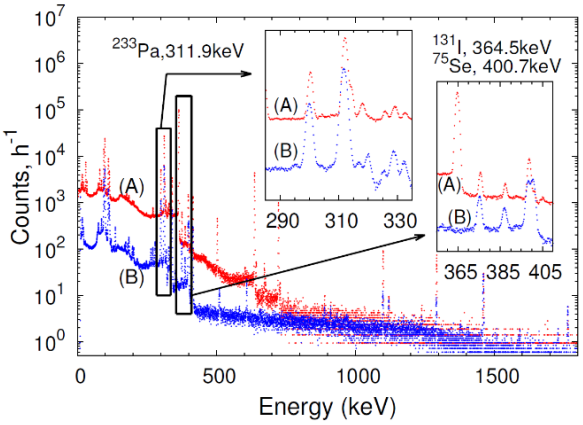

Figure 2. Comparison of γ-ray spectra in RNAA determination of ^{233}Pa in ^{82}Se. (A) – TOPO extraction method, (B) – TRU resin method.

Table 9. Comparison of LODs for ^{233}Pa determination in Cu with different methods (Povinec, 2017)

Method	LOD (μBq)
α-ray spectrometry	100
Underground γ-ray spectrometry	2400
BiPo-3 detector	1.4
ICP-MS	0.003
AMS	0.0003
RNAA	0.08

Uranium–238 ($T_{1/2}$=4.5x10^9 y)

The ^{238}U determination by NAA can be based on parameters given in Table 10.

Table 10. Nuclear parameters for ^{238}U determination

Nuclear reaction	σ (barn)	I_0 (barn)	$T_{1/2}$ of product	Main γ-line (keV); int. (%)
^{238}U(n, γ)^{239}U	2.7±0.7	280±10	23.5 min	74.7; 53.2
^{238}U(n, γ)^{239}U →^{239}Np	2.7±0.7	280±10	2.36 d	106.1; 25.3

For SuperNEMO experiment we also measured levels of ^{238}U in the enriched ^{82}Se and in Cu by RNAA. Of the two possibilities given in Table 10, the use of ^{239}U measurement was chosen, because this option has a higher potential for obtaining a better AF, it is faster and easier to perform. We employed the following irradiation and counting parameters: Φ_{th}= 2 x 10^{13} cm^{-2} s^{-1}, t_i = 3 min, t_d = 20–30 min, t_c = 3000–5400 s. Three versions of RNAA were used based on ^{239}U extraction with 50 % tributyl phosphate (TBP) in toluene from 7 M HNO_3. In the first version (denoted A in Figure 3), the organic phase was double scrubbed with 7 M HNO_3 in the presence of Se or Cu hold-back carrier before counting with a well-type HPGe detector (active volume of 150 cm^3, FWHM resolution 2.1 keV for the 1332.5 keV photons of ^{60}Co). A high ^{83}Br activity was present in the organic fraction separated from the irradiated ^{82}Se sample, which was created by the reaction ^{82}Se(n,γ)^{83}Se ($T_{1/2}$=22.3 min) → ^{83}Br($T_{1/2}$=2.4 h, E_γ=529.6 keV) and significantly increased background in the measured γ-ray spectra (cf. Figure 3). After stripping of ^{239}U with saturated solution of Na_2CO_3, the interfering activity of ^{83}Br (spectrum B in Figure 3) decreased. A further decrease was obtained by precipitation of the formed ^{83}Se as Ag_2SeO_3 and precipitation of ^{83}Br as AgBr prior to extraction of ^{239}U by TBP with ^{239}U stripping from the organic phase with saturated solution of Na_2CO_3 as the last separation step (spectrum C in Figure 3).

Using RNAA-C procedure, LODs for ^{238}U in Cu and ^{82}Se of 0.2 μBq and 0.6 μBq, respectively, were achieved (Kučera et al. 2017). A comparison of LODs for the ^{238}U determination in Cu with different methods (cf. Table 11) yields a similar picture as for the ^{232}Th determination (cf. Table 10): RNAA provides the third lowest LOD, after AMS and ICP-MS.

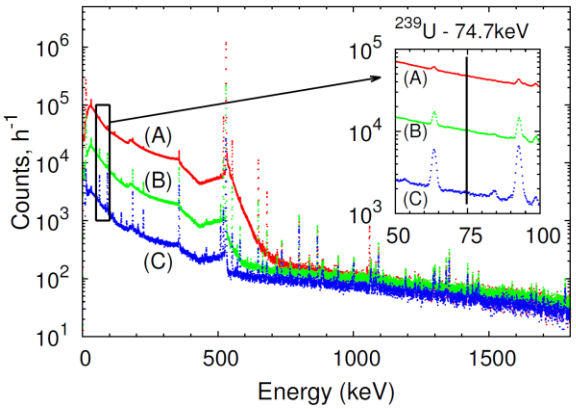

Figure 3. Comparison of γ-ray spectra in RNAA determination of ^{239}U in ^{82}Se. (A) – scrubbed TBP phase, (B) – stripped aqueous phase, (C) – stripped aqueous phase preceded by removal of ^{83}Se and ^{83}Br.

Table 11. Comparison of LODs for ^{238}U determination in Cu with different methods (Povinec, 2017)

Method	LOD (μBq)
α-ray spectrometry	100
Underground γ-ray spectrometry	2000
BiPo-3 detector	1.6
ICP-MS	0.010
AMS	0.0001
RNAA	0.2

Conclusions

Although the LODs of long-lived radionuclides by NAA have recently been surpassed by those achieved by ICP-MS and AMS, NAA as a primary method of measurement will keep its importance for quality control purposes. In most cases, no pre-irradiation chemistry is required (no risk of contamination of analyzed samples) and advanced post-irradiation chemistry (RNAA) has still a potential for further improvements of LOD values.

This work was carried within the CANAM infrastructure of the NPI CAS Řež supported through MŠMT project No. LM2015056.

Arnold, R. Augier, C., Baker, J. et al. 2010. Probing new physics models of neutrinoless double beta decay with SuperNEMO. *Eur. Phys. J., C*, 70, 927–943.

Byrne, A.R. and Benedik, L. 1999. Application of neutron activation analysis in determination of natural and man-made radionuclides, including ^{231}Pa. *Czech. J. Phys.* 49, S1, 263–270.

Fikrle, M. 2011. Development of methods for the ^{99}Tc determination in environmental samples. *Dissertation thesis*. Czech Technical University in Prague, Faculty of Nuclear Sciences and Physical Engineering (in Czech).

Hou, X.L., Dahlgaard, H., Nielsen, S.P., Kučera, J. 2002. Level and origin of Iodine-129 in the Baltic Sea. *J. Environ. Radioact.* 61, 331–343.

Hou, X., Malencheko, A.F., Kučera, J. et al. 2003a. Iodine-129 in thyroid and urine in Ukraine and Denmark. *Sci. Total Environ.* 302, 63–73.

Hou, X.L., Fogh, C.L., Kučera, J. et al. 2003b. Iodine-129 and Caesium-137 in Chernobyl contaminated soil and their chemical fractionation. *Sci. Total. Environ.* 308, 97–109.

Hou, X. 2008. Activation analysis for the determination of long-lived radionuclides. *Radioactiv. Environ.* 11, 371–405.

Hou, X. and Roos, P. 2008. Critical comparison of radiometric and mass spectrometric methods for the determination of radionuclides in environmental, biological and nuclear waste samples. *Anal. Chim. Acta* 608, 105-139.

Krausová, I. Kučera, J., Světlík, I. 2013. Determination of ^{129}I in bio-monitors collected in the vicinity of a nuclear power plant by neutron activation analysis. *J. Radioanal. Nucl. Chem.* 295, 2043–2048.

Kučera, J., Kameník, J., Povinec, P.P. 2017. Determination of ultra-trace levels of Th and U in components of SuperNEMO detector by radiochemical neutron activation analysis. *Proc. 6th Asia-Pacific Symposium on Radiochemistry (APSORC-2017), September 17-22, 2017, Jeju Island, Korea*.

Povinec, P.P. 2017. Analysis of radionuclides at ultra-low levels: A comparison of low and high-energy mass spectrometry with gamma-spectrometry for radiopurity measurements. *Appl. Rad. Isotopes* 126, 26–30.

Povinec, P.P., Benedik, L., Breier, R. et al. 2018. Ultra-sensitive radioanalytical technologies for underground physics. *J. Radioanal. Nucl. Chem*. 318, 677–684.

Rosenberg, R.J. 1993. Non-conventional measurement techniques for the determination of some long-lived radionuclides produced in nuclear fuel. A literature survey. *J. Radioanal. Nucl. Chem.* 171, 465–482.

Application of natural and artificial radionuclides for evaluation of sedimentation rate in the lake Khuko (West Caucasus)

N. Kuzmenkova[1], M.M. Ivanov[2,3], A. Grachev[3], A. Rozhkova[1], V. Golosov[2,3]

[1]Department of chemistry, Lomonosov Moscow State University, Moscow, 119991, Russia
[2]Department of geography, Lomonosov Moscow State University, Moscow, 119991, Russia
[3]Geography Institute RAS, Moscow, 119017, Russia
Keywords: natural & artificial radionuclides, sedimentation rate, Chernobyl, Cs-137, plutonium, americium
Presenting author, e-mail: kuzmenkova213@gmail.com

Some of fallout radionuclides (^{137}Cs, ^{210}Pb$_{ex}$) are quickly and strongly sorbed on the soils and sediments particles, and they widely used for the evaluation of erosion/deposition rates for the different time windows as a response to environmental changes. Ubiquitous in the environment are the natural radionuclides of the ^{238}U, ^{235}U and ^{232}Th families. The elements- members of the radioactive series differ in their chemical properties and geochemical behavior. Useful information can be provided by the ratio of the radioactivity of the members of the natural series. Goldberg (1963) proposed a ^{210}Pb dating method ($T_{1/2}$= 22.3 yrs), based on the imbalance between ^{226}Ra and the daughter radon atom. While the unsupported lead-210 has been employed for reconstruction of the sedimentation rate in lakes for a long time. This approach has several disadvantages. The daughter product of ^{226}Ra is radon gas, which constantly accumulates in the sediment. Under certain conditions, it can break out and disrupt the structure of the sediment and perturb the distribution of lead and radium (Appleby, 2008). Later on, an artificial radionuclide ^{137}Cs was used as a chronological marker following the nuclear bomb testing during 1954-1963. The interpretation of ^{137}Cs depth distribution in the bottom sediments of five lakes in England allowed to determine the sedimentation rate for two-time windows: 0.56 – 1.1 cm/year for 1963 – 1972 and 0.08 – 0.9 for 1954 – 1973. (Pennigton, 1973).

The aim of study was to evaluate lake sedimentation rate using artificial ^{137}Cs and unsupported ^{210}Pb. In addition, specific activity of ^{241}Am and ^{239,240}Pu in sediments were determined and were used for identification for the possible sources of artificial radionuclide fallout.

Lake Khuko is a mountain lake situated in the Caucasus natural reserve, within the mid-latitude belt at 1740 meters above sea level (a.s.l.) between the valleys of the Psheashkha (Psekha river tributary) and Shakhe rivers, 7 km northwest of Mountain Fisht. The lake's surface area is 27 500 m^2, length: 260 m, width: 150 m; maximal depth reaches 10 m. The area of the lake's catchment is around 120 000 m^2. The section of the Main Caucasus ridge adjoining the lake lies within the altitudes of 1700 – 1900 m a.s.l. The catchment area is primarily occupied by meadows and beech forest. The oval-shaped Lake Khuko is located within one of kettles formed by closed distinctive depressions. The lake's shoreline in not indented. Relative heights of the surrounding slopes vary in range 5 – 100 m. Microclimate of the lake kettle is rather severe with relatively low temperatures and high snow accumulation during cold part of year. Snow cover is preserved until the end of June, while certain ice floes can be still seen in July (Efremov, 1991). The lake's kettle represents a seasonally pronounced deposition environment for atmospheric aerosols. Drilling at Lake Khuko was carried out by the staff of the Glaciology Department of the Institute of Geography of the Russian Academy of Sciences in the Summer 2016. The same technique was used to collect samples at Lake Khuko in 2016. Total thickness of the core was 196 cm. Sediments are composed with loams with well-marked light and dark interlayers. In view of the small size of the catchment area and in the absence of permanent watercourses, even before sampling, it was expected to obtain low values of the rates of modern sedimentation in this reservoir.

Gamma-emitted radionuclides (^{210}Pb, ^{226}Ra, ^{232}Th, ^{137}Cs, ^{241}Am) were examined with gamma-spectrometer ORTEC GEM-C5060P4-B with HPGe detector. Bottom sediment samples were ashed (450°C, 8 hours) before plutonium separation and purification. 1 gram of samples was investigated. Complete acid decomposition was carried out. It was achieved by sequentially adding: 1) HF conc.; 2) 3:1 mixture of HF:HNO_3; 3) dry H_3BO_3 mixed with HCl conc.; 4) HNO_3 conc. With the 30% H_2O_2 addition. After each step, the resulting solution was evaporated to wet salts. At final stage, the obtained wet salts were dissolved in 7.5 M HNO_3. To separate plutonium from the bottom sediment, AB-17x8 anionite was used. To stabilize plutonium isotopes in the IV – valence state, crystalline $NaNO_2$ was added to the stock solution. The resulting solution was passed through a preconditioning resin column, then the column was washed sequentially with 7.5 M HNO_3, 9 M HCl, 7.5 M HNO_3 and distilled water. Plutonium isotopes were separated from the anion exchange resin by washing hydrochloric hydroxylamine heated to 40°C. To control the radiochemical yield, 10 µl of ^{236}Pu with (0.2 Bq) was added to the ashed sample. The plutonium coprecipitation with CeF_3 on a Resolve filter (Methods developed by Eichrom Technologies LLC) was used for alfa-spectrometry measurements preparation. The $^{236,238,239+240}$Pu concentration was detected by α-spectrometer of "ORTEC Alfa-Esemble-2" with a vacuum chamber, α- radiation detector (ENS-U900 silicon detector (UL-TRA-AS)) and pulse analyzer. The analysis of the ^{240}Pu/^{239}Pu ratio was carried out using ICP MS.

The depth distribution curve of atmospheric component ^{210}Pb$_{ex}$ (^{210}Pb – ^{226}Ra) in bottom sediments of the Lake Khuko indicates its relatively uniform accumulation due to precipitation from the atmosphere (Figure 1). The measurement error was no more than 8%. The ^{137}Cs dating fully confirmed the results obtained by the ^{210}Pb

dating of Lake Khuko bottom sediments. The maximum ^{137}Cs activity was found in the upper layer (0 – 0.5 cm) (Figure 2). According to the peak position in the upper 0.5 cm, the maximum period of this layer formation can be estimated at 30 years (sampling year: 2016), and the maximum accumulation rate for time window 1986 –2016 is 0.017 cm/year. So it is to conclude that sediment contribution from the lake's catchment area over the past 60 years has been very small due to high density of vegetation cover that protected soil from water erosion. The density of dry sediment varies from 0.57 to 0.75 g/cm^3. These densities are consistent with the idea that Lake Khuko sediments had mainly authigenic origin.

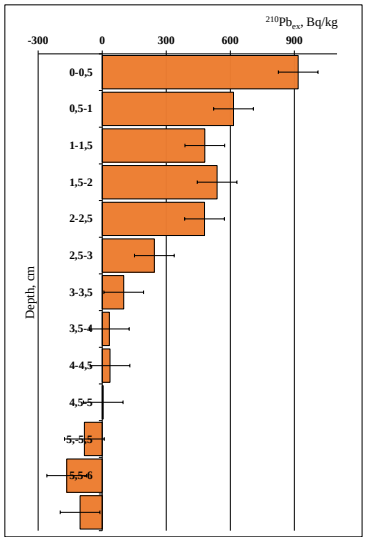

Figure 1. The depth distribution curves ^{210}Pb$_{ex}$ concentrations (Bq/kg) and their standard deviation in for the sediments from the Lake Khuko.

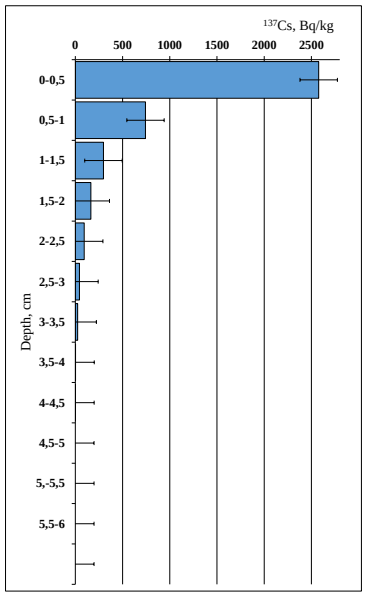

Figure 2. The depth distribution curves ^{137}Cs concentrations (Bq/kg) and their standard deviation in for the sediments from the Lake Khuko.

Based on the obtained data of the Lake Khuko bottom sediments, it can be argued that a significant part of ^{137}Cs was associated with the Chernobyl fallout. High precipitation is typical for the windward northern Caucasus macroslope and its western Black Sea sector especially. High concentrations of ^{137}Cs in Lake Khuko sediment (more than 3 kBq/kg) were very unexpected. This can indicate the presence of radioactive powerful source. Unfortunately, the low rates of sedimentation do not allow any opportunity for stratigraphic interpretation of possible sources of the radionuclides.

However, together with ^{137}Cs, the detectable amount of the technogenic ^{241}Am was identified (Figure 3), which could be the result of nuclear bomb tests or part of the Chernobyl atmospheric deposition. ^{241}Am is ^{241}Pu decay product, and its main source is the 1952 – 1963 nuclear weapons tests (Hirose, 2015). Due to the short half-life of the parent ^{241}Pu (14.7 years), the concentration of ^{241}Am (half-life 433 years) in the environment increases every year.

The ^{241}Am significant amount in the samples indicates the possibility of other plutonium isotopes presence, except ^{241}Pu. A relatively high concentration of the ^{239,240}Pu isotopes total activity was found (Figure 4).

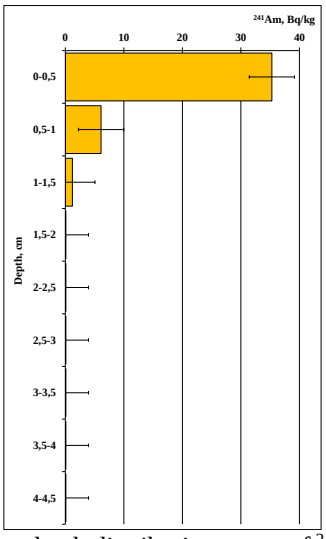

Figure 3. The depth distribution curve of ^{241}Am in the Lake Khuko bottom sediments and standard deviation.

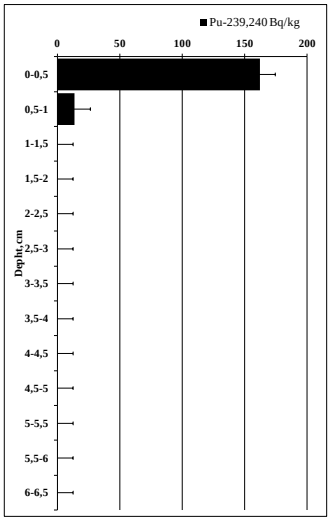

Figure 4. The depth distribution curve of $^{239.240}$Pu in the Lake Khuko bottom sediments and standard deviation.

For the surface layer the specific activity of the ^{239,240}Pu isotopes varied from 162.3 to 191.2 Bq/kg for two series

of samples, while in the layer 0.5-1 cm concentration of ^{239,240}Pu isotopes reduce up to 7.9-13.7 Bq/kg. In order to separate isotopes (239 and 240), the ICP-MS analyze was carried out. The mass spectrometric analysis results confirmed the plutonium isotopes specific activity levels and obtained ^{239}Pu – 85±2 ppt, ^{240}Pu –14±2 ppt. Plutonium isotopes 241 and 238 did not detect. Using various methods, in both cases, the values of ^{238,241}Pu specific activities and concentrations were below the detection limit.

Such high activity of technogenic radionuclides in this region was also recorded in the Adishi glacier cryoconite (Lokas et al., 2018). It should be noted, that the absolute artificial radionuclides activity values in the samples of bottom sediments and cryoconite coincide. Both objects appeared to be very effective storage for technogenic radionuclides. The mechanisms of technogenic radioisotopes accumulation, which may occur during the cryoconites formation, are not relevant to Lake Khuko bottom sediment. The value of natural ^{210}Pb in cryoconites in comparison with Lake Khuko bottom sediments is an order higher because of the high organics content. It can be argued that radionuclides high concentrations the upper layers of the Lake Khuko bottom sediments could not occur because of significant sedimentation rates since this would lead an atmospheric radioactive fallout "dilution" that received from the catchment.

Evaluation of the possible sources of artificial radionuclides in Lake Khuko sediments was performed based on the isotopic ratio analysis. Tropospheric and stratospheric events are distinguished in the works devoted to the determination of the source of radioactive contamination using the isotope ratio method. The so-called "global or bomb-derived fallout" correspond to the stratospheric events (atmospheric nuclear tests), whereas ground-based tests and accidents correspond to tropospheric events. As a result of this study, the isotopic ratios of artificial radionuclides in Lake Khuko were determined (Table 1).

Table 1. Artificial radionuclides isotopic ratios in the Huko lake bottom sediments and other researches (Dahlgaard et al. 2001, Lujaniene, 2009)

Source	^{239,240}Pu/^{137}Cs	^{241}Am/^{239,240}Pu	^{240}Pu/^{239}Pu
Huko	0,050-0,062	0,21-0,28	0,13-0,15
Global fallout	0,008-0,042	0,36-0,42	0,17-0,34
Chernobyl	$2{,}5\times10^{-6}$	0,08-0,19	0,35-0,42

The ^{239,240}Pu/^{137}Cs ratio is set equal to 0.012 in 1962 for global fallout events. This universal ratio is confirmed by numerous soil analyses (Everet, 2008; Sayles, 1992; Wan, 1987). For example, in the vicinity of «Mayak», the ratio of ^{239,240}Pu/^{137}Cs is known to be on average 0.0033 ± 0.002 for the silts of the Techa river, the bottom of the valley of which was subjected to severe local radioactive contamination (Trapeznekov, 1993), i.e. significantly lower than global fallout value. The dependence of this ratio on latitude has also been investigated: for 60-70 ° N, for instance, it equals 0.040 ± 0.005 (Hardy, 1973). The salinity of the reservoir can have a strong effect on the isotope ratio ^{239,240}Pu/^{137}Cs. It is known that the ratio of differs by an order of magnitude in the bottom sediments of fresh and saline water bodies. Values of ^{239,240}Pu/^{137}Cs 0.01-0.05 and 0.1-0.4 for freshwater and seawater respectively were established by Sanschi (1983). This is due to the transition of cesium into a dissolved state in seawater containing a substantial amount of salts (Sanschi, 1983; Livingston, 1979). The ratio ^{239,240}Pu/^{137}Cs could change significantly during the time that passed since the nuclear bomb tests, considering the half-life of ^{137}Cs (30.2 years).

Rarely used ^{241}Am/^{239,240}Pu isotopic ratio is an indirect confirmation of the isotopic input due to the Chernobyl accident (Lujaneine, 2009). The amount of americium in environmental objects is directly related to its parent isotope- ^{241}Pu (half-life is 14.3 years) and is constantly increasing over time. For example, in the vicinity of «Mayak», this ratio varies over very wide limits for different reservoirs because of liquid radioactive chemicals, and the americium content is often much higher than that of ^{239,240}Pu (Kuzmenkova, 2017). It is difficult to realistically assess the source of radioactive fallout according to the isotopic ratios of radionuclides having different chemical properties. Therefore, the ratio of different isotopes of plutonium is considered to serve as the best marker, as it includes only one element. The ^{238}Pu/^{239,240}Pu ratio is considered to range from 0.44 to 0.50 for the Chernobyl fallout (Lujaneine, 2009). It was not possible to reliably determine ^{238}Pu in the bottom sediments of Lake Khuko. The sample activity was below the detection limit of 0.05 Bq/sample, indirectly ruling out the Chernobyl fallout source. The ^{240}Pu/^{239}Pu ratio is most often used to determine the source of plutonium, which may be global or local (Cagno, 2013). The isotope ratio of plutonium entering to the environment during nuclear tests varied greatly depending on the power and type of nuclear bomb which was tested (Hirose, 2015). For an explosion of about 4 kilotons, atomic ratios of 0.0326 and 0.0011 are observed in atmospheric precipitation for plutonium isotopes ^{240}Pu/^{239}Pu and ^{241}Pu/^{239}Pu respectively (Skipperud, 2004).

It can be argued based on the isotopic relationships, that the data on the distribution of artificial radionuclides in Lake Khuko sediments are the result of global stratospheric depositions with the addition of local sources. Similar assumption was previously made based on the study of Caucasus cryoconites (Lokas et al., 2018). It is also obvious that part of the recent ^{137}Cs activity in the bottom sediments of Lake Khuko is associated with the Chernobyl fallout. Lake Khuko, located almost along the path of air mass passage had to be influenced by the Chernobyl accident. It should be noted, that a large amount of precipitation is typical for the subtropical climate of the Black Sea coast of the Caucasus. During the period from the end of April to the end of June 1986 a total amount of 162.6 mm of precipitation was recorded at the Sochi weather station, i.e. 9.7% of the annual average. Lake Khuko is located 43 km to the north from that weather station.

Using the isotopic ratios of technogenic radionuclides in upper layers of the Khuko Lake sediment it was not possible to unambiguously determine the contribution of different sources from atmospheric deposition. However, it is possible to suggest, that the main source of plutonium

and americium in bottom sediments can be considered the cumulative of all atmospheric fallouts that occurred since the beginning of open atmosphere nuclear bomb tests, including global stratospheric depositions, as well as Semipalatinsk, Kapustin Yar and Totsky tests. In order to study in more detail the possible sources of radioactive fallout, it is necessary to isolate uranium isotopes, search for possible "hot" particles in the bottom sediments of Lake Khuko, determine the extent of pollution, and create landscape-geochemical maps for the catchment of the Khuko Lake. In order to determine the forms of constituent artificial radionuclides, it is necessary to conduct a detailed analysis of the physicochemical properties of the sediments of Lake Khuko and to determine the organic matter content. It is also necessary to study the chemical and radionuclide composition of lake water.

It was established that sedimentation rates in the Khuko lake was very low during last 60 years due to insignificant sediment transport from the catchment area. High protection of soil surface by vegetation of catchment slopes is the main reason of very low sediment redistribution rates along the pathways from the slope to the lake.

This work was supported by Russian Science Foundation project RSF №19-17-00181.

Appleby, P., 2008. Three decades of dating recent sediments by fallout radionuclides: a review. *The Holocene* 18(1), 83-93.

Cagno, S., Hellemans, K., Lind, O., Skipperud, L., Janssens, K., Salbu, B., 2014. LA-ICP-MS for Pu source identification at Mayak PA, the Urals, Russia. *Environ. Sci.: Processes Impacts*. 16, 306-312.

Dahlgaard, H., Eriksson, M., Ilus, E., Ryan, T., McMahon, C. A. and Nielsen, S. P. (2001). Plutonium in the marine environment at Thule, NW-Greenland after a nuclear weapons accident. In: A. Kudo (ed.), Plutonium in the Environment. Elsevier Science Ltd, Oxford, UK, pp. 15-30.

Goldberg E.G. Geochronology with Lead-210. In: Radioactive Dating. IAEA. Vienna. 1963. P. 121.

Hardy, E., Krey, P., Volchok, H., 1973. Global inventory and distribution of fallout plutonium. *Nature* 241, 444-445.

Hirose, K., Povinec, P., 2015. Sources of plutonium in the atmosphere and stratosphere-troposhere mixing. *Sci. Rep.* 5 (15707), 1-9.

Kuzmenkova, N.V., Vlasova, I.E., Rozhkova, A.K., Romanchuk, A.Y., Petrov, V.G., Kalmykov, S.N., Osipov, D.I., Pryakhin, E.A., Plyamina, O.V., Grachev, V.A., Mokrov, Y.G., 2017. Distribution of radionuclides between biotic and abiotic components of radioactive contaminated reservoirs V-17 and V-4. *Radiation safety issues* 1, 54-66. (in Russian)

Livingston, H., Bowen, V., 1979. Pu and ^{137}Cs in coastal sediments. *Earth Planet. Sci. Lett.* 43, 29-45.

Łokas, E., Zawierucha, K., Cwanek, A., Szufa, K., Gaca, P., Mietelski, J., Tomankiewicz E., 2018. The sources of high airborne radioactivity in cryoconite holes from the Caucasus (Georgia). *Sci.rep*. 8, 1-10.

Lujaniene G., Aninkevicius V., Lujanas V. Artificial radionucledes in the atmosphere over Lithuania. *J. Envion. Radioactiv.* 2009. V. 100. P. 108-119.

Pennigton, W., Tutin, T., Cambray, R., Fisher, E. 1973. Observations on lake sediments using fallout ^{137}Cs as a tracer. *Nature* 242, 324-326

Santschi, P., Bolhalder, S., Farrenkothen, K., Lueck, A., Zingg, S., Sturm, M., 1988. Chernobyl radionuclides in the environment: tracers for the tight coupling of atmospheric, terrestrial, and aquatic geochemical processes. *Environ. Sci. Thech*. 22, 510-516.

Sayles, F., Livingston, H., Panteleev, G., 1997. The history and source of particulate ^{137}Cs and ^{239,240}Pu deposition in sediments of the Ob River Delta, Siberia. *Sci. Tot. Environ*. 202, 25-41.

Skipperud, L., 2004. Plutonium in the Environment: Sources and Mobility, PhD thesis, Norwegian University of Life Sciences, p. 28.

Trapeznikov, A.V., Pozolotina, V.N., Chebotina, M.Ya, 1993. Radioactive contamination of the Techa River, the Urals. *Health Phys.* 65, 481-488.

Wan, G.J., Santschi, P.H., Sturm, M., Farrenkothen, K., Lueck, A., Werth, E., Schuler, C., 1987. Natural (^{210}Pb, ^{7}Be) and fallout (^{137}Cs, ^{239,240}Pu, ^{90}Sr) radionuclides as geochemical tracers of sedimentation in greifensee, Switzerland. *Chem. Geol*. 63, 181-196.

Radionuclide determination by Accelerator Mass Spectrometry (AMS) in materials from decommissioning of nuclear facilities

J. M. López-Gutiérrez[1,2], E. Chamizo[1], C. Vivo-Vilches[1], J. I. Peruchena[1], C. Vockenhuber[3], M. García-León[1,4]

[1]Centro Nacional de Aceleradores (Universidad de Sevilla, Junta de Andalucía, CSIC), Avda. Thomas Alva Edison, 7, 41092 Sevilla, Spain
[2] Universidad de Sevilla, Departamento de Física Aplicada I, C/ Virgen de África 7, 41011 Seville, Spain
[3] Laboratory of Ion Beam Physics, ETH-Zurich, Otto Stern Weg 5, 8093 Zurich, Switzerland
[4] Universidad de Sevilla, Departamento de Física Atómica, Molecular y Nuclear, Avda. Reina Mercedes s/n, 41012, Sevilla, Spain
Keywords: Long-lived radionuclides, AMS, Decommissioning

Introduction

Disposal of radioactive wastes is a key environmental issue. An adequate classification of them is therefore important in order to provide a better protection of the environment and the public. And this is because the fate of them will depend on their characterization as low-, intermediate- or high-radioactive level wastes.

Decommissioning of nuclear facilities is becoming an important problem for the governments as the installations become obsolete with the time. These processes are known to generate a huge amount of radioactive wastes which have to be classified in order to be properly managed.

The classification of radioactive residues is based on their activity and on the half-life of the radionuclides that they contain. Their characterization determines the final destination of the residues. It is carried out through the measurement of its radioactivity by conventional radiation counting or mass spectrometry techniques. These well-established methods are known to be time consuming and sometimes dangerous for the professionals which have to deal, in many cases, with large sample amounts. Especially when long-lived radionuclides are involved which, on the other hand, play a very important role in the waste management problem. In addition, the conventional radiometric methods usually offer high limits of detection, and most mass spectrometry methods are unable to provide information on the isotopic abundance of the radionuclides of interest, which are essential to guess the origin of the residue and the operation of the nuclear facility. Obviously, new methodologies that overcome these drawbacks are welcome.

The capacity of Accelerator Mass Spectrometry (AMS) to provide more efficient measurements of smaller samples and of being able to measure extremely low isotopic ratios its high precision converts it in an ideal alternative to afford the problem of characterization of radioactive wastes.

In this paper, results are presented on the application of AMS to the determination of several radionuclides of interest in materials from the normal operation of Spanish Nuclear Power Plants (NPP) and the decommissioning of a mothballed Spanish NPP.

This work has been carried out within a long term collaboration project with ENRESA, the company which is responsible of the radioactive waste management in Spain.

Samples and Methods

Different samples taken during the normal operation of some NPP have been analysed. Some of them were resins used for the cleaning of cooling waters and other liquids, sludges obtained from the drying of wet residues in different containers or sinks, evaporator concentrates, etc. Additional analysis were done in materials coming from the decommissioning works of above mentioned mothballed NPP. They were concrete from its bioshield and smears used for surface contamination control of selected places.

The analysed radionuclides were ^{129}I, ^{41}Ca, ^{239}Pu and ^{240}Pu by using the 1 MV tandem AMS system at Centro Nacional de Aceleradores, Spain that has been operative during the last fifteen years. Details on the status of this facility can be found elsewhere (Chamizo et al. 2015), and, currently, radionuclides such as ^{14}C, ^{10}Be, ^{26}Al, ^{41}Ca, ^{129}I, Pu-isotopes, ^{236}U, ^{237}Np and others are measured on a routine basis. A recent upgrade of the system, which includes the use of He as stripping gas instead of Ar, and the substitution of the original ionization chamber by a miniaturized gas detector produced by the Ion Beam Physics group at the ETH (Zürich, Switzerland) have improved its overall performance as can be seen in (Scognamiglio et al. 2016).

Being the samples very different from those normally found in environmental studies, radiochemical methods in use have been adapted accordingly. Also, the concentrations levels are expected to be higher than environmental ones. For that, it is very important to process the samples in separate laboratory areas and with separate instruments, and even to carry out adequate AMS measurement protocols to avoid cross contamination effects

The radiochemical procedures can be found in (Vivo-Vilches 2018; López-Gutiérrez et al. 2013). Broadly speaking, a microwave digestion procedure of the sample and an extraction with $CHCl_3$ is used for the case of ^{129}I. This is back-extracted into $NaHSO_3$ and precipitated as AgI. After that the obtained material is dispersed into Nb to prepare the cathodes for the AMS determination. As for Pu isotopes, the sample is also digested in a microwave oven, then a chromatographic extraction is performed with TEVA® resins. Pu under PuO_2 form is dispersed into a Fe_2O_3 matrix mixed with Nb to prepare the cathodes for measurements. In the case of ^{41}Ca, the sample is digested with aqua regia and then precipitated as $Ca(OH)_2$. After, it is re-dissolved with HNO_3 and $CaCO_3$ precipitated. As explained in (C. Vivo-Vilches 2018) it is very convenient

to measure ^{41}Ca under CaF_2 form. For that the carbonates are re-dissolved with HNO_3 and some few drops of HF that are enough to precipitate the fluoride. This is dispersed into Ag to prepare the cathodes for AMS measurements.

Results and Discussion

In Table 1 results are given on the ^{129}I atom or activity concentration in different samples. All the samples in column one are resins with the exception of R-VD-9-02 and R-VD-9-03 which are dry sludges. The IAEA-375 and Soil samples (Ezerinskis et al. 2016) are environmental soils samples used for comparison. The superscript for each sample means number of replicate analysis in the same sample which gave and average value with a standard deviation that can be seen in the second and third column respectively.

Unfortunately, there are not very much data in current literature to compare those found in our work. Nevertheless, some conclusions can be derived.

Table 1. ^{129}I atom and activity concentrations (at/g or mBq/g respectively) for different samples from normal operation of Spanish NPP. Data taken from J. M. López-Gutiérrez et al. 2013.

Sample	Average ^{129}I concentration (at/g)	Average ^{129}I activity concentration (mBq/g)	Standard deviation
R-AS-07-04[9]	1.50×10^{11}	$2.07x10^{-1}$	54.2%
R-AS-08-01[10]	3.05×10^{10}	$4.21x10^{-2}$	88.2%
VD-10-01[2]	3.13×10^{9}	$4.32x10^{-3}$	51.6%
R-VD-9-01[2]	2.88×10^{10}	$3.97x10^{-2}$	6.7%
R-VD-9-02[2]	1.97×10^{10}	$2.72x10^{-2}$	11.5%
R-VD-9-03[2]	1.30×10^{10}	$1.90x10^{-2}$	11.2%
IAEA-375[3]	1.21×10^{9}	$1.67x10^{-3}$	7.8%
Soils	$\sim 10^{8} – 10^{9}$	$\sim 10^{-7} – 10^{-6}$	

Concentrations are in general higher than in environmental soils, even by two or three order of magnitudes in some cases. The individual uncertainties for each measurement were close to 2%, which is something impossible to reach by conventional techniques (see the activity concentrations). However, the replicate analysis gave clearly different results for each of the subsamples as it can be deduced from the standard deviations given in the third column. These high values clearly demonstrate how heterogeneous they are. Very likely this information can only be given by AMS and helps very much to characterize the type of residue that represent the sample.

In Table 2, a similar table is presented but for ^{239}Pu and ^{240}Pu. As in the previous one, all the samples in column one are resins with the exception of R-TR-08-02 which is a dry sludge. The superscript for each sample means number of replicate analysis in the same sample. In column 2 the summed activity concentration (mBq/g) of ^{239}Pu and ^{240}Pu is given for an easier comparison with data found in current literature. The standard deviation in column 3 corresponds to the average value obtained for the replicate analysis of Pu activity concentrations, while the standard deviation in column five corresponds to that obtained for the average value of the $^{240}Pu/^{239}Pu$ isotopic ratio in the same samples.

Table 2 ^{239}Pu and ^{240}Pu concentrations for different samples from normal operation of Spanish NPP. Data taken from J. M. López-Gutiérrez et al. 2013.

Sample	Average $^{239+240}Pu$ activity (mBq/g)	Standard deviation	Average $^{240}Pu/^{239}Pu$	Standard deviation
R-AS-07-04[4]	35.8	29.4%	0.246	0.4%
R-AS-08-01[5]	8.9	71.3%	0.225	8.4%
VD-10-01[3]	7.9	10.8%	0.281	6.2%
AS-06-03[3]	46.9	48.6%	0.355	1.1%
R-CO-09-05[3]	1235.5	13.1%	0.359	3.5%
R-TR-08-02	7.06	1.4%	0.1059	3.0%

Regarding the concentrations of Pu isotopes, we can make very similar comments to those presented for ^{129}I. Now a general level of less than 1 mBq/g in natural soils serves as a reference to compare the activities obtained for the samples (Salmani-Ghabesi et al., 2018). Again, the heterogeneity of the samples is clear from the dispersion of the data found for the different replicates. Note that very small masses, in the 0.001 – 0.1 range depending on the supplied information, were used for the AMS determinations. Thus, if samples were not homogenous, heterogeneities are likely to be observed. The large standard deviation in column 3 shows it, and this has to be compared to the low uncertainty associated to individual measurements which is no more than 2%.

The $^{240}Pu/^{239}Pu$ ratios measured in the samples are given in column 4 of Table 2. It is well known that this ratio is not accessible by conventional α-spectrometry, although it is with AMS. This is another specific contribution of AMS, besides the speed of analysis and the use of small amounts of samples.

According to the standard deviation of the average values, one can see that the ratios distribution is more homogeneous, although different from one sample to another. The values obtained, from 0.225 to 0.359 in resins and 0.106 for sludge, show expected differences which depend on the composition and irradiation history of the material and the fact that they are coming from different NPP. Of course, those ratios are significantly different from the one corresponding to global fallout in the Northern Hemisphere, with an average value of 0.18 (Kelley et al., 1999).

We have had also the opportunity of analyzing materials obtained during the decommissioning works of the José

Cabrera NPP. This NPP started operating in 1969 and stopped in 2006.

Some 30 wipes samples of surface smears carried out in the different parts of the such NPP were measured for ^{129}I. Needless to say that these determinations are not possible by conventional radiometric methods. Results shown an effective and heterogeneous dispersal of the ^{129}I contamination all along the NPP, with activities ranging from 10^{-2} to 10^{2} μBq. This variability is not strange and in an indirect way we can find it in others similar NPP. Indeed, in Figure 1 we compare the ^{129}I/^{137}Cs activity ratio experimentally obtained by us to calculated ratios in various NPP from France and USA. The data have been extracted from (Wang and Lee, 2006). In all the cases the ranges are wide and similar.

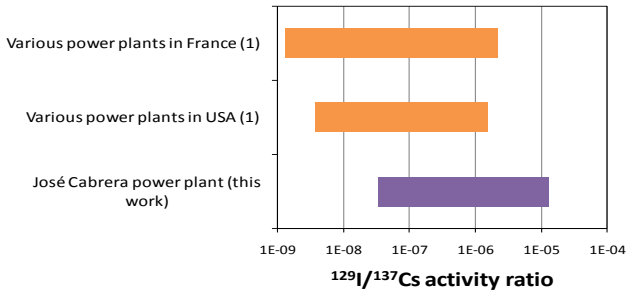

Figure 1. ^{129}I/^{137}Cs activity ratios obtained in the wipe measurements compared to the same ratio calculated in (K. H. Wang and K. J. Lee, 2006) for several NPP from France and USA. The Figure can be found in J. M. López-Gutiérrez et al. 2013.

Finally, ^{41}Ca/^{40}Ca isotope ratios have been measured in the bioshield of the José Cabrera NPP. The ratio cannot be measured at all by radiometric methods and since ^{41}Ca is produced by neutron activation of ^{40}Ca, it gives information on the neutron flux inside the reactor core. This can be done by applying well-known neutron activation equations. It has to be noted that the obtained neutron flux is mainly within the thermal range where the activation cross section is maximun.

A more detailed analysis of these data are in progress. However, as an example some results are presented in Table 3. There, we give ^{41}Ca/^{40}Ca ratios obtained at different depths in a deep concrete core extracted from the bioshield of José Cabrera NPP.

As expected, the ratio decreases with depth, starting from the surface, 0 cm, as the neutron flux decreases with depth due to its attenuation by the concrete.

^{41}Ca/^{40}Ca ranges from 10^{-5}, close to the surface, to 10^{-9} in the deepest layers. In all cases the ratio is higher than those expected from other anthropogenic sources, as in the case of thermonuclear weapon test sites, where ratios of around 10^{-10} have been measured.

The neutron flux for each depth can be obtained directly from the isotopic ratio. It decreases with depth as expected, and in general terms neutron fluences of around 10^{18} can be found. From the well-known exponential attenuation law, it can be calculated the attenuation coefficient for neutrons of the concrete for such an energy range.

Table 3. ^{41}Ca/^{40}Ca as a function of depth (column 1) in the concrete deep profile from the bioshield of the José Cabrera NPP. The thermal neutron fluence is given in column 3 for each depth and the obtained attenuation coefficient is given in column 4. Data from C. Vivo-Vilches, 2018.

Depth (cm)	^{41}Ca/^{40}Ca (x10^{-19})	Thermal neutron fluence (x10^{-15} cm^{-2})	Attenuation coefficient (x10^{-2} cm^{-1})
0	2054 ± 38	5710 ± 580	6.724 ± 0.096
27	289.7 ± 5.5	805 ± 82	
54	51.6 ± 2.1	143 ± 15	
81	7.33 ± 0.27	20.4 ± 2.2	
108	1.425 ± 0.029	3.96 ± 0.40	

Conclusions and perspectives

Several conclusions can be derived from this work. The main one being the fact that AMS is a very powerful tool to for the characterization and classification as wastes of materials coming from normal operation or from decommission of NPP. This due to the different advantages it poses as a very sensitive technique for the determination of radionuclides, especially long-lived ones, in a wide variety of samples. Indeed, AMS saves time in the analysis and avoids the radiation exposure of professionals due to the handling of small amounts of samples. AMS also can determine interesting isotopic ratios, which is almost impossible for conventional radiometric techniques. Furthermore, due to the possibility of measuring low sample masses, AMS can inform on the heterogeneity of samples which, in many cases, is very relevant for waste classification.

In our specific case we have measured ^{129}I, ^{239}Pu, ^{240}Pu and ^{41}Ca in several samples coming from normal operation of NPP or the decommissioning of a Spanish NPP. With the obtained results we are able to characterize the samples and inform on their origin and use of the residues. For this specific case it has been really important the determination of ^{240}Pu/^{239}Pu isotopic ratio in the samples. On the other hand, the measurement of ^{41}Ca/^{40}Ca isotopic ratio can inform on the neutron flux in the reactor core.

Being the results very promising, we have planned further developments for the close future. Beside works on refining the developed methodology for Pu-isotopes (including 239, 240, but also 241 and 242), ^{129}I or ^{41}Ca, new developments are planned for other radionuclides such as ^{233}U ^{236}U, ^{237}Np, ^{243}Am, ^{14}C in liquid wastes as well as the major U isotopes by ICPMS.

This work has been supported by ENRESA and the project FIS2015-69673-P of the Spanish government.

Chamizo, E.,. Santos, F. J, López-Gutiérrez, J. M., Padilla, S., García-León, M., Heinemeier, J., Schnabel, C., Scognamiglio, G. 2015, Satus report of the 1 MV AMS facility at the Centro Nacional de Aceleradores, *Nucl. Instr. Meth. Phys. Res. Sect. B361, 13-19.*

Ezerinskis, Z., Hou, X. L., Dutriekené, R., Puzas, A., Sapolaité, J., Gvozdaité, R., Gudelis, A., Buivydas, S., Remeikis, V. 2016, Distribution and source of ^{129}I, ^{239,240}Pu, ^{137}Cs in the environment of Lithuania, *J. Environ. Radioactiv. 151, 16-173.*

Kelley, J.M., Bond, L.A., Beasley, T.M., 1999 Global distribution of Pu isotopes and ^{237}Np. *Sci. Total Environ.*, 237–238,483-500.

López-Gutiérrez, J. M., Gómez-Guzmán, J.M., Chami-zo, E., Peruchena, J.I., García-León, M. 2013. Long-lived radionuclides in residues from operation and decommissioning of nuclear power plants, *Nucl. Instr. Meth. Phys. Res. Sect. B* 294, 647-651.

Salmani Ghabeshi, S., Chamizo, E., Christl, M., Miró, C., Pinilla-Gila, E., Cereceda-Balice, F. 2018. Presence of ^{236}U and ^{239,240}Pu in soils from Southern Hemisphere, *J. Environ. Radioactiv, 192, 478-484.*

Scognamiglio, G., Chamizo, E., López-Gutiérrez, J. M., Müller, A. M., Padilla, S., Santos, F.-J., López-Lora, M.. Vivo-Vilches, C.. García-León. M. 2016. Recent developments of the 1 MV AMS facility at the Centro Nacional de Aceleradores, *Nucl. Instr. Meth. Phys. Res. Sect. B* 375, 17-25.

Vivo-Vilches, C. 2018. ^{41}Ca measurement with Low Energy Accelerator Mass Spectrometry (LEAMS) at the Centro Nacional de Aceleradores. *PhD Thesis, Universidad de Sevilla*.

Wang, K. H. and Lee, K. J. 2006, Modelling the activity of ^{129}I and ^{137}Cs in the primary coolant and CVCS resin of an operating PWR, *J. Nucl. Mater. 350, 153-162*.

"Promoting technical cooperation among radioanalytical laboratories for the measurement of environmental radioactivity" – an International Atomic Energy Agency (IAEA) Technical Cooperation project RAF/7/017

I. Louw[1], M. Rozmaric[2], S. Haile[3,] I. Osvath[2]

[1]Analytical and Calibration Services, South African Nuclear Energy Corporation, Pretoria, South Africa
[2]Environment Laboratories, Department of Nuclear Sciences and Applications, International Atomic Energy Agency, Monaco, Principality of Monaco
[3]Division for Africa, Technical Cooperation Department, International Atomic Energy Agency, Vienna, Austria
Keywords: IAEA-TC project, Africa, environmental radioactivity
Presenting author e-mail: immanda.louw@necsa.co.za

Background

Monitoring of environmental radioactivity is implemented in several countries across Africa and has become more prominent with an increased awareness of the impact of the naturally occurring radioactive material (NORM) and nuclear related industries on the environment. Mining of different ores, gold, phosphates, petroleum and gas in the region may contribute to enhanced levels of natural radionuclides in the environment. Seventy percent of African countries have direct access to seafood, through which the population might be exposed to contaminants. There is however limited capacity for marine radioactivity monitoring and assessment on the continent.

The International Atomic Energy Agency's Technical Cooperation Department (IAEA-TC) has supported the environmental radioactivity monitoring programs of individual member states (MSs) in Africa through national projects aimed at establishing radio-analytical laboratories.

Some countries have been more advanced than others in utilizing these capabilities. The infrastructure of MSs in the African region varies from very basic (e.g. one gamma-ray spectrometry system used for analysis of foodstuff) to more advanced with well established laboratories having capabilities and infrastructure able to perform a wide spectrum of analysis required for environmental radioactivity monitoring. Measurement of environmental radioactivity remains a challenge in many countries due to many reasons including (i) complicated and time consuming methodology, (ii) expensive instrumentation and a lack of technical support, (iii) expensive and difficult to procure consumables, (iv) lack of highly specialized and specifically trained analysts and (v) legislation is often not in place and often not implemented.

Most developing MSs must be able to comply with national and international requirements for environmental radioactivity monitoring which can be significantly improved by the established cooperation at regional level.

Project objective, outcome and outputs

A regional project (RAF/7/017) was initiated by the African regional group of the ALMERA (Analytical Laboratories for the Measurement of Environmental RadioActivity) network of the IAEA to improve the quality of radioanalytical results produced by respective laboratories in the region. The project facilitates sharing of best practices between laboratories and serves to build a network of expertise among radioanalytical laboratories in Africa.

The project has been running for a period of 5 years from 2016-2020 and is managed by the Project Management Officer in the IAEA-TC department, Technical Officers from the Department of Nuclear Sciences and Applications of the IAEA, National counterparts of member states and the IAEA Programme Management and Project assistants.

The main objective of the project is to develop integrated quality-assured capability for the analysis of radionuclides in environmental samples. The expected outcome of the project is the enhancement of the competency of MSs in the monitoring and assessment of the environmental impact of nuclear- and NORM related industries.

Project outputs include strengthened regional capability in radio-analytical techniques, improved analytical quality of results produced by laboratories, progress toward implementation of a Quality Management System (QMS) for ISO-17025 accreditation, sustained capability to develop technology and continued and sustainable regional cooperation.

Activities and inputs

Project activities include (i) Regional training courses to enhance the radioanalytical capabilities of laboratories, to sustain human capacity and to ensure optimal use of equipment and infrastructure, (ii) Expert missions to advice on specific issues in respective countries and (iii) Participation in proficiency test exercises to ensure quality of produced data. Quality related training events form an important part of the project with the ultimate aim to prepare laboratories for ISO/IEC 17025 accreditation. To date almost 400 participants have participated in 24 events hosted in 14 countries. The events included 2 coordination meetings and 9 regional training courses. Participants in training activities received training in radio-analytical techniques (Table 1) and the quality management system (Table 2).

Support was given for attendance of the 4th African Conference on Quality Managements in Nuclear Industry and Research Laboratories (9-10 March 2017, Ethiopia) and the International Conference on Environmental Radioactivity (8-13 September 2019, Czech Republic). Participants from ALMERA laboratories from the African region participated in events organized by the IAEA-

ALMERA network (three meetings and two training courses).

Table 1. RAF/7/017 Technical training events.

Title	Venue	Date	Participants
Measurement of Naturally Occurring Radionuclides in Environmental and **NORM** Samples by **Gamma Spectrometry**	Karlsruhe, Germany	2016, 26 Nov to 2 Dec	20 from 20 MSs
Determination of Po-210 in environmental samples by **alpha-particle** spectrometry	Rabat, Morocco	2017, 24-28 Apr	34 from 27 MSs
Advanced training on Measurement of Naturally Occurring Radionuclides in Environmental and **NORM Samples by Gamma-ray Spectrometry**	Karlsruhe, Germany	2017, 17-21 July	19 from 19 MSs
Uranium isotopes in environmental samples by **alpha-**particle spectrometry	Pretoria, South Africa	2018, 18 Feb- 2 Mar	36 from 25 MSs
Naturally occurring radionuclides in environmental and **NORM samples by gamma-ray spectrometry**	Karlsruhe, Germany	2018, 16-27 July	24 from 24 MSs

Table 2. RAF/7/017 Quality training events.

Title	Venue	Date	Participants
ISO/IEC 17025 requirements and implementation in radio-analytical laboratories	Windhoek, Namibia	2016 26-30 Sep	27 from 23 MSs
Best Practices in Proficiency Tests for Measurement of Radionuclides in Environmental Samples	Addis Ababa, Ethiopia	2017 6-8 March	27 from 18 MSs
Method validation, Quality Assurance and Quality Control in alpha-particle and gamma-ray spectrometry	Arusha, Tanzania	2017 6-10 Nov	33 from 26 MSs
Uncertainty Estimation in nuclear analytical techniques	Rabat, Morocco	2018 9-13 Apr	27 from xx MSs
Preparation of **QMS documentation** according to ISO-17025 requirements	Mombasa, Kenya	2019 29 Apr-03 May	22 from 18 MSs

Expert missions

Five expert missions were conducted to establish national capabilities for environmental monitoring, to establish a national radio-analytical laboratory, to study the radioactivity baseline, to advice and train staff on QMS documentation for the purpose of accreditation and to assist with implementation of radiochemical separation methods.

Proficiency exercises

Two proficiency exercises were organized specifically for MSs participating in RAF/7/017. These included a proficiency test for determination of Sr-90, Cs-134, Cs-137 and H-3 in seawater, as well as an inter-laboratory study for determination of Po-210 in sediment, mussel and shrimp. Laboratories were also encouraged to participate in IAEA-ALMERA and IAEA-worldwide proficiency exercises.

Achievements, Challenges and Risks

The number of participating MSs has grown by more than 68 % to 32 since inception of the project in 2016, showing the great interest and need in the region. Of the participating member states only 8 laboratories are considered as advanced enough to be part of the ALMERA network.

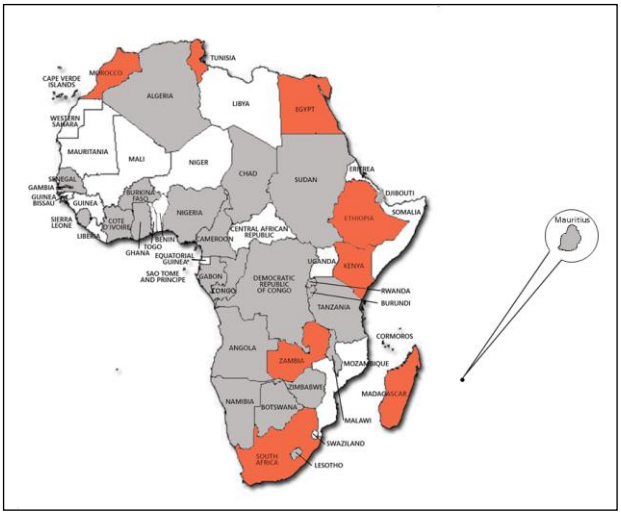

Figure 1. Participating member states.

RAF/7/017 is a well managed project with excellent technical support from the IAEA. The project supports national projects in capacity building. Excellent progress has been achieved in some countries, especially in those with strong government support. Training events have been relevant to enhance radio-analytical capabilities in the region. An increased participation in proficiency tests organized by the IAEA has been observed. There has been progress in Quality Management. Although only a single laboratory in the region is accredited, a good foundation has been given for MSs to be aware of quality principles and to follow good practises in the laboratory. RAF/7/017 serves as an important platform to share knowledge between laboratories in the African region and for support from more advanced to less advanced laboratories in the region. There has been better collaboration between radio-analytical laboratories within and between countries.

Due to the large number of participating MSs a limited number of participants can be trained per event, requiring repetition of specific training. It is expected of participants to share knowledge within their institute and country, which is not always the case. Different levels and subjects of training are required to address the needs of both advanced and just-established laboratories. This put a restraint on available resources. There is a lack of equipment, trained personnel and validated methodologies in some laboratories, which have to be addressed through national or other regional projects.

Future plans

Although is it expected to see some improvement in capabilities of laboratories, many will still not be at an advanced level after completion of the project in 2020. A project design for continuation of the project (Phase 2) in the 2022-2024 cycle is in preparation for submission to the IAEA-TC department for consideration.

This work is supported by the International Atomic Energy Agency.

Follow up the leaching efficiency of uranium series from high-grade granite sample with high concentration of sulfuric acid

A. Nada[1], N. Imam[2*], A. Ghanem[1]

[1] Physics Department, Faculty of Women for Art, Science and Education, Ain Shams University, 11757, Egypt.
[2] National Institute of Oceanography and Fisheries, Cairo, 11516, Egypt
Keywords: Leaching efficiency, Granite sample, Sulfuric acid
Presenting author, e-mail: noha_imam115@hotmail.com

Introduction

Uranium is the most representative actinide element that is of fundamental importance in the nuclear fuel cycle. Uranium is a naturally occurring radionuclide which has three isotopes (^{238}U ($t_{1/2}$=4.5x10^9 yr) 99.72 %, ^{235}U ($t_{1/2}$=7.1x10^8 yr) 0.0055 % and ^{234}U ($t_{1/2}$=2.5x10^5 yr) 0.72 %. It has several oxidation states tetravalent and hexavalent which dominant in the environment. Hexavalent uranium is more dissoluble and mobile than tetravalent uranium. Extraction of uranium is indeed a hydrometallurgical operation in which uranium is directly leached first by suitable acid or alkaline reagents (Kraiz et al., 2016). Acid leaching is more widely used than the alkaline one because of relatively coarse preparatory grinding, comparatively mild reagent concentration, shorter leaching times, applied under an ambient temperature and atmospheric pressure, the highest extraction efficiency, convenient for subsequent recovery processes (Kraiz et al., 2016; Nada et al., 2019). Leaching mining is a new type of deposit mining technology that includes a solid–liquid transfer process transmitting useful elements from the ore to the leaching solution.

The granitic rocks constitute about 60% of the total neoproterozoic outcrops of the Eastern Desert of Egypt. (El Gaby, 1975) classified the granites in Egypt into two groups: (a) synorogenic granitoids, and (b) younger granites, which include the post-orogenic pink and red granites. The younger granites of the Northern Eastern Desert found to be favourable for uranium mineralization and showed significantly higher level of radioactivity (Kraiz et al., 2016). Gabal Gattar area was located at Eastern Desert, the west of Hurghada city at the Red Sea coast. The younger granites of G. Gattar are highly fractured, sheared and subjected to hydrothermal alteration processes. The U-mineralization at this occurrence are mainly related to presence of some uranium minerals such as uraninite, pitchblende, uranophane, beta uranophane, clarkeite, zippeite, soddyite and kosolite as well as some U-bearing accessory and secondary minerals like zircon, sphene, chlorite, fluorite and iron-uraniferous grains (El-Galy et al., 2007). The main objective of the present investigation is studying uranium leaching efficiency of granite sample with high concentration of acid. In this type of study, Laboratory tests are used to evaluate a heap leach process using a batch type of testing methodology. We attempt to follow up the leaching efficiency of uranium isotopes from high-grade granite sample with high concentration of sulfuric acid at different interval time.

Materials and methods

Sample preparation

The red granite sample from Gabal Gattar, the Northern Eastern Desert (2352.8 ppm), was crushed and grinded into 63 mesh and then quartered to obtain representative sample. The mineralogical characterization of the granite sample was done using X-Ray Diffraction (XRD) (Model D8 discover manufacture by USA). The sample is measured by γ-spectrometry, using an HPGe-detector to determine the activity concentrations (Bq) of Uranium isotopes (^{238}U, ^{235}U, and ^{234}U), ^{230}Th and ^{226}Ra series. The conditions of the leaching procedures were 50 g of sample, 98 % (H_2SO_4) acid concentration, 60 min stirring time, 1:3 solid/liquid ratios at room temperature. The leaching procedures performed with two methods to determine the leaching efficiency. After the leaching process, the sample was filtered by using filter paper to get pregnant solution and the second method the sample without filter to get solution named total sample.

Analytical techniques

The leachate (pregnant solution) and total solution were measured by an HPGe detector at interval time for more than four months. The detector has a relative efficiency of about 50 % of the 3″x3″ NaI(Tl) crystal efficiency, connected to multichannel analyzer card (MCA) installed in a PC computer. The software program MAESTRO-32 was used to accumulate and analyze the data. The system was calibrated for energy to display gamma photo peaks between 63 and 3000 keV. The efficiency calibration was performed by using three well-known reference materials obtained from the International Atomic Energy Agency for U, Th and K activity measurements: RGU-1, RGTh-1and RGK-1 (IAEA, 1987). Uranium-238 activity was determined in directly from the gamma rays emitted by its daughter product ^{234m}Pa whose activity was determined from 1001 keV photo peaks (Sutherland and deJong, 1990). The uranium-235 activity was determined directly by its gamma ray peaks; 143.8, 163.4, 185.7, and 205.3 keV (Yucel et al., 1998). The ^{234}U activity was determined from the gamma rays emitted from this nuclide at energies of 53.2 keV and 120.9 keV (Yokoyama et al., 2008). Thorium-230 was determined from the 67.7 keV peak (Simpson, and Grün, 1998). The specific activity of ^{226}Ra was measured using the186.1 keV from its own gamma-ray (after the subtraction of the185.7 keV of ^{235}U). The specific activity of ^{214}Pb was measured using the 241.9, 295.2keVand 351.9 keV while the specific activity of ^{214}Bi was measured using the 609.3keV. The activity concentrations of these radionuclides were measured by using the relation given in equation (1) (Bakr, 2014).

$$A_i = \frac{N_{sY}}{B.R._Y * \varepsilon * t * M} \quad (1)$$

where:

A_i is the activity concentration of radionuclide (i) in Bq kg^{-1},

$B.R_Y$ is the emission probability of the gamma line corresponding to the peak energy (Y) of radionuclide (i),

ε is the spectrometer's efficiency corresponding to the peak energy (Y) at the specific geometry,

N_{sY} is the net count under the peak area of the selected gamma line for the measured sample,

t is the real counting time, and

M is the mass of the sample in kg.

The leaching efficiency of the radionuclides was calculated according to the following equation:

Leaching efficiency (%) = Activity concentration in leachate (Bq) / Activity concentration in the original sample (Bq) (2)

Results and discussion

Chemical analysis of Gabal Gattar granite sample

The mineralogical composition of the granite sample has a good source for the alkali oxides (K_2O + Na_2O) contained in potash feldspar minerals (orthoclase and microcline) and the sodic plagioclase feldspar mineral (albite) as shown in Table 1 and Figure 1. The chemical analysis of granite sample presented the major oxides of the sample Table 2. Oxygen and SiO_2 were the main major oxide of the studied sample and Al_2O_3 was the second major oxide. The studied red younger granite characterized enrichment in alkalis (K_2O+Na_2O) and albite.

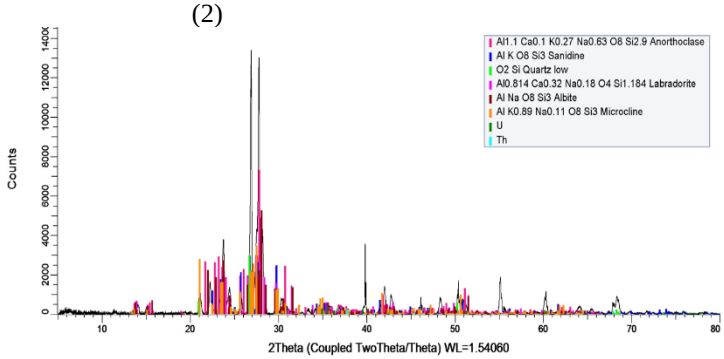

Figure 1. The XRD diffraction pattern of granite sample.

Table 1. The mineralogical characterization of G.Gattar granite sample.

Compound Name	Orthoclase	Albite	Microcline	U		Quartz low	Th
Wt (%)	43.6	29.5	23.6	0.5		2.7	0.1

Table 2. Chemical compositions of G.Gattar granite sample.

Chemical composition	Oxygen	Na_2O	Al_2O_3	SiO_2	K_2O	CaO	UO_2	ThO_2
Wt (%)	47.5	5.2	10.1	31.1	4.7	0.7	0.5	0.1

Radiometric measurement

The activity concentrations of solid, leaching and total sample are shown in Table 3. In solid sample, there was secular equilibrium between ^{238}U and ^{226}Ra and disequilibrium with ^{234}U that has the highest activity concentration. The sample indicated that preferential abundance of ^{234}U relative to ^{238}U may due to prevailing reducing conditions.

In leaching sample, the activity concentration of ^{238}U, ^{230}Th and ^{235}U started increasing from start point into 40 days and after that became slightly constant. On the other hand, ^{234}U has narrow change from start point to end of time; we can say no change with the time. This may due to hexavalent uranium is more mobile at higher acidity, and tetravalent uranium will oxidize and convert into hexavalent uranium. The ^{234}U on the surface of the granite sample was dissolved quickly the leaching solution increased rapidly to its maximum. On the same context, ^{226}Ra series has little changed from start point into 20 days and after that nearly slightly constant. This may due to lower solubility of these radionuclides. From Figure (2, 3), it's obvious that, ^{230}Th has highest activity concentration which may be due to alpha recoil (Shiobara et al., 2017) and the solubility of ^{230}Th increases in acidic aqueous solutions (Abdelouas, 2006).

The ARs of $^{234}U/^{238}U$ were higher than unity little changing from start until end of time as shown in Figure 4. This may be due to preferential release of ^{234}U from damaged lattice sites produced by α-recoil atoms of ^{234}U during the leaching period (Bonotto et al., 2001; Andersen et al., 2009). However, due to different oxidation states, ^{234}U forms more soluble U (VI) complexes and remains in solution, while ^{238}U present in the form of less soluble U (IV) complexes, precipitates (Pekala et al., 2010). The ARs of $^{230}Th/^{238}U$ were higher than unity started closed into unity and increased with the time. This may due to

solubility of ^{230}Th increased with time relative to ^{238}U. Furthermore, The ARs of ^{226}Ra/^{238}U were less than unity; this may due to different of chemical properties which effect on the mobility and solubility of ^{226}Ra. The ARs of ^{238}U/^{235}U were started with 20.47 and at the end of time became 18.08 which indicated increased ^{235}U relative to ^{238}U with time.

Table 3. Activity concentrations (Bq) of different radionuclides in pregnant solution (leaching) and total sample.

Sample	Days	Date	U-238	U-234	U-235	Th-230	Ra-226	Bi-214	Pb-214
Solid (Bq/kg)	-	-	29175.9± 99.6	35873.8±2931.8	1362.8±18.9	24679±1494	29488.49 ±76.5	25694.4 ± 32.3	26872.8 ± 21.9
Solid (50 g)			1458.8±5.4	1793.7±158.5	68.1±1.01	1234±74.7	1474.4±4.1	1284.7±1.7	1343.6±1.2
Leaching	0	10/12/2016	757.84±10.38	1084.01±70.00	37.01±0.64	840.8±53	788.22±3.59	349.01±0.98	369.50±0.66
	4	14/12/2016	780.49±20.51	1231.05±130.22	34.64±0.92	875.16±52.5	698.22±4.26	360.50±1.42	372.81±0.94
	11	21/12/2016	855.72±16.79	1190.77±176.41	39.77±0.96	979.14±58.7	736.21±5.15	542.40±1.67	539.95±1.11
	18	28/12/2016	832.13±3.98	1295.44±156.63	35.96±0.97	948±56.9	618.57±3.98	526.96±1.58	512.11±1.05
	23	2/1/2017	945.15±20.38	1117.04±143.40	42.51±0.83	1024.1±61.44	737.38±4.37	555.46±1.56	549.09±1.02
	32	11/1/2017	976.39±20.38	969.90±185.58	43.75±1.06	1093.72±65.6	720.43±5.52	564.53±1.90	555.92±1.21
	39	18/1/2017	1005.19±21.76	1211.83±202.91	52.58±1.36	1215.88±73	669.46±5.92	566.66±1.87	564.29±1.26
	45	24/1/2017	1007.40±27.44	1347.79±117.67	53.01±0.88	1204±72.2	732.71±4.96	583.06±1.58	578.88±1.07
	54	2/2/2017	1024.98±16.45	1234.06±117.54	53.01±0.94	1149.72±69	740.90±5.19	598.48±1.68	584.66±1.10
	61	9/2/2017	1045.73±21.28	1148.47±125.92	53.98±1.02	1192.24±71.5	753.70±4.84	587.83±1.75	582.3±1.15
	66	14/2/2017	1039.27±20.26	1138.30±142.67	54.03±1.22	1219.02±73.1	771.55±5.34	588.05±1.88	585.58±1.29
	73	21/2/2017	1037.94±22.65	1131.72±116.30	51.15±1.12	1269.28±76.2	785.74±5.53	596.84±1.69	593.23±1.12
	79	27/2/2017	1029.50±51.95	1220.29±286.36	54.20±3.56	1224.28±73.5	695.35±14.49	543.742±4.52	539.94±2.99
	87	8/3/2017	1042.49±17.05	1197.05±153.41	51.09±1.01	1222.2±73.3	804.26±4.68	553.86±1.55	546.51±1.04
	92	14/3/2017	1021.74±26.67	1141.50±134.96	46.61±0.90	1186.46±71.2	694.86±4.28	499.93±1.54	495.42±1.02
	99	20/3/2017	1031.66±25.33	1197.57±210.61	51.72±1.52	1332.66±80	732.36±6.24	535.36±2.36	535.02±1.57
	107	28/3/2017	1032.98±20.23	1243.28±197.64	54.92±1.18	1362.26±81.7	752.08±4.74	550.12±1.82	540.46±1.14
	115	5/4/2017	1043.42±18.02	1295.97±188.96	51.00±1.11	1336.56±80.2	810.32±5.33	534.59±1.80	518.57±1.21
	121	11/4/2017	1039.61±17.21	1226.65±143.17	57.49±0.84	1466.26±88	738.46±4.23	540.29±1.64	534.96±1.08
Total	0	12/10/2016	1298.69±22.59	1058.63±112.33	52.17±1.05	1289.67±77.4	1419.64±5.05	954.02±1.65	1015.50±1.09
	4	12/14/2016	1280.77±29.25	1177.51±122.21	49.33±0.87	1445.86±86.8	1241.13±4.96	1072.88±1.63	1080.88±1.09
	10	12/20/2016	1269.84±29.86	1239.13±245.14	49.38±1.83	1191.67±71.5	1232.68±8.39	1069.24±2.70	1085.17±1.85
	21	12/31/2016	1258.68±17.08	1208.16±109.45	48.65±0.98	1393.68±83.6	1252.24±5.39	1054.87±1.67	1073.38±1.14
	24	1/3/2017	1229.20±19.87	1349.64±178.17	49.49±1.13	1388.63±83.3	1274.85±6.14	1063.76±2.14	1073.46±1.42
	43	1/22/2017	1191.62±19.77	1156.30±177.31	48.57±1.29	1302.15±78.1	1174.45±6.95	1026.29±2.32	1027.11±1.52
	60	2/8/2017	1102.46±22.22	956.17±213.25	43.69±1.43	1126.37±67.6	1253.44±6.28	1054.96±2.23	1053.26±1.48
	65	2/13/2017	1103.48±21.97	1111.27±196.5	45.90±1.44	1357.45±81.4	1258.36±6.74	1035.85±2.21	1038.93±1.50
	75	2/23/2017	1127.63±20.68	1030.39±200.80	46.94±1.35	1309.38±78.6	1131.51±5.62	1006.02±2.31	994.84±1.56
	89	3/9/2017	1174.95±22.50	791.77±223.91	49.91±1.35	1640.31±98.4	1215.17±6.08	1006.72±2.27	1005.06±1.53
	115	4/3/2017	1180.10±19.97	964.10±240.28	46.94±1.30	1236.91±74.2	1128.29±5.92	928.95±2.21	922.74±1.47
	125	4/13/2017	1181.89±22.75	1000.25±201.83	49.26±1.58	1163.23±69.8	1247.29±7.46	998.66±2.28	993.69±1.55
	144	5/2/2017	1218.34±17.06	858.77±173.34	51.00±0.88	1769.50±106.2	1181.89±4.06	896.91±1.57	892.83±1.03

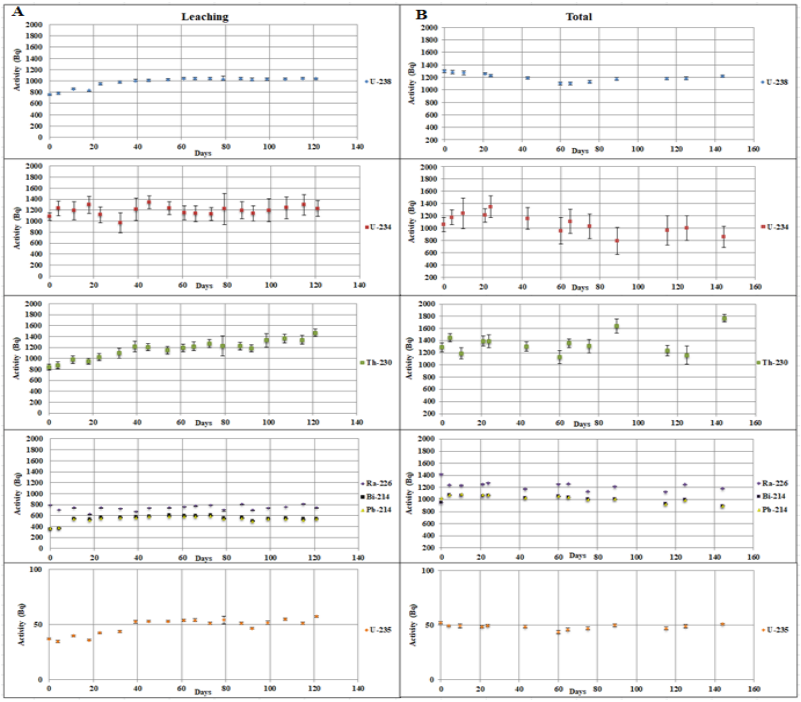

Figure 2. Activity concentrations of different radionuclides at interval time (A) pregnant solution (Leaching) and (B) total solution.

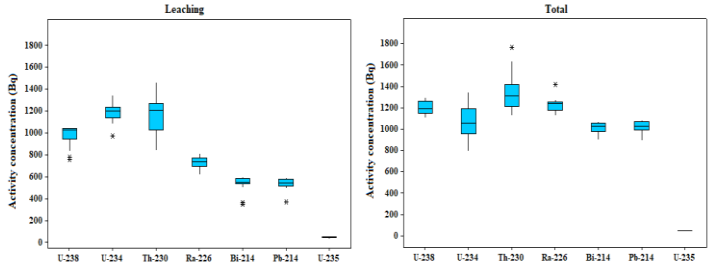

Figure 3. Box plot for activity concentrations of different radionuclides.

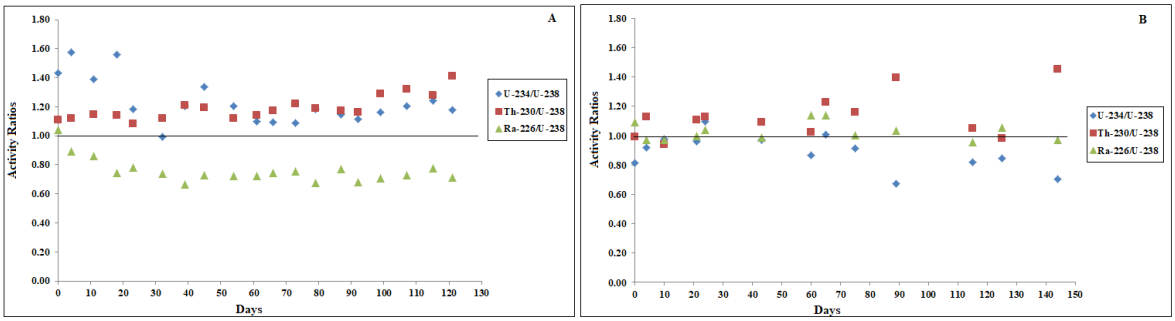

Figure 4. The Activity ratios of different radionuclides (A) leaching and (B) total.

The leaching efficiency (%) of the ^{238}U and ^{235}U series radionuclides at different interval time was demonstrated in Table 4 and Figure 5. The analysis of experiments showed that leaching efficiency decreased in order ^{230}Th > ^{235}U > ^{234}U > ^{238}U > ^{226}Ra > ^{214}B > ^{214}Pb. The leaching efficiency of ^{230}Th was the highest than that of other radionuclides, which may be due to alpha recoil and the solubility of ^{230}Th increases in high acidic solution. Also, uranium in liquid phase may be enriched by ^{235}U isotope relative to ^{238}U of the solid phase due to (1) the difference in energies of these nuclides bonds in crystal lattice of solid phase (Bondarenko and Sobotovich, 1998). (2) This is may be due to different mobility of ^{235}U and ^{238}U isotopes in leaching phase. ^{226}Ra, ^{214}Bi and ^{214}Pb were lower leachability than their parent ^{238}U, because these radionuclides have lower mobility in oxidizing conditions and combined with sulfate to form radium, bismuth and lead sulfate ($RaSO_4$, $BiSO_4$, and $PbSO_4$, respectively).

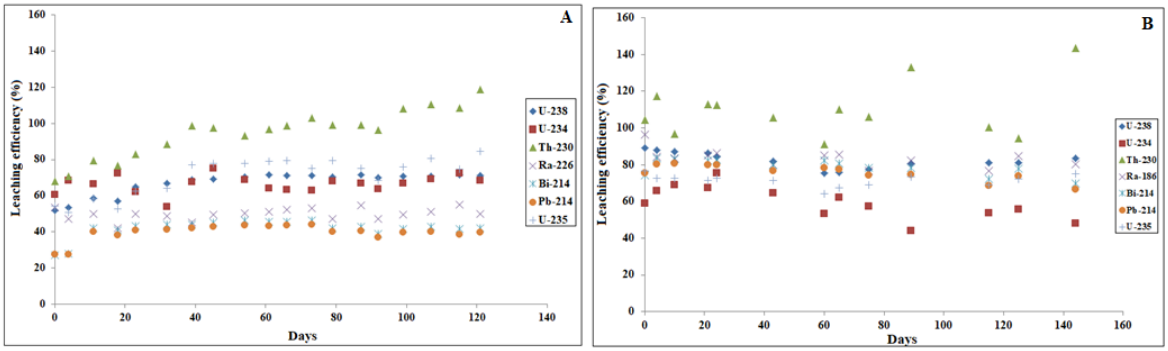

Figure 5. Leaching efficiency of different radionuclides in (A) leaching and (B) total.

Table 4. Leaching efficiency of different radionuclides at interval time.

	Days	U-238	U-234	U-235	Th-230	Ra-226	Bi-214	Pb-214
Leaching	0	51.95	60.43	54.32	68.14	53.46	27.17	27.50
	4	53.50	68.63	50.83	70.92	47.36	28.06	27.75
	11	58.66	66.39	58.36	79.35	49.93	42.22	40.19
	18	57.04	72.22	52.77	76.82	41.95	41.02	38.11
	23	64.79	62.28	62.39	82.99	50.01	43.24	40.87
	32	66.93	54.07	64.20	88.63	48.86	43.94	41.37
	39	68.90	67.56	77.17	98.53	45.41	44.11	42.00
	45	69.05	75.14	77.79	97.57	49.69	45.38	43.08
	54	70.26	68.80	77.80	93.17	50.25	46.58	43.51
	61	71.68	64.03	79.21	96.62	51.12	45.76	43.34
	66	71.24	63.46	79.29	98.79	52.33	45.77	43.58
	73	71.15	63.09	75.07	102.86	53.29	46.46	44.15
	79	70.57	68.03	79.54	99.21	47.16	42.32	40.18
	87	71.46	66.74	74.98	99.04	54.55	43.11	40.67
	92	70.04	63.64	68.40	96.15	47.13	38.91	36.87
	99	70.72	66.77	75.90	108.00	49.67	41.67	39.82
	107	70.81	69.31	80.60	110.39	51.01	42.82	40.22
	115	71.52	72.25	74.85	108.31	54.96	41.61	38.59
	121	71.26	68.39	84.37	118.82	50.09	42.06	39.81
Total	0	89.02	59.02	76.56	104.51	96.28	74.26	75.58
	4	87.79	65.65	72.40	117.17	84.18	83.51	80.44
	10	87.04	69.08	72.47	96.57	83.60	83.23	80.76
	21	86.28	67.36	71.40	112.94	84.93	82.11	79.89
	24	84.26	75.24	72.64	112.53	86.46	82.80	79.89
	43	81.68	64.47	71.28	105.52	79.66	79.88	76.44
	60	75.57	53.31	64.12	91.28	85.01	82.12	78.39
	65	75.64	61.95	67.37	110.00	85.35	80.63	77.32
	75	77.30	57.45	68.89	106.11	76.74	78.31	74.04
	89	80.54	44.14	73.25	132.93	82.42	78.36	74.80
	115	80.89	53.75	68.89	100.24	76.52	72.31	68.67
	125	81.02	55.76	72.29	94.26	84.60	77.73	73.95
	144	83.51	47.88	74.85	143.40	80.16	69.81	66.45

In Total sample, the activity concentration (Bq) of ^{238}U and ^{235}U series radionuclides in the sample was shown in Table 3 Figure 2. Total sample is the pregnant solution and the residual together without filtration. The activity concentration decreased in the following order of ^{230}Th > ^{238}U > ^{226}Ra >^{234}U > ^{214}Pb > ^{214}Bi, as shown in Figure 3. It's obvious that the activity concentration of ^{235}U was slightly changed from start into the end of time. Also, it is clear that ^{226}Ra, ^{214}Pb and ^{214}Bi were much closed into the activity concentration of ^{238}U, ^{234}U and ^{230}Th. This may due to these radionuclides were higher in the residual phase that made increasing in the total sample. The ARs of $^{234}U/^{238}U$, $^{230}Th/^{238}U$ and $^{226}Ra/^{238}U$ closed to unity from started into 60 days and dispersion far away from unity. On the other hand, the ARs of $^{238}U/^{235}U$ were nearly constant from started into the end of time which indicated ^{235}U and ^{238}U nearly slightly constant with time.

The leaching efficiency of different radionuclides was shown in Table 5 and Figure 5. It's obvious that the highest leaching efficiency was ^{230}Th radionuclide similar to leaching sample and the lowest leaching efficiency was ^{234}U radionuclide. Also, the leaching efficiency of ^{226}Ra-series closed into ^{238}U radionuclide; this is unexpected behavior. This is may be due to existence solution with solid sample for certain of time that may effect of the solubility of ^{226}Ra. Also, it can be estimated that ^{226}Ra, alpha-recoil atom like ^{234}U, migrated into deep part by alpha-recoil. As a result, alpha-recoil radium in the depths of ore grains was leached out, in strong acid condition (Morimoto, et al., 2003).Otherwise; ^{235}U leaching efficiency is more than at leaching sample but also there is no change from start into the end.

Conclusions

Feldspars (both of albite and k-feldspars represented by orthoclase and microcline) and quartz and U, Th represented the main constituents of the granite sample.

In leaching sample, the activity concentrations of ^{238}U, ^{234}U and ^{230}Th were effected with time interval until 40 days. Otherwise, the activity concentrations of ^{226}Ra series and ^{235}U not effected with time.

In total sample, the activity concentrations of ^{238}U, ^{226}Ra series and ^{235}U were not change with time nearly constant. But the activity concentration of ^{234}U and ^{230}Th change with time.

There is disequilibrium between ^{238}U and ^{226}Ra in pregnant solution but slightly equilibrium in the total sample.

There is a different fractionation in the activity concentrations of radionuclides for two samples where the highest leaching efficiency was ^{230}Th in the two samples. The leaching efficiency of uranium-series changed with time until 40 days in pregnant solution but in the total sample there is no change observed with time.

Uranium in liquid phase may be enriched by ^{235}U isotope relative to ^{238}U.

Abdelouas, A., 2006. Uranium Mill Tailings : and Environmental Impact. *Elements* 2(6), 335–342.

Andersen, M.B., Erel, Y., Bourdon, B., 2009. Experimental evidence for ^{234}U–^{238}U fractionation during granite weathering with implications for $^{234}U/^{238}U$in natural waters. *Geochim. Cosmochim. Acta* 73, 4124–4141.

Bakr, W. F., 2014. Analytical Method Validation of Gamma Spectrometric Procedure for the Determination of γ -Emitters in Environmental Samples. *Arab J. Nucl. Sci. Appl.* 47 (3), 130-138.

Bondarenko, G.N., and Sobotovich, E.V., 1998. Isotope fractionation of uranium in the process of leaching of nuclides of dispersed fuel of RBMK of the Chernobyl NPP (KURRI-KR--21). Imanaka, T. (Ed.). Japan.

Bonotto, D.M., Andrews, J.N., Darbyshire, D.P.F., 2001. A laboratory study of the transfer of ^{234}U and 238U during water-rock interactions in the Carnmenellis granite (Cornwall, England) and implications for the interpretation of field data. *Appl. Radiat. Isot.* 54, 977–994.

El-Gaby, S., 1975. Petrochemistry and geochemistry of some granites from Egypt. *N. Jb. Miner. Abh.* 124, 147-189, Stauttgart.

El Galy, M.M., El Feky, M.G., Roz, M.E., & Nada, A. 2007. Disequilibrium in U-Series at G-II Occurrence of Uranium Mineralization at Gabal Gattar Area, North Eastern Desert, Egypt; A Comparative Study using HP Ge and Nal-Detectors. *A. J. and Appl, S.* 40(1), 15-26.

IAEA, International Atomic Energy Agency, 1987. Preparation and Certification of IAEA Gamma Spectrometry Reference Materials, RGU-1, RGTh-1 and RGK-1. International Atomic Energy Agency. Report-IAEA/RL/148.

Kraiz, A. H., Fathy, W. M., Abu, H. A., Ramadan, A. M., & Moharam, M. R. 2016. Leachability of uranium from low grade uraniferous Granites, Eastern Desert, Egypt. *Int. Research. J. Eng. Technol.* 3(1), 775–782.

Morimoto, T., Banba, S., Ishikawa, K., Shinoda, Y., Hashimoto, T., 2003, Alpha-recoil nuclides in acid leaching experiments on radioactive ores, *Radioisotopes* 52(6), 269-276.

Pekala, M., Kramers, J.D., and Waber, H.N., 2010.$^{234}U/^{238}U$ Activity Ratio Disequilibrium Technique for Studying Uranium Mobility in the Opalinus Clay at Mont Terri, Switzerland. *Appl. Radiat. Isot.* 68:984–992.

Shiobara, R., Komatsubara, K., Kurihara, Y., Nomura, K., & Koike, Y. 2017. Radioactive characteristics and leaching behavior of Ra and Th isotopes on ishikawaite. *J. Radioanal. Nucl. Chem.* 313(2), 361–370.

Simpson, J. J., & Grün, R., 1998. Non-destructive gamma spectrometric U-series dating. *Quat. Geochronol.* 17(11), 1009–1022.

Sutherland, R.A., and DeJong, E., 1990. Statistical analysis of gamma-emitting radionuclide concentrations for three fields in Southern Saskatchewan, Canada. *Health Phys.* 58 (4), 417–428.

Simulation of ^{3}H concentration in coastal waters discharged from the spent nuclear fuel reprocessing plant in Rokkasho, Japan: Effects of input forcing data on simulation results

Kazuhiro Oshima[1*], Koichi Abe[1], Shinji Ueda[1], Shun'ichi Hisamatsu[1]

[1]Department of Radioecology, Institute for Environmental Sciences, Rokkasho, 039-3212, Japan
Keywords: ^{3}H, Coastal waters, Model simulation, Input forcing data
Presenting author, e-mail: oshima@ies.or.jp

Introduction

For an evaluation of radionuclides discharged from the first Japanese commercial nuclear fuel reprocessing plant in Rokkasho, we have developed an advanced environmental transfer and dose assessment model for the radionuclides in atmospheric, terrestrial, and aquatic environments around the plant (AdvETDAM; Hisamatsu et al. 2007, Ueda et al. 2006 & 2012). Hydrosphere components of the AdvETDAM consist of aquatic transfer models for the nearby brackish lakes of Obuchi and Takahoko, their catchments, and the coastal waters of Rokkasho. During the final test operation of the plant using actual spent fuel from 2006, a controlled amount of ^{3}H has been discharged into the atmosphere and the coastal waters from its main exhaust stack and marine discharge point (Figure 1).

Offshore currents on the Pacific side of the Shimokita Peninsula show clear seasonal changes. Associated with the Tsugaru Warm Current, intense southward flow along the coastline dominates during the winter and spring, whereas anticyclonic gyre flow dominates during the summer and fall (Conlon, 1982). Such seasonal changes in offshore currents affect the coastal current field and the advection-diffusion of radionuclides in coastal waters. In addition, our preliminary observations suggested that variations of the coastal current on timescales of a few days were affected by winds. Therefore, the wind forcing data is also important for simulating the coastal current field and radionuclide transfer in the Rokkasho coastal waters.

To improve the reproducibility of the simulation of ^{3}H transfer in Rokkasho coastal waters, we examined several types of lateral boundary conditions for offshore and wind forcing data over the study area, which are major input data for the coastal marine model.

Methods and Data

The coastal marine model simulates ocean current field and ^{3}H concentration in Rokkasho coastal waters, including the simplified calculation in Lake Obuchi, which is the brackish lake adjacent to the plant. The model solves three-dimensional ocean dynamics, including with tidal and wave effects, and the advection-diffusion equation for the radionuclides. The double-nesting of three simulation domains, with spatial resolutions of 1350 m, 450 m, and 150 m, are applied (Figure 1). The output interval of the model simulation is 1 hourly. There are five input data used in the model: the offshore boundary conditions (ocean current, water temperature, salinity, and sea surface height); meteorological data (air temperature, wind speed/direction, relative humidity, cloud amount and solar radiation); and observation data

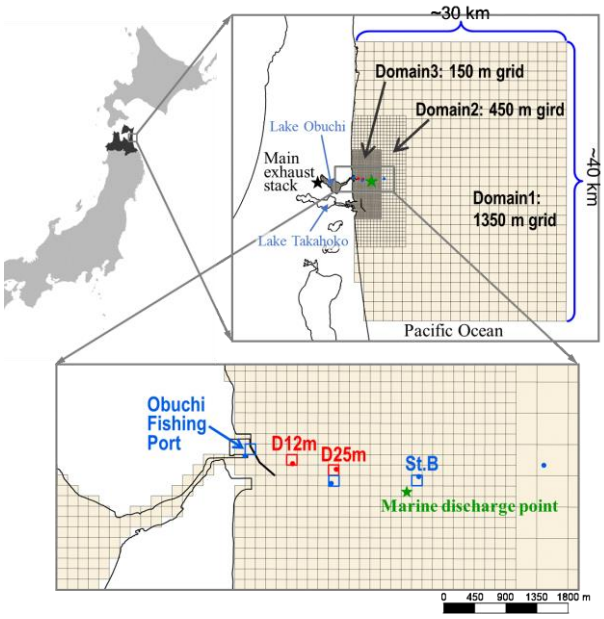

Figure 1. Simulation domain of the coastal marine model for Rokkasho coastal waters. Green and black stars denote the marine discharge point and main exhaust stack, respectively. In the bottom map, colored dots and squares represent observation site and evaluation grid, respectively. Red and blue markers are comparison sites/grids for the coastal current and ^{3}H concentration.

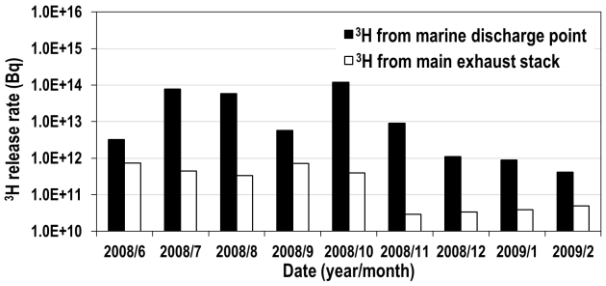

Figure 2. Time-series of ^{3}H release rates from the marine discharge point into the coastal waters (black bars) and from the main exhaust stack into the atmosphere (white bars) during June 2008 to February 2009 (JNFL 2019).

of ocean waves, the tide, and freshwater input from rivers. Details of offshore boundary conditions and wind forcing datasets are shown in Table 1. Figure 2 shows the monthly release rates of ^{3}H from the marine discharge point and the main exhaust stack (JNFL 2019). While those are monthly time-series, we used hourly oceanic release rates taking the delay between the measurement of ^{3}H

concentration at the plant and the release from the discharge point into account. The background ^{3}H concentration in all runs was set to 0.1 Bq L^{-1} based on our previous observations (Ueda et al., 2011). The coastal model simulation also includes ^{3}H discharged from land area through the river flowing into Lake Obuchi, but does not include the atmospheric deposition of ^{3}H over the coastal study area.

We carried out four runs of simulations using different input forcing data (Table 2). The first run used inputs of offshore boundary conditions data from the Japan Marine Science Foundation's (JMSF) model (In et al., 2007), and wind data from the Japan Meteorological Agency (JMA) weather station at Hachinohe, which is approximately 50 km south from the marine discharge point. This run is referred to as the JMSF run. The JMSF's model simulates three-dimensional ocean dynamics in the Rokkasho offshore area with 1.5 km spatial resolution, which is nested from ocean general circulation model covering the western North Pacific (In et al., 2007).

The second run, FORA, used ocean reanalysis data from FORA-WNP30 (Usui et al., 2017) as the offshore boundary conditions. While the JMSF's model simulation has finer spatiotemporal resolution than that of FORA data (Table 1), the FORA tended to have higher reproducibility of the offshore current field, like the anticyclonic gyre flow in the summer and fall. It is expected that such a different reproducibility of offshore current further affects the coastal current field simulated by our coastal marine model. In the model simulation, the FORA data were bilinearly interpolated from 5 km to 1.5 km in space and linearly interpolated from daily to 3 hourly in time. We compared the simulated results between those runs to examine the effect of offshore boundary conditions (Table 2).

The third and fourth runs adopted wind forcing data from meteorological operational analysis data of the JMA Mesoscale Model (MSM), and from regional meteorological reanalysis data of DSJRA-55 (Kayaba et al., 2016), respectively. These runs are referred to as the MSM and DSJRA-55 runs, and both simulations applied the same offshore boundary conditions as the JMSF run. These runs used grid point values of wind data from each of the MSM and DSJRA-55 datasets at 40.95°N and 141.5°E, located about 10 km off the Rokkasho coast within the simulation domain. Since the model calculation uses hourly wind data, the MSM was linearly interpolated from 3 hourly to 1 hourly. We compared the simulated results among the JMSF, MSM and DSJRA-55 runs to examine the effect of wind forcing data.

For the validation of runs, the simulated ocean currents were compared to the observed data from the ADCP (Acoustic Doppler Current Profiler) from June 2008 to February 2009 at the D25m and D12m sites shown in Figure 1. During the same period, seawater samples were collected nine times at the Obuchi Fishing Port at the mouth of the brackish lake Obuchi and twice at St. B site near the marine discharge point (Figure 1). Concentrations of ^{3}H in the seawater samples collected at 5 m depth were measured (Ueda et al., 2011) and compared to the simulated results at the 3-5 m depth layer of corresponding grids.

Table 1. Offshore boundary conditions and wind forcing data used in this study.

Input data	Dataset	Variables	Temporal & Spatial resolutions	Data available period
Offshore boundary condition	JMSF's model simulation	current, water temperature, salinity, sea surface height	3 hourly, 1.5km	2007/9 - 2009/3
	FORA, ocean reanalysis data	current, water temperature, salinity, sea surface height	daily, 10 km	1982/1 - 2014/12
Wind speed & direction	Hachinohe (JMA's observation)	wind speed & direction	1 hourly, (40.53N, 141.52E)	2007/3 - present
	MSM, meteorological operational analysis data	eastward & northward winds	3 hourly, 5 km	2006/3 - present
	DSJRA-55, regional meteorological reanalysis data	eastward & northward winds	1 hourly, 5 km	1958/1 - 2012/12

Table 2. Four types of the coastal marine model simulations.

Run	Offshore boundary condition	Wind speed & direction	Other input data
JMSF run	JMSF's simulation	Hachinohe	Meteorological data except for wind, ocean wave, tide & freshwater inflow: These input data were based on the observations and the same in all runs.
FORA run	FORA	Hachinohe	
MSM run	JMSF's simulation	MSM	
DSJRA-55 run	JMSF's simulation	DSJRA-55	

Results

At first, we compared the simulated currents with the observed ones on the Rokkasho coast. Figure 3 shows the time-series of coastal current speeds at the D25m site from June 1, 2008 to February 28, 2009. To compare the temporal changes over a few days, the current speeds of raw 1 hourly data were smoothed with a 73-hour (~3 day) running average. The observed coastal currents were dominated by the tidal flow and had current speeds in a range of 1.3 - 76.4 cm s^{-1} and 10.8 - 36.8 cm s^{-1} in the raw and smoothed data (black line in Figure 3), respectively. The simulated coastal current speeds on timescales of a few days were partially reproduced in all runs and could be reproduced at the order level throughout the entire calculation period.

The simulated current speeds of the FORA run overall tend to be underestimated compared to the other runs and the observation (Figure 3a). On the other hand, the simulated results of the JMSF, MSM and DSJRA-55 runs nearly match the observations during late June to mid-July and November (Figure 3b). However, all three runs underestimated the current speeds during late July to October 2008 and overestimated them after late December 2008. There were some large differences between the simulated and observed current speeds in January and February 2009, especially by the MSM and DSJRA-55 runs. Those large overestimations seem to be affected by cyclone activity and intense northwesterly wind related to the typical winter weather pattern. At the D12m site, the simulated coastal currents in all runs were almost like the above results at the D25m site (not shown).

Next, we compared the simulated ^{3}H concentrations in seawater with the observations. Figure 4 shows the time-series of ^{3}H concentrations at Obuchi Fishing Port from June 1, 2008 to February 28, 2009. Although the simulated ^{3}H concentrations by the JMSF run well reproduced before August and after November, there were some differences between these months (Figure 4a). The FORA run simulated the overall observed ^{3}H concentrations well, except in July (Figure 4a). In the FORA run, the current speeds were slightly smaller than in the JMSF run in July and early August (Figure 3a), inducing a weaker effect of advection-diffusion and higher ^{3}H concentrations (Figure 4a). Vice versa, the slightly larger current speeds in the FORA run in early September (Figure 3a) caused the lower simulated ^{3}H concentration than in the JMSF run (Figure 4a). During October to December 2008, the overall simulated ^{3}H concentrations by the MSM and DSJRA-55 runs were lower than those of the JMSF run, and reproduced the observations well (Figure 4b). The simulated current speeds by the MSM and DSJRA-55 runs during that period were slightly larger than those of the JMSF run (Figure 3b), thus inducing lower ^{3}H concentrations (Figure 4b).

There were only two observations at the St. B site with very low ^{3}H concentrations (~0.1 Bq L^{-1}) in June and September (data are not shown). The simulated results fitted to the observations in all the runs in June, but were overestimated in September in the JMSF, MSM and DSJRA-55 runs. In contrast, the FORA run simulated the low ^{3}H concentrations well in September, showing the effect of simulated current speeds.

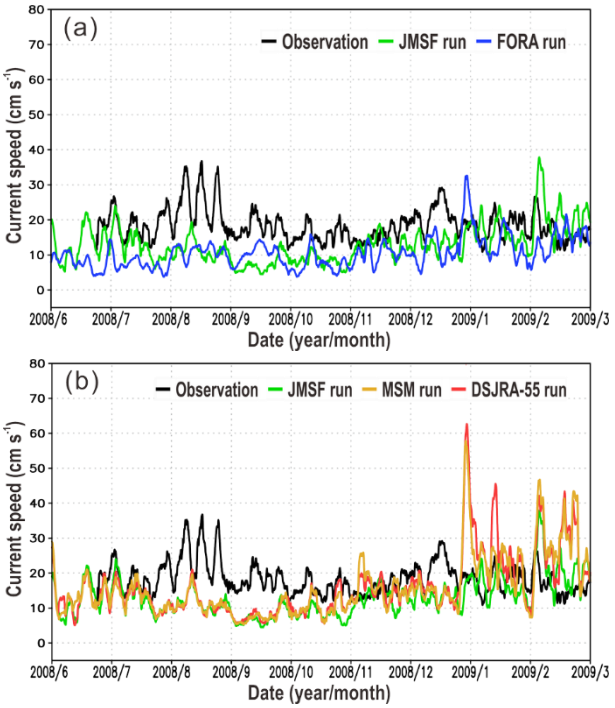

Figure 3. Time-series of simulated and observed current speeds at the D25m site. (a) Comparison in the offshore boundary conditions: observation (black line), JMSF run (green line), and FORA run (blue line). (b) Comparison of the wind forcing data: observation (black line), JMSF run (green line), MSM run (orange line), and DSJRA-55 run (red line). All data were smoothed with a 73-hour running average.

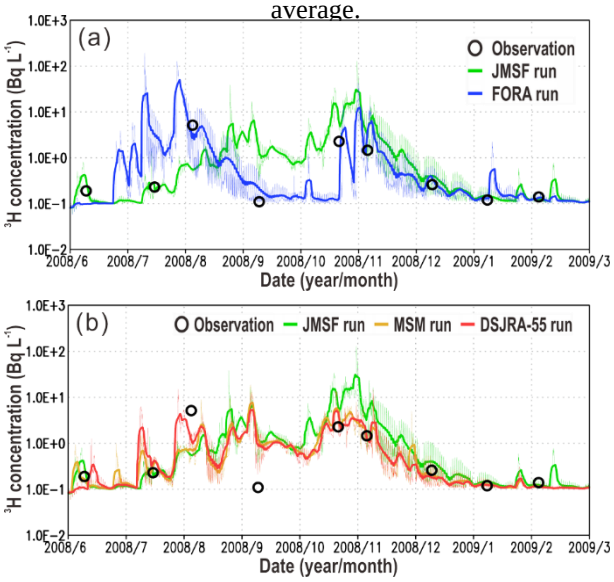

Figure 4. Same as Figure 3, but for the simulated and observed ^{3}H concentrations at Obuchi Fishing Port. (a) Comparison of the offshore boundary conditions. (b) Comparison of the wind forcing data. Circles denote the observations. The coloring convention of the lines is the same as in Figure 3. Thin and thick lines are raw data (1 hourly) and the 73-hour running average, respectively.

Figure 5 shows the scatter plot between the observed and simulated ^{3}H concentrations at Obuchi Fishing Port. Most of simulated ^{3}H concentrations were comparable to the observations and within factor-2, but there were several outliers. As mentioned above, there were some differences among the four runs. The simulated ^{3}H in lower concentrations (~1.0E-1 Bq L^{-1}) by the FORA run were closer to the observed values than those of the JMSF run. In comparison, the simulated ^{3}H in higher concentrations (> 1.0E+0 Bq L^{-1}) by the MSM and DSJRA-55 runs were closer to the observations.

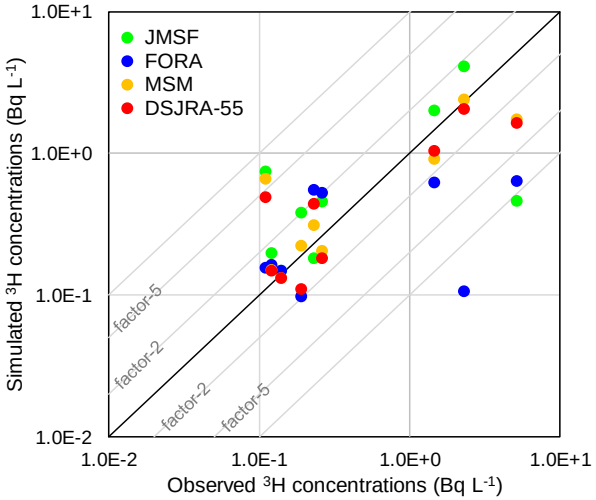

Figure 5. Scatter plot between the observed and simulated ^{3}H concentrations at Obuchi Fishing Port. Green, blue, orange, and red colored circles denote the concentrations from the JMSF, FORA, MSM, and DSJRA-55 runs, respectively.

Summary

We simulated ocean currents and ^{3}H concentrations in seawater by the Rokkasho coastal marine model to examine the effect of offshore boundary conditions and wind forcing data. The simulated coastal currents and ^{3}H concentrations in seawater were realistically reproduced in the coastal marine model. There were some differences among the four run types. In the examination of offshore boundary conditions for the coastal marine model, the FORA run reproduced the ^{3}H concentrations well in August and September 2008, better than the JMSF run, whereas the JMSF run was closer to the observations in the other time periods. These were due to the use of different offshore boundary conditions. Moreover, there was some effect due to the difference in wind forcing data. The MSM and DSJRA-55 runs reproduced the ^{3}H concentrations well during October to December 2008 compared to the JMSF run, whereas the reproducibility of those three runs were same degree in the other time periods. As a result, the changes in offshore boundary conditions and wind forcing data resulted in some higher reproducibility of the current speed and ^{3}H concentrations in coastal waters. The results imply that further tuning of the input data will improve the reproducibility of current fields and associated ^{3}H transfer in the Rokkasho coastal waters simulated by the coastal marine model.

This study was performed under contract with the Government of Aomori Prefecture, Japan.

Conlon, D.M., 1982. On the Outflow Modes of the Tsugaru Warm Current. *La Mer*, 20, 60–64.

Hisamatsu, S., T. Iyogi, J.-H. Chiang, H. Suwa, M. Koide and J. Inaba, 2007. Dose evaluation model for radionuclides released from the spent nuclear fuel reprocessing plant in Rokkasho. *Proceedings of International Symposium on Environmental Modelling and Radioecology*, 181–188.

In, T. T. Nakayama, Y. Matsuura, S. Shima, Y. Ishikawa, T. Awaji, T. Kobayashi, H. Kawamura, O. Togawa and T. Toyoda, 2007. The oceanic forecasting system near the Shimokita Peninsula, Japan. *Proceedings of International Symposium on Environmental Modelling and Radioecology*, 58–64.

Japan Nuclear Fuel Limited (JNFL), 2019. Our Business. http://www.jnfl.co.jp/ja/business/report/public_archive/safety-agreement-report/. Accessed 25 October 2019 (in Japanese)

Kayaba, N., T. Yamada, S. Hayashi, K. Onogi, S. Kobayashi, K. Yoshimoto, K. Kamiguchi and K. Yamashita, 2016. Dynamical Regional Downscaling Using the JRA-55 Reanalysis (DSJRA-55). *SOLA*, 12, 1–5. doi:10.2151/sola.2016-001.

Ueda, S., K. Kondo, J. Inaba, H. Kutsukake, K. Nakata, 2006. Development and application of an eco-hydrodynamic model for radionuclides in a brackish lake: Case study of Lake Obuchi, Japan, bordered by nuclear fuel cycling facilities. *Journal of Radioanalytical and Nuclear Chemistry*, 268, 2, 261–273, doi:10.1007/s10967-006-0163-0.

Ueda, S., H. Kakiuchi, H. Hasegawa and S. Hisamatsu, 2011. Validation of a Radionuclide Transfer Model in Brackish Lake. *Fusion Science and Technology*, 60:4, 1296–1299, doi:10.13182/FST11-A12668.

Ueda, S., T. Iyogi, H. Kutsukake, K. Nakata and S. Hisamatsu, 2012. Introduction of an ecosystem model into a transfer model for radionuclides in aquatic environments. *Journal of Advanced Marine Science and Technology Society*, 18, 1, 13–24, doi:10.14928/amstec.18.1_13. (in Japanese)

Usui, N., T. Wakamatsu, Y. Tanaka, N. Hirose, T. Toyoda, S. Nishikawa, Y. Fujii, Y. Takatsuki, H. Igarashi, H. Nishikawa, Y. Ishikawa, T. Kuragano and M. Kamachi, 2017. Four-dimensional variational ocean reanalysis: a 30-year high-resolution dataset in the western North Pacific (FORA-WNP30). *Journal of Oceanography*, 73, 205–233, doi:10.1007/s10872-016-0398-5.

Developing of the radioecological monitoring system of atmospheric air, terrestrial and freshwater ecosystems in the vicinity of Rooppur NPP (People's Republic of Bangladesh)

A.V. Panov, N.N. Isamov, V.K. Kuznetsov, D.N. Kurbakov

Russian Institute of Radiology and Agroecology (RIRAE), Obninsk, 249032, Russia
Keywords: radioecological monitoring, atmospheric air, terrestrial ecosystems, freshwater ecosystems.
Presenting author Alexey Panov, e-mail: riar@mail.ru

The Rooppur NPP with two VVER-1200 reactors and the total capacity of 2400 MW is being constructed under the Russian design, under General Contract dated 25 December 2015. The General Contractor for the Rooppur NPP is Atomstroyexport (the engineering division of Rosatom). Each construction stage of the Rooppur NPP in Bangladesh is closely monitored by the International Atomic Energy Agency (IAEA) and the national regulatory authority BAEC.

The Rooppur NPP site is located on the northern bank of the Padma (Ganges) River, 20 km east of the city of Pabna, 8 km south of the city of Ishwardi and 7 km northeast of the city of Veramar of Kushtia district, at a distance of about 160 km northwest of the city of Dhaka, the capital of Bangladesh. The site is situated near the settlement of Rooppur (Figure 1). There are two bridges near the Rooppur NPP site: the Harding railway bridge (constructed by Great Britain specialists in 1916) and the Lalon Shah motorway bridge (constructed by China specialists in 2004). These bridges (1.8 km) connect the northern and southern parts of Bangladesh. The selected site for NPP construction is very suitable: Padma river, railway, motorway and high voltage electricity system are near the site.

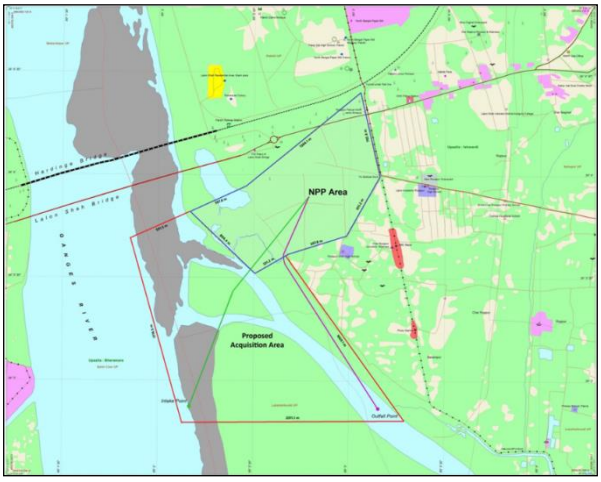

Figure 1. Schematic map of Rooppur NPP site.

The works in the vicinity of Rooppur NPP on engineering and environmental surveys and radioecological monitoring includes several interrelated blocks (Engineering surveys, 2012).

1. Engineering and environmental surveys in the vicinity of NPP:
- description of environmental conditions;
- description of the state of the environment;
- description of demography;
- description of the economic use of the territory, etc.

2. Development of the Programme and creation of the radioecological monitoring network in the vicinity of NPP.

3. Landscape characterization of the territory:
- description of aquatic and terrestrial ecosystems;
- soil studies;
- floristic and faunistic research;
- hydrobiological studies.

4. Detailed field survey of ecosystems for contamination detection (radionuclides, heavy metals, other toxicants):
- assessment of the surface layer of the atmosphere;
- assessment of terrestrial natural and agricultural ecosystems (soil, vegetation, agricultural products, food);
- assessment of aquatic ecosystems (surface and groundwater, sediments, water plants);
- route (vehicle and foot) studies (measurements of γ radiation exposure doses, noise, electromagnetic radiation) ;
- assessment of the radon hazard of the territory.

5. Radiation dose assessment for members of the public and reference animals and plants.

6. Development of maps and databases with the results of radioecological monitoring based on GIS technology.

7. Long-term forecast of changes in the radioecological situation in the vicinity of NPP.

In the period 2014 – 2017, based on a comprehensive survey of the 30-km zone of the Rooppur NPP, the system of radioecological monitoring of the atmospheric air, terrestrial (natural, anthropogenic and agrarian) ecosystems, as well as freshwater ecosystems, was developed. The detailed program of radioecological monitoring was developed; the observation sites were selected and examined; the objects of monitoring, a list of observable parameters, a schedule of observations, as well as the methods of monitoring and technical support were defined.

For the first stage, a network of radioecological monitoring of terrestrial natural, semi-natural and agricultural ecosystems consisting of 15 key sites covering the main landscapes of the territory has been created in the 30-km zone of the Rooppur NPP (Figure 2).

The peculiarity of Bangladesh is that it is a very densely populated country. The area of Bangladesh is 147.6 ths. km² and the population is 163 million. Consequently, more than 1 ths. people live on 1 km², and therefore, a significant part of terrestrial ecosystems are semi-natural and agrarian.

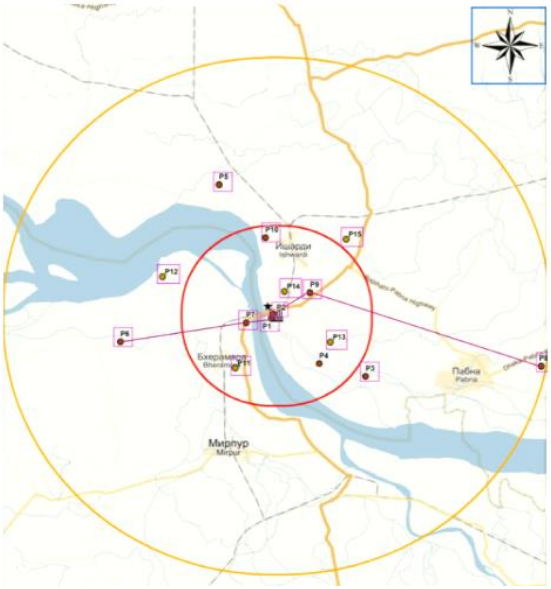

Figure 2. Schematic map of 15 key sites in the 30-km zone of the Rooppur NPP.

The territory of the NPP construction and the 30-km zone is located within the Padma River floodplain and presented by comprehensively developed agricultural areas. The vegetation of these areas is presented by agrocenoses with rather small fragments of secondary communities, and also plantations of trees and shrubs near roads and villages. The following crops of various species and breeds are cultivated in the region: cereals, including grain cereals, starch plants, sugar-bearing and oil-bearing plants, spices, fibrous species, vegetables, fruits, nuts, etc. The most wide-spread cultivated plants in the region are rice, jute, wheat, sugar cane, tobacco, mustard, turmeric, taro, beans, onion, garlic, different types of vegetables, etc. Even though the territory is highly developed in agricultural terms, it can be characterized with wide species diversity. In total, during the environmental survey, more than 170 species of plants (excluding aquatic) were found and identified at the site. These species belong to 55 families. 75 species of trees and shrubs were recorded. Most of this list is covered with cultivated species and plants used for economic purposes. There is plenty of weed species observed.

In the frame of environmental monitoring in the vicinity of the Rooppur NPP, there was conducted the landscape characterization of the territory, the description of freshwater and terrestrial ecosystems, soil, floristic, faunistic and hydrobiological studies. Hydrobiological monitoring in the vicinity of the Rooppur NPP included six different directions (Figure 3):

- Phytoplankton,
- Zooplankton,
- Periphyton,
- Zoobenthos,
- Macrophytes,
- Ichthyofauna.

Within 30-km area from the NPP construction site, valuable wetlands are missing. No rare or endangered species of plants were found in water bodies. The obtained fish catches contain 51 fish species:19 families, 10 orders.

As per species composition, the dominant ones are the Siluriformes (catfishes) order – 20 species, 6 families (moreover 10 species refer to Bagridae family (bagrid catfishes)) and Cypriniformes order (carp-like fishes) – 11 species, 1 family.

Figure 3. Schematic map of point samples of hydrobiological monitoring, water, aquatic flora and bottom sediments in the 30-km zone of the Rooppur NPP.

Basing on developed radioecological monitoring programme in period 2014 – 2017 conducted the assessment of the state of freshwater ecosystems (surface and underground waters, bottom sediments, aquatic flora) for the presence of pollutants (natural and artificial radionuclides, heavy metals and other toxicants). Table 1 presents some results of the monitoring of different components of freshwater ecosystems with the content of natural and artificial radionuclides for the period 2014-2017.

Table 1. The content of radionuclides in the components of freshwater ecosystems, Bq/kg (2014 – 2017).

Component	^{40}K	^{90}Sr	^{137}Cs	^{3}H
Surface water of Padma	0.3-2.3	0.03-0.23	0.01-1.5	0.8-2.1
Bottom sediments	350-852	0.05-3.5	0.01-3.1	<3
Aquatic flora	347-924	0.05-3.9	0.01-2.6	<3
Drinking water	0.45-1.1	0.01-0.07	0.01-0.08	0.4-1.2

Next direction of the radioecological monitoring is the assessment of the state of terrestrial natural and agricultural ecosystems including soil, vegetation, agricultural products, foodstuff on the presence of pollutants (natural and artificial radionuclides, heavy metals and other toxicants).

In the Rooppur NPP region, significant seasonal differences appear in climatic characteristics. Features of the three seasons are hot and humid spring (March-May), the warm season of tropical monsoons (June - October) and chilly arid winter (November - February). Air

temperature is +18...+25 °C in January and +23...+34 °C in April (the hottest month). The main difference is the amount of precipitation. Annual precipitation is 2000...3000 mm, in the north-east of the country - up to 5000 mm. About 80% falls from May to mid-October, which leads to river flood and flooding of territories.

The influence of climatic features led to the need to estimate the content of radionuclides in agricultural products and foodstuffs produced in dry and humid periods of the year (Table 2). Therefore, radioecological monitoring in the vicinity of the Rooppur NPP was conducted in the following periods: August (2014), April (2015), December (2016) and June (2017).

Table 2. The number of samples of agricultural products taken during radioecological monitoring in the vicinity of the Rooppur NPP in 2014-2017.

Type of product	Sampling period			
	2014 August	2015 April	2016 Dec.	2017 June
Arable lands				
Rice (straw)	8	7	7	1
Corn	1	6	-	-
Sugar cane	30	12	9	4
Jute	11	-	-	2
Tobacco	-	5	-	-
Wheat (straw)	1	17	-	-
Tarot	1	3	-	-
Pastures				
Forbs	55	9	1	-
Gardens				
Banana (leaves)	10	11	5	2
Bamboo (leaves)	3	5	-	-
Lychee (leaves	-	3	-	-
Mango (leaves)	-	2	-	-
Papaya (leaves)	-	-	-	1
Total samples	120	80	22	10

The samples of agricultural products together with soils were taken from arable lands, pastures and gardens at different periods of the year. Some of the products grow during the whole year (for example, rice and sugar cane), but some of them (for example, tobacco and vegetates) only for a short period.

The average content of natural radionuclides in the soils of agroecosystems in the vicinity of Rooppur NPP is ^{40}K - 717-855 Bq/kg, for ^{226}Ra - 44-52 Bq/kg, for ^{232}Th - 69-75 Bq/kg. The average content in the soil ^{90}Sr is in the range of 0.5-1.6 Bq/kg, and ^{137}Cs 1.2-2.5 Bq/kg. Results of determination of total and exchangeable content of heavy metals in soil samples correspond to global background values.

The content of radionuclides in agricultural products and foodstuffs was very low. The variability of data in the accumulation of radionuclides in agricultural products is due to both the varietal characteristics of plants and weather conditions (Table 3).

Results of spectrometric measurements of local foodstuff show that specific activity of ^{40}K corresponds to background values. Content of ^{137}Cs and ^{90}Sr does not exceed the values given in SanPin 2.3.2.1078-01 (Hygienic safety requirements, 2002). Therefore, all samples of feedstuff, as well as agricultural products, comply with the requirements of SanPiN 2.3.2.1078–01 and VP 13.5.13/06–01 (Veterinary and sanitary requirements, 2002).

Table 3. The content of radionuclides in agricultural products and foodstuffs, Bq/kg (2014-2017).

Product	^{40}K	^{90}Sr	^{137}Cs
Rice (straw)	466-923	0.9-5.2	0.8-2.9
Sugar cane	414-629	1.9-3.2	0.7-2.1
Jute	325-905	0.5-1.8	0.7-1.7
Banana (leaves)	688-938	0.7-3.4	0.8-1.7
Natural grass	222-601	1.8-2.6	1.3-1.6
Milk	37-76	0.01-0.2	0.01-0.08
Beef	49-143	0.01-0.7	0.02-0.1
Poultry	75-148	0.02-0.3	0.01-0.09
Eggs	38-45	0.01-0.1	0.07-0.9
Fish	78-124	0.01-0.8	0.01-0.3
Rice grain	12-40	0.3-1.4	0.1-0.8
Potato	103-183	0.17-0.3	0.04-0.6
Zucchini	34-67	0.01-0.3	0.01-0.08
Eggplant	59-84	0.02-0.2	0.01-0.1
Cabbage	47-61	0.14-0.7	0.03-0.06

The radioecological monitoring of surface air included the examination of the surface atmospheric layer on the presence of pollutants (natural and artificial radionuclides, heavy metals and other toxicants) using gas-analysers and aspirators. Air filtering unit (Aspirator PU-3E) consists of three filters:

- to measure dust content;
- to measure radionuclides content;
- to measure heavy metals content.

The investigation of aspirator filters on the content of radionuclides (^{40}K, ^{226}Ra, ^{232}Th, ^{90}Sr, ^{137}Cs) in atmospheric air showed that results of measurements were below the equipment detection limit, but the air was dusty at dry season (Table 4).

Table 4. The activity of radionuclides contained in the surface air in the vicinity of the Rooppur NPP in 2014 - 2017, Bq/m^3.

Year	^{90}Sr	^{137}Cs	^{40}K	^{226}Ra	^{232}Th
2014	$<1.3\cdot10^{-5}$	<0.002	<0.023	<0.008	<0.008
2015	$<1.3\cdot10^{-5}$	<0.002	<0.023	<0.008	<0.008
2016	$<1.2\cdot10^{-5}$	<0.001	<0.042	<0.014	<0.014
2017	$<1.3\cdot10^{-5}$	<0.001	<0.042	<0.014	<0.014

Gamma survey in the 30-km zone (1.6 thousand measurements by vehicle and foot) and at the construction site of the Rooppur NPP (370 measurements) was performed. The minimum detected dose rate was 0.08

μSv/h, and the maximum - 0.18 μSv/h. The average dose rate in the 30-km zone of Rooppur NPP was 0.13 μSv/h. The level of gamma dose rate in this region is due to the natural gamma background.

Next direction of the radioecological monitoring is radon hazard assessment at the site of Rooppur NPP. The obtained results of measurements of radon field density via the express-method proved the absence of radon hazard at the site. In all air samples (excluding one point) values of ^{222}Rn radon field density were below 80 mBq/s·m^2 (Figure 4).

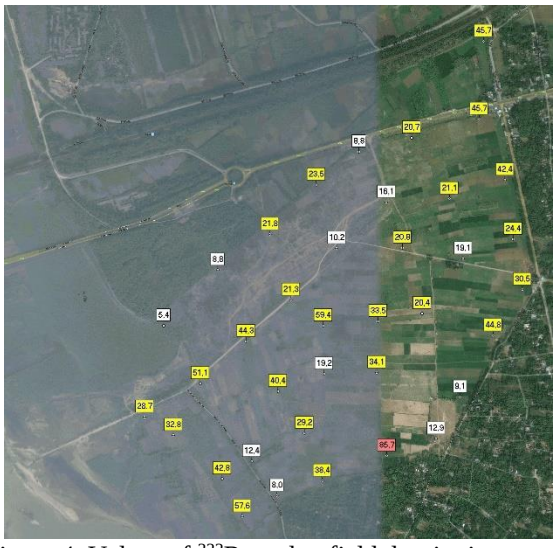

Figure 4. Values of ^{222}Rn radon field density in control point (White – Values of ^{222}Rn radon field density – 0…20 mBq/s·m^2; Yellow – Values of ^{222}Rn radon field density – 20…80 mBq/s·m^2; Red – Values of ^{222}Rn radon field density – 80…200 mBq/s·m^2).

However, hence radon field density at the soil surface depends on atmospheric pressure, humidity and ambient temperature, and radon measurements were done during monsoon period, it is recommended to perform such measurements also during dry period and update radon hazard assessment for the NPP area at the constructing stage.

For the first time, ever external radiation doses for members of public residing in the vicinity of Rooppur NPP construction site in Bangladesh were assessed using thermoluminescent dosimetry (Figure 5).

Figure 5. Schematic map of TLD dosimetry in the 30-km zone of the Rooppur NPP.

Investigation results show that these doses within 30-km zone around the NPP are determined by natural radiation sources and their value on average is 1.68 mSv/a (Panov et al., 2018). External radiation doses for members of public, as well as γ-radiation background are uniformly distributed around the investigated territory on different distances and directions from the construction site (Table 4).

Contribution of "transport" dose into dose accumulated by thermoluminescent dosimeters (TLD) for 6 months was in average 8.6%. It was observed that external radiation doses of the population living in stone buildings on the investigated area are lower than the same doses formed outside. Evidential differences in the formation of external radiation doses for public depending on professional occupation were not detected.

Table 4. External radiation doses in the settlements of the 30-km zone of the Rooppur NPP in 2016-2017.

Settlement	Direction and distance from NPP	Number of dosimeters	Exp. dose, μSv/h	Annual dose mSv/a
NPP site	-	1	0.25	2.21
Rooppur	S-E., 2.4	2	0.14	1.22
Kushtia	S-E., 20.3	1	0.29	2.54
Veramara	S-W., 7.7	1	0.14	1.20
Kutir	N-W., 1.2	12	0.19	1.65
Lalpur	N-W., 15.6	1	0.14	1.24
Bagra	N-W., 25.2	1	0.18	1.60
Radzhahi	N-W., 29.3	1	0.14	1.26
Gr.-City	N-E., 2.1	2	0.19	1.64
Ishurdi	N-E., 7.5	6	0.22	1.91

On the basis of the radioecological monitoring, conducted in 2014-2017 in the 30-km zone of the Rooppur NPP, it can be concluded that the ecological situation in this region is safe. The established radioecological monitoring system will make it possible to register a change of the ecological situation in the 30-km zone of the Rooppur NPP and identify the effect of the NPP operation on the ecological situation in this region.

This work was supported by the Russian Scientific Foundation under grant No. 18-19-00016.

SP 151.13330.2012. Engineering surveys for location, design and construction of NPP. Part I. Engineering surveys for the development of pre-project documentation (selection of a point and selection of a site for the location of nuclear power plants). Moscow, 2013. 187 p. (In Russian).

SP 151.13330.2012. Engineering surveys for location, design and construction of NPP. Part II. Engineering surveys for the development of design and working documentation and construction support. Moscow, 2013. 155 p. (In Russian).

Hygienic safety requirements and nutritional values of foodstuffs. Sanitary and epidemiological rules and norms

SanPiN 2.3.2.1078-01. M.: Ministry of Health of the Russian Federation, 2002.164 p. (In Russian).

Veterinary and sanitary requirements for radiation safety of feed, feed additives, feed raw materials. Permissible levels of radionuclides are ^{90}Sr and ^{137}Cs. Veterinary rules and regulations. VP 13.5.13/06-01 // Veterinary pathology. 2002. №4. pp. 44-45 (In Russian).

Panov A.V., Yakushkin V.S., Kurbakov D.N. Thermoluminescent dosimetry of public in the vicinity of Rooppur NPP construction site (People's Republic of Bangladesh) // Radiation and Risk, 2018, Vol. 27, №3. pp. 65-78 (In Russian).

Dose rate assessment at the submarine spring of Anavalos using ERICA Tool, Greece

F.K. Pappa, G. Eleftheriou, N. Maragos, C. Tsabaris

Institute of Oceanography, Hellenic Centre for Marine Research, Anavyssos, 19013, Greece
Keywords: submarine groundwater discharges, gamma-spectrometry, in-situ monitoring, radon daughters
Presenting author, e-mail: Filothei Pappa (fkpappa@hcmr.gr)

According to Burnett et al., (2003) and Moore (2010) as submarine groundwater discharge (SGD) can be defined the terrestrial groundwater discharging to the coastal area. Thus, groundwater serves as a pathway of nutrients from land to coastal regions, playing a significant role in coastal ecosystems and governing the coastal benthic environment. Although studies regarding the SGD influence in bacteria and biota were held by Vollberg et al. (2019) and Sugimoto et al. (2017), respectively, very little are known of the SGD radiological input. It is well known that good indicators of SGD areas are the natural radionuclides of ^{222}Rn and ^{220}Rn for the freshwater inflow and ^{40}K for the marine input (Tsabaris et al., 2012).
The main objective of this work was the radiological risk assessment in biota at an SGD site of Anavalos. Additionally, the hypothesis of utilizing the freshwater of this SGD spring taking into account the radiological assessment for aquaculture reasons was tested.

Study Area
Anavalos submarine underwater discharge (SGD) spring is one of the major springs of Nafplion city located at the coastal area of Argos, NE Peloponnese Peninsula in Greece. The spring is used for irrigation purposes and as an alternative water resource for Nafplio city. The groundwater originates from karst formations of the area and it is characterized by high levels of conductivity (low threshold) that indicates saline conditions. This saline environment can be attributed to either overexploitation of the water or leakage of the dam (Figure 1).

Figure 1. The dam surrounding the SGD spring of Anavalos. The main three "eyes" of the freshwater discharges are mentioned with blue. The aquatic plants grown in the dam are shown with green.

Methodology
In this work the activity concentrations in water (in Bq m^{-3}) and sediment (in Bq Kg^{-1}) of ^{40}K, ^{226}Ra, radon (^{214}Pb, ^{214}Bi), ^{228}Ra and thoron (^{208}Tl) progenies were utilized for the estimation of the dose rates receiving by marine biota.

Water
The activity concentrations in the water of ^{40}K, radon and thoron progenies were measured directly via in situ detectors of low (KATERINA) and medium (GeoMAREA) resolution. The average activity concentrations of the aforementioned radionuclides were utilized in the radiological assessment, takin into account the five-month measuring period. On the other hand, the activity concentrations of ^{226}Ra and ^{228}Ra in the water were determined by a well-established method in the laboratory, utilizing MnO_2 fibers (Wurl, 2009). The radionuclides of ^{226}Ra and ^{228}Ra, are characteristic of the coastal area, while the radon and thoron progenies represent an extra input due to freshwater discharge. Thus, through this methodology the supported radon and thoron, due to ^{226}Ra and ^{228}Ra presence, respectively, as well as the unsupported radon and thoron due to the freshwater input can be determined and taken into account.

Sediment
Similar approach was performed in the sediment measurements. The activity concentrations of ^{226}Ra and ^{228}Ra were calculated indirectly in the lab via their progenies ^{214}Pb / ^{214}Bi and ^{228}Ac, respectively assuming secular equilibrium (supported radon and thoron). In addition, the unsupported radon activity concentrations were estimated via the excess portion of ^{210}Pb. In brief the excess portion of ^{210}Pb was calculated by subtracting the supported portion of ^{210}Pb (^{226}Ra presence) from the total ^{210}Pb measured activity concentration in the sediment. Similarly, was calculated the unsupported thoron activity concentration (excess portion of ^{208}Tl).
Thus, the measured activity concentrations of natural radionuclides in the water and sediment were utilized, without using the default values of water-sediment distribution coefficient (Kd) provided by ERICA Tool. Alternatively, for the estimation of the activity concentration in the biota the default concentration ratios (CRs) were used, due to the absence of radioactivity measurements in the biota. Applying the aforementioned activity concentrations in all media, the dose rate calculation and assessment was performed via ERICA Assessment Tool. The radiological risk determination was performed for the biota inhabiting – or that are possibly inhabiting - in the freshwater of the SGD (fish, zooplankton, phytoplankton and vascular plant).

The ERICA Tool takes into consideration the progenies of a radionuclide if their half-lives are less than 10 days (Brown et al., 2008). However, the tool lacks in the estimation of dose rates due to the presence of noble gases (Vives i Battle at al., 2015) and little progress has been made regarding Rn, focusing only in air (Vives i Batlle et al., 2012). To the authors' knowledge the radiologic contribution of inert gases in the aquatic environment using ERICA, or other dose rate estimation models, is deficient. To overcome this problem two approaches were realized regarding the parent nuclides of radon and thoron progenies in the water. The first approach assumes that the parent nuclides are ^{222}Rn and ^{220}Rn, which are determined by the measured concentrations of ^{214}Pb / ^{214}Bi and ^{228}Ac, respectively. On the other hand, the second one considers ^{218}Po and ^{216}Po as the parent nuclides. With the first approach the CRs of the element Xe (IAEA, 2004) were utilized in order to describe Rn in the tool, as CRs for Rn are absent and Xe can be considered a good representative due to the fact that these elements have similar chemical characteristics. According to the second approach, the CRs of Po were inserted, which is a well-studied element for environmental radioactivity investigations.

Results and Discussion

The results of the total dose rates and the internal and external fraction for each approach are presented below. The results of the first methodology, where Rn (^{222}Rn, ^{220}Rn) is the parent nuclide are shown in Figure 2 a, b.

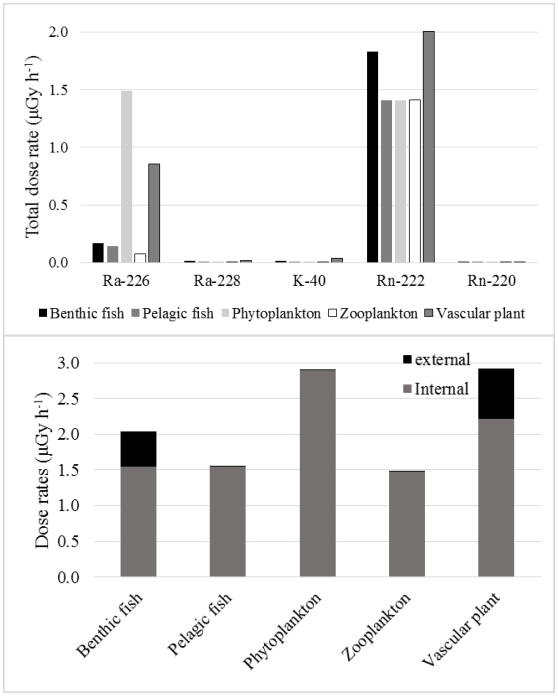

Figure 2. The total dose rates (a) and the internal and external fraction (b) estimated for freshwater biota at a submarine groundwater discharge, utilizing in situ gamma-ray measurements of KATERINA and GeoMAREA detectors. First approach results, where the noble gases (^{222}Rn and ^{220}Rn) are considered the parent nuclides for the dose rate estimation.

The total dose rates revealed that the highest dose rates can be attributed to ^{226}Ra and ^{222}Rn due to the high water-sediment distribution coefficient and the high activity concentrations, respectively describing these radionuclides. Additionally, the greatest fraction in the total dose rate can be attributed to the internal dose rate, as all the before mentioned radionuclides (^{226}Ra, ^{222}Rn, ^{228}Ra and ^{220}Rn) and their progenies, are mainly alpha emitters. Therefore, the dose rate input of a pure gamma-ray emitter (^{40}K) is negligible. The estimated dose rates were found well below the screening values (400 μGy h^{-1}) adopted by the ERICA Tool and proposed by IAEA (1992) and UNSCEAR (1996). For concentrations below the screening values (for chronic exposure situations) no measurable population effects would occur, thus the radiological risk is negligible.

The results of the second methodology, where Po (^{218}Po, ^{216}Po) is the parent nuclide are shown in Figure 3 a, b.

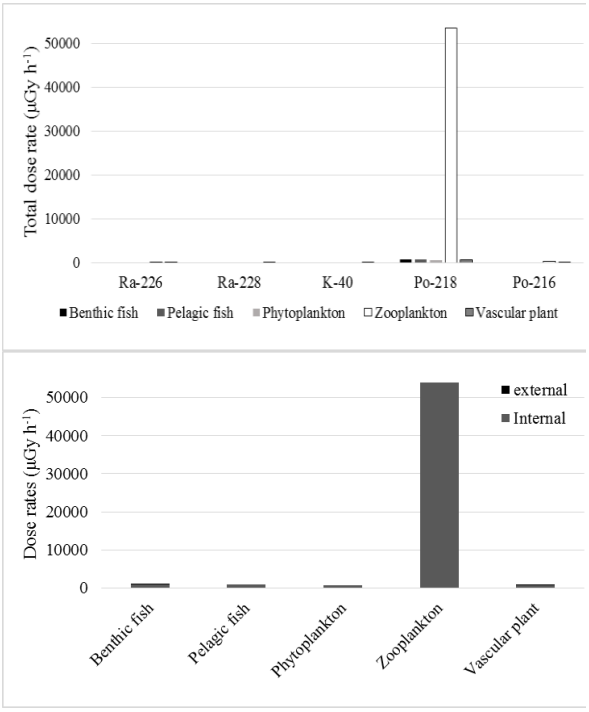

Figure 3. The total dose rates (a) and the internal and external fraction (b) estimated for freshwater biota at a submarine groundwater discharge, utilizing in situ gamma-ray measurements of KATERINA and GeoMAREA detectors. Second approach results, where the ^{218}Po and ^{216}Po are considered the parent nuclides for the dose rate estimation.

Similar observations with those of the first approach can be obtained, such as the external dose rate is negligible and the internal fraction is the main contributor to the total dose rate due to the high concentrations of ^{218}Po and the alpha-decay processes characterizing its progenies. Nevertheless, the total dose rates are orders of magnitude higher than those estimated with the first approach, as well as the adopted screening values (400 μGy h^{-1}) by ERICA. Therefore, the radiological risk is severe, and a more detailed assessment must follow based mainly on experimental data. The contradiction between the first and second approach reveal the importance of the inserted

default parameters (in this case the CRs) of the tool, as they may differ from region to region due to biochemical and physicochemical characteristics of the biota and the environment where they reside, respectively or due to lack of experimental data. In such cases the radiological problem must be further cautiously analyzed.
On the other hand, the problem of utilizing the default or experimental water-sediment distribution coefficient (Kd) values, was overcome via the use of experimental obtained activity concentrations in the water and sediment media. In Table 1 are given the experimental and default Kd values only for comparison reasons and in order to show the significance of having experimental data. The experimental data can be considered representative of the area assuming equilibrium between the media (water and sediment) so as to be compared with the default values.

Table 1. The experimental and default values of the water-sediment distribution (Kd) in (L kg^{-1}).

	Activity concentrations				
	Water ($Bq\ l^{-1}$)	Sediment ($Bq\ kg^{-1}$)	Exper.	ERICA	ratio
^{226}Ra	0.0054	60	11111	14034	0.79
^{40}K	0.5386	315	585	-	-
^{218}Po	12.518	940	75	17848	0.004
^{222}Rn*	12.518	940	75	1	75

The Kd values of radon are those of Xe, because the information regarding Kd data for Rn is absent and Rn and Xe have similar chemical characteristics as they both are noble gases.

It is well known, and it is especially mentioned in ERICA Tool that the Kd values, as well as CRs, differ among regions and thus the dose rate estimation is performed conservatively. However, in this work emerged the lack of experimental data needed to determine the Kd and CR parameters for natural radionuclides of interest, e.g. ^{222}Rn, ^{220}Rn resulting in ambiguous radiological assessments. For the time being it is not clear the radiological situation of the SGD spring and the scenario of utilizing the freshwater for aquaculture purposes cannot be supported yet. Thus, in order to verify one of the two approaches and clarify the radiological risk, aquatic plants were collected from the SGD spring inside the dam and radioactivity measurements are held.

The authors would like to thank the Municipality of Argos-Mykines and the Prefecture of Peloponnese for the continuous support regarding the organizing deployment in the study area. This work was supported by the project ANAVALOS “Development of an in-situ method for the study of submarine groundwater discharges at the coastal zone using radio-tracers” (MIS 5005218) through the Operational Program “Education and Lifelong Learning" of the National Strategic Reference Framework (NSRF) 2014-2020 co-financed by Greece and the European Union (European Social Fund ESF).

Burnett, W.C., Bokuniewicz, H., Huettel, M., Moore, W.S., Taniguchi, M. 2003. Groundwater and pore water inputs to the coastal zone. *Biogeochemistry* 66, 3–33

Brown, J.E., Alfonso, B., Avila, R., Beresford, N.A., Copplestone, D., Prohl, G., Ulanovsky A., 2008. The ERICA Tool. *J Environ Radioact.* 99, 1371-1383.

International Atomic Energy Agency (IAEA) 1992 Effects of ionising radiation on plants and animals at levels implied by current radiation protection standards. Technical Reports Series No. 332, Vienna

International Atomic Energy Agency (IAEA) 2004 Sediment distribution coefficients and concentration factors for biota in the marine environment. IAEA Report 422.Vienna

Moore, W.S. 2010. The effect of submarine groundwater discharge on the ocean. *Annu. Rev. Mar. Sci.* 2, 59–88.

Sugimoto, R., Kitagawa, K., Nishi, S., Honda, H., Yamada, M., Kobayashi, S., Shoji, J., Ohsawa, S., Taniguchi, M., Tominaga, O., 2017. Phytoplankton primary productivity around submarine groundwater discharge in nearshore coasts, *Mar. Ecol. Prog. Ser.* 563, 25–33

Tsabaris, C., Patiris, D.L., Karageorgis, A.P., Eleftheriou, G., Papadopoulos, V.P., Georgopoulos, D., Papathanassiou, E., Povinec, P. 2012. In-situ radionuclide characterization of a submarine groundwater discharge site at Kalogria Bay, Stoupa, Greece. *J. of Environ. Radioact.* 108, 50-59.

United Nations Scientific Committee on the Effects of Atomic Radiation (UNSCEAR) 1996 Effects of radiation on the environment. United Nations Scientific Committee on the effects of atomic radiation, report to the general assembly, annex I. United Nations, New York.

Vives i Batlle, J., Copplestone, D., Jones, S.R., 2012. Allometric methodology for the assessment of radon exposures to terrestrial wildlife, *Sci. Total Environ.* 427-428, 50-59.

Vives i Batlle, J., Jones, S.R., Copplestone, D., 2015. A method for estimating ^{41}Ar, $^{85,88}Kr$ and $^{131m,133}Xe$ doses to non-human biota, *J. of Environ. Radioact.* 144, 152-161.

Vollberg, F., Walther, M., Gardes, A., Moosdorf, N., 2019. Modeling the Potential of Submarine Groundwater Discharge to Facilitate Growth of Vibrio cholerae Bacteria, *Hydrology* 6, 1-15

Radon activity concentration assessment in Pozalagua Cave

S. Rozas, N. Alegría, R. Idoeta, M. Herranz, F. Legarda

Department of Nuclear Engineering and Fluid Mechanics, University of the Basque Country (UPV/EHU), Bilbao, 48013, Spain
Keywords: radon, electret, cave
Saroa Rozas, e-mail: saroa.rozas@ehu.eus

Introduction

Underground workplaces, such as touristic caves, are included among work activities covered by article 40 of Council Directive 96/29/Euratom (EU, 1996). Consequently, exposure of workers and members of the public in such places should be assessed, as there could be a significant increase of exposure, which cannot be disregarded from the radiation protection point of view, due to the presence of natural radiation sources.

Thus, in 2008, the Low Activity Measurements Laboratory (LMBA) of the University of the Basque Country (UPV/EHU) conducted a radiological study of radon in Pozalagua Cave (Legarda et al., 2010), which is located 52 km from Bilbao, in northern Spain.

The cave is an underground cavity formed by calcium carbonate, 125 m long, 70 m width and 19 m high (Sociedad de Ciencias Espeleológicas Alfonso Antxia, 2018), which holds world's largest concentration of eccentric stalactites. Natural ventilation was sealed some years ago, and hence, its usual air renewal conditions were disrupted. The sealing was done before 2008.

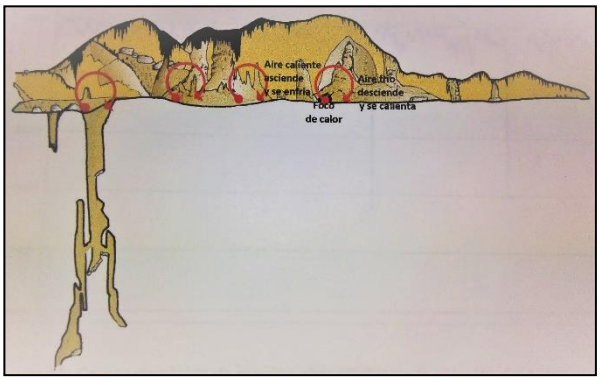

Figure 1. Pozalagua Cave (Sociedad de Ciencias Espeleológicas Alfonso Antxia, 2018).

Ten years later, in order to carry out a regulatory required validation of the results from that study, the LMBA measured again ^{222}Rn activity concentration in air at Pozalagua, from June 2018 to May 2019.

Materials and methods

This time, measurement has been undertaken using Rad Elec E-Perm® Long-Term (LT) Electrets (CSN, 2012). They have been placed 50 cm above ground in four different sampling points, these points have been chosen taking into account radon homogeneity, condensation and exposure time of workers and tourists along guided tour path. In each sampling point, three detectors have been used: two for radon measurement and the third one, inside a Mylar bag, for natural gamma radiation background measurement.

Once a month, electret voltage has been read and mean monthly ^{222}Rn activity concentration has been determined by Radon Report Manager Software 3.8.53 (RAD ELEC, INC., 2016).

Results and discussion

Obtained ^{222}Rn activity concentration, in Bq m^{-3}, at the different sampling points is shown in Table 1. Relative uncertainty of results is 5 – 10 %, detection limit 18 – 26 Bq m^{-3} and natural gamma radiation background 0.2 – 0.9 μGy h^{-1}. Temperature and humidity in the cave during electret voltage readings have been 16 °C and 100 %, respectively.

Table 1. ^{222}Rn activity concentration, in Bq m^{-3}, in different sampling points each month during a year.

Month	Point 1	Point 2	Point 3	Point 4
6	832	961	878	876
7	1025	1121	1064	903
8	821	832	811	868
9	766	653	680	726
10	791	779	546	527
11	-	342	351	283
12	500	523	594	569
1	1646	1154	1725	680
2	-	453	445	443
3	717	1178	764	414
4	365	604	407	482
5	800	754	1125	536

If we analyse the results for each month shown in Table 1, in most cases, there are no big differences among sampling points 1, 2 and 3; and therefore, it can be concluded that radon distribution in this cave is roughly homogeneous. This fact has been confirmed analysing environmental data (Sociedad de Ciencias Espeleológicas Alfonso Antxia, 2009 and 2018).

Moreover, radon concentrations for points 1, 2 and 3 have a mean value of 794 Bq m^{-3} and standard deviation of 329 Bq m^{-3}. This population follows a standard normal distribution, according to Shapiro – Wilk test, while activity concentrations for point 4 (the entrance) follows the observed air streams responsible for air exchange between the cave and the outdoor atmosphere, as seen in Figure 2 (Sociedad de Ciencias Espeleológicas Alfonso Antxia, 2009).

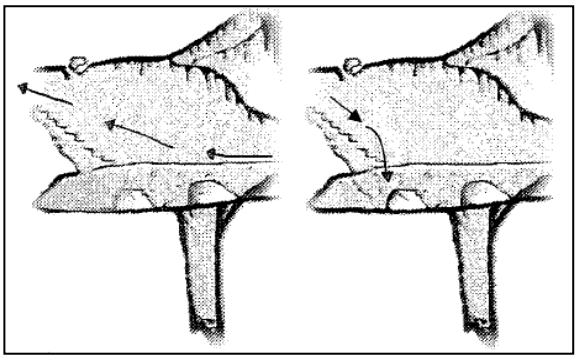

Figure 2. Air streams responsible for air exchange between the entrance and the outdoor atmosphere: during hot season (left picture) and cold season (right picture) (Sociedad de Ciencias Espeleológicas Alfonso Antxia, 2009).

The results for each sampling point show some radon seasonal variation: ^{222}Rn activity concentration decreases from summer to winter and increases from winter to summer, when the number of visitors is the largest, as shown in Figure 3.

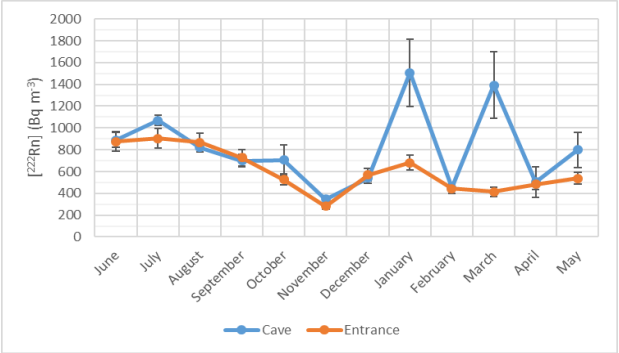

Figure 3. Variation of ^{222}Rn activity concentration, in Bq m^{-3}, in the cave and in the entrance, from June 2018 to May 2019.

The highest ^{222}Rn activity concentration in the cave was obtained in January 2019. This value could have been caused by heavy rainfall (328.8 L m^{-2}), which saturated the surrounding land and blocked usual gas flow through it, radon being concentrated in the cave.
Finally, it is important to note that these results are quite similar to those from 2008, they being between 200 and 800 Bq m^{-3}; and therefore, it can be concluded that exposure conditions in the cave have not changed since 2008.

We would like to thank the Council of Karrantza for giving us the opportunity to research this topic within a research contract.

Council Directive 96/29/Euratom. 1996. Official Journal of the European Communities L 159.

CSN. 2012. Metodología para la Evaluación de la Exposición al Radón en los Lugares de Trabajo. Guía de Seguridad 11.4.

Legarda, F. Idoeta, R., Alegría, N., Herranz, M. 2010. An active radon sampling device for high humidity places. *Radiat. Meas.* 45 (1), 122-128.

Radon Report Manager. 2016. RAD ELEC, INC. Frederick, MD 21704.

Sociedad de Ciencias Espeleológicas Alfonso Antxia, 2009. Estudio del microclima de la cueva Pozalagua. Bizkaia. Período de medición 2004 – 2009. Diputación Foral de Bizkaia.

Sociedad de Ciencias Espeleológicas Alfonso Antxia. 2018. Estudio del microclima de la cueva Pozalagua. Bizkaia. Período de medición 2016-2018. Diputación Foral de Bizkaia.

Exposure build-up factor studies of biological matrices in photon energies 0.05 to 3 MeV.

H. H. Saleh [1,2,*] , J.M. Sharaf[3].

[1]Department of Radiography/ Al-Hussein Bin Talal University, Ma'an, 71110, Jordan
[2]Department of Medical Imaging/ The Hashemite University, Zarqa, 13133, Jordan.
[3]Department of Physics/ The University of Jordan, Amman, 11942, Jordan.
Keywords: Exposure build-up factor EBF, Biological matrices, Effective atomic number.
[*]*Presenting author, e-mail: hanhas2002@gmail.com ; hanan_saleh@ahu.edu.jo*

Exposure build-up factors (EBF) have been calculated for some biological matrices including nine different tissues in the energy region 0.05 – 3 MeV up to a penetration depth of 40 mfp (mean free path). Geometric progression (G-P) fitting approximation has been used to calculate EBF of adipose, skin, muscle, brain, blood, lung, soft, compact bone, and cortical bone tissues. It has been observed that the examined biological matrices show variations in their EBF with incident photon energy, penetration depth, equivalent atomic number, and their elemental compositions of (O, C, Ca) with a significant difference in the intermediate region where Compton scattering dominates.

Introduction

Radiation interacts with material it passes by different types of interactions according to the incident energy range such as photoelectric absorption, coherent and Compton scattering, and pair production process. These interactions degrade photon energy and produce secondary photons that interpret the creation of build-up photons within the materials and it is estimated by build-up factors. Build-up factors are parameters include the geometry of the radiation field produced by the collided part of the beam used to correct the attenuation calculations of the radiation beam. According to the media of interest in which the detector response is sited, two types of build-up factors were defined namely energy absorption build-up factor (EABF) and exposure build-up factor (EBF). In energy absorption build-up factor, the quantity of interest is the deposited energy in the interacting material and the detector response function is that of interacting material. Meanwhile, in the quantity of interest in exposure build-up factor is the exposure and the detector response is that of absorption in air. (Dhillon et al., 2012). In order to calculate the received dose by material, many parameters are needed such as attenuation coefficients, effective atomic numbers and build-up factors. Different methods were estimated to calculate build-up factors in literature such as G-P fitting method (Harima et al., 1986), invariant embedding method (Shimizu, 2002) and Monte Carlo method (Sardari et al., 2009). Build-up factor for 23 elements, water, air and concrete at 25 standard energies in the energy range 0.015-15.0 MeV up to penetration depth of 40 mean free path using G-P fitting method were calculated in American National Standards. (ANSI/ANS 6.4.3, 1991)
In this work exposure build-up factors are computed using G.P. fitting method for some selected biological materials in humans includes of adipose, skin, muscle, brain, blood, lung, soft, bone (compact), and bone (cortical) tissues in the energy region 0.015 – 3 MeV up to a penetration depth of 40 mean free path (mfp). The calculated exposure build up factor has been studied as a function of incident energy, penetration depth and their elemental compositions of (O, C, Ca). The proper knowledge EBF at the surface or within depths of the human body can be useful for radiation control.

Materials and Method

Nine types of tissues were selected in the study as samples to make the calculations. These tissues were the main types which have the most biological effects after dose absorption. The chemical compositions of the samples used in the study with their weight fractions are presented in Table.1 as taken from ICRP website (ICRP, 1991).

Photon interaction parameters

The probability of photon interaction with any material is measured with the mass attenuation coefficient (μ_m) of that medium. WinXCom software presents the μ_m of all materials using the relation;

$$\mu_m = \sum_i w_i (\mu_m)_i \quad (1)$$

Where w_i is the fractional weight and the $(\mu_m)_i$ is the mass attenuation coefficient of the i-th element in the specific material, respectively. The linear attenuation coefficient (μ) is another parameter related the mass attenuation coefficient with the density (ρ) of the material ($\mu_m = \mu/\rho$) The average distance between two successive photon interactions in the material, known as mean free path (*mfp*), is given by the reciprocal of linear attenuation coefficient of these photons in the specific material (*i.e.* $mfp=1/\mu$).

Equivalent atomic number calculations

The Exposure build-up factors are calculated using the GP fitting parameters which can be obtained by the method of interpolation using the equivalent atomic number (Z_{eq}). The equivalent atomic number (Z_{eq}) for a specific material is a parameter describes the properties of its composition in terms of equivalent elements. Interaction of photons with materials is based occurrence of different partial photon interactions in the energy region but the build-up of these photons is due to Compton scattering. Hence, the equivalent atomic number (Z_{eq}) for a specific material is calculated first by matching the Compton ratio R contribution in the scattering process, where $R= \mu_{Comp}/\mu_{total}$, of the material at that energy with the corresponding ratio of an element at this energy. Harima (1983) proposed a relation for Z_{eq}, as follows;

$$Z_{eq} = \frac{Z_1(\log R_2 - \log R) + Z_2(\log R - \log R_1)}{\log R_2 - \log R_1} \quad (2)$$

Where Z_1 and Z_2 are the atomic numbers of elements corresponding to the (μ_{Comp}/μ_{total}) ratios, R_1 and R_2, respectively, and R is the ratio for the selected material at a particular energy, which lies between ratios R_1 and R_2. For this purpose, Geward et al. (2004) developed a computer program WinXCom which presents the values of these ratios for all elements, compounds and mixtures at any energy.

Exposure Build-up Factor calculations

The exposure buildup factors are calculated using G-P fitting, in which the estimated Zeq values were used to interpolate GP fitting parameters using the relation (Harima, 1983);

$$\alpha = \frac{\alpha_1(\log Z_2 - \log Z_{eq}) + \alpha_2(\log Z_{eq} - \log Z_1)}{\log Z_2 - \log Z_1} \quad (3)$$

Z_1 and Z_2 are the atomic numbers of elements between which the Zeq of the sample material lies, $\alpha_1$and α_2 are the G-P fitting parameters (*a, b, c, d and* X_k) corresponding to the atomic numbers Z_1 and Z_2, respectively, taken from the ANSI/ANS- 6.4.3 standard reference database, at the given specific energy. After all, the corresponding G-P parameters of each sample were used to calculate the exposure build-up factors using the relations (Harima et al., 1986);

$$B(E,x) = 1 + \frac{b-1}{K-1}(K^x - 1) \quad for\ K \neq 1 \quad (4)$$

$$B(E,x) = 1 + (b-1)x \quad for\ K = 1 \quad (5)$$

$$K(E,x) = cx^a + d\frac{\tanh(x/X_k - 2) - \tanh(-2)}{1 - \tanh(-2)} \quad for\ x \le 40mfp \quad (6)$$

E is the incident energy, x is the penetration depth measured in mean free path (*mfp*), the parameters (*a, b, c, d and* X_k) are the G-P fitting parameters, and K(*E,x*) represents the photon dose multiplication and the change in the spectrum shape.

Table 1. Elemental weight composition (%) of adipose, skin, muscle, brain, lung, soft, bone (compact), and bone (cortical) tissues (ICRP, 1991).

Element	**Adipose** ρ= 0.92 g/cm^3	**Bone, Cortical** ρ= 1.85 g/cm^3	**Bone, Compact** ρ= 1.85 g/cm^3	**Soft** ρ= 1.00 g/cm^3	**Lung** ρ= 1.05 g/cm^3	**Blood** ρ= 1.06 g/cm^3	**Brain** ρ=1.03 g/cm^3	**Muscle** ρ= 1.04 g/cm^3	**Skin** ρ= 1.10 g/cm^3
H	4.7234	6.3984	10.4472	10.1278	10.1866	11.0667	10.1997	10.0588	11.9477
C	14.4330	27.8000	23.2190	10.2310	10.0020	12.5420	12.3000	22.8250	63.7240
N	4.1990	2.7000	2.4880	2.8650	2.9640	1.3280	3.5000	4.6420	0.7970
O	44.6096	41.0016	63.0238	75.7072	75.9414	73.7723	72.9003	61.9002	23.2333
Na	0.0000	0.0000	0.1130	0.1840	0.1850	0.1840	00.0800	0.0070	0.0500
Mg	0.2200	0.2000	0.0130	0.0730	0.0040	0.0150	0.0200	0.0060	0.0020
Si	0.0000	0.0000	0.0000	0.0000	0.0030	0.0000	0.0000	0.0000	0.0000
P	10.4970	7.0000	0.1330	0.0800	0.0350	0.3540	0.2000	0.0330	0.0160
S	0.3150	0.2000	0.1990	0.2250	0.1850	0.1770	0.5000	0.1590	0.0730
Cl	0.0000	0.0000	0.1340	0.2660	0.2780	0.2360	0.0000	0.2670	0.1190
K	0.0000	0.0000	0.1990	0.1940	0.1630	0.3100	0.3000	0.0850	0.0320
Ca	20.9930	14.7000	0.0230	0.0090	0.0060	0.0090	0.0000	0.0150	0.0020
Fe	0.0000	0.0000	0.0050	0.0370	0.0460	0.0050	0.0000	0.0010	0.0020
Zn	0.0100	0.0000	0.0030	0.0010	0.0010	0.0010	0.0000	0.0010	0.0020

Table 2. Equivalent atomic numbers of adipose, skin, muscle, brain, lung, soft, bone (compact), and bone (cortical) tissues.

Energy (MeV)	**Adipose**	**Skin**	**Muscle**	**Brain**	**Blood**	**Lung**	**Soft**	**Bone, Compact**	**Bone, Cortical**
0.015	6.25	7.19	7.47	7.47	7.48	7.50	7.23	11.40	12.69
0.02	6.25	7.21	7.49	7.49	7.50	7.52	7.25	11.57	12.86
0.04	6.21	7.19	7.47	7.47	7.48	7.51	7.23	11.77	13.09
0.06	6.14	7.15	7.42	7.41	7.44	7.47	7.18	11.78	13.12
0.08	6.07	7.10	7.35	7.37	7.37	7.40	7.13	11.71	13.09
0.1	6.01	7.09	7.30	7.31	7.37	7.38	7.11	11.63	13.03
0.15	5.75	6.91	7.23	7.21	7.23	7.23	6.90	11.36	12.79
0.2	6.15	6.73	7.11	7.08	7.11	7.11	6.90	11.10	12.63
0.4	6.11	6.16	7.26	7.23	7.26	7.26	7.25	11.01	12.24
0.6	5.89	7.11	7.29	7.09	7.11	7.29	6.87	10.38	12.09
0.8	6.13	6.64	7.06	7.04	7.36	7.36	7.05	10.73	12.14
1	5.45	7.23	6.54	7.20	7.23	6.54	7.22	10.50	12.06
1.5	5.22	6.46	6.45	6.41	6.45	6.45	6.44	9.49	10.72
2	5.42	6.26	6.40	6.51	6.56	6.56	6.24	9.05	10.39

Results and discussion

XCOM software was used to obtain the mass attenuation coefficients and the partial coefficients related to Compton scattering for all samples in the energy ranges 0.05-3 MeV, so further calculations could be done. The equivalent atomic number (Z_{eq}) of adipose, skin, muscle, brain, blood, lung, soft, bone (compact), and bone (cortical) tissues in the energy region 0.015 – 3 MeV has been calculated and their variation with energy are shown in Table.2. The ranges of Z_{eq} are (5.22 – 13.14) and the maximum Z_{eq} is for bone (cortical) samples. For all the samples, equivalent atomic number decreases with the increase of the incident photons energy.

The Exposure build-up factors of adipose, skin, muscle, brain, blood, lung, soft, bone (compact), and bone (cortical) tissues were estimated in the energy region 0.015 – 3 MeV and their variation are shown in the Figure 1 (a – d), for different penetration depths (1, 10, 30 and 40) mfp, respectively. As seen from the figure, the obtained (EBF) values for all the selected tissues in the energy region of 0.05 – 3.0 MeV up to the penetration depth of 40 mfp are always greater than one. Also, increasing the incident photon energy increases the buildup factors with low rate at low energy region and with rapid increase in the intermediate region up to 0.1 MeV. After these maximum values, in the energy range (100 – 150) keV, its values return to decrease as the energy increases. The dominance of different photon absorption process such as photoelectric effect and pair production in the low and high energy regions, respectively, cause a total absorption of photons in these regions. Meanwhile, Compton scattering is the dominant process for the intermediate energies which results in multiple scattering that interprets the high increase in build-up factors. Adipose tissue has the highest build-up factor values and the bone (cortical) is the lowest for all photon energies because of the low Z_{eq} of the former and the high Z_{eq} values of the later.

The (EBF) values for the samples as a function of penetration depths for energies; 0.015, 0.15, 1.333 and 3 MeV are shown in Figure 2 (a – d), respectively. For all selected tissue samples, EBF values increase significantly with the increase in their penetration depth. Since increasing the penetration depth, thickness of the interacting material has been increased which results in increasing the scattering events that generate large number of low energy photons within the selected samples. For incident photon energy of 15 keV, build-up factors were very low, but greater than one, and their maxima were 14. The same figures show that the build-up factors for bone tissues (cortical and compact) are almost around unity compared with other tissues for all penetration depths. Increasing the energy, build-up factor values were increased. Again, the values of EBF return to be low after very high values in the intermediate energies, at (150) keV. At energies greater than 1 MeV, the difference between these factors for different samples diminished as the energy increased and become independent of the chemical composition of the selected tissues after 1.5 MeV.

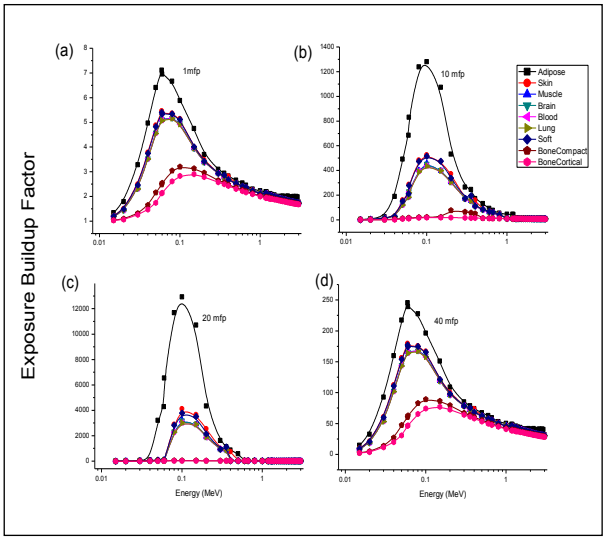

Figure 1 (a – d). The exposure build-up factor for; adipose, skin, muscle, brain, blood, lung, soft, bone (compact), and bone (cortical) tissues in the energy region 0.015 – 3 MeV at 1, 10, 30, 40 mfp.

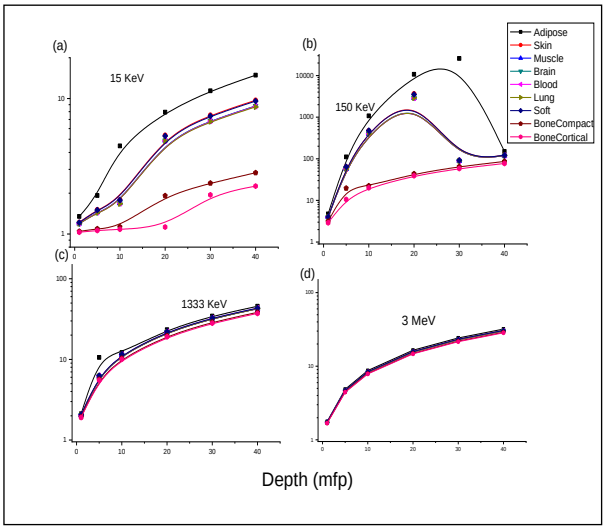

Figure 2 (a – d). The exposure build-up factor for; adipose, skin, muscle, brain, blood, lung, soft, bone (compact), and bone (cortical) variation with depth for energies; 0.015, 0.15, 1.333 and 3 MeV.

The effect of equivalent atomic number Z_{eq} of the samples for a specific energy is noticed to be indirect, i.e the highest Z_{eq} tissue such as bone (cortical) tissue has the lowest values of EBF and vice versa, the lowest Z_{eq} tissue such as adipose tissue has the maximum values of EBF. And this maximum EBF values shift toward the high Zeq tissues. Figure 3 (a & b) show the EBF variation with equivalent atomic number for various depths at energies; (a) 59.5 keV and (b) 2 MeV, respectively.

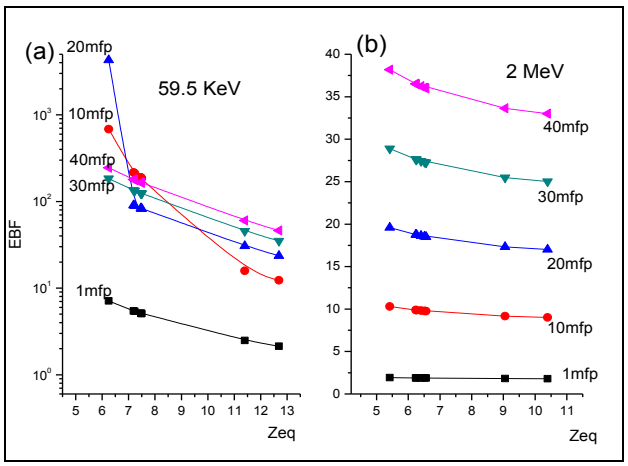

Figure 3. Exposure build-up factor variation with equivalent atomic number for various depths at energies; (a) 59.5 keV and (b) 2 MeV.

The effect composition fraction of Oxygen, Carbon, and Calcium, as main constitution of any types of tissues, on EBF at penetration depth of 40 mfp are shown in Figure 4 (a – c). As noticed from the Fig., increasing the weight fraction of O and C increases both build-up factors in the low photon energy regions but the relation becomes indirect with the weight fraction of Ca. Meanwhile there is no dependence on the three elements weight fractions in the tissues as the energy increased.

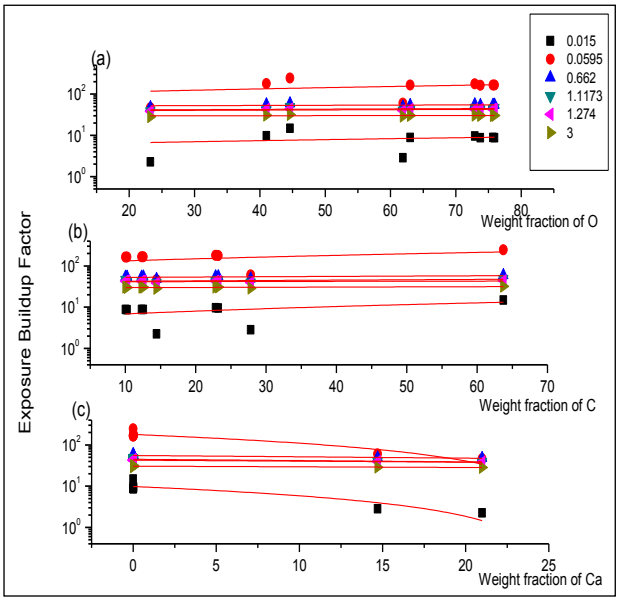

Figure 4 (a – c). The exposure build-up factor for; adipose, skin, muscle, brain, blood, lung, soft, bone (compact), and bone (cortical) tissues with weight fraction of (O), (C), and (Ca) at 40 mfp.

Conclusions

Selected biological matrices including nine different tissues have been examined to calculate their exposure buildup factors (EBF) in the energy region 0.05 – 3 MeV up to a penetration depth of 40 mfp using geometric progression (G-P) fitting approximation.

Adipose, skin, muscle, brain, blood, lung, soft, compact bone, and cortical bone tissues show variations in their EBF with incident photon energy, penetration depth and equivalent atomic number with a significant difference in the intermediate region where Compton scattering dominates. Samples of high Z_{eq}. have the minimum values of EBF meaning while other samples of low Z_{eq} have the maximum values of EBF.

Also, EBF values increases with the increase of the O and C weight fractions but with the decrease of Ca weight fraction presented in the selected tissues for low energies. But at high energies, the variations of EBF disappear and their values trend to be independent of the chemical compositions of the presented tissues. The presented factors can help people working with radiation in establish basic rules that protect their health from radiation hazards.

ANSI/ANS-6.4.3, 1991. Gamma ray attenuation coefficient and buildup factors for engineering materials.

Dhillon, J. S, Singh, B. and Sidhu, G. S., 2012. A comprehensive study on energy absorption and exposure buildup factors for some Vitamins and Tissue Equivalent Materials. *International Journal of Scientific and Research Publications* 2(9) ISSN 2250-3153.

Harima, Y., 1983. An approximation of gamma ray buildup factors by modified geometric progression. *Nucl. Sci. Eng.* 83, 299–309.

Harima, Y., Sakamoto, Y., Tonaka, S., Kawai, M., 1986. Valdity of geometric progression gamma ray buildup factors. *Nucl. Sci. Eng.* 94, 24–25.

ICRP Publication, 1991. Recommendations of the International Commission on Radiological Protection, Annals of the ICRP 60, Vol. 21, Pergamon Press, Oxford, UK.

Geward, L., Guilbert, N., Jensen, K., Levring, H.,2004. WinXCom-aprogramfor calculating X-ray attenuation coefficients. *Radiat. Phys. Chem.* 71, 653–654.

Sandari, D., Abbaspour, A., Baradaran, S., Babapour, F, 2009. Estimation of gamma and X-ray photons buildup factor in soft tissue with Monte Carlo method. *Appl. Radiat. Isot.* 67, 1438–1440.

Shimizu, A., 2002. Calculations of gamma ray buildup factors up to depths of 100 mfp by the method of invariant embedding, (I) analysis of accuracy and comparison with other data. *J. Nucl. Sci. Technol.* 39, 477–486.

A study on control of radioactive Cs elution from incineration fly ash by mixing soil

Y. Shimada[1], M. Yoneda[1], S. Fukutani[2], M. Ikegami[2]

[1]Department of Environmental Engineering, Kyoto University, Kyoto, 6158540, Japan
[2]Institute for Integrated Radiation and Nuclear Science, Kyoto University, Kumatori, 5900494, Japan
Keywords: Radioactive Cs, Elution, Incineration ash, Soil
Y. Shimada, e-mail: shimada@risk.env.kyoto-u.ac.jp

Introduction

Decontamination wastes with radioactivity more than 100,000Bq/kg caused by Fukushima Daiichi nuclear power plant accident are reduced with the volume by incineration. Toward the final landfill disposal of reduced decontamination wastes, it is demanded to control Cs elution from incineration ash. Our previous research (ERTDF 2017) revealed that elusion rate of radioactive Cs from Cs concentrated incineration fly ash is high in the range 64.1-89.1%. In the case of cement solidification of incineration fly ash, elusion rate of radioactive Cs is almost the same range 66.4-88.1%, obtained by the test based on Notification No. 46 of the Environment Agency, Japan. Our previous research revealed that Cs elusion rate of 500°C heat-treated forest soil is minimum value, under 0.2 % (ERTDF 2017). In this study, therefore, we considered the possibility of reducing the elusion rate of radioactive Cs from incineration fly ash by mixing soil.

Method and results

Forest soil used in this study was collected from Soil horizons of Iwate University Forest in Iwate Pref., Japan. The soil type is similar to the forest soil in Fukushima, Kuroboku soil according to the Japan soil classification.
First, we prepared 2 types of soil sample. One is added with small amount of radioactive Cs (2.6ng/kg Cs-134). Another is added with stable Cs (about 500μg/kg). Experimental results of elusion rate of Cs from these two soil samples didn't have a big difference (Figure.1). Therefore, we used the soil added with stable Cs.

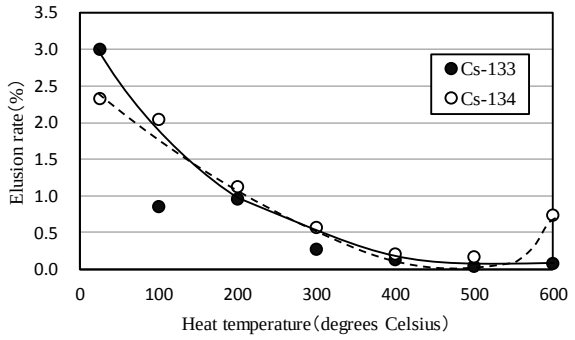

Figure 1. Elusion rate of stable Cs and radioactive Cs.

Cs elusion rates were measured under the condition of four cases; untreated soil added stable Cs mixed by simulated fly ash A (10 % KCl contained), simulated fly ash B (4% KCl contained), 500°C heat-treated soil added stable Cs mixed by fly ash A and 500°C heat-treated soil added stable Cs mixed by fly ash B, under the test based on Notification No. 46 of the Environment Agency, Japan. Reason why we set 500°C is that practical temperature for incineration of wastes including soils, minimum temperature for complete incineration of organic matter is 500°C and soil structure will be broken if soil is incinerated at more than 500°C.
The results are shown in Figure 2. Figure 2 shows that mixing ratio of soil should be about 90 % in order to reduce Cs elution rate to several %. This result revealed that mixing incineration fly ash with forest soil was not effective method for reducing Cs elusion rate.

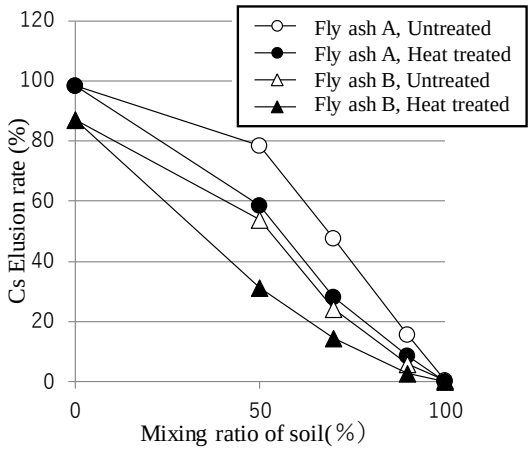

Figure 2. Measured elution rate of radioactive Cs from each incineration fly ash by mixing soil.

Discussion

There are 3 types of K^+ or Cs^+ adsorption sites in soil: adsorption site associated with organic matter (So), adsorption site associated with layerd structure of a clay mineral (Ss) and dsorption site associated with Frayed Edge Site (Sf). Considering competitive adsorption of Cs^+ and K^+, Langmuir equations are as follows:

$$[Cs\text{-}S] = [Cs\text{-}So] + [Cs\text{-}Ss] + [Cs\text{-}Sf] \quad (1)$$

$$[Cs\text{-}So] = [So_{max}]b_{Cs\text{-}So}[Cs^+] / (1 + b_{Cs\text{-}So}[Cs^+] + b_{K\text{-}So}[K^+]) \quad (2)$$

$$[Cs\text{-}Ss] = [Ss_{max}]b_{Cs\text{-}Ss}[Cs^+] / (1 + b_{Cs\text{-}Ss}[Cs^+] + b_{K\text{-}Ss}[K^+]) \quad (3)$$

$$[Cs\text{-}Sf] = [Sf_{max}]bCs\text{-}Sf[Cs^+] / (1 + b_{Cs\text{-}Sf}[Cs^+] + b_{K\text{-}Sf}[K^+]) \quad (4)$$

Where $[Cs^+]$ and $[K^+]$ are Cs^+ and K^+ concentration in solution respectively in meq/mL, [Cs-S] is amount of Cs adsorption to solid phase, [Cs-So], [Cs-Ss] and [Cs-Sf] are amount of Cs adsorption to So type adsorption site, Ss type adsorption site, Sf type adsorption site, respectively, $[So_{max}]$, $[Ss_{max}]$ and $[Sf_{max}]$ are the maximum amount of cation adsorption to adsorption site. $b_{Cs\text{-}So}$, $b_{Cs\text{-}Ss}$ and $b_{Cs\text{-}Sf}$ are equilibrium constant in mL/meq.
When the weight ratio of soil and water is 1/10 (g/mL), Cs elusion rate E_{Cs} (%) is expressed by Equation (5).

$$E_{Cs} = \frac{[Cs^+]}{[Cs^+]+\frac{1}{10}[Cs-S]} \times 100 \quad (5)$$

Representative measured value of CEC for the soil used in this study was 0.05 meq/g. It means that $[So_{max}]+[Ss_{max}]$ = 0.05 mmol/g. The value of $[Sf_{max}]$ is reported to be 0.0002 (meq/g) (Yamaguchi, 2014). Moreover, 1 g incineration fly ash A (10 % KCl contained) includes about 1.3 mmol K. Accordingly, the amount of K^+ in the eluate is about 30 times of the value of $[So_{max}]+[Ss_{max}]$ in the case that mixing ratio of soil and fly ash is 1:1. This result indicate that $[K^+] \gg [Cs^+]$.

When the ratio of mixing soil to fly ash is set to be *a*: 1-*a* ($0 \leq a \leq 1$), the maximum amount of cation adsorption to each adsorption site is extended to *a* times.

Neglecting Cs adsorption to fly ash, we rearranged Equation (1) – (4) as follows:

$$[Cs-S] = [Cs-So] + [Cs-Ss] + [Cs-Sf] \quad (1)$$

$$[Cs-So] = \frac{a[So_{max}]b_{Cs-So}[Cs^+]}{b_{K-so}[K^+]} \quad (6)$$

$$[Cs-Ss] = \frac{a[Ss_{max}]b_{Cs-Ss}[Cs^+]}{b_{K-Ss}[K^+]} \quad (7)$$

$$[Cs-Sf] = \frac{a[Sf_{max}]b_{Cs-Sf}[Cs^+]}{b_{K-Sf}[K^+]} \quad (8)$$

Regarding Cs^+, we assume that $[Sf_{max}]b_{Cs\text{-}Sf} \gg [So_{max}]b_{Cs\text{-}So}$, $[Sf_{max}]b_{Cs\text{-}Sf} \gg [Ss_{max}]b_{Cs\text{-}Ss}$. Regarding K^+, we assume that value of each $b_{K\text{-}So}$, $b_{K\text{-}Ss}$ and $b_{K\text{-}Sf}$ is not widely different. Under these assumptions, Equation (1) can be considered that [Cs-S] ≈ [Cs-Sf]. Equation (1) is consequently rewritten using Equation (8).

$$E_{Cs} = \frac{1000}{10+\frac{a[Sf_{max}]b_{Cs-Sf}}{b_{K-Sf}[K^+]}} \quad (9)$$

Observed value of $[Sf_{max}]b_{Cs\text{-}Sf}$ was about 10000 mL/g.

When the ratio of mixing soil to fly ash is set to be 0.5:0.5 (i.e. a=0.5), we obtain the following Equation (10)

$$E_{Cs} = \frac{1000}{10+\frac{5000}{b_{K-Sf}[K^+]}} \quad (10)$$

We assume that the amount of K adsorption to solid phase in soil, [K-S] (meq/g), is as follows:

Accordingly, $[K^+]$ is determined by the amount of K contained in incineration fly ash in the case that K » CEC. As shown above, representative measured value of CEC

$$[K-S] = [So_{max}] + [Ss_{max}] + [Sf_{max}] \approx [CEC] \quad (11)$$

for the soil used in this study was 0.05 meq/g and 1 g incineration fly ash A (10 % KCl contained) includes about 1.3 mmol K.

In the case that the mixture of 1g soil and 1g fly ash A is eluted with 20 mL water, K^+ concentration in the eluate from the soil (soil : water = 1 : 10), $[K^+]$ is (0.05+1.3)/20mL ≈ 0.067 meq/mL in the case of neglecting K adsorption to soil. Elution rate of 500℃ heat-treated soil added stable Cs mixed by fly ash A was measured to about 57 %. This measured result indicate that E_{cs} is equal to 57. When the values of E_{cs} and $[K^+]$ are substituted in Equation (10), $b_{K\text{-}Sf}$ is nearly equal to 10000 ml/meq. Accordingly, Cs elution rate of mixture of soil and incineration fly ash can be estimated by Equation (12).

In order to validate the estimation of Cs elution rate of mixture of soil and incineration fly ash using Equation (12), the elution ratio estimated by equation (12) was

$$E_{Cs} = \frac{1000}{10+\frac{a}{[K^+]}} \quad (12)$$

compared with observed value (Table 1)

Table 1. Comparison between the estimated and observed value of Cs elution rate of mixture of soil and incineration fly ash

	Mixing ratio Fly Ash : Soil	Elusion ratio of Cs (%) E_{cs}			
		Fly Ash A + 500℃ heat treated soil		Fly Ash B + 500℃ heat treated soil	
		Estimated	Observed	Estimated	Observed
Case 1	5 : 5 (a=0.5)	55.6	57.3	32.9	30.1
Case 2	3 : 7(a=0.7)	33.6	30.6	15.4	12.9
Case 3	1 : 9 (a=0.9)	8.6	6.9	1.0	2.9

According to Table 1, Cs elution rate of mixture of soil and incineration fly ash could be estimated with several % error on the assumption that competitive adsorption of K^+ and Cs^+ are only considered and neglected the other ions. But in the case 3 for Fly ash B, it is possible that the assumption "K ≫ CEC, $[K^+]$ is determined by amount of K in incineration fly ash" is not appropriate.

We estimated the $[K^+]$ in the case that elusion rate of Cs is 1 % at a=0.5 in Eq. (12). The estimated $[K^+]$ is 0.5×10^{-3} (meq/mL). This means that amount of K in incineration fly ash must be less than 1.0×10^{-2} (meq/g) (< CEC) in order to reduce the elusion rate of radioactive Cs to less than 1 %.

Conclusions

In this study, we analysed the possibility of reducing the elusion rate of radioactive Cs from incineration fly ash by mixing soil. As a result, it is difficult to reduce the elusion rate of radioactive Cs to less than 1% from incineration fly ash by mixing soil when incineration fly ash includes large amount of K. Therefore, it is necessary to reduce the K content in incineration fly ash by washing.

This work was supported by the Environment Research and Technology Development Fund (1-1702) of the Environmental Restoration and Conservation Agency of Japan.

ERTDF 2017. Final report of the Environment Research and Technology Development Fund (3K143009), ″Study on the Final Disposal Method mainly using Thermal Treatment of the Wastes Polluted with Radioactive Cs and Sr″.

Yamaguchi, N. 2014. Adsorption mechanism of radiocesium on soil. *J. Jpn. Soc. Soil Phys.* 126, 11-21.

Removal of heavy metals from contaminated water using nano-magnetic Prussian blue based on graphene oxide sorbent

I. Uogintė, G. Lujanienė, D. Valiulis

Center for physical sciences and technology, Savanorių ave. 231, LT-02300 Vilnius, Lithuania
Keywords: nano-sorbent, heavy metals, contaminated water
Presenting author, e-mail: ieva.uoginte@ftmc.lt

Introduction

The contamination of surface and ground waters by heavy metals and radionuclides became a serious environmental problem due to the rapid development of global industrialization. The main sources of these ions are mining activities, wastewater discharge, pigments, phosphate fertilizers, municipal waste, sewage waste and many others (Saleh et al., 2012). The Environmental Protection Agency (EPA) has set a maximum contaminant level (MCLs) as the standard for drinking water quality. Pollutants present above these levels have adverse health effects (Sun et al., 2015). Heavy metals tend to accumulate in living things and can even cause carcinogenic and mutagenic diseases even at low concentrations. Copper, cobalt, nickel and lead are common heavy metal ions occurring in our aquatic environment. Poisoning with divalent copper Cu (II) causes keratinization, dramatization, and itching of the hands and feet. Excessive consumption of cobalt can lead to bone defects, low blood pressure and even genetic mutations in living cells. Severe poisoning with Ni (II) causes dizziness, headache, nausea, and tightness or pain in chest, shortness of breath, dry cough, cyanosis and severe weakness. Similarly, lead Pb (II) can cause encephalopathy, anaemia and hepatitis. Conventional removal methods such as ion exchange, reverse osmosis, electrochemical treatments are costly and have disadvantages such as incomplete metal removal or disposal of secondary wastes. Adsorption is an alternative method, that can be used to remove toxic ions from aqueous solutions. Typically, materials that are capable of removing heavy metals from contaminated solutions contain oxygen, sulphur or nitrogen functional groups as binding sites. They should be low-cost and have high performance as well. Prussian blue (PB) has shown good sorption efficiency of radioactive Cs ions from wastewater (Gupta et al., 2013; Baiyang et al., 2012). The structure of PB consists of Fe^{3+}/Fe^{2+}coordinated to nitrogen/carbon atom ions linked through the bridging of cyanide ligands (Sasaki et al., 2012). Most of the adsorbed ions are introduced into the PB lattice and trapped there. Graphene oxide, with a single-layer sp2- hybridized carbon atoms, had attracted the attention of many scientists due to its specific chemical/physical properties, large surface area, and endless modification possibilities though the functional groups (-epoxy, -hydroxy, -carboxy) (Zhao et al., 2014; Lu et al., 2018; Wang et al., 2016). Some researchers used it to remove heavy metals and dyes from wastewater (Fan et al., 2013; Hosseinzadeh and Ramin, 2018).

Conventional sorbents of graphene oxide or Prussian blue can easily agglomerate in solutions and are difficult to separate after an adsorption-separation separation cycle. Magnetic materials may come in handy and solve this problem because of their ability to react to an external magnetic field, reducing secondary pollutions (Sun et al., 2015; Raza et al., 2018). Fe_3O_4 (magnetite) nano-sorbents have been recommended as economically feasible. Modification of magnetic graphene oxide with Prussian blue is expected to not only improve the stability and sorption efficiency of the nano-sorbent, but also facilitate its separation from the system.

The aim of this study was to modify magnetite nanoparticles (Fe_3O_4) with Prussian blue and graphene oxide and further employed it to remove Cu (II), Co (II), Ni (II) and Pb (II) ions. The batch studies were performed.

Experimental

Synthesis of MGO nano-sorbent

30 mg of graphene oxide (GO) and 0.3g magnetite (M) were separately dispersed in H_2O by ultrasonication. Then the two suspensions were mixed together and vigorously stirred for 10 min. The brown precipitate was collected with a magnet, rinsed three times with water and dried in an oven at 50°C.

Synthesis of MPBGO nano-sorbent (Figure 1)

The previously synthesized magnetic graphene oxide (MGO) was re-dispersed in 300 mL of water. 100 mL of $FeCl_3$ was added to the precipitate suspension under stirring, and then 50 mL of $K_4[Fe(CN)_6]$ was slowly added dropwise. The color of the mixture gradually changed from brown to dark blue, suggesting the formation of MPBGO nano-composite. The mixture was stirred for another hour. The precipitate was collected with a magnet, washed three times with water and dried in an oven at 50ºC.

Sorption experiments

Sorption experiments were performed by mixing a known amount of nano-sorbent with 10 mL of metal ion solutions. Sorption experiments were also carried out (when Cu (II), Co (II), Ni (II) and Pb (II) were present in the same solution). To study desorption, a sorbent loaded with metal ions was assembled from sorption experiments. and washed with water to remove the non-sorbed metal ions. Then, solid nanoparticles were mixed with a solution of HNO_3 at pH 4.0.

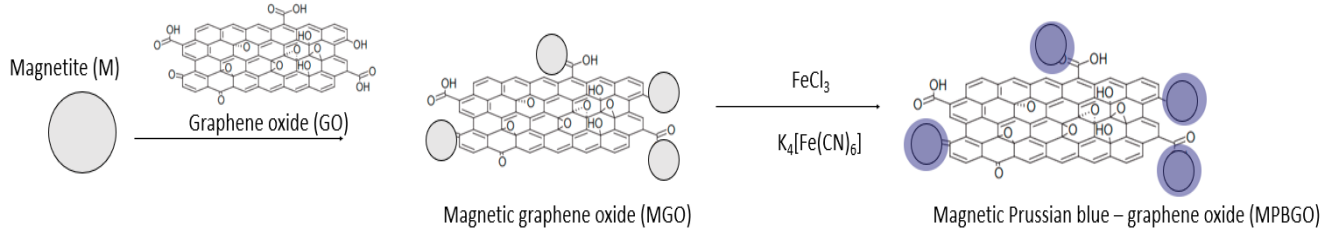

Figure 1. Synthesis of magnetic Prussian blue-graphene oxide nano-sorbent (MPBGO).

The effect of the sorbent dosage was investigated using 10-30 mg of MPBGO sorbent for 10 mL of an aqueous solution of heavy metals.

The sorption efficiency (E, %) and sorption capacity at equilibrium (q_e) of Cu(II), Co(II), Ni(II) and Pb(II) ions can be calculated using equations (1) and (2).

$$E\ (\%) = \frac{C_0 - C_e}{C_0} * 100\% \quad (1)$$

$$q_e = \frac{V(C_0 - C_e)}{m} \quad (2)$$

where C_0 and C_e are the initial concentrations of heavy metal; q_e is the amount of sorbed heavy metal per unit weight of MPBGO (mg/g), V is the volume of solution (L) and m is the weight of MPBGO (g).

Sorption experiments on real samples (Baltic Sea water)

The synthesized magnetic Prussian blue-graphene oxide nano-sorbent was used to investigate its suitability for the removal of Cu (II), Co (II), Ni (II) and Pb (II) metal ions from real water samples. For this purpose, seawater from the Baltic Sea was used. Seawater samples were taken from stations 4, 6, 7 and 64 located in the coastal waters of Lithuania in the Baltic Sea (Figure 2). The amount of nano-sorbent used in the experiment was 10 mg.

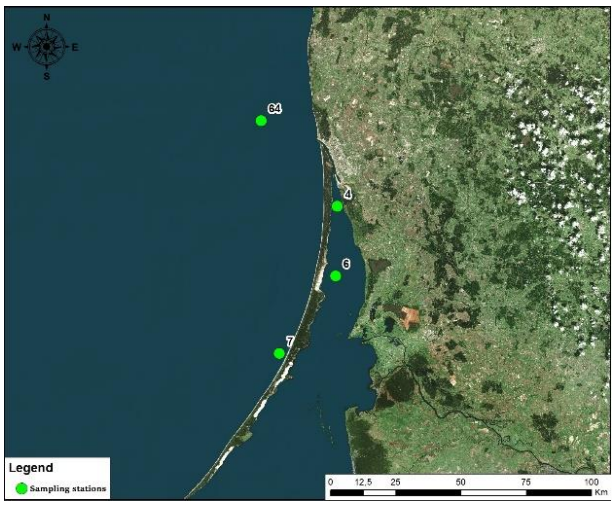

Figure 2. Sampling stations in the Baltic Sea.

Results and discussion

Effect of initial concentration

The initial concentration of heavy metal ions is one of the parameters, who has strong impact on sorption capacity. The effect of the initial concentrations was studied with 10 mg of MPBGO in 10 ml of a heavy metal solution. The concentration of Cu(II), Co(II), Ni(II) and Pb(II) ions for each sample was selected in the range from 0.05 to 1 mmol / L. All experiments were made triple time. Figure 3 shows the removal efficiency of heavy metals on magnetic Prussian blue with graphene oxide nano-sorbent. Sorption capacity increased relatively rapidly with the increase in the initial concentration of metal ions (Fig 3). Equilibrium sorption capacity of MPBGO for Cu(II) ions was 2.12 mmol/g, for Co(II) – 1.40 mmol/g, for Ni(II) – 2.55 mmol/g and for Pb(II) – 1.81 mmol/g. respectively.

The maximum adsorption capacities of the magnetic Prussian blue with graphene oxide sorbent were calculated using the Langmuir sorption isotherm. The correlation coefficients (Q_{max}, 1/n, and K_L) and linear regression coefficient values (R^2) for Cu(II), Co(II), Ni(II) and Pb(II) metal ion are summarized in Table 1.

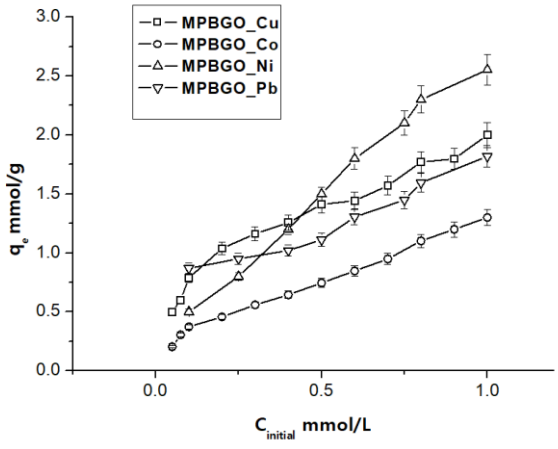

Figure 3. The initial concentration versus Q_e for sorption of heavy metal ions on MPBGO.

Table 1. Langmuir isotherm parameters for heavy metals sorption with MPBGO.

Langmuir	Cu	Co	Ni	Pb
R^2	0.954	0.894	0.815	0.931
Q_{max}	138	115	460	443
B	0.12	0.04	0.01	0.02
R_L	0.889	0.966	0.989	0.980

Effect of sorbent dosage

The effect of the dosage of the sorbent MPBGO on the removal of heavy metal ions was studied at initial metal concentrations of 100 mmol/L and a dosage of sorbent in the range of 10-30 mg. The pH of the solution was adjusted with 0.1 mol/L NaOH.

These results can be found in Figure 4. It is clearly seen, that the adsorption efficiency of Cu(II), Co(II), Ni(II) and Pb(II) metal ions raised with an increase in the initial amount of sorbent. Enhanced metal removal was observed with increasing dosage of the sorbent because more active sites were available for the binding metal ions. Uptake has increased from 41% to 97% for Cu(II), from 32% to 90% for Co(II), from 50% to 92% for Ni(II) and from 59% to 98% for Pb(II) metal ions, respectively.

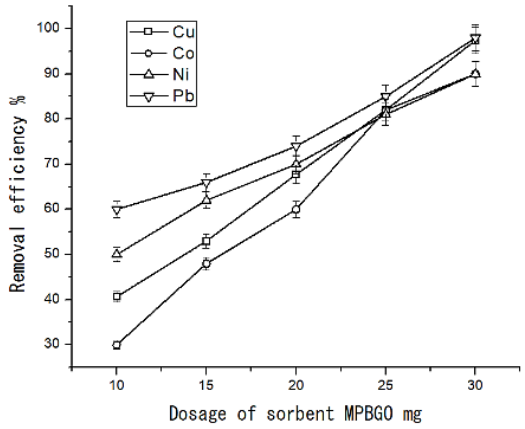

Figure 4. Effect of the sorbent dosage on the percentage removal of metal ions Cu(II), Co(II), Ni(II) and Pb(II) using MPBGO.

Desorption studies

The recovery of Cu(II), Co(II), Ni(II) and Pb(II) metal ions from magnetic Prussian blue with nanoparticles of graphene oxide was studied at pH 4 using HNO_3 acid as an eluting solution. The experiment was performed for three cycles (Figure 5). It was found that the removal efficiency of 90-98% was achieved in the first cycle for heavy metal ions. Removal efficiency decreased in the second and third cycles to 84% and 71% for Cu(II), 80% and 67% for Co(II), 77% and 69% for Ni(II), 85% and 68% for Pb(II), respectively. With each sorption-desorption cycle the removal efficiency decreases by about 10%. This can be explained by low pH values and the use of strong acid in the following desorption cycles, under which Prussian blue may dissolve. In addition, sorption efficiency decrease might be attributed to the loss of the sorbent due to washing after a sorption-desorption cycle. Moreover, active sites during sorption occupied by heavy metal ions could not be completely recovered by desorption.

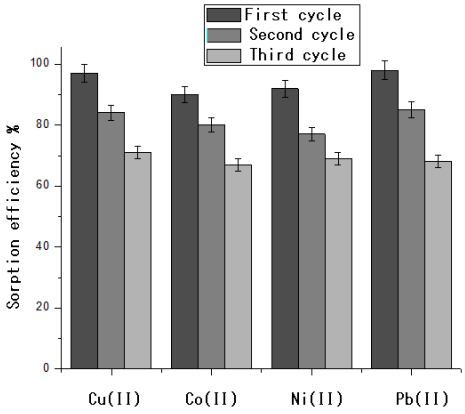

Figure 5. Regeneration of MPBGO after sorption of Cu(II), Co(II), Ni(II) and Pb(II) metal ions.

Sorption of heavy metals in Baltic sea water samples

Ground and surface waters contain a lot of different metal ions. These may influence the removal efficiency of Cu(II), Co(II), Ni(II) and Pb(II) by MPBGO nano-sorbent. High concentrations of Na^+, K^+, and other ions occur in seawater. The influence of co-existing ions is related to the hydration radio of cations and it decreases in the order as follows: K^+ (3.3Å), Na^+ (3.6Å), Pb^{2+} (4.02Å), Ni^{2+} (4.04 Å), Ca^{2+} (4.1Å), Cu^{2+} (4.19Å), Co^{2+} (4.23Å). The experiment was made with spiked sea water samples from 4 sampling stations in Baltic sea. Results are given in Table 2.

Table 2. Removal efficiencies of Cu(II), Co(II), Ni(II) and Pb(II) by MPBGO from Baltic Sea water samples.

Sample Station	Cu(II),%	Co(II),%	Ni(II),%	Pb(II),%
4st	63	51	63	82
6st	66	59	61	81
7st	61	52	58	83
64st	64	63	58	79

Removal efficiencies of Cu(II) (up to 66%), Co(II) (up to 63%), Ni(II) (up to 63%) and Pb(II) (up to 83%) using MPBGO was achieved. Higher removal efficiency can be obtained by increasing the dosage of MPBGO nano-sorbent. Thus, the results showed that MPBGO nano-sorbent can be used to remove Cu(II), Co(II), Ni(II) and Pb(II) or other heavy metals from complex environmental samples.

Conclusion

Magnetic Prussian blue graphene oxide (MPBGO) nano-sorbent was successfully synthesized and used for Cu(II), Co(II), Ni(II) and Pb(II) removal from water samples. The equilibrium sorption capacity was in the following order: Ni(II)>Cu(II)>Pb(II)>Co(II) with the values of 2.55 mmol/g, 2.12 mmol/g, 1.81 mmol/g and 1.40 mmol/g, respectively. Maximum adsorption capacities were evaluated using the Langmuir isotherm. The results revealed that the percentage of heavy metal

removal strongly depends on the optimal dosage of sorbent due to the increase in the number of binging sites on the surface. Even though the removal efficiency decreases with an increase in the number of sorption-desorption cycles, the obtained data showed that magnetic Prussian blue graphene oxide is re-usable and cost-effective nano-sorbent that can be used to remove heavy metals.

Baiyang, H., Fugetsu, B., Hongwen, Y., Abe, Y., 2012. Prussian blue caged in spongiform adsorbents using diatomite and carbon nanotubes for elimination of cesium. *J. Hazard. Mater.* 217-218, 85–91.

Fan, L., Luo, C., Sun, M., Li, X., Qiu, H., 2013. Highly selective adsorption of lead ions by water-dispersible magnetic chitosan/graphene oxide composites. *Colloids and Surfaces B Biointerfaces* 103, 523–529.

Gupta, V.K., Saleh, T.A., 2013. Sorption of pollutants by porous carbon, carbon nanotubes and fullerene- an overview. *Environ. Sci. Pollut. R.* 20 (5), 2828–2843.

Hosseinzadeh, H. and Ramin, S., 2018. Fabrication of starch-graft-poly(acrylamide)/graphene oxide/hydroxyapatite nanocomposite hydrogel adsorbent for removal of malachite green dye from aqueous solution. *Int. J. Biol. Macromol.* 106, 101–115.

Lu, L., Wang, J., Chen, B., 2018. Adsorption and desorption of phthalic acid esters on graphene oxide and reduced graphene oxide as affected by humic acid. *Environ. Pollut.* 232, 505–513

Raza, S., Yong, X., Raza, M., Deng, J., 2018. Synthesis of biomass trans-anethole based magnetic hollow polymer particles and their applications as renewable adsorbent. *Chem. Eng. J.* 352, 20–28.

Saleh, T.A., Gupta, V.K., 2012. Column with CNT/magnesium oxide composite for lead(II) removal from water. *Environ. Sci. Pollut. Res.* 19, 1224–1228

Sasaki, T., Tanaka, S., 2012. Magnetic separation of cesium ion using Prussian blue modified magnetite. *Chem. Lett.* 41, 32–34.

Sun, X.F., Liu, B., Jing, Z., Wang, H., 2015. Preparation and adsorption property of xylan/poly(acrylic acid) magnetic nanocomposite hydrogel adsorbent. *Carbohydrate Polymers* 118, 16–23.

Wang, J., Chen, B., Xing, B., 2016. Wrinkles and folds of activated graphene nanosheets as fast and efficient adsorptive sites for hydrophobic organic contaminants. *Environ. Sci. Technol.* 50, 3798–3808.

Zhao, J., Wang, Z., White, J.C., Xing,B., 2014. Graphene in the aquatic environment: adsorption, dispersion, toxicity and transformation. *Environ. Sci. Technol.* 48, 9995–10009.

Natural radioactivity in sediments along the middle region of red sea coast, Egypt

Hesham M. Zakaly*[1,2], Mostafa. Y. A. Mostafa[1,5*]. M. A. Uosif[2], Madkour.Hashim[3], Shams Issa[2,4] and Mahmoud Tamam[2].

[1]1Ural Federal University, Yekaterinburg, Russia.
[2]Faculty of Science, Al-Azhar University, Assuit branch, Egypt.
[3] National Institute of Oceanography and Fisheries, Hurghada, Egypt.
[4] Faculty of Science, Tabok University, Tabok, Saud Arabia.
[5]Department of Physics, Minia University, El-Minia, Egypt.
Keywords: Natural radioactivity, Sediment radioactivity, Coastal sediment, Radiation hazard, Red Sea
Presenting author, e-mail: mostafa_85@mail.ru

Nearly 85 sediment samples from 12 points in 4 cities along the Egyptian Red Sea coast were collected in order to investigate natural radioactivity. The cities were Ras Gharib, Hurghada, Safaga and Quseir from north to south of the Red Sea coast. The samples were collected from three points near the sea in each city. Gamma-ray spectrometer with a NaI (Tl) detector was used for measuring the activity of natural radionuclides. The activities values are well below the world average of 35 and 30 Bq/kg for ^{226}Ra and ^{232}Th, respectively. The results were compared with the reported ranges from other locations in the world. In Ras Gharib and Hurghada, the ^{40}K activity concentration values are relatively higher than the world average of 400 Bq/kg. The radiation hazard parameters were also calculated and compared with recommended levels from UNSCEAR reports. These results were compiled into the first database for natural radioactivity in coastal sediment samples from Egyptian Red Sea cites. The effective dose rate delivered to the particular organs (lungs, ovaries, bone marrow, testes and the entire body) from the air was estimated.

Introduction

The measurement of natural radionuclide concentrations (^{226}Ra, ^{232}Th, and ^{40}K) in sediments from water bodies (seas, rivers or oceans) is important for protecting the seawater ecosystem and human health from radiation. The Red Sea coast of Egypt is one of the most popular tourist spots in the world. Egypt has about 700 km of coastline along the Red Sea, which is of great environmental, economic and recreational value. Commercial and subsistence fisheries provide a living for a large part of the coastal population in Egypt. The major industries in the Red Sea region are oil exploration, oil production, oil processing, manufacturing industries (fertilizers, chemicals, cement), tourism, fisheries and oil-related maritime transport. Thanks to the rich marine life and favorable climate, tourism has become important for many Red Sea countries, with over 1 million tourists per year expected in the future. An extensive area of the coastline was developed to accommodate the increasing flux of tourists, especially in various areas along the Egyptian coastline (Nasr, 2003). On the Red Sea coast, there are two main centers for phosphate ore mining: Safaga and Quseir and three shipping harbors. Phosphate ore dust that spills into the sea during shipping is a continuous source of contamination in the Red Sea coastal environment (El Mamoney and Khater, 2004).

There is a lack of information about the radioactivity levels and characterization of coastal sediment in Egyptian Red Sea coastal cites (Ras Gharib, Hurghada, Safaga, and Quseir) (El-Taher et al., 2018). Recently, considerable attention has been given to the creation of a scientific database of radiological baseline levels in this coastal region. The baseline data can be used to assess any changes in the radioactivity background level caused by various activities involving radioactive materials or fallout in the near future. The measurement will also help in the development of guidelines. The data generated in this study can contribute to the database of natural radioactivity levels for this area: multivariate statistical techniques were applied to investigate the relationship between radionuclide and radiological parameters.

The aim of this work is to estimate the natural radioactivity of different sediments samples collected from four cities (Ras Gharib, Hurghada, Safaga and Quseir) along the Egyptian Red Sea coast. The samples were collected from 3 points in each city. The concentration of the natural radionuclide activity of ^{226}Ra, ^{232}Th, and ^{40}K in Bq/kg are investigated with a gamma-ray spectrometer (NaI (Tl) detector). The radiation hazard parameters, radium equivalent activity, annual dose, external hazard, excess lifetime cancer risk (ELCR) in mSv yr^{-1} and effective dose rate (D_{organ}) on different body organs and tissues were also estimated and compared with the recommended levels from UNSCEAR reports.

Experimental work

A total of 84 coastal sediment samples (upper 3 cm) were collected from sampling sites in 4 cities (Figure 1): there were 3 sites in Ras Gharib (18 samples), 3 in Hurghada (21 samples), 3 in Safaga (18 samples) and 3 in Quseir (27 samples). Nearly 1 kg of samples were washed in distilled water and dried at about 110 ^{o}C to ensure that moisture was completely removed (El-Taher et al., 2018; M. A. M Uosif et al., 2016). The samples were crushed, homogenized and sieved through a 200 mesh. The samples were weighed and placed in a polyethylene beaker. The beakers were completely sealed for four weeks to reach a secular equilibrium, where the rate of decay of the decay products becomes equal to that of the parent radium and thorium. This step is necessary for ensuring that radon gas confined within the volume and decay products also remains in the samples.

The sediment textures (gravel sand, mud) and total organic matter (TOM) content in representative sediment samples from each site are presented in Table 1. In general,

about 90% of these sediment samples was sand: mud constituted 0-2% and gravel from 4 to 14%. The TOM varied from 3-25 %.

Radioactivity measurements

Activity measurements were taken with a gamma-ray spectrometer containing a scintillation detector (3×3 inch). The set up was hermetically sealed and included a NaI (Tl) crystal, coupled to a PC-MCA Canberra Accuspec. To reduce gamma-ray background radiation, a cylindrical lead shield (100 mm thick) with a fixed bottom and a movable cover was used to shield the detector. The lead shield contained an inner concentric cylinder of copper (0.3 mm thick) in order to absorb X rays generated in the lead. In order to determine the background distribution of radiation in the environment around the detector, an empty sealed beaker was constructed in the same manner and with the same geometry. The measurement time was 43200 s. The background spectra were used to correct the net peak area of gamma rays from the measured isotopes. A dedicated software program, Genie 2000 from Canberra, was used to carry out on-line analysis of each measured gamma-ray spectrum. The ^{226}Ra radionuclide was estimated using a 351.9 keV (36.7%) γ-peak of ^{214}Pb and 609.3 keV (46.1%), 1120.3 keV (15%), 1728.6 keV (3.05%) and 1764 keV (15.9%) γ-peaks of ^{214}Bi. The 186 keV photon peak of ^{226}Ra was not used because of the interfering peak of ^{235}U with the energy of 185.7 keV. The ^{232}Th radionuclide was estimated using a 911.2 keV (29%) γ-peak of ^{228}Ac, 238.6 keV (43.6%) γ-peak of ^{212}Pb and 583.1 keV (84.5) γ-peak of ^{208}Tl. The ^{40}K radionuclide was estimated using a 1461 keV (10.7%) γ-peak from ^{40}K itself. All these procedures were described in previous publications (El-Taher et al., 2018; M A M Uosif et al., 2016; M. A. M Uosif et al., 2016).

Effective dose rate (D_{organ}) for different body organs and tissues

The effective dose rate delivered to a particular organ can be calculated using the following relation (O'Brien and Sanna, 1976):

$$D_{organ} = \text{AEDE} * F \quad (1)$$

where f is the conversion factor of organ dose from air dose. The energies of interest in the present work is 0.2E+03 MeV f, almost independent of energy. The average values of f for various organs and tissues are given in Table 1. Using these f values, D_{organ} was calculated by applying Eq. (1) (Darwish et al., 2015; El-Gamal et al., 2007).

Table 1. Average value of the f factor for different organs or tissues (Darwish et al., 2015; El-Gamal et al., 2007).

Organ or tissue	F
Lungs	0.64
Ovaries	0.58
Bone marrow	0.69
Testes	0.82
Entire body	0.68

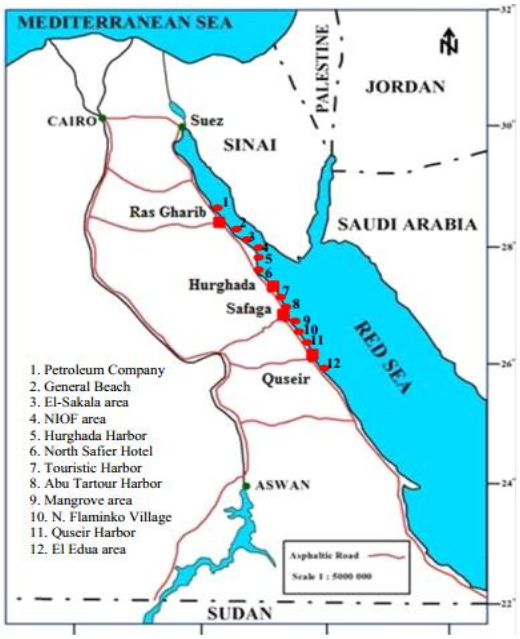

Figure 1. Study area along the red sea coast, Egypt (Ras Gharib, Hurghada, Safaga and Quseir).

Results and discussions

About 85 sediment samples from 12 points in four cities along the Egyptian Red Sea coast (see Figure 1) were collected and measured with gamma spectroscopy in order to investigate natural radioactivity. The concentration mean values with a range for ^{226}Ra, ^{232}Th, and ^{40}K (Bq/kg) for each city are listed in Table 2. The highest activities of ^{226}Ra, ^{232}Th, and ^{40}K are found in site 9 (a mangrove area), whereas the lowest mean activities are found in site 5 (Hurghada Harbor). The lowest activity values were found in 94.77% sandy sediments, while the highest values were found in 86.57% sandy sediments. This can be attributed to the difference in grain size texture. The concentrations of radionuclide activity increase as the particle size decreases because of the increase in surface area per unit of mass. The increase and decrease of radionuclides in soil and sediment samples are also affected by the amount and composition of the organic matter content, adsorption kinetics and the pH of the medium (Alfonso et al., 2014). The total organic matter content was highest in site 9. The activity concentrations of ^{226}Ra, ^{232}Th, and ^{40}K are higher than other points.

^{226}Ra activity ranged from Below Detection limit (BDl) to 57.8 ± 5Bq/kg for all samples. In case of the ^{232}Th, the range was from BDL to 51.5 ± 4 Bq/kg; for ^{40}K, it was from 17.8 ±1 to 1639.6 ± 90 Bq/kg. The average activity concentration values of ^{226}Ra, ^{232}Th and ^{40}K were found to be 23.8±3.8, 19.6±3.2, and 374.9±32 Bq/kg, respectively. A comparison of radionuclide activities in the sediment of the sites and in other coastal and aquatic environments in different countries is given in Table 3. The obtained results are considered to fall within in the range of natural radioactivity around the world. These values are below the world average of 35, 30 and 400 Bq/kg for ^{226}Ra, ^{232}Th and ^{40}K, respectively. In some samples, ^{232}Th concentration is found to be higher than ^{226}Ra concentration. This may be due to the low

geochemical mobility and insoluble nature of thorium in the water (UNSCEAR, 2008).

Radium equivalent (Ra_{eq})

Radium equivalent (Ra_{eq}) is calculated with equation 1. The values varied between 9 and 243 Bq/kg, with an average 80±35 Bq/kg (as listed in Table 2). Compared to the maximum permissible radium equivalent level of 370 Bq/kg (Beretka and Mathew, 1985), the Ra_{eq} values in the studied sites are very low, maintaining an external dose below 1.5 mSv y^{-1} as reported by UNSCEAR. The frequency normal distribution of Ra_{eq} for all samples under investigation is shown in Figure 2. Figure 3 illustrates the relationship between Ra_{eq} and ^{226}Ra activity with the fitted straight line. There is a positive and good correlation between ^{226}Ra activity concentration and the radium equivalent activity level in the area of interest.

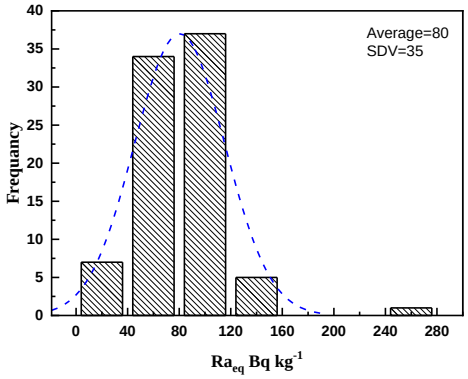

Figure 2. Frequency normal distribution of Ra_{eq}.

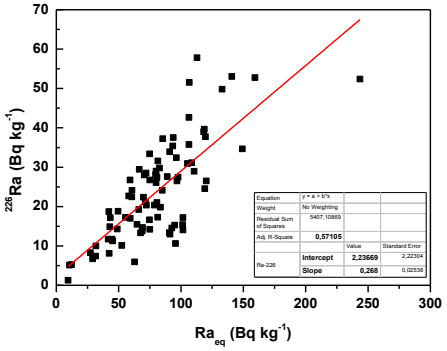

Figure 3. Correlation between ^{226}Ra and Ra_{eq} in all measured sites.

Absorbed Dose Rate (D)

The absorbed dose rates based on sediment samples ranged from 4 to 119 nGy/h, with an average of 38 ± 13 nGy/h. The dose rate values are presented in Table 2. The average absorbed dose rate (D) for all samples is lower than the world average (57 nGy/h) (UNSCEAR, 2008). Therefore, the sites studied do not pose any significant radiological threat to the population. The results attained in this study should be of considerable value as baseline data and a background reference level for Ras Gharib, Hurghada, Safaga and Quseir.

Representative Level Index (I_γ)

Iγ varies from 0.03 to .81 for all samples, as listed in Table 6. The values of the representative level index for all samples were lower than unity. However, the average value of the representative level index (Iγr) is less than unity.

Annual Effective Dose Equivalent (AEDE)

AEDE ranged from 5 to 146 µSv/y, with an average of 47±19 µSv/y (Table 6), which is comparable to the worldwide effective dose of 70 µSv/y UNSCEAR (UNSCEAR, 2008).

External Hazard Index (Hex)

Hex values for the sediment samples are all below unity, as given in Table 2. This indicates that these sediments pose no radiological hazard to the workers who handle them. Table 2. Concentration values of ^{226}Ra, ^{232}Th, and ^{40}K (Bq/kg) in sites of the present study.

Excessive Lifetime Cancer Risk (ELCR)

Excessive Lifetime Cancer Risk (ELCR) is ranged between 19 – 510, with an average of 163 ± 56: this ten times lower than the world average limit of 1450 (Qureshi et al., 2014). The obtained values of annual gonadal dose varied from 31 to 866 µSv y^{-1}, with a mean value of 272±81 µsv y^{-1}. The mean values were 440 mSv y^{-1} in Nigeria, 2400 µSv y^{-1} for other places in Egypt and 180 µsv $y^{-1}$for Saudi Arabia (Al-kaabi and Al-shimary, 1996). This means that the obtained results are quite safe. The effective dose rate delivered to particular organs (lungs, ovaries, bone marrow, testes and the entire body) from air doses indoors and outdoors are shown in Fig 4. D_{org} values are less than the set limit. We can also conclude that the testes have the highest radiation sensitivity while ovaries have the lowest radiation sensitivity. Therefore, males more affected than females by radiation.

Table 3. The average activity concentration of ^{226}Ra, ^{232}Th, and ^{40}K (Bq/kg) in sediment samples in different countries worldwide.

Country	^{226}Ra	^{232}Th	^{40}K	Reference
Egypt	23.8	19.6	374.9	This work
Venezuela	11.4	14.52	153.43	(Alfonso et al., 2014)
Korea	65.7	91.1	1,005	(Lee et al., 2009)
USA	21.4	45.3	609	(Powell et al., 2007)
Yugoslavia	71	49	520	(Bikit et al., 2005)
Greece	67	45	691	(Papaefthymiou et al., 2007)
Hong Kong	33	48	625	(Zare et al., 2012)
India	34	75	782	(Tripathi et al., 2013)
Turkey	19	-	387	(Ergül et al., 2013)
Malaysia	30	56	420	(Yii et al., 2011)
Spain	12	15	188	(Fernández et al., 2012)
UK	21	45	609	(Alfonso et al., 2014)
Thailand	9	42	963	(Malain et al., 2012)

Table 2. Concentration values of ^{226}Ra, ^{232}Th, and ^{40}K (Bq/kg) and the radiological hazard parameters in each city along the Red Sea coast.

City		Ra-226	Th-232	K-40	Ra_{eq}	D_{rate} (nGy h^{-1})	H_{ex}	I_γ	AEDE (μSv y^{-1})	ELCR (μSv y^{-1})	AGDE (μSv y^{-1})
Quseir	**Min**	1.3	3.9	17.8	9.4	4.3	0.0	0.03	5.3	18.6	30.8
	Max	57.8	47.2	627.9	149.3	69.6	0.4	0.50	85.4	298.8	496.6
	Av	25.6	20.7	240.4	73.7	34.2	0.2	0.25	41.9	146.7	241.0
Safaga	**Min**	7.4	6.3	195.7	31.5	15.3	0.1	0.11	18.7	65.5	110.8
	Max	53.1	33.8	821.0	140.7	65.9	0.4	0.47	80.8	282.8	465.7
	Av	22.2	19.2	477.6	86.5	41.4	0.2	0.29	50.8	177.9	298.9
Hurghada	**Min**	5.1	1.9	36.3	10.6	5.0	0.0	0.04	6.1	21.4	35.0
	Max	52.8	32.2	1119.9	159.4	78.9	0.4	0.53	96.8	338.7	574.3
	Av	19.1	15.1	432.0	74.0	35.7	0.2	0.25	43.8	153.2	258.0
Ras Gharib	**Min**	5.9	7.9	86.3	31.8	14.6	0.1	0.11	17.9	62.6	102.4
	Max	52.4	45.4	1639.6	243.5	118.8	0.7	0.81	145.7	510.0	866.3
	Av	28.0	23.9	381.4	91.5	43.0	0.2	0.31	52.7	184.6	306.1

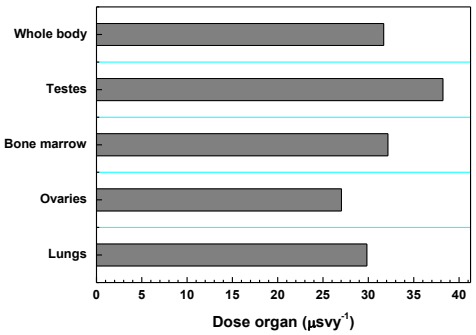

Figure 4. The effective dose rate delivered to particular organs (lungs, ovaries, bone marrow, testes and the entire body) from air doses outdoors.

Conclusions

The activity levels and distribution of natural terrestrial radionuclides of ^{226}Ra, ^{232}Th, and ^{40}K were measured by a gamma-ray spectrometry system in sediment samples collected from 12 points in 4 cities along the Egyptian Red Sea coast. The activity concentrations of ^{226}Ra, ^{232}Th and ^{40}K in the studied sediments were found to be normal. Our results suggest that the variation in grain-size distribution is one of the most important factors influencing the spatial variations of ^{226}Ra, ^{232}Th and ^{40}K in sediments. The extracted values are, in general, comparable to the corresponding ones obtained from other countries, and they all fall within the average worldwide ranges. All measured radiological parameters are lower than the permissible limit. Hence harmful radiation effects as a result of the natural radioactivity of beach sediments do not pose a danger to the public and tourists going to the beaches for recreation or to sailors and fishermen involved in activities in the area. This study can be used as a baseline for future investigations: the data obtained in this study may also be useful for natural radioactivity mapping and can be used as reference data for monitoring possible radioactivity pollution in the future.

Al-kaabi, M.A., Al-shimary, A., 1996. Study of the radiological doses and hazard indices in soil samples from Karbala city , *Iraq Abstract* : 1–9.

Alfonso, J.A., Pérez, K., Palacios, D., Handt, H., LaBrecque, J.J., Mora, A., Vásquez, Y., 2014. Distribution and environmental impact of radionuclides in marine sediments along the Venezuelan coast. *J. Radioanal. Nucl. Chem*. 300, 219–224.

Beretka, J., Mathew, P.J., 1985. Natural radioactivity of australian building materials, industrial wastes and by-products. *Health Phys*. 48, 87–95.

Bikit, I., Varga, E., Čonkić, L., Slivka, J., Mrda, D., Ćurčić, S., Žikić-Todorović, N., Vesković, M., 2005. Radioactivity of the Bega sediment - Case study of a contaminated canal. *Appl. Radiat. Isot.* 63, 261–266.

Darwish, D.A.E., Abul-Nasr, K.T.M., El-Khayatt, A.M., 2015. The assessment of natural radioactivity and its associated radiological hazards and dose parameters in granite samples from South Sinai, *Egypt. J. Radiat. Res. Appl. Sci.* 8, 17–25.

Degerlier, M., Ozger, G., 2008. Assessment of gamma dose rates in air in Adana/Turkey. *Radiat. Prot. Dosimetry* 132, 350–356.

El-Gamal, A., Nasr, S., El-Taher, A., 2007. Study of the spatial distribution of natural radioactivity in the upper Egypt Nile River sediments. *Radiat. Meas.* 42, 457–465.

El-Taher, A., Zakaly, H.M.H., Elsaman, R., 2018. Environmental implications and spatial distribution of natural radionuclides and heavy metals in sediments from four harbours in the Egyptian Red Sea coast. *Appl. Radiat. Isot.* 131, 13–22.

El Mamoney, M.H., Khater, A.E.M., 2004. Environmental characterization and radio-ecological impacts of non-nuclear industries on the Red Sea coast. *J.*

Environ. Radioact. 73, 151–168.

Ergül, H.A., Belivermiş, M., Kiliç, Ö., Topcuoğlu, S., Çotuk, Y., 2013. Natural and artificial radionuclide activity concentrations in surface sediments of Izmit Bay, Turkey. *J. Environ. Radioact.* 126, 125–132.

González-Fernández, D., Garrido-Pérez, M.C., Casas-Ruiz, M., Barbero, L., Nebot-Sanz, E., 2012. Radiological risk assessment of naturally occurring radioactive materials in marine sediments and its application in industrialized coastal areas: Bay of Algeciras, Spain. *Environ. Earth Sci.* 66, 1175–1181.

Gulan, L., Milenkovic, B., Zeremski, T., Milic, G., Vuckovic, B., 2017. Persistent organic pollutants, heavy metals and radioactivity in the urban soil of Priština City, Kosovo and Metohija. *Chemosphere* 171, 415–426.

Janković, M., Todorović, D., Savanović, M., 2008. Radioactivity measurements in soil samples collected in the Republic of Srpska. *Radiat. Meas.* 43, 1448–1452.

Lee, K.Y., Yoon, Y.Y., Cho, S.Y., Ko, K.S., Kim, Y., 2009. Regional characteristics of naturally occurring radionuclides in surface sediments of Chinese deserts and the Keum River area of Korea. *J. Radioanal. Nucl. Chem.* 281, 287–290.

Malain, D., Regan, P.H., Bradley, D.A., Matthews, M., Al-Sulaiti, H.A., Santawamaitre, T., 2012. An evaluation of the natural radioactivity in Andaman beach sand samples of Thailand after the 2004 tsunami. *Appl. Radiat. Isot.* 70, 1467–1474.

Nasr, M.A. and D.P., 2003. The Regional Organization for the Conservation of the Environment of the Red Sea and Gulf of Aden. Jeddah.

Njinga, R.L., Tshivhase, V.M., 2016. Lifetime cancer risk due to gamma radioactivity in soils from Tudor Shaft mine environs, South Africa. J. Radiat. Res. Appl. Sci. 9, 310–315. https://doi.org/10.1016/j.jrras.2016.02.003

O'Brien, K., Sanna, R., 1976. The Distribution of Absorbed Dose-rates in Humans from Exposure to Environmental Gamma Rays. *Health Phys.* 30, 71–78.

Papaefthymiou, H., Papatheodorou, G., Moustakli, A., Christodoulou, D., Geraga, M., 2007. Natural radionuclides and 137Cs distributions and their relationship with sedimentological processes in Patras Harbour, Greece. *J. Environ. Radioact.* 94, 55–74.

Powell, B.A., Hughes, L.D., Soreefan, A.M., Falta, D., Wall, M., DeVol, T.A., 2007. Elevated concentrations of primordial radionuclides in sediments from the Reedy River and surrounding creeks in Simpsonville, South Carolina. *J. Environ. Radioact.* 94, 121–128.

Qureshi, A.A., Tariq, S., Din, K.U., Manzoor, S., Calligaris, C., Waheed, A., 2014. Evaluation of excessive lifetime cancer risk due to natural radioactivity in the rivers sediments of Northern Pakistan. *J. Radiat. Res. Appl. Sci.* 7, 438–447.

Taskin, H., Karavus, M., Ay, P., Topuzoglu, A., Hidiroglu, S., Karahan, G., 2009. Radionuclide concentrations in soil and lifetime cancer risk due to gamma radioactivity in Kirklareli, Turkey. *J. Environ. Radioact.* 100, 49–53.

Taylor, K.G., Owens, P.N., 2009. Sediments in urban river basins: A review of sediment-contaminant dynamics in an environmental system conditioned by human activities. *J. Soils Sediments* 9, 281–303.

Tripathi, R.M., Patra, A.C., Mohapatra, S., Sahoo, S.K., Kumar, A. V., Puranik, V.D., 2013. Natural radioactivity in surface marine sediments near the shore of Vizag, South East India and associated radiological risk. *J. Radioanal. Nucl. Chem.* 295, 1829–1835.

UNSCEAR, 2008. Sources, Effects and Risks of Ionizing Radiation, Radiation Research. New York,.

Uosif, M A M, Hashim, M., Issa, S., Tamam, M., Zakaly, H.M., 2016. Natural Radionuclides and Heavy Metals Concentration of Marine Sediments in Quseir City and Surrounding Areas, Red Sea Coast-Egypt. *Int. J. Adv. Sci. Technol.* 86, 9–30.

Uosif, M. A. M, Issa, S., M.H. Zakaly, H., Hashim, M., Tamam, M., 2016. The Status of Natural Radioactivity and Heavy Metals Pollution on Marine Sediments Red Sea Coast, At Safaga, Egypt. *J. Nucl. Physics, Mater. Sci. Radiat. Appl.* 3, 191–222.

Wijesiri, B., Liu, A., Deilami, K., He, B., Hong, N., Yang, B., Zhao, X., Ayoko, G., Goonetilleke, A., 2019. Nutrients and metals interactions between water and sediment phases: An urban river case study. *Environ. Pollut.* 251, 354–362.

Yii, M.W., Wan Mahmood, Z.U.Y., Ahmad, Z., Nurrul, N.A., Ishak, K., 2011. NORM activity concentration in sediment cores from the Peninsular Malaysia East Coast Exclusive Economic Zone. *J. Radioanal. Nucl. Chem.* 289, 653–661.

Zare, M.R., Mostajaboddavati, M., Kamali, M., Abdi, M.R., Mortazavi, M.S., 2012. 235U, 238U, 232Th, 40K and 137Cs activity concentrations in marine sediments along the northern coast of Oman Sea using high-resolution gamma-ray spectrometry. *Mar. Pollut. Bull.* 64, 1956–1961.

Mass balance and latest fluxes of radiocaesium and tritium derived from Fukushima accident in the western North Pacific Ocean and coastal regions of Japan

Michio Aoyama[1], Daisuke Tsumune[2], Yayoi Inomata[3], Yutaka Tateda[2]

[1] Faculty of Life and Environmental Sciences, Univ. of Tsukuba, 305-8577, Japan
[2] Environmental Science Research Laboratory, Central Research Institute of Electric Power Industry, 1646 Abiko, 270-1194, Japan
[3] Institute of Nature and Environmental Technology, Kanazawa University, Kanazawa, 920-1192, Japan
Keywords: Radiocaesium, tritium, Fukushima accident, North Pacific Ocean, coast region of japan
Presenting author, e-mail: michio.aoyama@ied.tsukuba.ac.jp

Total amount of release radionuclides to the environment from the FNPP1 accident in March 2011 might be one of the big concerns about the FNPP1 accident as well as impact to human and non-human biota. In this paper, 1) we summarize total amount of released radiocaesium from the FNPP1 accident and mass balance of FNPP1 derived radiocaesium in the North Pacific Ocean and 2) present latest status of radiocaecium and tritium in the coastal region in Japan including close to FNPP1.

Mass balance of radiocaesium is a strong constrain to understand environmental impact of FNPP1 released radionuclides as below,

$\Sigma R_i = \Sigma I_j$ (1)

where R_i are released amount to each domain and I_j are inventory in each domain and

i: 1=atmosphere, 2=direct discharge

j: 1=atmosphere (now zero due to short residence time), 2= land, 3=ocean, 4=sediment 5= biota (negligible because maximum estimate of radiocaesium in biota based on fish catch amount of 20×10^6 kg around Fukushima and assuming an activity of 1×10^4 Bq kg^{-1} give us order around GBq.)

$R_1+R_2=I_1+I_2+I_3+I_4+I_5=<$total in the core (2)

We already proposed (Aoyama 2019) consensus values of Fukushima derived radiocaseum in the environments as below combining our results with other researchers.

1) R_1:Atmospheric release: 15-20 PBq , 2) R_2:Direct discharge: 3-6 PBq , 3) Atmospheric deposition in the North Pacific: 12-15 PBq, 4) I_2:Total on land: 3-6 PBq, 5) I_3:Total in the North Pacific Ocean: 15-18 PBq, 6) I_4:In the sediment: 130 ± 60 TBq.

The transport amount of ^{137}Cs from land to ocean were very small compared I[2], land deposition, and estimated to be 10–12 TBq y^{-1}.

Inomata et al. (Inomata et al. 2018) also discussed about distributions of radiocaesium derived from FNPP1 accident and the radiocaesium inventory in the surface layer and the subducted amount into the CMW were 8.6 ± 1.5 PBq and 2.5 ± 0.9 PBq, respectively. Radiocaesium inventory in the STMW was 4.2 ± 1.1 PBq (Kaeriyama et al. 2016) and the integrated amount of FNPP1-derived ^{137}Cs that entered the SOJ from STMW until 2017 was estimated to be 0.27 ± 0.02 PBq (Inomata et al., this conference).

Both at the inside the port (Monoageba) and 56N canal of FNPP1, the temporal variation of ^{137}Cs activity concentration are similar and ^{137}Cs activity concentration was low in winter (January - February) and high in summer-fall (July - October). There may be originated from the same source. The ^{137}Cs activity concentration in the port drops about one order of magnitude lower when the installation of the sea side barrier wall in 2015, the change at 56 N canal did not follow, so the leakage route to the port and 56N canal might be the same source and the routes of leakage may be different. After 2016 annual average of ^{137}Cs activity concentration at 56N canal were 100-140 Bq m^{-3} until 2018, which correspond 2-2.8 GBq day^{-1} flux of ^{137}Cs to open water from FNPP1 site.

Tritium activity concentration in Tomioka River decreased from ca. 1000 Bq m^{-3} in 2013 to ca. 400 Bq m^{-3} in 2018. Tritium activity concentration in seawater collected at Tomioka did not change and ranged from 90 to 160 Bq m^{-3} during the period from 2014 to 2018. Observed good linear relationship between ^{137}Cs and tritium in 2014 indicates that the source of both radionuclides should be liquid form and originated from same place.

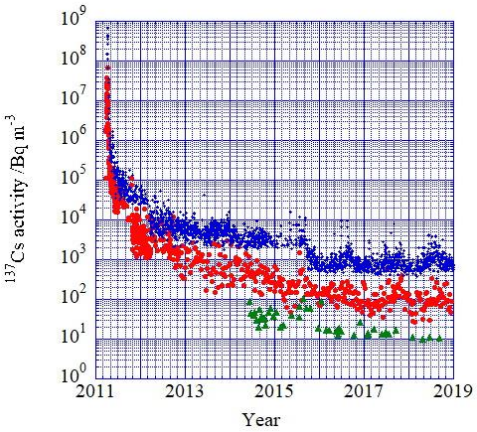

Figure 1. Temporal variations of ^{137}Cs activity concentrations. Diamond: Monoageba in the port of FNPP1, Square: 56North canal, Triangle: Tomioka.

Aoyama, M. (2019), 'Fukushima radionuclides in the marine environment from coastal region of Japan to the Pacific Ocean through the end of 2016', *Progress in Nuclear Science and Technology*, 6, 1-7.

Inomata, Y., et al. (2018), 'Estimate of Fukushima-derived radiocaesium in the North Pacific Ocean in summer 2012', *Journal of Radioanalytical and Nuclear Chemistry*, 318 (3), 1587-96.

Kaeriyama, H., et al. (2016), 'Intrusion of Fukushima-derived radiocaesium into subsurface water due to formation of mode waters in the North Pacific', *Sci. Rep.*, 6, 22010:DOI: 10.1038/srep10.

An ecosystem approach is mandatory to properly assess ecological risk from radiation

F. Bréchignac[1]

[1]Institute of Radioprotection and Nuclear Safety (IRSN) & International Union of Radioecology (IUR), Direction general, BP 17, 92262 Fontenay-aux-Roses cedex, France
Keywords: radiation, ecosystem, ecological risk assessment, environment protection
francois.brechignac@irsn.fr

There is still no consensus within the scientific community as to whether or not radioactive environmental contamination, such as resulting from the Chernobyl or Fukushima disasters, is promoting a deleterious ecological impact. This situation is critical as it is prone to favor unjustified distrust from society with respect to the ability of authorities to take adequate measures for mastering nuclear risk and protecting the environment. It is argued that one key challenge for radiation research when facing this general context is to widen traditional radiation biology, focused on DNA and cells of individual organisms, towards radiation ecology featuring an ecosystem-centered conceptualization. If life is driven by processes that act at subsystem level, i.e. the molecular engineering that founds the organisms' physiology, it depends as well on processes that act at system level, i.e. emergent properties of the ecosystem dimension such as life support, since both types of processes have jointly emerged through evolution. Organisms and populations of species only exist as embedded within an ecosystem featuring multispecies interactions (Figure 1).

Due to this basic consideration, environment protection measures that are developed exclusively from subsystem understanding (dose-response curves established for individual organisms) for practical reasons, as in current radioprotection guidance, may actually miss their protection objective and explain some recently reported discrepancies in assessing ecological impact (Figure 2).

A few examples will be discussed to illustrate that ecological impact of radiation (as well as of any stressor) cannot easily be understood if not addressing the issue also from an ecocentric perspective.

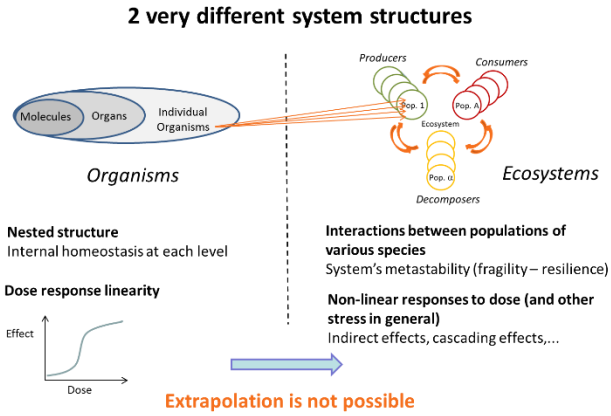

Figure 1: Organisms versus ecosystems: different responses to stress.

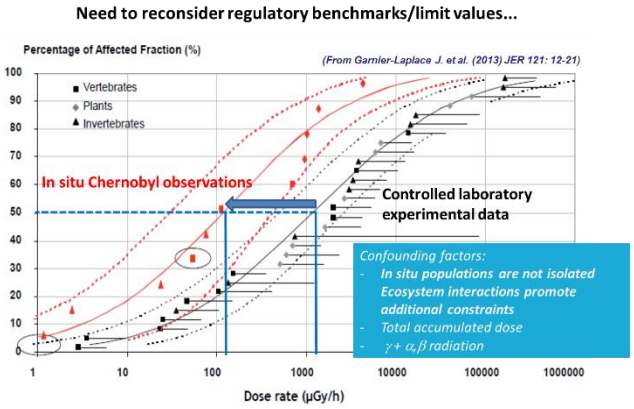

Figure 2. Mismatch between controlled laboratory experiments and field data obtained in Chernobyl contaminated territories.

Low background neutron activation: a high sensitivity technique for long-lived radionuclides determination in rare events physics experiments

M. Clemenza[1,2]

[1] INFN, Sezione di Milano-Bicocca, Milano, Lombardia, 20126, Italy
[2] Dipartimento di Fisica "G. Occhialini", Università degli Studi di Milano-Bicocca, Milano, Lombardia, 20126, Italy
Keywords: ^{232}Th, ^{238}U, Low background NAA, Physics of Rare Events,
Presenting author email: massimiliano.clemenza@mib.infn.it

Among the most recent developments in the elementary particles physics and in particular in astro-particle physics, the search for extremely rare events is of much importance. The direct search for dark matter [1], the experiments concerning neutrino physics (oscillation [2], solar neutrino [3]) and in particular the research on neutrino-less double beta decay NLDBD [4], need to use high sensitivity analytical techniques which are able to measure very low levels of radioactivity present in all components of experimental apparatus.

In support of these stringent requirements, there is a group of analytical techniques, the so-called "low level counting techniques" LLCT [5], that have appeared with the measure of very weak activity in the late 1940s by Willard F. Libby when he developed the radiocarbon dating method (^{14}C) [6]. These techniques are powerful tools in many different research fields such as geological and archaeological dating, measurements of natural and anthropogenic radioactivities in environment for radio-ecological study and nowadays they are increasingly applied in the study of fundamental particles physics. The capability of these techniques to measure very weak radioactivities and to continuously enhance the sensitivity to detect feeble signals characterized by low counting rates above the radioactive background has become more stringent than ever, in particular in the so-called Rare Events Underground Physics Experiments. Common radioactive background can often hide the signatures of extremely rare processes like those sought in astro-particle physics experiments. In order to increase the sensitivity of these experiments the constraints in radio-purity of the constituent materials are become more and more stringent, especially for primordial radionuclides which are always present in the experimental set-up; their decay products emit radiations which can have the same energy signature of rare processes such as neutrino-less double beta decay.

LBNAA provides very low detection limits for primordial radionuclides as demonstrated by the successful applications by several astro-particle physics collaborations (BOREXINO, CUORE, EXO, SUPER-NEMO, KAMLNAD) in radio pure materials selection to be utilized in the construction of rare events physics experiments. In particular, LBNAA may be really advantageous compared to ICP-MS and AMS as no preirradiation treatment is required avoiding possible contamination due to sample treatments. The possibility to improve detection limits by targeted post-irradiation radiochemistry can be utilized as complementary technique to the ultra low level gamma-ray spectrometry. Low-background neutron activation analysis has proven to be a very useful analytical method for the selection of low-radioactive materials used for the realization of "rare-events" physics experiments. The present work [7] reviews the main results obtained with neutron activation in the radio-pure materials selection by several research groups involved in underground astro-particle physics experiments [7].

1. Baudis L (2018) The search for dark matter. Eur Rev 26(1):70–81. https ://doi.org/10.1017/S1062 79871 70007 83

2. Capozzi F et al (2014) Status of three-neutrino oscillation parameters. *Phys Rev D* 89:093018

3. Nakahata M (2005) Future solar neutrino experiments. In: Suzuki Y, Nakahata M, Itow Y, Shiozawa M, Obayashi Y (eds) Neutrino oscillations and their origin. World Scientific, Singapore, pp 42–49. https ://doi.org/10.1142/97898 12701 824_0006

4. Avignone Frank T III, Elliott SR, Engel J (2008) Double beta decay, Majorana neutrinos, and neutrino mass. *Rev Mod Phys* 80:481

5. Oeschger H, Wahlen M (1975) Low level counting. *Tech Ann Rev Nucl Sci* 25:423–463

6. Arnold J, Libby W (1951) Radiocarbon dates. *Science*113(2927):111–120

7. Clemenza M. (2018) Low background neutron activation: a high sensitivity technique for long-lived radionuclides determination in rare events physics experiments ISSN 0236-5731 *J Radioanal Nucl Chem* DOI 10.1007/s10967-018-6333-z

Atmospheric impacts of the Fukushima Daiichi NPP accident: a review of eight-years studies in Japan

K. Hirose[1]

[1]Sophia University (retired), Tsukuba, Japan
Keywords: Fukushima, radiocesium, effects
e-mail: hirose45037@mail2.accsnet.ne.jp

In 2011, a severe nuclear accident happened in FDNPP after a gigantic earthquake and resulting destructive tsunami (Povinec et al., 2013). The major atmospheric emission of radionuclides started on 12 March 2011 and continued to the end of March 2011, although several peaks of radionuclide release occurred due to explosions in the FDNPP. Dominant radionuclides were volatile ones such as radioiodine and radiocesium (Total releases; ^{133}Xe: 11,000 PBq, ^{131}I: 160 PBq, ^{134}Cs: 18 PBq, ^{137}Cs: 15 PBq). About 20 % of radiocesium emitted in atmosphere was deposited on Honshu, the Japan's main island, whereas the remaining 80 % were transported towards the North Pacific Ocean. As a result of radioactivity deposition due to the FDNPP accident, high radioactive contamination area with a ^{137}Cs level exceeding 185 kBq m^{-2} spread approximately 1700 km^2 at Fukushima Prefecture and ^{137}Cs deposits exceeding 10 kBq m^{-2} extended over 24,000 km^2 [7]. The radioactive cloud spread in the northern hemisphere (as did the Chernobyl accident) where FDNPP-derived ^{133}Xe (half-life: 5.25 d), ^{131}I (half-life: 8.02 d), ^{134}Cs (half-life: 2.06 y) and ^{137}Cs (half-life: 30.1 y) were detected in surface air in North America, Europe and other regions by national and CTBTO networks (Hirose, 2016). The atmospheric effects of the FDNPP-derived ^{137}Cs rapidly decreased at a time scale of about 10 days and, after that its decrease rates were slowdown. The atmospheric effect continued more than 7 years after the FDNPP accident, although the area observed its effect, including Kanto plain where is the greatest population in Japan, covered less than 300 km from the FDNPP. The atmospheric effects of the FDNPP accident are still an ongoing issue. In this chapter, we focus on Japanese atmospheric monitoring activities of the FDNPP accident and describe its atmospheric effects observed in Japan.

Initial atmospheric release from FDNPP accident: radionuclide activities in the air

Outside of the FDNPP site, detailed features of FDNPP-derived ^{137}Cs in surface air of Fukushima Prefecture and Kanto area were depicted by analyzing filter-tapes of operational air pollution monitoring stations, in which continuous hourly-resolution time series of ^{137}Cs activities in surface air were obtained during the period of 12 – 25 March, 2011 just after the FDNPP accident (Tsuruta et al., 2018). Ten ^{137}Cs peak events were observed at Futaba (about 3.2 km northwest FDNPP) and Naraha (17.5 km south FDNPP) sites during the corresponding period. The highest ^{137}Cs activity in surface air (13.6 kBq m^{-3}) occurred at 15:00 on 12 March after a vent operation of reactor Unit 1.

Physical and chemical properties of radionuclide-bearing particles

For the FDNPP accident, hot particles have been discovered in airborne dust collected during the period of 15-16 March 2011 and soil by using gamma spectrometry, autoradiography and scanning electron microscopy with energy dispersive X-ray analysis. The FDNPP-derived hot particles in dust were characterized as spherical radiocesium-bearing particles (diameter: 2.6 μm), which were water less soluble than sulfate particles; radiocesium in hot particles were embedded into silicate.

Post-accident effects of the FDNPP-derived radionuclides

After rapid decrease of the FDNPP-derived radionuclides during the period of April to June 2011, the decrease rate of the surface ^{137}Cs slowed down and the surface ^{137}Cs level was still higher than pre-accident level at stations within about 200 km form the FDNPP until the end of 2016 (Doi et al., 2019). As did ^{137}Cs activities in surface air, the monthly ^{137}Cs deposition rates in the corresponding area until the end of 2018 was more than one order of magnitude greater than the pre-Fukushima level. Especially, the annual ^{137}Cs deposition in 2017 increased that in the previous year at several monitoring sites. To explain these findings, it is supposed that the post-accident ^{137}Cs in surface air and deposition is governed by resuspension and the atmospheric emission from the FDNPP including sporadic release events. However, detail processes remain to be solved.

Hirose, K. 2016. Fukushima Daiichi Nuclear Power Plant accident: Atmospheric and oceanic impacts over the five years. *J. of Environ. Radioact.* 157, 113-130.

Povinec, P.P., Hirose, K., Aoyama, M. 2013. Fukushima Accident: Radioactivity Impact on the Environment. New York, Elsevier.

Tsuruta, H., Oura, Y., Ebihara, M., Moriguchi, Y., Ohara, T., Nakajima, T. 2018. Time-series analysis of atmospheric radiocesium at two SPM monitoring sites near the Fukushima Daiichi Nuclear Power Plant just after the Fukushima accident on March 11, 2011. *Geochem. J.* 52, 103-121.

Doi, T., Takagi, M., Tanaka, A., Kanno, M., Dokiya, Y., Tao, Y., Masumoto, K. 2019. The variation of atmospheric radioactive caesium concentration from Fukushima Dai-ichi Nuclear Power Plant accident in Tsukuba and Iitate, and factors controlling its high concentration events. *Radioisotopes*. 68, 83-104.

Environmental radioactivity: analysis, distribution and trace studies of long-lived radionuclides

Xiaolin Hou [1, 2, 3]

[1] Technical University of Demark, Center for Nuclear Technologies Risø campus, Roskilde, 4000, Denmark
[2] Xi'an AMS Center, State Kay Laboratory for Loess and Quaternary Geology, Institute of Earth Environment, CAS, Xi'an, 710061, China
[3] School of Nuclear Science and Technology, Lanzhou University, Lanzhou, China
Keywords: Radionuclides, Environmental radioactivity, Environmental trace, soil, sediment, precipitation,
Presenting author, e-mail: xiho@dtu.dk

Since 1940's, large amount of radioactive substrances have been released to the environment through human nuclear activities, such as atmospheric nuclear weapons tests, reprocessing of spent nuclear fuel, operation of nuclear power plants and other nuclear facilities, nuclear accidents. After entered to the environment, these radionuclides were dispersed in the ecosystem and participate in the biogeochemical cycles with the stable isotopes of the corresponding elements. Besides the radiation impact in the highly contaminated regions, these radionuclides can be used as tracer to investigate the environmental process, such as the dispersion and migration pathway of pollutions and nutrition. Reliable determination of low-level radionuclides of and their species in various environmental media using radiochemical separation combined with sensitive measurement using radiometric and mass spectrometric techniques can provide the information of their distribution, sources and transport pathway. By analysis of time series samples, such as sediment core, ice core, tree rings, and coral samples, the variation of radionuclides with time can be obtained, which can be used to reconstruct the contribution and impact of the corresponding human nuclear activities. Based on the properties of each radionuclides, it can be also used to investigate the source, transport pathway and sink of different pollutions, and to study its environmental geochemical process. In the recent years, a number of analytical methods have been established in the author's groups, including the determination of ^{129}I, $^{234, 235, 236, 238}$U, $^{239, 240}$Pu in various environmental samples. Samples of soil and sediment cores, vegetation, tree rings, ice cores, time series precipitation and aerosols, river water and seawater collected from all over China and other areas have been analysed in the past years. These samples are being analysed for these radionuclides, which were used for mapping their distribution, and investigation of their source and impact, as well as to tracer environmental process (Zhang & Hou 2019, Zhou et cl. 2018, Zhao et al 2019, Zhang et al. 2017, 2018, Xing et al. 2017). Some aspects of these works are presented.

New development of the analytical method for the determination of low-level radionuclides in the environment using ICP-MS and chemical separation.

Sediment cores collected from high latitude in China to low latitude of south Asia were analysed for ^{129}I, to trace the dispersion of gaseous pollution from Europe to East Asia, and transport from north to south through the interaction of Westerlies and East Asian Monsoon.

Large number of surface soil samples were collected over China and analysed for ^{129}I and isotopes of plutonium and uranium. A large scale distribution of environmental radioactivity was mapped in China. The sources and contributions of different nuclear activities were estimated. The transport pathway, and the parameters influencing the transport, deposition, and retention of radionuclides are explored.

Time series of precipitation and aerosol particles were collected in different locations in China and analysed for ^{129}I, which was used to trace the dispersion and transport pathway of gas pollutions, and the formation of the heavy mist in China.

Zhang W.C., Hou X.L. Level, distribution and sources of plutonium in the coastal areas of China, *Chemosphere*, 2019, 230, 587-595.

Zhao X., Hou X.L., Du J.Z., Fan Y.K. Anthropogenic ^{129}I in the sediment cores in the East China Sea: Sources and transport pathways, *Environmental Pollution*. 2019, 245:443-452.

Zhou W.J., Du Y.J., Hou X.L., Chen P., Zhang L.Y., Fan Y.K., Zhang L., Niu Z.C., Gong G.C., Chen N., Li M. Long-lived radionuclides as chronometers and tracers of environmental processes at the Xi'an Accelerator Mass Spectrometry Center. *Chemical Geology*, 2018, 493:258-265.

Zhang L.Y., Hou X.L., Li., H., Xu, X. A 60-year record of ^{129}I in Taal Lake sediments (Philippines): Influence of human nuclear activities at low latitude region. *Chemosphere*, 2017, 193:1149–1156.

Zhang L.Y., Hou X.L. Cheng P., Chen N., Fan Y.K., Liu Q. Impact of North Korean nuclear weapons test on 3 september 2017 on inland China traced by 14C and 129I. *J. Radioanal. Nucl. Chem*., 2018, 316(1):383-388.

Xing S., Hou X.L., Aldahan A., Possernet G., Shi K.L., Yi P., Zhou W.J. Water circulation and marine environment in the Antarctic traced by speciation of ^{129}I and ^{127}I. *Sci. Rep*. 2017, 7:7726

Measurements of ^{129}I in coastal Pacific Ocean sites in California and US Pacific Northwest sites.

A. J. Timothy Jull[1,2,3*], Ching-Chih Chang[1,2], George S Burr[1,4], Li Cheng[1], Joellen Russell[2], Antra Priyadarshi[5], Mang Lin[5], Dan Crocker[5], Mark Thiemens[5] and Dana Biddulph[1]

[1] University of Arizona AMS Laboratory, University of Arizona, Tucson, AZ, USA
[2] Department of Geosciences, University of Arizona, Tucson, AZ, USA
[3] Isotope Climatology and Environmental Research Centre, Institute for Nuclear Research, Debrecen, Hungary
[4] Department of Geosciences, National Taiwan University Research Center for Future Earth, Taipei, Taiwan
[5]Department of Chemistry, University of California, San Diego, CA, USA.
**Correspondence to: A. J. Timothy Jull (jull@email.arizona.edu)*

Radionuclides such as iodine-129 released from nuclear activities and accidents into the ocean become entrained in surface ocean currents and subsequently are transported for great distances. In June 2011, a few months after the Fukushima Daiichi Nuclear Power Plant disaster, we began a surface ocean ^{129}I monitoring program, with samples from Scripps Pier, La Jolla, California, USA, with the expectation that surface currents originating off the east coast of Japan would eventually carry radionuclides to the La Jolla site. After 8 years of ocean transport, a distinct signal has not yet been positively identified, however we have recorded an interesting systematic seasonal ^{129}I time series record that stems from surface circulation variations along the California coast.

To provide a more comprehensive picture of the ^{129}I budget in coastal surface waters off the west coast of the U.S., we also included ^{129}I data from the Columbia River, and offshore sites along the coast of Washington State. Iodine-129 and other radionuclides are carried by the Columbia River into the Pacific Ocean from the vicinity of the decommissioned Hanford nuclear facility. We find highly elevated ^{129}I/^{127}I values in the Columbia River, downstream from the Hanford site, but this anthropogenic ^{129}I becomes significantly diluted once it reaches the Pacific Ocean. Nonetheless, its imprint persists in surface seawater off the west coast of the U.S. resulting in significantly higher ^{129}I/^{127}I levels than other surface sites in the Pacific Ocean.

This work is supported in part by US National Science Foundation grant EAR133588. AJTJ also acknowledges support by the European Union and the State of Hungary, co-financed by the European Regional Development Fund in the project of GINOP-2.3.2-15-2016-00009 'ICER'.

Radiocaesium contamination in seawater around the Korean Peninsula after Fukushima Nuclear Power Plant accident

S H. Kim[a], S. H. Lee[b*], G. H. Hong[a], H. M. Lee[a]

[a]Marine Environmental Research Center, Korea Institute of Ocean Science and Technology (KIOST), Busan 49111, South Korea
[b]Ionizing Radiation Center, Korea Research Institute of Standards and Science (KRISS), Daejeon, 34113, South Korea
Corresponding Author: Dr. Sang-Han Lee (s.lee@kriss.re.kr)

Surface seawater and deep water were collected in seas around the Korean Peninsula throughout 2011 to 2012 and radiocaesium (^{137}Cs and ^{134}Cs) was measured to evaluate the radioactive contamination level after Fukushima Nuclear Power Plant (FNPP) accident. ^{134}Cs was detected in the surface seawater and deep water around Korean peninsula from March to June 2011. The finding of ^{134}Cs in the seawater is attributable to the FNPP and this is supported by the analysis of air mass back trajectory and atmospheric pressure systems which the Fukushima-derived radiocaesium had predominantly reached South Korea from the west by surface westerlies from 11 March to 5 April. In this study, not only for the activity concentration of ^{134}Cs and ^{137}Cs in the surface and deep water around the Korean Peninsula but also will introduce details of activity concentration change over time before and after Fukushima.

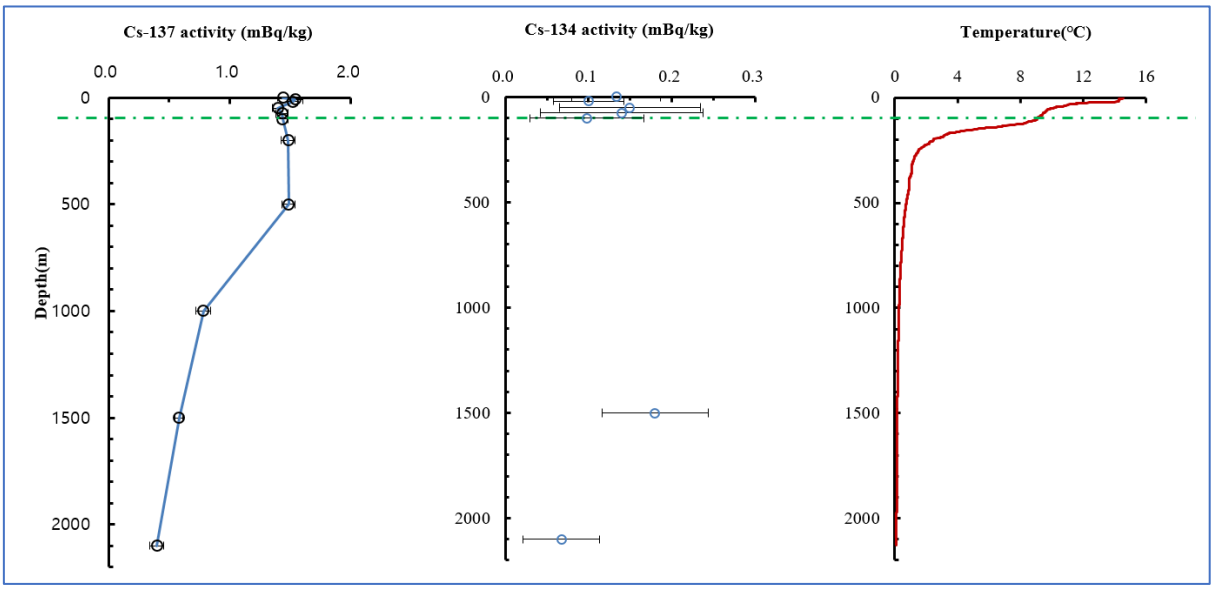

Figure 1 Vertical profiles of ^{134}Cs and ^{137}Cs activity concentration and water temperature at Stn. M (2011-06-01) in the Uleung Basin in the East Sea/Sea of Japan.

Measurements of low activity concentration of Fukushima-derived radiocesium in the western subarctic gyre of the North Pacific Ocean in summer 2017

Y. Kumamoto[1], M. Aoyama[2], Y. Hamajima[3], A. Murata[1]

[1]Research Institute for Global Change, Japan Agency for Marine-Earth Science and Technology, Yokosuka, 2370061, Japan
[2]Institute of Environmental Radioactivity, Fukushima University, Fukushima, 9601296, Japan
[3]Low Level Radioactivity Laboratory, Kanazawa University, Nomi, 9231224, Japan
Keywords: radiocesium, Fukushima accident, North Pacific
Y. Kumamoto, e-mail: kumamoto@jamstec.go.jp

The accident of Fukushima Dai-ichi Nuclear Power Plant (FNPP1) occurred on March 11, 2011, resulted in the release of 20-40 PBq radiocesium (^{134}Cs and ^{137}Cs) into the environment. It is estimated that 70-80% of the FNPP1-derived radiocesium deposited and discharged in the North Pacific Ocean and most of them are dissolved in seawater. Therefore, the FNPP1-derived radiocesium has been spreading throughout the North Pacific along with the surface water currents and diluted by seawater mixing. Previous studies revealed that the radiocesium deposited and discharged in the coastal area of Japan had been transported eastward to the international date line by summer 2012 along with the surface current in the subarctic area of the North Pacific Ocean (Kumamoto et al., 2016). Then, the high-concentration water mass was conveyed eastward continuously and had reached to the eastern subarctic gyre and the west coast of the North American Continent by 2015, about four years after the accident (Smith et al., 2017). On the other hand, in the western subarctic gyre of the North Pacific, the temporal change in the FNPP1-derived radiocesium after 2012 is not clear. We collected seawater samples for radiocesium measurements in the western subarctic gyre in summer 2017, about six years after the accident. Here we present our preliminary results of the radiocesium measurement using a Cs-resin on board.

We collected seawater samples at a station (41ºN/150ºE) during the cruise of R/V "Hakuho Maru" KH-17-3 in June 2017. Because the activity concentration of the FNPP1-derived ^{134}Cs has decreased to less than 1 Bq m^{-3} due to dilution and radioactive decay (its half-life is about 2 years), it should be concentrated before measurement. For the cesium condensation, a resin (potassium nickel ferrocyanate on polyacrylonitrile, KNiFC-PAN) manufactured by Triskem International (Sebesta and Stefula, 1990) was used on board. After adding cesium (^{133}Cs) chloride as a carrier to the seawater sample (concentration was about 100 ppb), about 40 L of seawater sample was passed through 5 ml (about 1 g dry) of the resin at a flow rate of 50 ml min^{-1} to concentrate the radiocesium in the resin. The recovery rate of radiocesium was estimated to be about 95% from the difference in the carrier (^{133}Cs) concentration before and after the cesium condensation. After washing the Cs resin with pure water, activity concentrations of ^{134}Cs and ^{137}Cs were measured using gamma-ray spectrometers (Ge semiconductor detectors) in Low Level Radioactivity Laboratory, Kanazawa University (Hamajima and Komura, 2004).

FNPP1-derived ^{134}Cs was detected at depths shallower than 200 m in the surface mixed layer (0.05~0.14 Bq m^{-3}), which correspond to 0.43~1.19 Bq m^{-3} of the activity concentrations decay-corrected to the accident day. The highest decay-collected concentration, 78.2 Bq m^{-3} was observed in surface water at a station near our station in June 2011 (Buesseler et al., 2012). Then the surface concentration decreased to 26.4 Bq m^{-3} in February 2012 (Kumamoto et al., 2014) and 1.47 Bq m^{-3} in July 2014 (Kumamoto et al., 2017), suggesting an exponential decrease in the FNPP1-derived ^{134}Cs between June 2011 and July 2014. This exponential decrease in the western subarctic gyre is consistent with the corresponding decrease in the eastern subarctic gyre. If the concentration in the west subarctic gyre decreased exponentially by June 2017, it could be 0.04 Bq m^{-3}, which is less than the detection limit. The higher ^{134}Cs concentrations observed in 2017 (0.43~1.19 Bq m^{-3}) indicate (1) re-circulation within the western subarctic gyre and (2) continuous addition from the FNPP1.

Buesseler, K., Jayne, S.R., Fisher et al, 2012. Fukushima-derived radionuclides in the ocean and biota off Japan. *Proc. Natl. Acad. Sci. USA.* 109, 5984-5988.

Hamajima, Y., Komura, K. 2004. Background components of Ge detectors in Ogoya underground laboratory. *Appl. Rad. and Isot.* 61, 179-183.

Kumamoto, Y., Aoyama, M., Hamajima, Y. et al. 2014. Southward spreading of the Fukushima-derived radiocesium across the Kuroshio Extension in the North Pacific. *Sci. Rep.* 4, 4276, doi:10.1038/srep04276.

Kumamoto, Y., Aoyama, M., Hamajima, Y. et al. 2017. Fukushima-derived radiocesium in the western North Pacific in 2014. *J. Radioanal. Nucl. Chem.* 311, 1209-1217.

Kumamoto, Y., Aoyama, M., Hamajima, Y. et al. 2016. Meridional distribution of Fukushima-derived radiocesium in surface seawater along a trans-Pacific line from the Arctic to Antarctic Oceans in summer 2012. *J. Radioanal. Nucl. Chem.* 307, 1703-1710.

Sebesta, F., Stefula, V. 1990. Composite ion exchanger with ammonium molybdophosphate and its properties. *J. Radioanal. Nucl. Chem.* 140, 15-21.

Smith, J.N., Rossi, V., Buesseler, K.O. et al. 2017. Recent transport history of Fukushima radioactivity in the Northeast Pacific Ocean, *Environ. Sci. Technol*. 51, 10494-10502.

Ultra-low background gamma-ray spectrometry and its applications

M. Laubenstein[1]

[1]Istituto Nazionale di Fisica Nucleare, Laboratori Nazionali del Gran Sasso, Via G. Acitelli 22, I-67100 Assergi (AQ), Italy

Keywords: gamma-ray spectrometry, ultra-low background, germanium detectors

Presenting author, e-mail: matthias.laubenstein@lngs.infn.it

The exceptional sensitivity and high resolution of high purity germanium detectors in gamma-ray spectrometry and their use in underground laboratories (Laubenstein et al., 2004) has increasing application because of the important science and technology that they allow to be studied.

In fundamental physics their application is focussed on rare phenomena, e.g. double beta decay, rare nuclear decays and Dark Matter search. In the past years there has been a growing number of underground measurements also in other fields such as environmental monitoring, surveillance of nuclear activities, benchmarking of other physical techniques, Life Science and material selection for equipment, which require materials with extremely low levels of radioactivity.

Here the state of the art in ultra-low background gamma-ray spectrometry with high purity germanium detectors is described (Laubenstein, 2017). Applications in underground laboratories are presented, especially measurements of very small samples (Povinec et al., 2015), searches for rare nuclear decays (Laubenstein, 2019), method validation (Nisi et al., 2009) and radiopurity (Aprile et al., 2017) as well as activation studies (Tzika et al., 2017) will be shown and explained on examples.

An outlook will be given on what contribution this technique can bring in the future to these and other fields of science.

M. Laubenstein et al., Underground measurements of radioactivity, *Appl. Radiat. Isot.* 61, No. 2-3, 167 (2004).

M Laubenstein, Screening of materials with high purity germanium detectors at the Laboratori Nazionali del Gran Sasso, *Int. J. Mod. Phys.* A 32, N. 30, 1743002 (2017)

P.P. Povinec et al., Cosmogenic radionuclides and mineralogcal properties of the Chelyabinsk (LL5) meteorite: What do we learn about the meteoroid? *Meteor. Planet. Sci.* 50, Issue 2, p. 273 (2015)

M. Laubenstein et al., A new investigation of half-lives for the decay modes of ^{50}V, *Phys. Rev. C* 99, 045501 (2019).

S. Nisi et al, Comparison of inductively coupled mass spectrometry and ultra-low level gamma-ray spectroscopy for ultra low background material selection, *Appl. Radiat. Isot.* 67, Issue 5, p. 828 (2009)

Xenon1Tollab. (E. Aprile et al.), Material radio assay and selection for the XENON1T dark matter experiment, Eur. *Phys. J. C* 77, p. 890 (2017).

F. Tzika etal., Coordinated underground measurements of gamma-ray emitting radionuclides for plasma physics research, ppl. *Radiat. Isot.* 126, p. 121 (2017).

Fifty years of Radiocarbon applications in modern Carbon cycle research

I. Levin, S. Hammer

Institut für Umweltphysik, Heidelberg University, Heidelberg, 69120, Germany
Keywords: Radiocarbon, global carbon cycle, fossil fuel CO_2
Ingeborg Levin, Ingeborg.Levin@iup.uni-heidelberg.de

Atmospheric nuclear weapon testing during the cold war in the 1950s and 1960s has been worrying in many aspects, however, it has been extremely beneficial for environmental sciences [Levin and Hesshaimer, 2000]. The artificial production of more than 6 x 10^{28} atoms or about 0.6 tons of ^{14}C, leading to a doubling of the $^{14}C/C$ ratio in tropospheric CO_2 of the Northern Hemisphere has generated a prominent spike in 1963 (Figure 1). This "bomb-spike" could be used as transient tracer in all compartments of the carbon cycle [Levin et al., 2010], but also to study atmospheric dynamics such as inter-hemispheric and stratosphere-troposphere air mass exchange. Today, the transient bomb-radiocarbon signal has levelled-off, and the anthropogenic input of radiocarbon-free fossil fuel CO_2 into the atmosphere has become the dominant driver, now diluting the $^{14}C/C$ ratio in tropospheric CO_2 by several permil each year. While this new transient atmospheric signal is often too small for tracer applications, it may still help scrutinising the total global release of fossil fuel CO_2 into the atmosphere. In this presentation we will review some prominent examples where the bomb ^{14}C disturbance has been successfully used to study dynamic processes in the carbon cycle and discuss current activities applying this unique isotope tracer for continental scale carbon cycle budgeting [Levin and Rödenbeck, 2008; Levin et al., 2011].

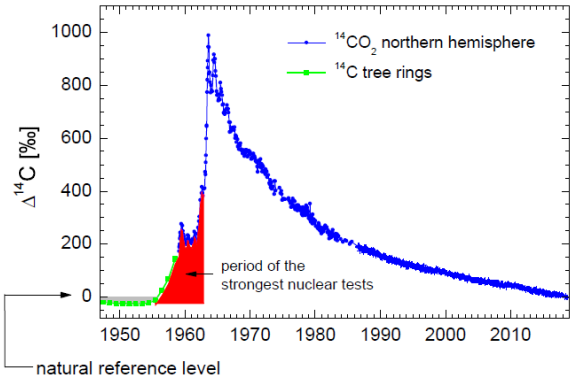

Figure 1: Long-term development of the $^{14}C/C$ ratio in atmospheric CO_2 in the Northern Hemisphere given as permil-deviation from an internationally accepted reference material. Zero $\Delta^{14}C$ approximately corresponds to the natural $^{14}C/C$ ratio in atmospheric CO_2, i.e. the equilibrium value between production in the upper atmosphere and decay in all carbon compartments.

Levin, I., Hesshaimer, V. 2000. Radiocarbon – a unique tracer of global carbon cycle dynamics. *Radiocarbon. 42,* 69-80.

Levin, I., Rödenbeck, C. 2008. Can the envisaged reductions of fossil fuel CO_2 emissions be detected by atmospheric observations? *Naturwissenschaften. 95(3),*203-208, DOI. 10.1007/s00114-007-0313-4.

Levin, I., Naegler, T., Kromer, E., Diehl, M., Francey, R. J., Gomez-Pelaez, A.J., Schäfer, A., Steele, L. P., Wagenbach, D., Weller, R., and Worthy, D. E. 2010. Observations and modelling of the global distribution and long-term trend of atmospheric $^{14}CO_2$. *Tellus.* 62B, 26-46, DOI: 10.1111/j.1600-0889.2009.00446.x.

Levin, I., Hammer, S., Eichelmann, E., Vogel, F. 2011. Verification of greenhouse gas emission reductions: The prospect of atmospheric monitoring in polluted areas. *Philosophical Transactions A.* 369, 1906-1924.

Carbon isotopes as tracers of organic and inorganic carbon in Baltic Sea sediments

G. Lujanienė

Department of Environmental Research, SRI Center for Physical Sciences and Technology, Vilnius, Savanoriu ave. 231, LT-02300, Lithuania
Keywords: Baltic Sea sediments, $\Delta^{14}C_{TOC}$, *Pseudomonas putida*, carbon sources
Presenting author, e-mail: galina.lujaniene@ftmc.lt

The objective of this study has been to estimate sources and fate of organic carbon (OC) in the coastal and open Baltic Sea as well as to use radiocarbon and lipid-derived biomarkers to trace toxic organic substances at chemical warfare agents (CWA) dumpsite. It has been expected that the release of CWA will lead to changes in carbon concentrations and in carbon isotope ratios since CWA were produced before World War II from petroleum, natural gas, and petroleum distillates and from coal. It was assumed that changes in the ratio of carbon isotopes could be a sign of CWA leakage into the environment.

Bottom sediment samples were collected during different sampling campaigns in 2010 – 2016 in Gotland Deep CWA dumping site, in the open sea and in the Lithuanian coastal region.

$\Delta 14C_{TOC}$ measurements in sediments and in different classes of organic substances (humic acids, total lipid extracts (TLE), glycol- and phospholipids) were carried out at the AMS facility (1.0 MV HVE Tandetron) in the Department of Geosciences of National Taiwan University (NTUAMS).

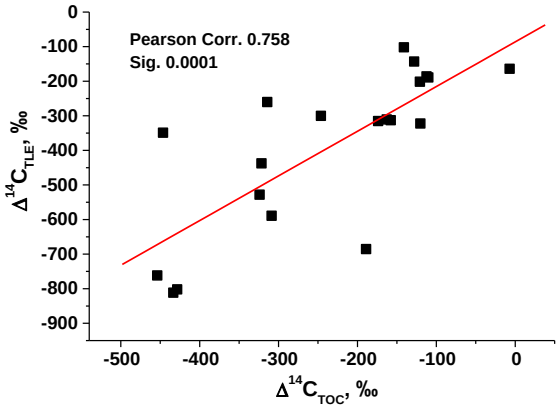

Figure 1. $\Delta^{14}C_{TOC}$ versus $\Delta^{14}C_{TLE}$ in bottom sediments.

Distributions of $\Delta^{14}C$ studied in bottom sediments in the Curonian Lagoon and in the open Baltic Sea indicated wide variations of $\Delta^{14}C_{TOC}$ (from –446.1‰ to –6.7‰) while $\Delta^{14}C_{TLE}$ values were more depleted with the average value of –536.0‰ (Figure 1) in bottom sediments (Lujanienė et al., 2015). The most depleted $\Delta^{14}C_{TOC}$ and $\Delta^{14}C_{TLE}$ values in bottom sediment samples were found at the CWA dumpsite located at the Gotland Deep and were attributed to the different carbon sources. Organic carbon sources in the sediments estimated using an End Member (EM) mixing-model for three sources of OC – continental, marine and fossil – on average were as follows: 26%, 53%, and 21% of the total, respectively, while the content of fossil carbon sources in the Gotland Deep sediments was higher (32%), as compared to the near shore zone with 13% (Lujanienė et al., 2016).

Plutonium isotope ratios have also been used to identify pollution sources in the coastal zone and in the open waters of the Baltic Sea (Lujanienė et al., 2017).

Microbial communities consisting of fungi and bacteria are responsible for the degradation, immobilization or mineralization of organic matter and, thus, could affect the carbon pathways in the marine environment. Estimation of effect of utilization of chemical compounds with different radiocarbon content on dating of sediments as well as $\Delta^{14}C$ analysis of organic fractions such as total lipid extracts and phospholipid-derived biomarkers have been applied.

The laboratory experiments on differential carbon utilization by *Pseudomonas putida* isolated from bottom sediments showed that microorganisms responsible for the degradation of organic matter may not necessarily use all compounds equally but choose easily assimilable OC from complex mixtures and provide differential involvement of various substances into the carbon cycle. (Lujanienė et al., 2018). Large ^{14}C depletions observed in sediments collected in the Gotland Deep of the Baltic Sea may indicate a leakage from the dumped chemical weapons.

The author would like to thank colleagues from Lithuanian institutions as well as Hong-Chun Li from the National Taiwan University and Pavel Povinec from the Comenius University for long-term collaboration. Financial support provided by the Research Council of Lithuania (contract No. MIP-080/ 2012) is highly acknowledged.

Lujanienė, et al., 2015. Δ14C and δ13C variations in organic fractions of Baltic Sea sediments. *Radiocarbon*, 57, 3, 479-490.

Lujanienė, et al., 2016. Δ14C and δ13C as tracers of organic carbon in Baltic Sea sediments collected in coastal waters off Lithuania and in the Gotland Deep. 2016. *J. Radioanal. Nucl. Chem.*, 307, 3, 2231-2237.

Lujanienė, et al., 2017. Carbon and Pu isotopes in Baltic sea sediments. *Appl. Rad. Isot.*, 126, 49-53.

Lujanienė, et al., 2018. Carbon isotopes as tracers of organic and inorganic carbon in Baltic Sea sediments. *Radiocarbon*, 60, 5, 1493–1505.

The European-scale ^{106}Ru detection event by the Ro5 network

O. Masson[1], G. Steinhauser[2]

1 Institut de Radioprotection et de Sûreté Nucléaire, Fontenay aux Roses, 92262, France
2 Leibniz Universität Hannover, Institute of Radioecology and Radiation Protection, Hannover, Germany
Keywords: ^{106}Ru, aerosols, Europe, event, 2017
Presenting author's e-mails: olivier.masson@irsn.fr and steinhauser@irs.uni-hannover.de

In October 2017, most European countries reported unique atmospheric detections of aerosol-bound radioruthenium (^{106}Ru). The range of concentrations varied from some tenths of µBq·m^{-3} to more than 150 mBq·m^{-3}. The study is based on a comprehensive survey aimed by an informal network, named Ring of Five (Ro5), working on a laboratory level. 1200 airborne and 200 deposition data from almost all European countries were gathered to assess the most likely release location and plume duration. Various possible release sources were considered including satellite disintegration. However, the widespread detection at such considerable (yet innocuous) level suggested a considerable release. In order to compare activity reports of airborne ^{106}Ru with different sampling periods, concentrations were reconstructed based on the most probable plume presence duration at each location (Fig. 1). Based on airborne concentration spreading (Fig. 2) and chemical considerations, it is possible to assume that the release occurred in the Southern Urals region (Federation of Russia). The ^{106}Ru age was estimated to be less than 2 years. It exhibited partly high solubility in aqueous media and volatility between 700 and 1000 °C, thus suggesting a release at an advanced stage in the reprocessing of nuclear fuel. The most likely candidate for a release would be the Mayak reprocessing facilities.

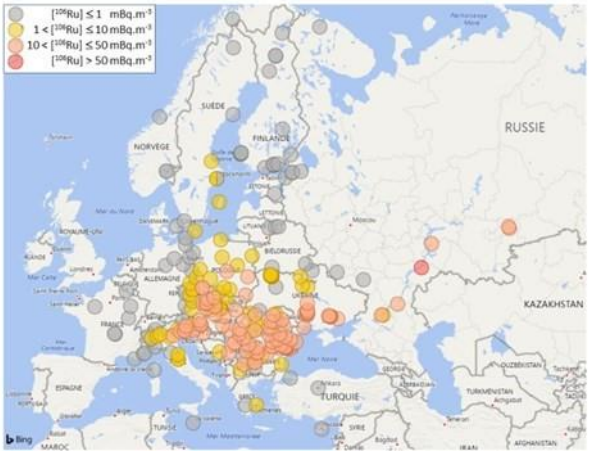

Figure 1. irborne ^{106}Ru corrected by the plume duration at each location.

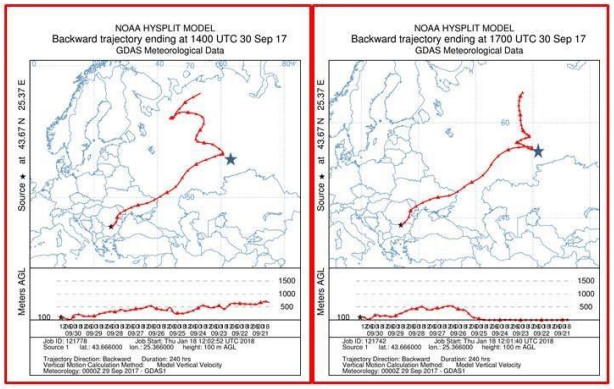

Figure 2. Backward air mass trajectories of ^{106}Ru ending at the location having the maximum registered activity.

Search for extinct natural radionuclides in kimberlite rock to verify the baryonic dark matter impact hypothesis

Jerzy W. Mietelski[1], R. Anczkiewicz[2], M. Paszowski[2], Peter Steier[3], B. Lehmann[4]

[1]Institute of Nuclear Physics, Polish Academy of Sciences, 31-342 Krakow, Poland
[2]Institute of Geological Sciencs, Polish Academy of Sciences, Krakow, Poland
[3]University of Vienna, Faculty of Physics, Isotope Research and Nuclear Physics, Vienna Environmental Research Accelerator, 1090 Vienna, Austria
[4]Mineral Resources, Technical University of Clausthal, 38678 Clausthal-Zellerfeld, Germany
Keywords: extinct natural radioactivity, kimberlites, baryonic dark matter, cosmic impacts
Presenting author, e-mail: jerzy.mietelski@ifj.edu.pl

Kimberlite pipes are perhaps the most unique geological structures present on Earth. These narrow features, a few m to a few hundred meters in diameter, but at least several tens of kilometers long, filled with ultramafic mantle breccia mixed with crustal xenoliths are connecting the deep mantle with the planet's surface. Almost 6000 such objects were found so far on Earth (Tappe et al., 2018). They are famous due to their diamond content, which is evidence for the direct mantle origin of kimberlite rock. The present state of knowledge cannot propose a widely convincing mechanism to explain how these structures were formed. An explanation based on the impact of an ultradense (density of nucleon) cosmic body of baryonic dark matter was proposed by us (Paszkowski & Mietelski, 2013). In this model, the high-energy massive projectile forms a narrow tunnel which is immediately enlarged by explosive degassing of deeper rocks. The empty tunnel is then filled up with pyroclastic material from mantle and crust. It was also proposed there, that during such an impact the energy was high enough to generate nuclear reactions. The idea of the existence of such kind of dark matter in space comes from astrophysicist Edward Witten (Witten, 1984). The search for nuclear traces of such an impact is the aim of this research. Possible evidence would be the presence of "extinct" long-lived natural radionuclides like: U-236 ($T_{1/2}$=23.4 Ma), Pu-244 236 ($T_{1/2}$=80.8 Ma), Cm-247 ($T_{1/2}$=15.6 Ma) or Sm-146 ($T_{1/2}$=64 Ma).

Four samples of bulk material originating from the kimberlite pipe of Fort à la Corne in Canada (Chalapathi Rao et al., 2017), dated at about 100 Ma, from a depth from 120 m to 180 m were the subject of investigation. After hot multiacid digestion (HF, HNO_3, HCl) of 40 grams from each sample, the following selected fractions were prepared using radiochemical procedures:

U for further AMS studies for U-236
Pu for further ICP MS or/and AMS studies for Pu-244
Cm/Am for further AMS studies for Cm-247
Sm for current alpha spectrometry and further ICP MS or/and AMS studies for Sm-146.

The accompanying blanks were made of reagents added during the radiochemical procedure. All above fractions have already been measured by alpha spectrometry to confirm proper separation. For Pu and Cm/Am the tracers Pu-242 and Am-243 in mili-Bqs level were added. No uranium tracer was added to minimalize the risk of introduction of trace amounts of U-236. The thorium fraction was separated (as by-product of Pu separation) and measured by alpha spectrometry. During radiochemical works some other by-product fractions (like Fe for instance) were collected. They were measured on a low-background gamma spectrometer with cosmic muons veto active shield in oder to look for any possible exotic gamma emitters like for example Nb-92 ($T_{1/2}$=34.7 Ma). In the time of preparation of the abstract the planned measurements are not finished yet; some of them will be performed in summer and their results will be available at the Conference.

Chalapathi Rao N.V., Lehmann B., Belyatsky B., Warnsloh J.M. (2017) The late Cretaceous diamondiferous pyroclastic kimberlites from the Fort à la Corne (FALC) field, Saskatchewan craton, Canada: petrology, geochemistry and genesis, *Gondwana Research* 44, 236-257

Paszkowski M. & Mietelski J.W. (2013) Are kimberlite pipes a kind of macroscopic nuclear tracks formed in collision with CUDO? *Acta Physica Polonica* B 44, 787-794

Tappe S., Smart K., Torsvik T., Massuyeau M., Wit M. (2018) Geodynamics of kimberlites on a cooling Earth: Clues to plate tectonic evolution and deep volatile cycles, *Earth and Planetary Science Letters* 484, 1–14

Witten E, (1984) Cosmic separation of phases, *Physical Review* D30, 272-285.

Quantifying fossil carbon load in urban vegetation using C-14 – a case study from Debrecen, Hungary

M. Molnár[1], T. Varga[1], P. Barnucz[1], I. Major[1], Zs. Lisztes-Szabó[1], E. László[1], J. Pénzes[3], A.J.T. Jull[1,3]

[1]Isotope Climatology and Environmental Research Centre, Institute for Nuclear Research, Hungarian Academy of Sciences (ATOMKI), Debrecen, H-4026, Hungary
[2]Department of Social Geography and Regional Development Planning, University of Debrecen, Debrecen, H-4001, Hungary
[3]Department of Geosciences, University of Arizona, Tucson, AZ 85721 USA
Keywords: fossil, radiocarbon, urban, vegetation
Presenting author, e-mail: molnar.miahly@atomki.mta.hu

The $^{14}C/^{12}C$ ratio in the atmospheric CO_2 is affected by both natural and anthropogenic sources and sinks. The dilution of atmospheric radiocarbon may occur by natural fossil emissions such as volcanic gases, but mainly induced by burning of fossil fuels, and this can be estimated using the formula devised by Suess (Suess 1955). Major anthropogenic fossil CO_2 sources are traditional fossil-fueled power plants, industrial facilities, cement production and road traffic.

There are many possible methods which are available for the monitoring and estimation of the carbon isotopic ratio of the atmospheric CO_2 (Molnár et al. 2007). The most sophisticated way of long-term monitoring is instrumental sampling, where a representative sample can be collected for a specific period of time, using calibrated electronic devices and high purity chemicals. On the other hand, plants can also collect the CO_2 from the air by photosynthesis. Thanks to this biochemical process, we can conduct cost-effective observations over a wide area during the growing season of plants (Janovics et al. 2013). CO_2 fixation by photosynthesis provides a way to estimate the proportion of CO_2 from magmatic activity, natural and urban CO_2 emissions, as well as traffic-derived fossil CO_2 emissions (Varga et al. 2018).

Deciduous tree leaf and grass samples were collected in Debrecen, the second largest city in Hungary. The aim of the study was to determine the rate of fossil fuel-derived carbon in urban vegetation. At the locations sampled, C3 and C4 plants close to roads were collected in September 2017. In total, 82 tree and grass leaf samples were gathered at 36 different sampling points all over the city of Debrecen. The ^{14}C results of the samples were compared to the local urban background atmospheric $^{14}CO_2$ data to determine the percentage of the fossil fuel-derived carbon in the plants.

The results from the courtyard of HEKAL, shows there is no clear difference compared to the $^{14}CO_2$ results of the local sampling station located here, consequently there is no significant fossil carbon contribution in this area during the vegetation period. Fossil carbon ratios were calculated for all samples and show a wide range of fossil and modern carbon load (from -1.9% to 9.6%). It is a narrower range in the case of tree leaves alone around a relatively relatively low average fossil carbon load ($0.9 \pm 1.2\%$, n=35). However, in grass leaf samples, the average fossil carbon content is $2.5 \pm 2.5\%$ (n=35). Our data show a realatively strong correlation between the grass leaf-tree leaf sample pairs and suggest that the tree leaves have just about 25% of fossil carbon content compared to their corresponding grass-sample pairs, in average. This might be an indication of how rapidly the traffic induced CO_2 emission can be diluted as a function of distance from the road. There are observable and higher fossil carbon load in local scale at the busy crossroads, as high as $9.6 \pm 0.7\%$ at ground level and $4.7 \pm 0.7\%$ at the height of tree leaves. In contrast, there is a clearly visible modern, post-bomb carbon emission from wood burning or soil CO_2 emission and litter decomposition in the suburbs, which can result in an apparently small negative fossil carbon load. Our study shows that the decidious trees and grass samples can easily applied for monitoring the radiocarbon level and fossil carbon load. This approach could be a reliable and relatively cheap method to monitor the local atmospheric radiocarbon level in CO_2 not just for close to nuclear facilities, but the vicinity of fossil loaded areas. Our results highlight the importance of collecting samples from the local vegetation as a record of local fossil-fuel and modern-carbon contributions to the CO_2 load.

The research was supported by the European Union and the State of Hungary, co-financed by the European Regional Development Fund in the project of GINOP-2.3.2-15-2016-00009 'ICER'.

Janovics R, Kern Z, Güttler D, Wacker L, Barnabás I, Molnár M. 2013. Radiocarbon impact on a nearby tree of a light-water VVER-type nuclear power plant, Paks, Hungary. Radiocarbon 55 (2-3): 826-832

Molnár M, Bujtás T, Svingor É, Futó I, Svetlík I. 2007. Monitoring of atmospheric excess ^{14}C around Paks Nuclear Power Plant, Hungary, Radiocarbon 49 (2) 1031-1043

Molnár M, Haszpra L, Svingor É, Major I, Svetlík I. 2010a. Atmospheric fossil fuel CO_2 measurement using a field unit in a Central European city during the winter of 2008/09. Radiocarbon 52 (2–3): 835–845

Suess HE, 1955. Radiocarbon concentration in modern wood. Science 122: 415–417.

Varga T, Major I, Janovics R, Kurucz J, Veres M, Jull AJT, Péter M, Molnár M. 2018. High-precision biogenic fraction analyses of liquid fuels by 14C AMS at HEKAL. Radiocarbon 60 (5): 1317-1325

Real-time RI Imaging of ^{14}C-carbon dioxide fixation and movement in a plant

T.M. Nakanishi

Graduate School of Agricultural and Life Sciences, University of Tokyo, Yayoi, Bunkyo-ku, Tokyo, 113-8657, Japan
Hoshi University, Ebara, Shinagawa-ku, Tokyo 142-8501, Japan
Keywords: real-time RI imaging, 14C, carbon dioxide gas, plant
Presenting author, e-mail: atomoko@mail.ecc.u-tokyo.ac.jp

We present the preferential movement of photosynthates after fixation of carbon dioxide in a plant by real-time RI imaging system (RRIS) we developed. After fixation of carbon in the mature leaves of a soybean plant, photosynthates moved preferentially to the youngest tissue, which movement was similar to the phosphate movement when absorbed from roots. In the case of Arabidopsis, when carbon was fixed at rosette leaves, the orientation of the photosynthates movement was either down to the roots or to the main stem tip. However, when carbon was fixed at smaller leaves other than rosette leaves, the photosynthates was not transferred to the roots or the main route but moved to the branch stem tip. Some of the gas fixation images in plants obtained by RRIS are presented.

There has been a lot of work for photosynthesis and the photosynthate has been studied to analyse photosynthesis itself. However, the real-time movement of the photosynthate in an intact plant is hardly known. We do not know whether there is any preference of photosynthate movement and accumulation or what could be the route of photosynthate actually moving in a living plant. To visualize the real-time movement of photosynthate in a plant, ^{14}C-labeled carbon dioxide was prepared by applying lactic acid to $NaH^{14}CO_3$ solution. Then produced $^{14}CO_2$ was supplied to the plastic bag prepared to cover the specific tissue of the plant.

The movement of the photosynthate was visualized by RRIS we have developed. The radioisotope imaging system is comprised of a scintillator and a CCD camera. The radiation from the plant, after application of a radioisotope, is converted to light by the scintillator and thus the radioisotope image of the plant is taken by a highly sensitive CCD camera.

One of the representative results is that, when carbon was fixed at mature leaves in a soybean plant the photosynthate was preferentially transferred to the youngest tissue. Figure 1 shows the the photosynthate movement image taken by our imaging. The $^{14}CO_2$ gas was supplied to the first trifoliate of a 20-day old plant for 30 min and the movement of the ^{14}C images was taken. As is shown in the figure, there was a specific route for the photosynthate produced in the trifoliate leaves. The metabolites were transferred preferentially to the youngest leaves (Fig. 1a). Even to the very small developing tissue of the young leaves, the photosynthate was selectively transferred to this meristem tissue and was accumulated (Fig. 1b). However, when the $^{14}CO_2$ gas was supplied only to the youngest leaves including meristem part, the photosynthate produced at this tissue remained at this site and hardly moved to the other tissue (Fig. 1c).

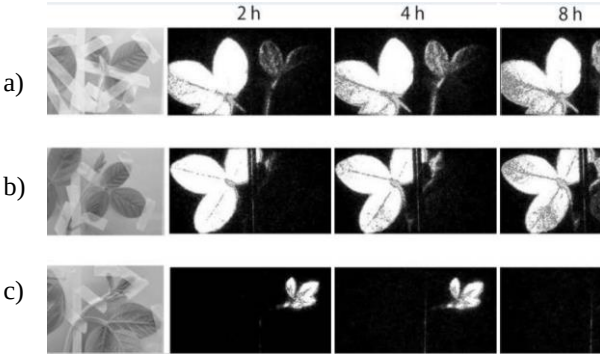

Figure 1. The photosynthate movements taken by RRIS[1)].

The other example is the case of Arabidopsis. When $^{14}CO_2$ gas was supplied to the up-ground part of the 14-day-old seedlings, the movement accumulation of photosynthates to the roots was visualized. The photosynthates produced in leaves was translocated to the meristematic root regions. A high ^{14}C signal intensity was detected around 200 and 800 μm distal to the main root tip. This region, suggested to be the major sink tissue in roots, can be considered as the part extending from the apical meristem to the elongation zone.

, Other result of Araibdopsis case was that the different route of photosynthates movement was visualized between the main stem and the branched stem according to the tissue where C was fixed.

Since plants live on inorganic ions, many kinds of element movements were also visualized using this system. Especially, the imaging of a gaseous radionuclide in our imaging system could drastically enhance the versatility of RRIS.

1) Sugita, R., Kobayashi, N.I., Tanoi, K., Nakanishi, T.M. Visualization of $^{14}CO_2$ gas fixation by plants. Journal of Radioanalytical and Nuclear Chemistry 318. 585-590 (2018)

2) Sugita, R., Kobayashi, N.I., Hirose, A., Iwata, R., Suzuki, H., Tanoi, K., Nakanishi, T.M. 2017. Visualization of how light changes affect ion movement in rice plants using a real-time radioisotope imaging system. *Journal of Radioanalytical and Nuclear Chemistry.* 312, 717-723

3) Sugita, R., Kobayashi, N.I., Hirose, A., Saito, T., Iwata, R., Tanoi, K., Nakanishi T.M. 2016. Visualization of uptake of mineral elements and the dynamics of photosynthates in Arabidopsis by Newly developed real-time radioisotope imaging system (RRIS). *Plant Cell and Physiology*. 57, 743-753

ICP-MS: radiopure material selection and applications for measurements of radionuclides in the environment

S. Nisi[1]

[1]Department of Chemistry, Laboratori Nazionali Gran Sasso, Istituto Nazionale Fisica Nucleare, Assergi (AQ), 67100, Italy

Keywords: ICP-MS, Material screening, Environmental radionuclides,

e-mail: stefano.nisi@lngs.infn.it

The sensitivity of the experiments looking for rare and low energy physics events is driven by the radioactive background of the whole experimental apparatus. Radiometric and mass spectrometric techniques have been widely used in order to select radio-pure materials suitable to build the experiments (Povinec, 2018). Simultaneous radio-purity assessment of materials through different techniques allows checking the secular equilibrium of the natural decay chains (Nisi et al., 2009). In fact, mass spectrometry is sensitive to primordial parent nuclides, while radiometric methods are suitable to detect shorter-lived progeny nuclides.

Thanks to the fact that the final measurement is fast, using ICP-MS can be carried out extensive assessment campaigns (Xenon Collaboration, Nisi S. 2017). On the other side, in order to achieve the best sensitivity, delicate and time-consuming sample treatment procedures are often needed, depending on the nature of the sample. The application of ICP-MS in screening of solid materials such as metals, alloy, crystals, polymers and composite material used for low background experiments are discussed here including the sample properly developed preparation procedures (Nisi et al., 2017).

Different ICP-MS equipment configurations and several optional accessories are nowadays available, such as laser ablation and desolvation systems, can be exploited to overcome issues related to specific applications.

The ICP-MS measurement of potassium in a NaI crystal used in an experiment looking for dark matter is a particular challenge due to the presence of isobaric interferences and the need of low detection limits (DL). Triple quadrupole mass spectrometry has successfully been used achieving sensitivities down to 10^{-9} g g^{-1} (Arnquist and Hoppe, 2017). Double focusing and quadrupole based mass spectrometers equipped with collision cells were tested and their performances were compared.

ICP-MS plays also an important role in the measurement of radionuclides for environmental applications.

A couple of examples are shown. The first is the determination of ^{226}Ra in groundwater for hydrogeological purposes. In this case the most critical drawbacks are the very low concentration of ^{226}Ra in the sample and the isobaric interferences risk due to the possible presence of some elements in the matrix.

After the optimization of the separation and pre-concentration method the detection limit of 0.002 fg mL^{-1} of groundwater sample have been reached (Copia et al., 2015).

The second application in the environmental field is related to the measurement of ^{90}Sr, which is one of the most dangerous fission products of uranium and plutonium. Its half-life is 29 years, and after a nuclear fallout ^{90}Sr is deposited in soil and water from where it enters the food chain. Most of the ^{90}Sr is expelled through the urine, but the rest tends to concentrate in the bones representing a serious health risk (Vonderheide et al., 2004). Applying on-line cascade separation and using a quadrupole based mass spectrometer it is possible to analyse a large number of samples reaching excellent sensitivity (Takagai et al., 2014).

Povinec P.P. et al. 2018. Ultra-sensitive radioanalytical technologies for underground physics experiments. *JRNC*

Nisi S. et al. 2009. Comparison of inductively coupled mass spectrometry and ultra low-level gamma-ray spectroscopy for ultra low background material selection. *Appl. Radiat. Isotopes*

Xenon Collaboration, Nisi S. 2017. Material radioassay and selection for the XENON1T dark matter experiment**.** *European Physical Journal* C 77(12)

Nisi S. et al. 2017. ICP-MS measurement of natural radioactivity at LNGS. *IJMPA* Vol. 32, No. 30 1743003 (23 pages) DOI:10.1142/ S0217751 X17430035

Copia L., Nisi S., Plastino W.,· Ciarletti M., Povinec P.P., 2015. Low-level 226 Ra determination in groundwater by SF-ICP-MS: optimization of separation and pre-concentration methods *J. of Analytical Science and Technology* 6:22

Arnquist I., Hoppe E., 2017. The quick and ultrasensitive determination of K in NaI using inductively coupled plasma mass spectrometry. *Nuclear Instruments and Methods in Physics Research A 851 15-19*

Vonderheide et al., 2004. Determination of ^{90}Sr at ultratrace levels in Urine by ICP-MS. *J. Anal. At. Spectrom. 19, 675-680*

Takagai Y., Furukawa M., Kameo Y., Suzuki K., 2014. Sequential inductively coupled plasma quadrupole mass-spectrometric quantification of radioactive strontiun-90 incorporating cascade separation steps for radioactive contamination rapid survey. *Analytical Methods 6-355*

Radioactive particle released into the environment - recent update

Brit Salbu[1], Sergey Fesenko[2], Alexander Ulanowski[3]

[1]CERAD CoE Environmental Radioactivity, Faculty of Environmental Sciences and Natural Resource Management, Norwegian University of Life Sciences (NMBU), Ås, 1432, Norway
[2]All-Russian Research Institute of Radiology and Agroecology Kievskoye shosse, 109 km, Obninsk, 249032, Russia
[3]International Atomic Energy Agency, IAEA Laboratories, Seibersdorf, A-2444, Austria
Presenting author, e-mail: brit.salbu@nmbu.no (B. Salbu)

Radioactive particles containing refractory radionuclides have been released from a series of sources associated with past nuclear events such as nuclear weapons tests (e.g., Marshall Islands; Semipalatinsk Test Site, Kazakhstan; Maralinga, Australia), non-criticality accidents involving nuclear weapons (e.g., Thule, Greenland; Palomares, Spain), military use of depleted uranium ammunition (e.g., Kuwait, Balkan countries), nuclear reactor accidents (e.g.,Windscale, UK; Chernobyl Nuclear Power Plant, Ukraine; Fukushima Daiichi Nuclear Power Plant, Japan), and as authorized discharges from nuclear installations to rivers (e.g., Techa River and Yenisei River, Russia) or to the sea (e.g., Irish Sea, UK; English Channel) as well as nuclear waste dumped at sea (e.g., Kara Sea, Russian Federation). Radioactive particles have also been identified at uranium mining sites for instance in Central Asia (e.g., Kazakhstan, Kyrgyzstan, Tajikistan) as well as at non-nuclear NORM industries such as phosphate or oil and gas industries. Ongoing research have shown that a significant fraction of radioactive material released from these kinds of sources still remains localized in the form of discrete particles varying in size, composition and structure in the environment.

To identify the phenomena associated with radioactive particles released during nuclear events, IAEA co-ordinated research on "Radiochemical, Chemical and Physical Characterisation of Radioactive Particles in the Environment" during 2000-2008. During 2013 – 2018 the scope was broadened in the succeeding IAEA CRP on "Environmental Behaviour and Potential Biological Impact of Radioactive Particles", which attracted more than 50 scientists from 16 countries worldwide. As documented by these IAEA CRPs, radioactive particles are more prevalent in the environment than it has previously been anticipated.

Environmental impact assessments are usually based on total activity concentrations of radionuclides in various compartments, assuming representative sampling. When particles are released, the deposition will be inhomogeneously distributed and representative sampling is difficult to obtain. Furthermore, particles are often inert and difficult to dissolve. Thus, analytical results may reflect partial leaching, and the actual inventory of a contaminated area can be underestimated. The inherent differences in mobility, bioavailability and ecosystem transfer of particle-bound radionuclides compared to simple ions have therefore to a large degree been ignored in radioecology and radiation protection.

To evaluate the impact of radionuclides in the environment, information on particle characteristics influencing particle weathering, as well as ecosystem transfer is needed. A series of available techniques for the collection, isolation and characterization of radioactive particles in the environment is available. Information on 2D distribution of elements/radionuclides on particle surfaces is obtained by electron microscopy, and 3D distribution within particles when EM is combined with microbeam X-ray emission techniques (e.g., SEM or TEM interfaced with EDX/WDX, X-ray tube micro-XRF), PIXE or 3D distribution by synchrotron radiation based microscopic techniques (SR-confocal μ-XRF) and micro-tomography (transmission and combined trans-mission XRF tomography). Information on 2D or 3D distribution of structures (SR-micro-XRD) or oxidation states (SR-micro-XANES) can also be obtained non-destructively, while destructive techniques such as mass spectrometric methods (e.g., ICP-MS, AMS, SIMS) are needed for source identification (atom or isotope ratios). To estimate ecosystem transfer, extraction techniques have also been developed and combined with solid-state techniques.

Soil and sediment will act as sinks for particles, while contaminated soil or sediments can act as diffuse source of radioactivity if particle weathering occurs over time. Information on particle weathering rates and the subsequent remobilization and ecosystem transfer of particle-associated radionuclides, depending on particle characteristics (e.g., composition, structure, oxidation state), is needed for assessing long-term consequences.

The work performed within the IAEA CRPs demonstrates that the particle composition will depend on the source (burn-up), while particle characteristics of relevance for ecosystem transfer and biological uptake will also depend on the release scenarios. The present paper will focus on radioactive particles released to the environment due to past nuclear events, as well as on advanced technologies needed to characterise relevant particle properties.

The advantages of measuring actinides with AMS

P. Steier[1], K. Hain[1], M.Kern[1], A. Wiederin[1], R. Golser[1]

[1]Isotope Physics Group, University of Vienna, Vienna, Austria
Keywords: Accelerator Mass Spectrometry, VERA, actinides, ^{236}U, ^{233}U, ^{237}Np
Peter Steier, e-mail: peter.steier@univie.ac.at

Interest in Accelerator Mass Spectrometry (AMS) of actinides has significantly increased recently due to the emergence of applications and improvements of the measurement technique.

We will discuss the main factors contributing to the technical progress, using our AMS facility VERA as an example. Compared to the previous setup at VERA, which was based on oxygen stripping and a time-of-flight detector, we have improved the sensitivity by more than an order of magnitude by switching to helium stripping and by installing a second 90° magnet in our analyzer beamline. The new setup has been successfully employed for several research projects.

We present the characterization of the upgraded spectrometer and benchmark measurements. The excellent suppression of neighboring masses allows e.g. measurements of ^{239}Pu in U-rich samples down to a level of ^{239}Pu/U = 10^{-14} (Figure 1), which makes previous chemical uranium suppression essentially unnecessary. In various projects, bulk precipitations of actinides have been used to measure several actinides from the same sputter sample (e.g. Quinto et al., 2017). For ^{236}U, the suppression of mass 239 vs. 238 suggests an instrumental sensitivity limit well below ^{236}U/^{238}U = 10^{-14}. Based essentially on the same principles, similar figures of merit may be achieved by forthcoming new instruments from the commercial AMS manufacturers.

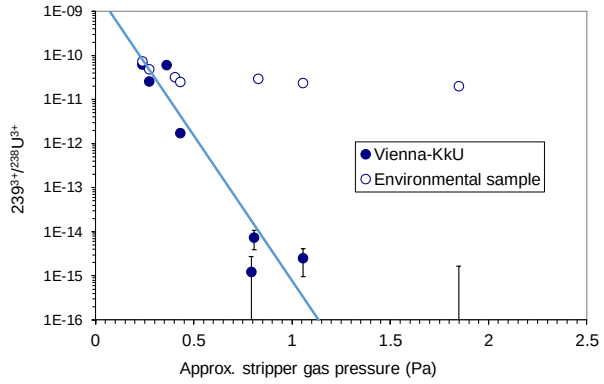

Figure 1. Destruction of interfering $^{238}U^{1}H^{3+}$ for the measurement of $^{239}Pu^{3+}$. Our in-house standard Vienna-KkU contains no ^{239}Pu, but $^{238}U^{1}H^{3+}$ mimics a ^{239}Pu/^{238}U ≈ 5×10^{-11} for low helium pressures, comparable to an arbitrarily chosen, archived environmental sample. The interference becomes negligible if the pressure is increased to ~1 Pa. The line is a guide to the eye.

In environmental samples, about one in 4500 sputtered actinide atoms is detected. In most cases, the sensitivity is limited by detection efficiency rather than instrumental background, therefore increasing the detection efficiency is presently in focus. Further improvements are expected e.g. from studies on the negative ion yield in the ion source (Kern et al., 2019; Prášek et al., 2019). Generally, this allows analysis of smaller samples and lower isotopic ratios. Low isotopic ratios are necessary for tackling natural ^{236}U for geologic applications, and e.g. the use of anthropogenic ^{236}U as ocean tracer will be possible with sample sizes less than 1 Liter of ocean water.

Other actinides profit from the higher sensitivity also. Especially, it has made the environmental concentration of the rare anthropogenic isotope ^{233}U detectable. The simultaneous measurement of two anthropogenic uranium isotopes, ^{233}U and ^{236}U, allows for fingerprinting of possible sources (Qiao et al., this conference).

The good suppression of neighboring ^{238}U also allows sensitive detection of ^{237}Np, at VERA and elsewhere. However, while ^{237}Np is readily detected in various environmental samples, no second Np isotope, suitable as a yield tracer, is available, which makes the quantitative determination difficult. This obstacle may be overcome for well-defined sample matrices by using ^{242}Pu as tracer, (López-Lora et al., 2019), but the general application demands an isotopic tracer.

The methodical aspects will be illustrated by current examples of application.

Kern et al. 2019. This conference.

Prášek et al. 2019. This conference.

Qiao, J., Steier, P., Hain, K. 2019. ^{233}U-^{236}U oceanic tracer studies in the Baltic Sea and the Arctic Ocean. This conference.

Quinto, F., Blechschmidt, I., Perez, C.G., Geckeis, H., Geyer, F., Golser, R., Huber, F., Lagos, M., Lanyon, B., Plaschke, M., Steier, P., Schaefer, T. 2017. Multiactinide Analysis with Accelerator Mass Spectrometry for Ultratrace Determination in Small Samples: Application to an in-Situ Radionuclide Tracer Test within the Colloid Formation and Migration Experiment at the Grimsel Test Site (Switzerland). *Analytical Chemistry* 89, 7182-7189.

López-Lora, M., Levy, I., Chamizo, E. 2019. Simple and fast method for the analysis of ^{236}U, ^{237}Np, ^{239}Pu and ^{240}Pu from seawater samples by Accelerator Mass Spectrometry. *Talanta* 200 (2019) 22–30.

Some speculations and their assessment about the release of radioruthenium in fall 2017

G. Steinhauser[1]

[1]Institute of Radioecology and Radiation Protection, Leibniz Universität Hannover, Hannover, 30419, Germany
Keywords: Ruthenium-106, Radioecology, Nuclear accident
Presenting author, e-mail: steinhauser@irs.uni-hannover.de

A sizeable, yet undeclared nuclear accident caused the release of radioruthenium (^{106}Ru) in fall caused elevated levels of this radionuclide in the European atmosphere (Masson et al., 2019). Some speculations about the cause of the accident have been discussed publicly and shall be evaluated with respect to their forensic value for the elucidation of the events from fall 2017. The most well-known hypothesis suggests a link of the release to the production of a high-power radioactive source of ^{144}Ce for a European neutrino experiment. This scenario exhibits a credible hypothesis for the causes of the accident and, so far, remains the most likely context of the release circumstances. In addition, we will discuss possible accident scenarios and how they reflect in the physico-chemical signatures of the release.

Masson, O., et al., 2019, *Proc. Natl. Acad. Sci. USA* in press.

Analytic progress in AMS and related opportunities for applications with long-lived radionuclides

Hans-Arno Synal

Laboratory of Ion Beam Physics, ETH Zurich, Building HPK, Otto-Stern-Weg 5, 8093 Zurich, Switzerland
Keywords: AMS, Radiocarbon, Long-lived radionuclides
e-mail: synal@phys.ethz.ch

Radioactive nuclides in nature can be detected, based on the emission of energetic radiation, with a sensitivity of the decay of a single atomic nucleus. However, due to their radioactivity, they can only occur if they are produced by natural processes or if they have been released into the environment by man-made nuclear activities. Depending on their half-life, the detection of these nuclides becomes increasingly difficult as the specific activity decreases and larger sample quantities have to be analysed. However, nuclides with long half-lives play a particularly important role in investigations of the Earth's cycles and adequate detection methods are needed to cope up with requirements of application based on tracing such nuclides in the environment. In a way, there is a close connection between analytical possibilities and the resulting fields of application and novel detection techniques enable new fields of science verse visa demands form possible applications will trigger new instrumental developments.

Here, the technical evolution of Accelerator Mass Spectrometry (AMS) instrumentation over the last ten years has boosted research with radioactive tracers in global environment. Of course, ^{14}C has been and still is the by far most important AMS nuclide but there is a great potential for applications of ^{10}Be, ^{26}Al, ^{36}Cl, ^{41}Ca, ^{129}I, and actinides measurements. Today, 1+ charge state is primarily used in case of ^{14}C detection, molecular interferences are destroyed in multiple collisions with He stripper gas atoms, and a high yield of atomic ions is reached at energies of a few hundred keV, only. Thus, instruments develop towards lab size or table-top devices and performance has improved with respect to overall detection efficiency and reproducibility of measurement conditions. In addition, the advent of hybrid ion source accepting sample materials as CO_2 in a He carrier gas stream (Fahrni et al., 2013) enabled the analysis of microgram sized samples making compound specific analyses possible.

He stripping has the potential to down size instruments for measurements of other radionuclides, too (Fifield et al. 2004). For the $^{10}Be/^{10}B$ pair, a significant isobar separation capability can be achieved already at particle energies of less than 1 MeV, by using passive absorber techniques and exploiting the quite large difference in energy loss of these isobar (Müller et al. 2010). Apart from this, only nuclides that are not interfered by nuclear isobars can be detected with new compact instruments. Modern simulation technique allows to optimize their designs and replace traditional accelerator technology by high-voltage platforms driven by commercial HV power supplies. These developments have launched the wide spread use of AMS in various research fields and has resulted in a boom of new AMS facilities which impact the wide variety of applications of AMS in modern research.

At the Laboratory of Ion Beam Physics (LIP) we have initiated a number of developments to improve AMS measurement technologies (Suter et al., 2000, Synal et al., 2000, Synal, 2013). The present status of the facility is shown in Figure 1. The versatile instrumental park allows to progress not only technical development, but also acts as an analytical backbone of new application fields. The recent technical development will be summarized and examples on specific applications will be discussed to highlight future perspective of research with long-lived radionuclides.

Figure 1. Impression of the AMS installation at ETH Zurich. There are four AMS spectrometers visible, the two multi-purpose systems Tandy (Stocker et al., 2005), MILEA (Maxeiner et al., 2019) covering the range of nuclides up to the actinides, and two MICADAS instruments (Synal et al., 2007) dedicated for radiocarbon analyses.

S. Fahrni et al. *NIM B* 294(2013) 320 - 327

K. Fifield et al., *NIM B* 223-24(2004) 802-806

A. Müller et al. *NIM B* 268 (2010) 2801-2807

M. Suter et al. *NIM B* 172 (2000) 144-151

H.-A. Synal et al., *NIM B* 172 (2000) 1-7

H.-A. Synal, *IJMS* 349 – 350 (2013) 192 - 202

M. Stocker et al., *NIM B* 240 (2005) 483-489

S. Maxeiner et al., *NIM B* 439 (2019) 84-89

H.-A. Synal et al., *NIM B* 259 (2007) 7-13.

Czech power industry in the European context

V. Wagner

Nuclear Physics Institute of Czech Academy of Sciences, Řež, 250 68, Czech Republic
Keywords: low-emission energy, nuclear energy,
V. Wagner, e-mail: wagner@ujf.cas.cz

Due to its geographical conditions, the Czech power sector has very limited possibilities for using renewable resources. The Czech Republic does not have windy seashore as north of Germany or Denmark. Also, the use of solar energy is not large enough due to its latitude. The use of biomass for energy production competes with food production and landscape ecological function. The potential of hydropower is also largely depleted.

Savings are also very important. However, given the need to switch to electromobility, it is not to be expected that electricity consumption will decrease.

The situation of the Czech electricity industry is also very strongly influenced by our neighbours. In the windy season, there are large surpluses of wind-generated electricity in the north of Germany. Conversely, resources are scarce at a time when the sun is not shining and blowing. The situation will worsen even further after the closure of all German nuclear power plants and a number of coal resources after 2022.

The European energy policy aims to reduce carbon dioxide emissions. The Czech Republic also needs to replace coal, which is currently the most used source. The reason is also the stock of this raw material. For the transition to low-emission energy, it is necessary to use all available low-emission sources in the Czech Republic as effectively as possible. The renewable resources described are suitable for decentralized use. Nuclear power plants, which currently account for about a third of production, will be used as large sources.

The State Energy Policy assumes that increased production of nuclear units and decentralized renewable resources will gradually replace coal-fired power plants. Low-emission sources will complement gas power plants. In 2040, it foresees an energy mix, with nuclear power plants producing between 46 and 58% and renewable sources between 11 and 21%.

The Czech Republic is thus counting on the long-term use of nuclear power plants in the future. Therefore, it must intensively support research on radionuclide emissions from nuclear installations and issues related to the management and storage of radioactive waste associated with the use of nuclear energy. The lecture will try to outline the possibilities of the development of the Czech energy sector and the challenges associated with it in the field of radionuclide studies not only in the environment.

Lessons learned from the radiological responses to TEPCO-Fukushima Daichi Nuclear Disaster

N. Yasuda[1] and H. Fukuo[1]

[1]The Research Institute of Nuclear Engineering, University of Fukui, Kanawa 1-3-33, Tsuruga, Fukui, 914-0055, Japan
Keywords: emergency preparedness and response, sheltering and evacuation, nuclear accident
Presenting author, e-mail: nyasuda@u-fukui.ac.jp

This paper looks back on Japan's response after the Fukushima Daiichi Accident caused by the Great East Japan Earthquake and tsunami that occurred on 11 March 2011, and on the lessons learned from the perspective of protecting the public from radiation.

Decision makings and countermeasures by the Government of Japan have been reported in the IAEA publication (IAEA, 2015). Until now, organizations and laws have been renewed, and a new disaster prevention system has been developed. Especially for protecting the public viewpoint, two off-site emergency zones (IAEA, 2002): the precautionary action zone (PAZ) and the urgent protective action planning zone (UPZ) have been adopted for making decision of sheltering and evacuation. The operational intervention levels (OILs), operational criteria, are also introduced to the new system (IAEA Safety Standards, 2015). However, there have been few verifications of these measures from the perspective of residents. For example, in preparedness phase, a uniform zone of the PAZ and UPZ based on the distance from the nuclear power plant was introduced into the municipalities with a population of tens of thousands to one million. For this reason, there is a current situation where the improvement of evacuation plans in areas with a large population is delayed or stopped. In the evacuation phase, a quantitative assessment of the risk trade-off between radiation exposure and evacuation after a nuclear power plant accident has been suggested that evacuation actions at the radiation level alone may increase the risk for the nursing home residents (Murakami et al., 2015). Thus, the new system does not fully reflect the points of improvement from the residents' point of view. A short review of failures, improvements, and problems on the countermeasures and system will be presented according to those in early phase on sheltering, evacuation, iodine thyroid blocking and relocation together with radiation monitoring strategy and system.

On the other hand, those activities must be evaluated based on some indicators to keep improving. The need for assessing the "coping capacity of local community on nuclear emergency preparedness and response" in some way is persistent in both academia and practice as similar to those for natural disasters. The component of the coping capacity is considered to be formed by three components of risk awareness, exposed capacity, and latent capacity (Birkmann, 2006). As prospects of coping capacity of local community evaluation research, Nagamatsu et al., described the research should be included: 1) the basis of shelter units as regional units, 2) evaluation of the local social structure itself, 3) risk awareness, exposed capacity, and latent capacity, 4) measures on improvement for coping capacity of local community based on evaluation, and 5) community-based approach. Thus, there is a need for measures to further improve the coping capacity of local community on nuclear emergency preparedness and response. For this, it is necessary not only for the improvement of the system but also the indicators for evaluating the system. Those lessons and knowledge should be integrated into the international framework. Recently, the IAEA has established an international training and educational network aimed at strengthening emergency preparedness and response around the world. This network will support the IAEA as it develops a model curriculum in EPR for a Masters-equivalent program and other postgraduate offerings.

This work was supported by the Grants-in-Aid for Scientific Research, JP18K02857.

IAEA publication, The Fukushima Daiichi Accident – Technical Volume (3/5), Emergency Preparedness and Response, 2015, and IAEA publication, The Fukushima Daiichi Accident – Report by the Director General, 2015.

IAEA publication, Preparedness and Response for a Nuclear or Radiological Emergency, IAEASafety Standards Series No. GS-R-2, 2002.

IAEA Safety Standards Series No. GSR Part 7, 2015.

Murakami, M., Ono, K., Tsubokura, M., Oikawa, T., Oka, T., Kami, M., Oki, T. 2015. Was the Risk from Nursing-Home Evacuation after the Fukushima Accident Higher than the Radiation Risk? *PLoS ONE* **10**(9): e0137906.

Birkmann, J. 2006. Measuring vulnerability to promote disaster-resilient societies. Conceptual frameworks and definitions, J. Birkmann ed. Measuring vulnerability to Natural Hazards, United Nations University Press, 9-54.

Nagamatsu, S., Nagasaka, T., Usuda, Y., Ikeda, S. 2009. How can the "Coping Capacity of the Local Community Against Disasters be Evaluated, Report of the National Research Institute for Earth Science and Disaster Prevention, 74, 1-11 (in Japanese).

Comprehensive radiological study on water and soil of high natural background area of Dehloran, Iran

M.E. Adelikhah[1], A. Shahrokhi[1], A. Peka[1], T. Kovács[1]

[1]Institute of Radiochemistry and Radioecology, University of Pannonia, 10 Egyetem str., H-8200 Veszprém, Hungary
Keywords: Radon concentration, Hot springs, Thermal bath, Natural radon radiation
Presenting author, Mohammademad Adelikhah

Hot spring spot area is an example of the high level natural radiation background source that includes high concentration level of ^{226}Ra, ^{222}Rn and ^{232}Th. However, health tourism including health care promotion and natural therapy becoming very popular, especially mineral water spa, mineral water therapy and lastly drinking of the mineral water. For example, the effective dose receives from natural radiation by residences in Ramsar of Iran is much higher than dose received by man in other part of Iran due high NORM materials concentration in Ramsar (Hajo and Ferid, 2009).

The largest fraction of annual effective dose to the general population from natural radioactivity is from radon, thoron and their short half-life progeny (EPA, 1980, 2003). In this paper, we determined concentration of three major natural radioactive materials in the farmland soil samples in Dehloran, is one of the cities of Ilam province located in western part of Iran, that are irrigated by hot spring water and compared with two others soil samples from same area but with differences irrigation water source. We also investigate the indoor ^{222}Rn and ^{220}Rn concentration of thermal water bathrooms due to tourist and patient's exposure. Likewise, the concentrations of dissolving of ^{226}Ra in water samples of 10 baths were measured to find distribution of ^{226}Ra between baths' thermal water.

To determine radon and thoron concentration, a Raduet selective radon and thoron chambers type with CR-39 detectors, were used. Concentration of dissolving ^{226}Ra in water samples were measured using emanation method by DURRDGE RAD7 radon detector with H_2O accessories. The K-40, Th-232 and Ra-226 were determined by HPGE detector.

Table 1 is shown the concentration of ^{40}K, ^{226}Ra and ^{232}Th present in the soil samples were irrigated by hot spring water (D-1 to D-3) and other source water (D-4 and D-5). The result shows a direct link between ^{226}Ra and ^{232}Th activity concentration in soil and irrigation source was discovered and for this reason the samples which were irrigated by hot spring water show higher concentration than soil samples that used other water source for irrigation.

Table 1. Concentration of NORMs in soil (Bqkg^{-1})

Sample ID	K-40	Ra-226	Th-232
D-1	238±7	320±12	80±10
D-2	227±6	293±10	68±5
D-3	228±6	298±8	49±8
D-4	240±8	278±9	31±8
D-5	100±8	285±12	20±8
Mean	**207**	**295**	**50**

The activate concentration of ^{226}Ra in water samples and Radon and thoron concentration in bath rooms are shown in table 2 and table 3, respectively.

Table 2. ^{226}Ra concentration in water samples (mBqL^{-1})

Water	Ra-226	SD
D-R1	418	±180
D-R3	423	±160
D-R5	422	±180
D-R7	408	±200
D-R10	416	±190
Mean	**417,4**	**±170**

Table 3. ^{222}Rn and ^{220}Rn concentration (Bqm^{-3}) in bath rooms

Bath Room	C_{Radon}	SD	C_{Thoron}	SD
D-R1	1982	±37	9	±4
D-R2	2012	±38	13	±3
D-R3	1880	±42	10	±3
D-R4	1890	±51	14	±2
D-R5	2150	±46	9	±5
D-R6	2450	±53	10	±3
D-R7	2010	±50	11	±4
D-R8	1890	±40	10	±2
D-R9	1895	±37	14	±2
D-R10	1937	±43	12	±3
Mean	**2010**	**±44**	**11**	**±3**

Radon concentration in bath rooms was measured in range of 1880±42 Bqm^{-3} to 2150±47 Bqm^{-3} which is significantly higher than reference levels. A direct link between the concentration of ^{222}Rn and area size of bath, frequency of using and the location of bath due to air pressure was discovered. The results of thoron concentration in bath rooms were out of expectation. Results of ^{220}Rn concentration were lower than expected value that may related to detector type and high humidity level in bath rooms.

Hajo, Z. and Ferid, S. WHO handbook on indoor radon: a public health perspective World Health Organization. (France: World Health Organization) (2009) ISBN 0 433 003502.

Office of Radiation and Indoor Air. EPA assessment of risks from raodn in homes. Washington DC, EPA 402-R-03-003, (2003).

U.S. Environmental Protection Agency. Prescribed Procedures for Measurement of Radioactivity in Drinking Water. EPA/600/4-80-032, (1980).

Stable isotope mass-spectrometer coupled graphite preparation laboratory for radiocarbon dating at Birbal Sahni Institute of Palaeosciences, Lucknow (India): A status report

Rajesh Agnihotri[1], S.K.S. Gahlaud[1], N. Patel[1], R. Sharma[2], Pankaj Kumar[2] and S. Chopra[2]

[1]BirbalSahni Institute of Palaeosciences, 53 University Road, Lucknow-226007, Uttar Pradesh, India
[2]Inter-University Accelerator Centre, Aruna Asaf Ali Marg, New Delhi-110067, India
Presenting author, e-mail: rajagni9@gmail.com

The conventional Radiocarbon dating laboratory at Birbal Sahni Institute of Palaeosciences, Lucknow was established in 1974 (Rajagopalan, 1978). The conventional ^{14}C dating is labour-intensive, time-consuming and requires several grams of dateable material. In contrast, advent of Accelerator Mass Spectrometry (AMS) revolutionized ^{14}C dating applications requiring only ~1 mg of solid carbon (in form of graphite) with analysis time <50 minutes (Fahrni et al., 2010). BSIP recently installed an Automated Graphitization Equipment (AGE) coupled with sample preparation units (i) Elemental Analyzer (EA) (for organic samples) and (ii) Carbonate Handling System (CHS) (for inorganic samples), along with an *in-line* Isotope Ratio Mass-Spectrometer (IRMS). The EA-IRMS was set up for generating stable isotopic data ($\delta^{13}C$, $\delta^{15}N$, $\delta^{34}S$). A suite of IAEA and *in-house* reference standards were used to achieve accuracy and analytical precision. Overall reproducibilities achieved were ~0.15‰ for $\delta^{13}C$ and ~0.20‰ for both $\delta^{15}N$ and $\delta^{34}S$. Both CN and CNS modes were set up while CN mode was used when samples are graphitized (for ^{14}C dating). Procedures were set up to prepare reproducible graphite targets from both organic and inorganic samples using EA and CHS systems respectively, following standard pre-treatment steps (Sharma et al., 2019) and using Inter university accelerator centre (IUAC)'s AMS (®NEC). A total of 27 samples were graphitized using EA-AGE equipment, nine of them were processed in duplicates and they yielded average coefficient of variation better than ~3.2% (in terms of measured pMC values). Eight samples were graphitized using both EA-IRMS-AGE combo (at BSIP) and EA-AGE at IUAC lab, finally measured for ^{14}C activities at AMS facility at IUAC. They yielded average coefficient of variation better than ~2% (Figure 1).

Ten graphite targets prepared at BSIP were measured at Direct AMS Lab (USA). Three samples of them were measured both at IUAC-AMS (New Delhi) and Direct AMS Lab. They revealed overall reproducibility better than 1%.

Four blanks (Anthracite powder) were prepared at BSIP's EA-IRMS-AGE facility which yielded ^{14}C ages between 39,072 to 42,215 years.

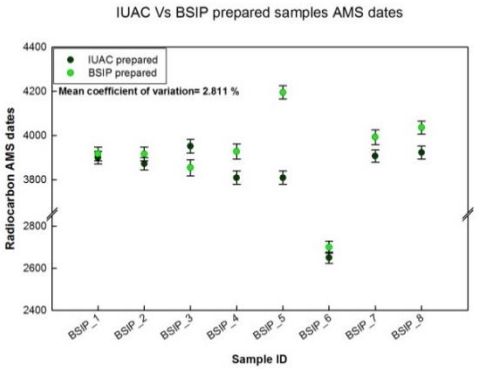

Figure 1. Reproducibility of graphite targets prepared at BSIP (Lucknow) and IUAC (New Delhi).

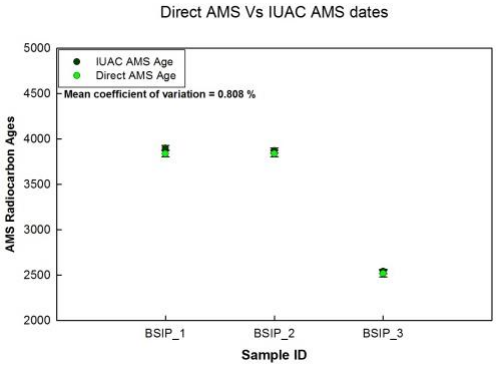

Figure 2. Reproducibility of graphite targets measured at IUAC and Direct AMS (USA).

Fahrni et al., Direct measurements of small ^{14}C samples after oxidation in quartz tubes, *Nuclear Inst. and Methods in Physics Research* B (2010), 268 (78), pp. 787-789.

Rajagopalan et al., Birbal Sahni Institute Radiocarbon Mesurments. I. *Radiocarbon* 20 (1977), pp. 398-404.

Sharma et al. AMS and upcoming geochronology facility at Inter University Accelerator Centre (IUAC), New Delhi, India. *Nuclear Inst. and Methods in Physics Research* B 438 (2019), pp. 124–130.

Development and calibration of a method for direct measurement of Thoron

F. Ambrosino[1,2], R. Buompane[1,2], V. Roca[2], C. Sabbarese[1,2]

[1] Centre for Isotopic Research on Cultural and Environmental heritage (CIRCE), Department of Mathematics and Physics, University of Campania "Luigi Vanvitelli", Caserta, 81100, Italy
[2]National Institute for Nuclear Physics (INFN), branch of Naples, Napoli, 80126, Italy
Keywords: Thoron chamber, non-ionized ^{220}Rn nuclei spectrum, Monte Carlo simulation, collection efficiency
F. Ambrosino, e-mail: fabrizio.ambrosino@unicampania.it

The interest in the measurement of Thoron (^{220}Rn) concentration activity in air has recently increased, with the attention for the development of standards for the calibration of measuring instruments (Buompane et al., 2013; Sabot et al., 2016; Tokonami, 2010). Due to its short half-life (55.8 s), consolidated techniques for the realization and use of controlled atmospheres of Radon (^{222}Rn) are not effective. New protocols in the case of Thoron are required. A method for the measurement of the Thoron reference activity based on the direct detection of the non-ionized alpha particles, at 6.3 MeV, produced by the decay of ^{220}Rn, from natural samples containing ^{232}Th salts, is developed. The possibility of acquiring an acceptable spectrum is entrusted to the realization of small measurement chambers, enough to reduce as much as possible the energy loss of the alpha particles that reach the Silicon detector inside such chamber.
In this regard, a cylindrical chamber model was implemented using the Monte Carlo simulation method (from FLUKA-Flair software). One of the two bases of the chamber is the active surface of a silicon detector for alpha particles having a diameter of 1.2 cm. Keeping the diameter and the specific activity of the Toron (primary starting particles source) constant in the chamber, many simulations were carried out with varying the height and, hence, the volume of the chamber. An example of spectrum is shown in Figure 1. The direct detection efficiency of the Thoron was obtained as a function of the chamber volume and is variable between 11% and 48% for distances of 4.8 cm and 0.2 cm, respectively.

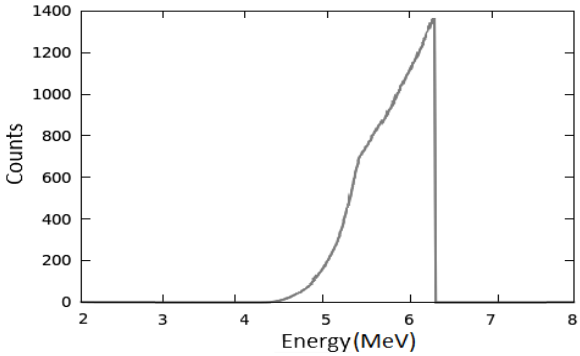

Figure 1. α-spectrum of ^{220}Rn nuclei at 6.3 MeV obtained from the silicon detector inside the small Thoron chamber, using a Monte Carlo simulation.

The prototype of the chamber (Figure 2) was made of brass with a height of 1.1 cm and a diameter of 1.2 cm. A high voltage is applied to the inner walls of the chamber to collect also the Toron decay products on the detector surface. Tests and measurements were performed in the Radon Chamber, where controlled Thoron atmospheres were created (Buompane et al., 2013). The ^{220}Rn α-spectrum is obtained by subtracting from the total spectrum (^{220}Rn+^{216}Po+^{212}Bi+^{212}Po) the spectrum collected after eliminating the Thoron from the chamber (containing only ^{212}Bi and ^{212}Po) that is achieved simply by turning the ventilation system off inside the Exposure Chamber. The contribution of the non-interfering ^{216}Po can be easily evaluated from total spectrum. The comparison of the spectra of non-ionized Thoron nuclei exhibit the similar shape, as well as the corresponding efficiencies, (32±3)% from simulations and (34±2) % from measurements, are compatible within the evaluated uncertainties.

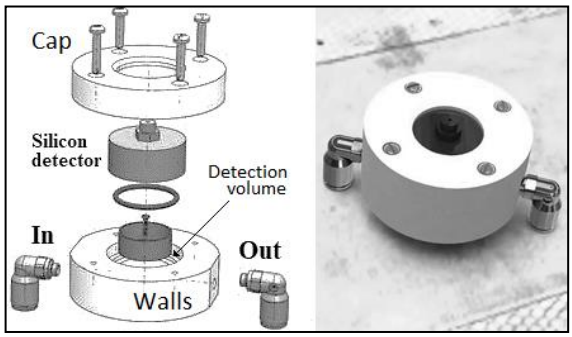

Figure 2. Exploded view of the assembly sequence of prototype of Thoron chamber (on the left); picture of the realized version (on the right).

The present results are in agreement with the results found in a similar way by Sabot et al. (2015). The methodology carried out for the direct measurement of ^{220}Rn can be very useful and effective to obtain for the characterization of reference atmospheres. In order to optimize the system, the realization of a new chamber having a double-sided Si detector, together with various simulation tests, are in progress.

Buompane, R., Roca, V., Sabbarese, C., De Cicco, F., Mattone, C., Pugliese, M., Quarto, M. 2013. Realization and characterization of a ^{220}Rn source for calibration purposes. *Appl. Radiat. Isot*. 81, 221-225.

Sabot, B., Pierre, S., Cassette, P., Michielsen, N., Bondiguel, S. 2015. Development of a primary thoron activity standard calibration of thoron measurement instruments. *Radiat. Prot. Dosim.* 167 (1-3), 70-74.

Tokonami, S. 2010. Why is ^{220}Rn (thoron) measurement important? *Radiat. Prot. Dosim.* 141 (4), 335-339.

Mass balances and transit times of artificial radionuclides transported from the Rhone River to the Mediterranean Sea

C. Antonelli[1], O. Radakovitch[2], F. Eyrolle[2], H. Lepage[2]

[1]PSE-ENV/SEREN, IRSN, BP3 - 13115 Saint-Paul-les-Durance, France
[2]PSE-ENV/SEREN/LRTA, IRSN, BP3 - 13115 Saint-Paul-les-Durance, France
Keywords: Mass balance, transit time, industrial releases, global fallout
Presenting author, e-mail: christelle.antonelli@irsn.fr

Many nuclear power plants are located along rivers in which they release artificial radionuclides through authorization or incident. Their behaviour is controlled by hydro-sedimentary processes, biogeochemical characteristics, potential sinks along the river and transit times. If these times can be extrapolated from hydrological model for water and dissolved radionuclide, it is more difficult to evaluate those of particles and particulate radionuclide.

The Rhone River (France) is one of the most nuclearized systems over the world with five nuclear power plants and two plants (Uranium conversion and spent fuel treatment) that have released radionuclides along 400 km of the river since the 50's. The reprocessing plant is responsible of the majority of these releases until now, even if an important decrease is experienced since the end of the 90's. Moreover, atmospheric fallout of radionuclides due to nuclear weapons tests and Chernobyl accident also affected the Rhone River catchment.

In this river, the transfer of particulate matter mainly depends on floods which transport up to 90% of the annual suspended matter flux in less than 10% of time. This could induce a disconnection between inputs and output fluxes because releases are not allowed during floods.

Since 2005, IRSN collects and measures dissolved and particulate radionuclide with an automatized station located 30Km upstream of the river mouth. This station also allows collecting specific samples during flood events, in order to better estimate the particulate radionuclide fluxes. This high frequency monitoring, combined with a performant metrology to measure trace element in both solid and liquid phase permits to constitute a long term and high resolution data for a large spectrum of artificial radionuclides.

The measured radionuclide output fluxes can thus be directly compared to the releases declared by the industrials, providing an opportunity to evaluate mass balance and transit times along the system. Important results are:

- Fluxes of radionuclide linked to releases and atmospheric fallouts (^{238}Pu, $^{239+240}$Pu, ^{241}Am, ^{137}Cs, ^{90}Sr) are slightly higher than those declared by the industries. This is partly due to leaching from the watershed soils but also due to resuspension of past sediment within the river, as evidenced by Pu isotopic ratios. - Fluxes of radionuclide only issued from the nuclear power plant releases (^{58}Co, ^{60}Co, ^{110m}Ag, ^{124}Sb, ^{125}Sb, ^{54}Mn, ^{244}Cm) are in equilibrium with those declared, traducing probably an efficient and rapid export from the system on a yearly basis, even for particulate radionuclide. Sometimes however a slight deficit is observed, which could be attributed to difficulties to measure radionuclides at trace-level and/or to temporary accumulation within the river.

Transit and resilience times of these radionuclides in the river system will be presented and discussed based on their origin and mass budgets.

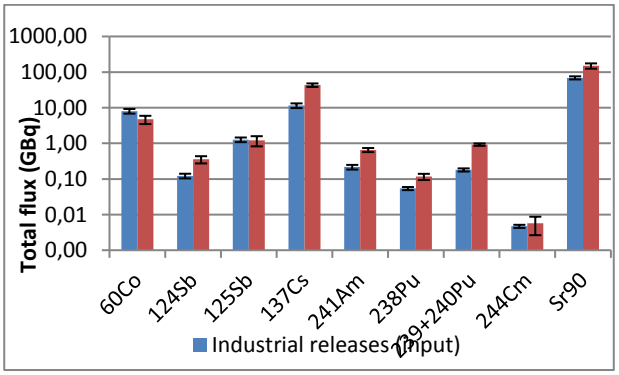

Figure 1. Mass balance between artificial radionuclides released into the Rhone and those delivered to the Mediterranean Sea (exemple for the year 2013).

This work was supported by the French Water Agency (Rhone Mediterranean Corsica Agency).

Variations of natural radionuclides as tracers of beach sedimentary dynamics

A.C. Arriola-Velásquez, A. Tejera, J.G. Guerra, I. Alonso, H. Alonso, M.A. Arnedo, J.G. Rubiano, P. Martel

Department of Physics, Instituto Universitario de Investigación en Estudios Ambientales y Recursos Naturales i-UNAT, Universidad de Las Palmas de Gran Canaria, Campus de Tafira, Las Palmas de Gran Canaria, 35017, Spain
Keywords: natural radionuclides, tracer, sedimentary processes, variability
Ana del Carmen Arriola Velásquez, ana.arriola101@alu.ulpgc.es

Natural and artificial radionuclides have been used as tracers of different marine sedimentary processes (Renfro, et al., 2016; Woszczyk, et al., 2017). The knowledge of coastal sedimentary dynamics is key to the sustainable management of high-value natural places for humans, such as beaches. Following this aim, the results from a three years study (from 2016 to 2019) of the spatial and temporal variability of natural radionuclides ^{226}Ra, ^{232}Th, ^{40}K, ^{210}Pb in Las Canteras beach, Spain, will be shown. This beach was selected due to its diverse sedimentary dynamic, combining the characteristic dynamic of a closed beach with that associated with a beach open to wave action (Alonso, 1994). Thus, this study could easily be extended to the management of other beaches of similar sedimentary dynamics.

For the spatial analysis a cluster and principal component analyses were performed by using stationary averages of the studied radionuclides activity concentrations and other quantities, such as grain size and or bulk density. The results show three zones of sediment distribution related to one of the main geomorphological characteristics of the beach (Figure 1).

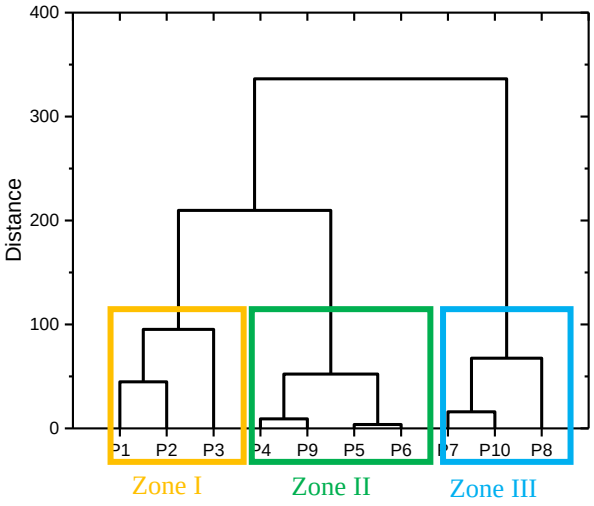

Figure 1. Dendrogram showing clustering for the different sampling points based on their activity concentrations of ^{226}Ra, ^{232}Th and ^{40}K.

The temporal analysis of the ratio ^{226}Ra/^{228}Ra (Dai et al., 2011) was used to stablish patterns of erosion and accumulation periods. The results agree with previous erosion/acucmulation studies at Las Canteras beach. Along with this ratio, ^{40}K is also analyzed as a tracer of the aforementioned sedimentary processes. Finally, relation of these potential tracers with some erosion and accumulation agents such as wave direction or the wave height, is studied (Figure 2).

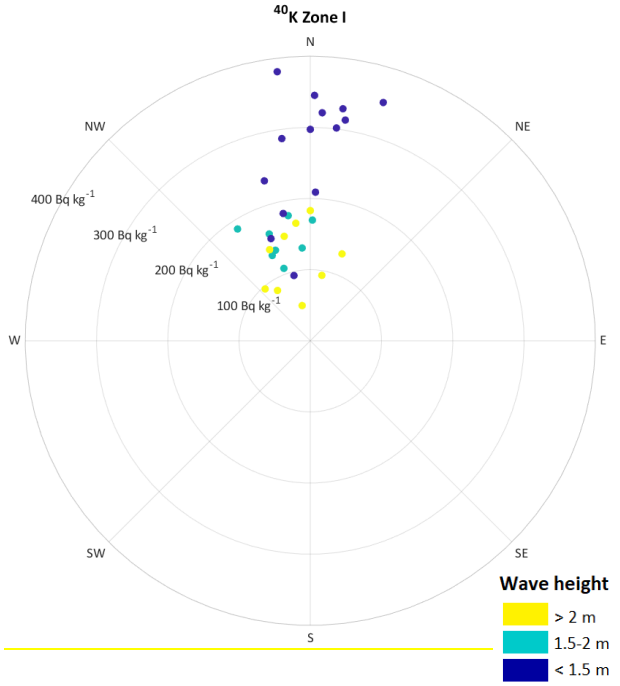

Figure 2. Azimuth plot of wave height and direction and activity concentration of ^{40}K for one of the established zones.

Alonso, I., 1994. Spatial beach morphodynamics. An example from Canary Islands, Spain. *Litoral* 94, 169–183.

Dai, Z.J., Du, J.Z., Chu, A., Zhang, X.L., 2011. Sediment characteristics in the North Branch of the Yangtze Estuary based on radioisotope tracers. *Environ. Earth Sci.* 62, 1629–1634.

Renfro, A.A., Cochran, J.K., Hirschberg, D.J., Bokuniewicz, H. J., Goodbred Jr, S.L., 2016. The sediment budget of an urban coastal lagoon (Jamaica Bay, NY) determined using ^{234}Th and ^{210}Pb. *Estuarine, Coast. Shelf Sci.* 180, 136–149.

Woszczy, M., Poreba, G., Malinowski, Ł., 2017. ^{210}Pb, ^{137}Cs and ^{7}Be in the sediments of coastal lakes on the Polish coast: Implications for sedimentary processes. *J. Environ. Radioact.* 169–170, 174–185.

Use of ^{137}Cs and $^{210}Pb_{ex}$ to assess soil redistribution in a cultivated site in western Algeria

A. Azbouche[1], B. Morsli[2], E. Fulajtar[3], S. Gouasmia[1], F. Gacem[4], F. Boussahoul[1], Z. Melzi[1]

[1]Nuclear Research Center of Algiers, 2 Bd Frantz Fanon Algiers, Algeria
[2]National Institute for Forest Research, BP 88 Mansourah, Tlemcen, Algeria
[3]Soil and Water Management &Crop Nutrition Section, Joint FAO/IAEA Division of Nuclear Techniques in Food and Agriculture, International Atomic Energy Agency, Vienna International Centre, PO Box 100, 1400, Vienna, Austria
[4]National Institute of Soils, Irrigation and Drainage (INSID), Avenue Pasteur –Hacène Badi –BP 148- 16200 El Harrach, Algiers, Algeria
Keywords: Fergoug Catchment; ^{137}Cs; ^{226}Ra-^{222}Rn equilibrium; $^{210}Pb_{ex}$, Gamma spectrometry; Conversion models; Erosion rate.
Corresponding author: A_Azbouche@yahoo.fr

Soil erosion and soil deposition represent a serious problem throughout the world, because of their impact on sustainable agriculture as well as on environmental conservation. ^{137}Cs and the ^{210}Pb are good radiotracers for documenting medium and long terms' soil erosion and deposition.

^{137}Cs and ^{210}Pb radiotracers' redistribution was studied in a cultivated area from Fergoug watershed, Mascara district (western Algeria) for their spatial distribution in order to assess soil loss. The study was carried out on a reference site where the surficial distributions of ^{137}Cs and $^{210}Pb_{ex}$ are uniform, and on a cultivated site with a slope of about 15%.

A total of 460 soil samples were sampled along three parallel transects using a motorized corer at a depth of 70 cm, and from a reference site for the determination of the reference activity with a coefficient of variation (CV) of around 20%. Soil samples were collected from the core each 2 cm till a depth of 20 cm, then each 5 cm between 20 and 40 cm depth. Beyond 40 cm, the samples are collected every 10 cm.

In laboratory, the soil samples preparation required drying, grinding and sieving at ≤ 2mm diameter then sealing for the ^{226}Ra-^{222}Rn secular equilibrium. They were afterwards packaged in cylindrical beakers for the measurements.

The measurement was carried out during 24 hours by means of a high resolution HPGe semi-conductor detector (1.8 keV for ^{60}Co 1332.5 keV line). The spectra were analyzed using the Genie-2000 software dedicated to the processing of gamma spectra. The detector efficiency calibration was simulated by Monte Carlo method using MCNP5 code.

The quantification of $^{210}Pb_{ex}$ was obtained after ^{226}Ra-^{222}Rn secular equilibrium by the subtraction of radium activity to the total activity of ^{210}Pb. The activity concentrations distribution of ^{137}Cs and $^{210}Pb_{ex}$ in the reference site are given in Table 1.

Table 1: ^{137}Cs and $^{210}Pb_{ex}$ at reference site

Depth (cm)	^{137}Cs activity concentrations (Bq kg^{-1})	$^{210}Pb_{ex}$ activity concentrations (Bq kg^{-1})
0-2	13.17 ± 0.43	26.9±0.21
2-4	12.61 ± 0.40	27.3±0.21
4-6	8.28 ± 0.34	24.4 ±0.19
6-8	5.16 ± 0.30	23.8±0.18
8-10	3.03 ± 0.23	22.4±0.18
10-12	1.88 ± 0.12	20.4±0.17
12-14	0.52 ± 0.07	18.9±0.16
14-16	0.45 ± 0.15	17.4±0.15
16-18	0.45 ± 0.14	17.2±0.15
18-20	0.14 ± 0.03	15.9±0.13
20-25	0.12 ± 0.03	12.3±0.11
25-30	0.17 ± 0.04	11.2±0.10
30-35	0.21 ± 0.04	11.3±0.10
35-40	< *DL	7.23±0.09
40-50	< *DL	2.17±0.09
50-60	< *DL	3.25±0.09
60-70	< *DL	1.23±0.09

*DL: Detection Limit

^{137}Cs and ^{210}Pb distributions in three transect (T_1, T_2, T_3) of Fregoug site are given in figure 1.

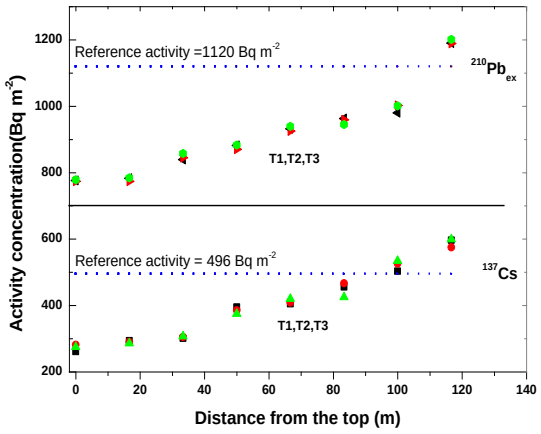

Figure 1: Distribution of ^{137}Cs and ^{210}Pb in Fergoug site

The specific activities of the ^{137}Cs and $^{210}Pb_{ex}$ obtained are then converted using both the proportional model and the mass balance model in order to quantify the erosion rate. The latter was estimated to range between 6.4 t ha^{-1} yr^{-1} and 24.9 t ha^{-1} yr^{-1}.

Influence of common decorporation agents on the speciation of trivalent f-elements in serum – a luminescence spectroscopic study

A. Barkleit[1], A. Heller[2]

[1]Institute of Resource Ecology, Helmholtz-Zentrum Dresden-Rossendorf, Dresden, 01328, Germany
[2]Molecular Cell Physiology and Endocrinology, Institute of Zoology, Faculty of Biology, Technische Universität Dresden, Dresden, 01062, Germany
Keywords: serum proteins, EDTA, DTPA, laser fluorescence spectroscopy
Presenting author, e-mail: a.barkleit@hzdr.de

The accidental release of radionuclides, especially actinides (An), in a nuclear facility or in the environment increases the risk of incorporation of these elements into the human body. Irrespective of the uptake pathway, via inhalation, ingestion, or through wounds or the skin, An are resorbed and transported by the bloodstream. Eventually, they are deposited in target organs (e.g., bone, liver or kidney) or partially excreted with urine or faeces. Fast and effective decorporation or chelation therapy is very important to minimize the health risk. To improve decorporation efficiency by choosing the right chelating agent or by designing new efficient chelators for different An, the understanding of their chemical speciation on a molecular level is crucial.

In this study, we investigate the chemical speciation of Cm(III) (as representative of An) and Eu(III) (as non-radioactive analogue for trivalent An) in blood serum. Subsequently, the alterations in speciation after spiking with common chelating agents often used for decorporation purposes, such as ethylenediaminetetraacetic acid (EDTA), or diethylenetriaminepentaacetic acid (DTPA), were studied and compared to biological ligands, such as citrate. Time-resolved laser-induced fluorescence spectroscopy (TRLFS) was used to perform the speciation investigations. Thermodynamic calculations were carried out to support the experimental results.

The dominant chemical species of Eu in serum were identified by comparing the Eu luminescence spectra and lifetimes in serum with those obtained in reference solutions with individual components of the serum, such as the proteins albumin and transferrin as well as the inorganic anions phosphate and carbonate. Linear combination fitting analysis (LCFA) on the sample spectra indicated that Eu is mainly coordinated by albumin (~50 %) and transferrin (~35 %), and to a lesser extent by inorganic anions like carbonate (~15 %).

The shape of the Eu luminescence spectrum in serum (Figure 1, black line) was only slightly influenced by adding citrate (red line) and EDTA (blue line), whereas the shapes of the pure ligand spectra differ strongly (dotted lines; Eu-citrate: red dots, Eu-EDTA: blue dots). This indicates that the speciation of Eu in serum was only slightly changed by these ligands. In contrast, DTPA caused a splitting of both the $^7F_1$ and $^7F_2$ peak (green line, compared to the black one), which is very similar to the Eu spectrum with the pure DTPA ligand (green dotted line), indicating a strong change of the Eu speciation in serum towards Eu-DTPA complexation. LCFA indicated that about 50 % of the Eu was coordinated by DTPA. The luminescence lifetimes and thermodynamic calculations as well as the Cm luminescence data show similar tendencies. Our results follow the trend of the respective complex stability constants of Am(III) complexes with chelating agents and the findings from ^{241}Am experiments with animals (Ansoborlo et al., 2007; Durbin 2008).

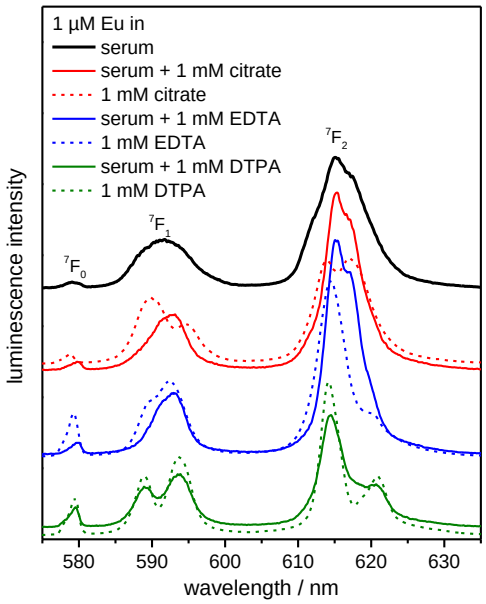

Figure 1. Luminescence spectra of Eu in serum and with different chelating agents. Luminescence bands are labelled with the respective ground state of the emission transitions.

This study combining TRLFS and thermodynamic calculations demonstrates a fast and easy way to screen the effect of several chelating agents towards (luminescent) An in vitro. In future, this could be a useful tool to improve decorporation methods.

Ansoborlo, E. et al., 2007. Review of actinide decorporation with chelating agents. *C. R. Chimie*. 10, 1010-1019.

Durbin, P. W. 2008. The quest for therapeutic actinide chelators. *Health Phys*. 95(5), 465-492.

High-resolution ^{129}I record of years 1956-2007 from an ice core in SE Dome Site, Greenland

A.T. Bautista VII[1], S.J.M. Limlingan[1], M. Toya[2], Y. Miyake[3], K. Horiuchi[4], H. Matsuzaki[2], and Y. Iizuka[5]

[1]Department of Science and Technology – Philippine Nuclear Research Institute (DOST-PNRI), Quezon City, 1101, Philippines
[2]Micro Analysis Laboratory, Tandem Accelerator (MALT), The University Museum, The University of Tokyo, Tokyo, 113-0032, Japan
[3]RIKEN Nishina Center for Accelerator-Based Science (RNC), Saitama, 351-0198, Japan
[4]Graduate School of Science and Technology, Hirosaki University, Aomori 036-8560, Japan
[5]Institute of Low Temperature Science, Hokkaido University, Sapporo 060-0918, Japan
Keywords: iodine-129, AMS, historical record, nuclear activities
Presenting author, e-mail: atbautistavii@gmail.com

^{129}I in ice cores, can be used to reconstruct the historical impact of human nuclear activities in the polar regions. Moreover, this information can be used as an age marker to confirm ice core chronologies, and as a tracer to better understand environmental processes. Here we show ^{129}I concentrations in an ice core from SE-Dome, Greenland for years 1956-2007 at a time resolution of ~4 months, the most detailed record to date. Results revealed ^{129}I bomb peaks in years 1959, 1962, and 1963, associated with tests performed by the former Soviet Union, one year prior, in its Novaya Zemlya test site. All ^{129}I bomb peaks were observed in winter (1958.9, 1962.1, and 1963.0), while tritium bomb peaks, another prominent radionuclide associated with nuclear bomb testing, were observed in spring or summer (1959.3, and 1963.6; Iizuka et al., 2017). These results indicate that ^{129}I bomb peaks can be used as annual and seasonal age markers for these years.

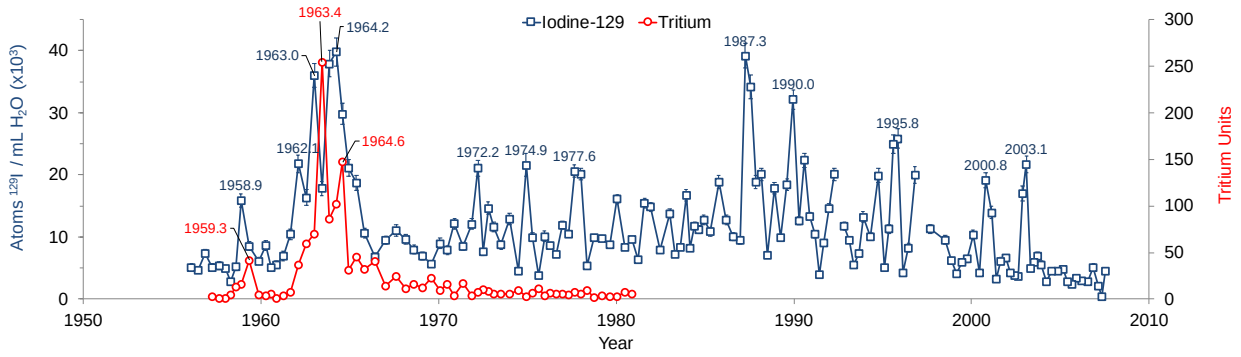

Figure 1. ^{129}I (in atoms x 10^3 / mL H2O) and tritium (in tritium units; from Iizuka et al., 2017) in the SE Dome ice core.

Reconstruction of Climate variations from Modern Warm Period in Balkan region by using ^{210}Pb chronology

R-Cs. Begy[1,2], Sz. Kelemen[1,2] ,J. Nikolov [3],N. Todorovic [3], N. Smječanin [4], M. Nuhanovic [4], M. Krmar [3], D.S. Veres[2]

[1]Faculty of Environmental Science and Engineering, "Babes-Bolyai", Cluj-Napoca, 400084, Romania
[2] Interdisciplinary research institute on Bio-Nano-Sciences, "Babes-Bolyai", Cluj-Napoca, 400084, Romania
[3]University of Novi Sad, Faculty of Sciences, Novi Sad, 210000, Serbia
[4] Department of Chemistry, University of Sarajevo, Sarajevo, 71000, Bosnia and Herzegovina
Keywords: Climate change, Peat bogs, 210Pb chronology
Robert-Csaba Begy, e-mail: Robert.begy@ubbcluj.ro

Climate Variability became more visible and attracts more attention in recent years. The late Holocene (last ca. 1400) encompasses some of the most striking variability events and/or alternations of climate that are claimed to be of importance in human history. These are the Dark Age Cold Period, the Medieval Climate anomaly, the little Ice Age and the Modern Warm Period. The Modern Warm Period (MoWP) is considered since the industrial revolution at 1850s, a warm shift has been predominant, and caused mainly by human-induced greenhouse gas emission, and characterized by fast glacial melt and extreme weather conditions, around the globe. The presented study has main goal to reconstruct the variation occurred in the climate in Balkan region of Europe during the MoWP. The perfect environments for climate reconstruction are the peat bog accumulations which grow rate are directly correlated with climate variations. Five peat bog deposits were chose for investigation from North and center part of Romania, from center and South part of Serbia and from center part of Bosnia and-Herzegovina. Peat samples were taken and LOI (Loss of Ignition) investigation was done for separation the organic material from the inorganic part. Radionuclide measurements (^{210}Pb, ^{226}Ra, ^{137}Cs, and ^{7}Be) were made by using gamma spectrometry with a HPGe Well-type detectors. By using the ^{210}Pb chronology each layer from the peat bog column was dated, and with organic material data the grow rates were calculated. The obtained grow rates reflect the changes between the humid and warm and dry cold periods. The figure below shows the increasing tendency in peat grows as an indicator of wet and warmer climate:

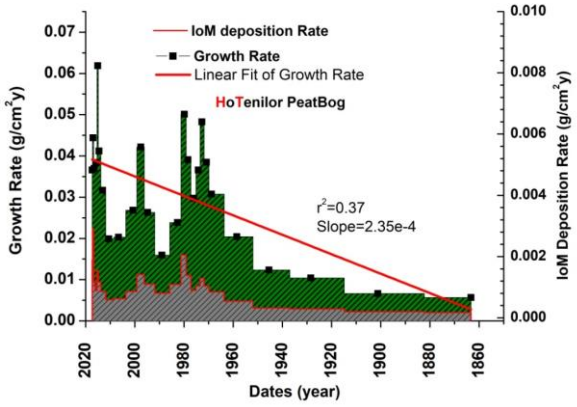

Figure 1. Peat bog growth tendency and variations.

Direct correlation can be found between the growth rate fluctuation and climatic events. From the organic material accumulation in the peat bog the cold/dry and warm/wet periods can be identified (they are marked in different ways in the graphs on Figures 2 and 3).

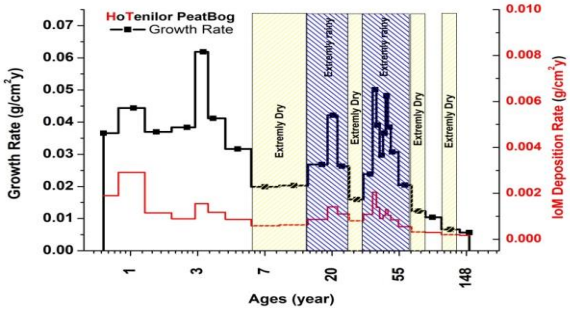

Figure 2. Climate variations for North part of Romania.

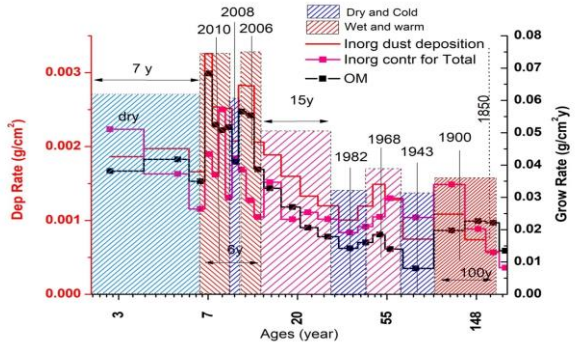

Figure 3. Climate variations for Centre part of Romania.

The marked periods are in good agreement with the ones presented in a multiannual report, published by the Romanian national meteorological agency in 2013.
The calculated peat bog (mosses OM) growth rate, clearly reflect the local climate changes, returns the micro-climate variations and in comparison with the Centre part peat accumulation (260 km distance) peat bog, the same variation can be recognized in each investigated region (North Vs Centre), and can be said that by Peat Bog Chronology, macro-climate can be clearly reconstructed for a given region (Transylvania, Romania). The investigation from other countries is currently on going.

This work was partially supported by the National Council Research under grant PN-III-P1-1.1-TE-2016-0814.

Decomposition of solid samples by various techniques with emphasis on actinides content

L. Benedik[1], A.M. Pilar[2], H. Prosen[2]

[1]Department of Environmental Sciences, Jožef Stefan Institute, Jamova 39, SI-1000 Ljubljana, Slovenia
[2]University of Ljubljana, Faculty of Chemistry and Chemical Technology, Večna pot 113, Ljubljana, SI-1000, Slovenia
Keywords: certified reference materials, decomposition, neutron activation analysis, alpha-particle spectrometry, isotopic composition
Presenting author, e-mail: ljudmila.benedik@ijs.si

One of the most important requirements in radiochemical analysis is complete dissolution of samples before isolation and radiochemical separation of the radionuclides of interest. It is well known that soil samples are often considered as one of the most difficult matrices to be dissolved. Uranium and thorium radioisotopes are incorporated into the structure of difficultly soluble minerals – such as zircon, apatite, titanite, allanite etc (Inn et al., 2016). These minerals are part of the soil and it is very important that they are completely decomposed during chemical treatment prior a radiochemical separation of the radionuclides of interest. On the other hand, most authors presume that the artificial radionuclides such as neptunium, plutonium and americium are attached to the surface of the sample particles which is probably not completely correct due to the growth of particles since the beginning of the nuclear era. This can also be said in the case when silicates accumulate in plants (Currie and Perry, 2007).

An overview of certificates of reference materials shows that various values are available for actinides and their radioisotopes: certified, noncertified, informational, recommended, etc. In the certification process the participated laboratories used various dissolution techniques, such as leaching, acid mixture dissolution, fusion, etc, as well as different measurement techniques using different amount of the samples taken for radiochemical analysis.

The aim of this study was to compare two dissolution techniques used in determination of actinides in environmental samples: conventional wet dissolution with mixtures of acids HNO_3, $HClO_4$ and HF and thermal fusion utilizing Li borate as a fusion agent and leaching with HNO_3 (Trdin et al., 2017). Certified reference material samples and samples from different interlaboratory comparison exercises, all with a significantly different composition were selected for determination of uranium, thorium, plutonium and americium radioisotopes. In the study various parameters, such as amount of the sample taken for analysis as well as addition of tracers before and after dissolution procedures, were investigated. For analyzing the content of actinides in samples as well as in obtained residues after dissolution, alpha-particle spectrometry and neutron activation analysis were used.

Figure 1 shows an example of Th-232 activity concentration in certified reference material NIST SRM 4357 (Ocean Sediment Environmental Radioactivity Standard) as a function of amount of the sample taken for analysis and type of dissolution. Its certified value in material is 13,0 ± 0,3 Bq/g, while its tolerance limit is in the range 11,6 – 14,3 Bq/kg (NIST, 1997).

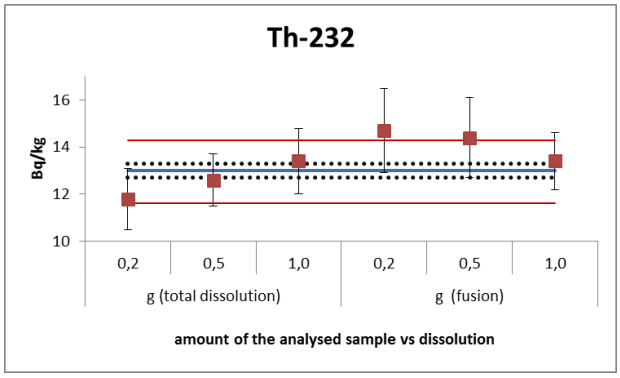

Figure 1. Dependence of Th-232 activity concentration in NIST SRM 4357 on amount of the sample and dissolution technique.

This work was supported by the Slovenian Research Agency (Research core funding No. P-0143).

Inn, K. G. W.; Robin Hutchinson, J. M.; Kelly, W. R.; Greenberg, R.; Norris, A.; Krey, P.; Feiner, M. S.; Fisenne, E.; Popplewell, D. S.; Gladney, E.; Beasley, T.; Huh, C. A.; Percival, D. R. *J Radioanal Nucl Chem* 2016, 307, 2513–2520.

Currie, H. A.; Perry, C. C. *Annals of Botany* 2007, 100, 1383–1389.

Trdin, M., Nečemer, M., Benedik, L. 2017. Fast decomposition procedure of solid samples by lithium borates fusion employing salicylic acid. Anal. Chem. 89, 3169-3176.

NIST, 1997. https://www.nist.gov/srmors/certificates/4357pdf

The Ruthenium-106 event, September-October 2017: A cold case

P. Bossew[1], F. Gering[1], E. Petermann[1], T. Hamburger[1], C. Katzlberger[2], M.A. Hernandez-Ceballos[3], M. De Cort[3], K. Gorzkiewicz[4], R. Kierepko[4], J.W. Mietelski[4]

[1]German Federal Office for Radiation Protection (BfS), Berlin and Munich, Germany
[2]Austrian Agency for Health and Food Safety (AGES), Vienna, Austria
[3]European Commission, Joint Research Centre (JRC), Ispra, Italy
[4]Department of Nuclear Physical Chemistry, Institute of Nuclear Physics, Polish Academy of Science (PAN), Kraków, Poland

Keywords: Ruthenium-106 incident, dose, nuclear forensics

Presenting author, e-mail: P. Bossew, pbossew(at)bfs.de

In late September 2017, traces of ^{106}Ru were recorded by air sampling stations in large parts of Europe. In some regions, over 100 mBq/m³ were measured as one-day means. Although resulting exposure was far below radiological concern, and, in addition, below detectability with the EURDEP dose rate network [1], the event aroused considerable interest, because this radionuclide is found only very rarely in environmental media. Earlier events involving ^{106}Ru were the Chernobyl accident and a few incidents in nuclear reprocessing plants.

The main exposure pathway was through inhalation, leading to up to about 0.3 µSv regionally. Other pathways are negligible in comparison. The geographical distribution of inhalation dose, inferred from monitoring results, is shown in Figure 1 (Bossew et al. 2019).

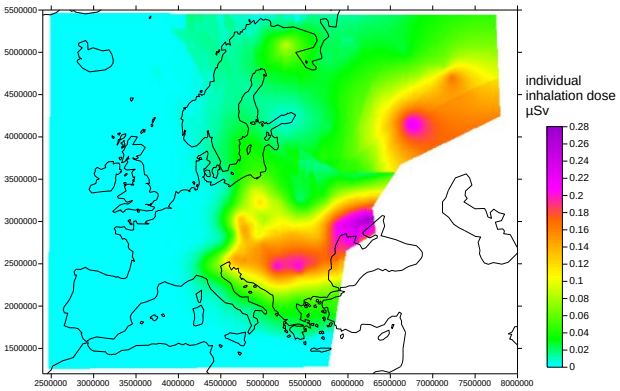

Figure 1. Geographical distribution of the individual inhalation dose. Blank areas: no interpolation possible. Axis units: m.

Two years later, the origin of the Ru is still a mystery. The Ru found in 2017 was not associated with other radionuclides except minute traces of ^{103}Ru. Therefore, a reactor accident can be excluded. Meteorological and dispersion calculations performed by several institutes (e.g. French agency for radiological protection (IRSN), German Federal Radiation Protection Agency BfS), unanimously led to a plausible region of origin in the Southern to Northern Ural region. However, Russian authorities denied any releases by civilian nuclear installations in the region.

In this presentation, we focus on summarizing dose calculations and the geographical distribution of dose. We also review documented accidents and incidents involving radioactive ruthenium. Finally, we report on talks with Russian authorities about the incident, and speculate about circumstances of the release and its likely origin as *argumentum e silentio*.

Although the incident has happened about 2 half lives of ^{106}Ru ago (376 days), we think that with today's possibilities of radiometric monitoring, and appropriate monitoring scheme, it should still be detectable in the environment in the trace of the plume not too far from the point of emission.

[1] https://remon.jrc.ec.europa.eu/About/Rad-Data-Exchange

Bossew P., Gering F., Petermann E., Hamburger T., Katzlberger C., Hernandez-Ceballos M.A., De Cort M., Gorzkiewicz K., Kierepko R., Mietelski J.W. 2019. An episode of Ru-106 in air over Europe, September–October 2017 – Geographical distribution of inhalation dose over Europe. *Journal of Environmental Radioactivity* 205–206, 79 - 92;

Development of certified reference materials in support of characterisation of naturally occurring radioactive material

E. Braysher[1,2], B. Russell[2], F. Dal Molin[3], D. Read[1,2]

[1]Department of Chemistry, University of Surrey, Guildford, GU2 7XH, UK
[2]Nuclear Metrology Group, National Physical Laboratory, Teddington, TW11 0LW, UK
[3]TATA Steel, Swinden Technology Centre, Rotherham, S60 3AR, UK
Keywords: NORM, CRM
Presenting author, e-mail: Emma Braysher, emma.braysher@npl.co.uk

Certified reference materials (CRM) are used to ensure quality control and metrological traceability through method validation and calibration of instruments (Parry 2012). Similarity in composition between a CRM and the material being analyzed is vital for the accuracy and precision of the measurement. Owing to the wide variety of sample types encountered across various industrial sectors, it is often difficult to find appropriate standards and there are currently insufficient CRM to support characterization and subsequent treatment of many radioactive materials.

One sector that suffers from a lack of CRM relates to those generating Naturally Occurring Radioactive Material (NORM) (Dal Molin et al., 2018), where accurate determination of the radionuclides present is vital to ensure operator safety and cost-efficient waste disposal. The aim of this project is to develop suitable CRM for NORM materials of major importance to the UK. Blast furnace slag from the steel industry and oil pipe scale from oil fields in Libya have been selected for processing and analysis as a CRM. Characterization of the materials was performed by gamma spectrometry, and homogeneity and stability testing were carried out on the materials to calculate an associated uncertainty. An inter-laboratory comparison exercise has been formulated to assist testing laboratories worldwide.

This work was carried out as part of a PhD project which was part-funded by the University of Surrey and the National Physical Laboratory. The National Physical Laboratory is operated by NPL Management Ltd, a wholly-owned company of the Department for Business, Energy and Industrial Strategy (BEIS).

Dal Molin, F., P.E. Warwick, and D. Read. 2018. Under-Estimation of Pb-210 in Industrial Radioactive Scales. *Analytica Chimica Acta*. 1000, 67–74.

Parry, Susan. 2012. Quality Assurance in the Nuclear Sector." *Radiochimica Acta*. 100, 495–501.

Monte Carlo simulation of HPGe detectors for radon measurements in the air using Marinelli containers

Róbert Breier[1], Miroslav Ješkovský[1], Veronika Palušová[1], Andrej Javorník[2,3], Jarmila Ometáková[2], Pavel P Povinec[1]

[1]Comenius University, Faculty of Mathematics, Physics and Informatics, 84248 Bratislava, Slovakia
[2]Slovak Institute of Metrology, Department of Ionizing Radiation, Karloveská 63, 842 55 Bratislava 4, Slovakia
[3]Slovak University of Technology in Bratislava, Faculty of Mechanical Engineering, Námestie slobody 17, 812 31 Bratislava 1, Slovakia
Keywords: Monte Carlo, HPGe, efficiency, background, radon, Marinelli container
Robert Breier, e-mail: breier@fmph.uniba.sk

Marinelli style gas containers (Fig.1) have been widely used for analysis of radon progeny in gas samples by gamma-spectrometry. Monte-Carlo simulations of the efficiency of HPGe detectors have been carried out with the aim to quantify the detection efficiency for various isotopes in the radon chain, and to compare it with experimental estimations.

Similarly, Monte-Carlo simulations have been used to compare measured gamma-spectra of HPGe detectors with the simulated ones (Povinec et al., 2008). However, all parameters needed for Monte-Carlo model are usually not well known. In the present study, a new Monte-Carlo based method to estimate unknown parameters has been proposed. Parameters obtained by the Monte-Carlo model has been used for calculation of peak efficiency of the HPGe detector (Canberra GC3200) with relative efficiency of 30%.

The detector was placed in a lead shield (cylinder size 500/200x600 mm). The samples were placed on the detector at 7 mm, 16 cm and 31 cm distances from the cryostat window. The detector model consists of germanium crystal, copper cryostat and lead shield (Fig. 1). The Marinelli container was placed on the top of the detector. For comparison, these mono-energetic etalons at distances of 16 and 31 cm were used in simulations: ^{241}Am, ^{139}Ce, ^{137}Cs, ^{54}Mn and ^{65}Zn for close geometry, and ^{29}I, ^{241}Am, ^{133}Ba, ^{57}Co, ^{139}Ce, ^{134}Cs, ^{152}Eu, ^{54}Mn, ^{88}Y, ^{65}Zn, ^{60}Co and ^{22}Na. For the Marinelli geometry ^{241}Am and ^{137}Cs have been used.

For the simulation of interactions of gamma-rays with the HPGe detector we used GEANT4 code developed at CERN for high-energy interaction studies (Allison et al., 2003; 2006). Depending on the definition of the physics list, we can optimize the simulation for specific applications (Breier and Povinec, 2009; 2016). We have been using a predefined physics list, QGSP_BIC_HP. This package allows a simulation of high-energy interactions of muons, and also includes low energy interactions of gammas.

The most important unknown parameter in the simulation is the thickness of the dead layer of the Ge crystal which has been parameterized in the GEANT4 geometry model (Fig. 1).

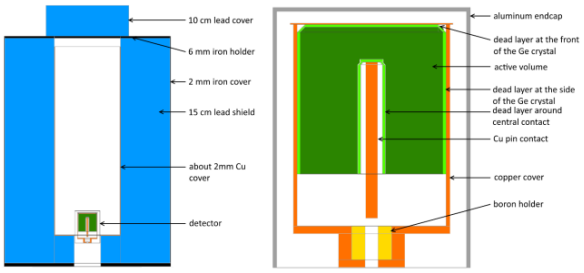

Figure 1. Schematic draw of GEANT4 geometry model.

The parametrization of the geometry model allows for changes in geometry options without recompilation of the model's code. The χ^2 values between simulation estimations and experimental values were stored for each run. This was then used for optimization of unknown parameters. The developed Monte Carlo model has been used for calculation of the detector efficiency for several energy regions and geometry configurations.

This work has been supported by the Slovak Research and Development Agency under the contract No. APVV-15-0017.

Agostinelli, S., et al., 2003. Geant4 - a simulation toolkit. Nucl. Instrum. Methods Phys. Res. A 506, 250–303.

Allison, J. et al., 2006. Geant4 developments and applications. IEEE Trans. Nucl. Sci. 53, 270–278.

Breier, R., Povinec, P.P., 2009. Monte Carlo simulation of background characteristics of low-level gamma-spectrometers. J. Radioanal. Nucl. Chem. 282, 799-804.

Breier, R., Hamajima, Y., Povinec, P.P., 2016. Simulations of background characteristics of HPGe detectors operating underground using the Monte Carlo method. J. Radioanal. Nucl. Chem. 307, 1957–1960.

Povinec, P.P., M. Betti, A.J.T. Jull, P. Vojtyla, 2008. New isotope technologies in environmental physics. Acta Phys. Slovaca 58, 1–154.

Semi mechanistic modelling of the long term soil to grass transfer of ^{137}Cs in French pastures

K. Brimo[*1], L. Pourcelot[1], M.A. Gonze[1]

[1]Institut de Radioprotection et de Sûreté Nucléaire (IRSN), LEREN, Cadarache, 13115 Saint Paul lez Durance, France
Keywords: cesium 137, uncertainty modelling, soil to grass transfer factor
[*] *khaled.brimo-PROMAN@irsn.fr*

The soil to grass transfer is one of the most important pathways leading to human ingestion of radiocesium 137 (^{137}Cs). A reliable prediction of the soil to grass transfer factor (*TF*) requires an accurate determination of both the labile distribution coefficient (*Kd*) at the soil-soil solution interface and the concentration factor (*CF*) at the soil solution roots interface, the values of which vary depending on the soil properties such as pH, clay content, organic matter content, and exchangeable K. An additional dynamic parameter named (*Dt*) is also needed which represents the decline in radiocesium bioavailability over time as result of its leaching and fixation in the root zone, defined as the percentage of bioavailable ^{137}Cs with respect to time. *Dt* is an essential information which is commonly described in literature by a kinetic equation involving three-parameters (k_{fast}, k_{slow}, P_{fast}) and two pools to mimic radioactivity declining rates for both the rapidly and the slowly declining fractions. Special attention should be paid to the estimation of *Dt* since its value may drastically influence the predicted *TF's*, especially on the long term after a nuclear accident. Up to now, the uncertainties associated to the aforementioned parameters and their impacts on the model prediction on the long term have not been addressed in the literature.

In this research, we first estimated the uncertainties associated to *Dt* at the slowly declining fraction (i.e. k_{slow}) deduced from a long term ^{137}Cs activity concentrations data in pasture soil, grass and milk collected from more than 25 years of monitoring programs at 10 different sites located in eastern France (Brimo et al., 2019). Based on an innovative Bayesian approach called "DREAM" (Vrugt et al., 2009) we then estimated the uncertainities related to *Dt* at the rapidely declining fraction (i.e. k_{fast}) using chronic data observed in 4 European countries (France, Germany, Austria and Czech Republic). To consider the effects of soil properties on plant uptake and the leaching rates of ^{137}Cs in a root zone soil and thereby on the imposed *CF* and *Kd* values, a set of empirical and semi mechanistic equations widely reported in literature were tested and evaluated (Absalom et al., 2001; Ota et al., 2016; Uematsu et al., 2015). The ^{137}Cs transfer factors to grass were finally predicted based on probabilistic simulations and compared to about 100 measurement data collected at dozen of French pasture sites. These sites were contaminated by the depositions from nuclear weapons tests and Chernobyl fallouts.

Our results showed a significant improvement in predicting *TF* which were in the whole comparable with those observed for all soils.

Absalom, J.P., Young, S.D., Crout, N.M.J., Sanchez, A., Wright, S.M., Smolders, E., Nisbet, A.F., Gillet, A.G., 2001.Predicting the transfer of radiocesium from organic soils to plants using soil characteristics. J. Environ. Radioact. 52, 31-43.

Brimo, K., Gonze, M.A., Pourcelot, L., 2019. Long term decrease of 137Cs bioavailability in French pastures: results from 25 years of monitoring. Submitted to J. Environ. Radioact. DOI: 10.1016/j.jenvrad.2019.106029

Ota, M., Nagai, H., Koarashi, J., 2016. Modeling dynamics of 137Cs in forest surface environments: application to a contaminated forest site near Fukushima and assessment of potential impacts of soil organic matter interactions. Sci. Total Environ. 551-552, 590-604.

Uematsu, S., Smolders, E., Sweeck, L., Wannijn, J., Hees, M. Van, Vandenhove, H., 2015. Predicting radiocesium sorption characteristics with soil chemical properties for Japenese soils. Sci. Total Environ. 524-525, 148-156.

Vrugt, J.A., ter Braak, C.J.F., Dike, C.G.H., Robinson, B.A., Hyman, J.M., Higdon, D., 2009. Accelerating Markov chain Monte Carlo simulation by differential evolution with self-adaptive randomized subspace sampling. J. Nonlinear Sci. Numer. Simul. 10(3), 273-290.

Characterization of Uranium containing particles originating from the Dounreay Nuclear Reprocessing Facility

I. Byrnes[1], O.C. Lind[1], E. Hansen[2], P. Dale[3], C. McGuire[3], K. Janssens[4], B. Salbu[1]

[1]CERAD CoE Environmental Radioactivity, Faculty of Environmental Sciences and Natural Resource Management, Norwegian University of Life Sciences (NMBU), Ås, 1432, Norway
[2]Norwegian Radiation and Nuclear Safety Authority (DSA), Østerås, 1361, Norway
[3]Scottish Environmental Protection Agency (SEPA), Stirling, FK9 4TR, United Kingdom
[4]Department of Chemistry, University of Antwerp, Antwerpen, 2020, Belgium
Keywords: U Particle, Particle Characterization, Nuclear Fuel Reprocessing
Presenting author, e-mail: ian.byrnes@nmbu.no

Since discovery in 1983, radioactive particles have been consistently recovered from the marine ecosystem and local beaches in the vicinity of the Dounreay Nuclear Reprocessing Facility in Scotland. These uranium containing, spent fuel particles were created during reprocessing practices in the 1950s, 1960s, and 1970s and, following deposition in the vicinity of the site, they represent a contamination risk to the environment. To properly assess the environmental impact and risk, information on particle characteristics such as elemental composition, structure, and oxidation state of the carrying matrix as well as contact doses is needed. In the present work, a collection of six Dounreay particles were characterized by a range of techniques. Scanning electron microscopy, with X-ray microanalysis, showed the structure and elemental composition of the surface of the particles. Semi-quantitative information on the elemental composition and distribution at higher penetration depths was provided by means of laboratory based micro X-ray fluorescence (see Figure 1).

The oxidation state of U in particle matrices was determined by synchrotron radiation based micro X-ray absorption near edge spectrometry. Subsamples of particles were digested to determine isotopic ratios of U, Nb, Nd, and Mo via triple quadrupole inductively coupled plasma mass spectrometry. Finally, the beta emissions from each particle were used to estimate beta activity. Along with gamma spectrometry, the results were used to assess the contact dose from each particle using the VARSKIN6 skin dose calculation tool. The results show two distinct types of particles (DFR and MTR) that originated from the same facility, but from different fuel types. Elemental and isotopic ratios vary considerably both between particles and within the matrices of single particles, and can be linked to the source and the release scenarios. The particle characterization presented here should provide a basis for improved assessments related to both human health and environmental impact of Dounreay particles in the environment. This work is also highlighting the usefulness of combining micro analytical x-ray techniques and mass spectrometry for source identification within both environmental chemistry, radioecology, and nuclear forensics.

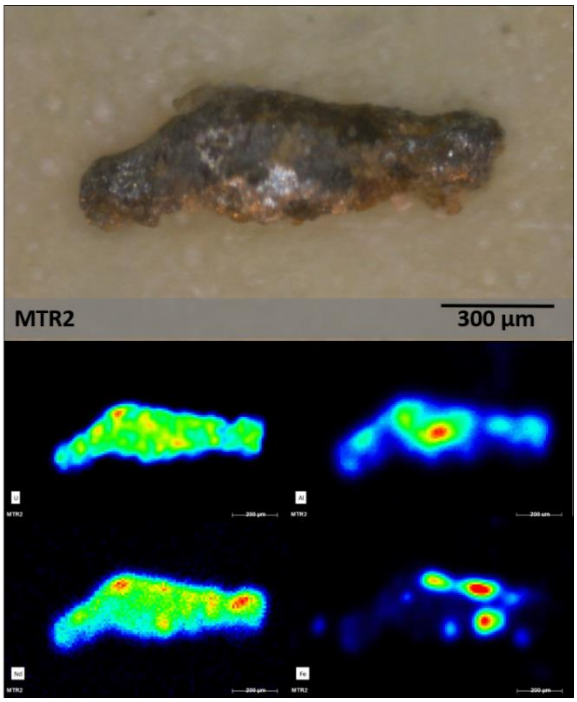

Figure 1. Elemental mapping (via benchtop µ-XRF) showing the distribution of U, Al, Nd, and Fe in Dounreay particle MTR2.

This study has been funded by the Research Council of Norway through its Centre of Excellence (CoE) funding scheme (Project No. 223268/F50).

Rapid and sensitive methods for transuraniuc radionuclides in environmental samples

X. Dai[1], M. Luo[1], D. Liu[1], Y. Wu[1], X. Shan[1]

[1] China Institute for Radiation Protection, 102 Xuefu Street, Taiyuan, 030006 China
Keywords: Transuranic radionuclides, sequential separation, ICP-MS, AMS, alpha spectrometry
Presenting author, e-mail: daixx@yahoo.com (Xiongxin Dai)

Radiochemical separation and analysis methods for transuranic radionuclides (e.g., ^{238,239,240,241}Pu, ^{237}Np, ^{241}Am and ^{242,244}Cm) in environmental samples are often required for research and for operational services in the fields of environmental monitoring, radiological protection, nuclear forensics, radioactive waste management and decommissioning, environmental radiochemistry and radioecology, etc. However, due to the very low levels of transuranic radionuclides in various complicated environmental matrices, fast, sensitive and accurate determination of these radionuclides in environmental samples is still a great challenge to radioanalytical chemists. Therefore, development of rapid and sensitive methods for transuranics in environmental samples, using modern radiometric and advanced mass spectrometric techniques in combination with emerging radiochemical separation technologies, is very much needed to shorten the sample analysis turn-around time, increase the analysis throughput, reduce the analysis cost, while obtaining good analytical accuracy and sensitivity.

This presentation will give a brief overview of some recently developed methods for the determination of Pu, Np, Am and Cm isotopes in water, liquid effluent, soil, aerosol and swipe samples etc (Dai et al., 2011, 2014 and 2016; Luo et al., 2018). In these methods, sequential separation procedures of transuranics using anion exchange and extraction column chromatography were utilized to speed up the radiochemical separation and purification processing and to allow for simultaneous determination of different radionuclides in single sample aliquot. The state-of-art source preparation methods for advanced mass spectrometric techniques including accelerator mass spectrometry (AMS) and inductively coupled plasma mass spectrometry (ICP-MS) as well as conventional alpha spectrometry counting techniques, have also been optimized to achieve ultra-low detection limits required for environmental samples. More details about these rapid and sensitive radioanlytical methods and their applications will be discussed in this work.

This work was supported by the Ministry of Science and Technology of China under grant No. 2015FY110800 and the National Natural Science Foundation of China under grant No. 11675150.

Dai, X., Kramer-Tremblay, S., 2011. Sequential determination of actinide isotopes and radiostrontium in swipe samples. *J. Radioanal. Nucl. Chem.* 289, 461-466.

Dai, X., Kramer-Tremblay, S., 2014. Five-column chromatography separation for simultaneous determination of hard-to-detect radionuclides in water and swipe samples. *Anal. Chem.* 86, 5441-5447.

Dai, X., Christl, M., Kramer-Tremblay, S., et al., 2016. Determination of atto- to femtogram levels of americium and curium isotopes in large-volume urine samples by compact accelerator mass spectrometry. *Anal. Chem.* 88, 2832-2837.

Luo, M., Xing, X., Yang, Y., et al. 2018. Sequential analyses of actinides in large-size soil and sediment samples with total sample dissolution. *J. Environ. Radioact.* 187, 73-80.

Analysis of Tritium on environmental levels in the area of Dresden, Germany

D. Degering; M. Kaden, M. Köhler

VKTA – Strahlenschutz, Analytik & Entsorgung Rossendorf e. V., Bautzner Landstraße 400, 01328 Dresden, Germany
Keywords: Tritium analysis, low-level analytical technique, liquid scintillation counting, Tritium in precipitation
Presenting author, e-mail: detlev.degering@vkta.de

The main source of Tritium in the environment is currently the production by nuclear reactions in the stratosphere at an altitude of 8 ... 18 km. Compared to the times of atmospheric nuclear weapons tests, anthropogenic emissions play at present a minor role. Tritium concentrations in environmental media (precipitation, surface and ground waters etc.) are consequently low and do not exceed levels of a few Bq l^{-1}. The analysis of such samples thus calls for the application of low-level techniques.

Low-level Tritium analyses are performed in the underground laboratory Felsenkeller, Dresden. The laboratory is located in the valley of the river Weißeritz in Dresden under an overburden of about 140 m w.e. of granite-like rock. At this location, the muon flux is reduced in the vertical direction by a factor of 50 whereas the integrated muon intensity is only reduced by a factor of about 30 due to the shape of the overlying rock (Niese, Köhler and Gleisberg, 1998; Ludwig et al., 2019).

Currently, the necessary sensitivity for Tritium in environmental media is achieved by applying an electrolytic Tritium enrichment in the aqueous samples followed by a LSC measurement using a Quantulus 1220 spectrometer. The electrolysis cells with a sample volume of about 200 ml allow total enrichment factors of 10 ... 15. Sample preparation and enrichment is controlled with respect to Tritium recovery and contamination by standard solutions and dead water samples, respectively.

Measurements with the low-level liquid scintillation counter Quantulus 1220 reach particularly low detection limits because of the reduced influence of cosmic radiation effects and the suppression of the Radon induced background by flushing its interior with nitrogen gas.

With the procedure described, detection limits according to DIN ISO 11 929 of about 0.1 Bq l^{-1} are currently achieved.

A further improvement of the sensitivity of Tritium analysis is expected by applying an AccuFLEX LSC-LB7 (Hitachi-Aloka). The instrument was installed underground at the beginning of 2019 and was extensively tested for its properties with respect to a minimised blank count rate and the reduction of detection limit by using large volume scintillation vials.

An example illustrating the necessity of low-level Tritium analysis is the determination of the Tritium concentration in precipitation as input function for hydrogeological investigations. Rainfall is collected as monthly composite samples on three locations in Saxony, Germany. The annual cycle of Tritium activity concentration in precipitation is characterised by a range of values between 0.5 and 2 Bq l^{-1} with a maximum in early summer. This behaviour is typical for any location worldwide and reflects exchange processes between strato- and troposphere.

Niese, S., Köhler, M., Gleisberg, B., 1998: Low-level counting techniques in the underground laboratory "Felsenkeller" in Dresden. *Journal of Radioanalytical and Nuclear Chemistry* 233 (1–2), 167–172.

Ludwig, F. et al., 2019: The muon intensity in the Felsenkeller shallow underground laboratory; *Astroparticle Physics* 112 24–34

Low-level measurements of environmental samples by gamma-ray spectrometry using well-type germanium detectors

A. de Vismes Ott[1], X. Cagnat[1], O. Masson[2], F. Eyrolle[3] and Ch. Ardois[1]

[1]PSE-ENV/SAME/LMRE, IRSN, Orsay, 91400, France
[2]PSE-ENV/SEREN/LEREN, IRSN, Saint-Paul-lez-Durance, 13115, France
[3]PSE-ENV/SRTE/LRTA, IRSN, Saint-Paul-lez-Durance, 13115, France
Keywords: Gamma-ray spectrometry, well-type HPGe, trace level, Monte Carlo simulations
Presenting author, e-mail: anne.de-vismes@irsn.fr

The French Institute for Radiation Protection and Nuclear Safety (IRSN) is responsible for the radiological environment monitoring program in France. In this context radioactivity in environment samples (biotas, waters, soils, aerosol filters…) is measured in the laboratory of environmental radioactivity metrology (LMRE). Many radionuclides are identified and quantified by low level gamma ray spectrometry, using 20 Hyper Pure Germanium (HPGe) detectors: the naturally occurring radionuclides and the artificial ones present at trace levels, due to the global fallout, or normally discharged by nuclear facilities, or potentially released in case of an incident or an accident.

These measurements can also be performed to support radioecology studies for a better understanding of the behaviour and transfer mechanisms of various naturally occurring or anthropogenic radionuclides in the environment. These samples are characterized by low activity concentrations but also often by very small quantities, implying very low activity per sample to measure. In this case we use well-type HPGe detectors allowing very high detection efficiencies thanks to their specific shape: indeed, the tube containing the sample is directly put inside the detector (see Figure 1, left).

This paper focuses on the use of the 3 well-type detectors of the laboratory, two with very low background installed in the deep underground laboratory in Modane (LSM), and the third one with very high resolution (SAGe well, Canberra) installed in our subsurface laboratory, located near Paris.

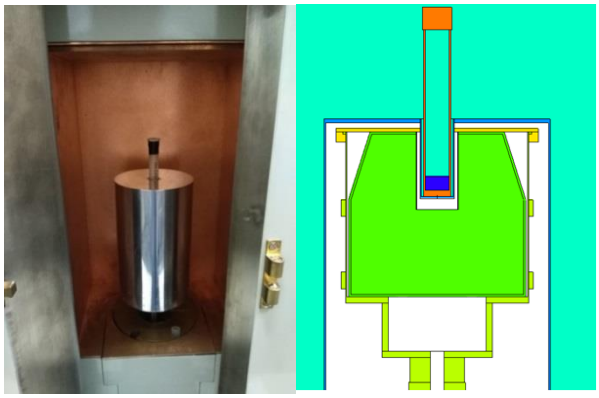

Figure 1. Picture (left) and Monte Carlo simulation (right) of the SAGe Well detector (Canberra) at LMRE (Orsay).

The detection efficiency has to be determined for each sample, accounting for the variability of the detection geometry due to the varying filling heights and of the attenuation correction due to the sample density and composition (organic matter, sediments, etc.). The detection efficiency is calculated by simulation using MCNP-CP, a Monte Carlo-type code of radiation matter interaction, which takes into account the radionuclide decay scheme and thus the True Coincidence Summing effect. The 3 detectors have been modelled (see figure 1, right) and models have been fitted by comparing simulated efficiencies and experimental efficiencies obtained with standard sources measurements.

The model is then used to calculate the detection efficiency by fixing the filling height of the tube, the mass and the sample matrix type. In routine the calculation is done automatically for 61 photon energies characterizing 32 radionuclides of interest and the sample matrix is chosen among 6 predefined material compositions (water, cellulose, ashes, soil…), but it can be performed whatever the radionuclide of interest and the sample matrix.

This paper describes this particular calibration method, validated with reference materials measurements. It will also show the achieved performances in terms of detection limits illustrated with measurement results of various environment matrices: sea water in the marine environment, suspended sediment sampled in rivers, or rain and cloud waters in the atmospheric field

The sample mass can be of few milligrams and even lower, and the total activity to be measured per sample is generally lower than 1 Bq, going down to few milliBecquerels.

For instance, the ^{137}Cs activity concentration in rain water samples can be determined down to 10 µBq/L and in cloud water samples down to few mBq/L via the measurement of a dry residue of less than 100 mg. Both measurements help so study the washout and rainout scavenging, and thus to improve the capability in modeling radionuclide deposition in case of a nuclear accident occurring in foggy conditions at lowland locations or in cloudy conditions at high altitude locations. Measurements of filtered waters sampled around Fukushima from only 1 L implied to determine ^{137}Cs activities down to 1 mBq and the suspended sediments mass from 2-5 L of water was lower than 1 mg. Both challenging measurements participated in the speciation of radioactive caesium in aquatic environment and quantification of fluxes to the ocean.

Baromembrane method for analysis of ultra-low concentrations of radionuclides in water sampling

A. Ekidin[1], M. Vasyanovich[1], A. Trapeznikov[2], A. Plataev[2]

[1]Radiation laboratory, Institute of Industrial Ecology UB RAS, Ekaterinburg, 620219, Russia
[2]Laboratory of General Radioecology, Institute of Plant and Animal Ecology UB RAS, Ekaterinburg, 620144, Russia
Keywords: baromembrane method, reverse osmosis, radionuclide, concentration.
M. Vasyanovich, e-mail: vasyanovich_maks@mail.ru

International documents indicate a possible negative environmental impact as a result of NPP liquid discharges of 31 radionuclides (IAEA, 2016). National requirements of the Russian Federation indicate the need for state regulation of 81 radionuclides in liquid discharges (Order of the Government, 2015). Analysis of available information demonstrate the necessity to take into account the background activity of radionuclides in water cooler system of nuclear power plants (Ekidin, 2016). Monitoring of liquid discharge sources allows to control background radionuclide concentration and determine the activity contribution in the water supply and waste water systems of nuclear power plants. The ultralow background concentrations of radionuclides in NPP water samples require special instruments and methods for their determination. The existing highly efficient methods for radionuclides sorption based on sulfides, dioxides and ferrocyanides of various metals are selective and can't be universal.

Using the baromembrane method based on an installation with osmotic membranes for determination ultralow radionuclide concentrations in liquid discharges of Russian nuclear power plants is demonstrated in this paper.

The standard control methods don't allow to authentically determine the radionuclides concentration in the form various metal salts in NPP liquid discharges due to the small amount of the initial sample (usually 10-20 liters). The proposed approach allows to concentrate of metal salts with osmotic membrane by 30-40 times, herewith the initial sample volume can be reduced from 1000 to 30 liters. After this, the remaining 30 liters of the sample should be evaporated until dry residue. It allows to measure Cs-137 with detection limit about $5.0 \cdot 10^{-4}$ Bq/l.

Method verification of concentrating radionuclides in water using baromembrane method was performed with another method. A natural sample of water with a volume of 500 liters was concentrated using an osmotic membrane and ordinary evaporation. The dry residues were analyzed with HPGe detector for evaluating Cs-137 concentration. This was made in the radiation laboratory of the Institute of Industrial Ecology (IIE UB RAS) and in the Laboratory of General Radioecology of the Institute of Ecology, Plants and Animals (IPAE UB RAS). The results this intercomparison is presented in table 1.

Table 1. Cs-137 concentration in natural water

Type of sample	IIE UB RAS, 10^{-3} Bq/l	IPAE UB RAS, 10^{-3} Bq/l
Evaporation 1	1.9±0.5	1.6±0.4
Evaporation 2	1.6±0.6	1.8±0.4
Osmotic membrane 1	2.2±0.7	2.8±0.8
Osmotic membrane 2	1.7±0.6	1.9±0.8

± *extended uncertainty*

The study of various liquid discharge sources made allows to obtain the results of the metal salts concentration of the main radionuclides that may be present in liquid discharges at Russian NPPs in the ranges:

Cs-137: from $1.5 \cdot 10^{-3}$ to $1.4 \cdot 10^{-2}$ Bq/l;
Sr-90: from $3.2 \cdot 10^{-3}$ to $3.8 \cdot 10^{-2}$ Bq/l.

Depending on the technological processes such radionuclides as Mn-54 and Co-60 are detected episodically in dry samples from liquid discharge sources.

This work was supported by the Ural Branch of the Russian Academy of Science Project 18-11-2-2.

IAEA, 2016. Nuclear Energy Series, No. NG-T-3.15. INPRO Methodology for Sustainability Assessment of Nuclear Energy Systems: Environmental Impact of Stressors IAEA, VIENNA.

The list of pollutants in respect of which measures of state regulation are applied in the field of environmental protection, 2015. Order of the Government of the Russian Federation of 08.07.2015, No. 1316-p. Moscow.

Ekidin A.A., Malinovskii G.P., Rogozina M.A., Vasil'ev A.V., Vasyanovich M.E., Yarmoshenko I.V., 2016. Evaluation of the contribution of technogenic radionuclides to the total activity of NPP emissions on the basis of a simulation model. *Atomic Energy.* 119, 271-274.

Continuous monitoring of submarine spring by means of gamma-ray spectrometry at Anavalos, Greece

G. Eleftheriou, F.K. Pappa, N. Maragos, C. Tsabaris

Institute of Oceanography, Hellenic Centre for Marine Research, Anavyssos, 19013, Greece
Keywords: submarine groundwater discharges, gamma-spectrometry, in-situ monitoring, radon daughters
Presenting author, e-mail: Georgios Eleftheriou (geoelefthe@hcmr.gr)

The freshwater flow through continental margins from the seabed to the sea, commonly known as submarine groundwater discharge (SGD), is a hydrological phenomenon with great impact on the coastal zone mainly due the transferred substances and pollutants. Especially in krast formations, SGD is often occurred through submarine springs with great amounts of discharged water. The systematic monitoring of such springs can provide valuable information about the total flux, the temporal variations and possible alterations in the water quality. In this effort, the application of in-situ underwater gamma-ray spectrometry has been proven a powerful tool since groundwater is rich in radon and its decay products are gamma-ray emitters, providing simultaneous quantitative determination of all radionuclides present in the emanating groundwater (Tsabaris et al., 2012). The monitoring of ^{40}K, radon (^{214}Pb, ^{214}Bi) and thoron (^{208}Tl) progenies can provide a mean for the estimation of groundwater discharge velocity and the degree of groundwater-seawater mixing, while recently the use of underwater gamma-ray spectrometry was proposed for the determination of groundwater residence time in the coastal zone (Eleftheriou et al., 2017).

In this work the radiological monitoring of Anavalos SGD site at NE Peloponnese, Greece is presented. Anavalos is an ideal test site for radiotracers applications since it is consisted of a number of swallow coastal submarine springs isolated from seawater by a curved dam, forming a freshwater well into the sea. Two submarine systems, the low resolution NaI(Tl) detector KATERINA and the new medium resolution $CeBr_3$ detector GeoMAREA (Tsabaris et al., 2019), have been deployed over a submarine spring in the seabed (Flux site) and 1.5 meter below the surface the well (Inventory site) for a 5 month period. Additional monitoring of salinity, conductivity, temperature and water level was performed, while over the submarine spring a mechanical flow-meter was also deployed and local meteorological data were systematically collected.

During the monitoring period the activity concentrations of the radon progenies varied from 3 to 30 kBq/m^3 while thoron progenies variations were significantly lower (4 – 10 kBq/m^3) and ^{40}K was almost constant (~ 0.5 kBq/m^3). The discharge rate, the groundwater and total water flux were estimated from radon and thoron progenies timeseries. The results were companied and correlated with all the additional acquired data. Water sampling and lab measurements of radium isotopes concentrations, heavy metals, major elements and nutrients were also performed in order to determine the quality of the discharged groundwater.

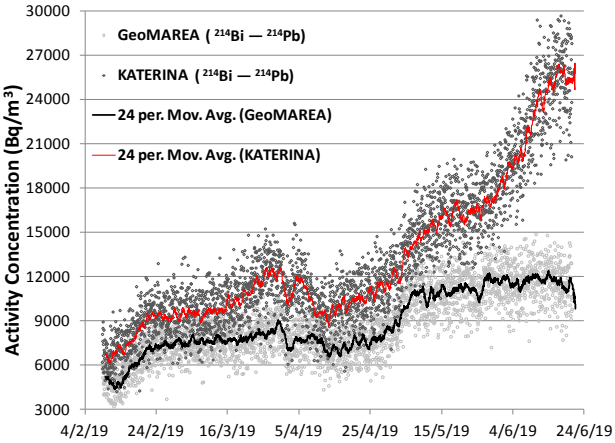

Figure 1. Radon progenies (mean of ^{214}Bi and ^{214}Pb) variations at the Flux (GeoMAREA detector) and Inventory (KATERINA detector) sites of Anavalos.

This work is supported by the national program "ΕΠ ΑΝΑΔ-ΕΔΒΜ" in the frame of the ANAVALOS project (MIS 5005218) entitled "Development of an in-situ method for the study of submarine groundwater discharges at the coastal zone using radio-tracers".

Tsabaris, C., Patiris, D.L., Karageorgis, A.P., Eleftheriou, G., Papadopoulos, V.P., Georgopoulos, D., Papathanassiou, E., Povinec, P. 2012. In-situ radionuclide characterization of a submarine groundwater discharge site at Kalogria Bay, Stoupa, Greece. *J. of Environ. Radioact.* 108, 50-59.

Eleftheriou, G., Tsabaris, C., Patiris, D.L., Androulakaki, E.G., Vlastou, R. 2017. Estimation of coastal residence time of submarine groundwater discharge using radium progenies. *Appl. Radiat. and Isot.* 121, 44-50.

Tsabaris, C., Androulakaki, E.G., Prospathopoulos, A., Alexakis, S., Eleftheriou, G., Patiris, D.L., Pappa, F.K., Sarantakos, K., Kokkoris, M., Vlastou, R. 2019. Development and optimization of an underwater in-situ cerium bromide spectrometer for radioactivity measurements in the aquatic environment. *J. of Environ. Radioact.* 204, 12-20.

Application of synthetic benzoic acid-7-^{14}C in environmental radiocarbon measurement

B. Feng [1,2#], C. Zhao,[2#], B. Chen[1], W.H. Zhuo[1], L.F. He[2], F.D. Tang,[2*]

[1]Institute of Radiation Medicine, Fudan University, Shanghai, 200032, CHINA
[2] Division of Chemistry and Ionizing Radiation Measurement Technology, SIMT, Shanghai, 201203, CHINA
Keywords: Radiocarbon, LSC, Benzoic Acid Synthesis, Environmental Radioactivity Measurement
Presenting author (Feng, B.), e-mail: 17111140002@fudan.edu.cn

Radiocarbon (^{14}C) monitoring is very important to assess the potential environmental impact by nuclear facility operation. The traditional techniques developed for high precision ^{14}C analysis are synthesized benzene method and AMS method. However, due to the limitation of cost and operability, these techniques are rarely considered in environmental-level monitoring. Although the gel suspension counting method and absorption counting method have been developed as alternative methods under the framework of radiation monitoring, the self-absorption of suspended particulate and the residues of organic amines (e.g. Carb-Sorb E) might have negative effect on these methods. Moreover, owing to physical quench, the performance of long-term stability in these two methods was also found not good enough in previous practice. Therefore, the development of a low-cost, reliable and practical method for environmental ^{14}C measurement is still of worth to study. Synthetic benzoic acid-7-^{14}C technique is classical in radiocarbon labeling and is widely used in biochemical and medical studies. Since benzoic acid has been confirmed to be soluble and steady in the toluene and 2,6-DIPN, it makes benzoic acid-7-^{14}C a promising sample medium in environmental ^{14}C measurement.

By using NaOH bubbler and combustion oven (if needed), the environmental ^{14}C containing samples were first stored in the form of $Na_2{}^{14}CO_3$. Sample preparation was mainly carried out in a self-developed vacuum instrument. In this vacuum instrument, the $^{14}CO_2$ gas was released from $Na_2{}^{14}CO_3$ solution by adding H_3PO_4, and reacted with phenylmagnesium bromide, producing benzoic acid-7-^{14}C solution. Subsequently, the purified benzoic acid was prepared following with extraction, filtration, and crystallization. Purity and yield were determined by HPLC for each synthetic sample. A total of 1.3 g synthetic sample was added in a low-potassium glass bottle and mixed with 20 ml of cocktail (Ultima-Gold-LLT) for 1000 min LS counting (Quantulus-1220).

To evaluate the radioactive analysis performance of this technique (e.g. detection limit, linear, and long-term stability, etc.), the background samples (blind coal) and the standard samples ($Na_2{}^{14}CO_3$, 4 activity levels in range of 1100~2200 Bq/kg C) were used for 5 batches of benzoic acid-7-^{14}C synthesis. To test the method's repeatability, additional 4 batches, including 2 background samples and 2 standard samples at a specific level, were prepared as well. In each batch of experiment (9 batches), the synthesis sample was considered to prepare three replicates LS samples for intra-group comparison. To further validate this technique in field ^{14}C monitoring, three $^{14}CO_2$ samples collected in a nuclear plant were parallelly converted to benzoic acid and graphite for LS and AMS measurement.

The synthetic procedure mentioned above is convenient and repeatable. Only about 2 hours were taken for sample's synthesis and purification. The purity of the synthetic benzoic acid crystal was 91.8%±2.4% (n=9) and the yield was about 85%. Under the adopted counting condition (100 min for one cycle measurement, 10 cycles for one LS sample; counting window 139–356 channels), the background counting rate was 1.63±0.04 cpm (n=9); the counting efficiency was 41.7%±0.5% (n=18) and the LLD was estimated to be 64.0 Bq/kg C. Figure 1a shows that the linearity of this method has a good performance (R^2=0.998, p<0.01) in a wider range of environmental ^{14}C level. In all measurement, the intra-group and inter-group deviations were 0.38%-3.06% and 1.24%-3.55%, respectively. Figure 1b illustrates that the counting rate of both background sample and standard sample are stable in 5 months. For the field experiment, the results showed that the specific activity of atmospheric $^{14}CO_2$ was in the ranges from 450.46 to 493.75 Bq/kg C, which is well consistent with the results measured by AMS (deviation within ±9%).

Although the synthetic benzoic acid technique was developed in the middle of last century, it is the first time being used in the environmental ^{14}C measurement. Our preliminary results showed that this method has many advantages, such as cost effective, easy operating and reliable. Besides, our sample system was confirmed to be well repeatable and long-term stability. In the field experiment, this method showed good performance in a wider range of environmental ^{14}C level despite its relatively higher detection limit. In short, this method is expected as an alternative approach in environmental ^{14}C measurement, particularly in routine ^{14}C monitoring near the nuclear power plant.

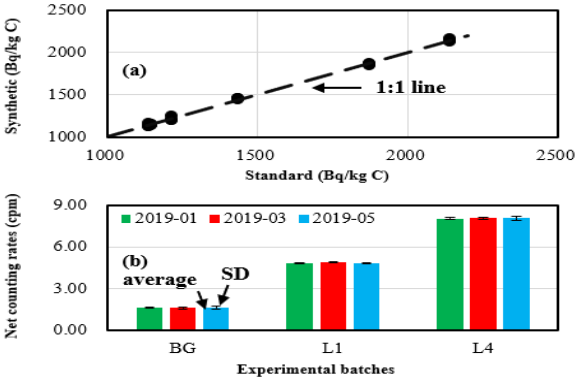

Figure 1. Radioactive analysis performance of synthetic benzoic acid method: (a) linearity; (b) long-term stability.

This study was supported by Shanghai Quality and Technical Supervision Research Program under grant No.2017-01.

A radiological data library for environmental impact assessments of accelerator facilities

R. Froeschl and P. Vojtyla

CERN, Geneva 1211, Switzerland
Keywords: Environmental impact assessment, radiological data, accelerator facilities, Monte Carlo simulations
Presenting author email: robert.froeschl@cern.ch

The radiological impact of an accelerator facility on its environment has to be assessed during the design phase of the facility and then monitored during its operation. This involves the calculation of the effective doses to members of the public (usually critical groups) and their subsequent comparison with dose constraints and regulatory limits (Vojtyla, 2009).

These assessments are carried out at CERN using dedicated computer codes for releases of activated air and discharges of activated water as well as Monte Carlo radiation transport codes such as FLUKA (Böhlen et al, 2014; Fassò et al. 2005). The source terms are also typically obtained by FLUKA Monte Carlo simulations and can comprise a huge variety of radionuclides, including β^+-emitters produced in high-energy spallation reactions that are not common in nuclear power plants.

Dose coefficients and dose conversion coefficients for all the relevant radionuclides are crucial for the calculation of the effective dose to members of the public from the given source term.

A dedicated radiological data library has been developed for the assessment of the environmental impact of accelerator facilities. The required radiological data consist of the physicochemical form, decay data (half-life, decay chains and γ-decay radiation), dose coefficients for inhalation and ingestion and dose conversion coefficients for several external exposure scenarios. The various data sets used as sources for the radiological data library will be presented.

The functional requirements for the radiological data library are 1) compliance with directives from national regulators; 2) coverage of all the relevant radionuclides; 3) integration of multiple data sets; 4) data sets for all relevant age groups; 5) handling of overlapping data sets; 6) traceability of all the data used in the final assessments; 7) extensibility for seamless integration of new data sets and 8) flexibility to provide the data in several output formats. The various requirements will be discussed in detail together with the strategies to ensure their implementation. This includes also the use of approximations when crucial data is not available.

The radiological data library is generated by a dedicated computer code that implements all these data sets and requirements and produces the required information for the traceability of all the coefficients. This code has been developed in the python programming language (Rossum, 2003).

As of May 2019, the library contains radiological data for 825 radionuclides from 97 chemical elements, satisfying the operational needs for environmental impact assessments of the CERN accelerator facilities.

Finally, foreseen updates and inclusions of newly available data sets as well as the use of these radiological data for other radiation protection assessments at CERN will be presented.

T.T. Böhlen, et al, 2014. The FLUKA Code: Developments and Challenges for High Energy and Medical Applications, Nuclear Data Sheets 120, pp. 212–214.

A. Fassò, A. Ferrari, J. Ranft, P.R. Sala, 2005. FLUKA: a multi-particle transport code, CERN-2005-10, INFN/TC-05/11, SLAC-R-773.

P. Vojtyla, 2009. Programmes for the evaluation of the environmental impact, Radiation Protection Dosimetry, Volume 137, Issue 1-2, November 2009, Pages 134–137, https://doi.org/10.1093/rpd/ncp197.

G. V. Rossum, 2003. The Python Reference Manual, Network Theory Ltd., September 2003.

Estimation of radiocesium concentration in brown rice using the soil exchangeable potassium content and soil radiocesium concentration

S. Fujimura[1], K. Yamamura[2], T. Ota[1,3], T. Shinano[4]

[1]Tohoku Agricultural Research Center, NARO, Fukushima, 960-2156, Japan
[2]Institute for Agro-Environmental Sciences, NARO, Tsukuba, 305-8604, Japan
[3] Bio-oriented Technology Research Advancement Institution, NARO, Kanagawa, 210-0005, Japan
[4] Graduate School of Agriculture, Hokkaido University, Sapporo, 060-8589, Japan
Keywords: brown rice, prediction, radiocesium, transfer factor.
Presenting author, e-mail: fujimu@affrc.go.jp

A large area of farmland in eastern Japan was contaminated by radiocesium (RCs) released from the Fukushima Dai-ichi Nuclear Power Plant owned by the Tokyo Electric Power Company after the accident on March 11, 2011. In Fukushima Prefecture, to reduce RCs levels of brown rice, large amounts of K fertilizer have been applied to paddy fields. RCs concentration in brown rice has not exceeded the standard limit (100 Bq kg^{-1}) since 2015. However, paddy field experiment conducted without K fertilizer in 2014 and 2015 indicates that concentration of RCs in brown rice could exceed the standard limit under low soil exchangeable K content (ExK) (below 80 mg-K kg^{-1}) (Ishikawa et al., 2017).

We previously constructed an equation to predict the concentration ratio (CR; RCs ratio of brown rice to soil) using ExK using field data obtained from 2012 to 2015 in 321 paddy fields distributed all over the Fukushima Prefecture (Yamamura et al., 2018). We found that the CR approximately follows a lognormal distribution under the given environmental conditions. Two factors are considered in predicting the logarithmic quantity of the CR: three districts in the Fukushima Prefecture and the year. The estimated parameters indicated that CR in Nakadori district was approximately 0.40-fold of those in Hamadori and Aizu districts under the same ExK. Calculated rate of decline of CR was 0.17 per year. In this study, we conducted subsequent survey of CR after 2015 and confirmed the prediction accuracy of the equation, and estimated the required appropriate ExK by using the equation that ensures the low risk of brown rice exceeding the standard limit.

The prediction accuracy of the equation was confirmed using field data obtained in 2017. We evaluated the goodness-of-fit by visually comparing the observed distribution with the predicted distribution. We can calculate the standardized CR by dividing each observed CR by the expectation of each observation. We found that the curve fit closely with the histogram considering the rate of decline by year (Figure 1).

By using estimated parameters, 95% quantile of RCs concentrations in brown rice are predicted (Figure 2). The prediction lines indicate that 95% quantile of RCs concentration in brown rice is less than 25 Bq kg^{-1} when ExK is 200 mg-K kg^{-1}, which is recommended value to inhibit translocation of RCs from soil to brown rice, while it is approximately 80 Bq kg^{-1} when ExK is 80 mg-K kg^{-1} under soil RCs concentration of 3,000 Bq kg^{-1}.

It is concluded that the equation derived by statistical analysis of field data precisely predict the distribution of CR, and ExK at harvest is estimated by the equation under the given soil RCs concentration and target value of 95% quantile of RCs concentration in brown rice.

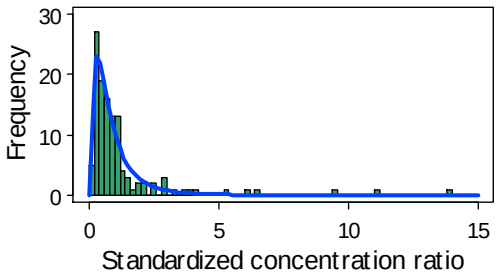

Figure 1. Comparison among observed and predicted distributions of CR in 2017. The histograms show the frequency distributions of standardized CR calculated by using the estimated parameters. The bold curve approximately indicates the predicted frequency distributions of detected observations.

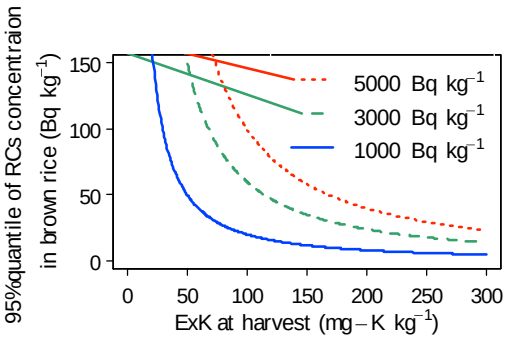

Figure 2. 95% quantile of RCs concentration in brow rice in soil RCs concentrations of 1000, 3000 and 5000 Bq kg^{-1} in 2017. The values were calculated using parameters for Hamadori in 2015.

This work was supported by the projects funded by the Ministry of Agriculture, Forestry and Fisheries, Japan.

Ishikawa, S. et al. 2017. Low-cesium rice: mutation in OsSOS2 reduces radiocesium in rice grains. *Sci. Rep.* 7, 2432.

Yamamura, K. et al. 2018. A statistical model for estimating the radiocesium transfer factor from soil to brown rice using the soil exchangeable potassium content. *J. Environ. Radioact.* 195, 114-125.

Radioecology in placer deposits: a case study

R.García-Tenorio[1,2], O.C.Lind[3], I.Vioque[2], M.C.Jimenez-Ramos[1], C.Bañobre[4] and B. Salbu[3]

[1]Centro Nacional de Aceleradores, CNA, Universidad de Sevilla-Junta Andalucía- CSIC, Sevilla, Spain
[2]Department of Applied Physics II, Universidad de Sevilla, Sevilla, Spain
[3] CERAD CoE Environmental Radioactivity, Faculty of Environmental Sciences and Natural Resource Management, Norwegian University of Life Sciences (NMBU), Ås, 1432, Norway
[4]Centro Universitario Regional del Este (CURE), Universidad de la República, Rocha, Uruguay
Keywords: Radioecology, NORM, particles, placer deposits
Presenting author, e-mail: R. Garcia-Tenorio, gtenorio@us.es

A placer deposit, or placer, is an accumulation of high density minerals formed during sedimentary processes by gravity based separation of particles originating from weathering of rocks, and subsequently by the effect of gravity on transporting particles. Different heavy minerals such as zircon, ilmenite, monazite, rutile and quartz can be found in such deposits, mostly in the form of independent grains or nodules. These minerals will in some cases contain enhanced amounts of radionuclides of the uranium and thorium series, and are chemical resistant to weathering and, consequently, are durable.

Alluvial placer deposits containing NORM heavy mineral particles constitute a challenge in radioecology because the behaviour of the natural radionuclides and their potential transfer to plant and water will be affected by their presence of a considerable fraction associated with individual inert particles. Measured values for Transfer Factor (TF) and distribution coefficient (Kd) for U and Th and their progenies in such deposits should be expected to be significantly lower (TF) and higher (Kd), respectively, than IAEA handbook values.

As a case study, this paper will focus on the Matamulas alluvial placer deposit located in the centre of Spain, being investigated from a radioecological point of view. This deposit is characterized by grey monazite nodules of 0.3 – 2.0 mm of diameter with a diagenetic metamorphic origin, found at concentrations of 2.5 – 3 kg/m^3. These nodules contain particularly enhanced Th concentrations compared with the typical concentrations found in soils.

Attending to the radioecological orientation of the study the work has been focused on:

1.-Performance of external gamma-dose rate measurements carried out along the deposit, and production of an associated radionuclide inventory map, the external gamma dose rates have been found moderates because the nodules enriched in Th are quite diluted in the deposit.

2.-Determination of the radionuclide grain-size distribution in soil aliquots collected in the area and its relation with the monazite nodules. The grain-size fraction from 0.3-1.5 contains in the form of nodules more than 90% of the Th associated to the soils

3.-Analysis of the morphological and elemental characterization of isolated grey monazite nodules by applying SEM-EDX as well as micro-XRF and micro-IBA techniques (Figure 1), The distribution of the Th in the monazite nodules is quite uniform while gradients of concentrations are observed for the associated rare-earths

4.-The application of leaching experiments to evaluate the potential mobility and bioavailability of the radionuclides from the NORM particles. These experiments show that the amount of Th leached from the nodules with groundwater collected in the area is negligible and extremely limited when solutions as 0.16M HCl are used. All the results obtained reinforce the idea that these monazite alluvial deposits have a quite limited radioecological impact.

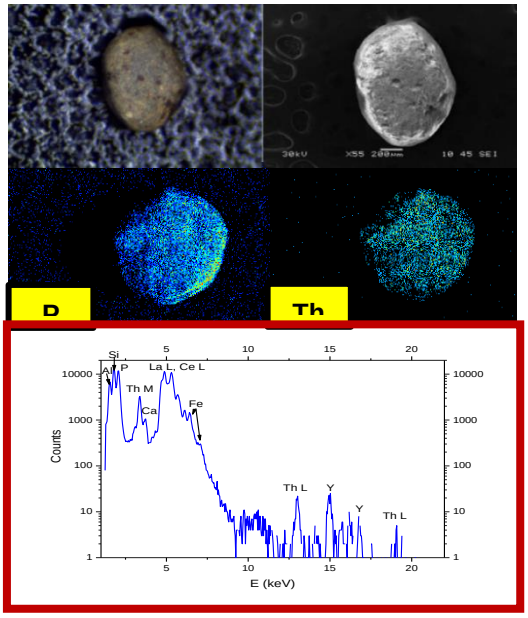

Figure 1.- Microscopic and SEM image of a monazite mineral grain (up), P elemental map obtained by micro-PiXE and Th elemental map obtained by micro-RBS (centre) and typical X-ray micro-PIXE spectra obtained by point analysis of the sample (down).

Is there migration of natural radionuclides from the phosphogypsum stacks into the underlying salt-marsh substrate?

J. L. Guerrero[1], I. Gutiérrez-Álvarez[1], S.M. Pérez-Moreno[1], F. Mosqueda[1], M. Olías[2], R. García-Tenorio[3], J. P. Bolívar[1].

[1] Department of Integrated Sciences, University of Huelva, Huelva, 21071, Spain.
[2]Department of Geodynamics and Palaeontology, University of Huelva, Huelva, 21071, Spain.
[3] Department of Applied Physics II, University of Seville, Seville, 41012, Spain.
Keywords: phosphogypsum, salt-marsh, natural radionuclides, pollution
Presenting author, e-mail: joseluis.guerrero@dfa.uhu.com

In the salt-marshes of the Tinto River (Estuary of Huelva, SW Spain), are stored in stacks around 100 Mt of phosphogypsum (PG), covering a surface of about 1000 ha, without any type of isolation and less than 1 km from the Huelva city (Figure 1), which produce an important impact in the surrounding environment.

Figure 1. Study area of the Huelva phosphogypsum stacks on the salt-marshes of the Tinto River.

Five acid phosphoric factories included in the industrial complex of Huelva were operative since 1965 until the end of 2010. The phosphate rock used in these factories for the phosphoric acid (PA) production contained U-series radionuclides concentrations of about 1500 mBq g^{-1} of ^{238}U in radioactive equilibrium with its daughters, as well as some chemical impurities as fluorine, phosphates, and some heavy metals (Bolívar et al., 2009). Due to their high content in natural radionuclides, PG are currently considered a NORM (Naturally Occurring Radioactive Material) material. In addition, the presence of residual PA trapped in the interstices of PG particles explains its acidic nature (pH about 3), and the high contaminant potential of this waste (Pérez-Moreno et al., 2018).

Despite the large number of studies developed in this area, none of them has analyzed the impact in the salt-marshes directly under the PG stacks. The aim of this study is to evaluate the deep pollution of the underlying salt-marsh sediments by natural radionuclides due to leachates from the stacks. For that purpose, 7 cores were collected from zones 2 and 3 of the stacks (Figure 1), and PG and sediments samples from different depths were analyzed. The concentrations of the main long half-live natural radionuclides of interest were determined by applying both gamma-ray and alpha-particle spectrometry radiometric techniques.

In order to better understand the influence of the PG leachates into the sediments, the mean value of the natural radionuclides in the salt-marsh sediments located in the first 20 cm under the contact and in the deeper samples were showed in Figure 2.

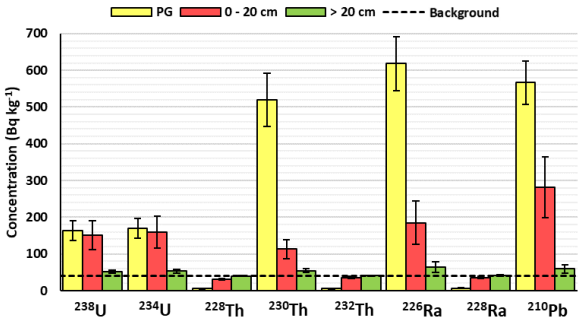

Figure 2. Comparison between mean value of natural radionuclides in the sediments located in the 20 first cm under the contact with the PG and in the deeper ones.

The main obtained conclusion is that salt-marsh sediments act as a "barrier" for the leachates from the PG and the affection by natural radionuclides ($^{234\text{-}238}U$, ^{230}Th, ^{226}Ra and ^{210}Pb) of the underlying sediments is restricted to the first 20 cm under the contact. The obtained results suggest that the projected perimeter channel in the restauration project, should has at least a deep of 1 m below the level of the PG stacks for assuring the complete collection of leachates from the stacks, and avoid their liberation into the Tinto River estuary.

Bolívar, J.P., Martín, J.E., García-Tenorio, R., Pérez-Moreno, J.P., Mas, J.L. 2009. Behaviour and fluxes of natural radionuclides in the production process of a phosphoric acid plant. *Appl. Radiat. Isot.* 67, 345-356.

Pérez-Moreno, S.M., Gázquez, M.J., Pérez-López, R., Vioque, J., Bolívar, J.P., 2018. Assessment of natural radionuclides mobility in a phosphogypsum disposal area. *Chemosphere* 211, 775-783.

Preliminary study on the estimation of minimum detectable activity and the efficiency for real-time marine monitoring system

S.Y. Han [1], S. Maeng [1], H.Y. Lee [1,2], S.J. Park[1], S.Y. Lim[1], S.H. Lee[1,2]

[1]School of Architectural, Civil, Environmental, and Energy Engineering, Kyungpook Nat'l Univ., Daegu, 41566, Korea
[2]Radiation Science Research Institute, Kyungpook Nat'l Univ., Daegu, 41566, Korea
Keywords: Seawater radioactivity monitoring system, Monte Carlo simulation, NaI(Tl), ^{137}Cs
Presenting author (S.Y. Han), e-mail: seuyou2@gmail.com

After the 2011 Fukushima accident in Japan, marine pollution has become a worldwide concern and the continuous monitoring of marine radioactivity began to play a fundamental role in radiation protection. The traditional monitoring method requiring a large number of samples and the skill of chemical pretreatment takes long counting time to get the quantitative results from high purity germanium detector. Thus, there is need of autonomous system for the marine monitoring even providing the early pollution warning.

For real-time marine radiation monitoring in Korea, the Korea Institute of Nuclear Safety (KINS) has chosen NaI(Tl) detectors which have been widely used for in-situ radioactivity measurement with high detection efficiencies and stable operation. However, the relatively poor energy resolution of NaI(Tl) detectors which can possibly leads to overlapping of the spectral lines so that makes the system difficult to identify precise peaks of the various gamma ray contributions. Also, there is still lack of the practical method of efficiency calibration for quantitative analysis of radioactivity in the marine environment.

In an attempt to develop the NaI(Tl) monitoring system for marine radioactivity, Monte Carlo simulation with the MCNPX code was performed to simulate the experimental setup of the 3" x 3" NaI(Tl) detector, taking into account the detailed geometry and the materials (Figure 1). Also, the certified sources in different types were used to test the reliability of the geometry. Simulation results were compared to experimental efficiency data except the aquatic measurement which will be conducted.

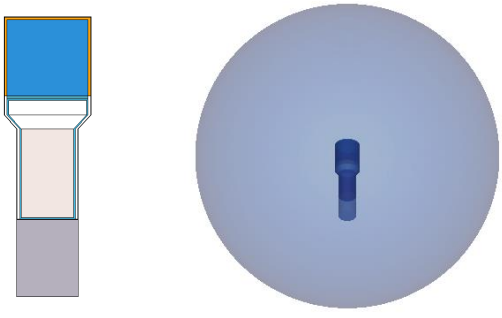

Figure 1. MCNP geometry of the 3" x 3" NaI(Tl) detector (left) and the concept geometry of detector in seawater sphere (right).

In addition to simulate the statistical broadening of the photopeak, the Gaussian Energy Broadening (GEB) option were used. The detection efficiency of the NaI(Tl) detector in different spherical volumes were simulated for determining the minimum detectable activities (MDA) of various radionuclides in the marine environment (Figure 2). The simulations of the NaI(Tl) detector in seawater were performed without consideration of its protective cover. To derive the validity of the simulation, it is imperative to consider the enclosure of the apparatus so that there is plan to accurately simulate the marine radiation monitoring system of KINS.

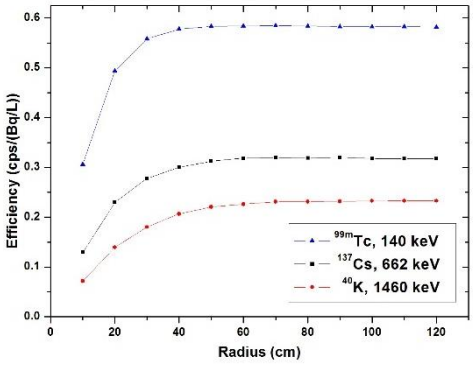

Figure 2. The detection efficiency for various radionuclides in the seawater simulated by MCNP.

This research can be used for the quantitative analysis of marine radiation monitoring with NaI(Tl) detector and provide the efficient design of system producing improvement in the operation.

At ENVIRA 2019 conference, the authors will present comparisons between measurement and simulations in the aquatic environment, ^{137}Cs detection efficiency in peak cps per Bq/L, and MDA of ^{137}Cs and its sensitivity to ^{40}K background levels.

Bagatelas, C., Tsabaris, C., Kokkoris, M., Papadopoulous, C. T., Vlastou, R. 2010. Determination of marine gamma activity and study of the minimum detectable activity (MDA) in 4pi geometry based on Monte Carlo simulation. *Environmental Monitoring and Assessment*. 165, 159-168.

Ren, G. X., Wei Z. Q., Liu. D. Y., Zhang. Y. Y. 2017. Marine radioactive field monitoring sensor based on NaI (Tl). *Water Resource and Environment*. 82, 012088.

^{210}Po bioaccumulation in Arctic seabirds

Violeta Hansen[1], Anders Mosbech[1], Flemming Ravn Merkel[1,2], Gert Asmund[1], Frank Rigét [1,2], Jens Søgaard-Hansen[3], Igor Eulaers[1]

[1]Department of Bioscience, Aarhus University, Frederiksborgvej 399, DK-4000 Roskilde, Denmark
[2]Greenland Institute for Natural Resources, Kivioq 2, Nuuk 3900, Greenland
[3]Danish Decommissioning, Frederiksborgvej 399, DK-4000 Roskilde, Denmark
Keywords: ^{210}Po bioaccumulation, absorbed and effective dose, arctic seabirds, Greenland
e-mail: viha@bios.au.dk

In this study, we report ^{210}Po activity concentrations in tissues, organs and feathers of seabirds collected from Greenland during autumn and winter of 2017 and 2018. The results of this study show significant intra and interspecific variability of ^{210}Po uptake behaviour in seabirds. Activity concentrations of ^{210}Po in seabird muscle ranged from 0.3 ± 0.1 Bq/kg w.w. in glaucous gulls to 26 ± 12 Bq/kg w.w. in thick-billed murre first winter birds. Mean ^{210}Po liver activity concentrations where typically higher than in muscle and ranged from 33 ± 9 Bq/kg w.w. in common eider to 132 ± 77 Bq/kg w.w. in thick-billed murre first winter birds. Tissues, organs and feathers of first winter thick-billed murre sampled in December 2018, show relatively high activity concentration of ^{210}Po in kidney (72 ± 67 Bq/kg w.w) and feathers (58 ± 21 Bq/kg w.w) with the lowest found in muscle (8 ± 9 Bq/kg w.w) and bone (4 ± 5 Bq/kg w.w). Arctic seabirds feeding at lower trophic levels (i.e. zooplanktonic crustaceans, mussels) bio-accumulate higher ^{210}Po than seabirds feeding at higher trophic levels (i.e. fish, birds eggs, chicks and adults of small species, small mammals, fishery discard and offal and carrion). The mechanism controlling polonium uptake and distribution in seabird tissues, organs and feathers is complex and is not entirely understood but some of the factors, which may control the uptake behaviour, have been identified (e.g. different feeding behaviour and diet, variability of ^{210}Po activity concentration in available prey items and temporal and spatial food availability).

Derived annual absorbed doses to breast muscle of seabirds from ^{210}Po ranged from 5 (glaucous gull) to 7.0 × 10^2 µGy (thick-billed murre first winter birds). Derived annual absorbed doses to liver of seabirds from ^{210}Po ranged from 9 × 10^2 (common eider) to 4 × 10^3 µGy (thick-billed murre first winter birds). Derived annual absorbed dose from ^{210}Po to whole body of thick-billed murre first winter bird were 3 × 10^2 µGy (3.2 × 10^{-2} µGy/h) which is low in comparison with ERICA Tool recommended benchmark of 10 µGy/h.

The annual effective dose due to ingestion of ^{210}Po in seabirds to the average adult and representative persons (most exposed - spare time hunters) in Greenland was estimated to be 14 µSv and 60 µSv, which is low and therefore, risk communication is not regarded necessary. In absence of other available data, the median values observed in this study may be used as background concentrations of ^{210}Po in seabirds in Greenland.

This work was supported by the Danish Environmental Protection Agency (EPA) under grant No. 20965/22711.

Nanoscale zero-valent Iron encapsulated in two-dimensional Titanium Carbides for removal of Cr(VI): A model for radioactive metal-oxo adsorption

L. He, G. Yue, J. Zhu, D. Huang, P. Zhao*

Institute of Materials, China Academy of Engineering Physics, Huafengxin, 621908, China
Keywords: MXene, adsorption, Chronium, radioactive
Pengxiang ZHAO, e-mail: zhaopengxiang@caep.cn

Two-dimensional (2D) early transition-metal carbides and/or nitrides, known as MXenes, are a new member of 2D materials that have attracted much attention since their first discovery in 2011 by the two groups of Gogotsi and Barsoum.(Naguib et al., 2011) Gernerally, MXenes are obtained by selective etching of "A" element from "MAX" phases. ("MAX" phases have a formula of $M^{n+1}AX_n$, where "M", "A" and "X" represent an early transition metal atom, a main group element atom, and C and/or N, respectively.) Owing to their specific structure that brings about unique and excellent physical and chemical properties, MXenes have been widely investigated including for photo- and electrochemical catalysis, sensors, capacitors, electromagnetic shielding and several other related fields. Particularly, due to their low density, unique interlayer structure and strong affinity for metal ions, MXenes are regarded as good candidates for heavy metal removal. More importantly, the precursor of MXene (MAX phase) have a very highly irradiation stability, thus the MXene are becoming a popular adsorbent for radioactive metal element, and recently a series of reports have emerged in this field (Ying et al., 2015). Although MXenes have a satisfactory removal capacity for metal ions, however, the small interlayer spacing and the lack of active site at the surface or interlayer (Zhu et al., 2017) is still a major drawback limiting the investigation of MXenes for metal ion adsorption.On one hand, the small interlayer spacing prevents the diffusion of heavy metal ions reducing the adsorptive capacity. On the other hand, the lack of active sites at the surface or interlayer would be negative for chemical adsorption of heavy metal ions. To overcome the disadvantages of conventional MXenes, the alkalinization intercalation of MXenes has been conducted in the present work. It provides the previously conducted introduction of OH groups in MXenes. Indeed in this way the interlayer distance in MXenes is enhanced and provides the active site for heavy metal adsorption (Peng et al., 2014). However, the OH groups on the surface of MXenes are only active for metal cations that form metal-OH bonds on the surface of MXenes. On the contrary, the OH group on the MXenes surface are not active with metal-oxo anions (e.g. $Cr_2O_7^{2-}$,ReO_4^-,TcO_4^-) and even provides adverse effect on adsorption (see experiment below). These metal-oxo anions are always toxic and highly pollutants, particularly, some of them (TcO_4^-) are radioactive, which is threatening for the environment and human beings. Therefore, a new strategy for metal-oxo anions adsorption *via* MXenes is called for. In this presentation, the Cr(VI) was chosen as a model contaminant herein, since its high toxicity and similar behavior as some radioactive metal-oxo anions. The design of nanoscale zero-valent iron (nZVI) intercalated Ti_3C_2 MXenes for Cr(VI) removal could be illustrated as followed(Scheme 1). Two advantages made this novel nanocomposite exhibit a very highly uptaken performance towards metal-oxo anions of Cr(VI).i) the increased interlayer of Ti_3C_2 nanosheet compared to that of untreated Ti_3C_2; ii) the introduction of nZVI into the Ti_3C_2 preventing the aggregation of nZVI and providing the synergistic effect that enhanced the uptake of Cr(VI).

This novel nano-composite should be a superb material for removal of heavy metal-oxo anions. Particularly, further development of promising applications of these materials is expected in particular to remove the radioactive metal-oxo anions for water purification and environmental remediation.

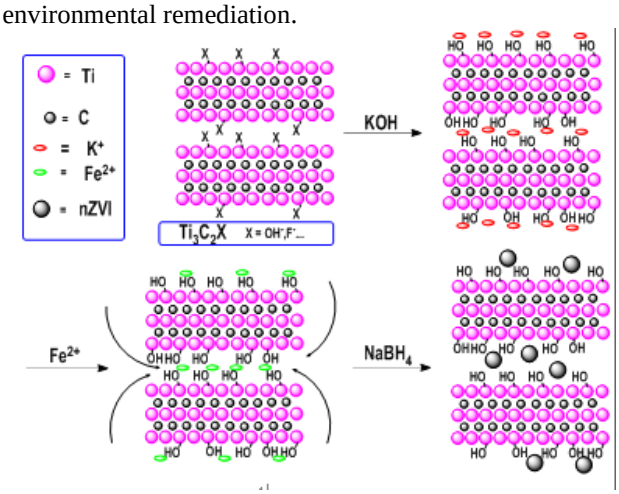

Figure 1. Synthetic route to nZVI-Alk-Ti_3C_2.

M. Naguib, et al., 2011. *Adv. Mater.* 23, 4248-4253.

Y. Ying, et al., *ACS Appl. Mater. Interfac.*, 2015, **7**, 1795-1803.

J. Zhu, et al., 2017. *Coord. Chem. Rev*. 352, 306-327.

Q. Peng, et al., 2014. *J. Am. Chem. Soc.* 136, 4113-4116.

Financial support from the Science and Technology Department of Sichuan Province (218JY0287), Natural Science Foundation of China (21806151), is gratefully acknowledged.

Caesium retention characteristics of KNiFC-PAN resin from river water

M. Hegedűs[1], H. Tazoe[1], G. Yang[1], M. Hosoda[1], N. Akata[1], S. Tokonami[1]

[1]Institute of Radiation Emergency Medicine, Hirosaki University, Hirosaki, 036-8203, Japan
Keywords: Caesium, KNiFC-PAN resin, Radiological monitoring, Fresh water
Presenting author, e-mail: Miklós Hegedűs, hegedus@hirosaki-u.ac.jp

The accident at the Fukushima Nuclear Power Plant sparked great interest in the improvement of both radioactive caesium (Cs) removal and Cs measurement techniques. Prussian blue was a prime target due to its selective Cs binding properties. The search for increased efficiency in Cs removal resulted in a wide selection of methods both in application, for example impregnated non-woven fabric, magnetic nanoclusters, hydrogels or different types of granules, and analogous compounds including different heteroatoms such as cobalt, copper, or nickel. Specifically, the KNiFC-PAN resin (potassium-nickel hexacyanoferrate in a polyacrylnitrile matrix) produced by the Czech Technical University has been utilized in a variety of seawater monitoring (Schmied et al., 2019; Breier et al., 2016), and it could be useful for freshwater monitoring as well.

To explore this possibility, 200 L river water was collected as the bulk sample for the experiment via a pump equipped with a 0.5 μm filter and it was acidified below pH 2 by the addition of HNO_3 for storage. 4 L aliquots of river water spiked with 125 ppb stable Cs as a yield tracer were pumped through the column with a bed of 2 mL wet KNiFC-PAN (TrisKem, particle size 100-600 μm) resin (1.3 cm Ø × 1.5 cm H resin in a 6 mL Agilent Bond Elut Reservoir) by a peristaltic pump with a variety of flow rates ranging from 2.5 to 400 mL per minute. The Cs concentration passing through the column was determined by ICP-MS. The 2 ml bed volume was selected to fit into the well type high purity germanium detector available for the planned measurements of radioactive Cs.

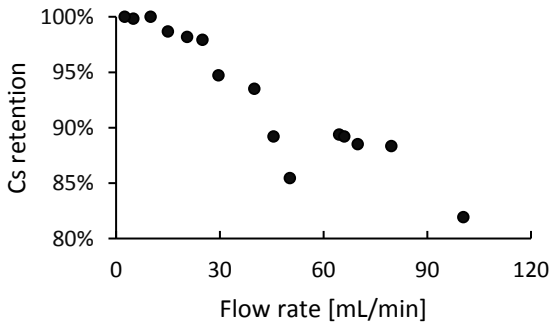

Figure 1. Caesium retention on KNiFC-PAN resin at low flow rates.

The KNiFC-PAN resin presented a nearly 100% retention of Cs at low flow rates (from 99.98% at 2.5 mL per minute to 97.89% at 25 mL per minute) and above 80% up to 100 mL per minute (Figure 1).

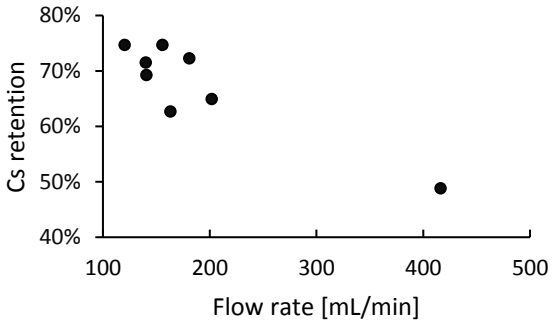

Figure 2. Caesium retention on KNiFC-PAN resin at high flow rates.

At 140 mL per minute and above the resin started being compacted by the water pressure, which might have influenced the results. At 400 mL per minute it still had close to 50% retention (Figure 2). The uncertainty of the data points is less than 1%, the variability between the data points is possibly due to the particle size differences in the resin, and the changes caused by the increasing pressure.

Based on the results, the KNiFC-PAN has the potential to be used for radioactive Cs determination in fresh water. An average 95% recovery of Cs was reported for a 5 ml resin from 20 L of sea water at 60 mL per minute in a 1.3 cm Ø × 5 cm H column (Breier et al. 2016) was reported for seawater previously. While increased amounts of resin would improve chemical yield in our setup as well, the loss in detection efficiency in the well-type detector would more than negate the benefits.

This work was supported by the Research on the Health Effects of Radiation organized by Ministry of the Environment Japan.

Breier, C. F., Pike, S. M., Sebesta F., Tradd, K., Breier, J. A., Buesseler, K. O. 2016. New applications of KNiFC-PAN resin for broad scale monitoring of radiocesium following the Fukushima Dai-ichi nuclear disaster. *J. Radioanal. Nucl. Chem.* 307, 2193–2200, doi: 10.1007/s10967-015-4421-x

Schmied, S.A.K., Meyer, A., Bendler, I. Šebesta F. 2019. Offshore concentration of caesium radioisotopes from large volume seawater samples using KNiFC-PAN. *Appl. Radiat. Isot.* 147, 197-203, doi: 10.1016/j.apradiso.2019.01.029

Effects of the cement production industry on NORM distribution in Nigeria

D. Heine[1], T. Weissenborn[1], F. Köhler[1], S. Bister[1], C. Walther[1], O. Ife-Adediran[2]

[1]Institut of Radioecology and Radiation Protection, Leibniz University of Hanover, 30167, Germany
[2]Radiation and Health Physics Research Group, The Federal University of Technology Akure, FUTA Rd, Nigeria
Keywords: Nigeria, cement production, NORM, contamination
Presenting author e-mail: heine@irs.uni-hannover.de

The growing need for construction infrastructure, rapid expansion of the construction industry and potential viability of cement production in West Africa and Nigeria particularly, are the recent realities of the cement manufacturing Industry.
The intensified efforts in meeting the local and global demands of cement in Nigeria have led to increased production capacities of existing plants and well as the establishment of new ones.
The highly industrial process of cement production also affects the environment where the plants are located. Exposures to natural radiation sources can be modified as well by anthropogenic activities such as, quarry activities, mineral processing, etc. causing enhanced natural radiation exposures. Furthermore, this influence on the distribution of NORM ("naturally occurring radioactive material") through various processes could result in a radiological risk to occupational and public exposure groups.
Different kind industrially influenced environmental samples (soil, water and plants) as well as samples from the cement production itself (raw-materials and cement) have been analysed in this study to determine the effects of the production processes on the distribution of NORM in the environment next to the production plants. In the first step, each sample was analysed by γ-spectrometry to determine the amount of ^{232}Th, ^{226}Ra and ^{228}Ra. In the next step the solid-samples were digested and ICP-MS was used to perform the quantification of uranium.
Table 1 shows the area of activity concentration for ^{232}Th and ^{226}Ra in soil and cement. While the values in the soil can vary by more than a factor of 15, the cement has a much smaller variance. Furthermore, the maximum activity concentration (a_{max}) which was found in soil is significantly higher than in cement.

Table 1. Activity concentrations in soil and cement.

Nuclide	a in soil [Bq/kg]	a in cement [Bq/kg]
a_{min} ^{232}Th	12.7	18.0
a_{max} ^{232}Th	186.1	66.8
a_{min} ^{226}Ra	8.71	23.5
a_{max} ^{226}Ra	127.0	46.1

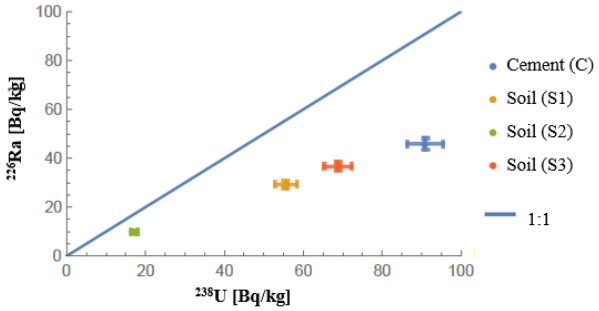

Figure 1. ^{226}Ra/^{238}U-ratio for soil and cement from one location.

While the activity concentrations in both kinds of samples can differ considerably, there is a similar deviation from the natural equilibrium of ^{226}Ra and ^{238}U in soil and cement from the same location (Figure 1).

This work was supported by the Siebold Sasse Foundation.

[1] WEISSENBORN, T.; Radiometric analysis of industrially influenced environmental samples from Nigeria. Leibniz University of Hanover, Institute for Radioecology and Radiation Protection; 2019

Effect of trivalent lanthanides and actinides on a rat kidney cell line

A. Heller[1], M. Acker[2], A. Barkleit[3], F. Bok[3], J. Wober [1]

[1]Molecular Cell Physiology and Endocrinology, Institute of Zoology, Faculty of Biology, Technische Universität Dresden, Dresden, 01062, Germany
[2]Central Radionuclide Laboratory, Technische Universität Dresden, Dresden, 01062, Germany
[3]Institute of Resource Ecology, Helmholtz-Zentrum Dresden-Rossendorf, Dresden, 01328, Germany
Keywords: cytotoxicity, f-elements, XTT, TRLFS
Presenting author, e-mail: anne.heller@tu-dresden.de

Exposure to trivalent lanthanides (Ln) and actinides (An) poses a serious health risk to animals and humans. Since both Ln and An are mainly excreted with the urine, we investigated the effect of La, Ce, Eu, and Yb (as representatives of Ln) as well as Am (as representative of An) exposure on a rat kidney cell line (NRK-52E) for 8, 24, and 48 h *in vitro*. Cell viability studies using the XTT assay and fluorescence microscopic investigations were combined with solubility and speciation studies using ICP-MS and time-resolved laser-induced fluorescence spectroscopy (TRLFS). Thermodynamic modelling was applied to predict the speciation of Ln and Am in cell culture medium.

All Ln show a concentration- and time-dependent effect on NRK-52E cells with Ce being the most potent element (see Figure 1). Effective Ln concentrations reducing the cell viability to 50 % (EC_{50} values) range from 340 µM for Ce to 1.1 mM for Eu. In general, light and heavy Ln seem to exhibit a greater effect than middle Ln.

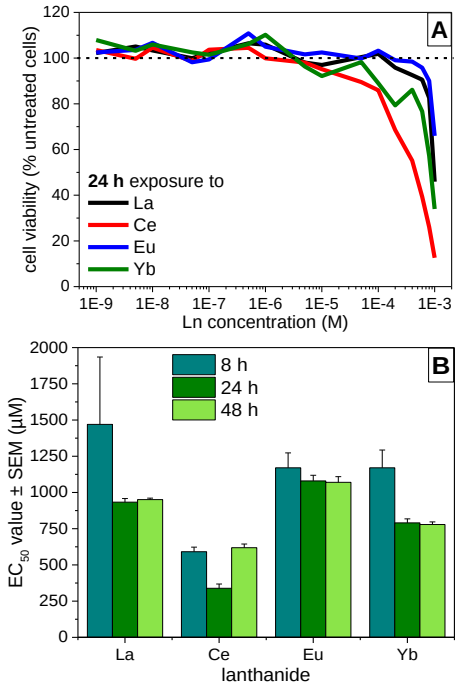

Figure 1: Dose-response curves of La, Ce, Eu, and Yb after 24 h exposure of rat NRK-52E cells (A) and derived EC_{50} values ± SEM at three exposure times (B). Values represent means of five to eight independent experiments, untreated cells equal 100 % cell viability (dotted line).

In cell culture medium with 10 % fetal bovine serum (FBS), the Ln are completely soluble and complexed with proteins from FBS. Ln speciation is time-independent (see Figure 2). Comparative experiments with Am are ongoing and will reveal analogies and/or differences in the effect of trivalent Ln and An on rat kidney cells.

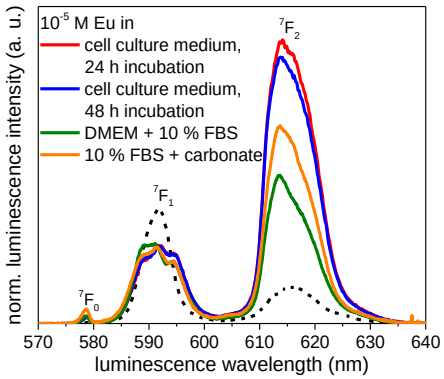

Figure 2: Steady-state luminescence spectra of Eu in cell culture medium and different model solutions. The dotted lines and open symbols represent data of the Eu^{3+} aqua ion; luminescence bands are labeled with the respective ground state of the emission transitions.

This is the first study revealing the effects of Ln onto mammalian kidney cells. Furthermore, our laboratory is one of the few worldwide, which is able to perform cell culture studies using radioactive elements like Am.

The results of this study underline the importance of combining biological, chemical, and spectroscopic methods in studying the effect of Ln and An on cells in vitro and may contribute to the improvement of the current risk assessment for Ln in the human body. Furthermore, they demonstrate that Ln seem to have no effect on rat renal cells in vitro at environmental trace concentrations. Nevertheless, especially Ce has the potential for harmful effects at elevated concentrations observed in mining and industrial areas.

This work was supported by the Deutsche Forschungsgesellschaft under grant No. HE 7054/2-1.

Heller, A. et al., 2019. Effect of four lanthanides onto the viability of two mammalian kidney cell lines. *Ecotox. Environ. Saf.* 173, 469-481.

Dispersion and ground deposition characteristics of radioactive material according to air mass classification for enhancing the preparedness to N/R emergencies

M.A. Hernandez-Ceballos[1], M. Sangiorgi[1], B. García-Puerta[2], M. Montero[2], C. Trueba[2]

[1]European Commission, Joint Research Centre, Ispra, Italy
[2] Department of Environment, Radiation Protection of Public and Environment Unit, Research Centre for Energy, Environment and Technology (CIEMAT), Spain
Keywords: Radionuclide impact, nuclear, radionuclide transport, radionuclide in the environment.
Presenting author, e-mail: Miguel-Angel.HERNANDEZ-CEBALLOS@ec.europa.eu

The large amount of radioactive material potentially to be released in a nuclear or radiological event is a big threat to the safety of public health and environment, and causes important socioeconomic consequences. The intent of minimizing its impact should imply preparedness activities that would largely rely, for instance, on an adequate knowledge of the dispersion patterns and an estimation of the potential levels of radioactive contamination.

In the present study, we present a method to identify wind patterns and to estimate the associated dispersion and ground deposition patterns. The framework of this study is the ANURE project, which aims at developing a methodology to elaborate nuclear risk maps integrating all these local factors, and is led by EC/DG JRC and CIEMAT.

We propose firstly to calculate the main transport directions by means the air mass trajectories calculated by the HYSPLIT model (Stein et al., 2015), and, secondly, the dispersion and the ground deposition characteristics associated with each wind pattern using the RIMPUFF model system (Mikkelsen et al., 1997). The method is tested based on the HYSPLIT trajectories and RIMPUFF simulations of the atmospheric dispersion and deposition during five consecutive years (2012-2016) at the Almaraz Nuclear Power Plant, in Spain.

3644 forward air mass trajectories were calculated (at 00 and 12 UTC, and with a duration of 36 hours) and 1387 simulations of the dispersion and ground deposition following an hypothetical release from Almaraz NPP were carried out from 2012 to 2016. The ISLOCA accident sequence, with 35 hours of offsite radionuclide release, was taken as reference. Each daily dispersion simulation was performed for 83 hours (35 hours of release and 48 hours of prognosis period). Ground contamination of ^{131}I, ^{90}Sr and ^{137}Cs were estimated at cell level on a non-homogeneous geographical grid spacing (radius of 800 km, and a minimum (maximum) cell size of 2 km (32 km)).

Figure 1a shows the eight clusters (air mass patterns) formed by using the cluster methodology implemented in the HYSPLIT. They represent five pronounced air mass patterns: to the east, to the north, to the northwest, to the southwest and nearby displacement.

Within each cluster, we have worked with "pure days", i.e. those in which trajectories at 00 and 12 UTC grouped into the same cluster. For each pure day within each cluster, we took the corresponding simulated spatial distribution of deposition at the 83rd hour. Therefore, for each cluster, and after considering the whole set of possible pure days and simulations, there is a vector of a certain number of total deposition values in each grid cell. In each vector, there is a large variability in the deposits. Figure 1b,c shows the spatial probability distribution of deposits for two air mass patterns (C2 to the east and C6 to the northwest) respectively.

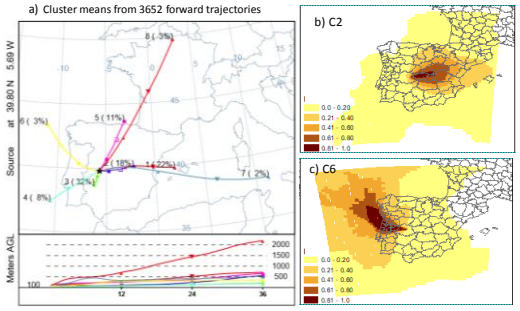

Figure 1. a) Mean cluster pathways (centroids). The percent of complete trajectories occurring in each cluster is in brackets, b) spatial probability distribution of total deposit for C2 (eastern) and C6 (northwestern) patterns.

In the nuclear preparedness field, these results can be used to estimate areas with high probability of being affected by high deposition values. Figure 2 shows an example of the different spatial coverage estimation of those areas needed to be decontaminated (> 1000 kBq/m^2) for each pattern, following the Nordic Guidelines and Recommendations 2014.

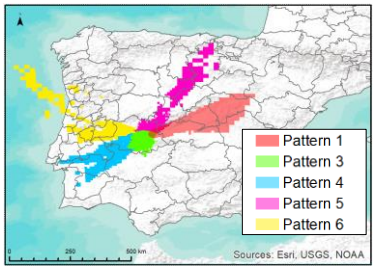

Figure 2. Spatial distribution of areas with a probability above 20 % of being contaminated by deposits over 1000 kBq/m^2.

This method would provide useful guidance in increasing knowledge of crisis and disaster management for improving responsiveness, as well as in the definition of Emergency Planning Zones (EPZ).

Stein, A.F., et al., 2015. NOAA's HYSPLIT atmospheric transport and dispersion modeling system, *Bull. Amer. Meteor. Soc.*, 96, 2059-2077.

Thykier-Nielsen, S., et al., 1997. RODOS SYSTEM, Analysing Subsystem: RIMPUFF, Stand Alone Version, *RIMDOS7, Users Guide*, RODOS(A)-TN(95)3.

Estimation of water seepage rate in the active crater lake system of Kusatsu-Shirane volcano, Japan, using radioactive cesium as a hydrological tracer

Y. Hirayama[1], A. Okawa[1], K. Nakamachi[2], T. Aoyama[1], Y. Okada[2], T. Oi[1], K. Hirose[1], Y. Kikawada[1]

[1]Department of Material and Life Sciences, Sophia University, Tokyo, 102-8554, Japan
[2]Atomic Energy Research Laboratory, Tokyo City University, Kawasaki, 215-0013, Japan
Keywords: Fukushima nuclear accident, hydrological tracer, crater lake, radioactive cesium
Presenting author, e-mail: y-kikawa@sophia.ac.jp

A crater lake to which hydrothermal fluids are supplied from its bottom, namely an "active crater lake," is one of the chief subjects of geochemical studies on active volcanoes. Water budget of such crater lakes is very complicated due to their hydrothermal activities. In this study, we tried to estimate the water seepage rate of "Yugama", a well-known active crater lake of Kusatsu-Shirane volcano, Japan, using radioactive cesium dispersed into the environment by the Fukushima Dai-ichi Nuclear Power Plant (F1NPP) accident in March 2011 as a hydrological tracer. Kusatsu-Shirane volcano is located about 240 km west-southwest from the F1NPP. Yugama is a lake with a diameter of about 300 m and the maximum depth of about 30 m, and the volume of its water has been kept at a certain level naturally.

We collected water samples of Yugama periodically at a fixed point since Nov 2011 until Nov 2014. The activities of ^{134}Cs and ^{137}Cs in the samples were measured by the gamma-ray spectrometry using a low-background Ge detector after selective extraction of cesium with 3M Empore "RAD Disk Cesium" filters from 10 L aliquots of the samples. The content of stable ^{133}Cs in the samples was measured by the ICP-QMS.

The contents of dissolved radioactive cesium are expected to be affected by the cesium adsorption equilibrium between lake water and bed sediments. To confirm this, we conducted adsorption experiments. A weighed bed segment of Yugama and a certain volume of ^{133}Cs-added Yugama water were placed in a glass tube, and the tube was sealed. The sealed tube was left at rest at the designated temperature for the predetermined period. The content of ^{133}Cs in the solution phase was determined after filtration.

The temporal changes in the cesium contents in Yugama water are shown in Figure 1. It is clearly seen that they are different between the radioactive and stable cesium (^{134}Cs, ^{137}Cs vs. ^{133}Cs).

The observed effective decreasing rates of the radioactive cesium are much larger than those based on the radiological half-lives of ^{134}Cs and ^{137}Cs. Based on the effective rate, the average residence time of radioactive cesium in Yugama was estimated as about 1000 days. Since there are no rivers flowing in and out from Yugama, dissolved radioactive cesium in the lake could be removed from the lake only due to seepage through the bed. Thus, the residence time of radioactive cesium in Yugama should reflect the seepage rate of the lake water. Accordingly, the seepage rate of the lake water is estimated to be about 0.1% of the total lake water volume per day.

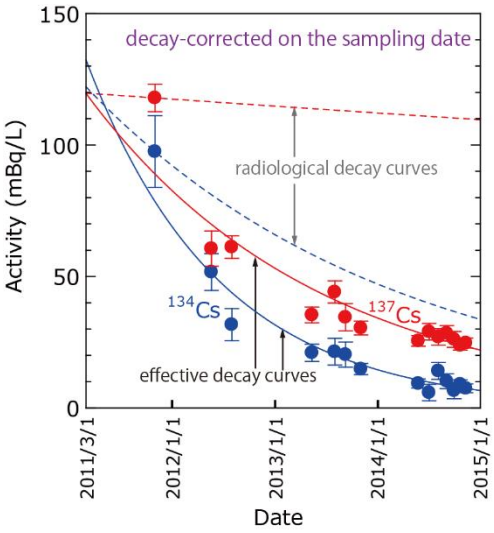

Figure 1. Temporal changes in the contents of radioactive cesium in Yugama water.

Another finding in Figure 1 is that the contents of radioactive cesium in Yugama seem to fluctuate seasonally. This is most probably caused by water temperature. The results of the adsorption experiments reveal that the adsorption equilibrium of cesium between the lake water and the bed sediment in Yugama is repeatedly going up and down in rapid response to the down-and-up change in water temperature.

Based on the decreasing rates of the radioactive cesium contents in Yugama water, it can be estimated that approximately 0.1% of the total dissolved radioactive cesium has leaked out through the lake bed together with the lake water per day. Thus, 0.1% of the total volume of the lake water, which approximately corresponds to 600~700 m^3, leaks through the bed per day. This value is smaller than the previous value of 1000~3000 m^3 (Ohba et al., 1994).

This work was supported by JSPS KAKENHI Grant Number 24654156.

Ohba, T., Hirabayashi, J., Nogami, K. 1994. Water, heat and chloride budgets of the crater lake, Yugama at Kusatsu-Shirane volcano, Japan. *Geochem. J.* 28, 217-231.

Modelling the partitioning of Am and Pu in agricultural soils using the geochemical code PHREEQC

V. Hormann[1*], H. W. Fischer[1]

[1]Department of Environmental Physics, University of Bremen, Bremen, Germany
Keywords: americium, plutonium, soils, modelling
**Presenting author, e-mail: vhormann@physik.uni-bremen.de*

Organic matter (OM) plays an important role in the speciation and partitioning of many radioactive isotopes in the environment. This is especially true for the transuranium elements americium (Tipping, 2002) and plutonium (Santschi et al., 2017). Recently, a multicomponent model (UNiSeCs) has been developed, successfully implemented into the geochemical code PHREEQC and validated (Hormann, 2015). This model has now been modified for the inclusion of Model VII by Tipping et al., 2016, which accounts for the binding of metal cations on humic substances. It has been validated for Am (see Figure 1) and Pu using results of batch experiments from the literature (Ramírez-Guinart et al., 2016; Miner et al., 1982).

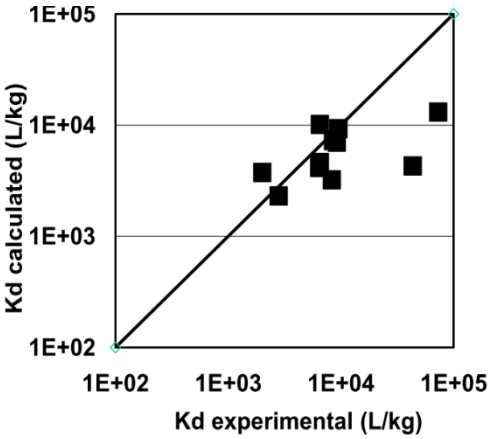

Figure 1. Calculated versus experimental K_d values for americium.

To evaluate the relative significance of OM and dissolved organic matter (DOM) in comparison to other soil components like clay minerals or hydrous ferric oxides, the modified model has been applied to a set of standard soils (REFESOLS, Kördel et al., 2009), varying the percentage of components within realistic margins. The results show that in almost all cases OM and DOM can be expected to dominate the partitioning of Am, whereas in the case of Pu, clay content and redox state may also play a significant role.

This model can be used for estimating the partitioning of Am and Pu in agricultural soils. This will be helpful in the larger project Trans-LARA (https://www.trans-lara.de), where the environmental transport of these elements will be predicted.

This work was supported by the German Federal Ministry of Education and Research (BMBF) under grant FKZ 02NUK051D.

Hormann, V.**:** Modelling Speciation and Distribution of Radionuclides in Agricultural Soils. 2015. In: C. Walther, D.K. Gupta (eds.), "Radionuclides in the Environment", 81 - 99, Springer International Publishing Switzerland 2015.

Kördel W, Peijnenburg W., Klein C.L., Kuhnt G., Bussian B.M., Gawlik B.M. 2009. The reference-matrix concept applied to chemical testing of soils. *Trends Analyt. Chem.* 28, 51–63.

Miner, F.J., Evans, P.A., Polzer, W.L. 1982. Plutonium behavior in the soil/water environment. Report for the U.S. Department of Energy, United States.

Ramírez-Guinart, O., Vidal, M., Rigol, A. 2016. Univariate and multivariate analysis to elucidate the soil properties governing americium sorption in soils. *Geoderma* 269, 19-26.

Santschi, P.H., Xu, C., Zhang, S., Schwehr, K.A., Lin, P., Yeager, C.M., Kaplan, D.I. 2017. Recent advances in the detection of specific natural organic compounds as carriers for radionuclides in soil and water environments, with examples of radioiodine and plutonium. *J. Env. Radioactivity* 171, 226-233.

Tipping, E. 2002. Cation binding by humic substances. Cambridge University Press, Cambridge, UK.

Tipping, E., Lofts, S., Sonke, J.E. 2011. Humic Ion-Binding Model VII: a revised parameterisation of cation-binding by humic substances. *Environ. Chem.* 8 (3), 225-235.

Development of *in vitro* testing methods with materials suitable for radiation exposure and internal contamination assessment including NORM materials

I. Hupka, V. Bečková

Department of Radiochemistry, National Radiation Protection Institute, Prague, 14016, Czech Republic
Keywords: solubility, lung fluids, NORM
Ivan Hupka, e-mail: ivan.hupka@suro.cz

The main purpose of this study is to determine the solubility and distribution of particles forming slag and ash containing naturally occurring radioactive materials, in simulated lung fluids (SLF). The experiments were performed to simulate the behaviour of radionuclides deposited in workers` lungs at sites, where the high risk of dust particles and aerosol inhalation is expected, especially at coal power plants. Solubility, transport and size of inhaled particles containing deposited radionuclides are crucial parameters for occupational internal contamination assessment. There are several studies concerning dissolution of aerosols in human lungs from workplaces, where the elevated concentrations of natural radionuclides and dust in air are present e.g. uranium mines, uranium reprocessing facilities (Duport, 1994; Bečková and Malátová, 2008). Procedure of using experimental data methods for calculation of dissolved fractions distribution in aerosols is described in the project document IDEAS (Doerfel et al., 2006). The actual clearance of radioactive aerosols from lungs to circulatory system is a complex process which depends on chemical and physical aspects associated to the dust dissolution kinetics in lungs. The dissolution and transport are key mechanisms for lung clearance (Metzger, 1996).

In this study, several samples of slags and fly ash were taken from fossil fuel power stations throughout the Czech Republic. The samples were sieved to obtain particle size <40 μm. Afterwards, the slag or fly ash aliquot was inserted between two cellulose nitrate filters of pore size 0.05 μm with additional layer of filter paper on each side. All the layers were then fixed in a Teflon disc-shape holder, where one side was exposed to 80 mL of filtrated SLF (Gamble`s solution) under stable conditions of pH 7.3. The whole assembly was left in a sealed beaker for a period of 30 days, while the solution was replaced by the fresh portion in planned intervals. The extraction time ranged from 1 hour up to 7 days. Prior to subsequent analysis extracts were acidified by a few millilitres of HNO_3, wet ashed, uranium and thorium were separated and measured using alpha spectrometry with PIPS detector. To calculate the dissolution rates and fractions of rapid and slow components a triexponential approximation was used:

$$A = f_1 e^{-\lambda_1 t} + f_2 e^{-\lambda_2 t} + f_3 e^{-\lambda_3 t} F = f_1 e^{-\lambda_1 t} + f_2 e^{-\lambda_2 t} A = f_1 e^{-\lambda_1 t} + f_2 e^{-\lambda_2 t}$$

where F is total undissolved fraction, f_1, f_2 and f_3 are a rapid, medium and slow fractions, respectively; λ_1, λ_2 and λ_3 are dissolution rates of rapid, medium and slow fractions, respectively.

Data for a slag sample containing uranium isotopes are presented in Table 1. For Th and Ra isotopes, no relevant data were obtained as the concentration of thorium and ^{226}Ra in solutions was less than the limit of quantification of the methods.

Table 1. Fractions and dissolution rates of rapid and slow components for ^{238}U and ^{234}U

Parameters	Radionuclides	
	^{238}U	^{234}U
f_1	0,035	0,031
f_2	0,047	0,047
f_3	0,918	0,922
λ_1 [d^{-1}]	81,7	102,0
λ_2 [d^{-1}]	0,818	1,111
λ_3 [d^{-1}]	0,0014	0,0019

Comparing the results with the data in ICRP Publication 71, both radionuclides are assigned to solubility class M, where the lung retention (the undissolved fraction of material) is considered to be from 13 to 87 % between 30 and 180 days.

Furthermore, detailed results from solubility of other NORM materials originating from different parts of power stations will be presented in this contribution as well as advanced method of *in vitro* testing of NORM behaviour in lungs and determination of the internal radiation dose for workers.

This research was financially supported by the Ministry of the Interior under project No. MV-32469-1/OBVV-2019.

Duport, P. 1994. Radiation protection in uranium mining: two challenges. *Rad. Prot. Dos*. 53, 13-19.

Bečková, V., Malátová, I. 2008. Dissolution behaviour of ^{238}U, ^{234}U and ^{230}Th deposited on filters from personal dosemeters. *Rad. Prot. Dos*. 129, 469-472.

Doerfel, H. et al. 2006. General guidelines for the estimation of committed effective dose from incorporation monitoring data. *Forschungszentrum Karlsruhe*.

Metzger, R. L. et al. 1996. Solubility testing of actinides on breathing-zone and area air samples. *NUREG*.

In soil radon anomalies and volcanic activity on Mt. Etna (Italy)

M. Ichedef [1], S. Giammanco[2], M. Neri[2], R. Catalano[3], G. Immè[4,5], D. Morelli[5], F. Murè[2], N. Giudice[4,5]

[1]Institute of Nuclear Sciences, Ege University, Bornova/Izmir, Turkey
[2]Istituto Nazionale di Geofisica e Vulcanologia - Osservatorio Etneo, piazza Roma, 2- 95125 Catania, Italy
[3]Istituto Nazionale di Fisica Nucleare - Laboratori Nazionali del Sud, via S. Sofia, 62 - 95123 Catania, Italy
[4]Istituto Nazionale di Fisica Nucleare - Sezione di Catania, via S. Sofia, 64 - 95123 Catania, Italy
[5]Dipartimento di Fisica e Astronomia "Ettore Majorana", via S. Sofia, 64 - 95123 Catania, Italy
Keywords: radon, magma, volcano
Presenting author, e-mail: josette.imme@ct.infn.it

For many years, we carried out several radioactivity investigations in the Mt. Etna area, a peculiar site characterized by both tectonic and volcanic features. In particular, we describe results extracted from continuous measurements of in-soil radon gas, carried out from 2015 until 2019, in three sites located both on the northern and on the southern flanks of Mt. Etna. During this period several volcanic events have occurred. The acquired raw data were properly filtered in order to remove non-volcanic factors, using band-stop filters on radon power spectra. This provided a robust methodology in order to verify a possible correlation between radon concentration anomalies and geodynamic events, in particular magma uprising, as observed in our previous published studies (Morelli et al., 2006), (Neri et al., 2006), (Giammanco et al., 2007), (Falsaperla et al., 2017).

Morelli, D., Immè, G., La Delfa, S., Lo Nigro, S., Patanè, G. 2006. Evidence of soil Radon as tracer of magma uprising at Mt. Etna. *Radiation Measurements* 41, 721-725.

Neri, M., Behncke, B., Burton, M., Giammanco, S., Pecora, E., Privitera, E., Reitano, D. 2006. Continuous soil Radon monitoring during the July 2006 Etna eruption. *Geophys. Res. Lett.* 33, L24316.

Giammanco, S., Sims, K. W. W., Neri, M. 2007. Measurements of 220Rn and 222Rn and CO2 emissions in soil and fumarole gases on Mt. Etna volcano (Italy): Implications for gas transport and shallow ground fracture. *Geochem. Geophys. Geosyst.* 8, Q10001.

Falsaperla, S., Neri, M., Di Grazia, G., Langer, H., Spampinato, S. 2017. What happens to in-soil Radon activity during a long-lasting eruption? Insights from Etna by multidisciplinary data analysis. *Geochem. Geophys. Geosyst.* 18.

Identification of Plutonium isotopes in radioactive particles released from the Fukushima Daiichi Nuclear Power Plant

J. Igarashi[1], J. Zheng[2], Z. Zhang[1], K. Ninomiya[1], Y. Satou[3], M. Fukuda[2], Y. Ni[2,4], T. Aono[2] and A. Shinohara[1]

[1]Graduate School of Science, Osaka University, Osaka 560-0043, Japan.
[2]Department of Radioecology and Fukushima Project, National Institutes for Quantum and Radiological Science and Technology, Chiba 263-8555, Japan.
[3]Collaborative Laboratories for Advanced Decommissioning Science, Japan Atomic Energy Agency, Fukushima 979-1151, Japan.
[4]State Key Laboratory of Nuclear Physics and Technology, School of Physics, Peking University, Beijing, 100871, China.

Keywords: Plutonium, Radioactive particles, ICP-MS, FDNPP
Presenting author e-mail: igarashij17@chem.sci.osaka-u.ac.jp

The Fukushima Daiichi Nuclear Power Plant (FDNPP) accident resulted in the large release of radionuclides into the environment. The release process and environmental behavior of volatile fission product such as radioactive Cs was mainly investigated. On the other hand, the studies of nonvolatile fuel elements, such as Pu, have still been limited.

It is known that the amount of Pu released from the FDNPP accident was much smaller compared with that of radioactive Cs [1]. However, the existence of Pu isotopes from the global fallout which was mainly derived from the atmospheric nuclear weapon tests makes it difficult to accurately assess Pu contamination from the FDNPP accident. In many environmental samples, Pu was affected not only by the FDNPP accident but also by global fallout. It is necessary to distinguish the source of Pu contaminations to assess the accurate Pu contamination from the FDNPP accident.

For identification of Pu contamination source, the Pu isotopic ratios provide important information. The ratios were completely different by the kinds of nuclear weapons and nuclear accidents. The Pu isotopic ratios were measured in some environmental samples around the FDNPP. However, the ratios varied by the researches due to the contamination by global fallout. Therefore, the ratios should be determined from the environmental samples which were not influenced by the global fallout.

In the FDNPP accident, radioactive particles which were insoluble in water and containing highly concentrated radioactive Cs were reported [2]. The radioactive particles were estimated to be formed in the reactor during the meltdown and directly released from the reactor. Due to its insolubility, the radioactive particles kept their elemental composition in the environment and retained the original property at the time of emission from the reactor. In other words, the radioactive particles are free from the contamination of global fallout. In this study, we identified Pu isotopes in radioactive particles found around the FDNPP.

We performed radiochemical analysis and inductively coupled plasma-mass spectroscopy (ICP-MS) measurements of Pu isotopes for radioactive particles. Figure 1 shows the scanning electron microscopy (SEM) image of the radioactive particle analyzed in this study. For this particle, $^{239+240}$Pu activity was $(1.70 \pm 0.20) \times 10^{-5}$ Bq with a ^{240}Pu/^{239}Pu atom ratio of 0.330 ± 0.077. The Pu isotopic ratio was higher than the ratio from global fallout (0.18) [3], but consistent with the simulation results from the ORIGEN code [4] and measurement results from some environmental samples around the FDNPP that were considered less influenced by global fallout [1]. We successfully determined the accurate Pu isotopic ratios from the FDNPP accident by analyzing radioactive particles.

In this presentation, the properties of the investigated radioactive particles will be presented, and detailed experimental method will also be shown. In addition, we will discuss about Pu isotopic ratios in radioactive particles and compare the results with other environmental samples.

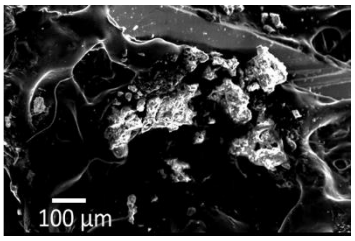

Figure 1. The SEM image of radioactive particle analyzed in this study.

[1] J. Zheng, K. Tagami, Y. Watanabe, S. Uchida, T. Aono, N. Ishii, S. Yoshida, Y. Kubota, S. Fuma and S. Ihara. Isotopic evidence of plutonium release into the environment from the Fukushima DNPP accident. Sci. Rep. 2, 304, 2012.

[2] K. Adachi, M. Kajino, Y. Zaizen and Y. Igarashi. Emission of spherical cesium-bearing particles from an early stage of the Fukushima nuclear accident. Sci. Rep. 3, 2554, 2013.

[3] J. Kelley, L. Bond and T. Beasley. Global distribution of Pu isotopes and ^{237}Np. *Sci. Total. Environ*. 238/238, 483-500, 1999.

[4] K. Nishihara, H. Iwamoto and K. Suyama. Estimation of fuel composition in Fukushima-Daiichi Nuclear Power Plant. JAEA-Data/Code. 2012-018, 65-117, 2012.

Trace elements and radioactive nuclides studied in the region of Northern Greece using *Hypnum cupressiforme* Hedw. as biomonitor

A. Ioannidou[1], Ch. Betsou[1], E. Tsakiri[2], K. Eleftheriadis[3], E. Diapouli[3], J. Hansman[4], M. Krmar[4], M. Frontasyeva[5]

[1]Aristotle University of Thessaloniki, Physics Department, Nuclear Physics Laboratory, Thessaloniki 54124, Greece
[2]Aristotle University of Thessaloniki, Biology Department, Division of Botany, Thessaloniki, Greece
[3]Institute of Nuclear & Radiological Sci.& Technol., Energy & Safety, NCSR "Demokritos", Athens 15341, Greece,
[4]University of Novi Sad, Physics Department, Faculty of Science, Trg Dositeja Obradovica 4, Novi Sad, 21000, Serbia
[5]Frank Laboratory of Neutron Physics, Joint Institute for Nuclear Research, Dubna, Moscow Region 141980, Russia
Keywords: atmospheric deposition, moss, Neutron Activation Analysis, source apportionment
Presenting author: Alexandra Ioannidou - e-mail: anta@physics.auth.gr

Mosses can be used as biomonitors for investigating the atmospheric deposition of radionuclides and heavy metals. They have the ability to retain particles from the air. Mosses receive most of their nutrients directly from wet and dry deposition. They have no rooting system, unlike the higher plants, the uptake from the substrate is normally not significant and the elements are absorbed entirely by their surface (Harmens et al., 2008; Berg and Steinnes, 1997). These properties make mosses an ideal low-cost method of monitoring the concentrations of heavy metals and radionuclides deposited from the air to terrestrial systems.

There are a lot of advantages using moss method, such as the simplicity of the sample collection and the ease of the analysis. Also, sampling can occur in remote areas easier and with lower costs than the sampling using the traditional methods.

Ninety-five (95) samples of *Hypnum cupressiforme* Hedw. were collected in the region of Northern Greece during the end of summer 2016. Samples were collected from different altitudes (30 to 1450 m above the sea level). During the sampling all the requirements of the Protocol of the European Survey ICP Vegetation were strictly followed (Harmens et al, 2008). After sampling all samples were analyzed to the content of heavy metals using Epithermal Neutron Activation Analysis (ENNA), while the concentrations of radionuclides were determined using gamma spectrometry.

The activity concentrations of ^{137}Cs, ^{40}K, ^{7}Be and ^{210}Pb were determined. Differences have been observed in the activity concentrations between mosses collected from ground surface, rocks, branches and roots. ^{7}Be and ^{210}Pb activity concentrations are higher in moss samples from the ground surface and rocks. ^{137}Cs concentrations are higher in mosses collected near roots and rocks.

Mosses were analysed to the content of heavy metals using ENAA, at the reactor IBR-2 of FLNP, JINR Dubna, Russia. The chemical composition database of the moss samples was further used for the application of source apportionment by Positive Matrix Factorization (PMF), and specifically by the EPA PMF 5.0 model. In total 30 species were used for source apportionment (Na, Mg, Al, Si, Cl, K, Ca, Sc, Ti, V, Cr, Mn, Fe, Co, Ni, As, Br, Rb, Sr, Mo, Cd, Sb, Cs, Ba, La, Ce, Tb, Hf, Ta and Th).

High concentrations of Al and V were noticed in areas where metal industries, coal fired power plants and lignite mining exist. Areas with manufacturing, electricity and heat production activities, showed an additional increase in concentrations of As, Cr and Ni elements. Finally, a high sampling density was achieved, providing information for the elemental and radionuclides deposition from the atmosphere to terrestrial systems over the region of Northern Greece.

Finally, a high sampling density was achieved, providing information for the elemental deposition from the atmosphere to terrestrial systems over the North Greece. The source apportionment results revealed contribution from five sources: Soil Dust, Aged Sea Salt, Vehicular Traffic, Heavy Oil Combustion and Mining Activities (Fig.1), with Soil Dust displaying the highest contribution to the measured metal concentrations among all other sources.

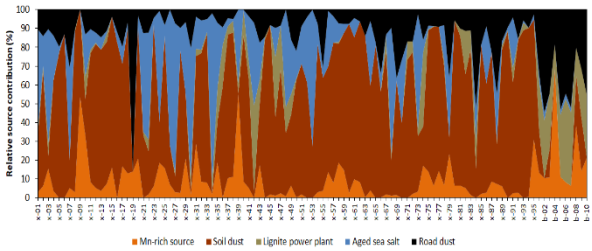

Figure 1. Relative source contributions per sample.

This work is supported by the Hellenic Foundation for Research and Innovation.

Berg, T., Steinnes, E., 1997. Use of mosses (Hylocomium splendens and Pleurozium schreberi) as biomonitors of heavy metal deposition: from relative to absolute values. *Environmental Pollution* 98, 61-71.

Harmens, H., Norris, D., Mills, G., and the participants of the moss survey (2013). Heavy metals and nitrogen in mosses: spatial patterns in 2010/2011 and long-term temporal trends in Europe. ICP Vegetation Programme Coordination Centre, Centre for Ecology and Hydrology, Bangor, UK, pp 63.

The Chernobyl-derived ^{137}Cs accumulation in artificial reservoirs in Central Russia as indicator of sediment sources

M.M. Ivanov[1,2], E.A. Konstantinov[2], N.N. Ivanova[1], A.S. Tsyplenkov[1], N.V. Kuzmenkova[3], A.L. Gurinov[1], A.V. Konoplev[4], V.N. Golosov[1,2]

[1]Faculty of Geography, Lomonosov Moscow State University, Moscow, 119991, Russia
[2]Institute of Geography, Russian Academy of Science, Moscow, 119017, Russia
[3]Faculty of Chemistry, Lomonosov Moscow State University, Moscow, 119991, Russia
[4]Institute of Environmental Radioactivity, Fukushima University, Fukushima, 960-1296, Japan
Keywords: Cs-137, Chernobyl contamination, reservoirs, sedimentation, migration of radionuclides
Presenting author, e-mail: ivanovm@bk.ru

Three artificial reservoirs of different size and area of their catchments were investigated in the Upa River basin, which is located in Chernobyl affected area in Central Russia (Tula region, so called «Plavsk hot spot"). Study area is characterized by temperate climate, plain topography and loamy soil cover (chernozems). Arable lands occupy the main part of reservoir's catchment areas. Soil erosion on the arable lands is the main process responsible for the ^{137}Cs transport from catchment area to rivers and reservoirs.

Evaluation of ^{137}Cs concentration changes in bottom sediment depth profiles may provide relevant information about changes of ^{137}Cs concentration in the different sediment sources over post-Chernobyl period.

A series of sediment cores was collected in January 2018 and February 2019 using piston sampler. Cores were sliced into sections of 2-3 cm, dried, grinded and gamma-spectrometry analysis measured with spectrometer ORTEC GEM-C5060P4-B with HPGe detector (relative efficiency 20%).

Peak of ^{137}Cs concentration was identified in the all cores (see Fig.1, as an axamples). The layer with maximum ^{137}Cs concentration can be attributed to period of the Chernobyl fallout from atmosphere. Sediments above this layer are supposed to be accumulated after 1986.

^{137}Cs depth distribution curves have different shape but they illustrate one basic tendency. In the first years after Chernobyl fallout concentration of ^{137}Cs in sediments drops in several times if it is compared with initial fallout and after that decrease of ^{137}Cs concentration decline smoothly. Such interpretation is consistent with direct observations of the particulate ^{137}Cs in the water of the Oka River and it's tributaries (Vakulovsky et al., 1995).

Nevertheless, ^{137}Cs concentrations in sediments accumulated in reservoir drained relatively small catchment area are characterized by more high fluctuation (Fig 1 A). It is associated with more high variation in the contribution of the different sediment sources.

The ^{137}Cs depth distribution in large reservoir are more smooth due to larger catchment area. It is promoted to more uniform ^{137}Cs concentration in river sediment due to mixing of sediments delivered from the different sediment sources (Fig 1 B).

If it is assumed that the mean rate of sediment accumulation for the post-Chernobyl period was uniform, temporal changes of particulate ^{137}Cs concentration in surface runoff in general can be described by convection-diffusion model (Crank, 1975; Prokhorov, 1981; Bulgakov et al., 2002). However, it is necessary to consider hydrologic, geomorphic and landscape features of the reservoir catchment area for improving of model calculation.

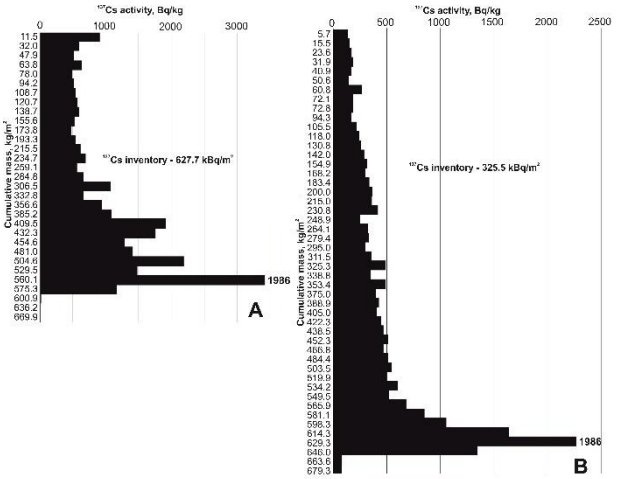

Figure 1. The ^{137}Cs depth distribution curves in bottom sediments of the Malyn (A) and Sheckino reservoirs (B).

This work was supported by the Russian Fund for Basic Research (RFBR project No. 18-55-50002) and Russian Scientific Fund (RSF project No. 19-77-00022).

Bulgakov, A.A., Konoplev A.V., Kanivets, V.V. and Voitsekhovich, O.V.: Modelling the long-term dynamics of radionuclides in rivers. *Radioprotection - Colloques*, 37(C1), 649-654, 2002.

Crank, J. 1975 The mathematics of diffusion. *London: Oxford University Press*, 56-61, 1975.

Prokhorov, V.M. 1981 Migration of radioactive contaminants in soils: physico-chemical mechanisms and modelling. *Moscow: Energoatomizdat*, 99 p., (in Russian)

Vakulovsky S.M., Nikitin A.I., Chumichev V.B., Katrich I.Yu., Voitsekhovich O.V., Medinets V.I., Pisarev V.V., Bovkun L.A., Khersonsky E.S. 1994. Cesium-137 and Strontium-90 Contamination of Water Bodies in the Areas Affected by Releases from the Chernobyl Nuclear Plant Accident: An Overview. *J. Environ. Radioactivity*, 23, 103-122.

Exploring uranium minor isotopes (U-233, U-236) as a new tracer to highlight uranium contamination downstream former uranium mine sites

H. Jaegler[1], A. Gourgiotis[1], A. Mangeret[1], P. Blanchart[2], G. Morin[3], K. Hain[4], P. Steier[4], R. Golser[4], C. Cazala[1]

[1]Institut de Radioprotection et de Sûreté Nucléaire - PSE/ENV - SEDRE/LELI, Fontenay-aux-Roses, 92262, France
[2]Institut de Radioprotection et de Sûreté Nucléaire - PSE/ENV - SEDRE/USDR, Fontenay-aux-Roses, 92262, France
[3]Institut de Minéralogie, de Physique des Matériaux et de Cosmochimie (IMPMC), UMR 7590 CNRS-Sorbonne Université IRD-MNHN, case 115, 4 place Jussieu, 75252 Paris Cedex 5, France
[4]University of Vienna, Faculty of Physics, Isotope Research and Nuclear Physics, Vienna Environmental Research Accelerator, Währinger Str. 17, 1090 Vienna, Austria
Keywords: former uranium mine, fingerprinting, ^{236}U, ^{233}U
Presenting author, e-mail: hugo.jaegler@irsn.fr

Uranium (U) is naturally occurring in the environment and its concentration ranges between 1 to 10 mg.kg^{-1} in the earth's crust. In the vicinity of former uranium mines, these concentrations can increase by several orders of magnitude, due to U remobilisation from mill tailings and waste rocks. Potential runoff and erosion after the rehabilitation of the mining sites could therefore explain this increase of U in the surrounding lands, watercourses and wetlands. However, high U concentrations have already been observed in sediments and soils in areas not influenced by U mining activities. In fact, organic matter and reducing conditions in sediments and soils can lead to an important U accumulation originating from the geochemical background. Therefore, identifying U origin (mine versus geochemical background) in the vicinity of former U mines is a key element for contribution to the assessment of uranium mining waste management strategies.

Natural processes like the alpha recoil effect and isotope fractionation limit the use of $^{234}U/^{238}U$ and $^{235}U/^{238}U$ isotope ratios as fingerprints to identify the U origin. In this work, the use of natural U minor isotopes was explored. The $^{236}U/^{238}U$ ratio of the geochemical background is estimated to be around 10^{-14}. On the contrary, in U ore, the higher neutron flux from (α, n) reactions leads to a significant production of ^{236}U by activation of ^{235}U. Consequently, uranium ores show distinct isotope signatures with typical $^{236}U/^{238}U$ isotope ratios ranging between 10^{-12} and 10^{-10}. However, ^{236}U has also been released in the environment by global fallout from atmospheric nuclear weapon tests in the 1960s. This anthropogenic input of ^{236}U in the environment increased the $^{236}U/^{238}U$ ratio of the geochemical background at levels close to U ore signature, thus limiting the use of this ratio as a fingerprint. Furthermore, natural ^{238}U concentration variations can also induce fluctuation of the $^{236}U/^{238}U$ isotope ratios.

In order to overcome these limitations, we investigated the use of environmental ^{233}U, for which detection became possible only recently. In nature, the main production process of ^{233}U is by neutron activation of ^{232}Th. In the geochemical background, the resultant concentration of ^{233}U is very low. In various U ores, measurements showed $^{233}U/^{236}U$ isotope ratios $\leq 10^{-4}$. The main origin of ^{233}U in the environment is global fallout from the atmospheric nuclear weapon tests with a typical $^{233}U/^{236}U$ isotope ratio of 10^{-2} (Hain et al., 2017) produced fusion neutrons via $^{235}U(n,3n)^{233}U$. This isotopic "contrast" between global fallout, the geochemical background and U ores makes the $^{233}U/^{236}U$ ratio a potential fingerprint to highlight U contamination of the environment by mining and milling activities.

Measurements of $^{233}U/^{236}U$ ratios were performed by Accelerator Mass Spectrometry (AMS) at the Vienna Environmental Research Accelerator (VERA).

First results of $^{233}U/^{236}U$ ratios in U ore samples, contaminated sediments from wetlands draining the former mine facilities and non-contaminated samples representing the geochemical background will be presented and discussed in this talk.

Hain, K., Steier, P., Eigl, R., Froehlich, M.B., Golser, R., Hou, X., Lachner, J., Qiao, J., Quinto, F., and Sakaguchi, A. 2017. "$^{233}U/^{236}U$ – A New Tracer for Environmental Processes ?" In *Envira2017*, 29.

Part of this work was supported by PF NEEDS Environment (Andra, CNRS, EDF, IRSN).

Initial radioecological and environmental state of Lithuanian transboundary area before the start of the operation of the NPP in Belarus

Jefanova O.*[,1], Baužiene I.[1], Mažeika J.[1], Petrošius R.[1], Skuratovič Ž.[1], Bridžiuvienė D.[1], Levinskaitė L.[1], Raudonienė V.[1], Švedienė J.[1], Paškevičius A.[1], G. Lujanienė[2]

1-State Research Institute Nature Research Centre, Akademijos str. 2, LT-08412 Vilnius, Lithuania.
2- State Research Institute Center for Physical Sciences and Technology, Saulėtekio av. 3, LT-10257 Vilnius, Lithuania.
Keywords: the NPP in Belarus, microorganisms, terrestrial ecosystems, radioecological state, H-3, C-14, Cs-137
Presenting author, e-mail: olga.jefanova@gamtc.lt

Knowledge of the background activity concentrations of anthropogenic radionuclides before the start of operation of the new Nuclear Power Plant (NPP) in Belarus is of great concern in neighbouring countries. The construction of a new NPP in Belarus (it is scheduled to begin operating in October 2019) is the issue of high importance for Lithuania, which causes not only the discussions but also the need of new investigations. The NPP in Belarus is located very close to Lithuanian border (20 km) and to country capital Vilnius (50 km). The part of 30 km zone of NPP is located on Lithuanian territory (Fig. 1).
The aim of this study is to investigate the pre-operational radioecological and environmental state of relevant terrestrial pine forest ecosystem located in that territory.

Figure 1. Location of sampling sites.

The observation system including 8 monitoring sites for terrestrial ecosystems (typical is pine forest) near Lithuanian-Belarussian border was justified. The samples from terrestrial ecosystems included higher plants (mosses, *Vaccinium myrtillus L.*, *Sorbus aucuparia L.*, *Artemisia sp.*) and forest litter-soil horizons (OL, OF and OH) as well as organic-mineral (A) soil horizon with analysis of Cs-137, H-3, C-14 distribution in 2017-2018. Additionally, it was analysed soil microorganism's distribution (*testate amoebae*, azotobacter, actinobacteria, yeasts and fungi).
The average value of H-3 in *Sorbus aucuparia L.* leafs is 15 ± 2.5 TU, vary from 13.2 ± 2.2 to 17.1 ± 2.3 TU. The average value of H-3 in *Vaccinium myrtillus L.* shrubs is 18.8 ± 2.5 TU, vary from 17.3 ± 2.2 to 20.8 ± 2.3 TU. H-3 values in plants are close to the level in precipitation, about 15 TU in Lithuanian latitude in summertime. C-14 values in flora samples (mosses, *Vaccinium myrtillus L.*, *Sorbus aucuparia L)* varied insignificantly. The average value is 98.6 ± 1.4 pMC. C-14 values were lower than modern level in all samples except in *Artemisia sp.*, fluctuated from 100.14 ± 0.75 to 102.40 ± 0.79 pMC. It shows fast modern C-14 metabolism in this species biomass.
Cs-137 distribution in soil horizons depends on forest plant succession and anthropogenic impact. In sites with forest growing for more than 100 years distribution of Cs-137 is usual. The most intensively Cs-137 is deposited in OH, soil litter horizon with the most dispersed organics and fine mineral fractions. Where younger forest grows, one can see perturbation of surface organic mineral A soil horizon and deeper penetration of Cs-137 fallout. The cumulated activity of Cs-137 in 15 cm topsoil vary from 593 to 1645 Bq/m^2 depending on different deposition level after Chernobyl accident, that is in order of magnitude observed in former studies (Mažeika, 2002). Direct positive correlation between Cs-137 and K-40 (Bq/m^2) in OF soil layer (r = 0.93) and direct negative correlation (r = 0.75) in mosses and OL top layers (less significant) is a feature of all studied profiles. The pH value in OF and OH soil horizons vary between 2.4 and 4.5. Due to low pH and presence of soil microorganisms (fungi, bacteria, etc.) Cs-137 bioavailability can be enhanced. Biodiversity, amount and correlation between the abundance of microorganism's groups were described in detail.
The Cs-137 specific activities in plants over ground biomass varied from 6.1 ±0.6 to 22.5 ± 1.0 Bq/kg dry mass in mosses; from 0.8 ±0.2 to 40.5 ± 1.8 in *Vaccinium myrtillus L.*; from 2.8 ± 0.5 to 18.9 ± 1.5 in *Sorbus aucuparia L.* leafs.

This work was supported by 2014-2020 Operational Programme for the European Union Funds Investments in Lithuania, under grant No. 09.3.3-LMT-K-712-13-0474.

Mažeika, J. 2002. Radionuclides in Geoenvironment of Lithuania. Vilnius, Institute of Geology, p. 216.

Performance evaluation of a European scale radon-in-water proficiency test

V. Jobbágy[1], M. Hult[1]

[1]European Commission, Joint Research Centre, Geel, 2440, Belgium
Keywords: proficiency test, radon, drinking water, environmental radioactivity
Presenting author, e-mail: viktor.jobbagy@ec.europa.eu

A European wide proficiency test (PT) on measurements of the massic activity of ^{222}Rn in drinking water was organised by JRC-Geel with the participation of 101 European environmental radioactivity monitoring laboratories in 2018. The proficiency test materials with elevated ^{222}Rn massic activity were collected in Austria.

A key problem when measuring an inert gas is the possibility of losing some of it during handling. Extra efforts were made to secure ^{222}Rn tightness throughout the whole process from sampling until measurement (Jobbágy, 2019 a), which also had been tested in a small scale pilot-PT (Jobbágy et al., 2019 b). The packaging and transport chain had to be established in a timely manner with short storage and delivery times. The process involved using all state-of-the art knowledge regarding sampling and transporting ^{222}Rn in water such as temperature controlled transport and use of radon tight containers.

During the European wide PT, two independent standard measurement methods (gamma-ray spectrometry and liquid scintillation counting) were used for the reference value determination, homogeneity and short term stability studies. The reference values were calculated from the power moderated means of measurement results at JRC-Geel. The uncertainty of the reference values included the uncertainties from sampling, stability, between-bottle homogeneity and characterization studies (ISO 17043, 2010).

The performance of the participating laboratories was evaluated with comparing to the reference value using percentage deviation, z-score, zeta-score (ISO 13528, 2015). It was found that 84 % of the participants' results were within the ± 20 % reference range and the general performance was acceptable as shown in Figure 1.

One can discern a small negative bias in the results which is most likely due to loss on radon when handling the sample, e.g. when transferring it to measurement containers. When the uncertainty budget was evaluated then less acceptable scores were found (76 % acceptable results). The results were further evaluated on the basis of applied methods to check for method dependency (gamma-ray spectrometry, liquid scintillation counting and emanometry).

Each of the applied methods seems to be adequate for radon-in-water measurements. A key observation is that radon loss is not perfectly taken care of in all laboratories and it should at least be included in the uncertainty budget. Underperforming measurement methods need to be checked to reduce ^{222}Rn loss during manipulation. In addition to this calibration procedures and uncertainty budgets need to be reviewed.

Sources of interferences were identified by PT the participants and the organizer as well. Participants already reported positive impacts as this PT helped to improve their QA system and was useful regarding the accreditation procedure.

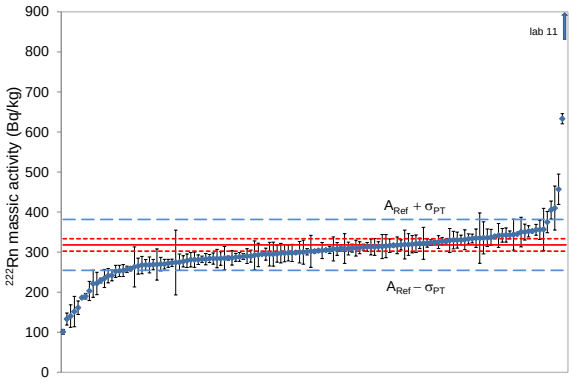

Figure 1. The reported ^{222}Rn massic activities with their combined standard uncertainties (Bq/kg).

Acknowledgments

This proficiency test exercise would not have been completed without the commitment and kind cooperation of Valeria Gruber, Dietmar Roth, Stefan Willnauer, Markus Bernreiter, Viktoria Schauer and Wolfgang Ringer from the Austrian Agency for Health and Food Safety (AGES) in Linz.

Jobbágy V., Stroh H., Marissens G., Hult M. 2019 a. *J. Environ. Radioact*. 197, 30-38.

Jobbágy V., Gruber V., Roth D., von Philipsborn H., Hult M. et al. 2019 b. Presented at the ICRM2019 conference.

ISO/IEC 17043:2010. Conformity assessment -- General requirements for proficiency testing, International Organization for Standardization, Geneva.

ISO 13528:2015. Statistical methods for use in proficiency testing by interlaboratory comparison, International Organization for Standardization, Geneva.

Temporal changes in the tritium and radiocarbon concentration in the western North Pacific Ocean (1993-2012)

J. Kaizer[1], Y. Kumamoto[2], M. Molnár[3], L. Palcsu[3], P.P. Povinec[1]

[1]Department of Nuclear Physics and Biophysics, Faculty of Mathematics, Physics and Informatics, Comenius University, 84248 Bratislava, Slovakia
[2]Research and Development Center for Global Change, Japan Agency for Marine-Earth Science and Technology, 2-15 Natushima-cho, Yokosuka, Kanagawa 237-0061, Japan
[3]Institute of Nuclear Research (ATOMKI), 4026 Debrecen, Hungary
Keywords: tritium, radiocarbon, WOCE, North Pacific
Presenting author e-mail: kaizer@fmph.uniba.sk

The aim of the World Ocean Circulation Experiment (WOCE) was to obtain data which could be used to develop models to study the role of circulation of the global ocean in climate change (Woods, 1985). In the framework project, which was conducted in the 1980s and 1990s, the stations in the western North Pacific were sampled as well. Besides physico-chemical characteristics such as temperature, salinity and oxygen content, ^{3}H and ^{14}C concentrations in water column were also determined, as both radionuclides have been recognized as useful oceanographic tracers.

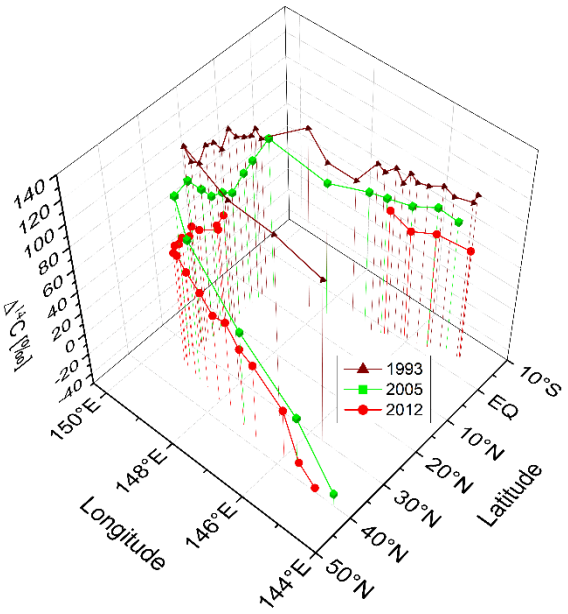

Figure 1. $\Delta^{14}C$ in surface waters of the western North Pacific in 1993-2012.

Here we shall present temporal changes in the tritium and radiocarbon concentration in seawater, sampled approximately along the 149°E meridian line, from the tropical to the subarctic region (4°S - 42°N). As part of the WOCE, the sampling sites were first visited in 1993. Twelve years later, another cruise was conducted along the line, however, tritium was not determined this time. The stations were re-visited once again at turn of the years 2011 and 2012, when an impact of the Fukushima Dai-ichi nuclear power plant (FDNPP) accident on the ^{3}H and ^{14}C level was investigated (Povinec et al., 2017; Kaizer et al., 2018).

Temporal changes in the radiocarbon concentration in surface waters in the western part of North Pacific Ocean are depicted in Figure 1. Similar decrease in the $\Delta^{14}C$ values was observed from 1993 to 2005 (Povinec et al., 2017) than from 2005 to 2012, though the effect of seasonal variation cannot be excluded due to different sampling periods. A latitudinal distribution pattern, which is typical for this region, did not change over the time, i.e. ^{14}C surface levels gradually increased from the subarctic area downwards to the South Equatorial Current. Vertical profiles of selected stations showed subsurface radiocarbon maxima at the depth of 100-200 m.
The situation is much different for tritium. All stations showed higher surface activity concentration in 2011/2012 than in 1993. This would suggest that the influence of the FDNPP accident on the ^{3}H level in the region was non-negligible, which is in concordance with our previous investigations (Povinec et al., 2017; Kaizer et al., 2018). Tritium and bomb-derived radiocarbon water column inventories will be presented and dis-cussed as well.

This work was supported by the EU Research and Development Operational Program funded by the ERDF (project No. 26240220004), and by the International Atomic Energy Agency (TC project SLR-1001).

Kaizer, J., Aoyama, M., Kumamoto, Y., Molnár, M., Palcsu, L., Povinec, P.P., 2018. Tritium and radiocarbon in the western North Pacific waters: post-Fukushima situation. *J. Environ. Radioact.* 184–185, 83–94.

Povinec, P.P., Liong Wee Kwong, L., Kaizer, J., Molnár, M., Nies, H., Palcsu, L., Papp, L., Pham, M.K., Jean-Baptiste, P., 2017. Impact of the Fukushima accident on tritium, radiocarbon and radiocesium levels in seawater of the western North Pacific Ocean: A comparison with pre-Fukushima situation. *J. Environ. Radioact.* 166, 56–66.

Woods, J.D., 1985. The World Ocean Circulation Experiment. *Nature* 314, 501–511.

Mobility of radionuclides from the spoil deposit No.1 of the abandoned uranium mine in Pécs, Hungary

L.H.N. Khumalo[1], Gy. Heltai[1], M. Horváth[1]

[1]Department of Chemistry, Szent István University, Gödöllő, 2100, Hungary
Keywords: Mobility, radionuclides, sequential exctraction, uranium mining
Presenting author, e-mail: lamlilekhumalo@gmail.com

The Hungarian uranium company in Pécs produced 22 000 tonnes uranium (tU) before ceasing production activities at the end of 1997, after 42 years of operation (International Atomic Energy Ageny, 2005). In 2006, there was a feasibility study of restarting uranium mining in the Mecsek Hills near Pécs (Malovics, 2014). According to International Atomic Agency (2005), during the Mecsek uranium mine remediation activity one of the biggest problems has been controlling erosion. During the process of soil covering, there was an erosion wounding occurrence on spoil deposit No.1 in Mecsek uranium mine. To follow the long-term effect, soil and plant samples were collected from four sampling points of the spoil deposit No.1; (1) at the top of the deposit - Rn-M11, (2) on the slope of the deposit – Rn-M12, (3) at the bottom field – Rn-M13 and (4) at the bottom edge of of the deposit - radioactive sample. Each soil core sample was taken from different depths: 0 – 25 cm, 25 – 50 cm, 50 – 75 cm and 75 – 100 cm.

The present research is joining the large monitoring program that is currently running at abandoned and recultivated Mecsek uranium mine. The main aim of this research is to study the effectiveness of soil covering layer in retardation of migration of radioactive substances on the cultivated soil deposit No.1. Radon measurement, gamma spectrometry and fractionation by sequential extraction of radionuclides were conducted to achieve the aim of this study.

This research is not yet completed. The fractionation by sequential extraction of radionuclides is still in progress.

Figure 1 indicates the summary of the results for ^{222}Rn activity concentration measurements in the soil samples and Figure 2 indicates the specific activity results for primordial radionuclides in soil and plant samples respectively.

Radon-222 results in Figure 1 indicate that the sampling point at the bottom of the deposit had higher radon activity concentrations compared to the points on top of the deposit. In Figure 2, elevated activity concentration of ^{238}U in soil and plant samples indicate that there might be a migration of radionuclides from the top of the spoil deposit No.1 to the lower area of the spoil deposit. It might also be an indication that the ^{238}U and some of its daughters might be available for biological uptake by plants.

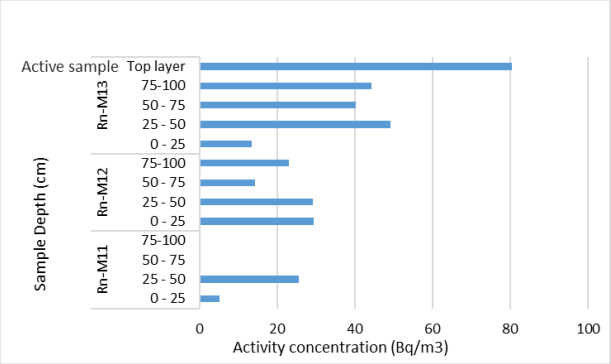

Figure 1. Radon results for soil samples.

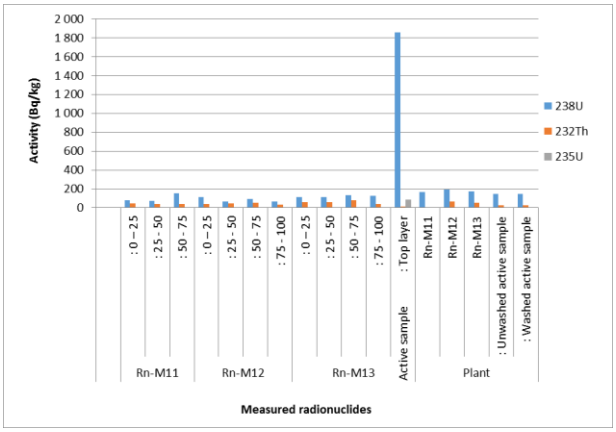

Figure 2. Specific activity results for primordial radionuclides in soil and plant samples.

This research is supported by Stipendium Hungaricum [Reg. No.: 238700] and by the South African Department of Higher Education and Training.

Malovics, G. 2014, 04 08. *Uranium mine opening in Pecs, Hungary*. Retrieved 09 24, 2017, from Ejatlas.org: http://ejalas.org/conflict/uranium-mine-reopening-in-pecs-hungary.

International Atomic Energy Agency. 2005. Recent developments in uranium exploration, production and environmental issues: Proceedings of a technical meeting organized by the IAEA in cooperation with the OECD Nuclear Energy Agency and DIAMO State Owned Enterprise held in Straz, Czech Republic, 6–8 September 2004. *IAEA-TECDOC-1463*, 6–8.

Heterogeneity of isotopic signatures of the FDNPP in the environmental samples

R. Kierepko[1]

[1] Department of Nuclear Physical Chemistry, Institute of Nuclear Physics, Polish Academy of Sciences (PAN), Krakow, 31-342, Poland
Keywords: FDNPP accident, actinides, distribution, nSM (n Sources Model)
Presenting author, e-mail: renata.kierepko@ifj.edu.pl

The accident of the Fukushima Daiichi Nuclear Power Plant (FDNPP) in 2011 caused released enormous radioactive isotopes into the atmosphere and in the aftermath to the terrestrial environment.

The chronology of events during this accident allowed to suppose that in isotopic signs assigned clearly to FDNPP should exist the subtle structure of the isotopic signatures connected with specific FDNPP reactors. The implementation of "deconvolution" by using the nSM (n Sources Model) opens new possibilities for the interpretation of the existed databases.

The mentioned analysis performed based on the actinides data set (^{238}Pu, $^{(239+240)}$Pu, ^{242}Cm, $^{(243+244)}$Cm), which was taken from a publication of Yamamoto et al., 2014, not only justify the coexistence of markers of specific FDNPP reactors but also determine the spatial range of isotopic traces of each reactor.

One of the most spectacular results of the conducted analyses was the discovery that in the considered sample material ("black substances"), selected as one of the best carriers of the "fresh" isotopic signs coming from the FDNPP (Kierepko et al., 2019), do not coexist simultaneously signatures coming from units no. 1, 2, and 3 of the FDNPP. This result was confirmed both using the model for 4 coexisting sources (4SM) in the statement: unit no. 1, 2, 3 and GF (global fallout) as well as using a model of 3 sources (3SM) in the statement: unit no. 1, 2, 3.

Other results showed that the most often identified combination of reactors in the environment of the Fukushima Prefecture was unit 2 and unit 3. Statistically, the most common actinides fraction came from unit 2, whereas the rarest was the fraction that came from unit 3. Finally, the obtained outcomes of mentioned analysis together with both geographical locations of sampling points and meteorological conditions during accident allowed to prepare maps of the distribution of actinides signatures belonging to the different FDNPP reactors.

Although the FDNPP accident happened eight years ago, the knowledge about some aspects of it remains incomplete. This presentation focuses on the details that were mention very rarely in the literature in the context of actinides and at the same time, applied methodology proposes a way to solve unexplained facts concerning the mixing of isotopic signs.

Yamamoto M., Sakaguchi, A., Ochiai, S., Takada, T., Hamataka,K., Murakami, T., Nagao, S. 2014. Isotopic Pu, Am and Cm signatures in environmental samples contaminated by the Fukushima Dai-ichi Nuclear Power Plant accident. *J. of Environ. Radioactivity*. 132, 31-46.

Kierepko, R., Sahoo, S., Hosoda, M., Tokonami, S., Sorimachi, A., Kim, E., Ohno, M. 2019. ^{238}Pu/$^{(239+240)}$Pu activity ratio as an indicator of Pu originating from the FDNPP accident in the terrestrial environment of Fukushima Prefecture *J. of Environ. Radioactivity*. 196, 133-140.

^{129}iodine in environmental samples: Analysis of river and sea water from the vicinity of the Sellafield reprocessing plant and insight into migration behaviour in the soil vadose zone

Fabian Köhler[1]*, Beate Riebe[1], N. Molkenthin[1], Clemens Walther[1]

[1]Institute of Radioecology and Radiation Protection, University of Hannover, 30419 Hannover, Germany
Keywords: iodine sorption, soil column, vadose zone, speciation
Fabian Köhler, e-mail: koehler@irs.uni-hannover.de

^{129}I is emitted continuously in large amounts by reprocessing plants in La Hague and Sellafield, which leads to an increase of the isotopic ratios ^{129}I/^{127}I from some 10^{-12} in the pre-nuclear age to 10^{-7} or above in parts of Europe, today [Daraoui et al., 2016]. With the long half-life (15 Mio y), ^{129}I is important to be considered for the long-term assessment of nuclear waste disposal, especially as it is a highly mobile fission product. Many aspects of iodine chemistry in the environment are already known [Kaplan et al., 2014; Hou, 2004], particularly the ability of ^{129}I to function as marine tracer and the dominant role of organics and clay in iodine retardation in soil. However, detailed process understanding, relevant for radioecological and geochemical modelling, is still missing for many aspects.

We report on the analysis of water samples taken in March 2019 from the direct vicinity of the Sellafield reprocessing plant and provide comparison regarding the iodine speciation with samples taken near La Hague 2016. ^{129}I/^{127}I ratios of 10^{-6} up to 10^{-5} were found for total iodine and IO_3^-, while ^{129}I/^{127}I ratios of 10^{-7} up to 10^{-6} were measured for the I^- fraction.

Furthermore, we conducted a long-term experiment with undisturbed natural soil columns of approx. 20 cm length, proving upwards migration of iodine in the vadose zone. The sampling site for the columns were in Hannover, Germany, and provides soil with rather low sorption capacities due to high sand content. In contrast to previous studies [Ashworth et al, 2006; Shimamoto et al., 2010], we extracted unhomogenized soil columns from natural soil matrix without preconditioning of the soil.

The experimental setup contained soil columns that were kept in contact with iodine solution over a period of 300 days at constant solution level at the bottom of the soil column before drying for the last 86 days. To achieve a homogeneous distribution of iodine throughout the column by capillary action, an air-filled space is kept on top of the soil inside the column. Relative iodine content (correlated with added amount of ^{125}I tracer) increased by factor 0.25 to 41 in the retardation zones of 4 to 14 cm above solution level. Detailed migration results are presented in Figure 1.

Concluding, we present combined results on iodine speciation in sea water and migration in undisturbed soil columns to give first insight into upwards migration from ground water in German reference soils [REF].

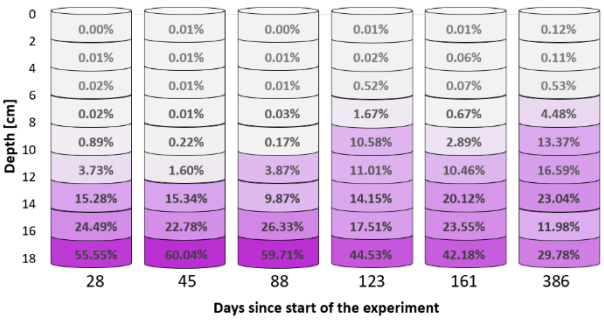

Figure 1. Upwards migration of iodine into the soil vadose zone of undisturbed soil columns over a period of 386 days. Values are given as percentage of total iodine in each column.

We acknowledge financing by the Siebold-Sasse-foundation.

Daraoui, A. et al. (2016). "Iodine-129, Iodine-127 and Cesium-137 in Seawater from the North Sea and the Baltic Sea." *Journal of Environmental Radioactivity* 162–163: 289-299.

Kaplan, D. I. et al. (2014). "Radioiodine Biogeochemistry and Prevalence in Groundwater." *Critical Reviews in Environmental Science and Technology* 44 (20): 2287-2335.

Hou, X. (2004). "Application of ^{129}I as an environmental tracer" *Journal Radioanalytical and Nuclear Chemistry* 262, No.1: 67-75

Ashworth, D. J. et al. (2006) „A comparison of the soil migration and plant uptake of radioactive chlorine and iodine from contaminated groundwater." *Journal of Environmental Radioactivity* 89: 61-80

Shimamoto, Y. S. et al. (2010) „Soil column experiments for iodate and iodide using K-edge XANES and HPLC–ICP-MS." *Journal of Geochemical Exploration* 107: 117-123

Vertical distributions of Chernobyl-derived ^{137}Cs and ^{241}Am in bottom sediments of water bodies in exclusion zone represent long-term dynamics of water contamination

A. Konoplev[1], G. Laptev[2], H. Lisovyi[2], Y. Igarashi[1], K. Nanba[1]

[1]Institute of Environmental Radioactivity, Fukushima University, Fukushima, 960-1296, Japan
[2]Department of Environment Radiation Monitoring, Ukrainian Hydrometeorological Institute, Kiev, 03028, Ukraine
Keywords: Chernobyl, radionuclide, bottom sediments, dynamics
Presenting author, e-mail: alexeikonoplev@gmail.com

Today, 33 years after the Chernobyl accident, the most relevant issue is long-term dynamics of radiocesium in the environment. Detailed analysis of Chernobyl data covering an extended time period can also serve the purpose of predicting long-term changes in environmental radioactivity in Fukushima contaminated areas.

Bottom sediments of lakes and reservoirs provide insight in understanding long-term dynamics of radionuclides strongly bound to sediment particles such as ^{137}Cs and ^{241}Am. With this in mind, in 2018 a number of cores of bottom sediments were collected to the depth of 40-70 cm (depending on site-specific bottom sediments characteristics) in the deep parts of Lake Glubokoe, Lake Azbuchin and Cooling Pond (CP) in close vicinity of the Chernobyl NPP. These water bodies were heavily contaminated as a result of the accident. The collected bottom sediment cores were sliced in 2-cm layers, dried and passed through 2-mm sieve, after which analyzed for ^{137}Cs and ^{241}Am using γ-spectrometry and by standard radiochemical technique for ^{90}Sr.

The obtained ^{137}Cs and ^{241}Am vertical distributions in sediment accumulation zones of the lakes and CP (Figure 1) suggest that almost no vertical mixing of sediments occurred, and the ^{137}Cs and ^{241}Am peaks are well-defined and not diffuse ones. Assuming that sediment accumulation rates after the accident are more or less uniform, layers of bottom sediments can be attributed to certain time of sedimentation. With ^{137}Cs activity concentration in a given layer of bottom sediments corresponding to ^{137}Cs concentration on suspended matter at that point in time, we were able to obtain the dynamics of particulate ^{137}Cs activity concentrations from 1986 to 2018. Over the time since the accident the particulate ^{137}Cs concentrations have decreased by 4-6 times, depending on a water body. Using experimental values of the distribution coefficient K_d, changes in the dissolved ^{137}Cs activity concentrations in the above water bodies have been estimated for the period of 32 years after the accident. The estimates of dissolved ^{137}Cs concentrations are in reasonable agreement with monitoring data. The general trend of the particulate and dissolved ^{137}Cs and ^{241}Am activity concentrations in all three water bodies apparently can be described by the semi-empirical "diffusional" model. All three water bodies exhibited a secondary maximum in estimated ^{137}Cs and ^{241}Am activity concentrations in water around year 2000, which is conceivably due to the shutdown of the Chernobyl NPP in case of CP and remediation activity in the surrounding areas in case of lakes Azbuchin and Glubokoe.

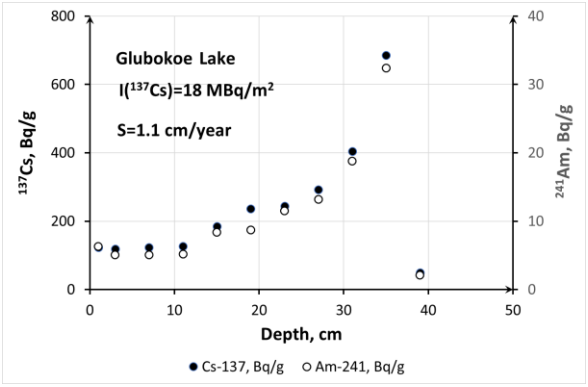

A

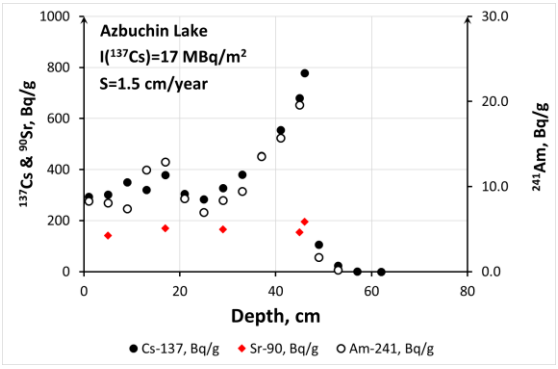

B

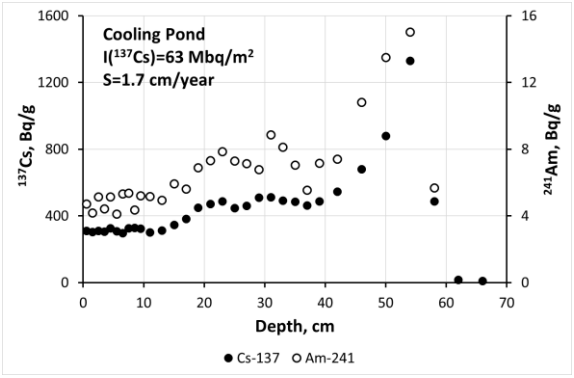

C

Figure 1. Vertical distributions of long-lived radionuclides in bottom sediments of Glubokoe Lake (A), Azbuchin lake (B) and Cooling Pond (C). I is radionuclide inventory in bottom sediments; S is estimated average sedimentation rate.

This research was supported by Science and Technology Research Partnership for Sustainable Development (SATREPS), Japan Science and Technology Agency (JST)/Japan International Cooperation Agency (JICA).

Radiocarbon analysis of carbonaceous aerosols in Bratislava, Slovakia

I. Kontuľ[1], J. Kaizer[1], M. Ješkovský[1], P. Steier[2], P. P. Povinec[1]

[1]Centre for Nuclear and Accelerator Technologies (CENTA), Faculty of Mathematics, Physics and Informatics, Comenius University, 842 48 Bratislava, Slovakia
[2]Vienna Environmental Research Accelerator (VERA), Faculty of Physics, University of Vienna, A-1090 Vienna, Austria

Keywords: aerosol, radiocarbon, source apportionment, AMS

Presenting author: Ivan Kontuľ, e-mail: ivan.kontul@fmph.uniba.sk

Aerosols dispersed in the atmosphere represent important factors influencing not only the environment, but also human health. Inhalation of aerosols containing combustion by-products contribute to respiratory and cardiovascular diseases (Pope and Dockery, 2006). From the environmental viewpoint, the concentration of aerosols in the atmosphere and their properties also influence the Earth's energy budget (Ramanathan and Carmichael, 2008). Carbonaceous aerosols are one of the main components of total atmospheric aerosols, and their sources are therefore of great interest. Several chemical analytical techniques can be used for source apportionment of carbonaceous aerosols, but radiocarbon analysis provides an excellent way to determine the fraction of fossil and non-fossil aerosols in the studied area (Currie, 2000).

Over the period of one-year (june 2017 - june 2018), we sampled atmospheric aerosol (size greater than 0.3 μm) in Bratislava, Slovakia and used the exposed quartz filters for radiocarbon analysis of the elemental carbon (EC) aerosol fraction. Accelerator mass spectrometry was used to measure radiocarbon content of the sampled aerosols. The sample preparation including the preparation of graphite targets was carried out at the CENTA laboratory of the Comenius University (Povinec et al., 2015). The accelerator mass spectrometry measurements were carried out at the VERA laboratory of the University of Vienna (Steier et al., 2004).

Using the radiocarbon analysis results for the EC aerosols, we calculated the relative contribution of their sources - biomass burning (f_{bio}) and fossil fuel combustion (f_{fos}). Figure 1 shows the obtained results from the studied time period.

The results show that on average the fossil fuel combustion is the dominant source of elemental carbon aerosol particles in Bratislava. In summer months, they represent more than half (65 - 80%) of the total EC aerosols. The relative amount of EC particles derived from biomass burning was 20 - 35% in summer, and then increased to 40 - 55% in winter months. The dominance of fossil fraction is caused by high degree of industrialisation and urbanisation of the city. The increase of biomass fraction in winter is probably caused by domestic wood burning in areas surrounding the Bratislava city.

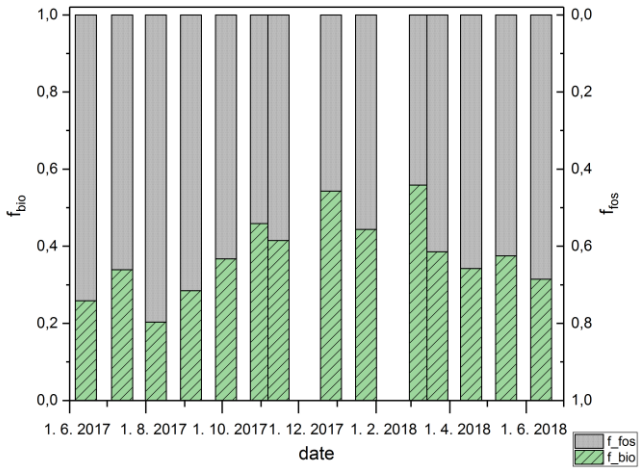

Figure 1. Fossil and biomass burning fractions of EC (elemental carbon) carbonaceous aerosols in Bratislava.

The authors acknowledge support provided by the EU Research and Development Operational Program funded by the ERDF (projects # 26240120012, 26240120026 and 26240220004), and by the International Atomic Energy Agency (project # SLR-1001).

Currie, L.A. 2000. Evolution and Multidisciplinary Frontiers of ^{14}C Aerosol Science. *Radiocarbon* 42, 115-126.

Pope, C.A., Dockery, D.W. 2006. Health effects of fine particulate air pollution: Lines that connect. *J. of Air and Waste Manag. Assoc.* 56, 709-742.

Povinec, P.P., Masarik, J., Ješkovský, M., Kaizer, J., Šivo, A., Breier, R., Pánik, J., Staníček, J., Richtáriková, M., Zahoran, M., Zeman J. 2015. Development of the Accelerator Mass Spectrometry technology at the Comenius University in Bratislava. *Nucl. Instr. Meth. B* 361, 87-94.

Ramanathan, V., Carmichael, G. 2008. Global and regional climate changes due to black carbon. *Nat. Geosci.* 1, 221-227.

Steier, P., Golser, R., Kutschera, W., Priller, A., Vockenhuber, C., Winkler, S. 2004. VERA, an AMS facility for "all" isotopes. *Nucl. Instr. Meth. B* 223-224, 67-71.

Participation in the international inter-laboratory comparison study for biogenic component in liquid fuels by the ^{14}C method

I. Krajcar Bronić[1], J. Kožar Logar[2], R. Krištof [2,3], J. Nikolov[4], N. Todorović[4], I. Stojković[5], J. Barešić[1], A. Sironić[1], D. Borković[1]

[1]Department of Experimental Physics, Ruđer Bošković Institute, 10000 Zagreb, Croatia
[2]Department of Low and Medium Energy Physics, Jožef Stefan Institute, 1000 Ljubljana, Slovenia
[3]Department of Sanitary Engineering, Faculty of Health Sciences, University of Ljubljana, 1000 Ljubljana, Slovenia
[4]Department of Physics, Faculty of Sciences, University of Novi Sad, Novi Sad, Serbia
[5]Faculty of Technical Sciences, University of Novi Sad, Novi Sad, Serbia
Keywords: liquid fuels, biogenic component, ^{14}C method, direct LSC technique
Presenting author: Ines Krajcar Bronić, krajcar@irb.hr

The ^{14}C method can be successfully applied for determination of biogenic component in any type of samples. For a special case of liquid fuels, the „direct LSC method“ for measurement ^{14}C activity by a liquid scintillation counter (LSC) has been recognized as a powerful and reliable method of determination of biogenic component. Laboratories of the Ruđer Bošković Institute (RBI) in Zagreb, the Jožef Stefan Institute (JSI) in Ljubljana, and at the Faculty of Science of the University of Novi Sad (UNS) in Novi Sad implemented the direct LSC method and optimized slightly different measurement and evaluation procedures (Krajcar Bronić et al., 2017, Krištof and Kožar Logar, 2013, Stojković et al., 2017). They defined limits of applicability of the direct LSC method by the values of the Standard Quench Parameter *SQP(E)* determined by the LSC Quantulus 1220.

The laboratories participated in the international inter-laboratory comparison study ILC/2018 „Content of biocomponent in liquid fuel samples“, which was organized in 2018 by the Institute of Ceramics and Building Materials (Opole, Poland). Here we present the results obtained by these 3 laboratories and compare the f_{bio} results with the expected $f_{bio\text{-}exp}$ values.

Seven samples of diesel type of fuel having different concentrations of biocomponent and different colours were obtained. The results for samples with the *SQP(E)* values well above the limits of applicability of the direct LSC method were satisfying in all three laboratories. Qualitatively acceptable, but quantitatively unacceptable results, were obtained for a sample in the *SQP(E)* region of limited applicability. One of the samples exhibited a high quench level, so the *SQP(E)* parameter was below the limits of applicability of the direct LSC method in all 3 laboratories, (*SQP(E)* < 600). The RBI laboratory applied accelerator mass spectrometry (AMS) technique to determine f_{bio} in this highly-quenched sample as well as in the sample without ^{14}C (*SQP(E)* > 800) and in the sample having *SQP(E)* in the limited region of applicability (600 < *SQP(E)* < 700). The JSI laboratory applied the direct absorption of CO_2 in an absorption-scintillation cocktail (DA) technique for the highly-quenched sample (*SQP(E)* < 600). The UNS laboratory used the biogenic oil for calibration and also the internal standard method (IntSt), and the latter resulted in better agreement with the expected values. In Figure 1 we compare the measured f_{bio} values in the intercomparison samples determined by all 3 laboratories and by all methods used with the $f_{bio\text{-}exp}$ values.

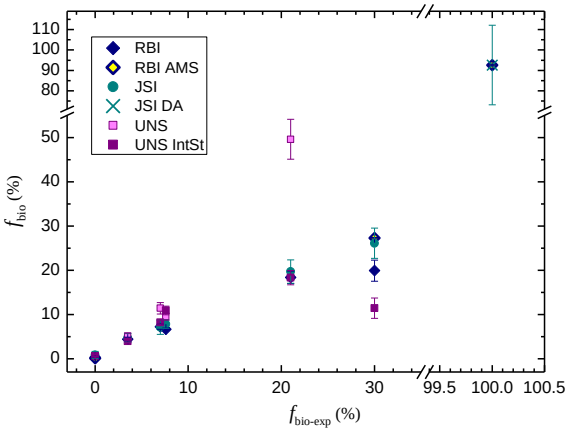

Figure 1. Comparison of the f_{bio} values with the expected $f_{bio\text{-}exp}$ in intercomparison ILC/2018 samples.

Although there were some differences in details of the applied direct LSC methods in the three laboratories, the presented intercomparison results showed that all the methods were suitable for determination of the f_{bio} in liquid fuels, providing the correctly defined limits of applicability for highly quenched samples. Laboratories that have possibility of applying a different ^{14}C measurement technique can satisfactorily determine f_{bio} also in highly quenched samples.

UNS thanks the Ministry of Education, Science and Technological Development (Serbia) for support under grants Nos. III43002 and OI171002.

Krajcar Bronić, I., Barešić, J., Horvatinčić, N., Sironić, A. 2017. Determination of biogenic component in liquid fuels by the ^{14}C direct LSC method by using quenching properties of modern liquids for calibration. *Radiat Phys Chem* 137, 248-253.

Krištof, R., Kožar Logar, J. 2013. Direct LSC method for measurements of biofuels in fuel. *Talanta* 111,183-8.

Stojković, I., Nikolov, J., Tomić, M., Mićić, M., Todorović, N. 2017. Biogenic fraction determination in fuels – Optimal parameters survey. *Fuel* 191, 330-338.

Interlaboratory comparison and OBT measurements in biota in the environment of NPPK

Romana Krištof[1,2], Jasmina Kožar Logar[1], Andreja Sironić[3], Ines Krajcar Bronić[3]

[1]Department of Low and Medium Energy Physics, Jožef Stefan Institute, Ljubljana, Slovenia
[2]Department of Sanitary Engineering, Faculty of Health Sciences, University of Ljubljana, Ljubljana, Slovenia
[3]Department of Experimental Physics, Ruđer Bošković Institute, Zagreb, Croatia
Keywords: organically bound tritium (OBT), Nuclear Power Plant Krško, (NPPK), agricultural produce, interlaboratory comparison
jasmina.logar@ijs.si

Slovenia and Croatia share the Nuclear Power Plant Krško (NPPK), situated on the left bank of the Sava River. Tritium in all types of water samples has been regularly monitored for decades. On some sampling points it shows measurable and slightly elevated concentration in comparison with environmental background but fairly below 100 BqL^{-1}.

Tritium in organic tissues has not been part of regular monitoring program yet. It has attracted our attention when the new Hydroelectric Power Plant Brežice (HPPB) few kilometres downstream of NPPK became the project under construction. The dam of HPPB came into operation in 2017 when the water surface area in the vicinity of NPPK enlarged for factor of 10, the groundwater level and its hydrodynamics changed and might affect also the local climate. First preliminary samplings of organic material and measurements of organically bound tritium (OBT) before the construction of HPPB dam were performed in 2016 (Krištof et al., 2017) when tissue free water tritium (TFWT) and OBT were determined. The observed trends correlate with the predicted modelled trends of NPPK emissions. The values and their ratios are in accordance with the similar studies worldwide (Korolevych et al., 2014).

Two tritium laboratories in Slovenia (JSI) and Croatia (RBI) decided to introduce the measurements of OBT into the inventory of their laboratory methods, check them in the international inter-laboratory inter-comparisons (Sironić et al., 2019) and harmonize both laboratories. Both laboratories proved their competence in determination of OBT (Table 1).

Table 1: Reported and true values at the 5th International OBT Exercise of both laboratories (RBI and JSI).

Lab	Observed value [Bq/L]	Uncertainty (1σ)	ζ
RBI	30.1	1.2	-0.7
JSI	32.2	0.9	-0.2
TRUE	32.8	1.9	/

Harmonized and confirmed methods were applied on agricultural produce, growing in the vicinity of NPPK. Samplings were performed in spring and autumn when the produce was in different growing stages.

Samples were collected on 17 sampling points, before and after the fully operational dam. Samples from each sampling point were split between both laboratories. Results of both laboratories are compared. The OBT values are not uniform for the whole sampling field and show similar correlation with the predominant wind direction. Rather similar behaviour (Figure 1) is known from the regular monitoring program of C-14 which is performed on regular basis since 2006 (Krajcar Bronić et al., 2017). The paper will focus on the OBT values, their correlation with C-14 values and therefore with predominant wind direction. The presented results cover the time period before and after the HPPB dam became operational. The differences and similarities observed in agricultural produce will be presented and discussed.

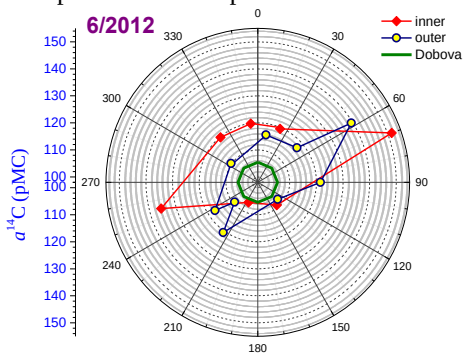

Figure 1: Polar diagram of relative specific C-14 activity (Krajcar Bronić et al., 2017), example for June 2012.

Korolevych, V.Y., Kim, S.B., Davis, P.A., 2014. OBT/HTO ratio in agricultural produce subject to routine atmospheric releases of tritium. *J. Environ. Radioact*. 129, 157–168.

Krajcar Bronić, I., Breznik, B., Volčanšek, A., Barešić, J., Borković, D., Sironić, A., Horvatinčić, N., Obelić, B., Lovrenčić Mikelić, I., 2017. Aktivnosti 14C u atmosferi i bilju u okolici Nuklearne elektrane Krško (NEK) – iskustva nakon 10 godina monitoringa, in: Radolić, V., Poje Sovilj, M., Krajcar Bronić, I. (Eds.), Zbornik Radova Jedanaestog Simpozija Hrvatskog Društva Za Zaštitu Od Zračenja. Hrvatsko društvo za zaščitu od zračenja, Zagreb, 231–237.

Krištof, R., Košenina, S., Zorko, B., Logar, J.K., 2017. Tritium in organic matter around Krško Nuclear Power Plant. *J. Radioanal. Nucl. Chem*. 314, 675–679.

Sironić, A., Krajcar Bronić, I., Kožar Logar, J., Krištof, R., 2019. Interlaboratorijske usporedbe aktivnosti organski vezanog tricija (OBT), in: Popić, J., Coha, I., Krajcar Bronić, I., Knežević Medija, Ž. (Eds.), Zbornik Radova Dvanaestog Simpozija Hrvatskog Društva Za Zaštitu Od Zračenja. Hrvatsko društvo za zaštitu od zračenja, Zagreb, 364–369.

Ion-Laser Interaction Mass Spectrometry: green light for a sensitive detection of long-lived radionuclides

J. Lachner[1], A. Wieser[1], M. Honda[1], O. Marchhart[1], M. Martschini[1], A. Priller[1], P. Steier[1], R. Golser[1]

[1]Faculty of Physics, University of Vienna, 1090 Vienna, Austria
Keywords: AMS, ILIAMS, ion-laser interaction, mass spectrometry,
Presenting author, e-mail: Johannes.lachner@univie.ac.at

Ion Laser InterAction Mass Spectrometry (ILIAMS, (Martschini et al., 2019)) is a new method that assists the analysis of long-lived radioisotopes with Accelerator Mass Spectrometry (AMS). This new isobar suppression method will widen the repertoire of sub-MV AMS facilities by including nuclides that are measured exclusively at larger facilities so far, e.g. ^{36}Cl. Furthermore, we currently develop measurement capabilities for novel AMS isotopes, i.e. among others ^{135}Cs, ^{137}Cs, and ^{90}Sr (Wieser et al., Marchhart et al., this conference).

This contribution will present the principle of operation and the experimental setup at the Vienna Environmental Research Accelerator (VERA), the key figures for routine AMS operation and first data on the performance with novel AMS isotopes.

ILIAMS takes advantage of the element selective photodetachment of a negative ion beam and thus offers a new way to strongly suppress isobaric interferences. To achieve this, the ion beam has to be decelerated electrostatically. This takes place in a radio-frequency quadrupole, where the beam is additionally cooled via collisions with a buffer gas (typically He).

ILIAMS thus serves as an additional elemental filter that is already successfully exploited for the separation of $^{36}Cl^-$ from $^{36}S^-$ (Figure 1) or $^{26}AlO^-$ from $^{26}MgO^-$ in routine AMS measurements. The additional isobar suppression allows for the use of lower charge states on the high energy side of the spectrometer (in the case of ^{36}Cl) or the use of more prolific negative molecules (AlO^- in the case of ^{26}Al). This improves the efficiency for ^{36}Cl and ^{26}Al measurements at VERA.

The sensitive analysis of the trace isotopes ^{135,137}Cs and ^{90}Sr in natural samples is of interest for environmental and radio-ecological studies. Here, the formation of suitable fluorine anions (Zhao et al., 2010) is one way to suppress the stable isobars, i.e. ^{135,137}Ba and ^{90}Y, ^{90}Zr. The fluorine anions of CsF_2^- and SrF_3^- can be transported through the ILIAMS setup, while the suppression of the isobars can be accomplished using a combination of several processes:

collisional detachment in a He buffer gas filled radiofrequency quadrupole

chemical reactions by admixing a small fraction of O_2 to the He buffer gas

photodetachment with 2.3 eV (λ = 532 nm) or 3.5 eV (λ = 355 nm) photons.

First ILIAMS assisted AMS measurements at VERA resulted in the successful detection of ^{135}Cs, ^{137}Cs and ^{90}Sr using in-house reference materials at concentration levels that can also be expected for natural samples. Tests using IAEA reference materials are in progress.

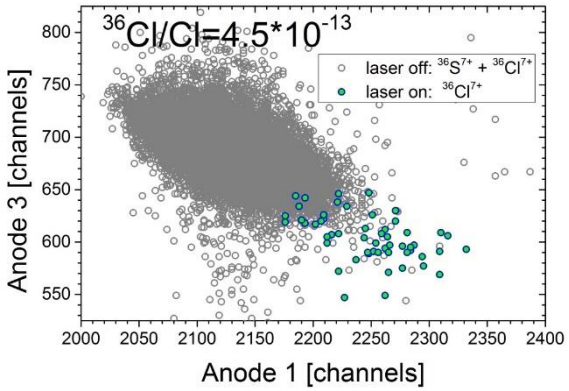

Figure 1. At a final beam energy of ca. 24 MeV the $^{36}Cl^{7+}$ is separated from $^{36}S^{7+}$ in the detection system. The application of ILIAMS completely removes the $^{36}S^{7+}$ interference and leaves only $^{36}Cl^{7+}$ to enter the detector. (Lachner et al, 2019).

Martschini, M., et al. 2019. The ILIAMS project – An RFQ ion beam cooler for selective laser photodetachment at VERA. *Nucl. Instrum. Meth. B.* https://doi.org/10.1016/j.nimb.2019.04.039

Wieser et al., 2019. *contribution at this conference.*

Marchhart et al., 2019. *contribution at this conference.*

Lachner, J. et al., 2019. ^{36}Cl in a new light: AMS measurements assisted by ion-laser interaction. *Nucl. Instrum. Meth. B.* https://doi.org/10.1016/j.nimb.2019.05.061.

Zhao, X.-L., Litherland, A.E., Eliades, J., Kieser, W.E., Liu, Q. 2010. Studies of anions from sputtering I: Survey of MF_n^- . *Nucl. Instrum. Meth. B.* 268, 807-811.

Artificial radionuclides in plants of steppe and forest ecosystems long after nuclear tests at Semipalatinsk test site

N.V. Larionova[1], A.O. Aidarkhanov[1], V.V. Polevik[2], Yu.S. Shevchenko[1], A.R. Ivanova[1]

[1]Branch "Institute of Radiation Safety and Ecology" of the RSE "National Nuclear Center of the Republic of Kazakhstan", Kurchatov, Kazakhstan
[2] Shakarim State University in Semey city, Semey, Kazakhstan
Keywords: Semipalatinsk Nuclear Test Site (STS), radioactive contamination, forest ecosystems
Presenting author, e-mail: Larionova@nnc.kz

Mainly radioactive contamination long after the nuclear tests at Semipalatinsk Nuclear Test Site (STS) is caused by the tests conducted at the «Experimental Field» site. From the 1949 till 1962 30 surface and 86 atmospheric nuclear tests were conducted at this territory. At that most of the radionuclides formed as the result of surface nuclear explosions remain in the epicenters of ıthe tests, and some part bound with relatively small ground or melted rock particles, was carried by wind to significant distance. The pine forest near Irtysh river is one of the territories having radioactive contamination resulted from the radioactive fallout «plume» that was formed more than 60 years ago (29th of August, 1949) as the result of the nuclear test conducted at the STS.

To assess accumulation of artificial radionuclides in the plants 20 spots were selected at the supposed hay-making areas and pasturelands in the zone of forest massif of the territory studied. In each point grassland vegetation represented by mixed samples of steppe herbs was sampled in the area of~ 2 sq. km. Additionally, a dominant grassland vegetation species – uncina (*Carex pilosa*) were sampled in 6 points of the forest area where increased concentrations of artificial radionuclides were found in soil. In 3 out of 6 points samples of pine (*Pinus silvestris*) aged 50-60 and 15-20 years were collected and separated into different parts (cones, branches, needles, cortex). Together with plants soil was sampled using an «кenvelope» technique (2×1 m) to the depth of 5 cm.

Specific activity of ^{137}Cs and ^{241}Am was determined by gamma-spectrometry, while ^{90}Sr and $^{239+240}$Pu – by radiochemical extraction with subsequent beta- and alpha-spectrometric measurements. For quantitative assessment of radionuclides intake from soil the transfer factor (TF) was used. Transfer factor is the ratio between a radionuclide concentration and a weight unit of plants and soil respectively.

Upon the result of laboratory analyses the content of ^{241}Am and ^{137}Cs radionuclides in mixed samples, collected in hay-making areas, pasturelands and individual forest areas, was found to be below the detection limit of the equipment used, ^{90}Sr value varies between 0,2 and 41±6 Bq/kg, $^{239+240}$Pu – between <0,1 and 2,3±0,3 Bq/kg. Specific activity of ^{241}Am and ^{137}Cs in soils collected together with plants, range between <1 and 5,1±1,1 Bq/kg and between 5,4±1,1 and 120±20 Bq/kg respectively. Specific activity of ^{90}Sr in soils ranges between 1,7±0,5 and 30±4 Bq/kg, and for $^{239+240}$Pu it varies greater (<1 to 270±20 Bq/kg).

According to concentrations of artificial radionuclides in uncina (*Carex pilosa*) and pine (*Pinus silvestris*), specific activity values of ^{241}Am in all the researched components are below the detection limits of the equipment used. Quantitative values of ^{137}Cs were found only in pine cortex (*Pinus silvestris*) (0,8±0,1 to 1,8±0,1 Bq/kg), in other cases these are also below the detection limits. Maximum values for $^{239+240}$Pu radionuclide were also registered in cortex (from 0,012±0,05 to 1,5±0,1 Bq/kg). The most interesting distribution pattern was observed for ^{90}Sr. Concentration of this radionuclide in uncina (*Carex pilosa*) is much higher, than in pine (*Pinus silvestris*), in particular in its individual parts studied.

For the purpose of quantitative assessment of radionuclides accumulation in uncina (*Carex pilosa*) transfer factors (TF) were calculated for ^{90}Sr and $^{239+240}$Pu. For ^{241}Am and ^{137}Cs no TF values was found due to lack of quantitative data. TF values for ^{90}Sr were found to be high enough (1,7-1,8) and these can be compared with TFs of this radionuclide, typical for the zones of radioactive streamflows and the venues where warfare radioactive agents (WRA) were tested (1,2-1,7). $^{239+240}$Pu TF values (0,0006-0,0085) obtained for the pine forest area were found to be lower than TFs for the conditionally «background» territories of the STS (0,019) and in most cases are comparable with TFs in the «plumes» of radioactive fallouts (0,0068).

A new approach to detect of low counting rate using an ultra-low-background HPGe detector

M. Laubenstein[1], S. Nagorny[2], S. Nisi[1]

[1]NFN-Laboratori Nazionali del Gran Sasso, Assergi, 67100, Italy
[2]Queen's University, Kingston, K7L 3N6, Canada
Keywords: rare alpha decay, gamma spectroscopy, low-background
Presenting author, e-mail: sn65@queensu.ca

Nowadays, a significant progress in registration of rare alpha decays could be noticed. It is triggered by applying of new experimental approaches for the low rate events registration (namely, cryogenics scintillating bolometers), as well as ultimate improvement of well-known detection technique (crystal scintillator detectors, proportional chamber). In such way was detected the alpha decay of ^{209}Bi ($T_{1/2}$ = 1.9×10^{19} y), ^{180}W (1.8×10^{18} y), ^{151}Eu (4.6×10^{18} y) and ^{148}Sm (4.6×10^{15} y). The ultra-low-background gamma spectroscopy with HP Ge detectors was applied to search for ^{190}Pt alpha decay to first excited state with $T_{1/2} = 2.3\times10^{14}$ y.

Summarizing the listed above results, one can say that in order to detect rare decays with $T_{1/2} > 10^{14}$ y, or in other words, with specific counting rate is about of few events per day, one should focus on detector, which possesses of lowest internal background in region of interest, flexibility with respect to investigation of different isotope of interest, possibility to utilize the sample of large mass, detector stability for the long period of data taking, good energy resolution, and high detection efficiency.

However, in case of decays to low-lying excited states \ (E < 250 keV) the conventional gamma spectroscopy cannot satisfy strict demands on the experimental technique, mainly because of abruptly reduction of the detection efficiency.

A new approach to detect such low-energy gammas, which occur in rare decays to low-lying excited states, is presented. The main feature of our concept is the ultra-nearest disposition of sample in certain simple geometry with respect to Ge detector. That eliminates of gammas absorption in the detector's holding materials and minimizes self-absorption in the sample, as well as simplifies calculation of the detection efficiency. The precise detection of ^{190}Pt alpha decay to the first excited state of daughter nuclide with $T_{1/2} = 4.6\times10^{14}$ y is first example of applicability of this technique. Future possible targets are under discussion.

Investigation of radioactive cesium level in seawater near Taiwan after the Fukushima nuclear accident

P.-F. Lee, W.-J. Huang, P.-J. Huang, M.-H. Lin, J.-J. Wang

Institute of Nuclear Energy Research, Atomic Energy Council, Taoyuan, 32546, Taiwan
Keywords: seawater, radioactive cesium, Fukushima nuclear accident
Presenting author, e-mail: mhlin@iner.gov.tw

Introduction

On 11 March 2011, the Great East-Japan earthquake occurred had caused the core meltdown accident in the Fukushima nuclear power plant followed by the leakage of radioactive materials into the air and ocean. Due to its long half-life of Cs-137, it becomes an important issue to assess the impact of marine ecosystems and public heath resulted by Cs-137 release.

Because Taiwan is geographically close to Japan, the radioactive materials discharged into the ocean by the Fukushima nuclear accident may diffuse to Taiwan through ocean currents. In order to investigate the impact of radioactive materials released into the ocean from the Fukushima nuclear accident, the seawaters near Taiwan were sampled during 2017 to 2018.

Method

In this study, two volumes of seawater (1 liter and 60 liter) were sampled near Taiwan for the content analysis of radioactive cesium during 2017 to 2018. Seawater samples were all filtered by glass microfiber filters with a pore size of 1.2 μm to remove suspended solids. 1 liter of seawater samples were collected by one-liter Marinelli beakers and then measured using HPGe spectrometers. 60 liter of seawater samples were analyzed by using an ammonium phosphomolybdate (AMP) co-precipitation method (The Oceanographic Society of Japan, 2019) and then measured using HPGe spectrometers.

Results and discussion

It was found that the radioactivity of Cs-134 and Cs-137 for all 1 liter seawater samples were less than 0.2 Bq/L. As for 60 liter seawater samples, it was found that the radioactivity of Cs-134 was all less than 1.0 mBq/L, while the radioactivity of Cs-137 was ranged from 0.72 mBq/L to 2.68 mBq/L (with an average of 1.82 mBq/L) as shown in Fig. 1. According to the results of the IAEA MARiS database during 2000 to 2010, the radioactivity of Cs-137 for western Pacific Ocean is about 1.7±0.6(2σ) mBq/L (IAEA, 2005). It showed that the radioactive material released to the ocean from the Fukushima nuclear accident had no significant impact on the seawaters adjacent Taiwan.

The RESRAD-BIOTA code developed by Argonne National Laboratory (ANL) was used to evaluate the radiological effect for aquatic fish from Cs-137 contained seawater. Among them, three different sizes of fish were selected from the common captured fish species to evaluate the maximum allowable concentration of radioactive cesium of seawater as shown in Table 1.

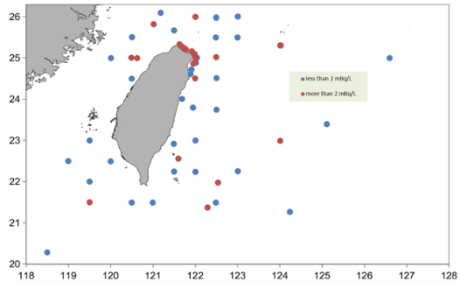

Figure 1. The distributions of Cs-137 for sixty-liter seawater samples taken from surface layer.

Table 1. Estimation results of the maximum allowable Cs-137 concentration of seawater for three different sizes of fish.

Aquatic fish	Mass(kg)	Geometry (cm)	Maximum allowable concentration (mBq/L)
Small size fish (Trachurus japonicas and Scomber australasicus)	1	45*8.7*4.9	108000
Medium size fish (Mugil cephalus and Katsuwonus pelamis)	10	50*26*13	84900
Large size fish (Makaira nigricans and Prionace glauca)	500	270*66*48	56900

It showed that the Cs-137 radioactivity in the seawater was currently 4-5 orders of magnitude lower than the maximum allowable concentration for Cs-137. Therefore, it was speculated that the radiological effect of Cs-137 on aquatic fish in Taiwan's adjacent sea area is not significant.

Conclusions

The average radioactivity of Cs-137 was about 1.82 mBq/L which is near the background level of Cs-137 (1.5±0.6 mBq/L) refer to IAEA MARiS prior to the Fukushima accident.

The radiological effect of Cs-137 on aquatic fish in Taiwan's adjacent sea area is not significant by the assessment results conducted by RESRAD-BIOTA.

The Oceanographic Society of Japan. 2016. Guideline of Ocean Observations Volume 9 Natural and Artificial Radioactivity. ISBN 978-908553-30-1, Japan.

IAEA (International Atomic Energy Agency). 2005. Worldwide marine radioactivity studies (WOMARS) Radionuclide levels in oceans and seas. IAEA-TECDOC-1429, Vienna.

Screening for radionuclide contamination from the Fukushima Accident by Iodine-129 measurement in corals from Baler

S.J. Limlingan[1], A.T. Bautista VII[1], A.M. Jagonoy[1], H. Kusuno[3], E. Dumalagan Jr.[2], F.P. Siringan[2], H. Matsuzaki[3]

[1]Philippine Nuclear Research Institute, Department of Science and Technology, Diliman, Quezon City, 1101, Philippines
[2]Marine Science Institute, University of the Philippines, Diliman, Quezon City, 1101, Philippines
[3]Micro Analysis Laboratory, Tandem Accelerator (MALT), The University Museum, The University of Tokyo, Bunkyo-ku, Tokyo, 113-0032, Japan
Keywords: iodine-129, Fukushima, coral, nuclear accident
Sophia Jobien Limlingan, e-mail: sophiajobien@gmail.com

Following the Fukushima Daiichi nuclear power plant accident of 2011, excessive amounts of toxic radioactive waste was deposited into the Pacific Ocean, consequently posing health risks to exposed individuals. Subsequent transport of this discharge material via circulation in the Pacific Ocean could eventually bring the radionuclides within the vicinity of Philippine coastal communities, potentially threatening marine life, domestic health, and aquatic livelihood. A research study was thus commenced to assess the degree and geographical extent of locally significant contamination with the use of iodine-129 as an environmental proxy for anthropogenic radionuclide transport. In this study, we present a time series profile of $^{129}I/^{127(stable)}I$ isotopic ratios in coral cores from the first of three target sites along the northeastern seaboard of the Philippines. Coral cores were collected from Baler, Aurora, age-modeled, and subsequently subsampled per annual growth band. From these, iodine was extracted from the calcium carbonate matrix via multi-stage solvent extraction procedures, and then analyzed via Accelerator Mass Spectrometry (AMS) and Inductively Coupled Plasma Mass Spectrometry (ICP-MS).

$^{129}I/^{127}I$ peaks corresponding to historical nuclear events such as the extensive above-ground bomb testing in the Pacific Proving Grounds (1952, 1954, 1956, 1958, 1962) and the Chernobyl Accident of 1986 (1998, with 12-year time lag) were clearly observed. Moreover, peaks from the Fukushima fallout may have been observed at around 2014, suggesting a three-year transport period via the Kuroshio Recirculation Gyre (KRG). However, high background $^{129}I/^{127}I$ levels in recent years (2000 – 2010) necessitate further validation from the two other geographical sites.

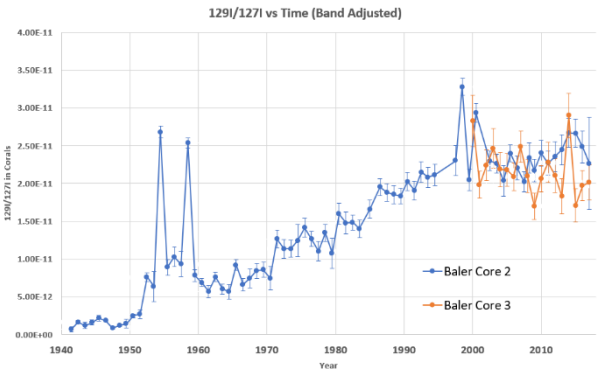

Figure 1. $^{129}I/^{127}I$ in corals collected in Baler.

This work was supported by the Philippine Council for Agriculture, Aquatic, and Natural Resources Research and Development (PCAARRD).

Bautista, A.T.V., Matsuzaki, H., Siringan, F.P. 2016. Historical records of nuclear activities from 129I in corals from the northern hemisphere (Philippines). *J. Environ. Radioact*. 164, 174-181.

Bautista, A.T.V., Miyake, Y., Matsuzaki, H., Siringan, F.P. 2017. A coral $^{129}I/^{127}I$ measurement method using ICP-MS and AMS with carrier addition. *Anal. Methods.* 164, 174-181.

Using AMS for speciation and source identification purposes within environmental radioactivity

O.C. Lind[1], D.H. Oughton[1], L. Skipperud[1], H.C: Teien[1], ,B. Salbu[1]

[1]CERAD CoE Environmental Radioactivity, Faculty of Environmental Sciences and Natural Resource Management, Norwegian University of Life Sciences (NMBU), Ås, 1432, Norway
Keywords: Long-lived radionuclides, size fractionation, combined techniques, ultra low level analysis
Presenting author, e-mail: olelin@nmbu.no

In order to assess the impact of radionuclide contamination of ecosystems, information on radionuclide species and their interactions in water-sediment or water-soil systems influencing mobility and biological uptake is essential.

In situ fractionation techniques of water samples and various extraction protocols for solid samples can provide information on potential mobility and bioavailability of radionuclides in the environment. However, the concentrations of the radionuclide analytes are often ultra low. Thus, extremely sensitive analytical techniques are required for analysis of fractions of total samples.

Accelerator Mass Spectrometry (AMS) offers ultra low level detection limits for determination of concentrations and atom ratios of long-lived radionuclides such as Pu isotopes, ^{236}U and ^{129}I. In the present work, we show examples of the use of AMS in combination with other analytical techniques such as air filtration (air filters collected in Norway during tropospheric fallout in the 50s and 60s (Wendel et al., 2013)), *in situ* and *at site* size fractionation of river, estuary, sea (Rivers Ob and Yenisei, Kara (Lind et al., 2006) and Barents Seas) and ground waters (Mayak (Salbu et al., 2001)) as well as sequential extractions of solid phases (Krasnoyarsk-26, (Skipperud et al., 2009)). Size fractionation is used to characterize radionuclide species according to particle size or molecular mass classes and in the present work this was performed using filtration and ultrafiltration prior to radiochemical separation and AMS analysis. By filtering water, particles are retained by 0.45 μm Millipore or 0.40 μm Nuclepore membranes, while hollow fibre ultrafiltration or tangential flow systems are efficient techniques for fractionating species in the colloidal 1-100 kDalton range. By interfacing *in situ or at site* ultrafiltration systems with ion chromatography, the ultrafiltered fraction was transferred to ion exchange columns with cation or anion exchange resins, respectively**.** Thus, Pu species in different size categories varying in charge properties could be obtained simultaneously.

Fractionation of radionuclides also include collecting particles from air using air filters, separation of particles from soils or sediments and distribution into individual sequential extraction fractions to provide information on binding mechanisms and chemical states (Geckeis et al., In press).

Because AMS in combination with fractionation techniques provides information on both the concentration as well as the provenance (by means of isotope ratios) of the Pu in an obtained fraction, it was in several cases possible to demonstrate that Pu isotopes exhibited different environmental behavior depending on the source and the scenario during which they were released. Thus, this combination can provide a significant improvement in the interpretation of data compared to analysis of total samples.

This study has been funded by the Research Council of Norway through its Centre of Excellence (CoE) funding scheme (Project No. 223268/F50).

Geckeis, H., Zavarin, M., Salbu, B., Lind, O.C., Skipperud, L., In press. Environmental Chemistry of Plutonium, in: Clark, D.L., Geeson, D.A., Hanrahan, R.J. (Eds.), Plutonium Handbook, 2 ed.

Lind, O.C., Oughton, D.H., Salbu, B., Skipperud, L., Sickel, M.A., Brown, J.E., Fifield, L.K., Tims, S.G., 2006. Transport of low (240)Pu/(239)Pu atom ratio plutonium-species in the Ob and Yenisey Rivers to the Kara Sea. *Earth and Planetary Science Letters* 251, 33-43.

Salbu, B., Lind, O.C., Børretzen, P.E., Oughton, D.H., 2001. Advanced speciation techniques for radionuclides associated with colloids and particles, in: Brechignac, F., Howard, B. (Eds.), Radioactive pollutants - Impact on the environment. EDP Sciences, pp. 243-260.

Skipperud, L., Brown, J., Fifield, L.K., Oughton, D.H., Salbu, B., 2009. Association of plutonium with sediments from the Ob and Yenisey Rivers and Estuaries. *J. Environ Radioact.* 100, 290-300.

Wendel, C.C., Fifield, L.K., Oughton, D.H., Lind, O.C., Skipperud, L., Bartnicki, J., Tims, S.G., Hoibraten, S., Salbu, B., 2013. Long-range tropospheric transport of uranium and plutonium weapons fallout from Semipalatinsk nuclear test site to Norway. *Environment International* 59, 92-102.

Environmental monitoring at CERN

F. Malacrida

CERN, Geneva 1211, Switzerland
Keywords: Monitoring of the environment, Radiological impact of research facilities
Presenting author email: fabrice.malacrida@cern.ch

CERN, the European Organization for Nuclear Research is the world's largest particle physics laboratory, located in the canton of Geneva in Switzerland and the Pays de Gex in France. Its premises consist of several fenced sites covering 200 hectares, some of them surrounded by fields and wooded areas owned by the Organization, for an additional 400 hectares.

CERN facilities include particle beam facilities, comprising accelerators, transfer tunnels, target and experimental areas. Such facilities are optimised from the radiation protection of the environment point of view. The activation by beam irradiation of the several matrixes lead to the production of relatively small quantities of radionuclides, the radiotoxicity of which remain low in general. Therefore, the operation of beam facilities leads to small releases of radionuclides as well as low levels of stray radiation outside the supervised areas. In addition, a long-term contamination of the environment is impossible. However, CERN facilities are unique, subject to continuous evolutions and, consequently, a proper environmental monitoring programme is required.

CERN, as the facility operator, carries out its own environmental monitoring programme, which is source oriented. This programme serves three purposes: The monitoring and evaluation of the source term (emissions), the surveillance of various environmental compartments (immissions) and the reporting of the results inside and outside the Organization (FOPH, 2018). The scope of the programme and associated methods are subject to an agreement by a tripartite committee composed of CERN staff and members from the Host States authorities, the Nuclear Safety Authority (F) and the Federal Office of Public Health (CH). In parallel, the CERN radiation protection code sets an effective dose objective (~0.01 mSv/y) and a limit (0.3 mSv/y) for the members of the public. The limit values are well in line with good practices and European regulations.

In the frame of the monitoring, the Environment Services exploit around hundred stations that are monitoring and/or sampling a fraction of atmospheric releases, ambient aerosols, water effluents and, outside supervised areas, the ambient dose equivalent induced by the stray radiation. These stations are transmitting more than 300 signals related to radiological parameters. In addition, about 3500 samples are collected and 4500 laboratory analyses are carried out yearly. These analyses mostly cover measurements of gross alpha-beta activity, liquid scintillation counting and gamma spectrometry. The parameters associated to the measurements allow minimising errors of the first and second types and offer a good compromise in terms of sensitivity. To calculate the effective dose received by the reference population groups, the quantities derived from the readings of the stations and the measurement results are combined with widely recognized dispersion and exposure models (Vojtyla, 2009).

In practice, members of the public living or working near CERN's sites are exposed to low levels of stray radiation (neutrons) originating in near-surface beam facilities and to the atmospheric releases of short-lived radioactive gases (^{11}C, ^{13}N, ^{14,15}O, ^{41}Ar). The contribution of other sources of artificial exposure remains minimal. Finally, the radiological signature of CERN activities in the local environment is low.

FOPH, 2018, Umweltradioaktivität und Strahlendosen in der Schweiz 2017

P. Vojtyla, 2009, Programmes for the evaluation of the environmental impact, *Radiation Protection Dosimetry*, Volume 137, Issue 1-2, November 2009, Pages 134–137, https://doi.org/10.1093/rpd/ncp197.

MILEA: a new compact 300 kV multi-isotope AMS system

Sascha Maxeiner[1], Arnold Milenko Müller[1], Marcus Christl[2], Philip Gautschi[2], Hans-Arno Synal[2], Christof Vockenhuber[2], Lukas Wacker[2]

[1]Ionplus AG, Lerzenstrasse 12, 8953 Dietikon, Switzerland
[2]Laboratory of Ion Beam Physics, ETH Zurich, Switzerland
Keywords: AMS, multi-isotope, actinides
Presenting author, e-mail: maxeiner@ionplus.ch

Multi-isotope AMS systems enable measurements of different long-lived radioisotopes on a single machine. Significant improvements in stripping techniques, molecule- and isobar suppression methods and advances in detector design over the last decade allowed lowering the ion energies while enhancing the efficiency at competitive background levels. A proof-of-principle experiment conducted at ETH Zurich showed that Tandem acceleration voltages of only 300 kV are sufficient for measuring of most radioisotopes measured by AMS today (Maxeiner, 2019).

Based on the experiences gained with the proof-of-principle experiment, a new compact multi-isotope AMS system was designed and taken into operation in 2018 at ETH Zurich as a collaboration between Ionplus and ETH. The MILEA (Multi-Isotope Low Energy Accelerator) system, based on a 300 kV vacuum insulated Tandem accelerator, is dedicated to the measurement of ^{10}Be, ^{14}C, ^{26}Al, ^{41}Ca (biomedical applications), ^{129}I and actinides (Pu, U, Th and others). With new models and simulation tools (Maxeiner, 2015), the stripper geometry and acceleration were optimized for He stripping at low energies. New approaches and developments were implemented in order to optimize the performance for all mentioned nuclides, resulting in a very small system footprint of 3.5 x 7 m^2 (Fig. 1).

During the last year, extensive tests and experiments were performed on the prototype instrument to determine its measurement performance regarding transmission, background and stability for the above-mentioned radionuclides. The obtained results confirm the outstanding power of this new multi-isotope AMS instrument. Based on the experiences gained with the prototype system, Ionplus was able to successfully commercialize MILEA. An overview of the most important system features will be given and the latest results for the different isotopes will be presented and discussed.

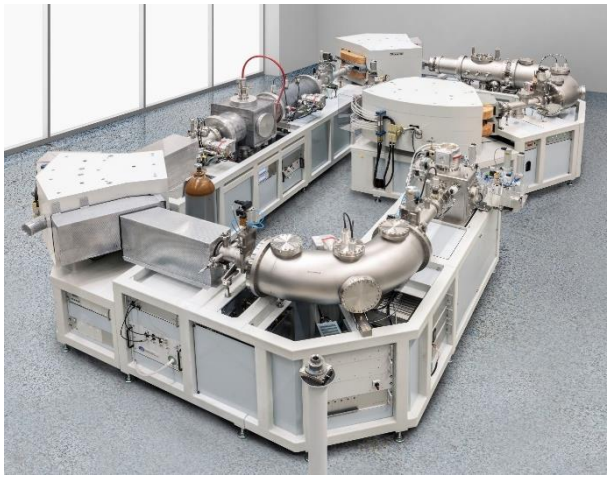

Figure 1. Perspective picture of the prototype version of the new, compact 300 kV multi-isotope AMS (MILEA) instrument. Footprint: 3.5 x 7 m^2.

Sascha Maxeiner et al., *NIM B* 439 (2019) 84-89

Sascha Maxeiner et al., *NIM B* 361 (2015) 237-244

Search for tritium in air in a room equipped with 14 MeV neutron generator with tritiated targets

M. Miecznik[1], W.J. Mietelski[1], K. Brudecki[1], A. Wójcik-Graguła[2]

[1]Department of Nuclear Physical Chemistry, Institute of Nuclear Physics PAN, Kraków, 31-342, Poland
[2]Department of Physics of Transport Radiation, Institute of Nuclear Physics PAN, Kraków, 31-342, Poland
Keywords: tritium, diffusion, radiation doses, LSC measurements, Wallac Guardian 1414
Presenting author: M. Miecznik, e-mail: magdalena.miecznik@ifj.edu.pl

In a room equipped with 14 MeV fast neutron generator IGN-14, 8 tritiated targets were stored. Targets total activity on 3rd Dec 2014 was 1500.97 GBq, while final activity on 31st May 2019 was 1166.56 GBq. During the working time the tritiated target is irradiated with deuterium beam. The maximum neutron output of the IGN-14 is $5*10^8$ n/s [1]. The aim of this work was to estimate the tritium content in the room atmosphere as well as the staff exposure to radiation. Tritium is a hydrogen isotope with one proton and two neutrons. It is a beta emitter with energy emission up to 18.7 keV and an average energy emission 5.7 keV. It decays with 12.3 years half-life [2]. The basic assumption of this work is that tritium from targets diffuses into the air where reacts immediately with oxygen forming vapor particles. Vapor enriched with tritium diffuses into open vessels with deionized water (120 ml plastic containers filled in a half) where gas exchange takes place. Fifty vessels were arranged along the length (every 0.50 cm) and width (every 1 m) of the room for 18 days. Additionally, five vessels were placed in the room for shorter time (4, 5, 7, 11 and 16 days) to define saturation curve. Each sample was measured for 45000 s (12 h 30 min), meaning that after 18 days to exposure for enriched tritium concentration, some samples were measured several days after. To prevent the situation when results are underestimated because some captured tritium already escaped, water from one sample was measured four times during the measurement period. The 5 ml of each sample was transferred to LSC vials (plastic 20 ml) and mixed with 15 ml scintillator Gold Star LT^2. In the scintillation technique a cocktail volume in the sample influences counting efficiency. Increasing cocktail volume increases counting efficiency [3],[4]. The Gold Star LT^2 scintillator was chosen for the experiment because this is a high-performance scintillator with low background in the low energy range [3]. As a background, detirated water was measured under the same conditions as samples. Measured activities were calculated in relation to the tracer sample. It was assumed that the titrated water/ water ratio in the sample was the same as the titrated vapour/ vapour ratio in the air when saturation was reached. Based on this assumption, value of tritium activity in measured samples was used to calculate spatial distribution of tritium activity in the room air. Based on the tritium activity, dosimetry dozes were calculated and will be presented on the conference.

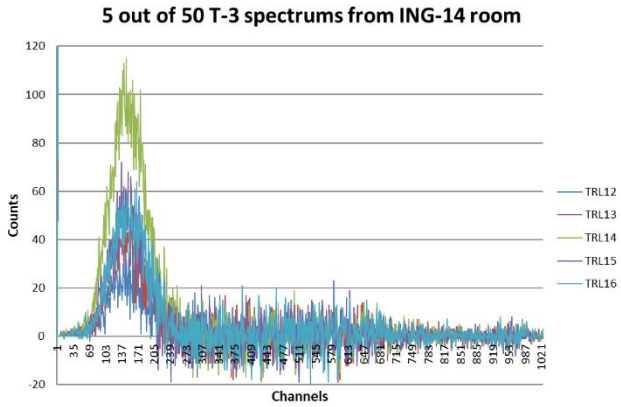

Figure 1. Examples of T-3 spectra measured in ING-14 room.

[1] https://www.ifj.edu.pl/dept/no6/nz61/A_pl_1.html. viewed 31.05.2019.

[2] Rashmi Nayak, S., Shiny D'Souza, R., Srinivas Kamath, S., Mohan, M.P., Bharath, S., Shetty, T., Sudeep Kumara, K., Narayana, B., Dileep, B.N., Ravi, P.M., Karunakara, N. 2019. Organically bound tritium: optimization of measurements in environmental matrices by combustion method and liquid scintillation spectrometry. *J Radioanal Nucl Chem.* 319, 917-926.

[3] Kleszcz, K. 2012. Nikiel-63 i technet -99 metodyka oznaczania i obecności w środowisku. PhD dissertation. Jerzy Haber Institute of Catalysis and Surface Chemistry, Polish Academy of Sciences.

[4] Komosa, A., Slepecka, K. 2010. Effect of liquid scintillatiing cocktail volume on ^{3}H and ^{14}C measurement parameters using a Quantulus spectrometer. *Nukleonika* 55(2), 155-161.

What was behind a mysterious Ru-106 contamination of European air observed in 2017?

Jerzy W. Mietelski[1], Pavel P. Povinec[2]

[1]Institute of Nuclear Physics, Polish Academy of Sciences, 31-342 Krakow, Poland
[2]Faculty of Mathematics, Physics and Informatics, Comenius University, 84248 Bratislava, Slovakia
Keywords: Nuclear jet engine; RTG, Ruthenium-106; radioactive contamination
Presenting author, e-mail: jerzy.mietelski@ifj.edu.pl

At the beginning of October 2017 radioactive ruthenium-106 (Ru-106) and its daughter rhodium-106 (Rh-106) were observed in many locations in air in Europe and at much lower levels also in America [IRSN, 2017]. The maximum Ru-106 levels in the air (180 mBq/m^3) were observed in Romania, followed by close to 60 mBq/m^3 in certain locations of Bulgaria, Czech Republic or Italy. Some very small traces of Ru-103 were found as well. There has not been yet a clear explanation of the origin of this Ru-106 contamination [IRSN, 2017].

The appearance of the Ru-106/Rh-106 contamination created general confusion in many agencies responsible for nuclear safety. The whole affair remains mysterious.

On the 1st of March 2018 during the official Presidential Address to the Federal Assembly of the Russian Federation President V.V. Putin said that Russia made successful in-flight and ground tests of a nuclear engine as a propulsion system of a cruise missile [Putin, 2018]. The aim of the presentation is to discuss the observed Ru-106 contamination in the European air as a result of a possible in-flight test of a nuclear-powered missile, and to point out on new challenges and possible consequences of such tests on radioactive contamination of the environment.

The concept of using nuclear energy for the propulsion of aircrafts and rockets originated already from the time of WW II. The reason is obvious – it is practically unlimited range of any kind of aircraft driven by such propulsion. In principle, the idea is simple: the thermal energy needed to drive the engine comes from a nuclear process instead of the combustion of a traditional fuel. Despite the obvious advantages of nuclear propulsion, primarily with unlimited range of an airplane, this concept was discontinued due to safety reasons in sixties of 20th century.

Ru-106 is a typical fission product present in spent nuclear fuel. The probability of production of the mass 106 in a fission of U-235 is 4.19 %. In routinely reprocessed nuclear fuel, the cooling time is in range of at least ten years, so the Ru-106 activity decreases by a factor of greater than 2^{10} (i.e., more than 1000 times). There is another Ru radioisotope produced in fuel, Ru-103, which has a shorter half-life time of 39 days. The probability of production of the mass 103 in a fission of U-235 is 3.10 %. To get pure Ru-106 one has to wait for enough Ru-103 half-life times – let say about two years. In the observed air contamination of Europe in October-November 2017 [IRSN, 2017], the activity of Ru-103 was by a factor of about 3500 lower than that of Ru-106/Rh-106, which in general supports the concept of about two years of cooling time of the spent fuel from which ruthenium was separated.

It can be calculated, that power required to drive cruise class missile should be at the level of 1 MW.If 1 MW power was obtained from the radioactive decay of Ru-106 simple calculations lead to results, that the required activity should be at the level of 5 EBq. From the dosimetry point of view this is a very difficult material for handling.

Another potential source of Ru-106 contamination of the European air will be discussed an accident in the Mayak nuclear fuel reprocessing facility.

The tests of nuclear propulsion systems in the open environment have serious consequences but also challenges for the world's nuclear safety national and international monitoring networks (e.g. the CTBTO network, the Ro5 network).

IRSN, Detection of ruthenium 106 in France and in Europe, http://www.irsn.fr/EN/newsroom/News/Documents/IRSN_Information-Report_Ruthenium-106-in-europe_20171109.pdf

Putin V.V. Presidential Address to the Federal Assembly, (2018), http://en.kremlin.ru/events/president/news/56957

Evaluation of radiochemical analysis method for ^{210}Po and ^{210}Pb in seafood sample using interlaboratory comparison

T. Miura[1], T. Ota[2], H. Terada[3]

[1]National Metrology Institute of Japan, AIST/ Tsukuba, 305-8563, Japan
[2]Japan Chemical Analysis Center/ Chiba, 263-0002, Japan
[3]Department of Environmental Health, National Institute of Public Health/ Wako, 351-0197, Japan
Keywords: ^{210}Po, ^{210}Pb, Method validation, Marine fish, Intercomparison, Alpha ray spectrometry, Extraction chromatography
Tsutomu Miura, e-mail: t.miura@aist.go.jp

Polonium-210 ($t_{1/2}$=138.4 d) occurs naturally via ^{210}Pb ($t_{1/2}$=22.2 y) and ^{210}Bi ($t_{1/2}$=5.012 d) in the ^{238}U decay series. Marine products such as marine fish are well known to contain ^{210}Po at relatively high concentrations (Ota et al., 2009). Therefore, it is important to precisely measure ^{210}Po and ^{210}Pb in marine products from the viewpoint of internal exposure dose evaluation attributable to food intake. In order to precise evaluation of internal exposure dose, it is desirable that analytical method to obtain measured value is evaluated in term of reliability. First of all in this study, the radiochemical analysis method of ^{210}Pb and ^{210}Po in environmental sample (Miura et al., 1999, 2000) was verified by the recovery experiment using the freeze dried fish sample after addition of known amount of ^{210}Po. Then the interlaboratory comparison using the homogeneous bonito powder sample also performed to validate the method. The aim of this study was to improve the reliability of ^{210}Po and ^{210}Pb measurements, which have a contribution to internal exposure dose evaluation.

Sample preparation for Po recovery experiment: The meat part of fish (Japanese flounder collected from sea of east Japan area) was freeze dried and homogenized. The fish was store over 5 years, so it is thought that initially existent ^{210}Po was decayed. *Procedure for Po recovery experiment*: Polonium-210 was separated from high purity Pb metal (FUJIFILM Wako pure chemical) using eichrom Sr resin column. The massic activity of the ^{210}Po solution was determined by α ray spectrometry and liquid scintillation counting. The radiochemical analysis method of ^{210}Pb and ^{210}Po (Miura et al., 1999, 2000) is consists from 3 steps (acid decomposition, extraction chromatography using eichrom Sr resin column, α ray measurement sample preparation by electrodeposition). Herein, ^{210}Po analysis of the above freeze dried fish sample was assumed, so a known amount of ^{210}Po was added to the sample before decomposition. The ^{209}Po was added on each separation step. Then, the recovery of ^{210}Po at each step was verified using ^{209}Po as internal standard.

Sample preparation for interlaboratory comparison: Five kg of dried bonito powder was purchased from TOMARU SUISAN Co. Ltd (Shizuoka, Japan) for interlaboratory comparison. After homogenising using V-type blender, the dried bonito powder (100 g each) was bottled in 500 mL polycarbonate bottle. Then the bonito powder sample in the bottle was sterilized by 20 kGy of ^{60}Co γ rays. The homogeneity for 10 bottle of dried bonito powder sample was studied using the above verified method. The homogeneity of dried bonito powder sample was evaluated according to ISO Guide 35. The measured homogeneities were shown in Table 1.

Table 1 The homogeneity of the bonito powder sample

	Massic activity *Mean*$\pm U$	s_{bb}	u_{bb}
^{210}Po	(12.5$\pm$0.92) Bq kg^{-1}	1.57 %	1.16 %
^{210}Pb	(0.55$\pm$0.33) Bq kg^{-1}	18.2 %	8.30 %

Interlaboratory comparison: The three bottles of sample and the analytical procedure were provided to the participants for interlaboratory comparison to validate the method.

Po recovery experiment: The loss of Po for each chemical separation step (acid decomposition, extraction chromatography, α ray measurement sample preparation by electrodeposition) of the analysis method was examined. As a result, there was no significant loss of Po in the chemical separation procedure. Therefore, it was confirmed that this method shows high reliability as ^{210}Po/^{210}Pb analysis method in marine fish sample.

Interlaboratory comparison: The reported values of ^{210}Po and ^{210}Pb by participants were in agreed the reference value within their uncertainty. The reliability of this method has been also confirmed from the interlaboratory comparison.

This work was supported by the JSPS KAKENHI Grant Number 15K00551.

T. Ota, T. Sanada, Y. Kashiwara, T. Morimoto, K. Sato. 2009. Evaluation for Committed Effective Dose Due to Dietary Foods by the Intake for Japanese Adults. *Jap. J. Health Physics*. 44, 80-88.

T. Miura, K. Hayano, K. Nakayama. 1999. Determination of Pb-210 and Po-210 in environmental samples by alpha ray spectrometry using an extraction chromatographic resin. *Anal.y Sci.*, 15, 23-28.

T. Miura, K. Kawabe, H. Kirita. 2000. Determination of ^{210}Po in reagent samples by alpharay spectrometry using extraction chromatographic resin. *J. Radioanal. Nucl. Chem.* 246, 327-330.

Interaction of curium(III) with plant cells (*Brassica napus*)

H. Moll[1], S. Sachs[1], J. Raff[1]

[1]Institute of Resource Ecology, Helmholtz-Zentrum Dresden-Rossendorf, Dresden, 01328, Germany
Keywords: curium, plant cells, luminescence spectroscopy, speciation
Presenting author, e-mail: h.moll@hzdr.de

The accumulation of radionuclides and toxic heavy metals into plants and thus into the food chain represents a potential pathway for human exposure. Hence, detailed knowledge of the fate of these elements in the ecosphere including the food chain is required for a reliable assessment of the resulting risk potential for humans and wildlife. Our aim is to explore the complex interaction of trivalent actinides with plant cells on a molecular level using curium(III) as an excellent luminescence probe. Suspension cell cultures received from callus cells are suitable models for studying cell metabolism processes in plants. They retain the ability to form metabolites characteristic of intact tissues for an adaptation to stress conditions, in this case curium.

We studied the response of canola (*Brassica napus)* cells to curium(III) exposure (0.7 µM). Time-resolved laser-induced fluorescence spectroscopy (TRLFS) was used as direct speciation technique to explore the Cm(III) speciation on the cells and in the supernatants. Liquid scintillation counting (LSC) was applied to measure the Cm(III) content in the supernatants. The possible release of plant cell metabolites was probed by solid phase extraction (SPE) with subsequent HPLC analysis.

The bioassociation experiments were performed in 0.154 M NaCl in a glove box over a time period up to 168 h. After 96 h 70% of Cm(III) was bioassociated corresponding to 6.7 nM Cm/$g_{fresh\ cells}$. After defined time steps the Cm(III) concentration in the supernatants was determined as well as luminescence spectra from washed cells and the supernatants were taken. The Cm(III) concentration in the supernatants as a function of time points to a multi-stage bioassociation process on the plant cells. Red shifted Cm(III) luminescence spectra (+8.6 nm compared to Cm^{3+}(aq)) in the supernatants indicated a Cm(III) complexation by substances that were released by the plant cells already after an exposure time of 5 h. Cell metabolites could be enriched and extracted by SPE. TRLFS studies (spectra and lifetime) showed a different Cm(III) speciation on cells compared to those found in the supernatants. To further describe the spectroscopic Cm(III) speciation in the *B. napus* system all spectra were evaluated with iterative transformation factor analysis (ITFA, Roßberg et al. 2003). The so obtained results (single component spectra and time-dependent species distributions) will be discussed in order to describe the fate of Cm(III) in the presence of plant cells (*B. napus*).

This new knowledge contributes to an improved understanding of trivalent actinide interactions with plants on a molecular level.

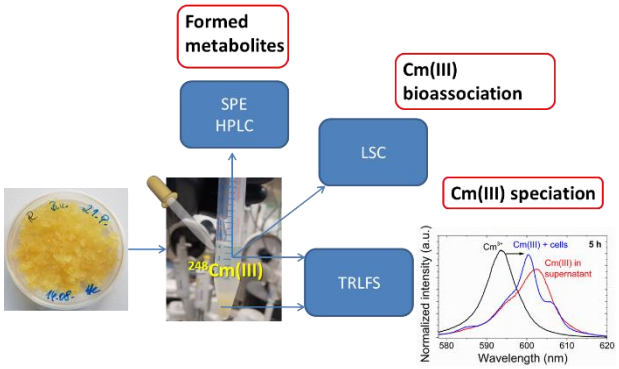

Figure 1. Investigation scheme of Cm(III) interactions with *Brassica napus* cells.

The authors are indebted to the U.S. Department of Energy, Office of Basic Energy Sciences, for the use of ^{248}Cm via the transplutonium element production facilities at Oak Ridge National Laboratory; ^{248}Cm was made available as part of collaboration between HZDR and the Lawrence Berkeley National Laboratory (LBNL). This study is part of the project TRANS-LARA which is funded by the Federal Ministry of Education and Research under contract number 02NUK051B.

Roßberg, A., Reich, T., Bernhard, G. 2003. Complexation of uranium(VI) with protocatechuic acid – application of iterative transformation factor analysis to EXAFS spectroscopy. *Anal. Bioanal. Chem.* 376, 631–638.

Towards a holistic approach to protection of inhabitants of contaminated environments: the role of non-targeted effects

Carmel Mothersill and Colin Seymour

Department of Biology, McMaster University, Hamilton L8S 4K1, Ontario Canada
Keywords: ecosystem approach, radiation protection, low dose, non-targeted effects, radiation effects
Presenting author, e-mail: mothers@mcmaster.ca

Recent moves within ICRP to develop an integrated approach to radiation protection of both humans and non-human biota are focused on regulating dose to exposed populations based on behavior, size, lifestyle and "radiosensitivity". Currently man and 12 reference organisms are used covering various taxonomic groups, behaviors, and exposure scenarios - e.g. marine, terrestrial, sediment or airborne. However most biologists agree that particularly in low dose exposure legacy sites, the factors determining effects and outcomes are far more complex that this simple framework suggests. The issue is developing reliable predictors of system or ecosystem health rather than relying on biomarkers that give information about effects on individual cells, organs or organisms. Approaches to this include the Adverse Outcome Pathway (AOP) developed as part of the CERAD project in Norway, which looks at multiple levels of organization from gene to ecosystem building a comprehensive picture of effects at multiple levels of organization in multiple species including humans. Various camera drone based ecosystem evaluation techniques have been developed in other areas of environmental management. These could be applied at legacy sites where damage to for example tree canopies or river flow patterns can be used to assess ecosystem health much like a CAT or MRI scan reveals structural changes in individual organisms systems. Another more focused approach used by our group is to look at the role of non-targeted effects such as genomic instability (GI) and bystander effects (BE). These mechanisms involve transmission of information between different levels of organization. In the case of BE signals from exposed to unexposed cells or organisms coordinate response at higher levels of organization permitting population responses to radiation to be optimized. GI is more complex as it involves not only signaling but also trans-generational transmission of genetic or epigenetic changes and may lead to long-term adaptive evolution. GI may also be involved in memory or legacy effects, which contribute a further component to the dose effect measured in legacy sites. Our recent analysis of the contributions of memory and legacy effects to the total effect using data sets from Chernobyl and Fukushima (voles, birds and butterflies) suggest this type of analysis may help reduce uncertainties over lab to field extrapolations. Given the clear discrepancy between actual data measured in the field and dose effects generated using databases populated mainly with acute lab based experimental data, it is imperative that we strive to develop meaningful holistic systems for protection of those living in contaminated ecosystems.

This work was supported by the Canadian Natural Sciences and Engineering Research Council Discovery Grants Programme, The Collaborative Research and Development Grants Programme, CANDU Owner's Group, Bruce Power, The National Chronic Fatigue and Immunedeficiency Foundation, Inc and the Canada research Chairs Program.

Determination of Water Equivalent Factor (WEQ_p) for evaluation of organically bound Tritium in environmental matrices

S.R. Nayak[1], R.S. D'Souza[1], S.S. Kamath[1], Bharath[1], Narayana B.[1], Dileep B. N.[2], Ravi P. M.[1,3], Karunakara N.[1*]

[1]Centre for Advanced Research in Environmental Radioactivity (CARER), Mangalore University, Mangalagangothri – 574199, India

[2]Environmental Survey Laboratory, Kaiga Generating Station, Kaiga-581 400, India

[3]Formerly with Health Physics Division, Bhabha Atomic Research Centre, Trombay, Mumbai – 400 085, India

Keywords: Organically Bound Tritium, Water equivalent factor, RADDEC pyrolyser

Presenting author: Rashmi Nayak S, corresponding author e-mail id: drkarunakara@gmail.com

Tritium (^{3}H) present in plant tissues can be classified into (i) Tissue Free Water Tritium (TFWT), and (ii) Tissue Bound Tritium (TBT) or Organically Bound Tritium (OBT). A part of OBT that does not exchange and have a long residence time in an organism is non-exchangeable OBT (NEOBT).The OBT concentration $(C_{pfw})_{OBT}$ in Bq kg^{-1}(fresh weight) of biota is computed as under (IAEA TRS 472, 2010; IAEA TecDoc 1616, 2009):

$$(C_{pfw})_{OBT} = \frac{(1-WC_p)WEQ_p\ R_p(C_{pfw})_{HTO}}{WC_p}$$

In the above expression, WC_p is the fractional water content of biota, WEQ_p is the water equivalent factor (gram of water produced per gram of dry matter combusted), R_p is partition factor, which accounts for reduction in dry weight concentration of OBT due to the presence of exchangeable Hydrogen in combustion water and also for isotopic exchange, $(C_{pfw})_{HTO}$ is HTO concentration in biota sample (w.r.t. fresh weight). Generally, WEQ_p is calculated from the knowledge of Hydrogen contents of protein, fat, and carbohydrate (7, 12 and 6.2%, respectively) and the fractions of protein, fat, and carbohydrate in the dry matter of the plant/organism (IAEA TRS 472, 2010; IAEA TecDoc 1616, 2009). However, WEQ_p may vary for tropical and temperate regions as well as among
different species and hence, the generation of site-specific data for this parameter is important. This paper presents WEQ_p for a large number of environmental samples, collected for Kaiga region of West Coast region of India, where a PHWR power plant is operating. This region experiences tropical monsoonal climate conditions and for such region, very limited data is available in the literature. The experimentally observed values of WEQ_p factors are compared with the theoretically generated values listed in TRS 472, and TecDoc 1616.

Thermal oxidation method (pyrolyser system, RADDEC, UK), was employed for the combustion of oven dried samples and extraction of water, which is the measure of water equivalent factor. The details of pyrolyzer system and its principle of operation was published earlier (Nayak et al., 2019). In this method, the sample is oxidized at a high temperature in the presence of air and oxygen to convert OBT into tritiated water (^3H_2O). Known weights of different types of samples were oxidized, the combustion water produced was weighed, and WEQ_p factors were determined experimentally. The results are presented in Table 1. The deviation between experimental data (generated in this study) and that listed in IAEA TRS 472, 2010; IAEA TecDoc 1616, 2009) was found to be up to 8%. This is the first systematic study aimed at generating comprehensive database on WEQ_p for tropical climate. The database would be valuable for the realistic environmental impact assessment in tropical countries.

Table 1: Comparison between experimentally generated and calculated values of WEQ_p for the biota samples

Sample Type	WEQ_p (Experimental values, present study) (gram of water per gram of sample, w.r.t. dry wt.)				WEQ_p (Theoretical Values,IAEA TRS 472, 2010; IAEA TecDoc 1616, 2009) (gram of water per gram of sample, w.r.t. dry wt.)				Deviation
	N*	Mean	Min	Max	N	Mean	Min	Max	
Non-leafy Vegetables	100	0.57±0.03	0.49	0.67	12	0.53	0.50	0.55	7%
Leafy Vegetables	44	0.56±0.02	0.52	0.68	10	0.51	0.47	0.55	8%
Nuts	8	0.52±0.02	0.49	0.54	No Data				
Root Crops	20	0.54±0.02	0.51	0.59	11	0.52	0.45	0.55	4%
Cereals	22	0.51±0.01	0.45	0.57	91	0.56	0.50	0.60	4%
Fruits	87	0.56±0.02	0.50	0.63					
Fish	6	0.68±0.04	0.62	0.74	4	0.65 (Nominal value)			5%

*N is the number of samples analyzed

International Atomic Energy Agency. 2010. Handbook of Parameter values for the prediction of radionuclide transfer in terrestrial and fresh water environment. Technical Reports Series, No. 472. Vienna

International Atomic Energy Agency. 2009. Quantification of radionuclide transfer in terrestrial and fresh water environment for radiological assessment. Technical Document series 1616.

Nayak, R., D'Souza, R., Kamath, S., *et al*., 2019. Organically Bound Tritium: Optimization of measurements in environmental matrices by combustion method and liquid scintillation spectrometry. *J. RadioanalNucl Chem.*2019, 319(3), 917-926.

Radiocesium deposition on agricultural products by resuspended matter

N. Nihei[1], K. Yoshimura[2], and T.M. Nakanishi[1]

[1] Graduate School of Agricultural and Life Sciences, The University of Tokyo, Tokyo, 113-8657, Japan
[2] Department of Environmental Sciences, Japan Atomic Energy Agency, 963-7700, Japan
Keywords: radiocesium, secondary fallout
Presenting author email: anaoto@mail.ecc.u-tokyo.ac.jp

Radiocesium dominated by ^{137}Cs was released by the Fukushima Daiichi Nuclear Power Plant (FDNPP) accident in 2011. Radiocesium contaminated forests, agricultural fields, and residential areas. To safely cultivate agricultural products in contaminated areas, decontamination works, i.e., the stripping of topsoil and inversion tillage, have been carried out for agricultural fields. However, they have not been completed in contaminated areas. Some of the deposited radiocesium, which are soil particles and Cs-bearing particles, have been in the contaminated ground surface and are continuously released into the atmosphere by wind (Ishizuka et al. 2017). Radiocesium activity in the resuspended matter is very low, but it can still be detected in highly contaminated areas (NRA Japan). Therefore, it is important to assess the radioactive deposition on plants (Hirose 2018). Nihei et al. (2018) reported that radiocesium deposited on agricultural products which just were cultivatedat a highly contaminated site. This deposition was considered to be caused by the resuspended radiocesium in the atmosphere. However, it is unclear how the crops are contaminated by radiocesium in the resuspended matter. Radiocesium deposition of crops includes not only external adsorption , in which radiocesium adheres to the above-ground part during cultivation periods, but also internal absorption, in which the adsorped radiocesium is absorbed from leaves and roots and transported into the interior of the crop. To resume agriculture in the contaminated areas, it is necessary to identify the radiocesium deposition pathways from atmosphere into agricultural products. However, there are few studies about radiocesium deposition by the resuspended matter, although there are many studies on the translocation and uptake of the deposited radiocesium in soil to plants. The purpose of this study was to assess the radiocesium depositionon crops caused by external adsorption and internal absorption and to analyze the resuspended matter to show the cause of radiocesium deposition.

Japanese mustard spinach (*Brassica rapa* L. var. *perviridis*) was cultivated using noncontaminated soil and water in a pot (measuring 30 × 30 × 30 cm) in 2018. Pots were set in six sites in the Fukushima Prefecture. After harvesting the ground part, half of the plants (unwashed plants) were measured for radiocesium concentration and the other half (washed plants) were washed with water and then measured. The radiocesium concentration of the washed crop was supposed to indicate internal absorption, and the amount of radiocesium calculated by subtracting the washed crop from the unwashed crop is regarded as radiocesium concentration on the external adsorption of the above-ground part. Basins were filled with water and placed at each site to catch the fallout matter during the cultivation period. The fallout matter trapped was separated to suspended and dissolved phases. Radiocesium in the samples was measured by Ge detector. The radiocesium concentrations of external adhesion (1–253 Bq kg^{-1}) and internal absorption (1–123 Bq kg^{-1}) varied with the cultivation place and time. Most radiocesium in the fallout matter was in the suspended phase (6–618 Bq m^{-2}); the radioactivity was low in the dissolved phase (1–84 Bq m^{-2}). The radiocesium concentration externally adsorbed was not correlated with the total radiocesium in the fallout matter and the suspended phase; however, the radiocesium concentration internally absorbed was highly correlated with the dissolved radiocesium in the fallout matter (r^2 = 0.71). Internal absorption is considered to absorb dissolved radiocesium in the fallout matter from leaves directly or from roots indirectly. External adhesion was assumed to have a correlation with the suspended radiocesium, but the correlation was not high because adhered radiocesium might have been washed away by rain during the cultivation period. A further detailed investigation is necessary.

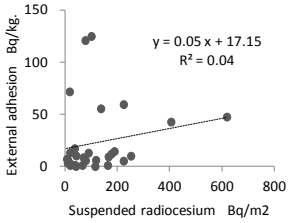

Fig.1 Suspended radiocesium and external adhesion radiocesium in crops.

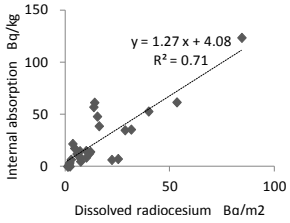

Fig. 2 Dissolved radiocesium and internal absorption radiocesium in crops.

Ishizuka M., et al. 2017. Use of a size-resolved 1-D resuspension scheme to evaluate resuspended radioactive material associated with mineral dust particles from the ground surface. *Journal of Environmental Radioactivity*, 166, 436-448.

Nuclear Regulation Authority, Japan webpage https://radioactivity.nsr.go.jp/en/

Hirose K. 2018. Long-term monitoring of radiocesium deposition near the Fukushima Dai-ichi nuclear power plant: effect of interception of radiocesium on vegetables. *Journal of Radioanalytical and Nuclear Chemistry*, 318, 65-70.

Nihei N., et al. 2018. Secondary radiocesium contamination of agricultural products by resuspended matter, *Journal of Radioanalytical and Nuclear Chemistry*, 318, 341-346.

Soil Air Radon Concentration in Bintan Island, Indonesia

Muttaqin Margo Nirwono[1,2], Ahmad Ciptadi Syuryavin[1,2], Seong Jin Park[1], Sang Hoon Lee[1,3]

[1] School of Architectural, Civil, Environmental, and Energy Eng., Kyungpook National Univ., Daegu, 41566, Korea
[2]Nuclear Energy Regulatory Agency of Indonesia (BAPETEN), Jl Gajah Mada 8, Jakarta, 10120, Indonesia
[3]Radiation Science Research Institute, Kyungpook National University, Daegu, 41566, Korea
Keywords: Radon Concentration, Bauxite, LR-115
Presenting author (M.M. Nirwono), e-mail: m.margo@bapeten.go.id

Bintan island had the first bauxite mining in Indonesia. It was located in Kijang and discovered since Dutch colonialization of 1924, mined and exported since 1935, and closed in 2013. Several mining areas in Teluk Bunyu District, Bintan Regency are still in operation.

Bauxite is one of concern about TENORM issues that releases radon gas (Hiswara, 2001; Tuka et al., 2005). The aim of this research is to identify concentration of radon in soil in bauxite area.

Soil air radon measurement used passive can technique of LR-115 detector at 30 cm depth as shown in Figure 1. A total of 24 detectors were installed for about 2-3 weeks measurement in Bintan Island that included four mining areas in Tembeling, Penaga and Bintan Bunyu vilages, Teluk Bintan District, Bintan Regency, and an office and two residence areas in Tanjung Pinang City, see Figure 2. Final process was sending LR-115 to the manufacture for reading of radon track.

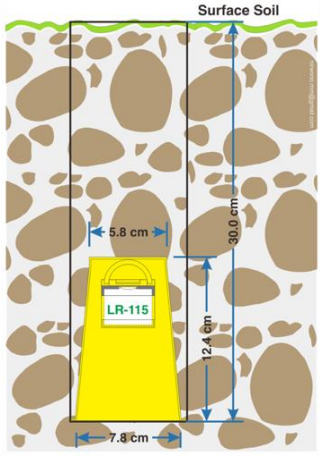

Figure 1. Arrangement of the LR-115 detector placed at 30 cm depth under the surface soil.

Table 1 shows the result of radon concentration in soil of studied area. The soil radon concentration from mining areas (No 1 to 19) range of 1,748 to 16,381 Bq.m^{-3}; office areas (No 20 to 23) range of 4,227 to 25,156 Bq.m^{-3}; and the residence areas had the lowest range of 1,919 and 3,093 Bq.m^{-3}. It is still below the reference level of WHO that radon concentrations in soil air/gas typically range from less than 10,000 up to 100,000 Bq.m^{-3} (WHO, 2010).

Radon concentration profile resulted from the passive method of LR-115 will be compared with active measurement using RAD7 based on three soil samples form site No 3, 7 and 11.

The result of the research is expected to give updated information about radon concentration in the specific area, and in general radon profile in Indonesia.

Table 1. Concentration of soil air radon.

No	Location	Concentration (Bq.m^{-3})
1	Tembeling, Teluk Bintan	8,136
2	Tembeling, Teluk Bintan	8,743
3	Tembeling, Teluk Bintan	6,454
4	Tembeling, Teluk Bintan	11,336
5	Tembeling, Teluk Bintan	11,056
6	Tembeling, Teluk Bintan	3,336
7	Tembeling, Teluk Bintan	11,383
8	Tembeling, Teluk Bintan	6,922
9	Tembeling, Teluk Bintan	1,748
10	Tembeling, Teluk Bintan	16,381
11	Penaga, Teluk Bintan	4,597
12	Penaga, Teluk Bintan	16,171
13	Penaga, Teluk Bintan	9,818
14	Penaga, Teluk Bintan	13,625
15	Bintan Bunyu, Teluk Bintan	11,593
16	Bintan Bunyu, Teluk Bintan	12,784
17	Bintan Bunyu, Teluk Bintan	8,954
18	Bintan Bunyu, Teluk Bintan	4,983
19	Bintan Bunyu, Teluk Bintan	3,126
20	Sei Jang, Bukit Bestari	25,156
21	Sei Jang, Bukit Bestari	13,187
22	Sei Jang, Bukit Bestari	4,227
23	Batu IX, Tanjungpinang Timur	1,919
24	Batu IX, Tanjungpinang Timur	3,093

M.M. Nirwono would like to thank the Ministry of Research, Technology, and Higher Education (RISTEKDIKTI) of Indonesia for granting a PhD scholarship through its Research and Innovation in Science and Technology Project (RISET-Pro) Program.

Hiswara, E. (2001). Impacts of the Application of Exemption Regulation to the Non-Nuclear Industry in Indonesia. In *Prosiding Seminar Nasional Keselamatan, Kesehatan dan Lingkungan I* (pp. 1–6). Jakarta: BATAN.

Tuka, V., Sandra, F., Susanti, D. A., & Purnama, A. S. (2005). *Laporan Hasil Kajian Pengkajian Konsepsi Sistem Pengawasan Keselamatan Radiasi di Instalasi Pertambangan, BAPETEN*. Jakarta: BAPETEN.

World Health Organisation (WHO). (2010). *WHO Guidelines for Indoor Air Quality: Selected Pollutants*. Copenhagen.

Convenient and rapid measurement of radiostrontium in seawater

Y. Ogata[1], H. Minowa[2], Y. Kato[3], S. Kojima[4]

[1]Radioisotope Research Center Medical Division, Nagoya University, Showa-ku, Nagoya, 466-8550, Japan
[2]Radioisotope Research Facility, The Jikei University School of Medicine, Minato-ku, Tokyo, 105-8461 Japan
[3]Measuring Systems Design Dept., Hitachi, Ltd. Mitaka-shi, Tokyo, 181-8622, Japan
[4]Aichi Medical University, Aichi, 480-1195, Japan
Keywords: radiostrontium, seawater, monitoring, ion exchange, plastic scintillator
Presenting author, e-mail: ogata.yoshimune@b.mbox.nagoya-u.ac.jp

Monitoring of radiostrontium, ^{89}Sr and ^{90}Sr, is important not only for nuclear accident but also for routine monitoring around nuclear facilities. Those nuclides are pure beta emitters. Since β-rays have continuous distribution and most gamma emitters also emit β-rays, strontium should be separated from other elements before the measurement. The conventional methods to estimate radiostrontium are time-consuming complicated procedures using lots of deleterious substances. Simple, quick and safety analysis of radiostrontium in environmental sample is desired. We tried to investigate the chemical procedure of Sr with the ion exchange coupled with measurement using plastic scintillator.

Artificial seawater and/or natural seawater sampled at Ise Bay, Japan, were used for the experiment. First, 100 mL of seawater was loaded to a cation ion exchange resin column (CV= 10 mL, Dowex 50W-X8, 200-400 mesh) to adsorb Sr. Next, Ca, Mg, Pb, etc. were rinsed with the mixture of ammonium acetate (15.4% W/V%) and methanol (1:1). Then, Sr was eluted with 4M-HCl. Finally, Sr was collected on a membrane filter and dried. The filter was laminated with a pair of polyethylene film (100 μmt) to avoid contamination. The sample was sandwiched with a pair of plastic scintillator (47mm×15mmt, EJ-200, Elijen Technology) and contained in a holder. The activity was measured with a low-background liquid scintillation system (AccuFLEX LSC-LB7, Hitach, Ltd.).

The chemical yields of Sr were estimated with a sample spiked with radiostrontium. The counting efficiencies, the linearity of the efficiencies, and the spectra of β-rays were measured. And, the counting stability of the background and the samples were investigated. The minimum detectable concentration (MDC Bq L^{-1}) was derived by the minimum detectable activity (MDA) estimated by the Currie's formula (Currie, 1968), i.e.;

$$MDA = \frac{2.33\sqrt{n_{BG} \times T}}{T} \times \frac{100}{\varepsilon} \quad (1)$$

$$MDC = MDA \times \frac{100}{y} \times \frac{1000}{V} \quad (2)$$

where n_{BG} is the background count rate (cps), T is the counting time (s), ε is the counting efficiency, y is the chemical yield, and V is the initial sample volume (mL).

The chemical yields of the stable elements, Ca, Mg, Pb, Na, and K, were measured with an ICP-AES (Thermo Jarrel Ash, IRIS/AP).

The chemical procedure took about seven hours and was safe and not so complicated. The average counting efficiency for the sample of ^{90}Sr on the equilibrium stage with ^{90}Y was 70%. The background count rate was 8.1 cpm. The chemical yields of Sr on the membrane filters ranged from 70 to 90%. The MDA was 0.01 Bq. Then the MDC was estimated as 0.15 Bq L^{-1} at 70% of the chemical yield. The MDC was 1/200 of the limit of the legal concentration for drain water; i.e., 30 Bq L^{-1}. Therefore, this method was probed to have sufficient sensitivity.

Usually, liquid scintillation counting method generates flammable organic liquid waste. However, the measurement method proposed here does not generate such organic liquid waste. Furthermore, the plastic scintillator can be used again and again. Therefore, this method is not only safe but also economical.

The method using plastic scintillator is not affected by the quenching effect, so that one can analyse the spectrum for nuclide discrimination, such as discriminate ^{89}Sr from ^{90}Sr.

It was confirmed that the method of ion exchange coupled with plastic scintillator measurement is valuable to monitor radiostrontium in seawater.

Professor Chisato Takenaka, Graduate School of Bioagricultural Sciences, Nagoya University helped us using an ICP-AES. This study was performed at Radioisotope Research Center Medical Division, Nagoya University.

Currie LA. 1968. Limits for qualitative detection and quantitative detection. *Anal. Chem.* 40, 586-593.

Actinides distribution in anoxic sediments close to Swedish nuclear facility

G. Olszewski[1,2,3], P. Törnquist[1], P. Lindahl[2], M. Eriksson[1,2], H. Pettersson[1]

[1]Department of Medical and Health Sciences, Division of Radiological Sciences, Linköping University, Linköping, 581 85, Sweden
[2]Swedish Radiation Safety Authority, Stockholm, 171 54, Sweden
[3]Department of Environmental Chemistry and Radiochemistry, Laboratory of Toxicology and Radiation Protection, University of Gdańsk, Gdańsk, 80-308, Poland
Keywords: plutonium, americium, curium, sediments, dating
Presenting author: G. Olszewski, e-mail: grzgorz.olszewski@liu.se

Radioactive releases from Swedish nuclear facilities are reported to and supervised by the Swedish Radiation Safety Authority (SSM). One of these nuclear facilities is Studsvik, located in the Trosa archipelago. Data on annual liquid radionuclide discharges from this facility are available, which gives an excellent opportunity to examine behavior of actinides in the marine environment. The recipient bay, Tvären, has high sedimentation rates (~1cm/y) and undisturbed sedimentation bottoms that enables detailed sediment chronology studies. By comparing inventories of different radionuclides in the sediment cores and the discharge data combined with sediment dating, a validation of the discharge records can be done. We will present radiometric sediment core data for α-emitting nuclides: ^{238,239,240}Pu, ^{241}Am, ^{242,243,244}Cm. The sediment cores have been dated using a ^{210}Pb model assuming constant ^{210}Pb flux and initial concentration.

The obtained data for analyzed actinides show high activity concentrations for ^{238}Pu, ^{239,240}Pu, ^{243,244}Cm and ^{241}Am (56±2, 39±1, 13±1 and 65±7 Bq/kg dry mass, respectively) and unique ^{238}Pu/^{239,240}Pu, ^{241}Am/^{239,240}Pu and ^{243,244}Cm/^{239,240}Pu activity ratios (0.2-1.6, 0.4-1.5 and 0.003-0.75, respectively. Integrated ^{239,240}Pu, ^{238}Pu and ^{241}Am inventories in analyzed sediment cores reach 800±3 Bq/m^2, 380 and 740 Bq/m^2, respectively.

Evaluation of the radon mass exhalation rate in Italian tuff using the closed chamber technique

J. Orbe[1-3], M. Capua[1,2], G. Durante[4], J. Castagna[5]

[1]Department of Physics, Università della Calabria, Cosenza, 87036, Italy
[2]INFN Gruppo Collegato di Cosenza, Laboratori Nazionali di Frascati, Italy
[3]Physics and Mathematics School, Escuela Superior Politécnica de Chimborazo, Riobamba, 060150, Ecuador
[4]Servizio Laboratorio Fisico Dipartimento di Cosenza/Agenzia Regionale per la Protezione dell'Ambiente della Calabria, Cosenza, 87040, Italy
[5] Istituto sulle Metodologie di Analisi Ambientali/Consiglio Nazionale delle Ricerche,Tito Scalo (PZ), 85050, Italy
Keywords: Closed chamber, gamma spectrometry, mass exhalation rate.
E-mail: jenny-orbe@hotmail.com

Extensive epidemiological studies have demonstrated a statistically significant increase in cancer risk from prolonged exposure to radon. The concentration of this gas can be very high in closed environments where it comes mainly from soil that is in contact with or beneath the basement or foundation. Radon indoor concentration can be increased by concrete and other building materials of mineral origin.

The recent EURATOM Directive 2013/59, considers the population and workers exposure to all kind of sources of radiation, including attention to the radon gas. According to the Directive, the usage of building materials should be restricted if their Activity Concentration Index (gamma index) (Annex VIII) is higher than a reference value.

However, even though in scientific literature there are indications that the internal dose received from radon exhaled from building materials can exceed the dose received from external radiation, there are no guidelines for radon in building materials.

In international standards and scientific literature, besides the respect of specific activities of 40K, 226Ra and 232Th (gamma index), introduced for building materials, reference to alpha dose index is considered for internal exposure to the radon gas (alpha index), the index depends on the content of radium in the materials.

As an alternative, the calculation of the mass exhalation rate, defined as the radon flux emitted from the building material per mass unit, can be performed (Chao and Tung, 1997).

The radon exhalation rate of a building material is influenced not only by the radium content but also by porosity, water content, permeability, emanation power, surface preparation, and covering. For this reason, can be more representative of the real hazard related to alpha-exposure. One of the limits of this method is the long time needed, varying from several days to about a month, for a measurement.

In this study, radon exhalation measurements using the closed-chamber technique were presented. Tuff samples, widely used in central Italy as a building material, were selected to test different procedures.

Chamber leakage and background radon concentration in the air inside the chamber are basic parameters for the chamber characterization and the of the mass exhalation rate extraction.

By studying the growth of radon activity with different radon measurement techniques and several internal and/or external detectors interfaced with the closed chamber, tuff exhalation rate has been extracted.

These studies show that short-term measurements, about a day, can be made without reducing the accuracy of the measurement. For completeness, gamma spectrometry measurements have been performed to calculate the corresponding alpha index.

European Atomic Energy Community (EURATOM). 2013. Laying down basic safety standards for protection against the dangers arising from exposure to ionizing radiation. *Council Directive 2013/59/EURATOM.*

Chao, C.Y., Tung, T.C.1997. Determination of radon emanation and back diffusion characteristics of building materials in small chamber tests. *J. of Building and Environment*. 32, 355-362.

Comparison between measurements techniques of radon concentration in spring water

J. Orbe[1-3], M. Capua[1,2], J. Castagna[4], G. Durante[5]

[1] Department of Physics, Università della Calabria, Cosenza, 87036, Italy
[2] INFN Gruppo Collegato di Cosenza,Laboratori Nazionali di Frascati; Italy.
[3] Physics and Mathematics School, Escuela Superior Politécnica de Chimborazo, Riobamba, 060150, Ecuador
[4] Istituto sulle Metodologie di Analisi Ambientali/Consiglio Nazionale delle Ricerche, Tito Scalo (PZ), 85050, Italy
[5] Servizio Laboratorio Fisico Dipartimento di Cosenza/Agenzia Regionale per la Protezione dell'Ambiente della Calabria, Cosenza, 87040, Italy
Keywords: Groundwater, radon closed chamber, radon measurement techniques.
E-mail: jenny-orbe@hotmail.com

Epidemiologic studies show a relationship between lung cancer and the inhaled radon (Lubin and Boice, 1997). The concentration of this gas can be very high in closed environments where it comes mainly from the soil that is in contact with or beneath the basement or foundation. Radon indoor concentration can be increased by the domestic use of spring water, used for example to showers, washing, etc. Furthermore, consumption of radon-containing spring water may increase the risk of stomach cancer (National Research Council, 1999).

This study presents a comparison between several techniques and instruments used for measures of the radon concentration in groundwater. For this purpose, water samples coming from a reference spring located in an area north of Calabria (Italy) have been used. This water source is monitored since summer 2013

The comparison includes, Lucas scintillation cells with emanometric tool, gamma spectrometry and electret techniques, an original not commercial method which uses a radon closed chamber in which the radon contained in the water sample degasses spontaneously.

The radon chamber was made of plexiglass with a gross volume of 125 liters and it is equipped with a gas-tight tap to insert the water sample, a removable side allows the entry of the necessary equipment.

A database and a dedicated program have been also realized for storing and first data analysis of the measurements. The program is particularly useful for monitoring in large scale surveys.

The results obtained show that the different techniques are well compatible using the sampling protocol and the measurement methodology proposed.

Lubin, J.H., Boice, J.D.1997. Lung cancer risk from residential radon: Meta-analysis of eight epidemiologic studies. *J. of the National Cancer Institute*. 89, 49-57.

National Research Council et al. 1999. Risk assessment of radon in drinking water. *National Academies Press.*

Radioactivity in the Irish Marine Environment – 35 years of monitoring

Currivan L., O'Toole S., O'Colmáin M., Hanley O., Kinahan A., & Fennell S.

Environmental Protection Agency, Office of Radiation Protection and Environmental Monitoring,
3 Clonskeagh Square, Clonskeagh Road, Dublin 14, D14 H424, Ireland.

Since the early-1980s, samples of marine environmental materials collected by the Environmental Protection Agency (and previously the Radiological Protection Institute of Ireland) around the Irish coast and from the Irish Sea have been analyzed to determine the concentrations of artificial radionuclides. This marine monitoring programme primarily monitors the effects of radioactive discharges from the Sellafield Nuclear Fuel Reprocessing Plant on the northwest coast of England.

The main objective of this programme is to assess the exposure to the Irish population resulting from radioactive contamination of the Irish marine environment and to estimate the associated risks to health. The artificial radionuclides of greatest concern from a dose point of view are caesium-137, technetium-99 and actinides (isotopes of plutonium and americium). In addition, the programme aims to assess the distribution of contaminating radionuclides and to identify long-term trends. To assess the exposure arising from this source, levels of radionuclides are measured in seawater, sediments and seaweed as well as fish and shellfish landed at ports along the north-east coast of Ireland, where the highest levels of radioactivity attributable to Sellafield are observed.

Fish and shellfish are monitored to determine exposure from the internal irradiation pathway, sediment is analyzed with relevance to external exposures and seawater and seaweed are sampled as environmental indicator materials.

A thorough review of the adequacy of the monitoring arrangements and a habits survey was carried out in 2009. This review provided information of possible changes in radiological exposure pathways affecting doses to people, an assessment of doses to people who consume large amounts of seafood and those who are exposed to external radiation over long periods. This led to some changes in the how the assessment of doses for the Irish population were derived from these pathways. The Irish marine monitoring programme has continued throughout the intervening years to the present time and is reviewed annually.

The objective of this paper is to provide concentrations of certain radionuclides in selected indicators (seafood, seaweed, seawater and sediment) and associated doses to the Irish population over a 35-year period. The concentration data have been compiled to assess the time trends from the early 1980s up to the present. This data gives a clear and broad picture of radionuclide trends in the Irish environment due to discharges of low level liquid radioactive waste from the UK's Sellafield Nuclear Fuel Reprocessing Plant.

Background sources in the Modane underground laboratory

V. Palušová[1], R. Breier[1], P.P. Povinec[1]

[1]Faculty of Mathematics, Physics and Informatics, Comenius University, SK-84248 Bratislava, Slovakia
Keywords: Underground laboratories, background sources, gamma-ray sources, neutron sources
Presenting author, e-mail: veronika.palusova@fmph.uniba.sk

The Modane underground laboratory (LSM) is the deepest operating underground laboratory in Europe. It is located under the Fréjus mountain in France, with average overburden of 4800 m w.e, (water equivalent), providing low-background environment for several experiments in nuclear and particle physics, astrophysics and environmental physics. As these experiments represent investigations of extremely rare events there is a need for understanding individual sources of background and to estimate each background component.

If detectors operate in deep underground laboratories, the cosmic-ray component should be negligible, as fluxes of secondary cosmic-ray particles are substantially decreased by surrounding rock. The residual cosmic-ray flux consists of high-energy muons induced by interactions of high energy cosmic rays in the upper atmosphere.

Background from U and Th decay chains and ^{40}K imposes severe constraints on the sensitivity of detectors and dominates over the cosmic-ray induced background by several orders of magnitude.

Several measurements and simulations of detectors background were performed in the past in order to study gamma and neutron fluxes in the LSM. Examples of measured and simulated spectra of NaI and HPGe detectors are presented in Figures 1 and 2.

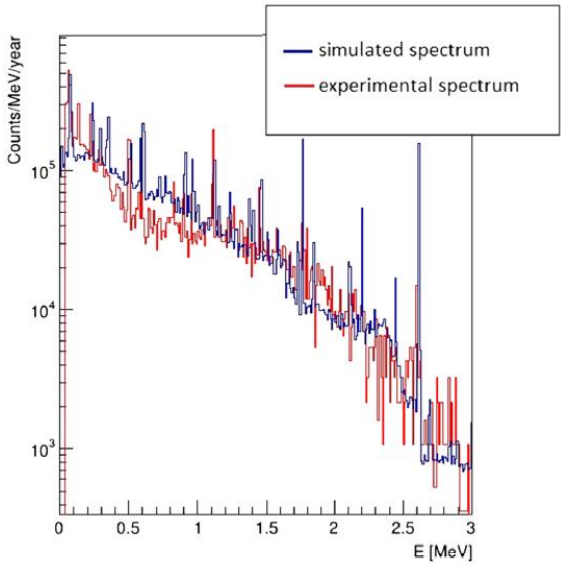

Figure 1: Simulated and experimental background γ-ray spectra of HPGe detector operating in LSM

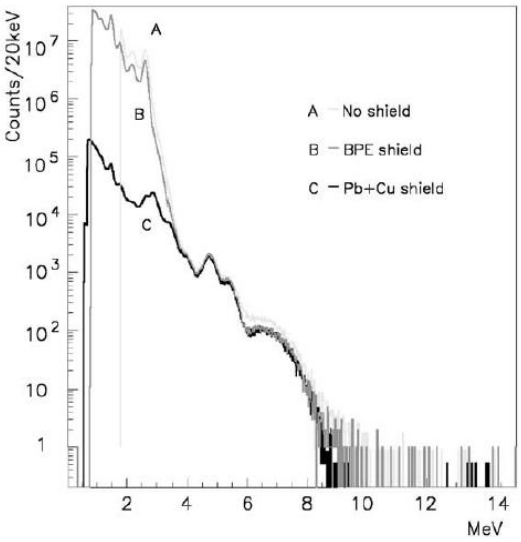

Figure 2: Large volume NaI scintillator energy spectra in the LSM with three different shielding configurations

This work discusses and analyses individual background contributions including residual cosmic-ray flux of high-energy muons, muon-induced neutrons and contributions to the background coming from primordial, cosmogenic and anthropogenic radionuclides present in the environment. Of the last mentioned, following sources are dominant: radioactive contamination and radioactive impurities of the laboratory (rocks, coatings) construction materials, and radon contamination of the laboratory air.

We shall focus on estimation of fluxes of low and medium energy gamma-rays from the environmental components, as well as on neutron fluxes produced in spontaneous fission processes of uranium and thorium in the rocks, and in (α,n) reactions.

P.P. Povinec et al. 2008. New isotope technologies in environmental physics". In: *Acta Phys. Slovaca* 58. pp. 1-154.

V. Palušová et al. 2018. Monte Carlo simulation of environmental background sources of a HPGe detector operating in underground laboratory. In: *Journal of Radioanalytical and Nuclear Chemistry* 318. pp. 2329–2334.

H. Ohsumi et al. 2002. Gamma-ray flux in the Frejus underground laboratory measured with NaI detector". In: *Nuclear Instruments and Methods in Physics Research, Section A* 482.3. pp. 832-839.

Assessment of tritium levels in man in Lund, Sweden, prior to the start of operation of the European Spallation Source

G. Pédehontaa-Hiaa [1], H. Holstein [1], S. Mattsson [1], C. L. Rääf [1] and K. E. Stenström [2]

[1] Medical Radiation Physics Malmö, Department of Translational Medicine, Lund University, Malmö, Sweden
[2] Nuclear Physics Division, Physics Department, Lund University, Lund, Sweden
Keywords: Tritium, European Spallation Source, Liquid Scintillation Counting, Isotope Ratio Mass Spectrometry
Guillaume Pédehontaa-Hiaa, e-mail: guillaume.pedehontaa-hiaa@med.lu.se

The European Spallation Source (ESS) is a neutron source under construction near the centre of Lund, Sweden. The spallation reaction in the ESS tungsten target as well as the activation of materials by its 5 MW linear accelerator will generate a wide variety of radionuclides including tritium (^{3}H). Tritium is expected to dominate the source term of continuous radioactive effluents (in $Bq \cdot year^{-1}$). The total tritium activity in the target system has been estimated to reach ~ 10^{15} Bq after 1 year of operation (Ene et al., 2015) and approximately $0.6 \cdot 10^{12}$ Bq is anticipated to be released annually through the main stack (Ene, 2016). Most of this tritium will be released in the environment as tritiated water (HTO).

Tritium is highly mobile in the environment, including in humans. The current levels of tritium in humans before the start of operation of the ESS were estimated by the analysis of human urine using liquid scintillation counting (LSC). Urinary HTO activity concentration were assessed in 55 participants divided in four groups: ESS staff members, neighbours of the ESS, members of Lund general public and exposed workers.

The participants provided a sample of morning urine as well as information about their beverage intake the day before the sampling. The collected samples were purified by filtration on activated charcoal followed by distillation before measurement by LSC. The effect of the sample preparation on the isotope fractionation of the urine samples was determined by isotope ratio mass spectroscopy (IRMS) of $^{2}H/^{1}H$. IRMS was also used to investigate the isotope fractionation in locally available tap and bottled waters consumed by the participants.

Activity concentrations for the ESS staff members, ESS neighbours and general public were found below the minimum detectable activity (MDA) of 2.1 $Bq \cdot L^{-1}$. Those values follow the general trend of a decrease of the global tritium levels since the bomb pulse in the 1960´s.

Only a few workers from facilities where tritium is handled showed an activity concentration above the MDA (2.1 $Bq \cdot L^{-1}$) up to 11 $Bq \cdot L^{-1}$. All of these workers were directly handling organic compounds labelled with tritium. They were thus occupationally exposed. Their contamination was however rather limited compared to that of other occupationally exposed workers and especially to those from heavy water reactors where the urinary activity concentration can reach up to 100 000 $Bq \cdot L^{-1}$ (Hou, 2011).

The data obtained during this study will be used as a reference to monitor the transfer of tritium to the local population once ESS will start its operation.

The study was approved by the regional ethical review board at Lund University (Dnr 2018/296). The samples were analysed for their isotopic composition at the Stable Isotope Service Lab, Department of Biology, Lund University. This work was partly funded by the Swedish Radiation Safety Authority (grant SSM2018-1636-1).

D. Ene, K. Andersson, M. Jensen, S. Nielsen, and G. Severin, 2015, Management of Tritium in European Spallation Source, *Fusion Sci. Technol.*, 67, 2, 324–327

D. Ene, 2016, Source Term to the Environment from the ESS Target Station, *Proceedings of SATIF13 workshop*, 32–47.

X. Hou, 2011, Analysis of Urine for Pure Beta Emitters: Methods and Application, *Health Phys.*, 101, 2, 159

Radioactive and radiological characterization of Spanish commercial bottled drinking water

S.M Pérez-Moreno[1], J.L Guerrero[1], F. Mosqueda[1], M.J. Gázquez[2] y J.P. Bolívar[1]

[1]Departament of Integrated Sciences, University of Huelva, Huelva, Spain.
[2]Departament of Applied Physic, University of Cádiz, Cádiz. Spain.
Keywords: *Bottled Drinking Water, Natural Radioactivity, Indicative Dose, Spain*
Presenting author, e-mail: silvia.perez@dci.uhu.es

The high consumption of commercial mineral water may pose a risk to the health of people due to the presence of natural radionuclides. The mineral composition and properties of natural mineral waters are regulated by the geological bedrock of the water. The presence of natural radionuclides in the host rock and its interaction with the water control the natural radionuclides concentrations in the water (Chau et al., 2011).

On the occasion of the recently Spanish regulations R.D. 314/2016, in which the control of the indicative dose is established, the radiological quality of a significant set of bottled waters of different Spanish brands with different geological origin have been evaluated. In addition, the behavior of the natural radionuclides (^{210}Po, ^{210}Pb, ^{234,238}U, ^{230,232}Th, ^{226,228}Ra) depending on their bedrock and physical-chemical conditions of the groundwater were also studied.

Both gross alpha and beta activities were measured in fifteen different brands of Spanish bottled water (Fig.1). They were also analyzed by ICP-MS, HPLC and alpha-particle spectrometry with PIPS detectors. The Indicative Doses (ID) were then determined according to procedure stablished in the Directive EURATOM (2013).

Figure 1. Lithology of Spain and location of waters.

The waters present pH around 6-7 (average = 6.9 ± 0.5), showing a neutral character. It is highlighted the high linear relation found between electrical conductivity and dry residue, as expected. According their chemical composition 57.1 % waters are classified as calcium bicarbonated, 21.4 % as sodium bicarbonated, 14.3 % as calcium chlorinated, and 7.1 % as sodium chlorinated.

The gross alpha activity varies from 10 up to 195 mBq L^{-1}. Waters that exceed the recommended value of 0.1 Bq L^{-1} have carbonate (#10) and granite substrate (#12, #15), while gross beta activity was always below 1 Bq L^{-1}.

The bottled mineral waters present a high variability in concentrations of natural radionuclides, which depend on characteristics of the aquifer. Several waters exceed of parametric value for gross alpha mainly due to ^{234}U, ^{226}Ra and/or ^{210}Pb concentrations (Fig. 2).

The highest activity concentration of ^{238}U was found in waters with carbonate substrate, where the uranium forms soluble complexes as $UO_2(CO_3)_2^{2-}$, and $UO_2(CO_3)_3^{4-}$. On the other hand, ^{226}Ra is very soluble in waters with a high concentration of Cl^-. And the highest activity of ^{210}Pb is found in granitic rock aquifers, especially those located in Extremadura.

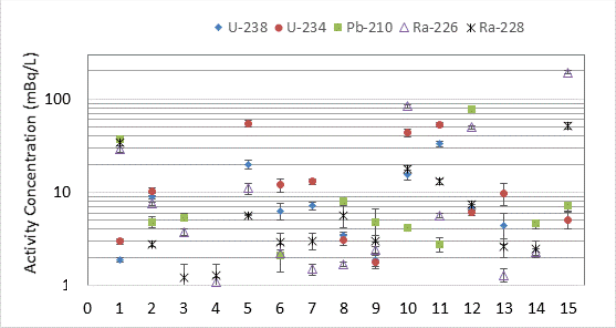

Figure 2. Activity concentrations of ^{238,234}U, ^{226,228}Ra and ^{210}Pb. Isotopes of Th <1 mBq L^{-1}.

The content of ^{226}Ra and ^{210}Pb in water specially contribute to the indicative dose. Only one of the waters (#12), exceeds the parametric value of 0.1 mSv. In view of this fact, it is suggested new investigations in order to evaluate the potential risk to human health.

This work was supported by the Spanish Ministry of Science, Innovation and Universities under grant No. CTM2015-68628-R, and No. EQC2018-004306-P.

Chau N. D., Dulinski M., Jodlowski P., Nowak J., Rozanski K., Sleziak M. and Wachniew P. Natural radioactivity in groundwater – a review. 2011. *Isot Environ Healt S*, 47, 415–437.

COUNCIL DIRECTIVE 2013/51/EURATOM of 22 October 2013 laying down requirements for the protection of the health of the general public with regard to radioactive substances in water intended for human consumption.

R. D.314/2016 por el que se regula la explotación y comercialización de aguas minerales naturales.

^{233}U-^{236}U oceanic tracer studies in the Baltic Sea and the Arctic Ocean

Jixin Qiao[1], Peter Steier[2], Karin Hain[2]

[1]Center for Nuclear Technologies, Technical University of Denmark (DTU Nutech), Roskilde, 4000, Denmark
[2] VERA Laboratory, Faculty of Physics – Isotope Research, University of Vienna, Vienna A-1090, Austria
Keywords: ^{233}U, ^{236}U, oceanic tracer, Baltic Sea, Arctic Ocean
Presenting author, e-mail: jiqi@dtu.dk

^{236}U is increasingly adopted as a new oceanic tracer. With the very recent achievement of detection of ^{233}U at environmental concentrations by Accelerator Mass Spectrometry (AMS), the application of ^{233}U-^{236}U as paired tracer system in oceanic studies opens up the possibilities for identifying the origin of anthropogenic U, and thus the water masses.

To understand the level, distribution, and source terms of ^{233}U and ^{236}U in the oceans, since 2012 we have continuously collected a large number of marine samples (seawater and sediment) in different regions of the Baltic Sea and Arctic Ocean and measured for ^{233}U and ^{236}U. Time series of seaweed collected from Danish marine environment since the 1980s have also been analyzed for ^{233}U and ^{236}U. This paper presents our recent progresses in ^{233}U-^{236}U oceanic tracer studies in the Baltic Sea and Arctic Ocean.

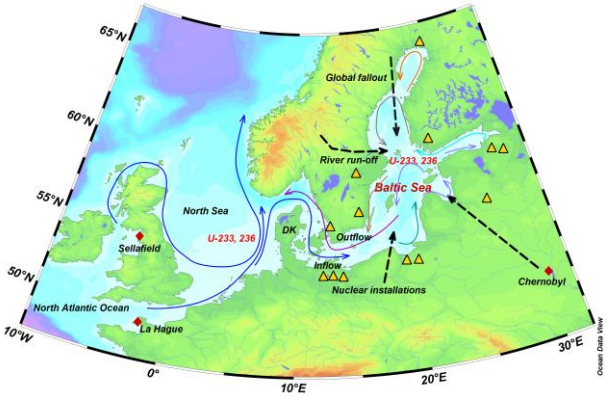

Figure 1. Map of the Baltic Sea and potential sources of ^{233}U and ^{236}U.

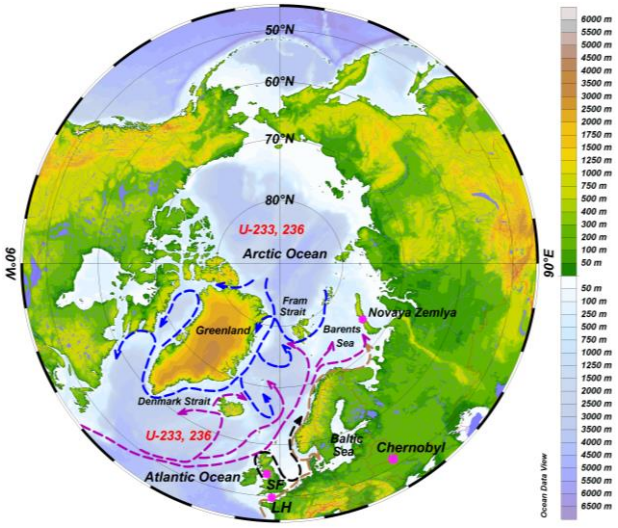

Figure 2. Map of the Baltic Sea and potential sources of ^{233}U and ^{236}U.

This work was financially supported by Danish Ministry of the Environment and Technical University of Denmark (DTU). J. Qiao wishes to thank Greenland Institute for Natural resources and National Institute for Aquatic Resources at DTU, Haitao Zhang (Northwest Institute of Nuclear Technology, China), Gideon Henderson (Oxford University, UK), Yiyao Cao (Zhejiang Provincial Center for Disease Control and Prevention, China) and all colleagues from Radioecology Section at DTU Nutech for contributions in sampling, sample process and discussion.

Linking heterogeneous distribution to mobility and potential bioavailability for radiocaesium in soils and pond sediments in the Fukushima Daiichi exclusion zone

E. Reinoso-Maset[1]*, J. Brown[2], F. Steenhuisen[3], B. Salbu[1], O.C. Lind[1]

[1]Centre for Environmental Radioactivity CoE, Faculty of Environmental Sciences and Natural Resource Management, Norwegian University of Life Sciences, Ås, 1432, Norway
[2]Centre for Environmental Radioactivity CoE, Norwegian Radiation and Nuclear Safety Authority, Østerås, 1361, Norway
[3]Artic Centre, University of Groningen, Groningen, 9718 CW, The Netherlands
Keywords: radiocaesium, radioactive particles, Fukushima
**Presenting author email: estela.reinoso.maset@nmbu.no*

During the Fukushima Daiichi Nuclear Power Plant (FDNPP) accident in 2011, an estimate of 6 to $20 \cdot 10^{15}$ Bq of ^{137}Cs were released from reactor units 1, 2 and 3 into the atmosphere (UNSCEAR, 2014). Radionuclide release occurred mostly as aerosols or gaseous phases and, due to interactions of volatile fuel with reactor internal containments, a significant portion was expected to be in the form of discrete radiocaesium particles of various sizes and compositions (Salbu & Lind, 2016). Subsequent wet and dry deposition processes at different phases of the accident resulted in a non-uniform radionuclide distribution in the near field (< 30 km) as well as large contaminated areas (50 – 70 x 20 km) in a north-western direction from the FDNPP (Saito *et al.*, 2015). Weathering of deposited particles is controlled by their specific characteristics (e.g., oxidation state, size, structure, elemental composition) and environmental conditions (e.g., soil pH, atmospheric and water transport), which can lead to heterogeneous contamination and, if omitted in environmental radioactivity calculations, can generate large uncertainties and significant errors in contamination risk and biological impact assessments. In this work, we aimed to elucidate the influence of speciation, including radioactive particles, on mobility and potential bioavailability of radiocaesium in soils and sediments from sites located in different directions and distances from the FDNPP.

Soil and sediment samples collected in September 2016 were fully characterized (pH, grain size, organic content) and subjected to two different leaching conditions, a simulated stomach juice to assess radiocaesium bioavailability and a sequential chemical extraction to evaluate the partitioning of radiocaesium between reversible and irreversible interactions with soil and sediment components. The ^{137}Cs and ^{134}Cs activities were determined in bulk, grain-sized and extracted soil/sediment fractions by gamma spectrometry, and the presence and distribution of radiocaesium containing particles was explored using digital autoradiography. Moreover, ambient equivalent air doses measured during sampling and radiocaesium surface contamination densities estimated from *in situ* gamma spectrometry using InSiCal software were compared to laboratory measurements of soils and sediments from the corresponding sites.

Results showed that the majority of the radiocaesium contamination was found in the upper layer of soils and sediments (< 5–6 cm). The Cs-isotopes were distributed among the grain-sized fractions, and were predominantly associated to the irreversibly bound and the inert fractions (>90 and ~84 % of the total activity in soils and sediments). Thus, the radioactive contamination in these soils and sediments was sparingly soluble under environmentally relevant conditions (i.e., water and exchangeable extractions). Digital autoradiography revealed that the inert fraction was predominately associated with heterogeneities in the form of radiocaesium-containing particles. The ^{137}Cs activity concentration in soil and sediments was correlated with the particle abundance, which was dependant on distance and direction from the FDNPP, and both were in good agreement with measured ambient equivalent dose rates in the associated sites. Moreover, contamination density estimations decay-corrected to the day of the FDNPP accident resulted in ^{134}Cs/^{137}Cs ratios that match the reported release and deposition plumes from the reactor units. These results demonstrated that the radiocaesium in the contaminated soils and sediments from the FDNPP's near field exhibit relatively low bioavailability and weathering, and that radiocaesium-containing particles are still an existing problem in the Fukushima area. Overall, this study highlights the importance of including radioactive particles in environmental impact assessments.

This work was supported by the Research Council of Norway through its Centres of Excellence funding scheme (project number 223268/F50).

Saito, K., Tanihata, I., et al., 2015. *J. Environ. Radioact*. 139, 308-319.

Salbu, B., Lind, O.C., 2016. *Integr. Environ. Assess. Manag.*, 12, 687-689.

UNSCEAR, 2014. *United Nations Scientific Committee on the Effects of Atomic Radiation*, New York, p. 321.

Reconstruction of the impact to biota of former releases of alpha emitters in the Loire River

S. Reygrobellet[1], P. Boyer[2]

[1]IRSN PSE-ENV/SEREN/LEREN, Bld 153, 13115 Saint-Paul-Lez-Durance cedex, France
[2]IRSN PSE-ENV/SRTE/LRTA, Bld 159, 13115 Saint-Paul-Lez-Durance cedex, France
Keywords: impact to biota, plutonium isotopes
Presenting author, e-mail: sophie.reygrobellet@irsn.fr, patrick.boyer@irsn.fr

Two accidents with fuel melt elements have occurred on the two carbon dioxide-cooled, graphite-moderated power reactors of Saint-Laurent-des-Eaux on October 1969, 17th and on March 1980, 13th. Additionally, on April 1980, 21st, a confinement´s loss occurred in a container stored in the spent fuel pool. These events have led to the radionuclide releases in the Loire River, among them ^{238}Pu and $^{239\text{-}240}$Pu. To search the traces of alpha emitters in the Loire River, IRSN sampled a sediment core in 2015 in which the vertical profile of plutonium concentrations allows to track these former releases. In this context, this abstract presents the exploitation of this sedimentary recording to rebuild impact to biota of these past events. The method consists first into the decomposition of activities of plutonium isotopes measured in this sediment coer according to the contributions due to the releases on one hand and to the atmospheric fallouts on another hand.

In a second step, the contributions of the releases are considered alone to deduce the possible range of activities of plutonium isotopes that they may have caused in the Loire River over the period from 1969 to 1983.
This chronicle is finally considered to assess the impact to biota over this period by applying the level two of ERICA tool and using the screening incremental dose rate of 10 μGy.h^{-1}. The results show that the hazard risk for aquatic ecosystems is nearly 8 times less than the reference level.

http://www.irsn.fr/FR/Actualites_presse/Actualites/Documents/IRSN_NI_Rejes-plutonium-Loire_17032016.pdf

www.erica-tool.com

Uranium toxicity on plant cells: Isothermal microcalorimetric studies for the differentiation between chemotoxic and radiotoxic effects of uranium

S. Sachs[1], J. Oertel[1], K. Fahmy[1]

[1]Institute of Resource Ecology, Helmholtz-Zentrum Dresden-Rossendorf, Dresden, 01328, Germany
Keywords: uranium, plant cells, toxicity, isothermal microcalorimetry
Presenting author, e-mail: s.sachs@hzdr.de

The transfer of radionuclides into the food chain is a central concern in the safety assessment of both nuclear waste repositories and remediation strategies in radioactively contaminated sites, such as legacies of the former uranium mining. The uptake and translocation of radionuclides, e.g., uranium, is speciation dependent and induces several stress response reactions, which changes the plant metabolism. Correlating molecular information on radionuclide speciation and biomolecular interactions with physiological performance is a major challenge for radioecology.

In our previous work we applied isothermal microcalorimetry as a sensitive real-time monitor to study the interaction of U(VI) with canola (*Brassica napus*) cells (Sachs et al., 2017). Applying this method, we were able to monitor the metabolic activity of the cells in the presence of U(VI) and to determine the U(VI) toxicity in *B. napus* cells. Those was correlated with the oxidoreductase activity of the cells and the U(VI) speciation in solution. Based on this work we are currently investigating the differentiation between chemotoxic and radiotoxic effects of uranium on *B. napus* cells applying natural uranium (U_{nat}) as well as ^{233}U as alpha emitter. To discriminate between these effects, the metabolic heat flow of the cells at a constant total uranium concentration of 5×10^{-5} mol/L is monitored by isothermal microcalorimetry applying increasing concentrations of ^{233}U (1×10^{-6}-1.5×10^{-5} mol/L), which correspond to increasing radiation doses. Applying liquid scintillation counting (LSC) we determine the amount of uranium that is bioassociated to the plant cells and estimate the respective ^{233}U doses for the cells.

Figure 1 shows the characteristic metabolic capacities (M_c) of *B. napus* cells as a function of the ^{233}U concentration. The M_c values provide a quantitative ranking of metabolic activities that is independent of cell number and largely unaffected by normal variations between experiments (Sachs et al., 2017). The data are normalized to M_c values of *B. napus* cells that were exposed to natural uranium only. In the presence of 2 µM ^{233}U a slight increase in the M_c values was observed, which indicates a slightly higher metabolic activity of the cells. Probably, this is an indication for a stress response of the cells to the radiotoxic effect of ^{233}U. With increasing ^{233}U concentration only a slight decrease of the M_c values was observed. This indicates only a slight effect of the alpha radiation on the cells compared to those cells that were exposed to natural uranium, which exhibits a predominant chemotoxic effect. These first results point to a high resistance of *B. napus* cells to the radiotoxicity of ^{233}U.

This presentation will demonstrate the potential of life cell microcalorimetry for radioecological studies. We will present the calorimetric determination of the U(VI) toxicity in *B. napus* cells that correlates with oxidoreductase activity and U(VI) speciation and will focus on the differentiation between chemotoxic and radiotoxic effects of uranium.

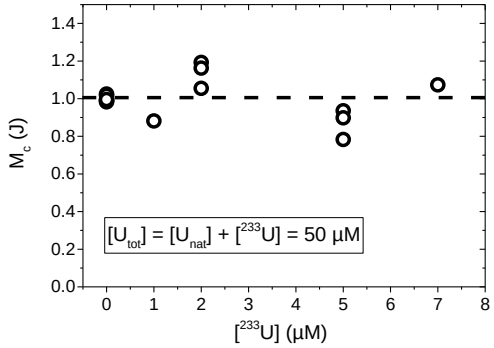

Figure 1. Characteristic metabolic capacity (M_c) of *B. napus* cells as a function of the ^{233}U concentration in solution.

We thank Dr. S. Taut for his support in dose estimation as well as J. Seibt, S. Heller, and J. Philipp for their valuable help with the performance of the experiments.

Sachs, S., Geipel, G., Bok, F., Oertel, J., Fahmy, K. 2017. Calorimetrically determined U(VI) toxicity in *Brassica napus* correlates with oxidoreductase activity and U(VI) speciation. *Environ. Sci. Technol.* 51, 10843-10849.

Chabazite, a promising zeolite material for radium removal from mining water

J. Schick[1], V. Luquet de Saint-Germain[2]

[1]Technical Direction, Orano mining, Bessines-sur-Gartempe, 87250, France
[2]Remediation and After-Mining Direction, Orano mining, Bessines-sur-Gartempe, 87250, France
Keywords: remediation, water, radium, zeolite
Joachim Schick, Joachim.schick@orano.group:

Numerous uranium deposits were exploited in France from 1947 to 2001. Nowadays, all these former mining sites are remediated and redeveloped. Natural uranium content in waters is low (around 0.5 µg/L), several anthropogenic activities (uranium exploration, mining) increase uranium concentration in the environment (Drozdzak et al., 2016). If needed, mining waters containing especially uranium and radium have to be treated before discharged into the environment.
Historical radium treatment consists in a barium addition and is removed with a $(Ba,Ra)SO_4$ double salt precipitation. In some cases (e.g. low sulfates content in water), this treatment is not very efficient. In addition to that, barium can be discharged due to an incomplete precipitation. Aluminosilicate zeolites with their negative charge framework have already been used for radium adsorbent (Chałupnik et al., 2013) (Litz and Williams, 2012) and could be an interesting alternative treatment.
The Bois-Nois site in France is a former uranium mine where tailings have been disposed below water, which contains 2 Bq/L radium. Three very common and low-cost zeolites have been chosen and tested to remove ^{226}Ra from mining water. Characteristics of this zeolite samples are presented in Table 1.

Table 1. Characteristics of zeolite samples

Zeolites	**Chabazite**	**Clinoptilolite**	**Faujasite**
Structural code	CHA	HEU	FAU
Origin	natural	natural	synthetic
Pore size (Å)	3.8 x 3.8	5.5 x 3.1	7.4 x 7.4
CEC (meq/g)	3.7	2.6	5.4
Specific area (m^2)	280	25	510

In batch experiment (Liquid /Solid ratio = 1000 mL/g), radium was totally (R = 100%) and quickly removed after 2 minutes contact time. No difference was observed between the three materials.

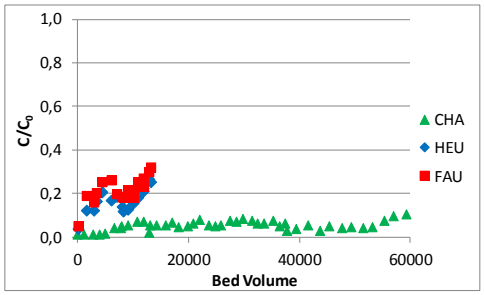

Figure 1. Radium removal from Bois-Noirs mining water on CHA, HEU and FAU (^{226}Ra = 2 Bq/L, F = 600 mL/h).

Column sorption experiments were carried out through a 13 cm length and 0.8 cm internal diameter vertical column. Zeolite bed volume (BV hereafter) corresponds to 26 mL. The influent was introduced down flow at 600 mL/h flow rate. Figure 1 represents radium removal on the three zeolite samples, with c_0 and c influent and effluent radium concentration respectively. Chabazite is the most efficient zeolite with a c/c_0 ratio below 0,1 until 60 000 BV. Chabazite is always efficient although radium content in material reaches 150 Bq/g.
^{226}Ra uptake was also tested at semi-industrial scale on a pilot plant (zeolite volume = 300 L, F = 2 m^3/h). Lab experiments results were confirmed, and more than 10 000 m^3 were successfully treated with a c/c_0 ratio below 0.1.
The environmental impact assessment of Ra-chabazite was characterized by using batch leaching tests made according to the standard NF EN 12457-2 as applied on all wastes. Ra-chabazite stability is excellent during this test: radium leaching is very low, less than 0,005%.
Radium removal efficiency can be decreased by channelling and partial clogging in zeolite filter due to a high suspended solids content in influent. In this case, a previous filtration system such as sand filter can be used to reduce particles entering in the zeolite filter.
Zeolites and specially chabazite tuff are very efficient and selective materials to remove radium from mining water in spite of very low concentration (~ 50 pg/L). After zeolite filtration, radium content in effluent is below 0.2 Bq/L and respects regulatory limit equal (c <0.37 Bq/L). This treatment is also an eco-friendly and sustainable process (no chemical) but also low-cost (water treated cost: 0,05 $ /m^3). In 2019, Orano mining will implement zeolites treatment on several former mining sites such as the Bois-Noirs site.

Chałupnik, S., Franus W., Wysocka, M., Gzyl, G. 2013. Application of zeolites for radium removal from mine water. *Environ Sci Pollut Res*. 20, 7900–7906.

Drozdzak, J., Leermakers, M., Gao, Y., M. Elskens, Phrommavanh, V. and Descostes, M. 2016. Uranium Aqueous Speciation in the Vicinity of the Former Uranium Mining Sites Using the Diffusive Gradients in Thin Films and Ultrafiltration Techniques. *Anal. Chim. Acta*. 913, 94 – 103.

Litz, J.E., Williams C.S. Radium removal from aqueous media using zeolite materials. 2018. US Patent 9 908 788 B1.

Spatial and vertical variability of ^{137}Cs activity in lake sediments of two dam lakes in Poland after the Chernobyl fallout

I. Sekudewicz, M. Gąsiorowski[1]

[1] Institute of Geological Sciences, Polish Academy of Sciences, Warsaw, PL-00818, Poland
Keywords: gamma spectrometry, lake ecosystems, cesium ^{137}Cs migration
Presenting author, e-mail: i.sekudewicz@twarda.pan.pl

Chernobyl nuclear power plant accident in 1986 caused radioisotopes pollution (including cesium-137) in a large area of Europe. The recent research has shown that due to the relatively long half-time of ^{137}Cs decay (30.08 y), its migration and accumulation in the natural environment may be observed even after 32 years from the Chernobyl fallout. In addition, ^{137}Cs research has been significantly developed due to its harmful effects on health, but also due to its suitability for dating, e.g. lake sediments.

The main goal of this study was to determine the spatial and vertical distribution of ^{137}Cs in lake sediments in Turawa Lake (50º43'19 N; 18º07'42 E) and Koronowo Lake (53º20'17 N; 17º57'39 E) after 32 years since the Chernobyl fallout. Studied reservoirs are characterized by similar limnological features, however, they are located in areas strongly (Turawa Lake) and weakly (Koronowo Lake) affected by radiocesium contamination. These dam lakes were chosen to the studies because they are characterized by a relatively high sedimentation rate (good vertical resolution) and intensive transport of sediments from the lakes' catchments.

In order to determine the spatial and vertical distribution of radiocesium in lake sediments in Turawa and Koronowo Lakes, the concentrations of ^{137}Cs and ^{40}K activity were measured using gamma spectrometry. In addition, the elemental analysis (C, H, N, and S) in organic matter in collected samples was performed using Vario CUBE elemental analyzer and the ammonia concentrations in pore water was measured with a calorimetric method.

The measurements showed that concentrations of ^{137}Cs activity in surface bottom sediments in studied reservoirs are still significant. Higher activity concentrations of this radioisotope were found in silt and clay fraction (<0.063 mm) than in coarse-grained (sands) sediments. The similar relationship was registered for ^{40}K activity measurements. Additionally, the strong positive correlation between ^{137}Cs activity concentrations and total organic nitrogen and total organic carbon was noticed. Based on obtained results, processes determining the spatial and vertical distribution of ^{137}Cs activity concentrations in lake sediments, as well as its eventual possibility of migration in the selected lakes' ecosystems have been described.

This work was supported by the Institute of Geological Sciences, Polish Academy of Sciences from the project for young scientists and from the internal project *'Turawa'*.

$^{135}Cs/^{137}Cs$ isotope ratio near the Fukushima Daiichi Nuclear Power Station

A. Shimada[1], T. Tsukahara[2], M. Nomura[2], T. Shimada[1], S. Takeda[1]

[1]Nuclear Safety Research Center, Japan Atomic Energy Agency, Tokai-mura, Naka-gun, Ibaraki, 319-1195, Japan
[2]Laboratory for Advanced Nuclear Energy, Tokyo Institute of Technology, O-okayama, Meguro-ku, Tokyo, 152-8550, Japan
Keywords: $^{135}Cs/^{137}Cs$ isotope ratio, Fukushima Daiichi Nuclear Power Station,
Presenting author, e-mail: shimada.asako@jaea.go.jp

Isotope ratio measurement is one of the strongest tools to identify the origin of radionuclides. $^{134}Cs/^{137}Cs$ (Chinone, M. et al., 2016) and $^{136}Cs/^{137}Cs$ (Fujiwara, T., et al., 2012) radioactivity ratios were measured relatively early period after the accident of the Fukushima Daiichi Nuclear Power Station (FDNPS). However, $^{135}Cs/^{137}Cs$ will be dominant after decades when nuclear facility sites will be released because of relatively short half-lives of ^{134}Cs and ^{136}Cs, 2.07 y and 12.97 d, respectively, and longer half-lives of ^{135}Cs and ^{137}Cs, 2.3×10^6 y and 30.2 y, respectively. Instead of γ-ray measurement for $^{134}Cs/^{137}Cs$ and $^{136}Cs/^{137}Cs$, chemical separation of Cs from soil and following mass spectrometry are required to determine $^{135}Cs/^{137}Cs$. Therefore, chemical separation method using calix[4]arene-bis(t-octylbenzo-crown-6) (BOBCalixC6) was developed in the present study. Triple quadrupole inductively coupled plasma mass spectrometry (QQQ) is available fast measurement of $^{135}Cs/^{137}Cs$ although precision is low. Whereas, thermal ionization mass spectrometry (TIMS) is available to obtain precise $^{135}Cs/^{137}Cs$ although measuring time is long. Required precision is discussed to identify the origin.

Soil samples were collected at the just outside of fence of FDNPS (shown in Fig.1). Organic materials in these samples were burned at 450℃ for 1 h. And then, the samples were transferred into Teflon bombs with each 50 ml of HNO_3. The Teflon bombs were inserted in pressure tight cases, and heated at 200℃ for 4 h. After filtration using 0.1 μm membrane filter, these filtrates were evaporated near dryness and dissolved in 3 M HNO_3. These 3 M HNO_3 solutions were contacted with 0.02 M BOBCalixC6 in 1-octanol solutions to extract Cs, and then, the organic phases were washed with 0.5 M HNO_3 to ensure the removal of Ba and Mo. Extracted Cs was recovered into 1 mM HCl solutions. At this time, 1-dodecanol was added into the organic phases to improve the back extraction of Cs. This separation procedure was repeated 2 times. $^{135}Cs/^{137}Cs$ isotope ratios were measured by TIMS and by QQQ to compare precision of these measurements.

Obtained $^{135}Cs/^{137}Cs$ isotope ratios were corrected to March 11, 2011 and shown in Fig.1. Only $^{135}Cs/^{137}Cs$ at the northwest direction showed higher value. This agrees with significantly different values of $^{134}Cs/^{137}Cs$ (Chinone, M. et al., 2016) and $^{136}Cs/^{137}Cs$ (Fujiwara, T., et al., 2012) in northwest direction. Major source of northwest direction is considered as Unit 1, therefore, the radiocesium isotope ratios differ from the other directions where major sources are considered as Unit 2 and 3.

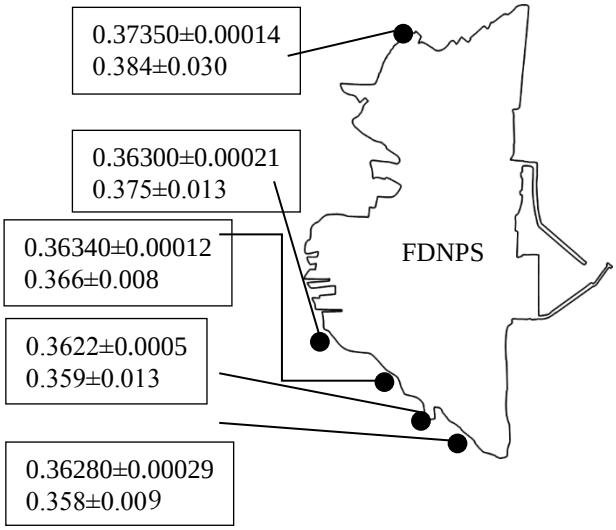

Figure 1. $^{135}Cs/^{137}Cs$ isotope ratio near FDNPS. Upper: TIMS, Lower: QQQ.

$^{135}Cs/^{137}Cs$ near the FDNPS except northwest direction was 0.3629±0.0005 (0.3622-0.3634) by TIMS measurement and 0.365±0.008 (0.358-0.375) by QQQ measurement. These values are agreed within the margin of error although values by TIMS measurement are an order of magnitude better precision than those by QQQ measurement. Using average value and standard deviation in this study, it was calculated how much ^{137}Cs originated from FDNPS in 1 and 20 Bq of ^{137}Cs is distinguished from another source. Where, $^{135}Cs/^{137}Cs$ of 0.3728 was assumed as another source. It is possible to guarantee that at least 0.74 and 16.6 Bq, respectively, originated from 1F is distinguished by TIMS measurement.

This research is funded by the Secretariat of Nuclear Regulation Authority, Nuclear Regulation Authority, Japan.

Chinone, M., Terada, H., Nagai, H., Katata, G., Mikami, S., Torii, T., Saito, K., Nishizawa, Y. 2016. Utilization of $^{134}Cs/^{137}Cs$ in the environment to identify the reactor units that caused atmospheric releases during the Fukushima Daiichi accident. *Scientific Reports*, 6, 1-39.

Fujiwara, T., Saito, T., Muroya, Y., Sawahata, H., Yamashita, Y., Nagasaki, S., Okamoto, K., Takahashi, H., Uesaka, M., Katsunuma, Y., Tanaka, S. 2012. Isotopic ratio and vertical distribution of radionuclides in soil affected by the accident of Fukushima Dai-ichi nuclear power plants. *J. of Environ. Radioact.* 113, 37-44.

Impact of dynamic speciation in model simulations of river-discharged radionuclides in the marine environment

M. Simonsen[1,2], O.C. Lind[2], Ø. Saetra[1], P.E. Isachsen[1,3], H.-C. Teien[2], J. Albretsen[4], B. Salbu[2]

[1]Norwegian Meteorological Institute, P.O. Box 43, Blindern, Oslo NO-0313, Norway
[2]Centre of Environmental Radioactivity CoE, Faculty of Environmental Sciences and Natural Resource Management, Norwegian University of Life Sciences (NMBU), P.O. Box 5003, NO-1433 Ås, Norway
[3]Department of Geosciences, University of Oslo, P.O. Box 1047, Blindern, NO-0316 Oslo, Norway
[4]Institute of Marine Research, P.O. Box 1870 Nordnes, Bergen NO-5817, Norway
Keywords: Dynamic Cesium-137 speciation, Hypothetic nuclear accident scenario, River discharges, Lagrangian coastal dispersion model
Presenting author: Magne Simonsen, e-mail: magnes@met.no

In the marine environment, the radionuclide transport is affected by a number of processes, such as hydrodynamic advection and diffusion, turbulent mixing, sedimentation and resuspension. As the environmental transport and toxicity depend on the distribution of physico-chemical forms (species), numerical models should ideally include relevant species and dynamic transformation processes to properly predict marine transport and environmental impact of radionuclides. Aiming to improving the understanding of the impact of biogeochemical and geophysical processes, a numerical model system for marine radionuclide transport was developed and utilized (Simonsen et al., 2019). A new numerical code describing the distribution and transformation of radionuclide species was implemented in the transport model. These processes have commonly been neglected in previous studies, but including them was assumed to reduce the overall model uncertainty as the model became more in line with reality. However, these implementations also introduced new uncertainties, due to relatively large uncertainties associated with the descriptions (parameterizations) of the transformation processes.

A case study was performed where the model system utilized ocean circulation fields at relatively high spatial (160 m × 160 m in horizontal direction) and temporal resolution (1 hour), considering a hypothetical accident scenario including river discharges of ^{137}Cs to the marine environment in the southwestern coast of Norway. Dynamic interactions between low molecular mass (LMM) species, suspended particles and sediments was considered, as well as slowly reversible forms of the particles and sediments.

The results from this case study showed that due to knowledge gaps related to descriptions of transformation processes and difficulties in transferring locally observed features to generic algorithms, there are still considerable uncertainty involved in the predictions. The present study (Simonsen et al., 2019) has identified some of the key factors contributing to such uncertainties and their impacts on the transport estimates in a hypothetical case involving coastal dispersion of river-discharged ^{137}Cs. The effects of including interactions with solid matter were found to be considerable, locally affecting the results with orders of magnitude. The predicted transport was found to be sensitive to factors affecting the particle affinity, especially the fraction slowly reversibly bound to particles, but also regarding the particle size distributions, as increased settling reduced the transport away from the discharge points and increased the total exposure near the river mouths with up to a factor 10.

This work was supported by The Research Council of Norway through its Centre of Excellence (CoE) funding scheme (Project No. 223268/F50).

Simonsen, M, Lind, O.C., Saetra, Ø., Isachsen, P.E., Teien, H.-C., Albretsen, J., Salbu, B. 2019. Coastal transport of river-discharged radionuclides: Impact of speciation and transformation processes in numerical model simulations. *Science of the Total Environment*. 669, 856-871.

Improving emergency preparedness - spiked reference material production and emergency proficiency testing

K. Sobiech-Matura[1]*, H. Emteborg[1], M. Fujak[2], M. Hult[1], G. Lutter[1], G. Marissens[1], P. McGinnity[2], I. Osvath[2], S. Tarjan[3], R. Van Ammel[1]

[1] European Commission, Joint Research Centre, Retieseweg 111, B-2440 Geel, Belgium
[2] IAEA Environment Laboratories 4a, Quai Antoine 1er, 98000 Monaco
[3] IAEA Environment Laboratories, Friedensstrasse 1, 2444 Seibersdorf, Austria
Keywords: emergency preparedness, proficiency testing, spiking, reference material
Presenting author e-mail: Katarzyna.SOBIECH-MATURA@ec.europa.eu

In the European Union (EU), monitoring of the environment is an obligation resulting from the European Atomic Energy Community (Euratom) Treaty (2012) and derived legislation. The monitoring data are collected in the European Radiological Data Exchange Platform (EURDEP). This platform is maintained by the Radioactivity Environmental Monitoring (REM) group of the European Commission (EC) Directorate General (DG) Joint Research Centre (JRC) in Ispra (Italy).
A well-structured way of collecting and sharing the monitoring results is especially important in the event of a nuclear emergency. It is also vital that the measurement results provided by the laboratories are reliable and of high quality. In order to verify that, proficiency tests (PTs) for the EU monitoring laboratories have been regularly organised by the JRC in Geel (Belgium) since 2003.
The reference material used in the PT organised in 2017 was blank maize powder spiked with radioactive solutions of anthropogenic radionuclides ^{131}I, ^{134}Cs and ^{137}Cs. The spiking procedure was first tested on a small amount of rice powder material (Sobiech-Matura et al., 2016) and adapted when applied on a large quantity of powder to obtain good homogeneity.
The homogeneity and short-term stability tests of the PT material were performed according to ISO Guide 35 (2017). As the initial results of the homogeneity test of the bottled material were not satisfactory the material was recollected into metal drums. It was then frozen in liquid nitrogen, cryomilled and rebottled. The homogeneity study was repeated and found satisfactory. The short-term stability study of the material was performed for 4 weeks at two temperatures (40 °C and 60 °C). The linear regression and Student t-test were applied to the obtained count-rates. No trend was observed, therefore the material was considered stable under these conditions.
The characterisation of the material was performed by 4 expert laboratories (CEA Saclay, IAEA Monaco, IAEA Seibersdorf and JRC Geel). Each laboratory received 2-3 bottles of the PT material and was asked to report the mean massic activity together with its uncertainty for each radionuclide of interest in this study. The reference values used in the PT were calculated as power moderated means of the results from the expert laboratories.
The laboratories participating in this PT reported results in two modes – routine (obligatory, up to one month from the sample receipt) and emergency (voluntary, within 48 h from the sample receipt). Out of 120 participating laboratories, 70 reported emergency results. The reported results were evaluated according to the ISO 13528 (2015). According to the *z* score the reported results for all three radionuclides were compatible with the reference values in 97% of the cases. The evaluation according to the zeta (ζ) score revealed problems with uncertainty estimation. The participants' results were consistent with the uncertainty of the reference value to a level of 73% for ^{131}I, 79% for ^{137}Cs and only 57% for ^{134}Cs. One possible explanation for the poor ^{134}Cs results is lack of performing coincidence summing corrections for the PT sample.
The presented method of reference material production could be used in a nuclear (or radiation) emergency to provide monitoring laboratories with a suitable reference material to control the quality of the reported results. The whole production process from spiking to bottling, including cryomilling, can be finalised within 4 days.

EURATOM. 2012. Consolidated version of the Treaty establishing the European Atomic Energy Community. OJ C 327/01:1-107.

ISO 13528:2015, Statistical methods for use in proficiency testing by interlaboratory comparisons. International Organisation for Standardization, Geneva, Switzerland.

ISO Guide 35:2017, Reference materials - Guidance for characterization and assessment of homogeneity and stability. International Organisation for Standardization, Geneva, Switzerland.

Sobiech-Matura, K., Máté, B., Altzitzoglou, T. 2016. Spiked environmental matrix for use as a reference material for gamma-ray spectrometry: Production and homogeneity test. *Applied Radiation and Isotopes*. 109, 126-128.

Environmental radioactivity baseline study for disposal facilities

T. Sojakka[1]

[1]Posiva Oy, Olkiluoto, Eurajoki, 27160, Finland
Keywords: disposal facility, releases, baseline, environment
Tiina Sojakka, e-mail: tiina.sojakka@posiva.fi

As nuclear facilities in Finland are obliged to monitor their radioactive releases and their dispersion and transport in the environment during operation, respective baseline studies are also required. The baseline study shall be implemented before the construction or operation of a new nuclear facility has an impact on the concentrations of radioactive substances in the environment. (STUK 2016).

Posiva is building the final disposal facility for the spent nuclear fuel at Olkiluoto. The disposal facility consists of two sections: aboveground encapsulation plant and underground repository. Posiva implements baseline study concerning the environment of both of these nuclear facilities.

During operational period of Posiva's nuclear facilities some atmospheric and aqueous releases will occur to environment. Atmospheric releases from the disposal facility disperse mainly from the ventilation stack of the encapsulation plant yet releases are expected to be minor (Rossi & Suolanen 2013). Aqueous releases can occur in the effluent of encapsulation plant and in the incident and accident cases in the outlet waters of repository (Paunonen et al. 2015). During normal operation no radioactive releases occur from the repository.

Sampling targets for the baseline study were chosen based on possible release locations. The atmospheric dispersion from the encapsulation plant was modelled based on the wind and other weather conditions. The soil, vegetation and deposition samples are collected from different sector and distances around the disposal facilities. The outlet waters from the repository are running in an open ditch to the sea. This outlet ditch, vegetation around it and sea environment near the release location of the ditch (including e.g. seawater, sediments, bottom fauna, fishes and periphyton) are sampled for the baseline study. The radiological baseline of groundwater of the disposal site is also investigated by sampling shallow and deep drillholes.

To differentiate the sources of observed radionuclides, it is also important to identify appropriate aquatic and terrestrial control areas not affected, or at least affected as little as possible, by releases either from the encapsulation plant and the repository or from the nuclear power plant. Regardless of the positioning of the monitoring locations, analysis of the results of the environmental radioactivity monitoring programme of the nuclear power plant is important due to the overlapping atmospheric deposition patterns and water mixing conditions in the sea. (Posiva 2012)

Posiva's environmental baseline study started in summer 2018. Sampling is planned to continue until 2020. The radionuclides to be monitored include H-3, Am-241, C-14, plutonium isotopes and gamma emitters like Cs-137 and Sr-90. These include those expected to be released during normal operation, those of global fallout and those of interest in detecting unauthorised diversion of nuclear materials (Posiva 2012). The first results of radionuclide analyses have been compared with the results of nuclear power plants. The results seem to be consistent. For example, Co-60, originating from nuclear power plants, can be detected in the kelp samples near cooling water channel and south side of Olkiluoto but not in outer sea or north side of Olkiluoto where outlet ditch of repository locates (Figure 1.)

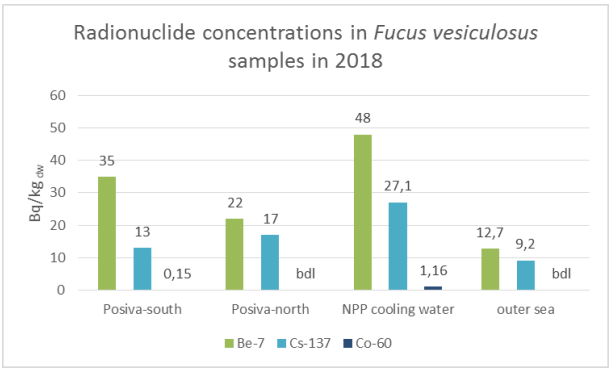

Figure 1. Radionuclide concentrations in Posiva's and nuclear power plant's kelp (*Fucus vesiculosus*) samples. (bdl= result **b**elow **d**etection **l**imit).

Paunonen, M., Nummi, O., Eurajoki, T. 2015. Waste Management of the Encapsulation Plant. Posiva Working Report 2015-51.

Posiva 2012. Monitoring at Olkiluoto – a Programme for the period before repository operation. Posiva Report 2012-01.

Rossi, J. & Suolanen, V. 2013. Operational safety analysis of the Olkiluoto disposal site (in Finnish). Posiva Working Report 2013-51.

STUK. 2016. Guide YVL C.7: Radiation monitoring in the environment of a nuclear facility. Radiation and Nuclear Safety Authority, Helsinki.

Rapid determination of polonium-210 for atmospheric application

L.J. Song, X.X. Dai*

China Institute for Radiation Protection, Taiyuan, 030000, China
Keywords:^{210}Po, Tellurium micro-precipitation, Stable element selenium; Source identification
L.J. Song, e-mail: songlj12@lzu.edu.cn

Polonium-210 (^{210}Po), an α-emitting radionuclide belong to the uranium-238 decay series with a half-life of 138 days, is of great concern due to its high toxicity: the lethal dose for ^{210}Po is only 1 μg for an adult (Harrison et al., 2007; Meli et al., 2017). As a highly volatile (evaporation occurs at 150 ℃) natural radionuclide, it could enter into the atmosphere through natural activities (Schmidt and Hamel, 2001) or human activities (Kim et al., 2005), and then undergo a long range transport with air masses (Nho et al., 1997). ^{210}Po is an effective indicator for tracing air-borne pollutants and has been widely used in investigating some atmospheric processes. For example, ^{210}Po has been applied to track the source of continental dust in an air mass, such as tracking dust transport from Africa (Bressan et al., 1973), and to study the removal or washout ratios, residence time, and exchange in air masses within or between the troposphere an stratosphere (Church et al., 2008; McNeary and Baskaran, 2007). Despite a vast amount of research on ^{210}Po in the atmosphere, very few studies have addressed the primary source of ^{210}Po in the metropolitan atmosphere due to its complex and diverse source components. However, prior to applying ^{210}Po as a tracer of air mass, especially air pollutants, it is critical to clearly identify its primary sources and its relationship with other elements or isotopes.

In our study, tellurium micro-precipitation was used to separate ^{210}Po from aerosol samples. Polonium-210 (^{210}Po) is studied in TSP and coal combustion samples for its potential application in tracing air pollutants. A significant seasonal variation of atmospheric ^{210}Po in Beijing was observed: winter > autumn > summer > spring. During the combustion of coal, ^{210}Po was highly enriched in fly ash but was depleted in bottom ash. Using selenium (Se) as an indicator of coal combustion, significantly positive correlation between ^{210}Po and Se in TSP samples (r2=0.705) revealed that coal combustion was a primary source of atmospheric ^{210}Po in Beijing. The mean emission factor of ^{210}Po from industry sector was found to be the highest (1.15 Bq kg^{-1}), followed by the residential (0.308 Bq kg^{-1}) and coal-fired power plant (0.0776 Bq kg^{-1}) sectors. The annual emission inventories of ^{210}Po from three coal consumer sectors (residential, coal-fired power plant, and industry) in 2016 in Beijing were estimated to be 1.49, 0.0729, and 1.36 GBq, respectively. The ratio of radioactive ^{210}Po and stable element Se (^{210}Po/Se) was creatively used as a combined indicator or fingerprint of coal combustion emission, which will contribute to the development of radioisotope tracer technology based on nuclide fingerprint database in the source identification of air pollutants.

This work was supported by China Institute for Radiation Protection (CIRP).

Harrison, J., Leggett, R., Lloyd, D., Phipps, A., Scott, B., 2007. Polonium-210 as a poison. *J. Radiol. Prot.* 27, 17–40.

Meli, M.A., Desideri, D., Roselli, C., Feduzi, L., 2017. ^{210}Po in human saliva of smokeless tobacco users. *Health. Phys.* 112, 28–32.

Schmidt, V., Hamel, P., 2001. Measurements of deposition velocity of radon decay products for examination of the correlation between air activity concentration of radon and the accumulated Po-210 surface activity. *Sci. Total. Environ*. 272, 189–194.

Kim, G., Hong, Y.L., Jang, J., Lee, I., Hwang, D.W., Yang, H.S., 2005. Evidence for anthropogenic 210Po in the urban atmosphere of Seoul, Korea. Environ. *Sci. Technol.* 39, 1519–1522.

Nho, E.Y., Cloarec, M. F.L., Ardouin, B., Ramonet, M., 1997. 210Po, an atmospheric tracer of long-range transport of volcanic plumes. *Tellus B* 49, 429–438.

Church, T.M., Sarin, M.M., 2008. Chapter 2 U- and Th-series nuclides in the atmosphere: supply, exchange, scavenging, and applications to aquatic processes. *Radioactiv. Environ.* 13, 11–47.

Bressan, D.J., Larson, R.E., Wilkniss, P.E., 1973. Atmospheric radon and dust, air mass trajectories and meteorological conditions over the Greenland Sea. *Nature*. 245, 74–77.

McNeary, D., Baskaran, M., 2007. Residence times and temporal variations of ^{210}Po in aerosols and precipitation from southeastern Michigan, United States. *J. Geophys. Res.* 112, D04208–D04218.

Direct speciation of radionuclides in plant parts by Time-resolved Laser Fluorescence Spectroscopy (TRLFS) and Desorption Electrospray Ionization Mass Spectrometry (DESI MS)

J. Stadler[1], A. Kogiomtzidis[1], M. Steppert[1], M. Schmidt[2], N. Huittinen[2], M. Weiss[1], F. Köhler[1], T. Stumpf[2], C. Walther[1]

[1]Institute of Radioecology and Radiation Protection, Leibniz University Hannover, Hannover, D-30419, Germany
[2]Helmholtz-Zentrum Dresden – Rossendorf, Institute of Resource Ecology, Dresden, D-01328, Germany
Keywords: TRLFS, DESI MS, Speciation, Radionuclides
Julia Stadler, e-mail: stadler@irs.uni-hannover.de

^{241}Am is an important radionuclide and currently the dominating α-emitter in the Chernobyl exclusion zone due to continuous buildup from its precursor ^{241}Pu ($t_{1/2}$ = 14.35 a) by beta decay. There is a high possibility, that americium transfers into plant parts via contaminated soil and eventually enters the human food chain. For a better understanding of the uptake mechanism on a microscopic scale, its chemical speciation has to be investigated. Bioavailability proves to differ for the various possible compounds that can be formed in soil and during the uptake process. Therefore, the ambient *Desorption Electrospray Ionization Mass Spectrometry* (DESI MS) (Takáts et al., 2004) technique was introduced for the speciation directly in plant parts. In combination with *Time-Resolved Laser Fluorescence Spectroscopy* (TRLFS) (Fellows et al., 2003), it represents a promising method for chemical speciation.

First results were obtained for europium as non-radioactive homologue for the trivalent actinides. Different crops were grown in a liquid HOAGLAND medium (Gupta et al., 2013) providing a controlled environment for plant growth and experiments. Eu was quantified (Inductively Coupled Plasma Mass Spectrometry) and localized (Scanning Electron Microscope with Element Dispersive X-ray analysis) in the plant parts root, stem, leaf, and fruit. The direct analysis with DESI MS shows the uptake of Eu in form of its Hoagland species (Figure 1). These species were identified by comparison of previous ESI MS measurements from the contaminated nutrition medium. Furthermore, TRLFS analysis exhibits high $^7F_1$ to $^7F_2$ ratios increasing from root > stem > leaf > fruit and differences in the speciation in fruit & leaf and stem & root (Figure 2). The signal splitting in the emission spectra from fruit and leaf indicates a well-defined coordination geometry of the Eu species, possibly a crystallization in a tetragonal symmetry. Based on the fluorescence lifetimes, Eu oxalate, phosphate and phytate were identified as possible species directly in plant parts, by comparison with reference solutions with different concentration ratios and pH.

Next steps will include the identification of further species and their determination with more DESI MS measurements. This direct analysis of radionuclides and their homologues proves to be a promising approach for speciation in complex matrices.

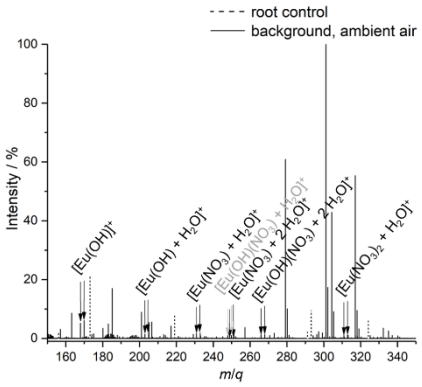

Figure 1. DESI MS spectrum of a root from *Secale cereal* (*L.*) and identified Eu HOAGLAND species.

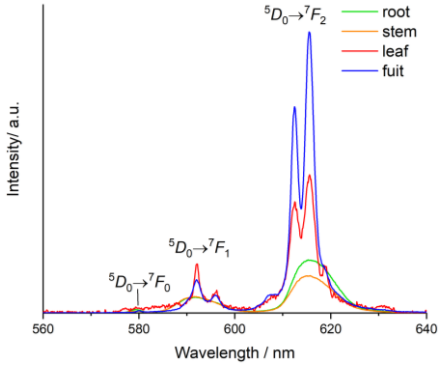

Figure 2. TRLFS spectra of the plant parts root, stem, leaf and fruit from *Phaseolus vulgaris* (*L.*).

This work was supported by the Siebold-Sasse-Foundation.

Takáts, Z., Wiseman, J.M., Gologan B., Cooks R.G. 2004. Mass Spectrometry Sampling Under Ambient Conditions with Desorption Electrospray Ionization. *Science*. 306, 471-473.

Fellows, R.J., Wang, Z., Ainsworth, C.C. 2003. Europium Uptake and Partitioning in Oat (Avena sativa) Roots as Studied by Laser-Induced Fluorescence Spectroscopy and Confocal Microscopy Profiling Technique. *Environ. Sci. Technol.* 37, 5247-5253.

Gupta, D.K., Inouhe, M., Rodríguez-Serrano, M., Romero-Puertas, M.C., Sandalio, L.M. 2013. Oxidative stress and arsenic toxicity: Role of NADPH oxidases. *Chemosphere*. 90, 1987-1996.

Beryllium from 7th heaven

P. Steinmann, D.M. Lienhard, and S. Estier

Swiss Federal Office of Public Health (SFOPH), Bern, CH-3003, Switzerland
Keywords: Be-7, Na-22, atmosphere
philipp.steinmann@bag.admin.ch

We explore the by now 25-year time series of weekly measurements of ^{7}Be in ground level air in Switzerland. We currently sample aerosol at 6 lowland stations in Switzerland using high volume samplers (HVS) which filter 100'000 to 150'000 m3 of air each week. The filters are pressed and then analysed using HPGe gamma spectrometry. A smaller sampler is operated at the alpine research station at Jungfraujoch (3'500 m a.s.l., 5'500 m3 weekly samples), while daily samples (700 m3) are taken at the HVS station in Berne. Although the main focus of our work is on the detection of artificial radionuclides, the natural ^{7}Be provides valuable information relevant for the proper interpretation of the data. This isotope's negative correlation with solar activity is clearly demonstrated by comparing the annual averages of ^{7}Be and cosmic neutron flux, respectively. Deviation from the expected behaviour can be explained by meteorological parameters like annual precipitation or average temperature. On a shorter time-scale the connection between cosmic radiation and ^{7}Be in ground level air becomes less apparent. Meteorological phenomena such as scavenging of aerosol particles during rain-events or increased vertical mixing during thunderstorms seem to be dominant factors in these smaller time windows. Yet we hypothesize that the lunar cycle and/or the solar rotation – both with a period of roughly one month – might also influence the distribution of ^{7}Be and therefore be visible in our data.

Looking at the ^{22}Na to ^{7}Be ratio of the samples confirms previous findings (Steinmann et al., 2013) of a maximum in May, consistent with an increased stratosphere-troposphere exchange at that time of the year. However, in the Swiss samples ^{7}Be continues to increase and stays high during the summer. This behaviour is not observed in more northern locations and not predicted by atmospheric circulation models. It may have to do with a more vigorous vertical convective air exchange close to the alps in summer.

Steinmann P., Zeller M., Beuret P., Ferreri G., Estier S., 2013. Cosmogenic ^{7}Be and ^{22}Na in ground level air in Switzerland (1994-2011). *Journal of Environmental Radioactivity* 124, 68-73.

Transfer of radiocesium from irrigation water to rice

Y. Suzuki[1], T. Iizuka[1], T. Matsubara[1], R. Inaba[1], S. Miyazu[2], T. Gomei[3], K. Ito[3], M. Shin[4], N. Yoshikawa[2], N. Nogawa[4], K. Suzuki[5], N. Harada[2]

[1] Graduate School of Science and Technology, Niigata University, Niigata, 950-2181, Japan
[2] Institute of Science and Technology, Niigata University, Niigata, 950-2181, Japan
[3] Aichi Tokei Denki Co., Ltd, Nagoya, 456-8691, Japan
[4] Faculty of Food and Agricultural Sciences, Fukushima University, Fukushima, 960-1296, Japan
[5] Institute for Research Promotion, Niigata University, Niigata, 950-2181, Japan
Keywords: ^{137}Cs, FDNPP accident, Irrigation water, Rice
Presenting author, e-mail: f17m001a@mail.cc.niigata-u.ac.jp

A large amount of radionuclides was released to the northeastern part of Japan by the Fukushima Daiichi Nuclear Power Plant (FDNPP) accident, and risk of radiocesium (^{134}Cs+^{137}Cs) contamination of crops is still concerned. We reported that ^{137}Cs concentration in rice collected near the water inlet was significantly higher than those collected at the centre of the rice fields and near the water outlet (Y. Suzuki et al., 2019). Considering that a large amount of water is used in paddy fields, this result suggests that irrigation water might be one of the sources of ^{137}Cs in rice. Here we conducted field and pot experiments to clarify effect of irrigation water on ^{137}Cs concentration in rice and investigated how to suppress ^{137}Cs uptake by rice.

[**Field experiment**] A field experiment was conducted in three decontaminated paddy fields in Fukushima, Japan, during 2016-2018. Three experimental treatment plots (each 5×80 m) were prepared as follows: 1) conventional cultivation (CT), 2) cultivation at four times planting density at 0-2 m from the inlet (DP_2), 3) cultivation with a no-planting zone until 50 m from the inlet (NP_{50}) (n=3). In the different year, two treatment plots were prepared as follows: 1) CT and 2) cultivation with a no-planting zone until 5 m from the inlets (NP_5) (n=3). Soil (0-15 cm), rice (brown rice + straw) and surface water samples were collected at several points according to the distance from the water inlet in each plot. ^{137}Cs concentrations in the samples were determined by an NaI(Tl) scintillator or a Ge semiconductor detector. As a result, ^{137}Cs concentrations in brown rice collected at 1 m point from the water inlet was 10.8 Bq/kg in CT, which were higher than 5.66 Bq/kg at 80 m point (Fig. 1). In DP_2, ^{137}Cs concentrations in brown rice collected in points away from 3 m were lower than those in CT. Suppression of ^{137}Cs concentration in rice by no-planting until 50 m from the inlet was not shown. ^{137}Cs concentrations in brown rice and rice straw collected 5-20 m from the inlet (0-15 m from the point with starting cultivation) in NP_5, were lower than those in CT. These results suggest that introduction of no-planting zones near the water inlets can reduce ^{137}Cs concentrations in brown rice.

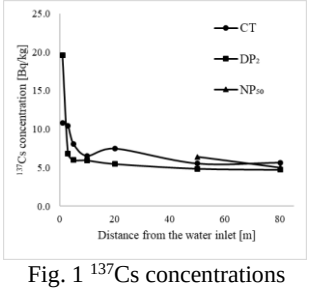

Fig. 1 ^{137}Cs concentrations in brown rice in the field experiment.

[**Pot experiment 1**] A pot experiment was conducted in Fukushima to clarify the effect of ^{137}Cs in irrigation water on ^{137}Cs uptake by rice. Soil samples collected from the rice fields in Fukushima (^{137}Cs: 2590 Bq/kg) and Niigata (^{137}Cs: 37.9 Bq/kg) were used. Each pot was placed in the containers (800×560×480 cm), and irrigation water pumped up from river was supplied to the containers. Soil and rice samples were collected at the harvesting and the ^{137}Cs concentrations were determined. As a result, the average ^{137}Cs concentration in brown rice grown in Niigata soil was 25.6 Bq/kg, which showed no significant difference from that in Fukushima soil (26.2 Bq/kg). This result indicates that ^{137}Cs in irrigation water can affect ^{137}Cs concentration in rice regardless of the soil ^{137}Cs concentration.

[**Pot experiment 2**] Another pot experiment was conducted in a green house in Niigata University to elucidate transfer of ^{137}Cs to rice from suspended solid in irrigation water. Soil was collected in Niigata prefecture and tap water was used as the water source. Bottom sediment collected from an agricultural dam in Fukushima was applied onto the soil surface of a pot at the transplantation (May), mid-summer drainage (June), heading stage (July) or ripening stage (August). The application rate was 400 Bq/pot. At the harvest, soil and rice samples were collected and the ^{137}Cs concentrations were measured. As a result, 0.3-2.2% of ^{137}Cs in the sediment was translocated into rice. When the sediment was applied at the heading stage, the highest ^{137}Cs uptake by rice was observed.

We confirmed that ^{137}Cs concentrations in rice near the water inlet was higher than other points. Furthermore, we found 3 new findings: 1) effect of irrigation water on ^{137}Cs concentrations in rice can be reduced by introduction of a no-planting zone or dense-planting zone with inedible rice near the water inlet, 2) ^{137}Cs in irrigation water can increase ^{137}Cs concentration in rice, even if the soil ^{137}Cs is low enough, and 3) ratio of ^{137}Cs transfer from suspended solid in irrigation water deposited onto soil surface to rice ranges between 0.3-2.2% and was highest at the heading stage.

Y. Suzuki, R. Shoji, T. Tsurumaki, T. Matsubara, S. Tamaki, K. Nakashima, R. Tsuruta, N. Yoshikawa, H. Ishii, N. Nogawa, M. Nonaka, N. Harada 2019. Yearly Changes in Rice and Soil Radiocaesium Concentrations in Minamisoma City, Fukushima Prefecture, Japan - Monitoring Results from 2013 to 2016-. *RADIOISOTOPES*. Vol.68, 1, 1-12 (Japanese).

Determination of radon leakage from sample container for gamma spectrometry measurement of ^{226}Ra

N.S. Syam[1,2], S.Y. Lim[1], H.Y. Lee[1,3], S.H. Lee[1]

[1]School of Architectural, Civil, Environmental, and Energy Engineering, Kyungpook Nat'l Univ., Daegu, 41566, Korea
[2]Nuclear Energy Regulatory Agency (BAPETEN), Jakarta, 10120, Indonesia
[3]Radiation Science Research Institute, Kyungpook Nat'l Univ., Daegu, 41566, Korea
Keywords: radon leak
age, gamma spectrometry, RAD7, HPGe
Presenting author (S.Y. Lim), e-mail: sy940103@gmail.com

Gamma spectrometry is widely used for natural radionuclide measurement including ^{226}Ra measurement because it is versatile, easy to implement, non-destructive, and relatively cheap method compared to other methods. By gamma spectrometry, ^{226}Ra can be determined directly using its energy peak of 186.21 keV or its decay products which are in secular equilibrium with the ^{226}Ra, i.e. ^{214}Bi and ^{214}Pb. However, both methods have challenges, as have been demonstrated in previous studies (Mauring and Gafvert, 2013). For direct measurement of ^{226}Ra, interfering from ^{235}U energy peak of 185.57 keV can add significant contribution to the 186.21 keV of ^{226}Ra gamma peak (Baumgartner, 2017; Lee et al., 2000). Consequently, to obtain an accurate result of radium concentration by direct measurement, accurate quantity of ^{235}U is needed, which not always can be obtained easily by some gamma spectrometry systems such as P-type HPGe (High Purity Germanium) detector. On the other hand, for indirect measurement using energy peaks of ^{214}Bi and ^{214}Pb, which are decay products of ^{222}Rn gas, longer time for their equilibrium (28 days) is needed than direct measurement. Also, the tightness of container from radon leakage must be ensured. In some measurements, the equilibrium could not be reached due to radon leakage from sample container.

Therefore, in this paper the radon leakage from three different sealing methods of Marinelli beaker is studied to determine the fraction of radon leaked from sample container, using radon accumulation chamber and RAD7, as shown in Figure 1.

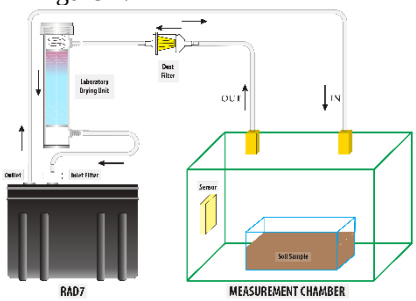

Figure 1. Experimental setup for released-radon measurement.

Soil sample taken from Uljin, county of Korea is used in this study. The soil was cleaned from physical impurities, crushed, and sieved to 2 mm and then dried at 110°C for 24 hours. The sample was then put in the two Marinelli beakers, sealed, and one measured by RAD7 and the other by HPGe detector. The three sealing methods are: without sealing (MB1), sealed with paraffin film (MB2), and sealed with vacuumed plastic bag (MB3).

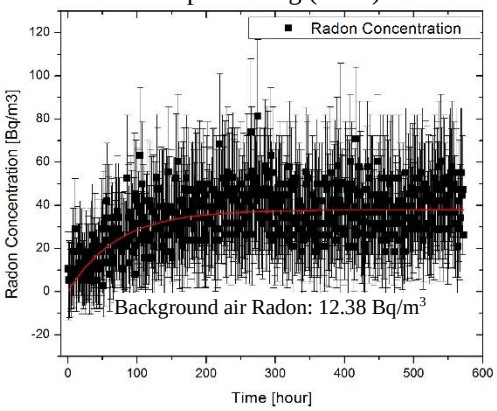

Figure 2. ^{222}Rn concentration build-up from MB1 measured by RAD7.

The radon concentration build-up inside the chamber for each of three different sealed Marinelli Beakers measured with RAD7, as shown in Figure 2 for MB1, is compared to the radon build-up from soil sample placed on an opened plate inside the chamber. The radon leakage rate from accumulation chamber and radon concentration in background air are also measured and considered for radon leakage determination.

This work was supported by KOREA HYDRO & NUCLEAR POWER CO., LTD (K-CLOUD Project 2017-TECH-08).
One of the authors (N.S. Syam) is granted a PhD scholarship through Research and Innovation in Science and Technology Project (RISET-Pro) from Ministry of Research, Technology, and Higher Education, Indonesia.

Mauring, A. and Gafvert, T. 2013. Radon tightness of different sample sealing methods for gamma spectrometric measurements of ^{226}Ra. *Applied Radiation and Isotopes*. 81, 92-95.

Baumgartner, A. Stietka, M. Kabrt, F. Wiedner, H. Maringer, F. J. 2017. Study of particular problems appearing in NORM samples and recommendations for best practice gamma-ray spectrometry. *Applied Radiation and Isotopes*. 126, 285–288.

Lee, K. Y. Yoon, Y. Y. Seo, B. K. 2000. A new aluminium container for γ-ray spectrometry analysis of radium and radon. *Analytical Science and Technology*. 13-6, 743-750.

Influence of humidity to exhalation of radon and thoron from building materials, and analysis of their radiological risk in indoor environment

A.C. Syuryavin [1,2], S.J. Park[1], M.M. Nirwono[1,2], S.H. Lee [1]

[1]School of Architectural, Civil, Environmental, and Energy Eng., Kyungpook National Univ., Daegu, 41566, Korea
[2]Nuclear Energy Regulatory Agency of Indonesia (BAPETEN), Jakarta, 10120, Indonesia
Keywords: radon exhalation, indoor environment, effective dose
Presenting author (A.C. Syuryavin), e-mail: a.ciptadi@bapeten.go.id

A part of radon, which is produced mainly on the surface layer of the minerals can eject out of the grains and may emanate into the interstitial space between them. These radon atoms exist in gaseous form and spread into the pore space driven by diffusion and advection. Some radon gas will eventually migrate upwards to the air interface and exhales out into the atmosphere. The characterization of this transfer process is crucial for the understanding of the following fate of the radioactive rare gas: either as trace substance in atmospheric dispersion or as accumulating contaminant in the indoor environment.

A German case control study on indoor radon (Wichmann et al., 2002) and the corresponding extrapolations of data from miners suggest that exposure to residential radon contributes in a relevant manner to the lung cancer risk in the general population. Even though it cannot be ascertained how significant the influence of radon and thoron on lung cancer, a more in-depth study of the exhalation of radon and thoron especially inside room still needs to be done to dig deeper information considering that nowadays about 80% of human time is in room.

When relative humidity of the ambient atmosphere is high the higher water content in the air will lead to greater deposition of aerosols on the internal building surfaces, which will lower the ^{222}Rn and ^{220}Rn emanation rates and reduce the gas concentrations (Janik et al., 2015). In this paper, we conduct an experiment on influence of humidity to the level of radon and thoron exhalation. For further research, it will be analyzed the annual effective dose caused by indoor radon and thoron to obtain how significant is radon or thoron contribution in environmental radiation.

To get more information and higher benefit, building materials from Indonesia and Korea which typically has different geological characteristic were chosen. Indonesia is a tropical country that is identical with active volcanoes (included in a Ring of Fire region), has many islands and seas, and prone to earthquakes; while Korea is a subtropical country with very few volcanoes and relatively safe from earthquakes.

The rate of exhalation of ^{222}Rn and ^{220}Rn has been obtained by the technique of accumulation in sealed chamber equipped with RAD7. The chamber has been characterized to determine the leak. To maintain relative humidity of the system, a desiccant is connected between RAD7 inlet and the accumulation chamber. In Figure 1 and 2 we show the equipment setup for the accumulation experiences and the accumulation curves of concentration ^{222}Rn and ^{220}Rn obtained.

Figure 1. System of exhalation measurement.

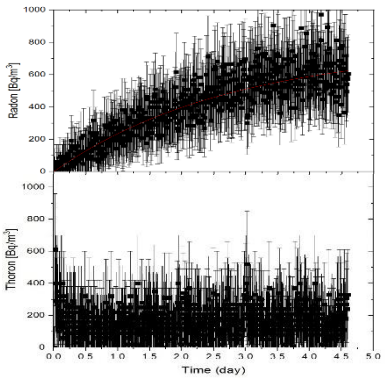

Figure 2. Radon and thoron concentration as a function of time in an accumulation chamber.

The activity concentrations of natural ^{226}Ra and ^{232}Th were measured using a p-type HPGe spectrometer model GEM15P4-70. The detector has 15% relative efficiency and it works coupled to an ORTEC Maestro-32 multichannel analyzer.

One of the authors (Ahmad Ciptadi Syuryavin) is granted a PhD scholarship through Research and Innovation in Science and Technology Project (RISET-Pro) from Ministry of Research, Technology, and Higher Education, Indonesia. This work is also supported by KOREA HYDRO & NUCLEAR POWER CO., LTD (K-CLOUD Project 2017-TECH-08).

Janik, M., Omori, Y., Yonehara, H. 2015. Influence of humidity on radon and thoron exhalation rates from building materials. *Appl. Rad. & Isotopes*, 95, 102-107.

Application biochar into the soil – if it influence for environmental radioactivity?

K. Szewczak[1], S. Jednoróg[2], K. Wołoszczuk[3], R. Szlązak[1], Z. Podgórska[3], A. Rafalska-Przysucha[1], Ł. Gluba[1], M. Łukowski[1]

[1] Institute of Agrophysics of Polish Academy of Sciences, Lublin,20-290, Poland
[2]Institute of Plasma Physics and Laser Microfusion, Warsaw, 01-497, Poland
[3]Central Laboratory for Radiological Protection, Warsaw, 01-194, Poland
Keywords: biochar, environmental radioactivity, activity concentration in soil
Presenting author, e-mail: Kamil Szewczak, k.szewczak@ipan.lublin.pl

The biochar find the broad application in the agriculture at the recent time. The properties of the biochar help to improve the quality of the soil by decontaminating from heavy metals or pesticides. The presented work shows the first results to improve the impact of the biochar for radiological condition of soil. We investigated the activity concentration of natural and anthropogenic radioisotopes at soil samples collected from field with various doses of biochar applied. In addition the direct measurements of radon exhalation rate were conducted. The analysis were performed using gamma spectrometry and active radon exhalation measurements utilizing accumulation box with AlphaGUARD instrument.

The increase trend of Bi-214 and Pb-214 as well as decrease of Ac-228 depending on the applied biochar were visualized. Rest of analyzed isotopes exhibited stable values.

The average increase by 6 mBq m^{-1} s^{-1} for radon exhalation rate depending on biochar dose was observed.

As a conclusion it was proved that the application of biochar into the soil have an observable influence for radiological condition of soil.

Concluding it was proved that application of biochar into the soils have observable influence on the radiological aspect of environment.

The research was partially conducted under the projects "Water in soil – satellite monitoring and improving the retention using biochar" no. BIOSTRATEG3/345940/7/NCBR/2017, which was financed by the Polish National Centre for Research and Development in the framework of "Environment, agriculture and forestry" – BIOSTRATEG strategic R&D programme.

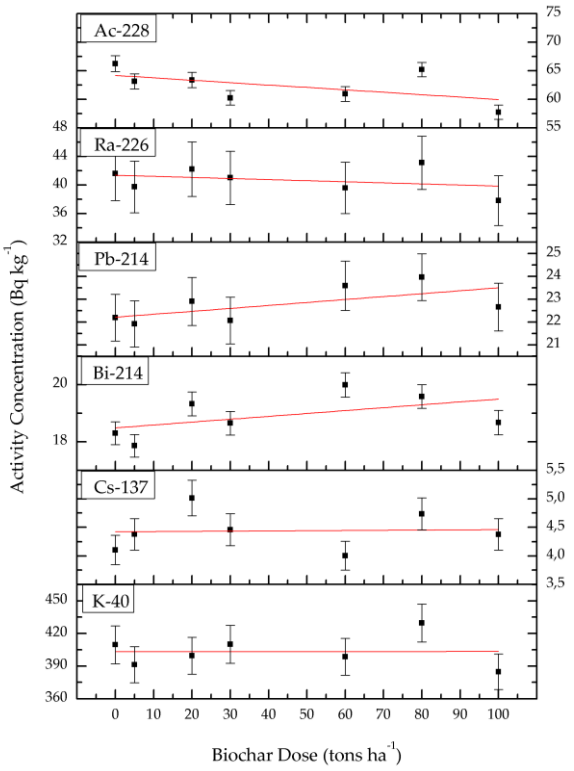

Figure 1. Fluctuation of activity concentration for six radioisotopes on soil samples depending on biochar dose.

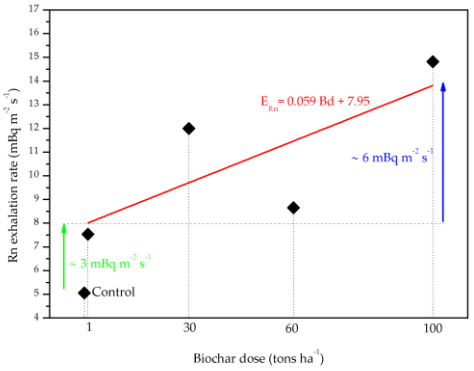

Figure 2. Influence of biochar applied into the soil for radon exhalation rate.

Iodine-129 as an environmental tracer for salinity origin in groundwater samples in Pampanga, Philippines

S.V. Tan[1], A.T. Bautista VII[2], N. DS. Mendoza[2], C.T. Racadio[2], M. Puthenpurekal[3], A.C. Resurreccion[1], H. Matsuzaki[4]

[1]Environmental Engineering Program, University of the Philippines, Quezon City, 1101, Philippines
[2]Department of Science and Technology - Philippine Nuclear Research Institute (DOST-PNRI), Quezon City, 1101, Philippines
[3]Department of Environment and Natural Resources - Mines and Geosciences Bureau (DENR-MGB), Quezon City, 1100, Philippines
[4]Micro Analysis Laboratory, Tandem accelerator (MALT), University of Tokyo, Bunkyo-ku, 113-8654, Japan
Keywords: ^{129}I, AMS, hydrology, water resource management
Presenting author, e-mail: spvtan@gmail.com

Assessing groundwater vulnerability to salinity contamination is important in order to meet the increasing demand for freshwater. Iodine-129 (^{129}I, half-life = 15.7 million years), a radioisotope of iodine, was used as an environmental tracer for possible origins of salinization in groundwater (i.e., natural rock weathering, seawater, connate water, contamination). In July 2017 (wet season), one hundred four (104) water samples were taken from production wells (90-150 meters below ground level), rivers and precipitation in Pampanga, a province in the Philippines that relies heavily on groundwater for freshwater source. Hydrogeochemical (mainly Cl) and stable water isotopes (δ^2H and δ^{18}O) were able to identify six (6) samples potentially affected by seawater intrusion. ^{129}I/^{127}I ratio vs. 1/^{127}I graph depicted the origin of the water samples and its interaction from various recharge sources (Figure 1). Iodine-129 vs. Chloride graph was capable of showing a clear distinction between different salinity origins (Figure 2). A conceptual model was produced to summarize the results (Figure 3). In addition, Iodine-129 spatial distribution map may also be indicative of groundwater age. The results of this study will be helpful to the government, civil society, and other organizations for monitoring, policymaking, and management of the groundwater and the subsurface formations that will be crucial to continuously supply the water needs of the present and future generation.

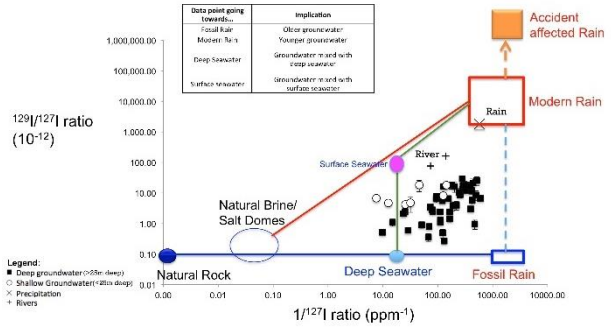

Figure 1. ^{129}I/^{127}I ratio vs. 1/^{127}I graph with groundwater, river and precipitation/rain data in Pampanga. The implication of data location is explained also in the table in the upper right of the figure.

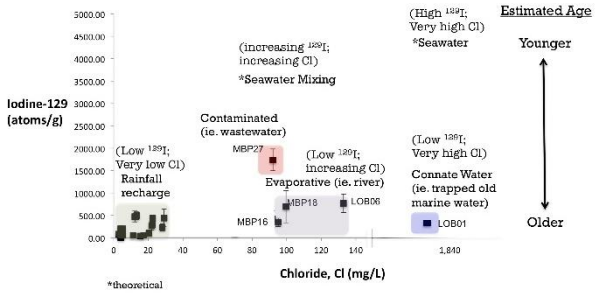

Figure 2. Iodine-129 vs. Cl graph identifies various salinization processes plotted results with error bars showing the 6 samples (with labels) identified of its salinity origin. Relative groundwater age is also implied.

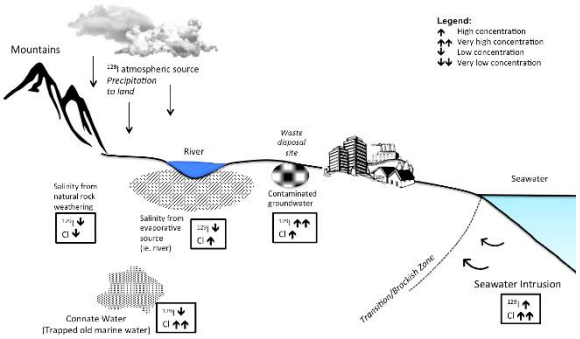

Figure 3. A cross section showing the conceptual model on different salinity origins in groundwater based on the samples taken in Pampanga for this research. Salinity from natural rock weathering, evaporative sources and connate water show low Iodine-129 due to non-exposure to Iodine-129 anthropogenic sources. Chloride (Cl) is relatively low for salinity derived from natural rock weathering and increases as salinity comes from an evaporative source (ie. river, lakes). Cl is notably high for connate water, as it is trapped old marine water. Contaminated groundwater shows an elevated value of Iodine-129, indicating it to be young water exposed recently from Iodine-129 anthropogenic source, with high Cl. Salinity from seawater intrusion has a signature of high Iodine-129 and very high Cl.

Removal of selected gamma and alpha radionuclides from aquatic solutions using *Chlamydomonas reinhardtii*, *Scenedesmus obliquus* and *Chlorella vulgaris*

D. Tatarová[1], D. Galanda[1], J. Kuruc[1], B. Gaálová[2]

[1]Department of Nuclear Chemistry, Faculty of Natural Sciences, Commenius University, Bratislava, 84215, Slovakia
[2]Department of Microbiology and Virology, Faculty of Natural Sciences, Commenius University, Bratislava, 84215, Slovakia
Keywords: microalgae, bioremediation, radioisotopes
D. Tatarová, e-mail: tatarova.d@gmail.com

Nuclear activities and accidents on nuclear facilities generate radionuclides which require processes for their decontamination. A variety of environmental restoration techniques have been developed but these methods may be expensive if large areas of lands and water are involved. For this reason, the research about bioremediation started with the need to develop and discover more suitable species for bioremediation of radioactively contaminated areas. The well-known species used for bioremediation are plants like hemp (*Cannabis sativa*) (Hoseini et al., 2012). However, microorganisms seem to be more effective in the terms of bioremediation as a unicellular organism well-known for radiation resistance. Microalgae with fast growth rates and small size provides low volume radioactive waste after removal of radionuclides from polluted area and are therefore promising alternative species for bioremediation of radioactive contaminated areas. They possess large cell wall surface, which is interesting for decontamination by biosorption and metabolic-dependent mechanisms. The 50% lethal dose (LD_{50}) of ionizing radiation for algae generally falls in the 30–1200 Gy range (IAEA, 1976) with exception of extremophilic microalga recently found in nuclear facilities, *Coccomyxa actinabiotis* nov. sp. which strongly accumulates radionuclides, including ^{238}U, ^{137}Cs, ^{110m}Ag, ^{60}Co, ^{54}Mn, ^{65}Zn, and ^{14}C (Rivasseau et al., 2013).

This paper is focused on radioactive removal using green microalgae *Chlamydomonas reinhardtii*, *Scenedesmus obliquus* and *Chlorella vulgaris*. *C. reinhardtii* is often used as a model organism to investigate various biological functions and removal of radionuclides was found out by authors Ciorba and Truta (2012). *S. obliquus* is suitable to produce biofuels, thanks to rapid cell growth, efficient CO_2 fixation, lipid accumulation, and the ability to grow in contaminated waters (Gris et al., 2014) and can uptake radionuclides (Adam and Garnier-Laplace, 2003). Removal of heavy metals (Fraile et al., 2004) and radionuclides (Vogel et al., 2011) have been also found in *C. vulgaris*.

Solutions for experiments with *C. reinhardtii* and *S. obliquus* consisted of microbial suspension of each microalga and mixture of ^{137}Cs and ^{60}Co in chloride form. Samples were prepared in different pH values (2–9). The main goal was to determinate removal of ^{137}Cs and ^{60}Co from aquatic solutions by measuring decrease of activity of radionuclides in time. The removal of radionuclides (^{241}Am and ^{239}Pu, respectively), in aquatic solutions using *C. vulgaris* was evaluated in alpha spectrometric system by measuring decrease of activity of radionuclides in time.

This work was supported by the Commenius University under grant UK/444/2019.

Hoseini, P.S., Poursafa P., Moattar F., Amin, M.M., Rezaei, A.H. 2012. Ability of phytoremediation for absorption of strontium and cesium from soils using *Cannabis sativa*. *Int. J. Env. Health Eng.* 1, 17.

Rivasseau, C., Farhi, E., Atteia, A., Couté, A. et al. 2013 An extremely radioresistant green eukaryote for radionuclide bio-decontamination in the nuclear industry. *Energy Environmental Science*, Royal Society of Chemistry. 6, 1230 – 1239.

Effects of ionizing radiation on aquatic organisms and ecosystems. Technical reports series 172, 1976. International Atomic Energy Agency. Vienna, Austria. 143 p. ISBN:92-0-125076-2.

Ciorba D., Truta A. (2012) Cytotoxic exposure of green algas Chlamydomonas Peterfii Gerloff in radon aerosols. *Romanian J. of Physics*. 58, 73-83.

Gris B., Morosinotto T., Giacometti G. M., Bertucco A., Sforza E. (2014) Cultivation of *Scenedesmus obliquus* in photobioreactors: effects of light intensities and light-dark cycles on growth, productivity, and biochemical composition. *Appl. Biochem. and Biotechnol.*, 172(5), 2377-89.

Adam, C., Garnier-Laplace, J. (2003) Bioaccumulation of silver-110m, cobalt-60, cesium-137, and manganese-54 by the freshwater algae *Scenedesmus obliquus* and *Cyclotella meneghiana* and by suspended matter collected during a summer bloom event. *Limnology and Oceanography*. 48, 2303–2313.

Fraile, A., Penche, S., González, F. et al. (2004) Biosorption of copper, zinc, cadmium and nickel by Chlorella vulgaris. *Chem.y and Ecology*. 21(1), 61-75.

Vogel M., Günther A., Gube M., Raff J., Kothe E., Bernhard G. 2011 Interaction of *Chlorella vulgaris* and *Schizophyllum commune* with U(VI). In: Merkel B., Schipek M. (eds) The New Uranium Mining Boom. Springer Geology. Springer. pp. 185-192. e-ISBN 978-3-642-22122-4

Reconstruction of temporal change of radiocesium level in demersal fish off Fukushima

Y. Tateda[1], K. Misumi[1], D. Tsumune[1], M. Aoyama[2], Y. Hamajima[3], and T. Aono[3]

[1]Environmental Science Research Laboratory, Central Research Institute of Electric Power Industry, Abiko, Chiba, 270-1194, Japan
[2]Center for Research in Isotopes and Environmental Dynamics, University of Tsukuba, Tsukuba, Ibaraki, 305-8577, Japan
[3]Low Level Radioactivity Laboratory, Institute of Nature and Environmental Technology, Kanazawa University, Nomi, Kanazawa, 923-1224, Japan
[2]National Institute for Quantum and Radiological Science and Technology, Inage, Chiba, 263-8555, Japan
Keywords: radiocesium, Fukushima accident, marine demersal fish, dynamic model
Presenting author, e-mail: tateda@criepi.denken.or.jp

The $^{134+137}$Cs were released to continental environment along eastern Japan by the accident of Fukushima Dai-ichi Nuclear Power Plant (1FNPP). The radiocesium level in seawater was decreased by diffusion (Tsumune et al., 2012), while the level in bottom sediment was remained substantial (TEPCO 2019). The radiocesium in marine sediment was suggested to transfer to benthos (Wang et al., 2016), and was hypothesized to contribute to the decrease rate delay of radiocesium level in demersal fish by feeding those benthos (Tateda et al., 2016). In this study, to evaluate sediment contribution in radiocesium transfer in benthic food chain, temporal change of radiocesium level in stomach content of demersal fish was analysed and reconstruct temporal radocesium levels demersal fish using dynamic model.

Using the absorption/desorption kinetic parameters in different pore size by sediment adsorption/desorption model (Misumi et al., 2014), temporal change of radiocesium concentrations in fine sediment (< 75 μm) at seabed surface off Fukushima were simulated using temporal seawater level simulated by the regional ocean model (Tsumune et al., 2012). The ^{137}Cs concentrations in benthos and sediment found in stomach content of demersal fish were analysed by the underground measurement facility of the Low Level Radioactivity Laboratory, Kanazawa University. By tuning the bioavailable fraction rate in sediment found in the stomach content of demersal fish, temporal radiocesium level in demersal fish was calculated, and was verified by the reported ^{137}Cs concentrations in demersal fish inhabiting within 30 km radius from the 1FNPP (TEPCO 2018).

Measured ^{137}Cs concentrations were within a range from 23 to 400 Bq kg-ww^{-1} in stomach content of demersal fish collected at the TEPCO monitoring point T-S4 during 2013 (Fig. 1-b). Fine sediment of 0.16 to 23 g was found in the stomach, and the concentrations were 6 to 790 Bq kg-d.w^{-1}. Using food composition as being primarily benthos with ingestion rate and assimilation rate of radiocesum, the ^{137}Cs level in demersal fish was simulated (Fig. 1-a). The reconstructed radiocesium levels in demersal fish was almost comparable with the measured concentrations, suggesting that the entrained sediment amount were assumed as several times larger than the ingested benthos.

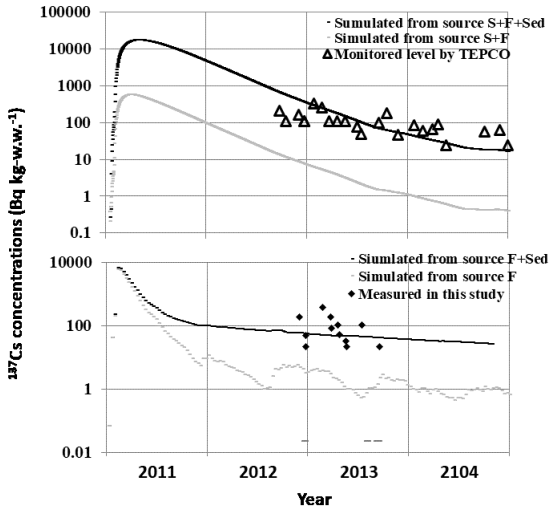

Figure 1. (a) Simulated and measured ^{137}Cs levels in demersal fish at T-S4. (b) Measured and simulated levels in the stomach content of the demersal fish collected at T-S4. The S, F, and SED being contamination source as seawater, food, and sediment, respectively.

Tsumune, D., Tsubono, K., Aoyama, M., Hirose, K. 2012. Distribution of oceanic ^{137}Cs from the Fukushima Dao-ichi Nuclear Power Plant simulated numerically by a regional ocean model. *J. Environ. Radioact.* 111. 100-108.

Misumi, K., Tsumune, D., Tsubono, K., Tateda, Y., Aoyama, M., Kobayashi, T., Hirose, K. 2014. Factors controlling the spatiotemporal variation of ^{137}Cs in seabed sediment off Fukushima coast: implications from numerical simulations. *J. Environ. Radioact.* 136. 218-228.

Tateda, Y., Tsumune, D., Tsubono, K., Misumi, K., Yamada, M., Kanda, J., Ishimaru, T. 2016. Status of ^{137}Cs contamination in marine biota along the Pacific coast of eastern Japan derived from a dynamic biological model two years simulation following the Fukushima accident. *J. Environ. Radioact.* 151. 495-501.

Improvement of the detection efficiency for ^{210}Pb determination in water samples by Cherenkov radiation

N. Todorović[1], J. Nikolov[1], I. Stojković[2], B. Tenjović[1], M. Vraneš[3], S. Gadžurić[3]

[1]Department of Physics, Faculty of Sciences, University of Novi Sad, Novi Sad, 21000, Serbia
[2]Faculty of Technical Sciences, University of Novi Sad, Novi Sad, 21000, Serbia
[3]Department of Chmistry, Faculty of Sciences, University of Novi Sad, Novi Sad, 21000, Serbia
Keywords: ^{210}Pb, detection efficiency, Cherenkov radiation, LSC, ionic liquids
Presenting author, e-mail: natasa.todorovic@df.uns.ac.rs

^{210}Pb determination in aqueous systems is being carried out for radiological safety estimations as well as in studies of different environmental and marine processes. It requires methods which are rapid, sensitive and precise since its ^{210}Pb natural levels can be very low, and measurement assumes previous chemical separations in samples. Direct measurement of ^{210}Pb is quite challenging through beta counting, gamma spectrometry and liquid scintillation counting (LSC), due to the low detection efficiencies of low energy beta and gamma-rays of ^{210}Pb and the interferences from rapid in-growth of its daughter nuclide ^{210}Bi ($T_{1/2}$ = 5.013 d).

Investigation of a simple method for ^{210}Pb content estimation directly without any sample pre-treatment, via Cherenkov radiation detection in a liquid scintillation counter Quantulus 1220 is presented. The analysis of ^{210}Pb by Cherenkov counting is possible only through the detection of the Cherenkov photons produced by the daughter nuclide ^{210}Bi, which reaches secular equilibrium with its parent nuclide. The Cherenkov counting efficiency of the ^{210}Pb/^{210}Bi without wavelength shifters is reported to range between 14%-18%. Sodium salicylate and ionic liquids, acting as a wavelength shifters, have been used to improve the detection efficiency of Cerenkov photons.

Salicylates in the form of the ionic liquids have been tested since their unlimited solubility in water.

Possibilities to improvement of minimum detectable activity (MDA) and detection efficiency were explored: increment of the initial sample volume to be evaporated, prolonging the sample measurement time and adding sodium salicylate and ionic liquids to the vial in order to increase efficiency detection. The preliminary results presented in Table 1. Efficiency variation will be further explored by adding greater volumes of ionic liquids to the vial.

The problem of spectral interference with other naturally occurring radioisotopes (radium in particular) was discussed as well.

In this study, we found that the addition of sodium salicylate and ionic liquids could significantly increase the counting efficiencies of ^{210}Pb/^{210}Bi in aqueous samples due to the production of more scintillation light. These findings clearly demonstrate the potential of this method for the detection of ^{210}Pb content in the areas where its natural levels are increased, for example, in waters polluted by mining activities.

Table 1. Detection efficiency and MDA limit.

Method used	Sample volume (L)	Counting time (min)	Detection efficiency ε (%)	MDA BqL^{-1}
Direct method	0.02	1000	15.3(4)	0.80
Direct method – longer counting times	0.02	2000	15.3(4)	0.56
Direct method – evaporation of larger volume	0.2	1000	15.3(4)	0.08
Direct method – addition of 0.2 mg ionic liquid: sodium salicylate	0.02	1000	42.2(25)	0.29
Direct method – addition of 86.1 mg ionic liquid: sodium salicylate	0.02	1000	31.4(5)	0.39
Direct method – addition of 30 μL ionic liquid: I-buthyl-3-methylimidazolium salycilate	0.02	1000	25.0(4)	0.49
Direct method – addition of 30 μL ionic liquid: 3-methylpiridnium salicilate	0.02	1000	28.8(5)	0.42

This work was supported by the Provincial Secretariat for Higher Education and Scientific Research, Republic of Serbia within the project "Radioactivity in drinking water and cancer incidence in Vojvodina", no. 142-451-2447/2018, the Ministry of Education, Science and Technological Development of the Republic of Serbia within the projects no. OI171002 and III4300; the International Atomic Energy Agency (IAEA) via IAEA Research Contract No. 23159/R0 .

and the Provincial Secretariat for higher education and scientific research within the project No. 142-451-2793/2018.

Underwater in-situ gamma-ray spectrometry using medium and low resolution detection systems

C. Tsabaris, F.K. Pappa, N. Maragos, G. Eleftheriou

Institute of Oceanography, Hellenic Center for Marine Research, Anavyssos, 19013, Greece
Keywords: medium resolution γ-ray spectrometry, submarine springs, radon daughters
Presenting author, e-mail: Christos Tsabaris (tsabaris@hcmr.gr)

The available underwater sensors that are widely applied in the marine environment consist of low resolution crystals (such as NaI, BGO). A well know system named KATERINA (Tsabaris et al., 2009) is applied for monitoring and studying marine processes in various marine compartments worldwide (Med, Baltic, Kaspia, and Black Seas). Nowadays a new detection system named GeoMAREA is developed and applied for measuring marine radioactivity using a 2'x2' $CeBr_3$ medium resolution crystal (Tsabaris et al., 2019). This apparatus is designed for smart operation providing qualitative and quantitative radionuclide measurement in aquatic environments with maximum operational depth of deployment at 600m. A detailed study for the software development is presented to support real-time applications as well as to provide sequential data for continuous monitoring in a stand-alone mode. The spectrometer was calibrated first using point sources for energy, energy resolution and efficiency parameters and particular attention was paid on the factors that affect them. The system offers activity concentrations of all detected gamma-ray emitters in Bq/m^3 using the marine efficiency calibration, which is estimated by the MCNP5-CP simulation code (Tsabaris et al., 2019). Two experimental points were used for validating the theoretical estimation for a large energy range. The experimental data were obtained by diluting two reference sources (^{137}Cs and ^{40}K) in a special-designed tank and acquiring for specific period of time for background and foreground spectra. The underwater detector is combined in the field with salinity meter regarding the acquiring of radon daughters (^{214}Pb and ^{214}Bi) at a closed marine system where submarine groundwater discharge takes places (Anavalos, Kiveri, Greece). A first estimation is also given for the intrinsic background at the area of ^{40}K which is around 0.16 cps for the energy window of ^{40}K.

The intrinsic efficiency is calculated by combined measurements at the specific area (cold spring) and the laboratory tank. More specifically, the solution of the system equation

$$CPS_{\text{int}} = CPS_{tot} - \varepsilon_{1461}(I_{\gamma\,214Bi}^{1461} A_{214Bi} + I_{\gamma\,40K} A_{40K})$$

$$CPS_{int} = CPS'_{tot} - \varepsilon_{1461}\left(I_{\gamma 214Bi}^{1461} \cdot A'_{214Bi} + I_{\gamma 40K}^{1461} \cdot A_{40K}'\right),$$

provides the intrinsic and the photopeak efficiency at 1461 keV. In the above system of equations the CPS_{int} represents the intrinsic contribution in cps, ε_{1461} is the system photopeak efficiency, I_γ is the respective gamma-ray intensities and A is the activity concentration for ^{214}Bi and ^{40}K, respectively.

One of the main advantages of the medium resolution detection system GeoMAREA is the capability to distinguish photopeaks with neighbouring energies. To demonstrate this, a spectrum was acquired using two Cs isotopes (^{134}Cs at 605 and 796 keV and ^{137}Cs at 662 keV) positioned in a close distance from the crystal window (~ 10 cm). The results are depicted in Fig. 1. The energy resolution for 605, 662 and 796 keV was found to be 29, 30 and 33 keV, respectively. It is obvious that the photopeaks of ^{134}Cs and ^{137}Cs are well distinguished, making the detection system capable to identity clearly the key fission by-products after a nuclear accident and provide support for the scientific community to further study the dispersion processes of radio-pollutants in the marine environment. Due to the half-life differences for these radionuclides, the simultaneous activity concentration determination of both radionuclides may provide the period of incidence or the origin of Cs in the water.

GeoMAREA is an effective marine sensor for radioactivity measurement and in the near future the detection system will be applied for smart monitoring purposes that will be operated in different modes in areas with enhanced industrial activity.

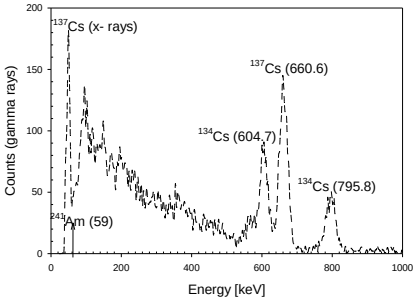

Figure 1. ^{134,137}Cs spectra as detected by the GeoMAREA system (Tsabaris et al., 2019).

All authors would like to acknowledge the national program "EDBM34" for supporting the measurements campaigns and exercises performed in the frame of the ANAVALOS project (MIS 5005218).

Tsabaris, C., Androulakaki, E.G., Prospathopoulos, A., Alexakis,S., Eleftheriou, G., Patiris, D.L., Pappa, F.K., Sarantakos, K., Kokkoris, M., Vlastou, R., 2019, "Development and optimization of an underwater in-situ cerium bromide spectrometer for radioactivity measurements in the aquatic environment", *J Environ Radioact.* 204, 12-20.

Tsabaris, C., Bagatelas, C., Dakladas, Th., Papadopoulos, C.T., Vlastou, R., Chronis, G.T. 2008, "An autonomous in situ detection system for radioactivity measurements in the marine environment", *Appl Radiat Isotopes* 66, 1419-1426.

Impacts of direct release and riverine discharge on oceanic ^{137}Cs derived from the Fukushima Dai-ichi Nuclear Power Plant accident

Daisuke Tsumune[1], Takaki Tsubono[1], Kazuhiro Misumi[1], Hikaru Miura[1], Yutaka Tateda[1], Yasushi Toyoda[1], Yuichi Onda[2], Michio Aoyama[2]

[1]Central Research Institute of Electric Power Industry, Abiko,270-1194, Japan
[2] Center for Research in Isotopes and Environmental Dynamics, University of Tsukuba, Tsukuba, 305-8572, Japan
Keywords: Fukushima Dai-ichi Nuclear Power Plant accident, 137Cs, River input, Regional Ocean model
Presenting author, e-mail: tsumune@criepi.denken.or.jp

A series of accidents at the Fukushima Dai-ichi Nuclear Power Plant (1F NPP) following the Great East Japan Earthquake and tsunami of 11 March 2011 resulted in the release of radioactive materials to the ocean. Measured ^{137}Cs activities in the coastal zone of Fukushima are still higher than the one before the accident because sources to the ocean are still existing from 1F NPP site and/or rivers. The Regional Ocean Model System (ROMS) was employed for regional-scale simulation of ^{137}Cs activity in the ocean offshore of Fukushima (Tsumune et al., 2013), the sources of radioactivity being direct release, atmospheric deposition, the inflow of ^{137}Cs deposited into the ocean by atmospheric deposition outside the domain of the model, and river discharges. Direct release of ^{137}Cs was estimated from 26 March 2011 to 31 August 2018 by comparing simulated results and measured activities adjacent to the accident site. In addition, riverine discharge rates of ^{137}Cs for 17 rivers were also estimated by multiplication between river flow simulation rates and estimated decreasing rate of ^{137}Cs activities from 2013 to 2016 for 4 years in this study because there were few data in the river before 2012. Simulated atmospheric deposition to the ocean was employed by atmospheric transport model. Inflow of ^{137}Cs from boundary sections was set by the results of the North Pacific scale ocean model.

Simulated ^{137}Cs activity attributable to direct release was in good agreement with measured data in the coast zone adjacent to the 1F NPP from 26 March 2011 to 31 August 2018, because the effect of direct release was dominant. Direct release rate has decreased from 10^{14} Bq/day at 26 March 2011 to 10^{9} Bq/day at the end of August 2018. Apparent half-life of direct release rated is about 1 year from 2012 to 2016.

We compared impacts of direct release and the one of river input on ^{137}Cs activity in the ocean from 2013 to 2016. Horizontal distribution of ^{137}Cs activity changed with time complexly due to meso-scale eddy. On the other hand, annual averaged horizontal distribution patterns of ^{137}Cs activity are similar in 2013 to 2016. Simulated annual averaged ^{137}Cs activities without river inputs are in good agreement with observation in 2013 (Fig.1) and other years. Impacts of river input on annual averaged ^{137}Cs activities are negligible because impacts of direct release are still dominant. Simulated results attributable to inflow from boundary sections were slightly underestimated to the measured data offshore area. This suggests that recirculation of subducted ^{137}Cs to the surface layer was underestimated in the North Pacific model (Tsubono et al., 2016).

Apparent half-life of direct released and river discharged ^{137}Cs activity were estimated to be about 1 year and 2 years, respectively. And apparent half-life of inflow of ^{137}Cs activity was much longer due to time scale of dilution process in the North Pacific. Apparent half-life of each source should be similar to the measured one attributable to each source. Apparent half-life of measured ^{137}Cs activity adjacent to the 1F NPP was about 1 year. Apparent half-life of measured data was about 2 years in front of the Uda river mouth where is far from the 1F NPP, therefore impacts of river input was dominant. Simulated ^{137}Cs activitiy with river input was underestimate one fifth of observations. There is a brackish lagoon, Matsukawa-ura in front of Uda river mouth. The observed ^{137}Cs activities in the Matsukawa-ura were 3-5 times larger than the one in the Uda river. This suggests the removal process of ^{137}Cs from particle and/or sediment to dissolved form in the brackish lagoon may be important.

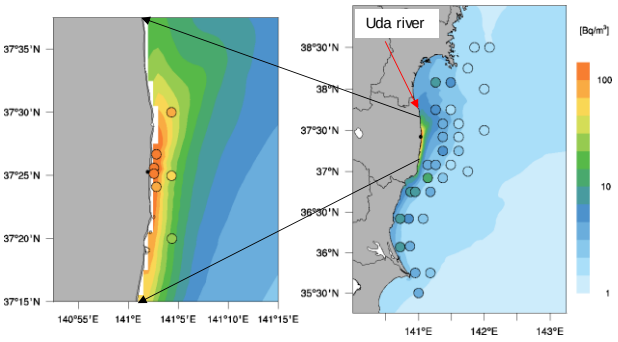

Figure 1. Annual averaged ^{137}Cs activity in 2013. Contour shows simulation without river input, circle shows observation.

Tsumune, D., Tsubono, T., Aoyama, M., Uematsu, M., Misumi, K., Maeda, Y., Yoshida, Y., Hayami, H. 2013. One-year, regional-scale simulation of ^{137}Cs radioactivity in the ocean following the Fukushima Dai-ichi Nuclear Power Plant accident, *Biogeosci.*, 10, 5601-5617.

Tsubono, T., Misumi, K., Tsumune, D., Bryan, F. O., Hirose, K., Aoyama, M. 2016. Evaluation of radioactive cesium impact from atmospheric deposition and direct release fluxes into the North Pacific from the Fukushima Daiichi nuclear power plant, *Deep Sea Res.I*, 115, 10–21.

Correlations between ^{7}Be dry deposition and meteorological data

R. Uhlář[1], P. Haroková[2], P. Alexa[3], M. Kačmařík[4]

[1]Department of Physics, VŠB-Technical University of Ostrava, 17. listopadu 2172/15, Ostrava, 708 00, Czech Republic
[2]ŠKODA JS a.s., Orlík 266, Plzeň, 316 00, Czech Republic
[3]Department of Physics and Institute of Clean Technologies, VŠB-Technical University of Ostrava, 17. listopadu 2172/15, Ostrava, 708 00, Czech Republic
[4]Department of Geoinformatics, VŠB-Technical University of Ostrava, 17. listopadu 2172/15, Ostrava, 708 00, Czech Republic

Keywords: cosmogenic nuclides, annual variations, meteorological data, sunspot number

Presenting author, e-mail: radim.uhlar@vsb.cz

^{7}Be is a natural radioisotope with a half-life of 53.22(6) days produced in cosmic-ray spallation processes mainly in the lower stratosphere and upper troposphere. It is removed from the atmosphere by radioactive decay and by wet and dry deposition. The deposition depends mainly on total precipitation, precipitation rate, atmospheric convection (temperature), latitude and incident cosmic-ray flux (Ioannidou and Papastefanou, 2006; Mohan et al., 2019).

PM10 aerosol particles were accumulated using the HVS Digitel DA 80 sampler equipped with a Whatman glass microfiber filters (GF/C, 150 mm diameter) during the period of one year from September 2015 to August 2016 at Ostrava, Czech Republic. One filter was deposited to the air flow of about 32 m^{3}/h in the sampler for 24 h. PM10 concentrations were measured gravimetrically in each filter and the ^{7}Be content was determined for two filters (48 h frequency) that is shorter compared to a standard 7-day frequency of routine ^{7}Be measurements. Relevant meteorological data were recorded by a Thies CLIMA laser precipitation monitor (rainfall amount, rain rate, particle size and speed) and by an automatic meteorological station Davis Vantage Pro 2 (temper-ature) located at a distance of about 1 km from the sampler. ^{7}Be activity was measured using a 30% HPGe gamma spectrometer. The measured ^{7}Be, PM10 and sunspot number (SILSO, 2019) are shown in Fig. 1.

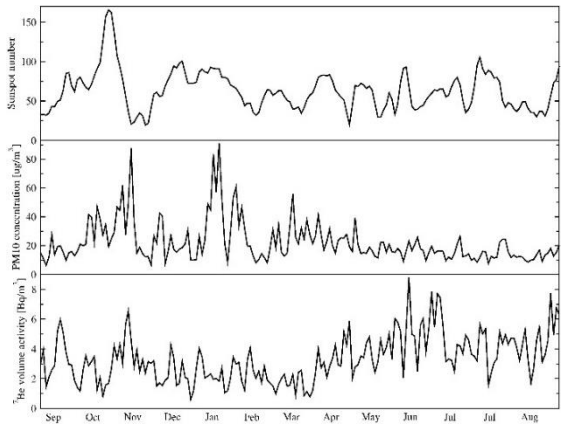

Figure 1. 2-day variations of ^{7}Be volume activity, PM10 concentration and sunspot number.

Weighted linear regression analysis was applied to the ^{7}Be volume activity, the measured meteorological explanatory variables and the sunspot number. Temperature and precipitation-particle speed were found to be the most statistically significant explanatory variables. A significant correlation as quantified by Pearson's correlation coefficient was found also between the ^{7}Be volume activity and PM10 concentration.

The tree model (Crawley, 2007) proves temperature as the most important explanatory variable and predicts the threshold value separating low and high temperatures at about 13°C (2-day average).

A simple two-layer (stratosphere and troposphere) atmospheric model was then applied to the data analysis. In the model, ^{7}Be production rates are supposed to be solar modulation potential dependent (Usoskin and Kovaltsov, 2007). ^{7}Be is removed from stratosphere by decay and surface-temperature induced stratospheric-tropospheric convection and from troposphere by decay and dry and wet deposition. The model is also applied to our previous dry and wet deposition measurements (Uhlář et al., 2015).

This work was supported by the projects SP2019/26 and the National Programme for Sustainability I (2013-2020), identification code LO1406.

Ioannidou A., Papastefanou C. 2006. Precipitation scavenging of ^{7}Be and ^{137}Cs radionuclides in air. *J. of Environ. Radioactiv.* 82, 121-136.

Mohan M.P. et al. 2019. Influence of rainfall on atmospheric deposition fluxes of ^{7}Be and ^{210}Pb in Mangaluru at the Southwest Coast of India. *Atmospheric Environment* 202, 281-295.

SILSO, 2019. On-line Sunspot Number catalogue: http://www.sidc.be/SILSO/, '2015-2016'.

Crawley M.J. 2007. The R book. Wiley, Chichester.

Usoskin I.G., Kovaltsov A. 2008. Production of cosmogenic ^{7}Be isotope in the atmosphere: Full 3-D modeling. *J. Geophys. Res.* 113, 1-12.

Uhlář R. et al. 2015. Short-term variations in ^{7}Be wet deposition in the eastern part of the Czech Republic. *J. Radioanal. Nucl. Chem.* 304, 89–93.

Geochemical behaviour of Uranium and Thorium in soils and sands from a natural high background radiation area of Odisha coast, India

N. Veerasamy[1,2], S.K. Sahoo[1], K. Inoue[2] and M. Fukushi[2]

[1]Department of Radioecology and Fukushima project, National Institutes for Quantum and Radiological Sciences and Technology, 4-9-1 Anagawa, Inage-ku, Chiba, 263-8555, Japan
[2]Department of Radiological Sciences, Tokyo Metropolitan University, 7-210 Higashiogu, Arakawa-ku, Tokyo 116-8551, Japan
Keywords: Uranium, Thorium, HBRA, ICP-MS
Presenting author, E-mail: nimelanveerasamy@gmail.com

Uranium (U) and thorium (Th) are the primordial radionuclides ubiquitously present in the Earth's crust. Both U and Th play a significant role in environmental sciences to study natural radioactivity and monitor radiation dose whereas in geological sciences to understand the sedimentary processes and geochronology. Indian coastal areas are rich in heavy minerals deposits such as ilmenite, rutile, monazite and zircon etc. Odisha coast is one of the well-known high background radiation areas in India since it is rich in monazites and rutile (Sahoo et al., 2016). Therefore, Odisha coast was selected to study geochemical characteristics of U and Th in soil and sands.

The main goal of the study is geochemical approach to find the source of enhanced radiation level in the environment. The concentration of U and Th were measured using inductively coupled plasma mass spectrometry (ICP-MS). The mean concentration of U and Th is 6.9 ± 6.7 µg g^{-1} and 217 ± 233 µg g^{-1}, respectively which higher than the bulk continental crust (Wedepohl, 1995). Major element concentrations were carried out using X-ray fluorescence spectroscopy to understand the mineralogical composition and chemical weathering of the samples.

A behavioural study of Th/U and Th/K cross plot (figure 1) was performed to identify mineralogical properties and geochemical facies (Anjos et al., 2010). The ratio of Th/U and Th/K varies from 4 to 37 and 3 to 2663 respectively. Th/K ratios are widely used for the recognition of heavy and clay mineral associations. Th/U ratios are useful to interpret the mobilization, transportation and fixation of sedimentary cycle. Th/U ratios are varying from 0 to 2 in anoxic environment, whereas ratios varying from 2 to 7 in strongly oxidizing environments. The obtained results clearly indicate that the samples from the coastal region are formed in oxidizing and intense chemical weathering terrestrial environment with an enrichment of radiogenic heavy minerals (monazites and zircon) and clay mineral association. Since majority of samples undergoes intense weathering in oxidizing environment, uranium is leaching from the soil matrix. Eventually, thorium resides in the matrix and contributes major exposure of radiation to the environment. The high ratios of Th/U suggest that the inclusions of placer deposits with enrichment of Th bearing radioactive mineral (monazite) in the samples.

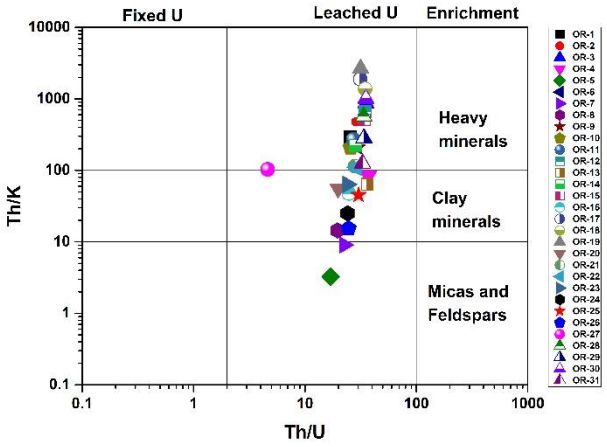

Figure 1. Cross plot of Th/U and Th/K ratios from High Background Radiation Area Soil and sand samples.

I (NV) am thankful to "Tokyo Human Resources Fund for City Diplomacy, Tokyo Metropolitan Government, Tokyo, Japan" for the award of Doctoral fellowship at Tokyo Metropolitan University.

Sahoo, S. K., Kierepko, R., Sorimachi, A., Omori, Y., Ishikawa, T., Tokonami, S., Prasad, G., Gusain, G. S. and Ramola, R. C. 2016. Natural radioactivity level and elemental composition of soil samples from a high background radiation area on eastern coast of India (Odisha). *Radiat. Prot. Dosim.* 171, 172-178.

Wedepohl, K. H. 1995. The composition of the continental crust. *Geochim. Cosmochim. Acta*. 59, 1217-1232.

Anjos, R. M., Macario, K. D., Lima, T. A., Veiga, R., Carvalho, C., Fernandes, P. J. F., Vezzone, M. and Bastos, J. 2010. Correlations between radiometric analysis of Quaternary deposits and the chronology of prehistoric settlements from the southeastern Brazilian coast. *J. Environ. Radioact.* 101, 75-81.

Investigation of elevated radiation exposure from debris of a renovation project

W.-H. Wang[1], J. Robinson [2], A.M. Hamideh[2]

[1]Center for Energy Studies, Louisiana State University, Baton Rouge, Louisiana, 70803, USA
[2]Radiation Safety Office, Louisiana State University, Baton Rouge, Louisiana, 70803, USA
Keywords: clay tile, NORM, lessons learned
Presenting author, e-mail: weihsung@lsu.edu

Planning, preparation, and training for radiation safety staff responding to radiological incidents are not only prudent, but also vital for regulatory compliance. Practical lessons regarding the effectiveness of preparedness, and actions in response to a radiological event, often are learned best as a result of actual involvement in such an event. This presentation reviews a case of scrap metal with elevated radioactivity from an academic administration building during renovation. We describe the handling of this event by radiation safety professionals through the planning, recognition, and evaluation phases.

A load of scrap metal in a dumpster was returned to the construction site, because the load had set off the radiation monitor at the scrap metal recycling facility. The radiation safety emergency responders were notified and arrived on scene to investigate. The dumpster was about 15 m^3 and contained mainly metal sheets, ventilation ducts, and conduits from the renovation project. A preliminary survey of the contents, using calibrated detectors with Geiger Mueller and sodium iodide probes, did not indicate elevated radiation exposure. It was then decided that the first step would be to determine whether the content in the dumpster or the dumpster itself had triggered the radiation monitor at the recycling facility. After moving the content out of the dumpster, a pile of broken clay roof tiles was found at the bottom of the dumpster. Subsequently, the tiles were removed from the dumpster and bagged, because they were not supposed to be shipped to the recycling facility. The remaining debris was loaded to a new dumpster and shipped to the recycling facility. This load of scrap metal passed through the radiation monitor successfully. Furthermore, the potentially questionable dumpster itself went through the radiation monitor without triggering the alarm. It appeared that the clay roof tiles set off the radiation monitor at the recycling facility. In general, clay tiles tend to have slightly elevated radioactive contents, due to the inherent presence of naturally occurring radioactive materials. The radiation level from clay tiles depends on both the raw materials and the glazing materials. It is not unusual to observe higher radioactivity concentration in the tiles than the average concentration of the earth's crust. About 30 bags of disposed clay roof tiles were surveyed and slightly elevated exposure rates were observed. In addition, three tiles were collected from those bags for further characterization using a high-purity germanium counting system. The radioanalysis indicated uranium, thorium, and potassium in the tiles that are typical naturally occurring radionuclides. These radionuclides are commonly present in the raw materials for building and construction materials. The concentration for these radioisotopes in the tiles was found to be significantly less than the regulatory exempt quantity. Also, the naturally occurring radionuclide compositions in the clay tiles had not been technologically enhanced. Thus, the clay roof tiles were disposed as normal construction debris. We believe that the radiation monitor threshold at the scrap metal recycling facility was set too low, thus triggering a radiation monitor response to the clay tiles in the dumpster.

Figure 1. Renovation debris in the dumpster.

Selective separation of Cerium(Ⅲ) by Sodium Bismuthate nano-sheets

Ning Wang, Chu-Ting Yang and Sheng Hu

Institue of Nuclear Physics and Chemistry, China Academy of Engineering Physics
64# Mianshan Road, Mianyang City, Sichuan Province, People's Republic of China
Keywords: $NaBiO_3$, Nano-Sheets, Separation
Presenting author: Ning Wang, e-mail: wangn@caep.cn

The separation of trivalent americium (Am^{3+}) is fairly hard because its chemical behavior is almost identical to that of its related trivalent lanthanide and actinide elements in the nuclear fuel cycle. As a strong oxidant, bismuthate has been used to oxidize and separate valuable elements (Hara and Suzuk, 1977) $NaBiO_3$ oxidizes Am^{3+} to $[AmO_2]^{2+}$ which can then be isolated from other chemically-similar fission products (Ln^{3+}) by solvent extraction with several phosphate and phosphonate ligands. The extracted $[AmO_2]^{2+}$ can then be either disposed safely or repurposed in fast reactor fuel. In this paper, Ce^{3+} was employed an acceptable surrogate of Am^{3+} to futher evaluate the mechanism of oxidation and separation.

The $NaBiO_3$ nano-sheets were synthesized by a facile method of oxidizing Bi^{3+} in alkaline solution. The as-synthesized products were used to adsorb Ce^{3+} in solution and characterized by XRD, SEM, TEM and XPS. The results show that the synthesized products have nano-sheets structure with a size of ~50 nm（Figure 1） and high selective adsorption performance on Ce^{3+}. After adsorption of Ce^{3+}, all Na cations in $NaBiO_3$ nano-sheets have been fully exchanged and replaced by Ce cations and the chemical state of Ce and Bi were Ce^{4+} and Bi^{3+} in the generated products. The XPS analysis shows that Bi^{5+} species were changed into Bi^{3+} species in the adsorption process of Ce^{3+}(Figure 2). So the adsorption process of Ce^{3+} contains two process of the ion-exchange between Ce^{3+} and Na^{+} cations and the oxidation of Ce^{3+} species, and the selective adsorption process of Ce^{3+} ion was achieved by an ion-exchange and redox reaction process.

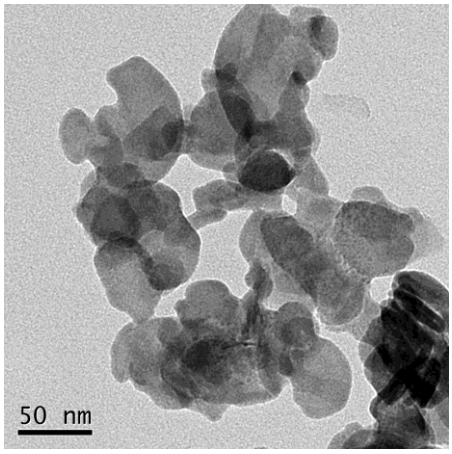

Figure 1. TEM image of as-prepared $NaBiO_3$.

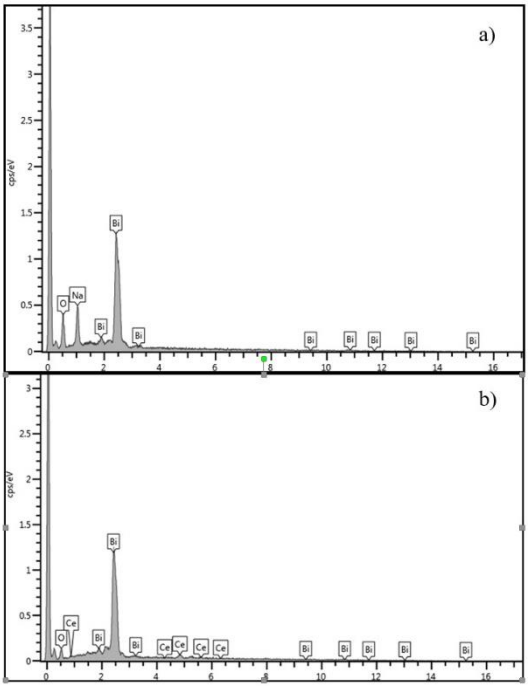

Figure 2. EDS spectrum of (a) as-prepared $NaBiO_3$ and (b) after Ce^{3+} adsorption.

M. HARA, S. SUZUK, *Journal of Radioanalytical Chemistry*, Vol. 36 (1977) 95-104

Karoly Kozma., T. Wesley Surta, et al. *Journal of Solid State Chemistry* 263 (2018) 216–223

Phosphorylcholine compounds as chemosensors for recognition of UO_2^{2+} and selective adsorption of uranyl

Jun Wen, Zeng Huang

[1] Institute of Nuclear Physics and Chemistry, China Academy of Engineering Physics, Mianyang, 621900, Sichuan Province, China

Keywords: Phosphorylcholine, Uranyl, chemosensors, selectivity

Presenting author, e-mail: junwen@caep.cn

Uranium is a representative element of an actinide metal that has naturally radioactivity and widely distributed in the environment (Gongalsky, 2003). Uranium is one of the main fuel in nuclear energy generation, and it also has been used in nuclear weapons (Corn, 1993). With the growing human demand for nuclear energy, the worldwide uranium consumption is continuous increasing. For uranium, the most stable and common ionic form is appears as a complex of the uranyl ion (UO_2^{2+}), because uranyl is water soluble, it is readily migrated to environment. Unfortunately, uranium is radioactive and chemically toxic, it was reported that human exposure to uranium could give rise to lung cancer, urinary system disease and genetic diseases.

Considering the widespread use of uranium and its toxic properties, the development and improvement of analysis methods for the determination of uranium are vital. Therefore, many techniques have been used for the determination of uranium. Among these analysis methods, colorimetric detection is a simple, rapid, highly selective, and low-cost method for metal ion determination. However, only few reports on the application of this technique to uranium ion analysis have been published.

Herein, a phosphorylcholine substituted tetraphenylethene compound (**TPE-PC**) was prepared as chemosensors for recognition of uranium. This sensor has excellent selectivity and anti-interference ability, which can efficient identification and analysis of uranyl ions under complicated conditions. Meanwhile, phosphorylcholine functionalized fiber was synthesized by Atom-Transfer Radical Polymerization. This adsorbent exhibits high selectivity for uranyl and good adsorption capacity. This work illustrates phosphorylcholine has potential applications in environmental systems for uranyl ion detection and extraction.

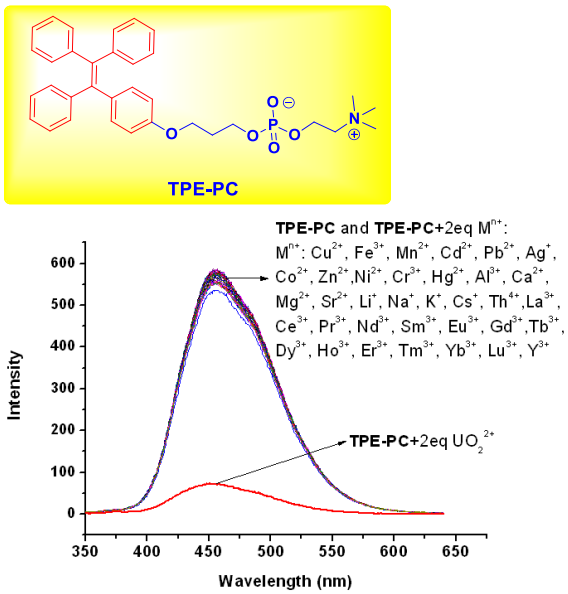

Figure 1. Fluorescence spectra of **TPE-PC** (1.0×10^{-5} M) in the presence of metal cations (each at 20μM) in 25mM HEPES buffer (with 1% EtOH, pH=7.4).

This work was supported by the National Natural Science Foundations of China No. 21876162.

Gongalsky, K .B. 2003. *Environ. Monit. Assess.*, 89, 197.

Corn, M. D. Handbook of Hazardous Materials, 1993, Academic Press, San Diego.

Speciation of global fallout plutonium isotopes in natural soil particles and the implications for environmental tracing studies

Y.H. Xu[1], Y. P. Hao[2] and S. M. Pan[2]

School of Geography and Turism, Anhui Normal University, Wuhu 241002, China
School of Geographic and Oceanographic Sciences, Nanjing University, Nanjing 210023, China
Keywords: Pu isotopes, Soil particles, Speciation, behavior
Presenting author email: yhxu@ahnu.edu.cn

Plutonium isotopes (^{239}Pu and ^{240}Pu, with half-lives of 24110 and 6561 years, respectively) were recently used by some researchers as substitutes for ^{137}Cs for investigation of soil erosion, due to their long half-lives, dominating source of global fallout worldwide, as well as their high particle reaction in soil. However, compared with ^{137}Cs, behaviors of Pu isotopes in natural soils are more complicate and still not very clear. In order to apply the Pu isotopes tracing method in soil erosion studies more scientifically, a systematical study of the behavior of Pu isotopes in natural soil particles is needed.

In this work, speciation of the $^{239+240}$Pu in natural soils including surface soils with different particle size and profile soils with different layers was analyzed by using sequential extraction method combined with ICP-MS measurements. Results generally showed that Pu isotopes were most observed in the residue fraction in all surface and profile bulk soils (Figure 1 and 2) as well as soil particles with different sizes (Figure 3), followed by the organic matter fraction. The percentages of plutonium in the water soluble and exchangeable (including carbonates) fractions was generally least in all soils. Fe/Mn oxides fraction in all soils also contained very small percentage of plutonium. Compared with bulk soils, speciation of plutonium in soil particles with different particle sizes showed that the smaller the particle size of soil particles, the more plutonium contained in the residue fraction, indicating that plutonium in natural soils primarily bounds to clay minerals very well. However, the speciation results of plutonium in grass clippings showed most of the $^{239+240}$Pu distributed in the organic matter fraction, indicating that plutonium also bounds to organic matter well. Different proportions of plutonium in organic matter fraction in the two grass clippings indicating the composition of organic matter might be the important factor for its adsorption of plutonium.

The results of this research gave implications for application of plutonium as a tracer for soil erosion study in different soil types as well as erosion types, such as in black soils, or in water erosion and wind erosion area, impact factors considered are different. More discussions will be showed in the presentation.

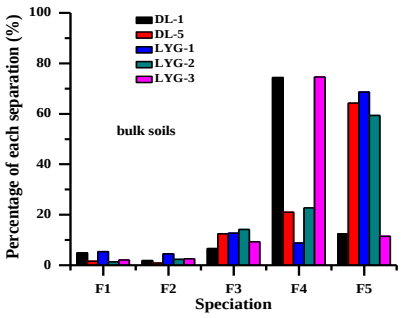

Figure 1. Speciation of plutonium in bulk surface soils.

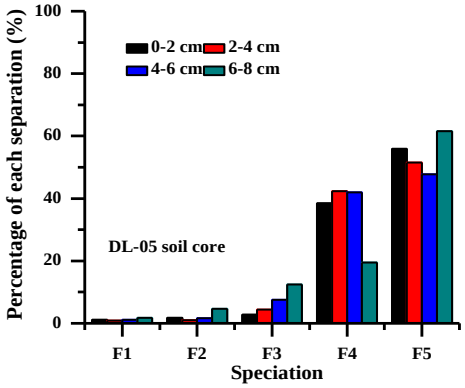

Figure 2. Speciation of plutonium in different layers of soil profile.

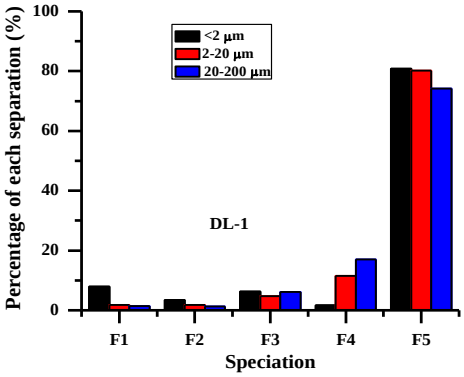

Figure 3. Speciation of plutonium in soil particles with different sizes.

The separation of Am^{III} from Cm^{III} with pyridine-type chromatographic material

Chu-Ting Yang,[1] Hai-Zhu Yu[2] and Xiao-Lin Wang[1]

[1] Institute of Nuclear Physics and Chemistry, China Academy of Engineering Physics Mianyang 621900 (P. R. China)
[2] Department of Chemistry and Center for Atomic Engineering of Advanced Materials, Anhui University, Hefei 230026 (P. R. China)

Keywords: Nuclear fuel waste, Actinides, Separation

Chu-Ting Yang, e-mail: yangchuting@caep.cn

With increased implementation of nuclear energy, nuclear fuel waste disposal has recently attracted extensive research interest. The main components of nuclear waste are lanthanides and uranium (98.5 wt%), which generally do not pose a long-term hazard. By contrast, tiny amounts of minor actinides (such as plutonium, americium and curium) exhibit high radioactivity and toxicity. To remove the highly threatening minor-actinides from nuclear waste, many strategies have been developed in the past few decades such as PUREX (Plutonium and Uranium Extraction), TRUEX (transuranic extraction). To date, the most challenging problem in reprocessing the spent nuclear fuels lies in the separation of Am^{III} from Cm^{III}, because these two elements show high similarity in the ion radius, charge density, electronic structure and chemical reactivity. Furthermore, Am^{III} is the main component to account for heat emission after 100 years, while Cm^{III} requires careful shielding treatment in each time of operation due to its high neutron emission activity. The separation of Am^{III} and Cm^{III} will contribute to reducing α-waste volume and long-term environmental hazards (Panak, P. J. and Geist, A., 2013).

Although the pyridine resins frequently suffer from the poor Am/Cm selectivity, the resins have become promising materials for Am/Cm separation.[6] In order to improve the selectivity, a series of pyridine resins with different substituents embedded in silica beads were synthesized (Yang, C. T., et al., 2018). We found that: 1) The Am/Cm separation factors ($SF_{Am/cm}$) decreased with electron-donating groups (Me, OMe), and this was probably due to the enhanced basic and complexing ability of the nitrogen atom. 2) By contrast, the resin with the CF_3 group revealed the best Am/Cm selectivity ($SF_{Am/cm}$=4.2), due to the softer nitrogen atom. 3) Interestingly, the resins with Cl groups exhibited high Cm selectivity. The separation factors were calculated as $SF_{Cm/Am}$ = 2 and 5 with mono-Cl and di-Cl substituents, respectively. With the improved resins, baseline separation of Am^{III} from Cm^{III} was achieved

We further analyzed the Cm-selectivity through density functional theory calculations of the optimized structure, formed by the simplified ligand model (2-Cl-Py) and metal centers (Am, Cm). The Am-N bond length was longer than Cm-N bond length in the optimized structures (2.843 Å versus 2.832 Å), indicating a weaker interaction between Am and the pyridine ligand. Furthermore, frontier molecular orbital analysis revealed comprehensive interactions between Cl(*p*) orbital and the Cm(*f*) orbital, which was significantly weaker in the Am-system (See the Supporting Information). In addition, the corresponding frontier orbital energy of the Cm complex was significantly lower than that of the Am-complex, and the HOMO-LUMO energy gap of the Cm system was greater, which helped to improve the stability of the Cm complex (Yu, J., et al., 2019).

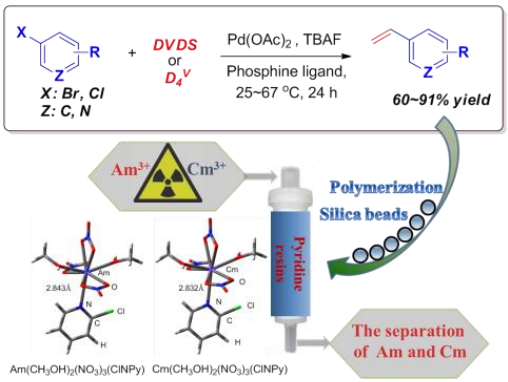

Figure 1. The separation of Am^{III} from Cm^{III} with pyridine-type chromatographic material.

This work was supported by the Science Challenge Project (TZ2016004), and the National Natural Science Foundation of China (Nos. 91426302, 21672001).

Panak, P. J., Geist, A., 2013, *Chem. Rev.*, 113, 1199–1236.

Yang, C. T., Han, J., Liu, J., Li, Y., Zhang, F., Yu, S. Hu, H. Z., Wang, X. L., 2018, *Chem. Eur. J.*, 24, 10324-10328.

Yu, J., Ma, J., Yang, C. T., Yu, H. Z., 2019, *Dalton Trans.*, 48, 1613-1623.

Polyvinyl alcohol （PVA）based porous organic polymers for Iodine adsorption and mechanistic aspect

G. Z. Yue*, P. Huang, D. S. Huang, J. Zhu, P. X. Zhao

Institute of Materials, China Academy of Engineering Physics, Huafengxin, 621908, China
Keywords: Aero Gels, adsorption, radioactive iodine
Guozong Yue, e-mail: yueguozong@caep.cn

Iodine isotopes, including ^{129}I ($t_{1/2}$ = 8 days) and ^{131}I ($t_{1/2}$ = 1.6 × 10^7 years) are mainly generated through uranium fission process and nuclear accident. Iodine compounds are highly environmental mobile, which could be gathered in living organisms, particularly in thyroid gland, and cause severe damage to human metabolic system (Kulyukhin et al., 2008). Thus, the removal of iodine for environmental remediation gains a lot of attentions. Compared with conventional inorganic or metal based iodine adsorbents (activated carbons, silver zeolite, oxide materials, etc.), rising porous materials (POPs, MOFs, COFs) have been significantly involved in recent years due to their unique porous structure with functionality. Among them, porous organic polymers (POPs) including amorphous hyper-crosslinked polymers, conjugated microporous polymers, and polymers of intrinsic microporosity, are a new family of porous materials with high surface area, low density, controllable functionality and remarkable stability. Up to now, various POPs have been applied for iodine uptake (Huve et al., 2018; Ping et al., 2018). According to previous works, heteroatoms (N, S, etc.) are high affinity to iodine for their lone electron pair have interactions with iodine, thus iodine uptake performance could be improved effectively. In this presentation, two novel PVA-based porous organic polymers (POP-1 and POP-2) were obtained through the cross-linking of modified PVA side chains. The as-prepared POPs present ultrahigh iodine uptake capacities. Noteworthy, the uptake capacities of POP-2 arrives at 5.9 g/g in iodine vapor, which is the best among all the porous organic polymers in literatures.

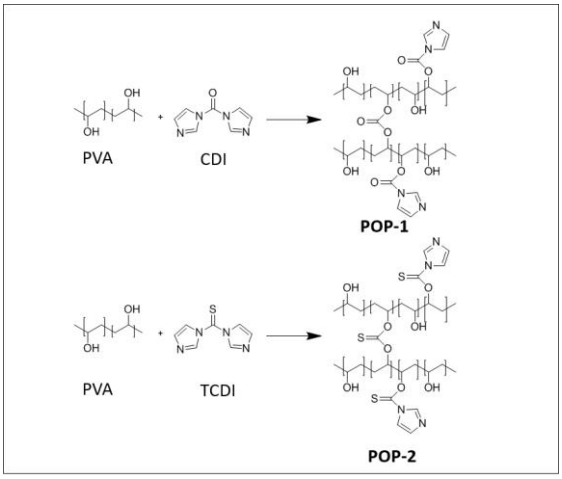

Scheme 1. Synthetic route to PVA-based POPs.

Subsequently, the mechanistic studies revealed that *N* atoms of imidazole are the dominant affinity sites for I_2 molecules, that is verified by the X-ray photoelectron spectroscopy (XPS). In addition, the unique porous structure of POP-2 that illustrated in Figure 1 also provides the positive effect for I_2 uptake. In summary, our strategy provides a novel efficient way for I_2 uptake for environmental remediation.

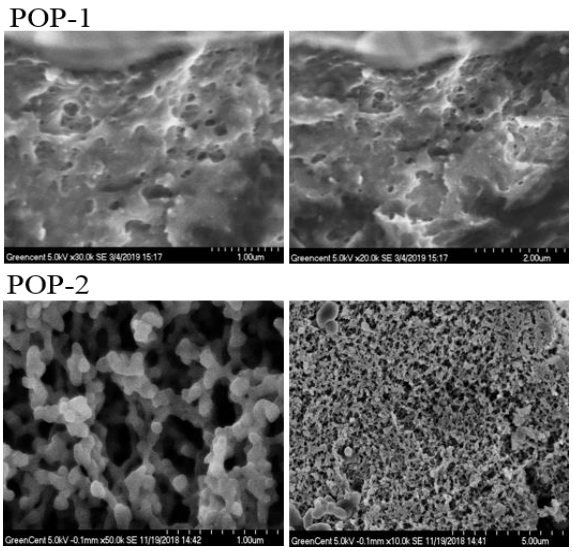

Figure 1. SEM of **POP-1**, **POP-2**.

Financial support from Natural Science Foundation of China (21601166) is gratefully acknowledged.

Kulyukhin, S. A.; Kamenskaya, A. N.; Mikheev, N. B.; Melikhov, I. V.; Konovalova, N. A.; Rumer, I. A. Basic and applied aspects of the chemistry of radioactive iodine in a gas medium. *Radiochemistry*. 2008, *50*, 1-20.

Huve, J.; Ryzhikov, A.; Nouali, H.; Lalia, V.; Augé, G.; Daou, T. Porous sorbents for the capture of radioactive iodine compounds: a review. *RSC Adv*. 2018, 29248-29273.

Ping, W.; Qing, Xu.; Zhongping, Li.; Weiming, J.; Qiuhong, J.; Donglin, J. Exceptional Iodine Capture in 2D Covalent Organic Frameworks. *Adv. Mater*. 2018, *30*, 1801991-1801997.

Development of methods for AMS analysis of long-lived radionuclides at the CENTA facility

J. Zeman[1], M. Ješkovský[1], J. Pánik[2], J. Kaizer[1], I. Kontuľ[1], P.P. Povinec[1]

[1]Centre for Nuclear and Accelerator Technologies (CENTA), Faculty of Mathematics, Physics and Informatics, Comenius University, Bratislava, 842 48, Slovakia
[2]Institute of Medical Physics, Biophysics, Informatics and Telemedicine, Faculty of Medicine, Comenius University, Bratislava, 813 72, Slovakia
Keywords: AMS, radionuclides, ^{10}Be, ^{26}Al, ^{232}Th, ^{238}U
Jakub Zeman, e-mail: jakub.zeman@uniba.sk

Accelerator Mass Spectrometry (AMS) is being widely used for investigation of radionuclides' abundance in specimen of different origin. With the detection limit of ~ ppt the AMS has been a powerful tool for investigations in environmental and material physics. The environmental studies at the CENTA laboratory have focused mainly on ^{14}C investigations around nuclear power plants, while the material research focused on radiopurity measurements of construction materials for underground physics experiments.

We shall discuss in detail AMS measurements of ^{10}Be using an ionisation chamber with a SiN foil stack used for ^{10}B isobar background suppression. The detection limit of 10^{-12} was reached even without using a high-resolution analysing magnet since the AMS line at the CENTA facility has not been installed yet (Ješkovský et al., 2015).

The research dedicated to analysis of ^{26}Al consists of multiple phases. Suitable materials as targets for AMS measurements were investigated in the first phase, motivated by previous studies which indicated that AlN targets could have higher yields. Following compounds were analysed: Al_2O_3, AlF_3, AlN, $Al_2(SO_4)_3$ together with a pure aluminium wire, all Alfa Aesar products. The idea behind these studies was to suppress the isobaric interference from the ^{26}Mg ions. Results of obtained beam currents are shown in Table 1 (Pánik et al., 2019).

As can be seen, the yiels for AlN was ~ 1.8 times higher than for Al_2O_3. The AlF_3 and $Al_2(SO_4)_3$ were not suitable since the currents were at the detection limit of the system.

In the second phase, the AMS measurements were carried out for ^{26}Mg isobaric suppression investigation. The obtained results for AlN matrix showed that further suppression is needed. Moreover, it was observed that ^{26}Mg production rate depends on the matrix of the ion source target material.

The purpose of ^{232}Th and ^{238}U investigation is to determine their concentration in materials which can be used as detectors' construction materials with very low background. Such detection systems are required for neutrino experiments, dark matter search and other experiments which are looking for signals coming from rare events.

Table 1. Comparison of ion beam currents for aluminum.

Material	Ion	HRIBF	PRIME	CENTA
		Beam current (nA)		
Al_2O_3	Al^-	147	100	30 - 35
	AlO^-	1830		900 - 1100
AlN (no exposure to air)	Al^-	234	100 - 150	55 - 60
	AlO^-	600		600 - 650
	AlN^-	1260		650 - 700
AlN (1 h exp. to air)	Al^-	1000	500	
	AlO^-	3100		
	AlN^-	7600		
AlN (2 days exp. to air)	Al^-	290	350	
	AlO^-	725		
	AlN^-	2050		

Primordial radionuclides ^{232}Th and ^{238}U and their decay products contribute significantly to the background of detectors operating underground. Since these radionuclides are present in the environment, the screening of detectors' material is necessary. In the CENTA facility, several measurements of possible materials have been carried out, with the main focus on the investigation of suitable targets and production of clusters in the ion source.

This work was supported by the Slovak Research and Development Agency (under the contract APVV-15-0576) and by the EU Research and Development Operational Program funded by the ERDF (projects no. 26240120012, 26240120026 and 26240220004).

Ješkovský, M., Steier, P., Priller, A., Breier, R., Povinec, P.P., Golser, R. 2015. Preliminary AMS measurements of ^{10}Be at the CENTA facility. *Nuclear Instr. Methods Phys. Res. B* 361, 139-142.

Pánik, J., Ješkovský, M., Kaizer, J., Steier, P., Zeman, J., Povinec, P.P. 2019. Investigation of suitable targets for accelerator mass spectrometry of ^{26}Al. *Nuclear Instr. Methods Phys. Res. B* 438, 101-106.

A study on natural radioactivity accumulation and aerosol mean transit time from their area of origin to the Canadian Arctic region with monitoring data of both radon and thoron progeny

W. Zhang

Radiation Protection Bureau of Health Canada, Ottawa, K1A 1C1, Canada
Keywords: $^{212}Pb/^{210}Pb/^{210}Po$, tracer, residence time of aerosols, Arctic
Presenting author, e-mail: Weihua.zhang@canada.ca

In this study, the activity concentrations of ^{210}Pb and ^{210}Po on the 22 daily air filter samples, collected at CTBT Yellowknife station from September 2015 to April 2016, were analysed. To estimate the time scale of atmospheric long-range transport aerosol bearing ^{210}Pb in the Arctic during winter, the mean transit time of aerosol bearing ^{210}Pb from its origin was determined based on the activity ratios of $^{210}Po/^{210}Pb$ and the parent-progeny decay/ingrowth equation. The activity ratios of $^{210}Po/^{210}Pb$ varied between 0.06 and 0.21 with a median value of 0.11. The aerosol mean transit time based the activity ratio of $^{210}Po/^{210}Pb$ suggests longer mean transit time of ^{210}Pb aerosols in winter (12 d) than in autumn (3.7 d) and spring (2.9 d).

Ten years ^{210}Pb and ^{212}Pb monitoring results and meteorological conditions at the Yellowknife station indicate that the ^{212}Pb activity is mostly of local origin, and that ^{210}Pb aerosol in wintertime are mainly from outside of the Arctic regions in common with other pollutants and sources contributing to the Arctic. The activity concentration ratios of ^{210}Pb and ^{212}Pb have a relatively constant value in summer with a significant peak observed in winter, cantered in the month of February. Comparison of the $^{210}Pb/^{212}Pb$ activity ratios and the estimated mean ^{210}Pb transit time, the mean aerosol transit times were real reflection of the atmosphere transport characteristics, which can be used as a radio-chronometer for the transport of air masses to the Arctic region.

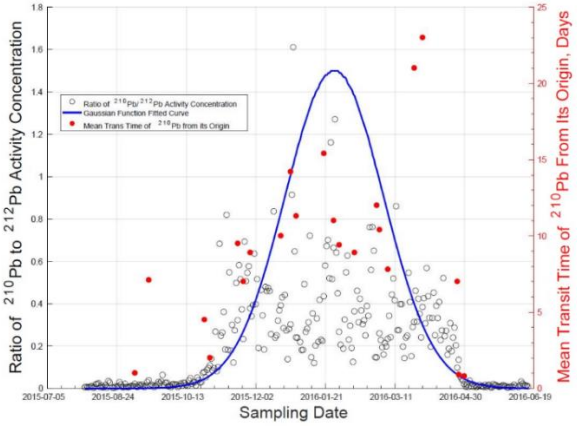

Figure 1. The Gaussian distribution function fitted to the profile of ^{210}Pb and ^{212}Pb concentration ratios obtained in the winter of 2015, and the determined mean aerosol transit time from its origin to the Yellowknife.

Table 1. Activity ratios of $^{210}Po/^{210}Pb$ and aerosol mean transit time from its origin by 22 air filter sample collected at Yellowknife station from September 2015 to April 2016.

Sampling date	Po/Pb ratio	mean transit time, d
2015-09-06	0.18	1.0
2015-09-16	0.17	7.1
2015-10-26	0.09	4.5
2015-10-30	0.06	2.0
2015-11-19	0.13	9.5
2015-11-23	0.07	7.0
2015-11-28	0.08	8.9
2015-12-20	0.11	10.0
2015-12-27	0.11	14.2
2015-12-31	0.07	11.3
2016-01-20	0.17	15.4
2016-01-27	0.11	11.0
2016-01-31	0.08	9.4
2016-02-12	0.13	8.9
2016-02-28	0.10	12.0
2016-02-29	0.09	10.4
2016-03-06	0.21	7.8
2016-03-25	0.18	21.0
2016-03-31	0.17	23.0
2016-04-25	0.11	7.0
2016-04-26	0.08	0.9
2016-04-30	0.06	0.8

Nuclear Forensics around the Ruthenium-106 Release in Fall 2017 above Europe

D. Zok[1], G. Steinhauser[1], D. Degering[2], J. H. Sterba[3], M. W. Cooke[4], T. Hopp[5]

[1]Institute of Radioecology and Radiation Protection, Leibniz Universität Hannover, Hannover, 30419, Germany
[2]VKTA – Strahlenschutz, Analytik & Entsorgung Rossendorf e.V., Dresden, 01328, Germany
[3]Atominsitut, Technische Universität Wien, Vienna, 1020, Austria
[4]Radiation Protection Bureau, Health Canada, Ottawa, K1A 1C1, Canada
[5]Institut für Planetologie, Westfälische Wilhelms-Universität Münster, Münster, 48149, Germany
Keywords Ruthenium-106, Radioecology, Incident, Monitoring, Radiochemistry, Speciation
Presenting author, e-mail: zok@irs.uni-hannover.de

In October 2017, European atmospheric radionuclide monitoring stations noticed the abnormal presence of Ru-106 and Ru-103 in their filter systems. Since no official statement clarified the release of these radionuclides, the source of the radioruthenium is still subject to speculations. It became clear in multiple radiometric measurements that the ruthenium was realised in a very pure radiochemical state: no other typical fission product or radionuclide was found to be present in elevated concentrations during this periode.

We collected some environmental samples in the middle of October 2017 in Vienna and Hanover, including leaves from various trees as well as grass samples to estimate the deposition of Ru-106 on vegetation. In all of these environmental samples, small activity of Ru-106 were detectable and quantifiable, typically below 1 Bq/kg dry mass.

More importantly, in this study, an air filter obtained from a high-volume sampler from Vienna, Austria, was investigated to provide more information on the state of the ruthenium. This included stepwise heating of the filter material. The results suggest that the radioruthenium on the filter exhibits low volatility. In addition, a different behaviour in the solubility of the filter could be observed by extraction experiments with different agents. By neutron activation analysis, the filter was checked for any elemental anomalies, however, none were found. Chemical complexation reactions were performed with derivatives of pyridine to get more information about the chemical state of the radioruthenium. Combined with some previous results of the extraction, it may be concluded that various ruthenium species are present on the filter.

Finally, we want to test the presence of a stabile ruthenium isotope anomalies by multi-collector sector field mass spectrometry. Results on this task are currently pending.

This work was supported by the Volkswagen Stiftung.

Zok, D., Sterba, J.H. & Steinhauser, G., 2018, *J Radioanal Nucl Chem* 318: 415.

Time-dependent trends of artificial radionuclides in fish, zoobenthos, and aquatic moss of the Yenisei River (Siberia, Russia)

T. Zotina[1,2], E. Trofimova[1], D. Dementyev[1]

[1]Institute of Biophysics, Krasnoyarsk Science Centre SB RAS, Krasnoyarsk, 660036, Russia
[2]Institute of Fundamental Biology and Biotechnology, Siberian Federal University, Krasnoyarsk, 660041, Russia
Keywords: ^{60}Co, ^{137}Cs, ^{144}Ce, ^{152}Eu, Arctic grayling, Northern pike, Siberian dace
Tatiana Zotina, e-mail: t_zotina@ibp.ru

The Yenisei River is contaminated with artificial radionuclides due to the operation of the Mining and Chemical Combine (MCC), which has been producing weapon grade plutonium since 1958. The MCC is housing three uranium-graphite reactors, a radiochemical plant for irradiated fuel reprocessing, and storage of radioactive wastes (Vakulovsky et al., 1995). The last reactor of the MCC was shut down in April 2010, thus stopping the discharges of the majority of isotopes with neutron-induced activity to the Yenisei (Shershakov et al., 2010-2016). We investigated time-dependent trends of artificial radionuclides in aquatic moss (*Fontinalis antipyretica*), zoobenthos (amphipods *Eulimnogammarus viridis* and caddisfly larvae *Apatania crymophyla*), and three abundant wild fish species (Northern pike *Esox lucius*, Arctic grayling *Thymallus arcticus*, and Siberian dace *Leuciscus baicalensis*) inhabiting the Yenisei River in the vicinity of the radioactive discharge site. Samples of biota, water and sediments were collected from the Yenisei in 2007-2015. Activity concentrations of radionuclides in samples were measured using an HPGe-gamma-spectrometer (Canberra). For calculations, we used publicly available data on ^{137}Cs concentration in water of the Yenisei River and data on annual discharges of radionuclides to the Yenisei (Radiation situation…., 2007-2016). From our research, we learned that concentrations of short-lived radionuclides (^{24}Na, ^{46}Sc,^{51}Cr, ^{54}Mn, ^{58}Co, ^{59}Fe, ^{60}Co, ^{65}Zn, ^{103}Ru, ^{141,144}Ce, ^{152,154}Eu, ^{154}Eu, ^{239}Np), whose discharges to the Yenisei either stopped or ceased after the shutdown of the reactor plant at the MCC, decreased in biota samples as well. The ecological half-life (EHL) of ^{65}Zn (0.4-0.7 y) was similar to the physical half-life of this isotope, while the EHLs of ^{60}Co (1.2-2.1 y) and ^{152}Eu (1.8 y) were shorter than the physical half-lives of these isotopes. Concentration of ^{137}Cs did not decrease significantly in biota of the Yenisei after the shutdown of the last reactor plant because the discharges of this radionuclide to the Yenisei continued at the same level. On a longer-term scale (since 1973 and since 1991), concentration of ^{137}Cs in fish muscle had significantly decreased, following the decrease in annual discharges of this radionuclide to the Yenisei, and the EHL of ^{137}Cs was estimated as 6.5-12.8 y. Statistically significant correlation with annual discharges of ^{137}Cs was revealed for the concentration of this radionuclide in grayling (bodies and muscle); dace (muscle), and amphipods (Table 1). Despite their ability to accumulate high concentrations of ^{137}Cs, aquatic moss and caddisfly larvae (analyzed together with their stony casings) were not sensitive to interannual fluctuations in the releases of this radionuclide to the Yenisei.

Among the analyzed fish species of the Yenisei, the highest activity concentration of ^{137}Cs was revealed in pike, indicating biomagnification of this radionuclide in the top level of trophic chain. Concentration of ^{137}Cs in pike tended to decrease with increasing weight of the fish, indicating negative "size effect" (Figure 1).

Table 1. Correlation between activity concentration of ^{137}Cs in samples of biota of the Yenisei River (Bq kg^{-1} f.w.) and annual discharges of this radionuclide to the Yenisei (Bq year^{-1}) during 2007-2015.

Sample of biota	*n*	*R*	*p*
Arctic grayling, body	23	**0.69**	0.0003
Arctic grayling, muscle	26	**0.44**	0.026
Siberian dace, body	24	0.23	0.281
Siberian dace, muscle	17	**0.51**	0.037
Aquatic moss	13	0.32	0.288
Caddisfly larvae with casings	8	-0.03	0.948
Amphipods	12	**0.65***	0.021

p – Confidence level, n – number of samples. *Amphipods were collected from 2009 onwards.

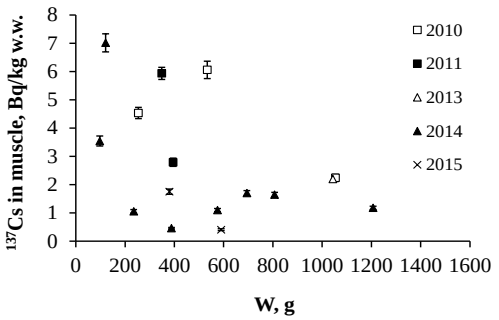

Figure 1. Concentration of ^{137}Cs in muscle of pike of the Yenisei River (Bq·kg^{-1} w.w.) vs. total fresh weight of the fish body (W, g).

This work was supported by the Russian Foundation for Basic Research and Krasnoyarsk Scientific Foundation under grant No. 18-44-240003 and the State Assignment for Fundamental Research.

Vakulovsky, S. M., Kryshev, I. I., Nikitin, A. I., et al. 1995. Radioactive contamination of the Yenisei River. *J. Environ. Radioactiv.* 29, 225–236.

Radiation situation in Russia and neighboring countries in 2007-2015. A yearbook. Shershakov, V. M., et al. (Eds.). 2008-2016. FGBU NPO Typhoon, Obninsk.

Ecological transfer of wet-deposited radiocaesium and radiostrontium on Chinese vegetable

Han Baohua, Zhang Chao, Li Jianguo, Cao Shaofei, Zhang Sheng, Wang Huijuan, Ma Binghui, Wang Xuewen

Department of nuclear environmental science, China Institute for Radiation Protection, Taiyuan,030006, China
Keywords: ecological transfer, wet-deposited, radionuclides, eggplant
Presenting author, Han Baohuo, e-mail: hbaohua918@126.com

Interception of wet-deposited radionuclides by vegetation is a key process in radioecological models assessing ingestion doses to the population following radioactive releases to the atmosphere. The process of radionuclide deposition involves parameters such as interception fraction, translocation factor and transfer factor, which is the important part of environmental assessment.

The purpose of this study is to establish a database of radionuclide transfer parameters in the subtropical regions of China. In this experiment, the rain scenarios were simulated in the artificial climate chamber. Eggplant (flowering stage) was used as experimental material in 2018. Soil was collected near a nuclear facility in Southern China. A new artificial rain sprinkler was used to simulate light and moderate radioactive rain, the rainfall was 3 mm and 15 mm respectively. The activity concentration of ^{137}Cs in rainwater was 564Bq/L,^{90}Sr was 464Bq/L. The layout of the experiment was showed in table 1.The volume of light rain is 6.6L, 220mL per pot of vegetable, the volume of moderate rain is 33L, 1.1L per pot.

Table 1. Layout of the deposition experiment.

Deposition date	Deposition to vegetable	Sampling date	Radinuclides deposited amount
2018.7.11	light rain-Interception	2018.7.13	^{137}Cs : 1652Bq/m^2,^{90}Sr : 1359 Bq/m^2
2018.7.11	light rain - translocation	2018.8.8	
2018.7.11	moderate rain-Interception	2018.7.13	^{137}Cs : 8518Bq/m^2,^{90}Sr : 7008 Bq/m^2
2018.7.11	moderate rain-translocation	2018.8.8	

* eggplant was sowed at 2018.3.6.

The interception, translocation of radionuclides during the flowering stage of eggplant were studied, and the corresponding transfer parameters were obtained. The interception fraction(f) of ^{137}Cs in light /moderate radioactive rain on Eggplant leaves surface at flowering stage were 0.19 and 0.073, respectively (means are from three replicates). The interception fraction of ^{90}Sr in light /moderate rain on eggplant leaves surface at flowering stage were 0.21, 0.061 respectively (Fig.1).

When the soil surface was covered with cotton and plastic film, The translocation factors(f_{tr}) of ^{137}Cs in light rain/moderate rain were 12.7% and 12.3% in flowering stage of eggplant, while those of ^{90}Sr in light rain/moderate rain were 1.0% and 2.0%, respectively. When the soil surface was not covered, the translocation factors of ^{137}Cs in the light /moderate rain were 13.0% and 10.8% during flowering stage of eggplant, respectively, and the translocation factors of ^{90}Sr in the light/moderate rain were 1.4% and 1.6%, respectively (Fig. 2).

At the flowering stage of eggplant, for the same nuclide, the interception fraction (f) of light rain was significantly higher than that of medium rain. Interception of rain by vegetable is closely linked to the water storage capacity, Interception increases during a rainfall event until the interception capacity is achieved. Under the same experimental conditions, the translocation factor (f_{tr}) of ^{137}Cs is much larger than that of ^{90}Sr. For eggplant, radionuclide ^{137}Cs is easier to transfer to fruits than ^{90}Sr. These transfer parameters will be compiled in the transfer parameter database of China in the future.

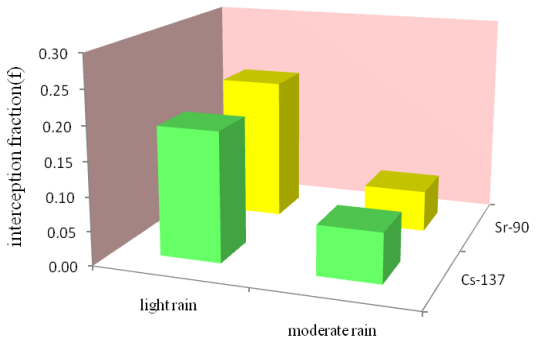

Figure 1. The interception fraction(f) of ^{137}Cs and ^{90}Sr.

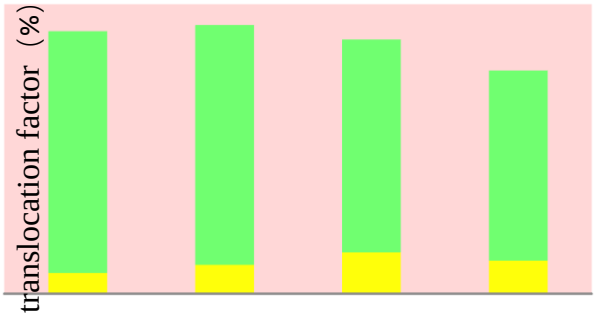

Figure 2. The translocation factors(f_{tr}) of ^{137}Cs and ^{90}Sr.

IAEA. Handbook of parameter values for the parameter values for the prediction of radionuclide transfer in terrestrial and freshwater environments [R]. *IAEA technical reports series* No. 472, 2010.

Rosén K, Vinichuk M. Interception and transfer of wet-deposited ^{134}Cs to potato foliage and tubers[J]. Journal of Environment Radioactivity, 2016,151:224-232.

Sorption of strontium on the Czech bentonite in the presence of synthetic granitic water

L. Baborová, K. Štamberg, D. Vopálka

Department of Nuclear Chemistry, Czech Technical University in Prague, Prague, 11519, Czech Republic
Keywords: strontium, sorption, bentonite, granite
L. Baborová, e-mail: Lucie.Baborova@fjfi.cvut.cz

Within the project of the deep geological repository (DGR) in the Czech Republic, the local Mg/Ca bentonite named BaM (Bentonite and Montmorillonite) has been tested with the aim to assess its sorption qualities for the performance assessment (PA) of the repository with regard to cations. Sorption batch experiments present a tool to the estimation of sorption coefficients, which provides an useful information on the transport properties of barrier materials.

Batch sorption experiments of Sr were performed on the loose bentonite BaM (Červinka *et al.* 2015) contacted with the synthetic granitic water (SGW), which was suggested earlier as a representative of the deep circulation of ground-waters in the granitic massive and its composition corresponds with the mean composition of ground water in the *Underground Research Facility* Bukov. The water is of Ca-HCO_3 type and its ionic strength is about 5 mmol·L^{-1} (Červinka *et al.* 2016). Radiotracer method with the use of ^{85}Sr was employed for the determination of Sr concentration in the liquid phase. Activity of samples was measured relatively against standard solution with known activity.

Kinetic study was performed for Sr concentrations (C_0 [mol·L^{-1}]) 10^{-5} and 10^{-3} mol·L^{-1} and four values of solid-to-liquid ratio (m/V [g·mL^{-1}]). The results showed that Sr concentration in liquid phase initially drops as the cation is taken up by the adsorbent but after 24 hours a small amount of Sr (< 5 %) is released again to the solution and desorption process continues until about 42 days. An attempt was made to fit the experimental data with the kinetic model of film diffusion, as shows Figure 1.

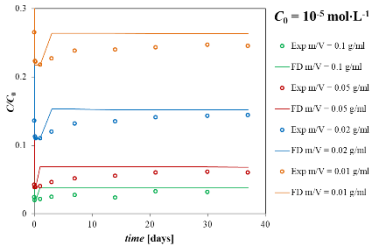

Figure 1. Kinetics of Sr relative concentration in liquid phase evaluated by film diffusion model.

Based on the results of kinetic study, equilibrium experiments were led 42 days with four Sr concentrations in the range from 10^{-6} to 10^{-3} mol·L^{-1} and four values of solid-to-liquid ratio. The resulting relations between Sr concentration taken up by solid phase (q [mol·kg^{-1}]) and concentration remaining in liquid phase (C [mol·L^{-1}]) were fitted by linear and Freundlich sorption model, as shows Figure 2. It was found out that the Freundlich model is more appropriate, although linear model can be also conveniently applicable.

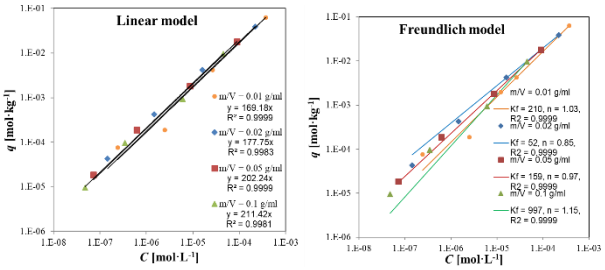

Figure 2. Equilibrium sorption data of Sr evaluated by linear (left) and Freundlich (right) sorption model.

Finally, K_d values obtained as a slope of the sorption isotherms were found to be increasing with the value of solid-to-liquid ratio. According to the power function in Figure 3, it is then possible to estimate the K_d value applicable for the conditions of compacted bentonite, which is proposed as a buffer material in the DGR, with high solid-to-liquid ratio.

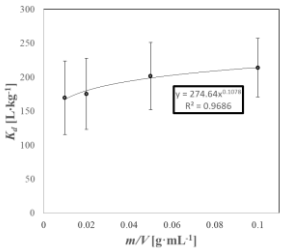

Figure 3. K_d values in dependence on solid-to-liquid ratio.

This work is partially a result of Radioactive Waste Repository Authority project „Research Support for Safety Evaluation of Deep Geological Repository“ and partially a result of grant No SGS19/193/OHK4/3T/14 provided by the Grant Agency of the Czech Technical University in Prague.

Červinka R., Vopálka D., etal., 2015: Transport radionuklidů z úložiště / Vstupní parametry a procesní modely pro hodnocení transpor tu radionuklidů přes inženýrské bariéry: 1. Průběžná zpráva. *TR nr. 24/2015.*

Červinka R., Gondolli J., Havlová V., Rukavičková L. 2016: Výběr reprezentativních podzemních vod a příprava jejich syntetických ekvivalentů. *TR nr. 41/2016.*

Independent development of ESS tungsten target radionuclide composition modelling

V. Barkauskas[1], K. Stenström[1]

[1]Division of Nuclear Physics, Lund University, Lund, 221 00, Sweden
Keywords: spallation, FLUKA, ESS, tungsten
E-mail: vytenis.barkauskas@nuclear.lu.se

The European Spallation Source (ESS) is a large-scale user facility currently under construction in Lund, Sweden. It will be a powerful neutron source for studies of the structure and dynamics of the materials. An inevitable side effect of the neutron generation is the production of various radionuclides, resulting from spallation in the proton accelerator and target, as well as from neutron activation of surrounding structures, soil, and air. A fraction of the radionuclides produced in ESS may be released to the environment during normal operation, as well as in potential accidents.

We present an independent assessment of radionuclides production in ESS target that might be used as a source term for further radiological impact assessment. Despite the number of recent publications, knowledge about ESS target radionuclide composition during and after irradiation still remains limited (Mora et al., 2018). Our objective is to bring more clarity to this field of study with our ESS-independent contribution which may be further employed by regulatory institutions and researchers. We are also intending to specify and justify radionuclide list, which may be relevant for environmental monitoring during and after operation. For example, evaluation of production rate and activity of ^{148}Gd is of vital importance as it is one of the most toxic alpha emitters which will be produced in ESS. ^{3}H has low dose factors, however it is produced in high quantities and it is very mobile in the environment, therefore quantification of ^{3}H production is essential from the perspective of environmental radiological protection. It is estimated that the total activity content of ^{3}H in the tungsten target after 5 years of operation will be $3 \cdot 10^{15}$ Bq (Ene et al., 2015), i.e. in the same order of magnitude as the annual ^{3}H release from an operational heavy water reactor.

A simplified model of one ESS target sector was used to demonstrate possible application of FLUKA code (Böhlen et al., 2014). FLUKA is a general purpose tool for calculations of particle transport and interactions with matter using Monte Carlo method. Major components of ESS target were included in the model, but with simplified geometries.

We have calculated activities of all radionuclides after 5 years of operation (designed lifetime of target-wheel). The obtained activity concentration of radionuclides in the front part (facing the proton beam) of target wheel are presented in Fig. 1. Most of the radionuclides are short-lived and only a minor part of the produced radionuclides is relevant for long-term radiological effect evaluation.

The particular attention was paid to the production levels of alpha-emitter ^{148}Gd. Relatively high discrepancies between our calculation results and those of other authors were found. Our calculations show one order of magnitude higher activities of ^{148}Gd. Preliminary evaluation results show that content of ^{3}H generated in the target is in the same orders of magnitude as in other publications. The addition of impurities to the tungsten target composition did not significantly affect the concentrations of most radionuclides in the target.

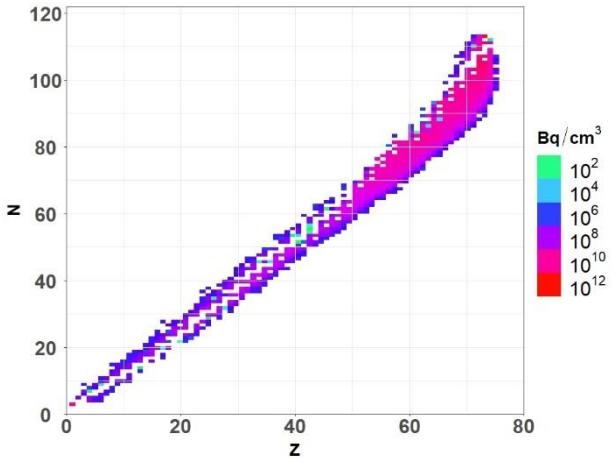

Figure 1. Activity concentrations of radionuclides in the front part of ESS tungsten target.

Currently the model needs some further verification activities which may include uncertainty and sensitivity analysis, and possibly use of other calculation codes. These activities are foreseen in the future.

This work is supported by Swedish Radiation Safety Authority (SSM), grant No. SSM2018-1636-1.

Mora, T. et al. 2018. An evaluation of activation and radiation damage effects for the European Spallation Source Target. *J. Nucl. Sci. Technol*. 55, 548-558.

Ene, D. et al. 2015, Management of Tritium in European Spallation Source. *Fusion Sci. Technol*. 67, 324-327.

Böhlen, T. T. et al 2014. The FLUKA Code: Developments and Challenges for High Energy and Medical Applications. *Nucl. Data Sheets*. 120, 211-214.

Long-term and multivariate correlation analysis of air dose rate with meteorological parameters in Japan

T. Batgerel[1], K. Yoshida[1], T. Nomura[1] and N. Yasuda[1]

[1]Research Institute of Nuclear Engineering, University of Fukui, Tsuruga, 914-0055, Japan
Keywords: air gamma dose rate, variation, meteorological parameter, analysis
T. Batgerel, turbatgerel@gmail.com

Continuous measurement of the air gamma dose rate (air dose rate) is one of the screening methods for making a decision of sheltering and/or evacuation under nuclear emergency with an atmospheric radioactive release. In a normal situation, long-term measurement is also useful as an indicator to recognize situation change to be an emergency situation and to educate resident how to behave under the disaster (Batgerel et al., 2019). There are many researches to characterize the air dose rate with a meteorological parameter. For example, the air dose rate in surface air is mainly originated from natural radioactive decay in the ground and the secondary cosmic rays (Beck et al., 1972) and fluctuation of air dose rate is usually expected from radon and its progenies in the surface air (Wissmann, 2006), which is affected mainly by meteorological conditions. Precipitation causes a noticeable increase in air dose rate owing to scavenging of short-lived radon progenies, mostly ^{214}Pb and ^{214}Bi (Fujinami, 1996; Inomata et al., 2007), and strong correlation with contributing air mass (Mercier et al., 2009). Snow cover also causes the fluctuation of air dose rate due to attenuation of the primary radiation in the snow cover (Omori et al., 2019). Thus, the correlation between the air dose rate with multiple meteorological parameters was rarely reported in the past years.

In this paper, with aim of understanding how the air dose rate varies over almost 50 years and is affected by natural phenomena, we statistically analysed as Big Data of the time series of air dose rate, continuously measured at six radiation monitoring stations in Akita, Niigata, Fukui, Nagoya, Kochi and Miyazaki prefectures in Japan. The air dose rate (in nGy/h) has been monitored routinely and stored into the Environmental Radiation Database, which is publicly available. The typical meteorological parameters considered in this work were precipitation (in cm), snow cover (in cm), temperature (in ºC), humidity (in %), pressure (in hPa), and wind speed (in m s^{-1}) and direction obtained from the meteorological measurement system at the corresponding weather observation site and were supplied by database of Japan Meteorological Agency.

To explore the correlations between air dose rate and meteorological parameters their mean monthly values were statistically calculated using the arithmetic average value. We used the Pearson`s correlation since it is available to evaluate the linear relationship between two continuous variables. The correlation coefficients were varied by the range of each meteorological parameter. Relatively high correlation coefficients between the air dose rate and the meteorological parameters obtained were below. The correlations with precipitation were 0.77 and 0.71 in Akita and Niigata, respectively. Snow cover also strong negatively correlated with the air dose rate in Akita (-0.74) and Fukui (-0.71). The correlations with temperature were moderately positive in Akita (0.53) and negative in Miyazaki (-0.53). In the case of humidity, the calculation produced a correlation coefficient of 0.42 in Nagoya. For the pressure correlation coefficients were moderately positive in Nagoya (0.43) and Miyazaki (0.46). The correlations with wind speed were mainly negative, -0.68, -0.67, and -0.52 in Nagoya, Kochi, and Akita, respectively.

In conclusion, correlation coefficients between the air dose rate and multiple meteorological parameters vary in different locations. This study had revealed the observable phenomenon of correlation between the air dose rate and the meteorological condition in a different location. It will be useful to consider sheltering and evacuation order after the nuclear accident.

This work was supported by the Grants-in-Aid for Scientific Research, JP18K02857.

Batgerel, T. et al., 2019. Environmental gamma radiation monitoring in Japan. in First International Conference on Applied Sciences and Engineering, Ulaanbaatar, Apr. 2019 pp.631-634.

Beck, H.L. et al., 1972. In situ Ge (Li) and NaI (T1) gamma-ray spectrometry. P00066834.

Fujinami, N., 1996. Observational study of the scavenging of radon daughters by precipitation from the atmosphere. *The Natural Radiation Environment VI 2*, 181–185.

Inomata, Y. et al., 2007. Seasonal and spatial variations of enhanced gamma ray dose rates derived from ^{222}Rn progeny during precipitation in Japan. *Atmospheric Environment, 41(37)*, pp.8043-8057.

Mercier, J.F. et al., 2009. Increased environmental gamma-ray dose rate during precipitation: a strong correlation with contributing air mass. *Journal of environmental radioactivity, 100(7)*, pp.527-533.

Omori, Y. et al., 2019. Reduction in ambient gamma dose rate from radiocesium due to snow cover. *Radiation protection dosimetry*.

Wissmann, F., 2006. Variations observed in environmental radiation at ground level. *Radiat. Protect. Dosim. 118 (1)*, 3–10.

Elevated seawater $^{129}I/^{127}I$ ratios in the West Philippine Sea

A.T. Bautista VII[1], S.J.M. Limlingan[1], J. Munar[2], H. Matsuzaki[3], F.P. Siringan[2]

[1]Department of Science and Technology – Philippine Nuclear Research Institute (DOST-PNRI), Quezon City, 1101, Philippines
[2]Marine Science Institute, University of the Philippines, Quezon City 1101, Philippines
[3]Micro Analysis Laboratory, Tandem Accelerator (MALT), The University Museum, The University of Tokyo, Tokyo, 113-0032, Japan
Keywords: iodine-129, AMS, South China Sea
Presenting author, e-mail: atbautistavii@gmail.com

Iodine-129 (^{129}I) is a long-lived fission product that is predominantly released by human nuclear activities (HNA) such as nuclear weapons testing and manufacture, nuclear fuel reprocessing, and nuclear accidents. In the marine environment, it can act as a proxy for detecting HNAs and as an oceanographic tracer for quantifying ocean circulation and seawater mass exchange.

In a previous study, ^{129}I measurements in corals from the Philippines (Bautista et al., 2016) show that the West Philippine Sea (WPS) may have higher concentrations of ^{129}I than that observed from the east side of the country (i.e., Pacific Ocean side). This situation merits further investigation to study possible sources of ^{129}I in the WPS and its application as an oceanographic tracer of the complicated and interesting WPS circulation.

Here we present ^{129}I concentrations of 34 seawater samples collected along a transect in the WPS (Figure 1). Results show that $^{129}I/^{127}I$ ratios in the WPS are in the range of 2.4 to 3.7 x 10^{-11} (average of 3.1 x 10^{-11}). These values are 1.5x higher than that from the Pacific Ocean side of the Philippines, which is at an average of 2.2 x 10^{-11} (based on coral measurements). Seawater samples taken from 5m depth show that $^{129}I/^{127}I$ ratios from locations along the seawater circulation appear to have higher $^{129}I/^{127}I$ ratios than those observed in the middle parts of the WPS. This finding suggests that ^{129}I is being carried by the prevailing ocean circulations and may come from sources that directly feed the mentioned current. Moreover, these results support that ^{129}I may be used as a quantitative tracer for the complicated WPS circulation. An even more extensive seawater sampling across the WPS and the whole South China Sea may help ascertain the source of ^{129}I in the region.

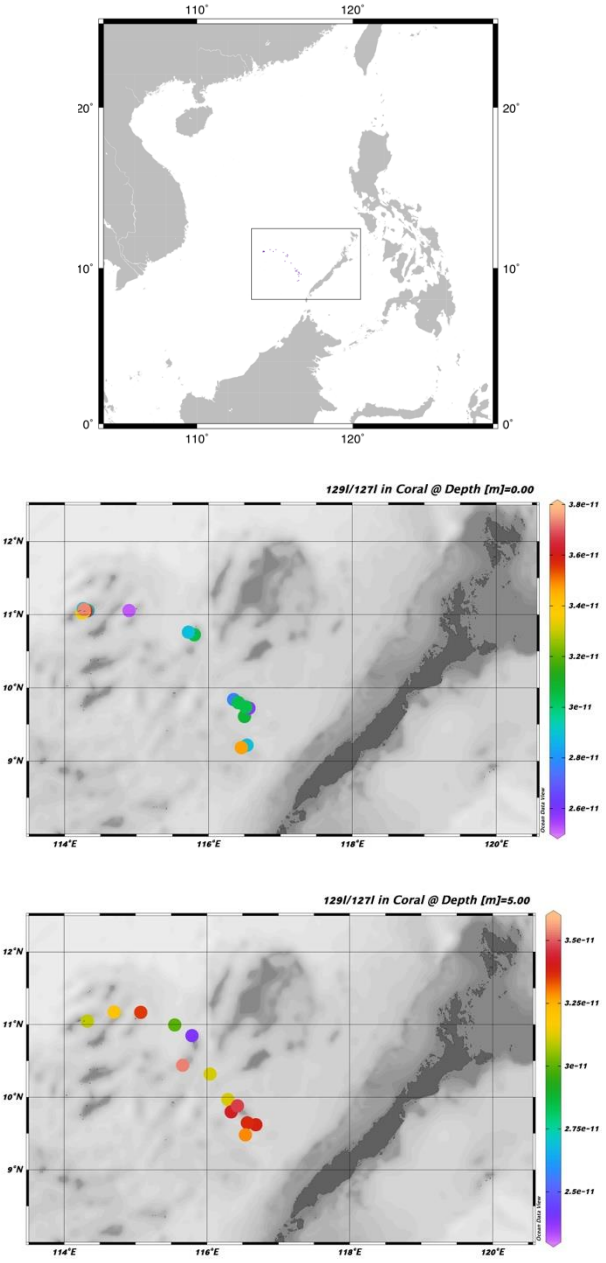

Figure 1. (top) sampling sites; $^{129}I/^{127}I$ ratio of seawater from the West Philippine Sea at depths of (middle) 0m, and (bottom) 5m.

Bautista, A.T., Matsuzaki, H., Siringan, F.P., 2016. Historical record of nuclear activities from 129I in corals from the northern hemisphere (Philippines). *J. Environ. Radioact.* 164, 174–181. doi:10.1016/j.jenvrad.2016.07.022

Estimation of ADER from aerial measurements by the drone equipped with gamma spectrometer

Daniel Bednář[1, 2], Petr Otáhal[1], Ladislav Němeček[1], Eva Geršlová[2]

[1]National Institute for Nuclear, Chemical and Biological Protection (SUJCHBO), Kamenná 71, 262 31 Milín, Czech Republic
[2] Department of Geological Sciences, Masaryk University, Faculty of science, Brno, Kotlářská 2, 602 00, Czech Republic
Keywords: ADER, drone, radiation, spectrometer
Daniel Bednář: bednar@sujchbo.cz

Radiation monitoring is increasing in demand whatever it is monitoring in the surroundings of nuclear power plants, monitoring of former uranium mines or areas before and after remediation. During the traditional way of field monitoring – walking measurements – it is possible to encounter inaccessible or dangerous areas. For these cases the drones equipped with proper device can be used to determine the radiation levels during the field monitoring. For this type of monitoring the National Institute for Nuclear, Chemical and Biological Protection (SUJCHBO) has created the methodology of aerial measurement of ambient dose equivalent rate (ADER) using the drone with gamma-spectrometer.

Drones found great use during the radiation monitoring after Fukushima disaster (Sanada and Torii 2015, Sanada et al. 2016).

The goal of this research was to evaluate new custom made spectrometer for aerial measurements and to test the reliability of method for estimation of ADER near the ground by aerial measurements.

The gamma spectrometer D230A was tested in special testing room provided with radioactive source in form of concrete walls (in the corner) which has higher concentration of radionuclides from uranium decay series. There is a bench with ruler attached to the walls pointing to the center of the room. The values of ADER on the bench goes from approx. 200 nSv/hr to 1650 nSv/hr. There is also a cell made of lead bricks to simulate lowest possible ADER with values under 40 nSv/hr. Device were compared in 5 measuring points – 4 on the bench in the range 4 m, 2.5 m, 1.5 m and 0.7 m from source and 5th in the lead cell. The results were compared with our verified spectrometer GT-40.

Spectrometer was then tested on the testing field.

This testing field (Figure 1) is characterized by area in the south-west corner formed by material from uranium waste dump with increased amount of natural radionuclides from uranium series with higher values of ADER – maximum approx. 1200 nSv/hr. There are also parts with values of ADER lover than 200 nSv/hr. This makes the Heliport an ideal place for testing devices suitable for measuring and mapping the distribution of ADER.

The flights on the testing field were done at altitude of 6, 11 and 16 meters. The measured data are presented as the maps. Foer each height the 25th, 50th, 75th, 90th and 95th percentile were calculated and based on this the values of ADER at altitude of 1 meter were calculated (Figure 2). Then the calculated values were compared to values measured by walking measurement at altitude of 1 m.

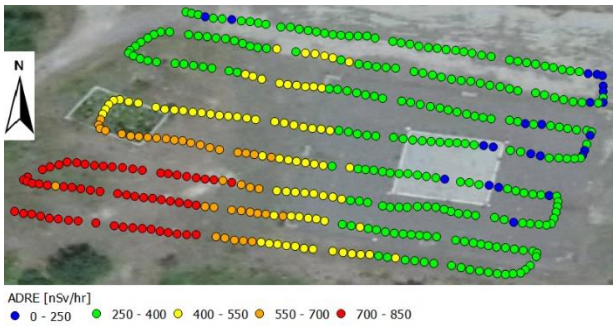

Figure 1. Example of ADER distribution on heliport measured via D230A from altitude 6 m.

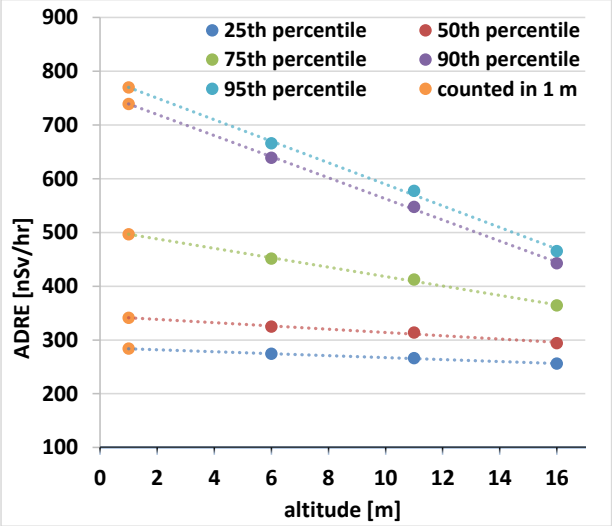

Figure 2. Values of percentiles for each height.

Sanada, Y., Orita, T., Torii, T. 2016. Temporal variation of dose rate distribution around the Fukushima Daiichi nuclear power station using unmanned helicopter. *Appl. Radiat. Isot.* 118, 308-316.

Sanada, Y., Torii, T. 2015: Aerial radiation monitoring around the Fukushima Dai-ichi nuclear power plant using an unmanned helicopter. *J. Environ. Radioact.* 139, 294-299.

Development of fluoride target matrices for ^{26}Al determination with AMS

M. Bilous[1], K. Fenclová[1], T. Prášek[1], M. Němec[1], J. Tecl[2], J. Kučera[2]

[1]Department of Nuclear Chemistry, Czech Technical University in Prague, 115 19, Czech Republic
[2]Nuclear Physics Insitute, The Czech Academy of Sciences, Husinec - Řež, 250 68, Czech Republic
Keywords: Accelerator Mass Spectrometry, Aluminium, Fluoride
M. Bilous, e-mail: biloumar@fjfi.cvut.cz

Accelerator mass spectrometry (AMS) is one of the most sensitive methods for determination of ultratrace concentrations of long-lived radionuclides in environment. In addition, AMS measurements using fluoride matrices have a significant advantage in terms of interference reduction since fluorine is a monoisotopic element. The determination of ^{26}Al is used in areas such as meteorite dating or time exposure of rocks to cosmic radiation (Kutschera, 2013). The fluoride matrix for determination of ^{26}Al was selected on base of Na_3AlF_6 because of its precipitation properties and possibility to produce high ion currents. Experiments were performed using the detection system of linear tandem accelerator system Tandetron 4130 MC. For these measurements, sputter targets of pure Na_3AlF_6 and its mixtures with powdered Ag, W, Cu, CaF_2 or PbF_2 were used. Resulting ion currents were examined after sputtering the target samples in a caesium ion source. The assessment of the suitability of the prepared matrices was based on obtained mass spectra, where the most promising molecular ion was identified as AlF_4^-. This ion mass was then selected and accelerated at terminal voltages 1, 1.5 and 2 MV, respectively, and analysed for beam composition and positive ion yields. Currently performed experiments are focused on determination of critical isobaric interferences between ^{26}Mg and ^{26}Al.

This work was supported by project No. CZ.02.1.01/0.0/0.0/16_019/0000728: RAMSES.

Kutschera, W. 2013. Applications of accelerator mass spectrometry. *International Journal of Mass Spectrometry*. 349-350 (2013) 203-218.

How the distribution coefficient of ^{238}U in natural soils is affected by the method used to obtain the soil solution

P. Blanco Rodríguez[1], F. Vera Tomé[1], J.C. Lozano[2]

[1]Natural Radioactivity Group. University of Extremadura, 06071 Badajoz, Spain
[2]Laboratory of Ionizing Radiations. University of Salamanca, 37008 Salamanca, Spain
Keywords: Uranium, Distribution coefficients, Centrifugation
Presenting author, e-mail: pbr@unex.es

The process of absorption-desorption between a soil and the soil solution are described by means of the distribution coefficient K_d ($L \cdot kg^{-1}$), that represents the partition of the radionuclide between the solid phase in the soil ($Bq \cdot kg^{-1}$) and its solution ($Bq \cdot L^{-1}$). The K_d coefficient is commonly used to assess the mobility and residence times of radionuclides in soils, and is an input for the transfer models. The use of the K_d coefficient assumes that the distribution of the radionuclide between the two phases follows equilibrium conditions in a reversible process. However, there is ample evidence that such equilibrium conditions are not always met and that the value of K_d tends to increase over time.

An approach based on the use of a high performance centrifuge and specifically designed devices has been proposed (Lozano et al., 2019) to obtain the most realistic possible values of the K_d of soil. With this in mind, in a previous work (Blanco Rodríguez et al., 2018), different experiments were designed to determinate the available fraction of ^{226}Ra in soils collected in a mineralized uranium zone located in western Spain. In the present work, the same experimental design was performed but with the aim of obtaining the distribution coefficient of ^{238}U in soils.

Therefore, the main objective of this work is to reduce the level of the uncertainty regarding the K_d parameter. For this, we initially performed a systematic study on the influence of parameters, such as incubation time, solid/liquid ratio and centrifugation speed, on the distribution coefficients of ^{238}U. Also, in order to clarify the influence of particle size on the K_d value, a systematic study has been performed on three soil fractions with different structural characteristics. With the aim of eliminating other sources of uncertainty, due to the soil type, three soil subsamples from a natural single soil have been obtained through dry sieving processes.

The soil sample was collected from an area with natural uranium mineralization located in the south-west region of Castilla y Leon, in Spain (40°43'N; 6°42'E).

The aqueous extracts from each soil subsample were obtained by centrifugation using an ultracentrifuge (Beckman-Coulter, Avanti 25I), a fixed-angle rotor (Beckman-Coulter, JLA 16.250) and devices specially designed to adapt the positioning of soil specimens to the fixed-angle rotor (Lozano et al., 2019). In order to study the influence of the three parameters in the determination of the K_d for ^{238}U, three values were selected for each parameter: 1, 7 and 30 days for the incubation time; 50%, 75% and 100% for moisture level; and 2200, 5000 and 12000 rpm for centrifugation speed, which correspond to the ranges of suction and mean values (kPa) of [32-41] (36), [153-193] (168) and [760-938] (827), respectively, depending on the characteristics of each sample. Additional details regarding this experimental design have been previously described (Blanco Rodríguez et al., 2018; Lozano et al., 2019).

The activity concentration of ^{238}U (for the three soil fractions and for every soil solution extract) was determined by using the alpha spectrometry technique.

An analysis of variance (ANOVA) was performed in order to assess the influence of the studied factors on the distribution coefficient of ^{238}U.

The results indicate that the level of moisture is the most important factor to be taken into consideration when designing procedures for determining uranium-K_d. The statistical analysis conducted also shows that (in the ranges considered in this study) both the incubation time and centrifugation speed have no influence on the uranium concentration in the soil solution. This indicates that short incubation times are sufficient for ^{238}U-K_d determination, and that an increase in the suction applied does not increase the concentration of uranium in solution. Furthermore, the influence of moisture on the K_d for uranium depends on the structural characteristic of the soil.

We thank the Spanish Ministry of Education and Science, Plan Nacional de I+D+I (CTM2011-25400 project), for providing financial support.

Blanco Rodríguez, P., Lozano, J.C., Vera Tomé, F., Prieto, C., Medeiros, A. 2018. Influence of soil conditions on the distribution coefficients of ^{226}Ra in natural soils. *Chemosphere* 205, 188-193.

Lozano, J.C., Blanco Rodríguez, P., Vera Tomé, F., Maldonado, R., Medeiros, A.S., Prieto, C. 2019. A system for obtaining soil solution extracts and soil water retention curves using a bench centrifuge with fixed angle rotors. Submitted for publication.

Monte-Carlo simulation of HPGe spectrometer background at low energies

Róbet Breier[1], Veronika Palušová[1,2], Holger Kluck[3,4], Valentyna Mokina[4], Fabrice Piquemal[2], Pavel P Povinec[1]

[1]Faculty of Mathematics, Physics and Informatics, Comenius University, SK-84248 Bratislava, Slovakia
[2]Université de Bordeaux, CNRS/IN2P3, CENBG, F-33175 Gradignan, France
[3]Atominstitut, Vienna University of Technology, A-1020 Wien, Austria
[4]Institut für Hochenergiephysik der Österreichischen Akademie der Wissenschaften, A-1050 Wien, Austria
Keywords: Monte-Carlo, HPGe, Background, muon, cosmic rays, contamination, radon
Presenting author, e-mail: breier@fmph.uniba.sk

The best non-destructive and widely used method in environmental radioactivity measurements is gamma-spectrometry. To improve the accuracy of these measurements, detectors with high efficiency, good resolution and high sensitivity are needed. Large volume HPGe detectors meet these requirements. The important parameter which influences the detection limit is radionuclide background, consisting mainly of (i) cosmic rays, (ii) intrinsic contaminations of the detector materials, and (iii) ambient contaminations of the laboratory (Breier et al., 2016).

Cosmic-ray induced background can be eliminated to a large extent by placing the detector in an underground laboratory. The background induced by soft component of cosmic rays (electrons, positrons, gamma-rays) and by radionuclide contamination can be decreased by using passive shielding made of radiopure materials. Neutron-contribution to background is effectively shielded by materials with low Z. On the other hand, materials with high Z effectively absorb gamma-rays (Povinec et al., 2008).

The optimization of the shielding configuration is often a hard challenge, therefore Monte-Carlo (MC) simulations represent a useful tool to solve this task. However, MC simulations are often inaccurate in the low energy range (<300 keV). This range is very important for measuring radionuclides from the ^{238}U and ^{232}Th decay chains, as well as of cosmogenic origin. The low energy range is also important for material screening for low-energy dark matter experiments. GEANT4 MC simulations are influenced by geometric parameters (cryostat thickness, material of the cryostat and detector holder, dead layer thickness of the Ge detector), which are used in the parameters of the physics list.

Under investigations was the Obelix HPGe detector which is operating in the Laboratoire Souterrain de Modane (LSM) in France at the depth of 4800 m w.e. (Breier et al., 2018). It is a p-type coaxial detector with a diameter of 93.5 mm and a length of 89.6 mm. The useful volume is 600 cm^3 and the relative detector efficiency is 162%. The resolution of the detector is 1.12 keV at 122 keV, and 1.98 keV at 1332 keV. The cryostat and the detector holder are made from Al-4%Si alloy; the thickness of the entrance window is 1.6 mm. Oxygen free high conductivity copper was used for production of the cold finger. The inner shield (thickness of 12 cm) of the HPGe detector was made of Roman archeological lead. The outer shield (thickness of 20 cm) was made from low activity lead.

All simulations were carried out with the GEANT4 toolkit developed at CERN (Allison et al., 2006). Radioactive alpha, beta$^+$ and beta$^-$ decays of contaminants were simulated with the G4RadioactiveDecay module of Geant4. The nuclear de-excitation of the excited daughter product was simulated using G4PhotoEvaporation class. The module is empirical, and it uses data from Evaluated Nuclear Structure Data File (ENSDF). The position of radioactive decays was simulated in various parts of the HPGe detector (Fig. 1).

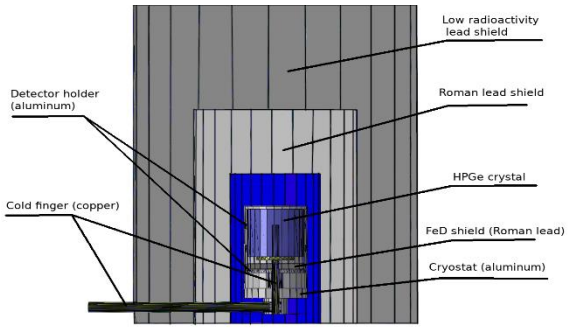

Figure 1. Obelix HPGe detector.

GEANT4 properties relevant to low energy simulations are mainly: the selected physics list, cut value, and atomic processes (Augers electrons, X-ray emission, etc.). The evaluation of the impact of these parameters on the HPGe detector background was a goal of this work.

This work has been supported by the Slovak Research and Development Agency (SK-AT-2017-0019), and by the Austrian Agency for International Cooperation in Education and Research (SK 06/2018).

Allison, J. et al., 2006. Geant4 developments and applications. *IEEE Trans. Nucl. Sci.* 53, 270–278.

Breier, R., Hamajima, Y., Povinec, P.P., 2016. Simulations of background characteristics of HPGe detectors operating underground using the Monte Carlo method. *J. Radioanal. Nucl. Chem*. 307, 1957–1960.

Breier, R. et al., 2018. Environmental radionuclides as contaminants of HPGe gamma-ray spectrometers: Monte Carlo simulations for Modane underground laboratory. *J. Environ. Radioact.*190-191, 134-140.

Povinec, P.P., M. Betti, A.J.T. Jull, P. Vojtyla, 2008. New isotope technologies in environmental physics. *Acta Phys. Slovaca* 58, 1–154.

Nuclide-specific directional environmental radiation mapping of the vicinity of FRM II

H. Breitkreutz, D. Bruev[1], M. Schmidt, A. Kastenmüller[2]

[1]Envinet GmbH, Hans-Pinsel-Str. 4, 85540 Haar, Germany
[2]Forschungs-Neutronenquelle Heinz Maier-Leibnitz (FRM II), Technische Universität München, Lichtenbergstr. 1, 85748 Garching, Germany
Keywords: Environmental radioactivity mapping, radioactive source localization, mobile gamma spectroscopy
harald.breitkreutz@envinet.com

The emissions of nuclear reactors and radio-isotope production facilities into the environment are strictly limited by demanding legal requirements and under close surveillance to ensure the containment of radiation sources inside these facilities and appropriately licensed controlled areas. At the Forschungs-Neutronenquelle Heinz Maier-Leibnitz (FRM II), in addition to on-site monitoring installations, an external ring monitoring network is operated independently by the Bayerisches Landesamt für Umwelt (LfU). The network consists of 12 Geiger-Müller-based ENVINET MIRA devices to reliably measure H*(10) at all times.

In March 2019, an ENVINET MONA system consisting of 2x4l NaI scintillators, mounted in a car and connected to a GPS, was used to produce a detailed, nuclide-specific radiation map of the surrounding of FRM II. Spectra have been acquired in 1s-intervals and analysed regarding nuclide-specific activities and contributions to the ambient dose rate equivalent. This way, natural and artificial radiation sources could well be discriminated. Variations in the environmental background dominate the map and reveal patterns depending on asphalt, building density and other installations. Very minor contributions from artificial sources could be identified in the privately-operated facility for radioisotope production, i.e. Lu-177 and Ga-68. No artificial contributions were found from the two reactors (FRM and FRM II) and the nuclear fuel laboratory.

Since the MONA consisted of two separate detection units, the directional information was extracted by means of an analysis of the overall count rate of both detectors. The detected direction clearly correlates with the main radiation sources (Figure 1).

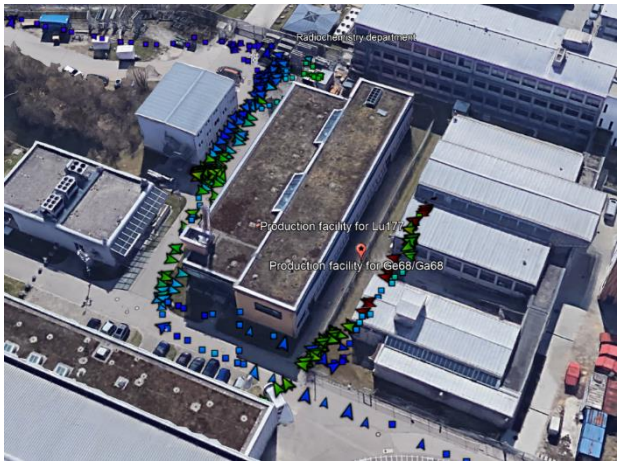

Figure 1: Ambient dose rate (colour-scale) and direction of radiation sources in the vicinity of a radioisotope production facility.

MONA has been calibrated such that the ambient dose rates can be calculated from the recorded spectra. These were in agreement with those from the MIRA ring monitoring network. The results demonstrate the reliability of the current monitoring installations as well as the advantages of spectroscopic measurement techniques and nuclide-specific environmental mapping. Furthermore, the directional sensitivity of a multi-detector MONA can be well exploited to localize radioactive sources.

A buoy-based radioactivity monitoring system for gamma emitters in seawater

Jong-In Byun, Seok-Won Choi, Myeong-Han Song, Byeong-Uk Jang, Yong-Jae Kim

Department of Environmental Radiation & Radioactivity Assessment, Korea Institute of Nuclear Safety, Daejeon, 34142, Republic of Korea
Keywords: Seawater, Radioactivity, Gamma-ray spectrometry, In-situ, Buoy, MDA
Jong-In Byun, e-mail: k975bji@kins.re.kr

Conventional method for analysis of gamma emitters in seawater involves the seawater sampling at the site and their transfer to laboratory for the preparation and analysis. So, this may be time consuming and may not detect radiological events in a timely manner, such as illegal ocean disposal of radioactive waste or unexpected discharges of radionuclides from nuclear facilities. In-situ gamma-ray spectrometry is not as accurate as laboratory analysis with sampling, but it can rapidly analyse radionuclides. The purpose of this study is to implement a buoy-based real-time radioactivity monitoring system for gamma-ray emitting radionuclides in seawater. The monitoring system consists of four core functions: 1) buoy, 2) gamma-ray measurement, 3) system control with a real-time communication (RTC), high voltage supply and GPS, 4) solar power generation. The buoy is a shallow water light type (LL-28) with a body 2.8 meters in diameter and 2 meters in height. To measure gamma-rays, a 3″Ø × 3″ NaI(Tl) scintillator coupled to a photomultiplier with a multi-channel analyser was used, which was enclosed in a 2 mm thick stainless steel cylinder for waterproofing. The detector assembly was attached to the stabilizing pole of the buoy so that the NaI(Tl) scintillator could be placed approximately 2 meters below the water surface. The system control parts and solar power generator were installed on the buoy's mast. The whole system deployed in the marine environment is shown in figure 1(a). A total of three monitoring system was installed at different sites in the Donghae (East Sea). The data measured at each site is sent to the Korea Institute of Nuclear Safety (KINS)'s server every 15 minutes via code-division multiple access (CDMA) way.

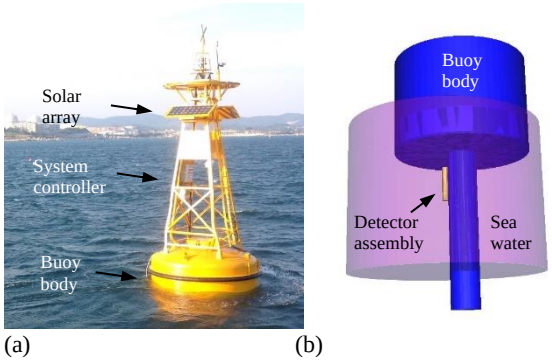

(a) (b)

Figure 1. (a) The underwater radioactivity monitoring system and (b) MCNP model for efficiency calculation of NaI(Tl) detector.

Detection efficiency of the system was determined using Monte Carlo simulation with the MCNP code. Figure (b) shows the geometrical model and the pulse height tally 'F8:P' with the default physics option in the MCNP code was used to simulate the full energy peak (FEP) efficiency. To validate the MCNP modelling, seawater samples were collected at the sites and analysed for ^{40}K using a high purity germanium detector (HPGe) system with a 30% relative efficiency in a laboratory. The FEP efficiency of the HPGe detector for was calibrated with a certified gamma-ray source.

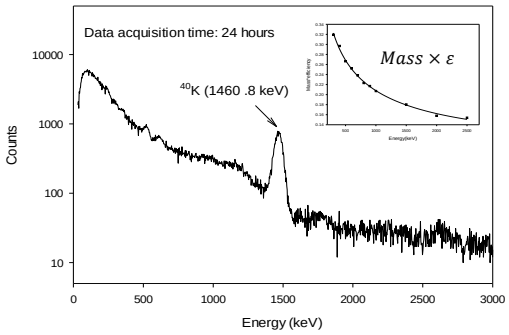

Figure 2. Gamma-ray energy spectrum obtained by the monitoring system for 24 hours. Inset plots shows 'mass (kg)×FEP efficiency' of the system.

Figure 2(a) shows gamma-ray energy spectrum obtained for 24 hours at one of the sites and ^{40}K full energy peak is showed apparently. Figure 2(b) shows simulated 'mass (kg)×FEP efficiency' for the range between 300 keV and 2500 keV.

Table 1. Comparison of radioactivity analysis by in-situ and sampling analysis for ^{40}K in seawater at the sites.

Site No.	Radioactivity concentration (Bq/kg)*		In-situ/ Sampling
	In-situ measurement	Sampling analysis	
1	11.3 ± 0.1	10.4 ± 0.2	1.09
2	10.8 ± 0.1	10.6 ± 0.2	1.02
3	10.5 ± 0.1	11.2 ± 0.2	0.94

*The uncertainty was estimated only for the 1 σ statistical uncertainty

Table 1 shows in-situ radioactivity analysis results using the suggested monitoring system and sampling analysis results for ^{40}K at the three sites. The radioactivity estimated using the in-situ and sampling analysis methods agreed within 10%. The minimum detectable activity (MDA) for ^{131}I and ^{137}Cs was estimated as 22 mBq/kg and 27 mBq/kg under the condition of $k_\alpha = k_\beta = 1.645$ and 24-hour measurement, respectively. Although the MDA of the monitoring system is higher than of the sampling analyses, it can be effective to timely detect abnormal events with higher radioactivity that can occur in the ocean.

Derivation of in-situ gamma-ray measurement time for the Target MDA

J.I. Byun[1], G.H. Chae[1], M.H. Song[1], D.J. Kim[1], J.B. Lee[1], J.H. Lee[1], C.S. Kim[1], G.H. Cho[2], J. S. Hwang[2], B.S. Kim[2], R.S. Park[2], B.H. Ryu[2], S.H Yang[2]

[1]Department of Environmental Radiation & Radioactivity Assessment, Korea Institute of Nuclear Safety, Daejeon, 34142, Republic of Korea
[2]Korea Hydro & Nuclear Power, Gyeongju, 38120, Republic of Korea
Keywords: Radiation emergency, Radioactivity, In-situ gamma-ray spectrometry, HPGe
Jong-In Byun, e-mail: k975bji@kins.re.kr

A portable high purity germanium (HPGe) detector has been widely used as one of emergency measurement instruments due to relatively high resolution and recently improved electric cooling system. In radiological or nuclear emergencies, freshly deposited radionuclides on the ground can be estimated by in-situ gamma-ray spectrometry using the HPGe detectors. For rapid preparedness and response for those situations, the measurement time to reach a target minimum detectable activity (MDA) should be preliminarily determined. However, it can be time consuming to determine MDAs of various HPGe detectors with different detection efficiency for similar type areas. Therefore, it is needed to obtain more effective way to determine the measurement time to reach consistent MDAs for the detectors with varied efficiency. The purpose of this study is to determine the correlation factor between HPGe detectors with varied relative efficiency, and to derive the measurement time to reach the target MDA.
The information of portable HPGe detectors (Mirion Technologies Inc., or AMETEC Inc.) used in this study is shown in Table 1.

Table 1. The information of portable HPGe detectors used in this study.

No.	Detector information		
	Relative efficiency (%)	Crystal length (mm)	Crystal diameter (mm)
1	20	60	30
2	30	62.5	39.5
3	40	65	50
4	45	67	52.7

To obtain the consistent full energy peak (FEP) efficiency for the source distribution with α/ρ = 6.25 cm^2 g^{-1}, the analytical method suggested by Helfer and Miller (1988) was applied to all the detectors. For in-situ gamma-ray measurements, an open field with the radius more than 50 m with almost flat surface was chosen considering the effective field of view of the detector. Gamma-ray spectra were obtained using each HPGe detector placed at 1 m above the ground surface for 3600 seconds. Figure 1 shows the normalized FEP efficiency, $\mu_B{}^{-1/2}$ and MDA to values estimated for the HPGe detector with 20% relative efficiency, for background counts (μ_B) covering 2.5 times the full width of half maximum (FWHM) of 662 keV. Here, the MDAs were estimated using the Currie method (1968) with the confidence level of 95%. As the detector's relative efficiency increases, the background count rate increases, but since the MDA is proportional to the square root of the background counts and inversely proportional to the measurement efficiency, the MDA tends to decrease with the detection efficiency.

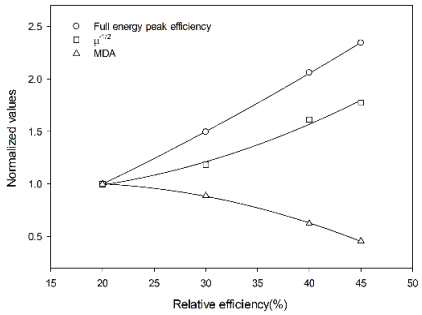

Figure 1. Relative efficiency vs. normalized detection efficiency, $\mu_B{}^{-1/2}$ and MDA for freshly deposited ^{137}Cs.

The correction factors with relative efficiency as a variable derived through the normalized MDA can be used to determine the target measurement time of the detector with any other detection efficiency. The measurement time (T_{ST}) with target MDA (M_T) can be derived as

$$T_{ST}(s) = 0.5\left(\frac{2\,a\,M_T}{\varepsilon I_\gamma} + \frac{b^2\dot{\mu_B}}{\varepsilon^2 {I_\gamma}^2} + \sqrt{\frac{4ab^2 M_T \dot{\mu_B}}{\varepsilon^3 {I_\gamma}^3} + \frac{b^4 \dot{\mu_B}^2}{\varepsilon^4 {I_\gamma}^4}}\right)/{M_T}^2 \quad (1)$$

where the detection limit is $L_D = a + b\sqrt{\mu_B}$, $\dot{\mu_B}$ is background count rate, ε is FEF efficiency, and I_γ is gamma-ray emission probability. The target measurement times with specific relative efficiency (REF) can be derived using Eq. (1) and correction factor ($C_{MDA}(REF)$) as

$$T_T(s) = T_{ST} C_{MDA}(REF). \quad (2)$$

The preliminary estimation method of the measurement time to reach the target MDA can be useful in establishing strategies for environmental radioactivity assessment in radiological or nuclear emergencies.

Helfer I., Miller K.M. 1988. Calibration factors for Ge detectors used for field spectrometry. *Health Phys.* 55, 15-29.

Currie L.A. 1968. Limits for qualitative detection and quantitative determination. Application to radiochemistry. *Analytical chemistry*. 40(3), 586-593.

Tomography of thorium-rich particles from Norwegian NORM sites (Fen area)

S. Cagno[1], K. Janssens[2], J. Jaroszewicz[3], G. Nuyts[2], J. Mrdakovic Popic[4] B. Salbu[1], L. Skipperud[1] F. Vanmeert[2], and O.C. Lind[1]

[1]CERAD, Norwegian University of Life Sciences, Aas, Norway
[2]Department of Chemistry, University of Antwerp, Antwerp, Belgium
[3]Department of Materials Engineering, Warsaw University of Technology, Warsaw, Poland
[4] Norwegian Radiation and Nuclear Safety Authority (DSA), Oesteraas, Norway
Keywords: thorium, tomography, mining
Simone Cagno, simone.cagno@nmbu.no

In this study we performed microscopic characterization of thorium-rich soil particles. These were collected in the thorium-rich Fen Complex in Norway and were selected according to their radioactivity by means of autoradiography.

The external gamma dose in the Fen area is among the highest in Europe. While the worldwide median content of Th in soil is estimated to 7-8 mg/kg, the measured concentrations of ^{232}Th in Rødberg rocks and soils collected at locations within or near the Fen Fe-mine range between 97 and 3000 mg/kg (Sundal and Strand 2004).

Extensive mining (e.g. Fe) has been conducted in the past, and mine waste contains significant amounts of Th and U as well as other metals (Mrdakovic Popic et al. 2012). In the Fen complex, the presence of Th in small mineral grains and its consequent separation to obtain satisfactory enrichment are the main challenges concerning Th extraction potential.

For the characterization of the particles, data obtained with X-ray absorption micro-CT, micro-XRF and micro-XRD, both in bi- and in three-dimensional (tomographic) mode were combined. The measurements were obtained with a combination of synchrotron and laboratory measurement sessions.

The results consistently show a heterogeneous distribution of radionuclides and heavy metals in Th-containing aggregates. Micro-XRF data showed that thorium is present in highly concentrated inclusions, associated with several heavy metal hotspots (e.g. REE, Nb, Pb), and in some cases with uranium. Micro-XRD measurements allowed the identification of different minerals present in the Th-rich inclusions, such as synchysite ($CaCe(CO_3)_2F$) and ferrocolumbite ($FeNb_2O_6$).

Upon weathering due to human or environmental factors, Th-hotspots could result in the formation of radioactive particles which represent point sources of exposure. Besides the chemical/mineral composition of the Th and lanthanide containing inclusions, this work determined also the size of the inclusions (diameter range 20-100 µm, with a few inclusions over 100 µm). All these data are needed to assess their environmental mobility and extractability, also in the context of possible mining activities in the Fen Complex. Toxic and radioactive waste generated from mining activities can have a high impact on licensing and disposal costs.

Considering the abundance of recent investigations and the potential for future mining activities at the Fen complex, the radioecological and radioanalytical impact of heterogeneous distributions of radionuclides and metals at these sites should be taken into account when environmental impact is assessed. The present work also demonstrates that radioecological studies should benefit from the use of micro- and nanoanalytical techniques.

This project was supported by the Research Council of Norway through its Centres of Excellence funding scheme, project number 223268/F50.

Mrdakovic Popic J., Bhatt C.R., Salbu B., Skipperud L., 2012, *J. Environ. Monit*. 14, 193-201

Sundal A.V. and Strand T., 2004. *J. Environ. Radioact*., 77, 175-189

Long-term study of BE-7 activity in Pleurozium Schreberi

R. Černý[1], K. Johnová[1], M. Šimeček[1]

[1]Department of Dosimetry and Application of Ionizing Radiation, Faculty of Nuclear Sciences and Physical Engineering, Czech Technical University in Prague, Prague 11519, Czech Republic
Keywords: BE-7, moss, environmental monitoring
Presenting author, e-mail: Radek.Černý, radek.cerny@fjfi.cvut.cz

Presented work summarizes results of long-term monitoring of radionuclides concentration in samples of moss – specifically Pleurozium Schreberi.

The samples of moss are collected regularly every autumn at 29 sampling points that are distributed in circles around Czech Nuclear Power Plant Temelin. (Thinova et al., 2006). The outer circle of sampling is 20 km in radius and the sampling point closest to the NPP is less than 3 km away of Temelin NPP.

Every year the samples are collected during autumn season – mainly in September and October. The results presented in this work cover 12 years long period of monitoring (2007-2018).

When taking samples, the upper part of the moss is cut with scissors in order to prevent soil and lower dry parts of the moss to get into the sample. The samples are then dried at the room temperature and cleared from impurities, like other types of moss (other than Pleurozium Schreberi) and grass.

Prepared samples are filled into 500 ml Marinelli beaker and measured at 30 % HPGe coaxial detector with acquisition time set to 24 hours. In this work we evaluate the concentration of BE-7 that is produced by spallation reactions through the interaction of cosmic ray in the atmosphere. Aside of BE-7 concentration of CS-137 (trace after Chernobyl accident fallout) was estimated.

The relatively long period of monitoring together with non-changing methodology of sampling and evaluation of the samples allows us to observe and analyse long-term variations in BE-7 concentration and their possible origin. The variations are associated with changes in solar activity and therefore with the production rate of BE-7, however the changing cosmic ray flux is not the only parameter that influences those variations. After their production BE-7 atoms are adsorbed onto aerosol particles and move through layers of atmosphere in a complicated way before their final sedimentation by dry or wet deposition.

The activity of BE-7 in moss is also influenced by the physiology of the moss itself. Unlike other plants terrestrial mosses do not have a rooting system, therefore uptake of the nutrients from the substrate is very low. Mosses absorb the nutrients from air a so they are considered to be a useful tool for heavy element and other pollutants monitoring. (Rühling and Tyler, 1973).

Using available data, we are trying to map all possible parameters that influence the long-term variations in BE-7 concentrations in moss samples. The stable methodology and fixed sampling sites through the whole period of monitoring allows us to focus on the true parameters with a minimum of systematic errors of measurement and fluctuations caused by changes in sampling site characteristics through the years. The mosses are widely used as bioindicators of trace elements and radionuclides, therefore it is necessary to study in detail the physiology of the elements transport into the moss body. The long-term studies are recognized as one of the most useful tools for obtaining the deeper knowledge of the transport process.

The analysis of CS-137 concentration may provide some additional useful information as is effective half-life that is strongly influenced by the characteristics of the sampling site.

The work was supported from European Regional Development Fund-Project "Center of Advanced Applied Science" No. CZ.02.1.01/0.0/0.0/16-019/0000778.

Thinova, L., Cechak, T., Kluson, J., Trojek, T. 2006. Use of Gamma Spectrometry Method for Environmental Monitoring in the area of NPP. *Journal of Physics: Conference Series. 41*. 569. 10.1088/17426596/41/1/071.

Rühling, A., Tyler, G., 1973. Heavy metal deposition in Scandinavia. Water, *Air and Soil Pollution 2*, 445e455.

Seasonal variations in precipitation rates of fine aerosol revealed using ^{7}Be as a tracer

J.S. Chae[1,2], G. Kim[1]

[1]School of Earth and Environmental Sciences, Seoul National University, 1 Gwanak-ro, Gwanak-gu, Seoul 08826, Republic of Korea
[2]Korea Institute of Nuclear Safety, 62 Gwakak-ro, Yuseong-gu, Daejeon, 34142, South Korea
Keywords: ^{7}Be, precipitation, aerosol
Presenting author, e-mail: jschae@kins.re.kr

Beryllium-7 is a naturally occurring cosmogenic radionuclide produced by the by the spallation processes of atmospheric nuclei. After production, ^{7}Be is rapidly adsorbed onto fine aerosol particles and removed to the Earth's surface by dry and wet fallout. The ^{7}Be concentrations are affected by various factors such as the air exchange between the stratosphere and the troposphere, scavenging by precipitation, and horizontal transport. Thus, ^{7}Be has been used to trace the intrusion of stratospheric air into the troposphere and to trace the deposition velocity of aerosols.

Particulate matter (PM) is a key air pollutant for air quality. Many modelling studies have been conducted to locate the pollution sources and predict PM occurrences. However, there are still large discrepancies between modelling results and observations due to unknown sources and removal processes. In this study, the ^{7}Be data collected for the surface air and precipitation in Korea were analysed to determine the seasonal variations in precipitation rates of fine aerosol.

The ^{7}Be concentrations in the surface air were relatively higher in spring (March, April, May) owing to tropopause folding. However, they were relatively lower in summer owing to efficient removal by precipitation. The monthly average concentrations of ^{7}Be decreased as the precipitation amounts increased showing a negative correlation against the precipitation amount. The monthly depositional fluxes of ^{7}Be showed a positive correlation against the amount of precipitation. These results suggest that the precipitation plays a major role on the ^{7}Be depositional flux in the surface air.

The monthly deposition velocities of fine aerosols, based on the ^{7}Be mass balance model, showed a large seasonal variation, with its maximum value of 1.9 cm s^{-1} in July and minimum value of 0.22 cm s^{-1} in March. These results imply that the concentrations of fine aerosols in the dry season (winter; December, January, February) can be five-fold higher than those in summer if the input terms of fine aerosols remain the same over the year.

Dissolved uranium and radon in groundwater of the Goesan area, Korea

B.W. Cho

Korea Institute of Geosciences and Mineral Resources (KIGAM), 124, Gwahakro, Yuseonggu, Daejeon, Korea
Keywords: Uranium, Radon, Concentration, groundwater
Presenting author email: cbw@kigam.re.kr

Uranium and radon concentration were measured in 200 groundwater samples taken from Goesan area known as contains Ogcheon metamorphic rock zone (OG2) which partly include coal bed bearing high uranium content of 361 ppm (Shin and Kim, 2011). Well depth ranged from 10 to 220 m having an average depth of 82 m. The geology of the area was classified as three metamorphic rock zones (OG1, OG2, and OG3) and two granite zones (Cretaceous granite and Jurassic granite).

Uranium and radon in groundwater is originated from uranium in bedrock. To see uranium content of rocks of the 5 zones, equivalent of uranium (eU) in rocks was measured using portable gamma ray spectrometer (GR-320A) at the groundwater sampling point if possible (Table 1). Higher median value of eU (8.2 ppm) was found on CGR outcrops. The median eU value of OG2, known as having high uranium content at some point, was not as high as that of CGR and similar to those of JGR, OG1, and OG3.

Table 1. Eequivalent of uranium (eU) of the 5 zones in the area (ppm).

Zone	Samples	Min.	Max.	Med.
JGR	56	1.1	6.8	3.8
CGR	25	3.8	11.6	8.2
OG1	43	1.1	8.0	3.5
OG2	38	1.4	14.9	3.9
OG3	38	1.7	6.8	3.1

The uranium level in groundwater of the area ranged from 0.02 to 293.0 μg/L with a median value of 0.87 μg/L. The uranium level in groundwater was highest in CGR zone (Figure 1) and it is well consistent with the results of uranium content of rocks (Table 1). Most of the samples were found to have uranium concentrations below 30 μg/L, the WHO guideline value based on its chemical toxicity (WHO, 2011), and only four samples from granite zones (JCR and CGR) exceeded 30 μg/L.

The radon level in groundwater of the area was found to vary from 1.8 to 1,540.9 Bq/L with a median value of 58.8 Bq/L which is similar to the national median radon level of 52.1 Bq/L (NIER, 2015). The percentage of samples having radon concentration equal to or greater than 100 Bq/L of WHO guideline value (WHO, 2011) was found to 25.5 %. The radon concentration was high in the samples from the CGR (range of 18.9-1,540.9 Bq/L) and JGR zones (range of 3.3-523.9 Bq/L) (Figure 2). The percentage of samples having radon level above 100 Bq/L in CGR zone was 64.0 % while those in JGR, OG2, OG1, OG3 zones were 39.3, 18.4, 9.3, and 5.3 %, respectively. Although there is still no guideline value for radon in drinking water in Korea, it is highly recommended to reduce radon concentration of groundwater having greater than 100 Bq/L before drinking, especially in granite zone.

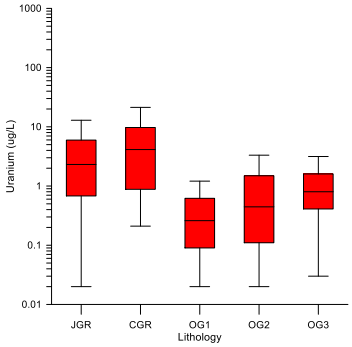

Figure 1. Uranium levels in groundwater from 5 geology.

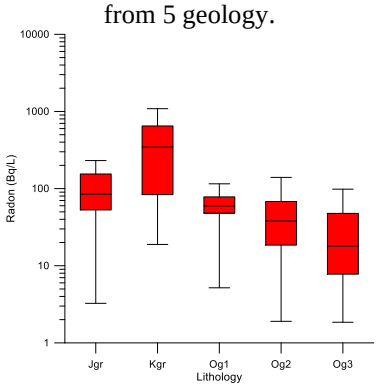

Figure 2. Radon levels in groundwater from 5 geology.

This work was supported by the National Institute of Environmental Research (NIER-SP2015-386) and Korea Institute of Geosciences and Mineral Resources (Gp2015-014-2016(2))

Shin, D. B., and Kim, S. J., 2011. Geochemical characteristics of black slate and coaly slate from the uranium deposit in Deokpyeong area. *J. of Econo. Environ. Geol.*, 44, 373-386.

NIER, 2015. Studies on the naturally occurring radionuclides in groundwater in the multi-geologic areas. NIER Report No. SP2015-386, 235.

WHO, 2011. Guidelines for drinking water quality. Chapter 9. Radiological aspects, 4th edition. World Health Organization, Geneva.

European Atlas of Natural Radiation data: an overview of digital and printed version

G. Cinelli[1], P. Bossew[2], M. De Cort[1], V. Gruber[3], M.A. Hernandez-Ceballos[1], T. Tollefsen[1]

[1] European Commission, Joint Research Centre (JRC), Ispra, Italy
[2] German Federal Office for Radiation Protection, Berlin
[3] Austrian Agency for Health and Food Safety, Department for Radon and Radioecology, Linz
Keywords: natural radiation, mapping, Atlas, Europe
Presenting author, e-mail: M.A. Hernandez-Ceballos, Miguel-Angel.HERNANDEZ-CEBALLOS@ec.europa.eu

Over ten years ago the Joint Research Centre (JRC) of the European Commission embarked on the long-term project of generating a European Atlas of Natural Radiation (EANR) (De Cort et al., 2011). Previously, 20 years ago, an atlas about the Chernobyl fallout over Europe was published (De Cort et al., 1998). Another mapping project maintained by REM is EURDEP, which shows ambient dose rate at several thousand locations over Europe in near-real time (https://remon.jrc.ec.europa.eu/). All these efforts are aimed to provide insight into geographical variability of the respective exposure components, and appreciation of their relative importance for total exposure to ionizing radiation.

The EANR is intended to familiarise the public with the natural radioactive environment, to give a more balanced view of the annual dose that it may receive from natural radioactivity and to provide reference material and generate harmonised data for the scientific community. The legal base of this project is the Euratom Treaty (European Union, 2016) which requires the EC to collect, validate and report information on radioactivity levels in the environment of the EU Member States.

Since 2017, a first online version of the European Atlas of Natural Radiation is available at https://remon.jrc.ec.europa.eu/ (Cinelli et al., 2019). The current (spring-2019) digital version of the EANR includes maps of the following quantities:

- European Annual Cosmic-Radiation Dose map;
- U, Th and K concentration in European topsoil and bedrock;
- European Annual Terrestrial Gamma Dose Rate;
- European Indoor Radon Map: radon concentration and number of measurements.

The maps are partly incomplete, reflecting the data situation, whichhowever is steadily improving, given the substantial but necessary experimental efforts.

As a next step, a printed version is under way (planned for end of 2019), which contains detailed information about the quantities displayed in the maps. Moreover, it reports background information on natural sources of radiation not yet mapped (i.e. food and water).

In the present work, the digital version and the structure of the printed version will be shown and described.

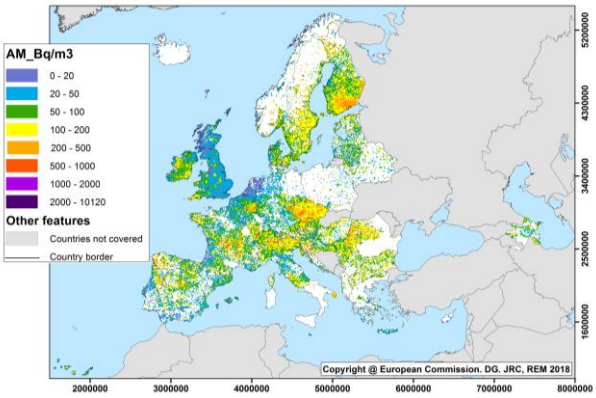

Figure 1. Arithmetic means over 10 km x 10 km cells of long-term radon concentration in ground-floor rooms. (The cell mean is neither an estimate of the population exposure, nor of the risk.). Last version, September 2018.

De Cort M., Gruber V., Tollefsen T., Bossew P. & Janssens A. (2011) Towards a European Atlas of natural radiation: goal, status and future perspectives. Radioprotection. 46, 737–743 (DOI: doi.org/10.1051/radiopro/20116871s).

De Cort et al. (1998): Atlas of Caesium deposition on Europe after the Chernobyl accident. Report EUR 16733 EN/RU, ISBN 92-828-3140-X; https://rem.jrc.ec.europa.eu/RemWeb/Browse.aspx?path=Atlas

European Union (2016), Consolidated version of the Treaty establishing the European Atomic Energy Community, Official Journal of the European Union, C 203, 07.06.2016, p. 1 – 112, https://eur-lex.europa.eu/legal-content/EN/TXT/?uri=OJ:C:2016:203:TOC

Cinelli G., Tollefsen T., Bossew P., Gruber V., Bogucarskis K., De Felice L., De Cort M., 2019. Digital version of the European Atlas of Natural Radiation, *Journal of Environmental Radioactivity*.Vol.196, 240-252. https://doi.org/10.1016/j.jenvrad.2018.02.008.

Content of technogenic radionuclide's in water bottom sediments and benthos of the Kara sea and shallow bays of the Novaya Zemlya archipelago.

Emelyanov A.[1], Lavrinovich E.[1]

[1]Vernadsky Institute of Geochemistry and Analytical Chemistry of Russian Academy of Sciences
Keywords: Environmental radiochemistry, radioecologie, Arctic region, technogenic radionuclides.
Presenting author PhD Student Emelyanov, Alexander Mikhailovich, E-mail: ksander93@mail.ru

Arctic regions play an invaluable role on the planet in stabilizing biosphere processes and climate. The nature of the Arctic zone is extremely vulnerable to anthropogenic interference due to the slow cycle of the level of mass and energy exchange in the cold latitudes. Radioactive contamination of the water environment of the Arctic basin in addition to discharges of radioactive waste of the nuclear fleet, is caused by the influence of atmospheric deposition of the products of the Chernobyl accident, the transfer of radionuclides by sea currents from Western European radiochemical enterprises, as well as river transport of the Ob and Yenisei rivers products of nuclear power complexes located in the Urals and Siberia. The most relevant direction of modern radioecological studies of the Arctic region is the study of the laws of man-made radionuclides, the assessment of the migration capacity of the latter and their accumulation in the shelf zone.

Samples were taken in the course of expeditionary research on the NIS "Academician Mstislav Keldysh" in the Kara sea and in various bays of the Novaya Zemlya archipelago, as well as the mouths of the Ob and Yenisei rivers. The works were carried out in the places of radioactive waste disposal, in the areas accessible (in depth) for the passage of the vessel and deck works.

The concentration of neptunium in solutions was determined by the method of luminescent analysis on a fluorescent filter analyzer in the near IR range (1713 nm). Plutonium was determined alpha-spectrometric, 137Cs-gamma-spectrometric.

Studies have shown that the content of plutonium in water is slightly higher than global. At the same time, 238Pu was not detected in the water, which shows a low isotope ratio of 238 and 239+240 plutonium. This suggests that global deposition is likely to be the main source of plutonium entering the marine environment. Although the content of neptunium in global deposition is almost two orders of magnitude lower than the content of plutonium, we found that the activity of neptunium in water is an order of magnitude higher than the activity of plutonium (0.76-1.89 Bq / m^3).

The benthic study showed that the content of radiocesium and plutonium in the selected samples is below the detection limit at a sample weight of 100-200 g of raw weight (0.1 Bq for 137Cs and 0.001 Bq for 239.240 Pu). Therefore, the content of these radionuclides in benthos is lower than 1 Bq/kg for 137Cs and 10-2 for 239,240 Pu. However, the content of neptunium in benthic samples is above the detection limit (1-80 Bq / kg wet weight). This is typical only for the bays of the Novaya Zemlya archipelago, where radioactive waste was buried. This content of neptunium in benthos may be one of the indicators of radioactive contamination of the marine environment, along with the content of plutonium and radiocesium in bottom sediments

This work is supported by the Russian Science Foundation project №17-17-01212

Comparison of two air sampling methods for determination of the radiocarbon level in the atmosphere

I. Faurescu[1], OG Duliu[2], C. Varlam[1], D. Faurescu[1], I. Vagner[1], D. Costinel[1]

[1]National R&D Institute for Cryogenics and Isotopic Technologies-ICSI Rm. Valcea, 4, Uzinei Str., 240050, Ramnicu Valcea, Romania
[2]University of Bucharest, Faculty of Physics, Department of Structure of Matter, Earth and Atmospheric Physics and Astrophyisics, 405, Atomistilor Str., PO Box MG-11,
077125, Magurele (Ilfov), Romania
Keywords: radiocarbon, atmosphere, direct absorption method, liquid scintillation counting
Presenting author, e-mail: ionut.faurescu@icsi.ro

The paper presents results of a comparison study of two air sampling methods for determination of the radiocarbon level in the atmosphere. The first sampling method involved static absorption of atmospheric CO_2 on the saturated carbonate-free NaOH solution (Kianpour et al 2012). Second method involved active absorption of the atmospheric CO_2 by bubbling the air NaOH aqueous solution. This kind of comparison has not been done. Static absorption of atmospheric CO_2 is not a routine procedure in the environmental radioactivity monitoring laboratory, due to various unknown factors that appears during the CO_2 absorption process. The only advantage, but essential, is that of no request of different facilities as electric power, pump, or high-volume protective cage. It can be used from mountain's pasture to wild plain. The second method, widely used in radiocarbon laboratory, can quantify the performances evaluation of static absorption method of atmospheric CO_2.

The samples were collected in various periods in the vicinity of the Experimental Pilot Plant for Tritium and Deuterium Separation (PESTD) from the Institute of the Cryogenics and Isotopic Technologies (ICSI) placed about 10 km south from the Ramnicu Valcea city (Romania), in the Govora industrial area. This facility is an experimental project in the national nuclear energy research program, which has the aim of developing technologies for tritium and deuterium separation. Until now, PESTD normal operation was with heavy water and tritiated water below exemption level approved by Romanian legislation. Foreseen experiments will be done with tritiated heavy water moderator from Cernavoda NPP (two CANDU-6 reactors), known to contain about half of the ^{14}C production of a Heavy Water Reactor. The largest contributor (>95%) to the production of ^{14}C in CANDU reactors is neutron activation of ^{17}O in the heavy-water moderator. Considering the fact that one of the important releases of PESTD is gaseous radioactive effluents, the baseline of atmospheric C-14 was a must for environmental program. It should be noted that in the Govora industrial area operates a 315 MW Coal-Fired Thermoelectric Power Plant and two chemical plants. This site is a particular one due to the Suess effect caused by continuously production of fossil CO_2.

For static absorption of CO_2, initially a thin layer of solid NaOH (around 80 g) was put in a plastic tray so it rapidly absorbs air humidity becoming saturated carbonate-free NaOH solution. The plastic tray was placed outside at the first floor of a three-floor building. The distance between sampling location and the coal-fired thermoelectric power plant was approximately 400 meters. The tray was left outside for a certain period after that the sodium hydroxide was changed. For active absorption of the atmospheric CO_2 was collected by bubbling the air through two flasks filled with 500 mL of 3M NaOH solution (Svetlik et al 2010) in the same location as the plastic tray for static absorption. We choose NaOH because it can easily react with CO_2 as alkali solution, and it has a high absorption efficiency (92%-99%).

For both methods the samples were processed by acid carbonate decomposition, CO_2 purification followed by direct absorption into liquid scintillation cocktail, and measurement by liquid scintillation method. This consists in measuring ^{14}C contained in a known quantity of carbon, as carbon dioxide, obtained from a sample, standard or background material, counted in an ultra-low-level liquid scintillation counter Quantulus 1220. ^{14}C results were normalized for deviation of the measured $\delta^{13}C$. The $^{13}C/^{12}C$ ratio was measured by isotope ratio mass spectrometry on a Delta V IRMS on small aliquots of sodium carbonate resulted from absorption of CO_2. Values are given relative to the VPDB standard, with overall precision typically ±0.1 ‰. $\delta^{13}C$-corrected $\Delta^{14}C$ data are given relative to NBS oxalic acid activity, corrected for decay. The measured $\Delta^{14}C$ levels have demonstrated the similarity of the two methods.

This work was supported by a grant of Ministry of Research and Innovation, CNCS - UEFISCDI, project number PN-III-P1-1.1-PD-2016-0532, within PNCDI III and monitoring program of Tritium Removal facility PESTD.

Kianpour M, Sobati MA, Shahhosseini S. 2012. Experimental and modeling of CO_2 capture by dry sodium hydroxide carbonation. *Chem. Eng. Res. Des.* 90(11), 2041:2050.

Svetlik, I., Povinec, P.P., Molnár, M., Vána, M., Šivo, A., Bujtás, T. 2010. Radiocarbon in the air of Central Europe: Long-Term investigations. *Radiocarbon*. 52, 823-834.

Development of station for artificial gamma activity measurements in surface water bodies

M. Fejgl[1], M. Hýža[1], I Hupka

[1]Department of radiochemistry, National Radioation Protection Institute, Prague, 140 00, Czech Republic
Keywords: Artificial radioactivity, caesium, water contamination, monitoring
Presenting author, e-mail: Michal.fejgl@suro.cz

The construction of the autonomous station for artificial gamma radioactivity measurement in surface water bodies (SAGMA) is a crucial part of the Czech Ministry of the Interior project. General purpose of this project is to develop the detection technique of SAGMA and to establish a monitoring network comprising several SAGMAs around the Czech Republic. Ultimately, it will lead to formation of a system for continuous gamma activity monitoring (SCOMO).

Chernobyl and Fukushima accidents revealed that system measuring gamma activity in water environment in real-time conditions would be a favourable instrument under such circumstances. The SCOMO system will enable a prompt and reliable detection of the artificial radioactivity contamination of the surface water bodies, which cover more than 50 % of all drinking water sources in the Czech Republic. At the same time, this system can provide additional information about radioactive air plume behaviour.

The principal component of SAGMA is an unshielded scintillation NaI(Tl) probe designed to be fully immersed directly in deep water of the examined river or lake. The station is powered by combined solar and wind source, with added satellite data transfer feature. Development of detection methods proceeded in accordance with activity concentration levels of gamma emitters of the highest interest (e.g. ^{137}Cs and ^{131}I) expected on basis of the aforementioned accidents experiences and with respect to the requirements of the Czech legislation.

For spectra analysis, a method of noise adjustment singular value decomposition (NASVD) was employed to reduce the background fluctuation related to various radon progenies present in water due to weather variations. The resulting level of minimal detectable activity concentration (MDAC) was below 1 Bq/L for measurement lasting one hour, which is comparable with more complicated monitoring systems equipped with lead shielding. The MDAC level meets the requirements of the Czech governmental emergency preparedness system.

Detection capabilities of SAGMA tool and current stage of the SCMO construction will be presented in this poster.

This contribution is supported by research programme VI20172020083.

Sorption and desorption capacity of heat-treated soil for radioactive cesium

S. Fukutani[1], M. Ikegami[1], T. Kubota[1], Y. Shibahara[1], Y. Shimada[2] and M. Yoneda[2]

[1]Institute for Integrated Radiation and Nuclear Science, Kyoto University, Kumatori, Osaka, 5900494, Japan
[2]Departament of Environmental Engineering, Kyoto University, Nishikyo, Kyoto, 6158540, Japan
Keywords: Soil, Heat treatment, Radiocesium Interception Potential (RIP), Frayed Edge Sites (FES)
Presenting author, e-mail: fukutani@rri.kyoto-u.ac.jp

Great East Japan Earthquake and following the nuclear accident in 2011 generated a huge amount of disaster waste and decontamination waste including soil. To reduce volume of these waste, incineration treatment has been conducted, and such stripped soil from paddies, fields, and forests is planned to be heat treatment. These soils contain radioactive cesium which come from Fukushima Daiichi nuclear power plants accidents, and it is important to understand the behavior of radioactive cesium in the soil in incinerating or heat treating. In this study, especially from the aspect of sorption and desorption capacity of soil, such as Radiocesium Interception Potential (RIP) (A. Cremers, et al, 1988), Frayed Edge Sites (FES) and Cation Exchange Capacity (CEC), effects of heat treatment on soil for cesium desorption were discussed. As for the experiments material, soil samples were collected at the forest (Iwate prefecture) and at the cultivated field (Osaka prefecture), and carrier free radioactive cesium was made by (γ, p) reaction at the electron linear accelerator (KURRI-LINAC) (T. Kubota, et al., 2018), as follow, $BaCl_2$ (^{135}Ba, ^{137}Ba, ^{138}Ba) (γ, p) ^{134}Cs, ^{136}Cs, ^{137}Cs.

One of experiments is shown in the Table 1. That is changes of distribution ratio of radioactive cesium, defining concentration in soil over concentration in liquid phase, of 4 kinds of the forest soil before and after processing of the 1000 °C heat treatment.

Table 1. Changes of distribution ratio of radioactive cesium in heat treatment.

Soil Sample	Distribution ratio ($L \cdot kg^{-1}$)			
	No heat treatment		1000 °C	
	^{134}Cs	^{137}Cs	^{134}Cs	^{137}Cs
A	5.5E+02	5.2E+02	4.9E+01	5.2E+01
B	4.2E+02	4.1E+02	3.6E+00	3.4E+00
C	5.5E+02	5.4E+02	5.0E+01	5.3E+01
D	4.3E+02	5.0E+02	7.9E+01	8.4E+01

The distribution ratios of after 1000 °C heat treatment were approximately one order smaller than those of before processing.

This research was supported by the Environment Research and Technology Development Fund (1-1702) of the Ministry of the Environment, Japan.

A. Cremers, A. Elsen, P. De Preter and A. Maes, Quantitative analysis of radiocaesium retention in soils, *Nature*, 335, 247–249 (1988).

T. Kubota, S. Fukutani, Y. Shibahara and T. Ohta, Production and purification of ^{43}K and ^{136}Cs, KURRI Progress Report 2017, 209, (2018).

Determination of radiological parameters of drinking water in large cities, and evaluation of doses received by its consumption for people of different age categories

A. Fulara[1]

[1]Department of Radiation Hygiene, Central Laboratory for Radiological Protection, Warsaw, 03-194, Poland
Keywords: water, tritium, gross beta
Presenting author, e-mail: Fulara@clor.waw.pl

Water consumed by humans may contain radioactive isotopes.

In Poland, the quality of water is regulated by the Ordinance of the Minister of Health of 7 December 2017. Monitoring of radioactive contamination of tap water in 2018 included samples of water coming from the main water intakes in Warsaw, Lublin and Poznan. Purified water pumped into the network was collected into polyethylene containers with a volume of 10 dm^3. Twenty liters of water were collected from each point. The water delivered to the laboratory was distributed for testing as follows:

- 15 dm^3 of water was allocated to the ^{137}Cs and ^{90}Sr content tests. The samples were pre-evaporated to approx. 0.5 dm^3. First, ^{137}Cs content was determined, followed by ^{90}Sr.
- 4 dm^3 of water was dedicated to the study of total alpha and beta radioactivity.
- the remaining 1 dm^3 of water was allocated to the tritium content tests.

Collected and analyzes were performed in the waters coming from 11 water treatment plants.

The results of ^{137}Cs and ^{90}Sr determinations in drinking water collected in three cities indicate, that both ^{137}Cs and ^{90}Sr concentrations were at low level, for ^{137}Cs ranging from values 1.75±0.25 $mBq \cdot l^{-1}$ (water treatment plant Praga in Warsaw) to 3.26±0.61 $mBq \cdot l^{-1}$ (water treatment plant Gruszczyn in Poznan). The average concentration of ^{137}Cs calculated for the examined water samples was 2.69±0.49 $mBq \cdot l^{-1}$.

In case of ^{90}Sr that range was from values 2.02±0.28 $mBq \cdot l^{-1}$ (water treatment plant Filtry in Warsaw) to 5.81±0.82 $mBq \cdot l^{-1}$ (water treatment plant Poznan). The average concentration of radioactive ^{90}Sr in drinking water tested was 4.17±1.08 $mBq \cdot l^{-1}$. The tritium concentration in drinking water did not exceed the detection limit (0,5 $Bq \cdot l^{-1}$) only for three of the eleven water samples tested.

The total beta radioactivity in investigated water samples was very low and ranged from 0.10±0.02 $Bq \cdot l^{-1}$ to 0.27±0.03 $Bq \cdot l^{-1}$. The average total beta radioactivity in investigated water samples was 0.16±0.05 $Bq \cdot l^{-1}$.

The total radioactivity exceeded the detection limit of α (0.015 $Bq \cdot l^{-1}$) only for three of the eleven water samples tested.

Pursuant to the Agreement, in case of exceeding 0.1 $Bq.l^{-1}$ of total α radioactivity, ^{226}Ra, uranium isotopes (^{238}U, ^{234}U, ^{235}U) had to be determined, while in the case of β 1.0 $Bq.l^{-1}$ exceeded the total radioactivity β, determine the concentration of ^{40}K and ^{228}Ra.

In none of the waters tested, total α and β radioactivity exceeded the above values. Therefore, ^{226}Ra, uranium isotopes (^{238}U, ^{234}U, ^{235}U), ^{40}K and ^{228}Ra were not carried out.

Based on the concentrations of ^{137}Cs and ^{90}Sr, the annual absorption of these isotopes with water in age groups was calculated: up to 1 year of age (water intake of 250 l. $year^{-1}$), 1 -10 years (intake of 350 $l \cdot year^{-1}$), 11 up to 17 years (intake 540 $l \cdot year^{-1}$) and adults (consumption 730 l. $year^{-1}$).

On the basis of these data, the average annual absorption was calculated. These absorptions were 0.67 ± 0.12 $Bq \cdot year^{-1}$; 0.94 ± 0.17 $Bq \cdot year^{-1}$; 1.46 ± 0.27 $Bq \cdot year^{-1}$ and 1.97 ± 0.36 $Bq \cdot year^{-1}$ for ^{137}Cs. The ^{90}Sr absorption in appropriate age groups was: 1.04 ± 0.27 $Bq \cdot year^{-1}$; 1.46 ± 0.38 $Bq \cdot year^{-1}$; 2.25 ± 0.58 $Bq \cdot year^{-1}$ and 3.05 ± 0.79 $Bq \cdot year^{-1}$.

Based on the annual absorption and appropriate conversion factors expressed in $Sv \cdot Bq^{-1}$, given in Table 4 (Regulation of the Council of Ministers of January 18, 2005 on the ionizing radiation limit doses, Journal of Laws No. 20, item 168), calculated weighing effective doses.

Doses from absorption of ^{137}Cs range from 0.010 to 0.026 $\mu Sv \cdot year^{-1}$, which is a small percentage (0.0010-0.0026%) of the annual border dose for people from the general population specified in the Regulation of the Council of Ministers dated January 18, 2005 on the radiation dose limits of ionizing radiation Dz. U. No. 20, item 168 (1 $mSv \cdot year^{-1}$).

From ^{90}Sr absorption, the doses range from 0.085 to 0.240 $\mu Sv \cdot year^{-1}$, which is 0.0085% - 0.0240% of the limit dose.

The results obtained indicate that these doses are negligibly small and the tap water in all examined cities meet the requirements set out in the Regulation of the Minister of Health of 7 December 2017.

The work was carried out in accordance with Agreement No. 26 / OR / 2018/99 concluded on June 25, 2018. between the State Treasury - the President of the National Atomic Energy Agency and the Central Laboratory for Radiological Protection.

Environmental radiation level and radioactivity in the Ryukyu Archipelago, southwestern part of Japan

M. Furukawa[1], S. Nakasone[1], A. Ishimine[1], K. Nakamura[1], Y. Shiroma[1], Y. Tamakuma[2], T. Suzuki[2], M. Hosoda[2], N. Akata[2], S. Tokonami[2], T. Sanada[3]

[1]Graduate School of Engineering and Science, University of the Ryukyus, Nishihara, Okinawa 903-0213, Japan
[2]Institute of Radiation Emergency Medicine, Hirosaki University, Hirosaki, Aomori 036-8565, Japan
[3]Hokkaido University of Science, Sapporo, Hokkaido 006-8585, Japan
Keywords: gamma radiation, radionuclide, radon, red soils, eolian dust, Ryukyu Archipelago
Presenting author, e-mail: m_furu@sci.u-ryukyu.ac.jp

In order to estimate the exposure due to the natural radiation and the 2011 Fukushima Dai-ichi neclear power station accident for the Ryukyu Archipelago that stretches over Kagoshima and Okinawa prefectures (Fig. 1), comprehensive study of the environmental radiation and radioactivity have been conducted by our research group. Also geo-scientific setting for the radiation environment in the archipelago has been studied to understand the origin and dynamics of the radioactivity. Summary of the results for recent research is shown in this presentation, including reported matters.

Gamma radiation

In situ measurement and car-borne survey for the gamma radiation dose rate in air have been conducted at about 8,000 points in the archipelago. A part of the results was reported by Furukawa *et al*. (2015). Arithmetic mean, minimum and maximum of the dose rates (nGy h^{-1}) at 1m in height from the unpaved soil ground were estimated to be 41, 8 and 165, respectively. This arithmetic mean is lower than that of the whole Japan, 50 nGy h^{-1} (Furukawa and Shingaki, 2012). Relatively high dose rates, >100 nGy h^{-1}, were particularly found in Miyako-jima and Daito Islands which are mainly composed of the uplifted coral reef, the Quaternary Ryukyu limestone. Comparative study of the gamma radiation data obtained prior to and subsequent to the 2011 accident suggested that the accident has no impact on the archipelago.

Natural radionuclides of soils

Analyses for ^{238}U, ^{232}Th and ^{40}K have been performed on the red soils collected from the wide area of the archipelago, and the ranges of the concentration (Bq kg^{-1}) were estimated to be 42-220, 33-112 and 370-740, respectively. These indicate that the concentrations are relativery high in Japan. Also the result for the comparison of the results with the concentrations of soils in China (Furukawa *et al*., 2005) suggested that the basic material of the red soils developed on the Ryukyu limestone is not weathering residual from the limestone, but the eolian dust deposits from the high background radiation area in the southeastern part of China.

Atmospheric radon

In Yomitan-son, a village of Okinawa-jima, the highest annual average of indoor radon (^{222}Rn) concentration in Japan, 220 Bq m^{-3}, has been observed in a private residence by a nationwide survey (Sanada *et al*., 1999). So in this study, to estimate the distribution of the high indoor radon concentration, annual and short-term measurements were conducted in 10 dwellings in the village. The highest concentration, 211 Bq m^{-3}, was observed by a short-term measurement during winter season in a private house. Our results for radon and gamma radiation suggested that the main radon source is the red soil distributed on the Ryukyu limestone.

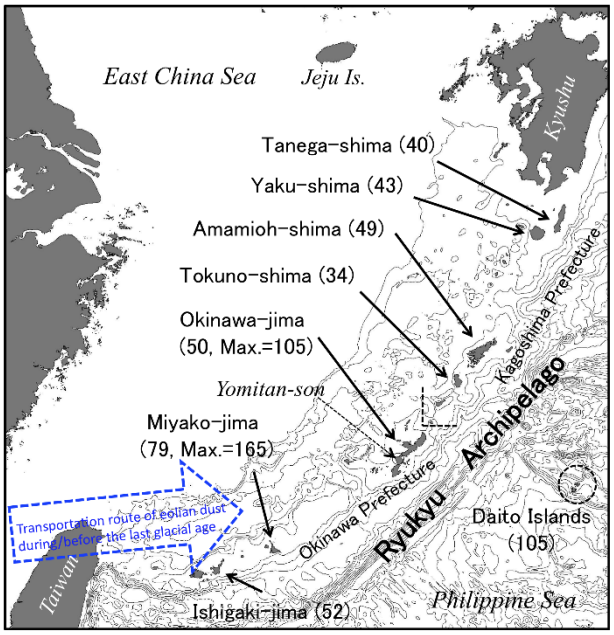

Figure 1. Map of study area. Values in paretheses are average of gamma radiation dose rate in air (nGy h^{-1}).

Furukawa, M. *et al*. 2005. Characteristics on natural radioactivity of loess and eolian dust origin soils in East Asia. *J. Aerosol Res.* 20, 306-312.

Furukawa, M. *et al*. 2015. Terrestrial gamma radiation dese rate in Ryukyu Islands, subtropical region of Japan. *Radiat. Protection Dosim*. 167, 223-227.

Furukawa, M., Shingaki, R. 2012. Terrestrial gamma radiation dose rate in Japan estimated before the 2011 Great East Japan Earthquake. *Radiat. Emergency Med*. 1, 11-16.

Sanada, T. *et al*. 1999. Measurement of nationwide indoor Rn concentration in Japan. *J. Environ. Radioact.* 45, 129-137.

Method for ultra-trace Determination of Tc-99 from Large Seawater Samples

F. Gülce[1,3], T. Feastermann[2], K. Hain[3], G. Korschinek[2], M. Martschini[3], J. Pitters[3], F. Quinto[4], G. Rugel[5], P. Steier[3], G. Wallner[1], J.M. Welch[6]

[1]Institute of Inorganic Chemistry, University of Vienna, Vienna, 1090, Austria
[2]Physics Department, Technical University of Munich, 85748, Garching, Germany
[3]VERA Laboratory, Faculty of Physics, University of Vienna, Vienna, 1090, Austria
[4] Institut für Nukleare Entsorgung, Karlsruher Institut für Technologie,76344, Germany
[5] Helmholtz-Zentrum Dresden-Rossendorf, 01328, Dresden, Germany
[6]Atom Institute, TU Wien, Vienna, 1020, Austria
Keywords: ^{99}Tc, AMS, liquid-liquid and chromatographic extraction
Presenting author e-mail: fadime.guelce@univie.ac.at

^{99}Tc is a long-lived ($T_{1/2}$ = 2.11×10^5 a) fission product which has been released into the environment by atmospheric nuclear weapon tests, nuclear fuel reprocessing plants and also by nuclear medicine. Owing to its high solubility in its predominant form as pertechnetate ion (TcO_4^-), it may provide valuable information as a marine tracer to study circulation of water masses.

Since environmental levels of ^{99}Tc are still low, sensitive detection methods are necessary. To date, both radiometric and mass spectrometric methods have been applied (Shi et al. 2012). Whereas radiometric methods are mainly limited by the low specific activity of environmental samples, mass spectrometric techniques have to cope with the interference of the stable isobar ^{99}Ru and the lack of a stable isotope for normalization.

Because of its ability to suppress isobaric background, accelerator mass spectrometry (AMS) is the most sensitive technique at the moment. In this way a detection limit for ^{99}Tc of 5×10^6 atoms can be reached (Quinto et al. 2019). The application of this method to environmental samples requires a careful Tc purification to remove the sample matrix and reduce interfering isobars.

In this work, we have developed a highly efficient two-step procedure for the pre-concentration and purification of ^{99}Tc from 10 l seawater samples (Figure 1).

This procedure utilizes a bulk extraction step with 5% TIOA-XYLENE to efficiently reduce sample volume by nearly two orders of magnitude and remove the seawater matrix followed by extraction chromatography with TEVA resin to remove unwanted impurities (Ru, Mo). The Tc recovery of this method was tested on artificial seawater samples by application of ^{99m}Tc ($T_{1/2}$ = 6.0 h) as tracer and was found to be around 70%.

Furthermore, 20 ml of the IAEA-381(443) reference material and two samples spiked with ^{99}Tc (TCZ44, NH_4TcO_4 in H_2O, Eckert and Ziegler, Nuclitec.) were treated by this method and subsequently analysed by AMS using the set-up at the 14MV tandem accelerator at the Maier-Leibniz-Laboratory in Munich. The agreement of the measurement results with the expected values is very good (see Table 1), therefore the method is now being applied to obtain depth profiles of ^{99}Tc in the Pacific Ocean.

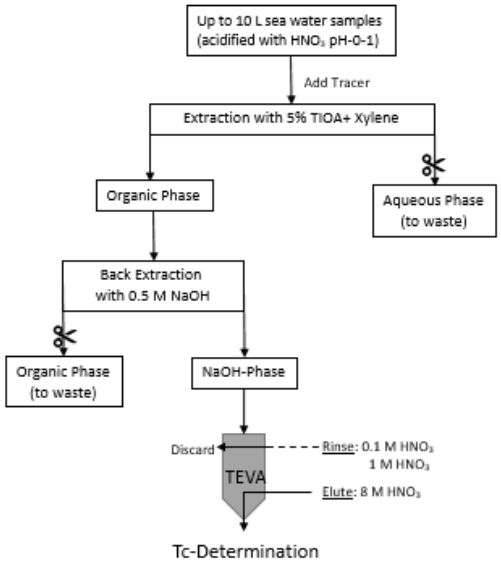

Figure 1. Chemical process for Tc preconcentration and purification.

Table 1. Preliminary AMS results for IAEA-381(443) and spiked samples.

Test Material	Expected number of atoms ^{99}Tc	Observed Value ± Uncertainty
IAEA-381	(2.08 ± 0.1) × 10^9	(2.42 ± 0.7) × 10^9
Sample-1	(5.06 ± 0.15) × 10^8	(3.32 ± 0.9) × 10^8
Sample-2	(5.30 ± 0.16) × 10^8	(6.47 ± 1.9) × 10^8

This work is funded by the Austrian Science Fund (FWF): [P 3161421].

Shi, K. et al. 2012. *Anal. Chim. Acta* 709 (2012) 1-20.
Quinto, F. et al. *Anal. Chem*. 2019, 91, 4585-4591.

Applying cluster analysis to investigate Radon behaviour

I. Gutiérrez Álvarez[1], J.L. Guerrero[1], J.E. Martín[1], J.A. Adame[2], A. Vargas[3], J.P. Bolívar[1]

[1]Department of Integrated Sciences, University of Huelva, Huelva, Spain
[2]Atmospheric Sounding Station – El Arenosillo, Atmospheric Research and Instrumentation Branch, National Institute for Aerospace Technology, INTA, Mazagón-Huelva, Spain
[3]Institut de Tècniques Energètiques, Universitat Politècnica de Catalunya, Barcelona, Spain
Keywords: Atmospheric radon, WRF Model, HYSPLIT, K-means clustering, Phosphogypsum
Isidoro Gutiérrez-Álvarez, isidoro.gutierrez@dfa.uhu.es:

Outdoor radon was measured in Huelva (South-West Spain), where a phosphogypsum repository is located, from March 2015 to March 2016. The hourly mean values of this gas oscillate between 5.6 and 10.9 Bq m^{-3} while the maximum ranged between 36.4 and 53.4 Bq m^{-3}. Radon concentration shows the expected monthly variation with higher levels in November and December. Typical daily evolutions were also observed, with maximum between 06:00 and 08:00 UTC and minimum around noon.

To extract daily radon patterns, the K-means clustering technique was applied. Radon behavior was grouped in 5 clusters which described the radon outline throughout the year. Based on this classification, four different "events" were analyzed in detail, describing two with high radon levels and two with low radon. Local meteorology, back-trajectories computed with the HYSPLIT (Hybrid Single Particle Lagrangian Integrated Trajectory) model and meteorological fields from the WRF (Weather Research and Forecasting) model, were used to analyze these periods selected.

Clustering classification showed that low radon periods are characterized by the arrival of air masses from the Atlantic Ocean with the higher wind speeds, whereas high radon events occur during the night under pure sea-land breezes, extending through the day if there is high atmospheric stability. Factors such as meteorology or local emission sources alone could not be enough to justify the high radon events in the area. Other factors could be playing a role in the radon levels. The obtained results indicate that high radon events occur simultaneously to the arrival of Mediterranean air masses transported from medium long range. This suggests that the Gulf of Cadiz could act as a radon trap and the continental areas around the Western Mediterranean Basin could act as a radon source.

This research was partially supported by the Spanish Ministry of Science, Innovation and Universities, by the research project ‘ ‘Fluxes of radionuclides emitted by the PG piles located at Huelva; assessment of the dispersion, radiological risks and remediation proposals" (Ref.: CTM2015-68628-R), and the infrastructure project with Ref.: EQC2018-004176-P.

López-Coto, I., Mas, J.L., Vargas, A., Bolívar, J.P., 2014. Studying radon exhalation rates variability from phosphogypsum piles in the SW of Spain. *J. Hazard Mater.* 280, 464–471.

Grossi, C., Arnold, D., Adame, J.A., López-Coto, I., Bolívar, J.P., De La Morena, B.A., Vargas, A., 2012. Atmospheric 222Rn concentration and source term at El Arenosillo 100 m meteorological tower in southwest Spain. *Radiat. Meas.* 47, 149–162.

Beaver, S., Palazoğlu, A., 2006. A cluster aggregation scheme for ozone episode selection in the San Francisco, CA Bay Area. *Atmos. Environ.* 40, 713–725.

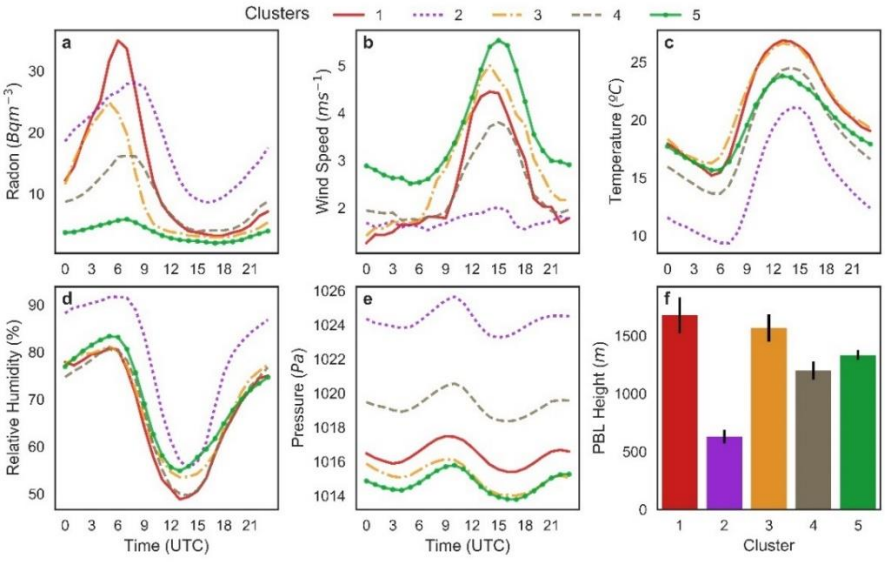

Figure 1. Radon, wind speed, temperature, relative humidity, pressure and PBL daily patterns associated to the five clusters.

Localization of radioactivity in dried shiitake mushrooms (*Lentinula edodes*).

M. Hachinohe[1], T. Yamada[2], A. Hachisuka[3], K. Soga[3], S. Horii[1], T. Miura[4]

[1] National Agriculture and Food Research Organization, Tsukuba, 3058642, Japan
[2] Kindai University Atomic Energy Research Institute, Higashiosaka, 5770818, Japan
[3] National Institute of Health Sciences, Kawasaki, 2100821, Japan
[4] National Institute of Advanced Industrial Science and Technology, Tsukuba, 3058560, Japan
Keywords: radiocaesium, shiitake mushroom, distribution, homogeneity
Presenting author, e-mail: mhach@affrc.go.jp

Since the Fukushima Dai-ichi nuclear power plant (FNPP) accident, radioactive substance inspection for domestic foodstuffs has been introduced in Japan. Radiocaesium measurement is being performed by many laboratories to ensure the food safety using the gamma-ray spectrometry technique with a germanium detector, scintillation spectrometers, or non-destructive radioactive contamination food monitors.

Heterogeneous localization of radioactive material in agricultural product has been concerned as one of the factors affecting the result of radioactivity measurement. Therefore, understanding the localization of radioactive substances in agricultural product is important as it can be an index for evaluating the homogeneity of the measurement sample. In this study, we clarified the localization of radioactivity in dried shiitake mushrooms (*Lentinula edodes*) containing radiocaesium and examined the effect of the localization on the homogeneity of the dried shiitake powder.

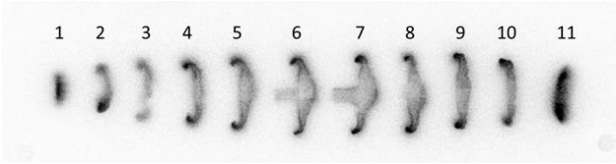

Figure 1. IP image of the inside of a contaminated dried shiitake mushroom (DM-3). The mushroom was sliced longitudinally from the left edge, and the numbers indicate the order of slicing.

Seven dried shiitake mushrooms (DM-1 to 7) cultivated domestically were used. Each of them was sliced approximately 5-7.5 mm thick in the vertical to the pileus surface, and the sliced ones were placed with the slice-surface down. The internal distribution of radioactive substances was examined by Imaging Plate technique (BAS SR2040E, FUJIFILM). In all 6 samples, the distribution of radioactivity inside the mushrooms was not uniform. It was shown to be localized a higher at the edge of the pileus of mushroom and lower at the central part of it (Figure 1). As a result of analyzing the intensity of radioactivity at the edge of the pileus and the central part using image analysis technology (ImageQuant TL, GE Healthcare), the radioactivity difference between edge and central part in individual shiitake mushrooms was estimated to be approximately about 2.8-27.4 times. (Table 1) This result suggests that the radioactivity of radiocaesium may have the similar distribution as this result. In order to evaluate the homogeneity of the dried shiitake powder sample packed in U-8 container, we calculated the homogeneity (u_{hom}) associated with the between-bottle homogeneity based on ISO Guide 35: 2006. (Table 2)

Table 1. Estimated radioactivity ratios of edge to central part in dried shiitake mushrooms.

Sample No.	DM-1	DM-2	DM-3	DM-4	DM-5	DM-6	DM-7
Radioactivity ratio*	3.3	2.8	3.9	3.9	27.4	4.0	6.3

The shiitake mushrooms grown in the same farm were milled to a uniform particle size by an ultracentrifuge mill equipped with a sieve (ZM200, Retsch), and the mushroom powder was thoroughly mixed. Then, 35 U-8 containers filled with the dried shiitake powder were prepared, and 20 of them were used for measurement. The mean of mass is 30.00 g (RSD 0.2%), and the mean of sample height is 48 mm (RSD 1.4%). Each of 20 samples were measured twice by ORTEC GEM20-70 and GEM25-70 to determine the activities of ^{134}Cs and ^{137}Cs.

Table 2. Evaluation a homogeneity for dried shiitake mushroom filled in the U-8 container.

		s_r	s_{bb}	u_{bb}
^{134}Cs	Bq·kg-1	7.14%	3.22%	2.19%
^{137}Cs	Bq·kg-1	4.27%	2.90%	0.48%

The u_{hom}s of the dried shiitake mushroom powder were 3.22 % for ^{134}Cs and 2.90% for ^{137}Cs. This result is greater than that of activities in CRM IAEA-473 (milk powder, ^{134}Cs: 1.65% and ^{137}Cs: 1.65%) (IAEA, 2015) and wheat flour (^{137}Cs: 0.34%) (Furukawa et al., 2018). The localization of radioactivities in milk and wheat flour is considered to be more homogeneous than dried shiitake mushroom. Therefore, these results suggest that the heterogeneous distribution of radioactive material in dried shiitake mushroom may affect the homogeneity of radiocaesium in the mushroom powder sample.

IAEA, 2015. Internal report NAEL/RM/001, Certification of massic activities of ^{89}Sr, ^{90}Sr, ^{134}Cs and ^{137}Cs in CRM IAEA-473 (milk powder) sample. International Atomic Energy Agency.

Furukawa, R., Unno, Y., Miura, T., Yunoki, A., Hachinohe, M., Hamamatsu, S. 2018. Homogeneity of wheat flour in 5ml containers for certified reference materials. *Appl. Radiat. Isot.* 134, 32-34.

Using barium-133 as a surrogate for iodine-131 in a silver zeolite cartridge for air sampling

A.M. Hamideh[1], W.-H. Wang[2]

[1]Radiation Safety Office, Louisiana State University, Baton Rouge, Louisiana, 70803, USA
[2]Center for Energy Studies, Louisiana State University, Baton Rouge, Louisiana, 70803, USA
Keywords: iodine-131, air sampling, silver zeolite, barium-133
Presenting author, e-mail: weihsung@lsu.edu

Iodine-131 (I-131) is a major fission product among other radionuclides released during a nuclear incident. This radioiodine has a half-life of 8.02 days and the primary organ of uptake through ingestion or inhalation is the thyroid gland. For these reasons, nuclear power plants must routinely monitor I-131 through air sampling. Currently, there are two adsorbing media to collect gaseous I-131: activated charcoal and silver zeolite cartridges. Silver zeolite cartridges are generally used during a post nuclear incident due to its affinity for iodine while not adsorbing noble gases such as krypton-85 and xenon-135. After an air sample is collected from a plume, the cartridge is taken to a low radiation background area for measuring the activity of I-131. This is usually done by using a γ-spectroscopy detection system. To use these detectors, the system must be calibrated using the same source geometry as in the field. Source geometry refers to source to detector orientation when counting. Because of licensing issues, radiation protection requirements, and financial concerns, it is common to use a single barium-133 (Ba-133) sealed point source on top of a silver zeolite cartridge as a calibration standard for air sampling purposes. This method does not reflect the actual gaseous I-131 distribution in the silver zeolite cartridge. Consequently, gaseous I-131 activity would be underestimated due to different source geometries (i.e., counting efficiencies).

This study compares various geometrical arrangements of both Ba-133 and I-131 spiked filter media in a silver zeolite cartridge to mimic the gaseous I-131 distribution found in the field in order to establish conversion factors back to a Ba-133 sealed point source geometry for calculation of proper counting efficiencies. The results of this study indicate that nine is the most appropriate conversion factor for estimating gaseous I-131 activity measured in the field using a Ba-133 sealed point source under specific calibration conditions.

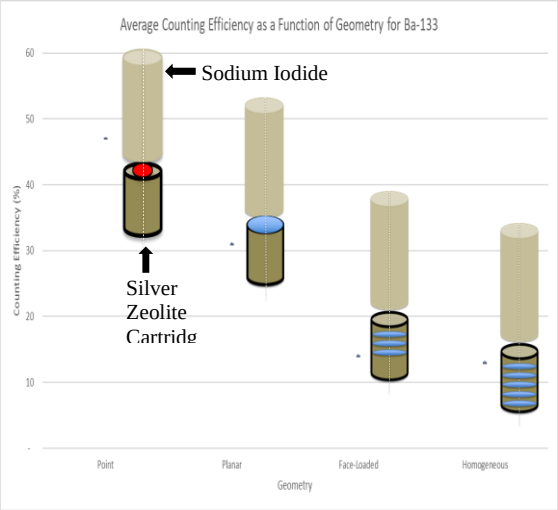

Figure 1. Counting efficiency vs. source geometry.

This work was supported by Louisiana Sea Grant.

Natural radioactivity of urban surface deposited sediments in three different urban environments

Mohamed Y. Hanfi [1,3*], Ilia V. Yarmoshenko [2], Andrian A. Seleznev [2], Michael V. Zhukovsky [2]

[1] Ural Federal University, Mira St 19, Ekaterinburg, 620002, Russia
[2] Institute of Industrial Ecology UB RAS, S. Kovalevskoy St., 20, Ekaterinburg, 620219, Russia.
[3] Nuclear Materials Authority, Maadi, 520, Egypt.
Keywords: gross beta activity, dust; fine sand; coarse sand.
Presenting author, e-mail: m.nuc2012@gmail.com

Study of gross beta activity was conducted in three Russian cites; Ekaterinburg, Rostov and Nizhny Novgorod. The cities are located in different geographical and climate zones. Samples of the urban surface deposited sediments were collected in autumn in each city. The bulk urban samples were fractionated with three size fractions: dust (0.002-0.1 mm), fine sand (0.1-1 mm), and coarse sand (> 1 mm). Measurement setup equipped with beta radiometer BDPB-01 was designed to measure the low levels of gross beta-activity in a small amount of the obtained size-fractionated samples. According to results of the study, the gross beta activity depends on the size fraction and the city. Highest beta activity concentration was found in the dust fraction which is about the same in all cities 0.8-0.9 Bq g^{-1}. In size fractions of fine sand and coarse sand the beta activity depends on the city. Among other cities, the highest average concentration was found in Ekaterinburg (0.8 and 0.6 Bq g^{-1} in fine and coarse sand fractions, respectively), while the lowest – in Nizhny Novgorod (0.28 and 0.44 Bq g^{-1}, respectively). In Nizhny Novgorod, the relationship of beta activity concentration with mineral and chemical composition is studied. Average beta activity in the different fractions of the surface deposited sediment correlates with uranium, thorium and organic matter concentration. High concentration of potentially harmful elements was found in the dust fraction as well: mean Pb concentration – 48 mg kg^{-1} (220% of concentration in the fine sand fraction), Cu – 135 mg kg^{-1} (490%) and Zn – 338 mg kg^{-1} (610%). Thus, the gross beta activity may be considered as indicator of high contribution of dust and high pollution with Pb, Cu, and Zn in the urban environment.

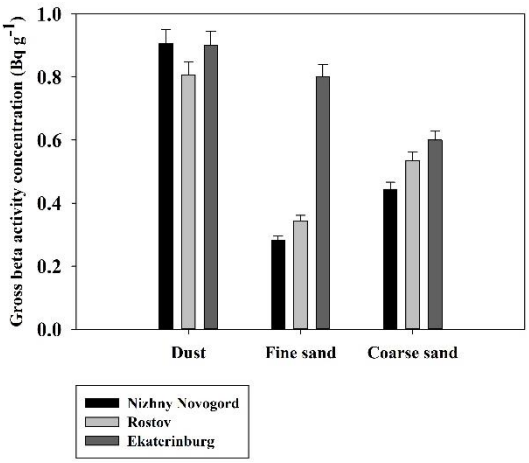

Figure 1. The average gross beta activity concentration (Bq. g^{-1}) ith error bar at different fraction size in three diferent cities.

The study was supported by Russian Science Foundation (grant No. 18-77-10024).

Seleznev, A.A., Yarmoshenko, I. V., 2014. Study of urban puddle sediments for understanding heavy metal pollution in an urban environment. *Environ. Technol. Innov*. 1–2, 1–7.

Seleznev. A. A., 2015. Environmental and geochemical assessment of the urbanized environment based on the study of sediment deposited in depressed landscape areas (on the example of Ekaterinburg).

Ogundare, F.O., Adekoya, O.I., 2015. Gross alpha and beta radioactivity in surface soil and drinkable water around a steel processing facility. *J. Radiat. Res. Appl. Sci*. 8, 411–417.

Occurrence of geogenic Radium in aquifers from Central Africa

D. Heine[1], F. Köhler[1], S. Bister[1], C. Walther[1], F. Wagner[2]

[1]Institut of Radioecology and Radiation Protection, Leibniz University of Hanover, 30167, Germany
[2]Federal Institute for Geosciences and Natural Resources, 30655, Germany
Keywords: Radium, aquifer, γ-spectrometry
Presenting author e-mail: heine@irs.uni-hannover.de

Uranium and its decay products are naturally occurring radioactive elements which can be found everywhere in the environment. Thus, the different isotopes of uranium and other radionuclides derived from the three natural decay series are naturally also present in aquifers. The concentrations can vary greatly depending on the nature of the host rock. In addition to uranium, the two radium isotopes ^{226}Ra ($t_{1/2}$=1600 y) and ^{228}Ra ($t_{1/2}$=5.75 y) are of particular interest for the radiological evaluation of a groundwater reservoir in terms of drinking water abstraction due to their dose relevance.

Since both isotopes are products of the natural decay series of ^{232}Th and ^{238}U, the presence of radium as well as the ^{226}Ra/^{228}Ra-ratio in groundwater is also depending on the presence of thorium and uranium in the host rock.

In this study groundwater from different locations in Burundi and Namibia have been analysed. All samples have been up concentrated and radium where chemically separated. The determination of radium (^{226}Ra and ^{228}Ra) was performed with γ-spectrometry using high purity germanium detectors (HPGe-detectors). Furthermore, the uranium-content was determined by ICP-MS.

Table 1 shows the activity concentrations of radium and ^{238}U in the groundwater-samples of six different locations. While the concentrations of both radium isotopes for all locations are <1 Bq/kg, the uranium-activities up to 9.7 Bq/kg can be found. Since the occurrence of radium is mainly influenced by α-recoil at the solid/fluid interface, the U- and Th-concentration in the host rock has a much greater influence on the distribution of radium as well as the ^{226}Ra/^{228}Ra-ratio in groundwater. To get more information on the underlying processes leading to the distribution of dissolved radium in groundwater, the aquifers host rock is also of particular interest.

Therefore, additional measurements were done on solid-samples, which were taken from the drilling for the groundwater-samples from three locations with enhanced uranium concentration. The solid-samples were also analysed regarding activity concentrations of the different radium isotopes, as well as other products from the three natural decay chains using γ-spectrometry and ICP-MS.

Table 1. Activity concentrations in groundwater.

	^{226}Ra	**^{228}Ra**	**^{238}U**
Sample	a in Bq/kg	a in Bq/kg	a in Bq/kg
Bu-1	0,468	0,039	8,215
Bu-4	0,620	0,560	9,737
Bu-7	0,607	0,322	8,253
Bu-10	0,635	0,470	0,508
Bu-11	<0,09	0,128	0,233
Bu-12	0,155	0,585	0,286

This work was supported by the Siebold Sasse Foundation.

[1] Szabo, Z.; Occurrence and geochemistry of radium in water from principal drinking-water aquifer systems of the United States. *Applied Geochemistry*. 27 (2012) 729–752.

[2] MÜHR-EBERT, E.-L.; Literary research on the occurrence and spread of geogenic uranium and radium levels in groundwater. Leibniz University of Hanover, Institute for Radioecology and Radiation Protection; 2017.

Distribution and environmental hazard parameters of radionuclides in river sediments and rocks in the Lomonosov diamond deposit area (NW Russia)

E.Yu. Iakovlev[1], A.I. Malov[1], S.V. Druzhinin[1], E.N. Zykova[1], A.S. Orlov[1], E.A. Karmanova[2]

[1] Laboratory of Environmental Radiology, N. Laverov Federal Centre for Integrated Arctic Research of Russian Academy of Sciences, Arkhangelsk, 163000, Russia
[2] Department of Geography and Hydrometeorology, Northern (Arctic) Federal University, Arkhangelsk, 163000, Russia
Keywords: radionuclides, sediments, hazard parameters
Presenting author, e-mail: yakovlev_eu@inbox.ru

Radioecological studies of river sediments were conducted in the area of the Lomonosov diamond deposit located in the Arkhangelsk region. This area is part of the Arctic zone of Russia. The Lomonosov diamond deposit is the largest deposit with commercially exploitable reserves in Europe. The Zolotitsa River is the main river flowing around the deposit. The Zolotitsa River has a special conservation status; it is the largest spawning ground for Atlantic salmon in the White Sea basin. Villagers use the waters of the Zolotitsa for drinking. The only man-made object that can pollute the aquatic ecosystem of the Zolotitsa River is the mining and beneficiation complex of Lomonosov diamond deposit (Karpenko, 2008). Currently, the deposit is under active development involving the extraction of large volumes of ore, including a full enrichment cycle, various measures to ensure the functioning of the mining and processing industry (the construction of dumps and tailings, water decrease, cleaning water used for washing of the concentration plant, and the construction of filtration fields). Therefore, radioecological research in this area is extremely important.

Radionuclide activity in bottom sediments and rocks was measured using low-background semiconductor gamma spectrometry with HPGe high-purity germanium detector, and isotopes ^{234}U and ^{238}U in bottom sediments and waters are studied using alpha spectrometry. The granulometric composition of the bottom sediments was determined using the vibrating screening machine. In samples of river sediments, physicochemical parameters were determined, such as the content of organic matter, water-soluble salts, carbonates (CO_3^{2-}), and the pH of the aqueous extract.

Average activity concentrations ^{137}Cs, ^{226}Ra, ^{232}Th and ^{40}K amounted to 5.4, 9.0, 11.2, 318.8 $Bq \cdot kg^{-1}$. Rocks extracted from quarries and stored in rock dumps contain, on average, almost twice as much ^{226}Ra and three times more ^{232}Th than river sediments. The influence of mining and beneficiation complex on the increase in activity radionuclides in bottom sediments of Zolotitsa River was found. The maximum average values of physicochemical parameters and radionuclides are observed in site of Zolotitsa River where drainage water is being unloaded into the riverbed from peatbog-filtration fields. Unloading of mineralized drainage water in this area, containing significant amounts of clay particles, leads to an increase in the proportion of clay component, organic matter, carbonates, water-soluble salts and natural radionuclides. Filtration of drainage waters through the swamp massif also leads to an increase in the mass fraction of organic matter in the bottom sediments, the source of which are organic peat compounds. An increase in organic p eat organic matter, in turn, leads to an increase in the activity of technogenic 137Cs in bottom sediments, since organic complexes of peat deposits fix global fallout radionuclides (Rosern et. al., 2009).

The radiation hazard parameters of bottom sediments and rocks from quarries were calculated. The average absorbed dose rate of gamma radiation D_R of river sediments was 24.4 $nGy \cdot h^{-1}$. Radium equivalent Raeq for bottom sediments averages 47.3 $Bq \cdot kg^{-1}$. Raeq and D_R are slightly higher for rocks from quarries than for those in bottom sediments. The maximum average values of Raeq and D_R are characteristic of sandy-clay Vendian deposits (V_2) and are 87.2 $Bq \cdot kg^{-1}$ and 41.5 $nGy \cdot h^{-1}$, respectively. The calculated external hazard index H_{ex} for river sediments and rocks extracted from quarries does not exceed 1. The total alpha activity in water does not exceed the established values of 0.2 Bq/l for drinking water (NRB 99/2009). The values of the radiation hazard parameters are, on average, at a level below the world average and do not represent a significant danger to the mining complex personnel and the population of the mining camp (UNSCEAR, 2000). However, in the future, with increasing ore production, deepening of quarries, increasing pumping volumes and salinity of drainage waters and with an even greater decrease in the sorption capacity of peatbog-filtration fields, we can expect an increase of radioactivity in bottom sediments of the Zolotitsa River.

This work was supported by the Russian Ministry of Education and Science (project no. № AAAA-A19-119011890018-3), the UB RAS (project no. 18-5-5-26), the Russian Foundation for Basic Research (projects no. 19-55-04001_Bel_mol_a; 18-05-60151_Arctic; no. 18-05-01041_A).

Karpenko, F.S. 2008. The influence of saponite on the stability of hydraulic structures of tailings in the Lomonosov deposit. *Geoecology*. 3, 269-271.

NRB – 99/2009. 2009. Radiation Safety Standards. Moscow. 72 p.

Rosern, K., Vinichuk, M., Johanson, K.J. 2009. ^{137}Cs in a raised bog in central Sweden, *J. Environ. Radioactivity*. 100, 534–539.

UNSCEAR, 2000. Sources and effects of ionizing radiation. United Nations, NewYork: Report to the General Assembly with Annexes.

Possibilities of the new scintillation $CeBr_3$ for radiological environmental monitoring

R. Idoeta, M. Herranz, N. Alegría and F. Legarda

Dpto. de Ingeniería Nuclear y Mecánica de Fluidos, ESI de Bilbao, Universidad del País Vasco UPV/EHU,
Plaza Ingeniero Torres Quevedo, 1, Bilbao, 48013, Spain
Keywords: $CeBr_3$, radiological environmental monitoring, gamma-ray spectrometer.
Presenting author, e-mail: raquel.idoeta@ehu.eus

Gamma-ray spectrometry dealing with low and very low level gamma ray activities is a fundamental part of the radiological environmental monitoring equipment. High energy resolution and cryogenically cooled semiconductor detectors like HPGe are routinely chosen for this monitoring purpose with the aim of obtaining the finest quality gamma-ray spectrometry and the maximum possibilities of quantifying any gamma-ray emitter in any matrix.

Alternatively, Cerium bromide ($CeBr_3$) detectors are part of a new group of scintillators able to be used for medium energy resolution gamma-ray spectrometry at room temperatures. This medium resolution could be enough to satisfy the analysis of the different emissions of important radioisotopes involved in radiological environmental monitoring, like I-131 and Cs-137, and they result a cheaper option than that of the more expensive HPGe detectors.

In this sense, these $CeBr_3$ detectors can result particularly attractive for routine tasks in radiological environmental monitoring because part of the radiological environmental monitoring is done after selective sampling process like the one done with collection filter cartridges specific for Iodine or after radionuclide chemical isolation, both cases implying that only some specific radionuclides should appear in the obtained spectrum, so that this medium energy resolution allows for distinguishing their gamma-rays. Also samples that contain more radionuclides, typically those belonging to the natural radioactive chains, can be measured by using these CeBr3 detectors if the radionuclides that we want to analyze do not present strong overlapping between their gamma-ray energies and those belonging to other radionuclides present in the sample.

This work establishes the measurement conditions under which a 1.5" $CeBr_3$ detector can serve for routine analysis in radiological environmental monitoring, for example, in the analysis of I-131 in I selective sampling in filter cartridges and the analysis of I-131 and Cs-137 in cellulose filters from conventional air-particulates sampling.

Specifically, a 1.5" $CeBr_3$ detector from Scionix, with a 2" Hamamatsu photomultiplier, surrounded by a 10 cm Pb shield has been used for this study. Its nominal energy resolution is 4.3% at 662 keV (^{137}Cs). It has a 0.5 mm thick Al housing and an external 45 mm diameter. For the multichannel analyzer, 512 channels have been selected.

Appropriate calibrations for radioiodine collection filter cartridges and particulate filters (cellulose nitrate) have been done. The calibration sources contained 10 radionuclides, having 12 different gamma ray energies with an energy range between 59.54 and 1836.05 keV. The Full Width at Half Maximum (FWHM) values found, although with larger values compared with those typical found in HPGe detectors, are sufficiently small to allow correct separation of the calibration peaks. They range between 8 keV at 59.5 keV to 43 keV at 1836 keV. This resolution is enough to resolve the 364.5 keV (81.2% intensity) from I-131 from other emissions coming from the other iodine radioisotopes (I-132, I-133 and I-135) and that of Cs-137 (661.62 keV) from that of Cs-134 (604.72 keV).

Different test samples have been measured and activities, uncertainties and detection limits have been calculated. Detection limits have been calculated using the ISO standard 11929 method (ISO, 2010).

In the examples cited before, for I-131 in the radioiodine collection filter cartridges, the detection limit found for I-131 is about 6.5 10^{-4} Bq/m^3 for a measuring time of two days, well below the mandatory value of 1.0 10^{-3} Bq/m^3 established by the *Consejo de Seguridad Nuclear*, (Spanish Nuclear Safety Council, CSN, 1993).

In the case of cellulose nitrate filters, the measurement of I-131 gives a detection limit of 5.8 10^{-4} Bq/m^3 and for Cs-137 the detection limit achieved is 1.5 10^{-4} Bq/m^3, for a measuring time of one day, both of them below the required values of 1 10^{-3} Bq/m^3 and 2 10^{-4} Bq/m^3, respectively, established by the Spanish Nuclear Safety Council, (CSN, 1993).

So, one or two days of measurement, depending on the test sample, with this detector is sufficient to achieve the requirements of I-131 and Cs-137 for air monitoring purposes.

So, this small detector that operates at room temperature and is largely cheaper than traditional HPGe detectors could be considered as an option for simple routine tasks associated to radiological environmental monitoring as it shows an excellent performance in assessing highly important selected radionuclides that must be continuously monitored in the environment.

ISO, 2010. Determination of the characteristic limits (decision threshold. detection limit and limits of the confidence interval) for measurements of ionizing radiation -- Fundamentals and application, ISO 11929. International Standards Organization, Geneve.

CSN, 1993. Guía de Seguridad no 4.1. Diseño y desarrollo del programa de vigilancia radiológica ambiental para centrales nucleares, Madrid.

Short-term metabolism of ^{125}I in bastard halibut (*Paralichthys olivaceus*) after ingestion of biologically incorporated ^{125}I

S. Imai[1], T. Tani[1], Y. Tako[1], Y. Takaku[1], S. Hisamatsu[1]

[1]Department of Radioecology, Institute for Environmental Sciences, Rokkasho, Kamikita, Aomori, 039-3212, Japan
Keywords: biologically incorporated radioiodine, biomagnification, bastard halibut, ingestion pathway
Presenting author e-mail: imais@ies.or.jp

A commercial, large-scale nuclear fuel reprocessing plant in Rokkasho, Aomori Prefecture, Japan is now under final safety assessment by the Nuclear Regulation Authority. ^{131}I is an important radionuclide in the safety assessment of the plant, as is ^{129}I, which is discharged by the normal operation of the plant, because certain marine organisms are known to accumulate radioiodine. In this study, we developed a short-term metabolism model of ^{125}I in bastard halibut (*Paralichthys olivaceus*), a commercially important fish in the coastal waters of the Aomori Prefecture, using retention data after ingestion of ^{125}I incorporated into a freshwater fish (medaka, *Oryzias latipes*).

We used ^{125}I (half-life, 60 days) as a tracer in this experiment. Because adult bastard halibuts are piscivores, we selected medaka as an appropriate feed. Medaka samples (mean body weight ± SD, 0.28 ± 0.11 g) were placed for 7 days in freshwater containing 200 Bq g^{-1} ^{125}I and radioactivity was measured using a NaI auto-gamma detector. The mean radioactivity of the exposed medaka was 1.2 ± 0.6 kBq.

Bastard halibuts (12.9 ± 6.5 g) were used ≥159 days after hatching for the ingestion experiment. Each bastard halibut was placed in a closed acrylic tank (400 mm wide × 300 mm deep × 350 mm high, 8 L water, 20 L air), individually. The tank was filled with seawater, which did not contain ^{125}I, and aerated. During the experimental period (12 days maximum), bastard halibuts were fed only medaka containing ^{125}I. One medaka containing ^{125}I was fed to each bastard halibut up to six times, after measuring the radioactivity in the individual medaka, and bastard halibuts consumed the medaka immediately after feeding. Bastard halibuts were separated into experimental groups (n = 4–6) with different feeding periods (1–6 days). The excreta were removed and the ^{125}I concentration in the tank water was negligible.

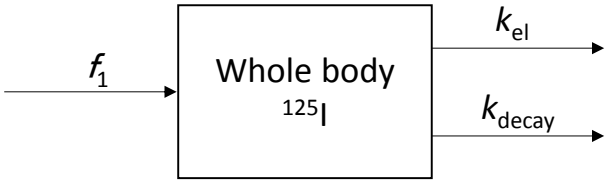

Figure 1. Diagram of the compartment model.

The gastro-intestinal absorption ratio (f_1) and elimination rate constant (k_{el}, h^{-1}) are unknown parameters, and the decay constant (k_{decay}) is 0.00049 h^{-1}.

Bastard halibuts were collected 24 h after the last feeding, and the radioactivity was measured in the tissues. In addition, certain fish in the group fed medaka for 6 days were sampled 3 and 6 days after the last feeding.

Whole-body retention of ^{125}I (excluding that in the gastro-intestinal (GI) tract) increased with each feeding day and quickly decreased after the last feeding. Using the retention data, we constructed a single compartment model to simulate ^{125}I uptake and metabolism (Fig. 1). Here, we assumed that the ^{125}I ingested was promptly absorbed from the GI tract. The GI absorption ratio (f_1) and elimination rate constant from the whole body (k_{el}) were obtained using the least squares method. f_1 and k_{el} were estimated to be 0.41 and 0.010 h^{-1}, respectively. The estimated radioactivity in the whole body of individual bastard halibuts was plotted against that measured (Fig. 2). As shown in Fig. 2, the model adequately simulated the short-term behaviour of ^{125}I. The biological half-life of ^{125}I was short (approximately 3 days) and indicated the rapid metabolism of radioiodine in bastard halibut.

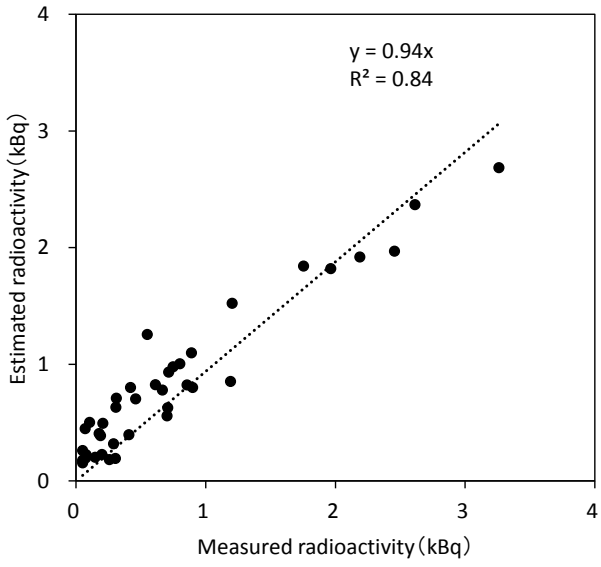

Figure 2. Comparison of the estimated radioactivity using the compartment model with measurements in bastard halibut after ingestion of biologically incorporated ^{125}I.

This study was performed under a contract with the government of Aomori Prefecture, Japan.

Portable radiation detectors used in in-situ gamma spectrometry for radiological characterization of a contaminated site near a coal power plant in Northern Greece

Ioannidou Alexandra

Aristotle University of Thessaloniki, Physics Department, Nuclear Physics Laboratory, Thessaloniki 54124, Greece
Keywords: in-situ gamma spectrometry, environmental radioactivity, remediation
Presenting author: Alexandra Ioannidou - e-mail: anta@physics.auth.gr

The traditional characterization procedures of radiologically impacted environments are time and money consuming by collecting, preparing and analyzing big number and amount of samples, while the In-Situ technique offers certain advantages by fast determination, cost reduction and optimization of the sampling strategies. The present work reviews the results of an environmental radioactivity study carried out by the Nuclear Physics Laboratory, Aristotle University of Thessaloniki (NPL-AUTH), by the use of specific portable radiation detection instruments.

Radioactivily contaminated sites due to anthropogenic activities by various industrial activities, or pollutants related with Technologically Enhanced NORM (TENORM) lead to the exposure of members of the public to ionizing radiation resulting in negative health effects.

The method of In Situ technique has been chosen to characterize such a site in a cost and time effective manner, without time consuming sample collection, preparation and analysis in the laboratory, in order to allow immediate spatial quantitative information of key gamma-ray emitters enriched in the soil. Furthermore, this work will allow the validation of this in-situ method, by comparing the results with analysis of soils samples in the lab.

The site that studied is in the region of Northern Greece, with coal power plants of total power of 2800MW. The experimental work performed by using portable gamma ray spectrometers, studying an area of 25000m^2 in a grid of 500x500m in places that were accessible and 1000x1000m at non accessible places.

Three different instruments have been used: 1) Saphymo-Stel 1'' NaI(Tl), 2) Thermo FH 40 Survey Meter, 3) Identifier, target system electronic gmbh (Figure 1). In each sampling point, we recorded the dose rate (nSv h^{-1}) at 1 m above the ground. Radiological map is given in Figure 2, with values in nSv h^{-1}.

The In-Situ measurements had been cross-checked with measurements of soil samples in the lab by Ge-detectors. The first results show that in higher contaminated areas the concentrations of ^{238}U, ^{235}U, ^{226}Ra were higher too.

Figure 1. Portable detectors used for the in-situ survey.

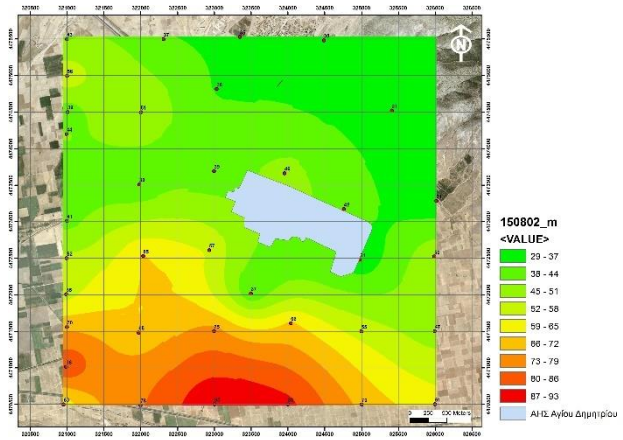

Figure 2. Radioliogical map around the CPP Ag. Dimitiros, Northern Greece.

With a first approximation, the measured external doses are in agreement with the estimated external doses.

The observed external doses 30-93 nSv h^{-1} are in agreement with the population-weighted average absorbed dose rate in air from terrestrial gamma radiation 57 nGy h^{-1} (UNSCEAR 1993) the reported in Greece average absorbed dose rate in air from terrestrial gamma radiation 42 nGy h^{-1} (UNSCEAR 1993)

The results can be used as a reference point for radiological mapping of the studied area.

The validation of the in-situ method near a coal power plant could have as a result a fast mapping characterization of a site near a coal power plant.

UNSCEAR 1993. Sources and Effects of Ionizing Radiation. *United Nations Scientific Committee on the Effects of Atomic Radiation, United Nations*, New York.

Relationship between the radon concentration of dripping water in limestone cave and the amount of precipitation observed in Okinawa, subtropical region of Japan

A. Ishimine[1], S. Nakasone[1], Y. Shiroma[1], N. Akata[2], M. Furukawa[1]

[1]University of the Ryukyus, 1 Senbaru, Nishihara, Okinawa 903-0213, Japan
[2]Hirosaki University, 66-1 Hon-cho, Hirosaki, Aomori 036-8564, Japan
Keywords: radon concentration, limestone cave, dripping water, precipitation
Presenting author, e-mail: akiishimine3@gmail.com

Radon (^{222}Rn) is a radioactive noble gas with a half-life of 3.8 days, which has radium (^{226}Ra) as a parent nuclide. Radon exists around us. Soluble from soil to water. And it is supplied to the cave as seepage water. When the supply of radon cuts off while passing through the limestone with a very few contents of radium, it decays according to the half-life and the radon concentration decreases. Therefore, the radon concentration in the groundwater changes with time, and the residence time of the groundwater estimated from the concentration decreases (Komae, 1995). Radon concentration increases in enclosed spaces with low ventilation rates, such as in caves and indoors (Furukawa *et al*., 2004). It also shows high concentration even in Gyosen-dou, a limestone cave formed in the southern part of Okinawa Island (Tanahara *et al*., 1997). The amount of radium contained in the limestone forming the cave is lower than the detection limit. It suggested that the source of radon is likely to be soil deposited in the above of limestone layer. There have been few examples of measurement of radon concentration in dripped water from straw generated on the roof of the cave. In the case of Shiroma *et al*. (2016) has few data, and the examination of the radon concentration and the amount of precipitation in the dripping water was insufficient.

Continuous observation of monthly radon concentration in dripping water has been carried out from July 2016 in a limestone cave, Gyokusen-dou, located in the southern part of Okinawa Island. 10 ml of dripping water was collected directly from the straw using the plastic syringe. The collected samples were placed in glass vial contains 10 ml of a mineral oil scintillator in advance and were measured using Quanturus 1220 (PerkinElmer). The amount of precipitation date used “Itokazu” (AMeDAs). Furthermore, in order to compare the radon concentration with the dripping water that was converted for one month. In this study, continuous observation is conducted for the purpose of clarifying the relationship between the amount of precipitation and the radon concentration in the dripping water.

The arithmetic means ± standard deviation for the radon concentration of dripping water samples were estimated to be 9.8 ± 0.8 Bq L^{-1}. The amount of dripping water and radon concentration increased with the amount of precipitation during the rainy season from May to June 2017. However, from May to June 2018, the amount of dripping water decreased less than 10 mm, but the radon concentration increased to 1.0-2.0 Bq L^{-1}. If the amount of monthly precipitation exceeds 300 mm, the amount of dripping water increases and the average amount of dripping water in 2.9 mm min^{-1}. When there is the amount of monthly precipitation over 600 mm, the amount of dripping water over 4.6 mm min^{-1} can be confirmed, and radon concentration also increased. However, the radon concentration increased even if the monthly mean precipitation did not exceed 300 mm. Simple moving averages were taken and compared to make it easier to compare the relationship between radon concentration and the amount of precipitation. There is a relationship between precipitation and radon concentration because of the similar trend of variations (Fig. 1). The radon concentration rises when the amount of precipitation is large. Radon concentration is low when there is little precipitation. The radon concentration in the dripping water variations depending on the amount of precipitation.

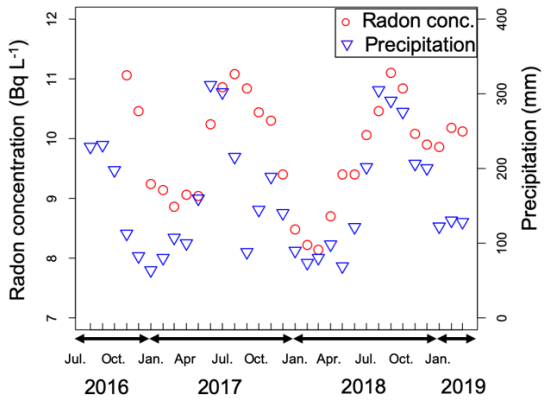

Figure 1. Variations of radon concentration for dripping water in a limestone cave, Gyokusen-dou, and amount of precipitation observed in Okinawa Island.

The authors thank S. Ooka, Nanto of Nanto Co. Ltd, A. Kato of National Institute for Fusion Science for their cooperation. This work was supported by JSPS KAKENHI Grant number 18K14543.

Furukawa, M. Zhuo, W. Tokonami, S. 2004. Radon and Tron concentrations in the atmosphere of Miyakojima, Okinawa, *Radioisotopes*., 141-147.

Komae, T. 1995. Application of radon to hydrological analysis, *Radioisotopes*.,715-724.

Shiroma, Y. Shiroma, M. Kina, S. Hosoda, M. Yasuoka, Y. Akata, N. and Furukawa, M. 2016. Sourece of Atmospheric Radon in the Gyokusendo, a Limestone Cave in Okinawa, Japan, *Jpn. J. Health Phys*., 218-226

Tanahara, A. Taira, H. and Takemura, M. 1997. Radon distribution and the ventilation of a limestone cave on Okinawa, *Geochem. J*., 49-56.

Radiation survey of fossil fuel in the Philippines

K. Iwaoka[1], E.B. Enriquez[2], T.Y. Garcia[2], R.J. Aniago[2], L.J.H. Palad[2], M. Hosoda[3], S. Tokonami[3], H. Yonehara[4], C.P. Feliciano[2], R. Kanda[1]

[1]National Institutes for Quantum and Radiological Sciences and Technology,4-9-1 Anagawa, Inage, Chiba, 263-8555, Japan.
[2]Health Physics Research Section, Atomic Research Division, Department of Science and Technology – Philippine Nuclear Research Institute (DOST-PNRI), Commonwealth Avenue, Diliman, Quezon City, 1101, the Philippines.
[3]Hirosaki University,66-1 Honcho, Hirosaki, Aomori 036-8564 Japan.
[4]National Institute of Radiological Sciences,4-9-1 Anagawa, Inage, Chiba, 263-8555, Japan.
Keywords: Natural radiation, NORM, fossil fuel
Kazuki Iwaoka, e-mail: iwaoka.kazuki@qst.go.jp

A material containing a significant number of natural radioactive nuclides such as ^{238}U series and ^{232}Th series is referred to as a naturally occurring radioactive material (NORM). The relevant values for the safe handling of NORM of 10 Bq g^{-1} for ^{40}K and 1 Bq g^{-1} for all other radionuclides of natural origin were given in the International Atomic Energy Agency (IAEA) Safety Guide (IAEA, 2004). Recently, the fossil fuel such as coal has been used with industrial development. In some countries, data on activity concentration of natural radioactive nuclides in coal has been reported. In the Philippines, although coal is imported and used as an industrial raw material for coal-fired power plants, information related to radiation exposure in coal-fired power plants is scarce. In this study, measurements of activity concentration of natural radioactive nuclides of industrial materials, the ambient dose equivalent rate as well as ^{222}Rn decay products concentration in a coal-fired power plant in the Philippines were performed.

A coal-fired power plant in the Philippines was selected for this study. This coal-fired power plant is one of the typical plants handling coal in the Philippines. The processes of work sites in the plant are illustrated in Figure 1. Measurements of the ambient dose equivalent rate and ^{222}Rn concentration in the work sites as well as measurements of the activity concentrations in raw materials and by-products were performed. A NaI(Tl) scintillation survey meter was used for measuring the ambient dose equivalent rates in each work site. Each measurement was performed at a height of 1 m from the floor. The activity concentrations of the ^{238}U series, the ^{232}Th series and ^{40}K in samples were determined by inductively coupled plasma mass spectrometry (ICP–MS) and gamma-ray spectrum analyses. A measurement of ^{222}Rn decay products were performed by collecting them on a filter in each work site. The values of ^{222}Rn decay products concentration (Equilibrium equivalent radon concentration: EERC) were calculated from their alpha counts.

The activity concentrations of the ^{238}U series and ^{232}Th series in the raw materials and by-products were lower than the relevant values in the IAEA Safety Standards. The values of the ambient equivalent dose rate in the work sites was less than an average value of those in the Philippines. The values of the EERC in work sites were not quite different to those in BG.

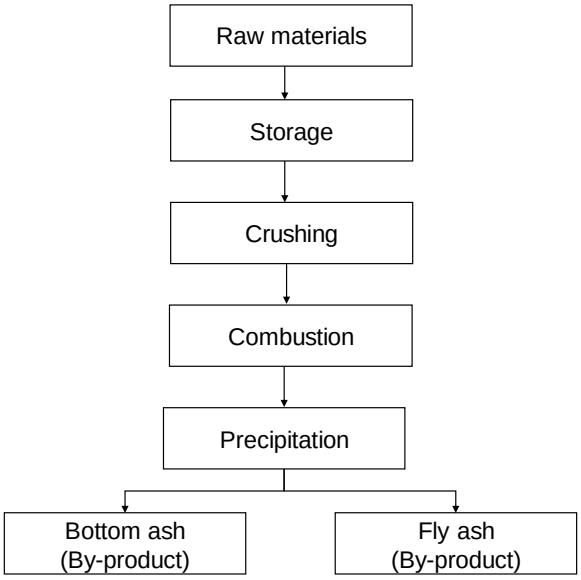

Figure 1. Process of operation in the plant.

IAEA. 2014. Safety Standards, Radiation Protection and Safety of Radiation Sources: International Basic Safety Standards. General Safety Requirements Part 3. Vienna.

Experimental study on concentration ratio of ^{90}Sr and ^{137}Cs in crab (Scylla serrata)

Li Jianguo, Han Baohua, Wang Huijuan, Ma Binghui, Cao Shaofei

Department of Nuclear Environmental Science, China Institute for Radiation protection, Taiyuan, 030006, China
Keywords: ^{90}Sr, ^{137}Cs, Concentration Ratios, Crab
Li Jianguo: lijianguo@cirp.org.cn

The inland nuclear facilities are located near the rivers and lakes. During the operation of the nuclear facilities, radioactive pollutants inevitably enter the rivers, which may have impact on aquatic organisms and thus contribute to the public radiation dose. ^{90}Sr and ^{137}Cs are important radionuclides discharged from nuclear facilities. In this project, the freshwater crab (*Scylla serrata*) were selected as experimental organisms, and water bodies recycled in glass aquarium were used. By adding ^{90}Sr and ^{137}Cs in the water, the transfer behaviour of ^{90}Sr and ^{137}Cs in water-organism system were studied. The ^{90}Sr and ^{137}Cs radioactivity concentration in water was 300Bq/L at the beginning of the experiment. After one week equilibrium time, young crab and adult crab were raised in the aquariums. The biological and water samples were collected regularity. The CR (the Concentration Ratio of radionuclide concentration in organism to that in water, L/kg) of ^{90}Sr and ^{137}Cs in different parts of adult crab, young crab (as a whole) were obtained.

The CR variation of ^{137}Cs in the adult crab meat and carapace were showed in Figure1 and Figure 2.

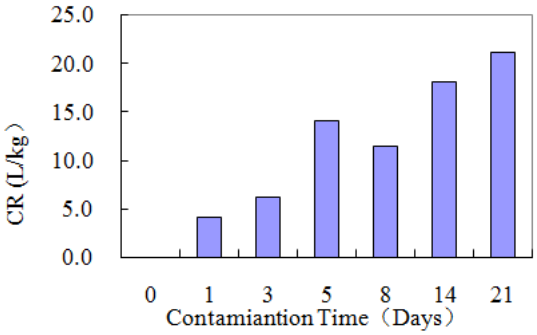

Figure 1. The concentration variation of ^{137}Cs in the adult meat.

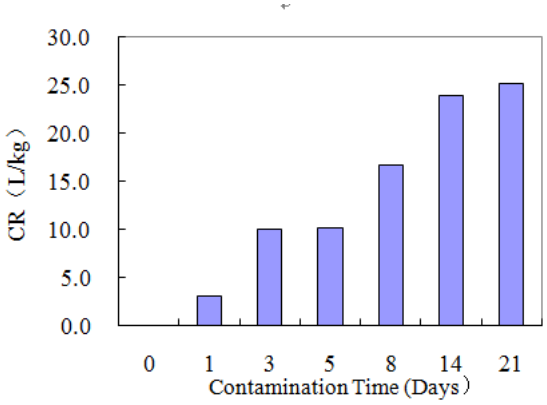

Figure 2. The concentration variation of ^{137}Cs in the adult carapace.

The results showed during the 21-days contamination experiment, the CR of different parts of adult crab increased significantly over time. The maximum concentration ratios of ^{90}Sr and ^{137}Cs in adult crab meat (the edible part) of were 21.1L/kg and 8.5L/kg respectively, and the maximum concentration ratios of ^{90}Sr and ^{137}Cs in the carapace of adult crab were 15.4L/kg and 25.1L/kg respectively. The results showed ^{90}Sr in water was more concentrated in crab carapace than that in crab meat, and the concentration of ^{137}Cs in crab meat and carapace were in the same order.

The CR variation of ^{137}Cs in the young crab was showed in Figure 3. During the 95-day contamination experiment, the maximum concentration ratios of ^{90}Sr and ^{137}Cs of young crab (as a whole) were 123.3lL/kg and 146.2L/kg respectively, which showed the CR of ^{90}Sr and ^{137}Cs of young crab were significantly higher than that of adult crab.

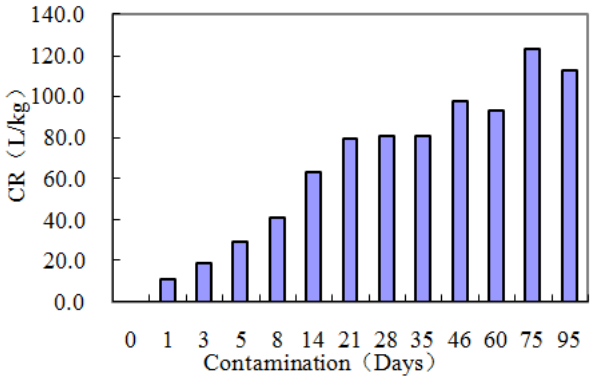

Figure 3. The concentration variation of ^{137}Cs in the adult carapace.

The CR for freshwater invertebrate (eg., Sr, 77~1300) of IAEA Handbook (2010) and other literatures are quite in a wide range.

Further studies would be focused on the method to estimate the concentration ratio under equilibrium in experimental conditions.

IAEA. 2010. Handbook of parameter values for the parameter values for the prediction of radionuclide transfer in terrestrial and freshwater environments. IAEA technical reports series No. 472.

Qin Suyun, Li Shuqin, Zhou caiyun, Qi Yong et.al. 1995. On the Concentration Factors of Some Radionuclides in Aquatic Organisms in Freshwater Environment. *Radiation Protection*.Vol. 15. No. 5.

Monte Carlo model of Czech calibration facility for gamma-ray spectrometers

K. Johnová[1]

[1]Department of Dosimetry and Application of Ionizing Radiation, Faculty of Nuclear Sciences and Physical Engineering, Czech Technical University in Prague, Prague 11519, Czech Republic
Keywords: calibration facility, Monte Carlo, field gamma spectrometry
Presenting author, e-mail: Kamila Johnová, kamila.johnova@fjfi.cvut.cz

Gamma ray spectrometry is one of the most widely used analytical method that utilizes ionizing radiation, covering a large region of different scientific and industrial fields.

Each gamma spectrometer in order to provide reliable data needs to be calibrated correctly. While the energy calibration is usually very simple, we are only dealing with efficiency calibration here. In laboratory conditions the efficiency calibration is usually rather simple compared to the field measurement. The standard of activity for every calibration needs to approximate the real sample as closely as possible, which means that for the field spectrometry we usually need quite large and relatively high activity standards when comparing to laboratory conditions.

The field gamma spectrometers - instruments designed for borehole measurement included - are usually calibrated on large calibration pads with certified activities. The requirements and recommendation for calibration pad construction are summarized in (IAEA, 2013).

The Czech gamma spectrometer calibration facility is located in Straz pod Ralskem in the site of DIAMO state enterprise. (Rojko and Zeman, 1975). The facility provides the possibility for calibration of field and borehole spectrometers. The field spectrometers are calibrated on 3 concrete pads (each of them with enhanced content of K-40, U-238 and TH-232) and one background pad (filled with low activity sand). For borehole spectrometers there are again three concrete standards (each with enhanced content of K-40, U-238 and TH-232) and one background standard. Apart of these there are two cylindrical layered standards for borehole instruments.

The activities measured at each standard are regularly verified through control measurements and the concentrations measured at these standards were also compared to measurements (with the same instruments) at other European calibration facilities. Recently an intercomparing measurement between Czech and Chinese calibration facility was organized.

Due to careful measurements the calibration facility provides very accurate certified values that can be used for calibration of spectrometers with a construction closed to the one that was used for the control measurement. Even though the corrections on distance between the crystal of the detector and ground were previously established, with new detectors being designed, the calibration facility will soon be unable to cover the needs of calibration for newly available detectors.

In order to extend the portfolio of the detectors that can be calibrated at this facility a model for Monte Carlo simulation of the whole facility was created. The model includes all the calibration pads, walls (divided into brick and different layers of plaster), door, floor and all other important objects in the building. The activities of radionuclides (K-40, U-238 and TH-232) in these objects were estimated by sampling and performing a laboratory spectrometry. With known structure of the spectrometer that needs to be calibrated, this model may be used to calculate correction of the calibration coefficients. Using this model the utility of the Czech calibration facility may be extended to practically any kind of field spectrometer.

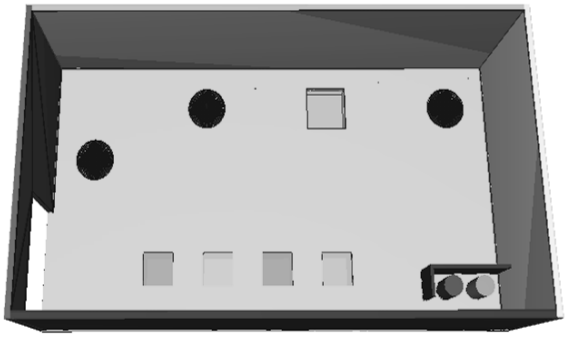

Figure 1. The visualization of the calibration facility model.

The work was supported from European Regional Development Fund-Project "Center of Advanced Applied Science" No. CZ.02.1.01/0.0/0.0/16-019/0000778.

IAEA, 2013. Guidelines for radioelement mapping using gamma ray spectrometry data, July 2003, *TECDOC-1363*

Rojko, R., Zeman, J., Josovic, M., Stanek, M. 1975 Building of the calibrating facility for the field gamma-ray spectrometers, *Final report of the project*, Liberec, GPUP

Uranium concentrations in drinking waters in Greece

K. Kehagia, D.C. Xarchoulakos, A. Papathanasiou, C. Potiriadis

Department of Environmental Radioactivity, Greek Atomic Energy Commission, Agia Paraskevi, 15310, Greece
Keywords: drinking water, uranium isotopes, a-spectrometry
Konstantina Kehagia, e-mail: konstantina.kehagia@eeae.gr

In the Council Directive 2013/51/EURATOM of 22 October 2013, laying down requirements for the protection of the health of the general public with regard to radioactive substances in water intended for human consumption, determination of several radionuclides is required.

The main sources of drinking water consumed by the population of Greece are mostly spring water, groundwater, mainly from drilling operations and surface water.

Waters play an important role in the migration, diffusion and redistribution of natural radionuclides in the earth`s crust. Since these radionuclides are present in soil and rock, they can also be found in ground and surface water. Among the natural radionuclides that have to be determined for the estimation of the Indicative Dose that has to be less than the parametric value of 0.1 mSv, are the uranium isotopes U-234 and U-238, which are from great interest because of their multiple characteristics.

Uranium is a natural constituent of the earth crust and occurs in all of its rocks, soils and fluids. Due to its radiological and chemical toxicity leads to health effects in exposed population. Intake of natural uranium can be obtained through air, which is low, through food and drinking water. The concentration of uranium in water is typically very small, but varies from region to region, depending on the type of minerals in the soil and bedrock. Uranium gets into drinking water sources when groundwater dissolves minerals that contain uranium. Elevated levels of uranium are more likely to be found in groundwater, rather than in surface water supplies.

In this study the uranium results which derive from about 1750 water samples of 152 municipalities in Greece are presented. These measurements have been performed from 2016 until today and are depicted on a map. The map has been constructed by the use of the software tool "Microsoft Power Map for Excel".

The uranium activity concentrations in the drinking water samples have been determined after radiochemical analysis by means of a-spectrometry and ICP-MS.

Considering the results, we observed that the uranium activity concentrations in the northern part of the country are higher than in the south, even though a few of them exceed the derived concentrations for radioactivity issued in the above mentioned Council Directive. This can be attributed to the fact that the main source of drinking water in the north part is mainly groundwater from drilling operations. The activity ratios $^{234}U/^{238}U$ for dissolved uranium ranges from 1.1 to 3.5. No correlation between drinking water activity concentrations and incidence rates of several groups of diseases has been studied yet.

EURATOM (2013), Council Directive 2013/51/ EURATOM.

WHO (2005), Guidelines for Drinking – water Quality, Uranium in Drinking – water, WHO/SDE/03.04/118.

Investigation of the anthropogenic land using effect on the Pănăzii lake (Romania) catchment area used Cs-137 and Pb-210 radionuclides

Sz. Kelemen[1,2], D. Veres[2,3], O-L. Muntean[1], C.V. Malos[1], R-Cs. Begy[1,2]

[1] Faculty of Environmental Science Engineering, University of Babes-Bolyai, Cluj-Napoca, 400294, Romania
[2]Interdisciplinary Research Institute on Bio-Nano-Sciences, University of Babes-Bolyai, Cluj-Napoca, 400271, Romania
[3] Romanian Academy, Institute of Speleology "Emil Racoviță", Cluj-Napoca, 400006, Romania
Keywords: Land use effect, Soil erosion, Pb-210 dating
Presenting author, e-mail: kelemen_szabolcs@ymail.com

Soil erosion impact on the environment have interested increasing attention in the last few years, and there is a very important to need to know more information about the soil erosion processes. For the investigation of the soil erosion can be use Cs-137 and Pb-210 as a tracer for this geomorphology process. Among the different existing tracers, the fallout component of the radioisotope Pb-210, also termed unsupported or excess Pb-210 (Pb-210xs) when referring to its presence in soil or sediment, arguably offers the broadest potential for environmental applications, due to its origin and relatively long half-life. (Matisoff 2014)

The aim of this study is to examine the anthropic land using effect (grazing, roads and agriculture) on the soil erosion and the lake sedimentation process in the Pănăzii natural lake (Romania) catchment area. The lake situated in the center part of Romania in Alba County on the 450 m latitude. The lake has relatively small catchment area (1.2 km^2) and the surface of the lake is 0.016 km^2, this catchment area was used for the agricultural and the grazing activity. The position and the environmental attributes in the studied area is qualified to modeling the anthropogenic land use erosion processes. The using model including estimates of the depositional flux of Pb-210xs to the soil surface and the post-depositional mobility of Pb-210 are also discussed. In order to have a time table about this catchment aria erosion process was applied the Pb-210 and Cs-137 dating method on the sediment cores (Appleby and Oldfield, 1978). For the Pb-210 measurements was used the alpha spectrometry method when the Pb-210 activity concentration was determined from they daughter element (Po-210) activity concentration. The determination of the Cs-137 activity concentration applied the high-purity Germanium coaxial well Photon detector system (Begy et al 2018). The catchment area erosion map was made in GIS (Geographic Information System) software.

This work is financially By PN-III-P1-1,1-TE-2016-0814 project, "Studies on the effects of land use changes on soil erosion and increased sedimentation using radionuclides" National project, initiated by the Romanian Government.

G. Matisoff, (210)Pb as a tracer of soil erosion, sediment source area identification and particle transport in the terrestrial environment *Journal of environmental Radioactivity (2014)*

P.G. Appleby, F. Oldfield, The calculation of lead-210 dates assuming a constant rate of supply of unsupported ^{210}Pb to the sediment *Catena, 5 (1978), pp. 1-8*

R-Cs. Begy, H. Simon, Sz. Kelemen, L. Preoteasa, Investigation of sedimentation rates and sediment dynamics in Danube Delta Lake system (Romania) By 210 Pb dating method *Journal of environmental Radioactivity (2018)*

Increased negative ionization yield for the detection of ^{236}U and ^{233}U by AMS

Michael Kern[1], Peter Steier[1], Karin Hain[1], Maki Honda[1], Andreas Wiederin[1], Xiaohe Zhang[1], and Robin Golser[1]

[1]University of Vienna, Faculty of Physics – Isotope Physics, VERA Laboratory, Währinger Straße 17, 1090 Vienna, Austria

Keywords: AMS, Actinide, Fluoride, Ionization Yield

Michael Kern, e-mail: a01247822@unet.univie.ac.at

^{236}U ($T_{1/2}$ = 2.342(4) x 10^7 years) and ^{233}U ($T_{1/2}$ = 1.592(2) x 10^5 years) are trace nuclides found in environmental samples due to releases from nuclear fuel reprocessing and from atmospheric nuclear weapon tests. ^{236}U originates from thermal neutron capture ^{235}U(n,γ)^{236}U or the fast neutron induced reaction ^{238}U(n,3n)^{236}U. ^{233}U is produced by ^{235}U(n,3n)^{233}U, as well as by ^{232}Th(n,γ)^{233}Th followed by β$^-$-decay. Typical ^{236}U/^{238}U ratios as low as 10^{-9} were found in the north-east Pacific (Eigl et al., 2016) using acellerator mass spectrometry (AMS). The limiting factor in uranium AMS measurements is the relatively low detection efficiency (ca. 10^{-4}), with the negative ionization yield being the main loss factor. Increasing this, is especially important for the recently established measurements of ^{233}U (Hain et al., 2017) which is typically two orders of magnitude less abundant than ^{236}U. The combined determination of anthropogenic ^{233}U and ^{236}U in environmental samples is a promising method for source assessment of antropogenic radionuclides.

For AMS, U is usually extracted as UO^- from an Fe_2O_3 matrix using a Cs sputter ion source. For routine analysis of environmental samples the final preparation step is a co-precipitation with at least 1 mg of Fe meaning that the sample is not consumed in a usual measurement of 4 h. This can be achieved with an improved sample preparation giving ionization yields of 0.3% (Eigl et al., 2016). This yield needs to be increased substantially to facilitate the detection of ^{233}U with reasonable effort.

However, investigations of AMS ionization yields are very time consuming as the samples must be completely consumed, which typically takes several hours. With the recently installed ILIAMS beamline (Lachner et al., 2019) at VERA, an additional injection system became available, which allows measurements in parallel to routine AMS operation. About one month of beam time for the investigation of ionization yields became thus available, and over 100 different samples were analyzed as described in the following.

To set the starting value, the in-house standard Vienna-KkU-D30 (U:Fe 1:30, wt. ratio both as oxides) was mixed with different materials in order to change the negative ion formation behaviour. The maximum achieved $^{238}U^{16}O^-$ negative ion yield peaked at 0.74%. Furthermore, under consideration of an improved formation of superhalogen anions like UF_5^- (Zhao et al. 2010), we tested a mixture of Vienna-KkU-D30 and PbF_2 (1:9, wt. ratio). This increased the negative ion yield of $^{238}U^{19}F_5^-$, up to 2.49%. The comparison of UO^- and UF_5^- anion current characteristics in figure 1 shows nearly an 18-fold increase in peak current for UF_5^- (blue) to UO^- (black) alongside with UO^- current of a sample which corresponds to standard preparation method (red).

Around 95% of total extractable UF_5^- ions (within 4 h) were already ionized in less than 1.5 h of sputter duration. Additionally, extraction of UF_5^- delivers excellent suppression of $^{238}UH^{3+}$ allowing for a measurement of ^{239}Pu in U-rich samples down to ^{239}Pu/U = 10^{-14}, using the whole VERA AMS instrument setup (Steier et al., 2019). The above measurements for UF_5^- enable us to proceed towards smaller sample sizes, increased throughput for routine measurements and higher sensitivity for even lower ^{236}U/^{238}U ratios as well as investigations of samples containing ^{233}U.

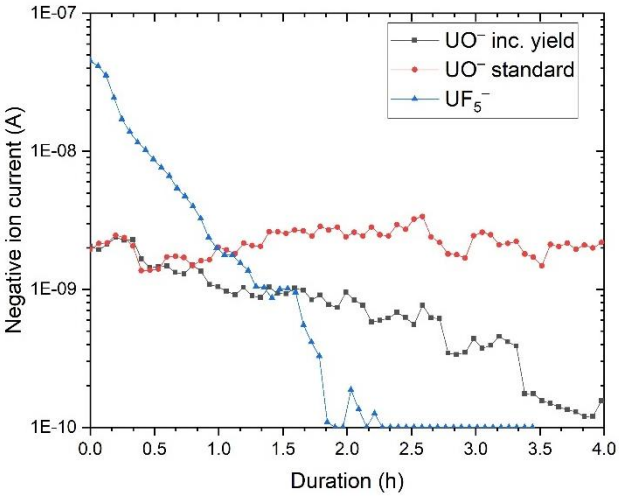

Figure 1. Comparison of UF_5^- (blue) and UO^- (black, red) negative ion current (log) vs sputter duration.

Eigl, R. et al., 2016. First study on U-236 in the Northeast Pacific Ocean using a new target preparation procedure for AMS measurements. *J. Environ. Radioact*. 162, 244-250.

Hain, K. et al., 2017. ^{233}U/^{236}U a new tracer for environmental processes? *ENVIRA 2017*. 29.05.17.

Lachner, J. et al., 2019, This conference.

Zhao, X.-L. et al., 2010. Studies of anions from sputtering I: Survey of MFn-. *Nucl. Instr. Meth.* B 268. I 7–8, 807-811.

Steier, P. et al., 2019. This conference.

The effect between background gamma dose rates and radionuclides by height in the near-ground level

Chang-Jong Kim[1], Jong-Myoung Lim[1], Wanno Lee[1]

[1]Korea Atomic Energy Research Institute
Presenting author, e-mail: Chang-Jong Kim, cjkim@kaeri.re.kr

The study of background radiation in the environment is significant for an objective of establishing reliable baseline data on the background radiation level. Background radiation originates from a variety of sources, both natural and artificial. These include both cosmic radiation from space and terrestrial radiation from ground. The Terrestrial radiation emitted from natural sources is largely due to primordial radionuclides, mainly Th-232 and U-238 series, and their decay products, as well as K-40, which exist at trace levels in the earth's crust. Gamma dose rates are affected by both terrestrial radiation and cosmic radiation, and the effects of terrestrial radiation is dominant in the near-ground level. In this paper, in order to verify the effect between background gamma dose rates and radionuclides by height, gamma dose rates and gamma-ray spectrum were measured at a height of the meteorological tower between 0 and 70 meters using high pressure ionization chamber (HPIC) and HPGe detector. The gamma dose rate and peak count of Th-232, U-238 series and K-40 decrease as the height increases. It seems that above the near-ground level there is more contribution from terrestrial radiation compared to cosmic radiation.

Radiocarbon in tree rings from a clean air region of Low Tatras in Slovakia

I. Kontuľ[1], M. Molnár[2], P. P. Povinec[1], I. Svetlik[3]

[1]Centre for Nuclear and Accelerator Technologies (CENTA), Faculty of Mathematics, Physics and Informatics, Comenius University, 842 48 Bratislava, Slovakia
[2]Institute of Nuclear Research (ATOMKI), 4026 Debrecen, Hungary
[3]Department of Radiation Dosimetry, Nuclear Physics Institute CAS, 180 86 Prague, Czech Republic
Keywords: radiocarbon, tree rings, Suess effect, bomb peak
Presenting author, e-mail: ivan.kontul@fmph.uniba.sk

Atmospheric radiocarbon in the form of $^{14}CO_2$ is absorbed by trees during photosynthesis and incorporated into the wood's structure during the growing season. This link between radiocarbon in the atmosphere and biosphere allows to study past ^{14}C levels by measuring radiocarbon concentration in the annual growth rings. Tree-ring records can therefore provide decades of reconstructed radiocarbon data.

The natural radiocarbon levels in the atmosphere and biosphere in the last 100 years were significantly affected by anthropogenic factors - increasing fossil CO_2 emission and nuclear technologies. The fossil CO_2 is radiocarbon-free and its input into the atmosphere dilutes ^{14}C concentration in the atmosphere (Suess effect). Nuclear technologies represent a new source of ^{14}C excess which has been found in the environment. The nuclear weapons tests carried out in 1950s and 1960s in the atmosphere were a significant source of anthropogenic ^{14}C, increasing its activity in the atmosphere by almost 1000 ‰ (the bomb peak).

In order to study radiocarbon levels in a clean air location with no significant local anthropogenic effects, we took tree ring samples from a tree in the vicinity of Jasná recreational area in the Low Tatras region in the central part of Slovakia. There are no significant local fossil fuel emission sources, and therefore these samples can represent regional clean air background for other tree ring series from Slovakia. The growth rings from the sampled tree cover the period from 1911 to 2016. Radiocarbon content of the sampled tree rings was measured by accelerator mass spectrometry and the results of these measurements are shown in Figure 1. The first part of the data (1911 - 1950) represents relatively stable radiocarbon levels influenced by Suess effect. The following period exhibits a sudden increase in radiocarbon levels due to atmospheric nuclear weapon tests, and the gradual decrease from the bomb peak maximum characterized by an exponential trend.

We used the data from Jasná as a reference for comparison with two modern tree ring data sets from Slovakia - Žlkovce (in the vicinity of Bohunice Nuclear Power Plant; Ješkovský et al., 2015) and Vysoká pri Morave (close to Bratislava city; Kontuľ et al., 2017). This comparison showed that radiocarbon levels at both locations are lower than clean air reference values, indicating the influence of local and regional fossil fuel emissions. In the case of Žlkovce tree rings, this shows that the Suess effect at this location is stronger than the increase due to ^{14}C releases from Bohunice Nuclear Power Plant.

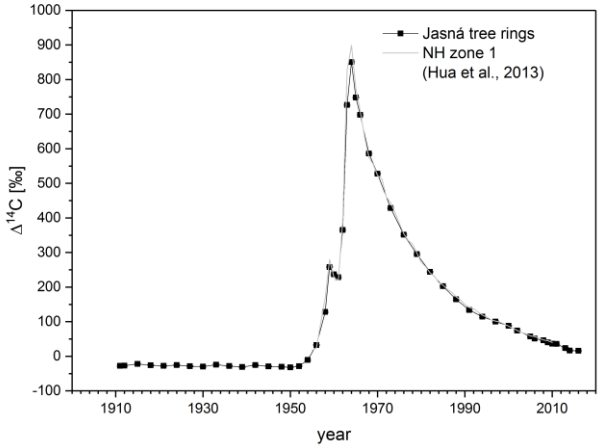

Figure 1. $\Delta^{14}C$ in tree rings (squares) from Jasná in Low Tatras mountains compared with the radiocarbon data for northern hemisphere NH zone 1 (Hua et al., 2013).

The authors acknowledge support provided by the EU Research and Development Operational Program funded by the ERDF (projects # 26240120012, 26240120026 and 26240220004), and from the International Atomic Energy Agency (project # SLR-1001).

Hua Q., Barbetti, M., Rakowski, A.Z. 2013. Atmosoheric radiocarbon for the period 1950-2010. *Radiocarbon* 55, 2059-2072.

Ješkovský, M., Povinec, P.P., Steier, P., Šivo, A., Richtáriková, M., Golser, R. 2015. Retrospective study of 14C concentration in the vicinity of NPP Jaslovské Bohunice using tree rings and the AMS technique. *Nucl. Instr. Meth. B* 361, 129-132.

Kontuľ, I., Ješkovský, M., Kaizer, J., Šivo, A., Richtáriková, M., Povinec, P.P., Čech, P., Steier, P., Golser, R. 2017. Radiocarbon concentration in tree-ring samples collected in the south-west Slovakia (1974-2013). *Appl. Rad. Isot.* 126, 58-60.

Uranium concentrations in sediment pore waters of Lake Neusiedl, Austria

Regina Krachler, Rudolf Krachler, Fadime Gülce, Gabriele Wallner

Department of Inorganic Chemistry, University of Vienna, Vienna, A-1090, Austria
Keywords: uranium, isotope activity ratios, pore water
Presenting author, e-mail: gabriele.wallner@univie.ac.at

The goal of the present investigation was to measure for the first time $^{234}U/^{238}U$ activity ratios in pore waters of Lake Neusiedl, Austria, in order to learn more about uranium in groundwaters of the Lake Neusiedl/Seewinkel region. We analyzed sediment pore waters (at 1 m depth) in the littoral zone of Lake Neusiedl. Our samples were collected from pristine sites that were not influenced by fertilized fields or vineyards. Uranium isotopes were extracted from 1.5 L of sediment pore water and measured by α-particle spectrometry. Uranium concentrations were unexpectedly high (up to 853 µg L^{-1}) especially in pore waters of salt-rich locations where halophytes thrive. $^{234}U/^{238}U$ activity ratios were between 0.91 and 1.09 for all pore water samples, irrespective of their origin from the east or west littoral zones of the lake.

Uranium and mineral salts concentrations were strongly correlated. ^{222}Rn concentrations were low (between 22 and 42 Bq L^{-1}). We conclude that brines containing both, high mineral salts concentrations (mainly sodium sulphate, sodium chloride and sodium hydrogen carbonate) and high uranium concentrations, ascend locally from deep Tertiary strata along faults.

Borylo, A., Skwarzec, B. 2014. Activity disequilibrium between ^{234}U and ^{238}U isotopes in natural environment. *J. Radioanal. Nucl. Chem.* 300 (2), 719-727.

Liesch, T., Hinrichsen, S., Goldscheider, N. 2015. Uranium in groundwater – fertilizers versus geogenic sources. *Sci.Total Environ. 536*, 981-995.

Wallner, G., Jabbar, T. 2010. Natural radionuclides in Austrian bottled mineral waters. *J. Radioanal. Nucl. Chem.* 286 (2), 329-334.

Citizen Monitoring Network in the Czech Republic – project RAMESIS

P. Kuča, J. Helebrant

Department of Emergency Preparedness, National Radiation Protection Institute, Prague, 16000 Czech Republic
Keywords: citizen monitoring, monitoring network, radiation protection, gamma doserate
Presenting author, e-mail: P. Kuča, petr.kuca@suro.cz

The paper summarizes results achieved during solution of the RAMESIS project aimed at supporting of Citizen monitoring in the Czech Republic. The main accent was given to collaboration with schools and other selected institutions and general public, resulting into establishing a national-wide Citizen Monitoring Network.
The RAMESIS project covers design and development, or selection, and implementation of equipment for fix-station based monitoring - see Fig. 1, suitable equipment for mobile monitoring, web-based RAMESIS central application for data storage, processing and presentation of measured data.

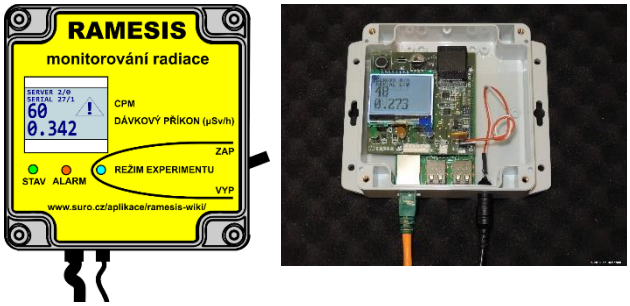

Figure 1. Equipment for fix-station based monitoring.

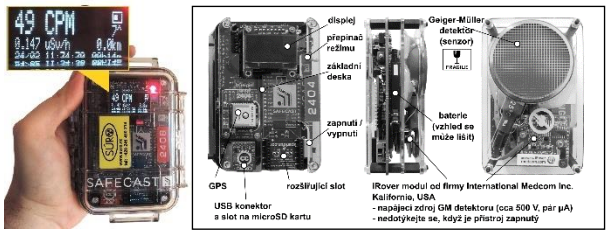

Figure 2. Equipment for mobile monitoring.

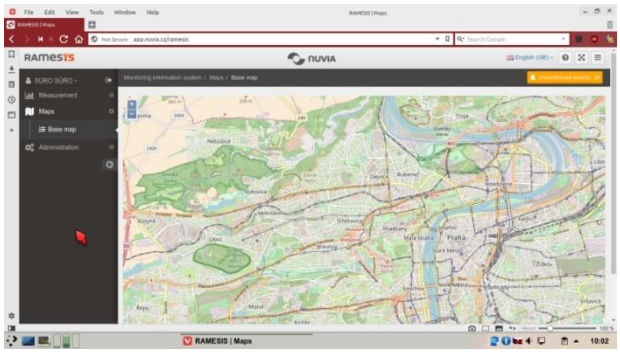

Figure 3. RAMESIS central application – example tools for monitoring results local processing and presentation on on-line or off-line map background.

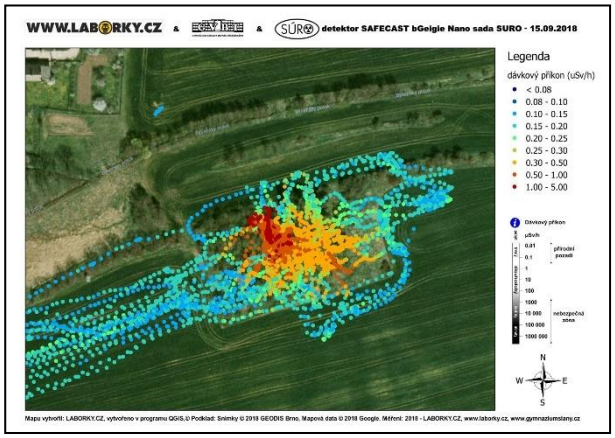

Figure 4. Local presentation of monitoring results – example.

RAMESIS-wiki web portal for providing information, guides, manuals, tools etc. for both users and public.

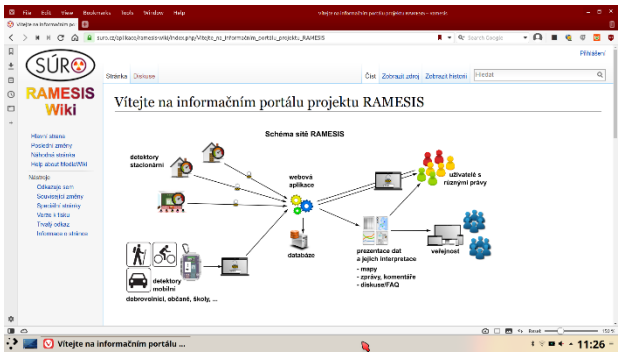

Figure 5. Web-portal RAMESIS wiki - example.

Equipment for both types of monitoring as well as access to the RAMESIS Central Application is provided to participating schools, institution and public on a free-of-charge basis on condition of sharing results of monitoring. Tools provided to public are completely based on open-source approach.
Successful fulfilment of all project tasks and its acceptance of both public and the authorities gives a good base for future progress and expansion of citizen monitoring in the Czech Republic.

This work was supported by Ministry of Interior of the Czech Republic in the frame of Security research program under grant No. VI20152019028.

^{210}Po and ^{210}Pb distribution in the south central western part of the Tropical Indian Ocean

Hyun Mi Lee*, Suk Hyun Kim, Intae Kim, Gi Hoon Hong

Korea Institute of Ocean Science and Technology, Busan ,49111, South Korea
Keywords: ^{210}Po, ^{210}Pb, Indian Ocean.
**Presenting author, e-mail: hmlee@kiost.ac.kr*

Three vertical water column profiles of dissolved (<1.2 μm) and particulate (>1.2 μm) ^{210}Po and ^{210}Pb were measured in the south central western Indian Ocean (5° S at 60° E to 67° E and 20° S 67° E) in April 2018 (Fig. 1). Our three stations are located within the tropical gyre surrounded by South Equatorial Current, Northeast Madagascar Current and South Equatorial Countercurrent. Dissolved ^{210}Po and ^{210}Pb activities were in the ranges of 6.0 - 17.9 dpm 100kg^{-1} and 8.4 - 21.5 dpm 100kg^{-1}, respectively. Dissolved ^{210}Po and ^{210}Pb values are rapidly decreased in the surface mixed layer (<100m) and ^{210}Po/^{210}Pb activity ratio in the dissolved phase was approximately 0.8 - 1.0 in the surface layer and 0.8 - 1.1 in the deep water (>2000m) of the St. 19 and St. 34. But the ^{210}Po/^{210}Pb activity ratio in the deep water was 1.2 - 1.8 at St. 13 probably due to the elevated decomposition of organic matter in the oxygen deficient deep waters. Particulate ^{210}Po and ^{210}Pb to total ^{210}Po and ^{210}Pb account for about 7 to 29 % for ^{210}Po and about 3 to 17 % for ^{210}Pb with lower values in the surface and higher values near the bottom in the south central western Indian Ocean. The earlier GEOSECS in 1978 sampled thoroughly the eastern and western and southern parts of the Indian Ocean except the tropical gyre. We attempted to plot the basin wide distribution of dissolved ^{210}Pb and the activity ratio of ^{210}Po/^{210}Pb in the surface waters of the Indian Ocean based on our measurements and the earlier GEOSECS data collected in 1978 (Fig. 2, Fig. 3). Both ^{210}Pb activities and ^{210}Po/^{210}Pb activity ratios reveal higher in the center of tropical gyre and lower at its edges and this spatial pattern is similar to those of the Pacific Ocean.

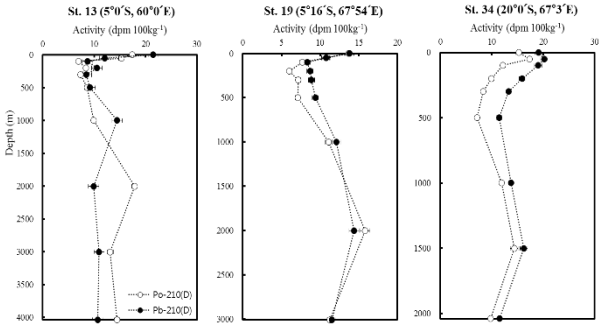

Figure 1. Vertical distributions of dissolved ^{210}Po and ^{210}Pb in the south central western Indian Ocean (April 2018).

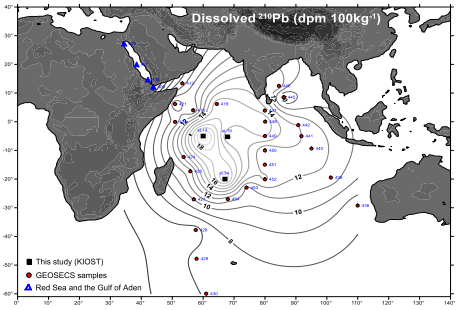

Figure 2. The distribution of dissolved ^{210}Pb activity (dpm 100kg^{-1}) in the surface of the Indian Ocean.

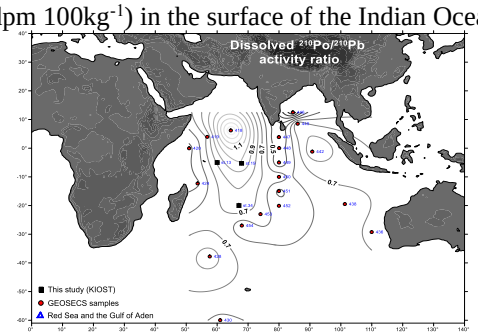

Figure 3. The distribution of dissolved ^{210}Po/^{210}Pb activity ratio in the surface of the Indian Ocean.

This work was supported by the Korea Institute of Ocean Science & Technology (PE99712).

Y. Chung, R. Finkel. 1988. ^{210}Po in the western Indian Ocean: distributions, disequilibria and partitioning between the dissolved and particulate phases. *Earth and Planetary Science Letters*. 88, 232-240.

J.K. Cochran, M.P. Bacon, S. Krishnaswami, K.K. Turekian. 1983. ^{210}Po and ^{210} Pb distributions in the central and eastern Indian Ocean. *Earth and Planetary Science Letters*. 65, 433-452.

Y. Chung, R. Finkel. 1987. ^{210}Pb in the western Indian Ocean: distribution, disequilibrium and partitioning between dissolved and particulate phases. *Earth and Planetary Science Letters*.85, 28-40.

Y. Nozaki, J. Thomson, K. K. Turekian. 1976. The distribution of ^{210}Pb and ^{210}Po in the surface waters of the Pacific Ocean. *Earth and Planetary Science Letters*.32, 304-312.

Inspection and radiation dose evaluation results of Radon bed mattress in Taiwan

M.-H. Lin, Y.-H. Lu, P.-J. Huang

Institute of Nuclear Energy Research, Atomic Energy Council, Taoyuan, 32546, Taiwan
Keywords: Radon, mattress, radiation dose
Presenting author e-mail: mhlin@iner.gov.tw

Introduction

In addition to smoking, radon is stipulated as the second leading cause of lung cancer by the World Health Organization (WHO, 2009). In May 2018, South Korea discovered that the mattress produced by a manufacturer added monazite powder containing natural radioactive substances. The thoron formed by the decay of the thorium contained in the monazite causes the radiation dose above the dose limit of 1 mSv/year for the public in South Korea. In August 2018, the competent authority of Atomic Energy Council (AEC) in Taiwan conducted an audit of the radiation content of commercial mattresses which may contained monazite powder.

Method

The concentration of radon (included thoron) was determined by using a radon meter (RAD 7) and the internal radiation dose resulted from the progenies of radon was evaluated by using the model reported in ICRP Publication 115 (ICRP 115, 2010).

Results and discussion

Among them, the sample with the highest internal dose evaluation results was further tested for the content of radon at different heights above the mattress and air conditioning environments. The measurement condition of 2 cm above the surface is to assume that a user is lying face down and breathing, while the 10 cm is to assume that a user is lying on their back and breathing. In the 2 cm (face down) situation, we found out that when window and air conditioning both being off, the internal dose was 78.39 mSv/yr. Then air conditioning being on, then the internal dose was down to 13.10 mSv/yr, decreased 83%. Then if open the window, the internal dose was down to 4.83 mSv/yr, decreased 94%. And opening window is more effective than using air conditioning because of the wind disturbance.

In the case where the window is closed and no air conditioning, the measured concentration of thoron at a distance of 10 cm from the surface of the mattress was about 5 times lower than that measured at a distance of 2 cm from the surface of the mattress. The concentration decrease of thoron gas with increasing height from the surface of the mattress was mainly due to the short half-life (55.6 second) of the thoron gas.

In this study, by the end of June 2019, a total of 48 mattresses were tested for the content of radon and 18 of which exceeded the dose limit (1 mSv/year) for the public in Taiwan.

It was also found that, except for one specific mattress which the monazite powder was embedded in the inner layer of the mattress to shield the emission of the beta/gamma rays, the concentration of thoron measured from the other mattresses was linear with the surface radiation dose rates measured by the surface contamination monitor, as shown in Figure 1. The above findings have been found to be useful for rapid screening of the concentration of thoron gas from the mattresses which were contained monazite powder.

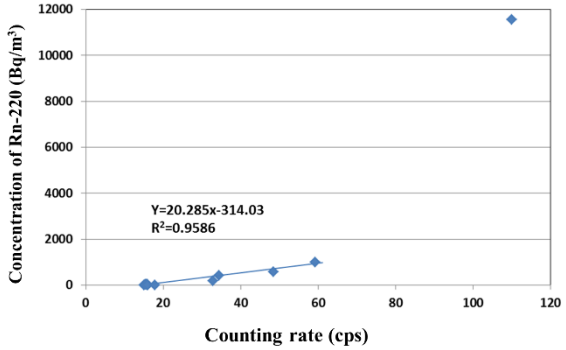

Figure 1. Conc. of Rn-220 versus surface counting rate.

Conclusions

From the result of radon concentration versus different airflow conditions, the concentration decrease of thoron gas with increasing height from the surface of the mattress was mainly due to the short half-life (55.6 seconds) of the thoron gas. And radon concentration was influenced by airflows, opening windows was better than using air conditioning.

In our study, we find the linear correlation between the surface counting rate and the concentration of Rn-220 for general mattress, the CoMo 170 is useful for rapid-scanning the monazite powder contained mattress.

WHO, 2009. In: Zeeb, H., Shannoun, F. (Eds.), Handbook on Indoor Radon.

ICRP 115, 2010, Lung Cancer Risk from Radon and Progeny and Statement on Radon. ICRP Publication 115, Ann. ICRP 40(1).

Potential radiological impact of the phosphate industry in South Africa on the public and the environment

I. Louw[1]

[1]Analytical and Calibration Services, South African Nuclear Energy Corporation, Pretoria, 0001, South Africa
Keywords: Phosphate industry, environmental monitoring, dose
Presenting author e-mail: immanda.louw@necsa.co.za

Phosphate rock is mined on a large scale as a source material for fertilizers and other phosphorous containing products, such as phosphoric acid and gypsum. The potential problem of high concentrations of natural occurring radionuclides in the phosphate industry has been recognized for many years (Wymer, 2007). The industry is responsible for the production of millions of tons of phosphogypsum waste, which is usually stockpiled and might impact the surrounding environment.

Although many studies have been conducted on phosphogypsum and the phosphate industry worldwide, limited information is available for South African products. The presented study aims to assess the natural radioactivity concentrations in raw and waste sub-products from phosphate mining and fertilizer production in South Africa.

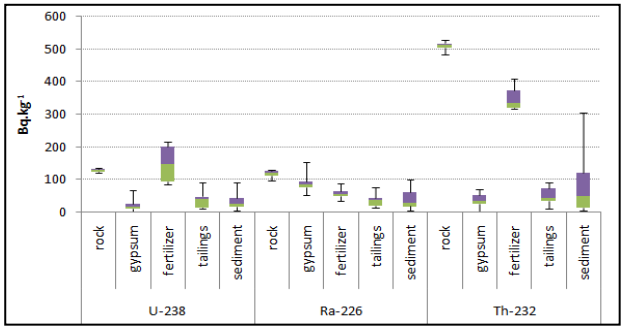

Figure 1. Activity concentrations for solids from the phosphate industry (Bq.kg^{-1}).

Activity concentrations of ^{238}U, ^{226}Ra and ^{232}Th in phosphate rock, fertilizer, phosphogypsum, tailings and sediment (Figure 1) were found to be similar to values reported in previous studies conducted in SA (Van der Westhuizen, 2007). The concentrations in all solids were less than the 1000 Bq.kg^{-1} exclusion value proposed internationally for regulation of NORM.

The activities of the industry may lead to enhanced levels of natural occurring radioactivity in the environment. A preliminary risk assessment of environmental contamination resulting from the activities of a phosphate fertilizer plant in South Africa was performed, evaluating the dose to both humans and biota. The ERICA tool was used to predict radiation dose rates and associated risk to selected reference organisms in the aquatic ecosystem using default parameter settings.

Activity concentrations in water from the environment around the phosphate mining industry were low and comparable to background values. Concentrations similar to background were measured in soil from the area, whereas some sediment samples showed enhanced concentrations of Th-series nuclides.

Studies from literature have shown that discharge of phosphogypsum and effluent waste of phosphate fertilizer plants into water may result in significantly elevated levels of radioactivity in seawater, sediments and biota and the practice of discharging was therefore discontinued in Europe. In many other countries (including SA) effluent is still discharged to water bodies (IAEA, 2013). Although significantly elevated levels were not observed in the results presented here, further environmental monitoring in the vicinity of the discharge point is encouraged.

The results suggested that members of the public were unlikely to receive any significant dose from the use of phosphate rocks and fertilizers. However, the high concentrations measured in some of the products and environmental media confirmed the need for continuous control and monitoring of the industry, especially where by-products such as phosphogypsum are utilized in agriculture or as building material.

International Atomic Energy Agency, IAEA (2013). *Radiation protection and management of NORM residues in the Phosphate industry.* Safety Reports Series No. 78, IAEA, Vienna, Austria.

Van der Westhuizen, A.J. (2007). Public exposure from mines operating and igneous ore body. *Proceedings of the fifth international symposium on naturally occurring radioactive material (NORM V),* Seville, Spain, 19-22 March 2007. IAEA publication 1326.

Wymer, D. (2007). Managing exposure to NORM. *Proceedings of the fifth international symposium on naturally occurring radioactive material (NORM V),* Seville, Spain, 19-22 March 2007. IAEA publication 1326.

Plutonium isotopes in Baltic Sea sediments

G. Lujanienė[1], B. Šilobritienė[2], D. Tracevičienė[1], S. Šemčuk[1], V. Stirbys[3], V. Romanenko[1], G. Garnaga-Budrė[4]

[1]Department of Environmental Research, SRI Center for Physical Sciences and Technology, Vilnius, Savanorių pr. 231, LT-02300, Lithuania
[2]Ministry of Environment, A. Jakšto g. 4, LT-01105 Vilnius, Lithuania
[3]Marine Research Institute, Klaipėda University, Herkaus Manto str. 84, LT-92294 Klaipėda, Lithuania
[4]Environmental protection agency, A. Juozapavičiaus g. 9, LT-09311Vilnius, Lithuania
Keywords: Pu isotopes, sediments, Baltic Sea.
Presenting author, e-mail: galina.lujaniene@ftmc.lt

The most significant sources of anthropogenic radioactivity in the Baltic Sea are the global fallout after the nuclear weapon tests and the Chernobyl NPP accident in 1986. A large number of nuclear tests resulted in the globally distribution of plutonium isotopes (^{239}Pu – 6.52 PBq, ^{240}Pu – 5.35 PBq, ^{241}Pu – 142 PBq) worldwide while during the Chernobyl NPP disaster 6.1 PBq of Pu isotopes were introduced into environment. Satellite accident (SNAP-9A) over the South Pacific in 1964 released ~ 0.6 PBq of ^{238}Pu into the atmosphere. The amount of Pu isotopes introduced into the Baltic Sea after the nuclear weapon tests was estimated at about 16-19 TBq (HELCOM 1995) whereas the total Pu derived from the Chernobyl NPP releases was found to be as less than 10% (Holm, 1995). According to different researchers, another important source of ^{238}Pu and ^{239,240}Pu the Baltic Sea was river runoff (Bergström & Carlsson, 1994; Skwarzec et al., 2011).

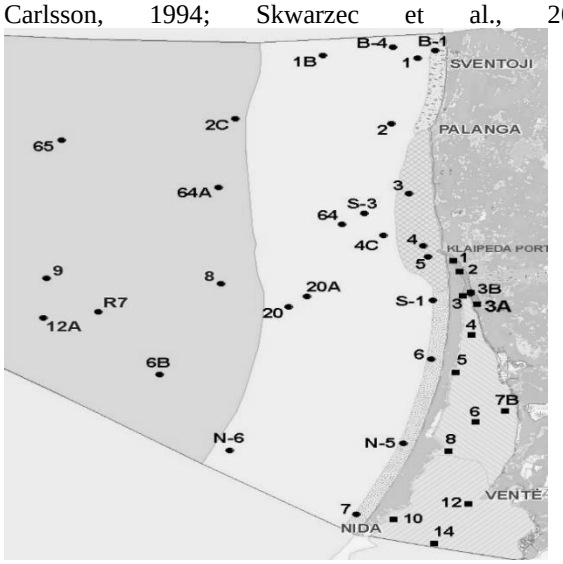

Figure 1. Sampling locations in the Curonian Lagoon and the Baltic Sea.

In addition, measurements of Pu isotopes in the waters of Polish rivers showed that the Vistula and the Odra, and as to a lesser extent, the Pomeranian Rivers are the most important sources of ^{241}Pu isotopes in the southern Baltic Sea with an annual contribution of 2,418 MBq (Strumińska-Parulska & Skwarzec, 2013).

To assess the contribution of various sources, Pu isotopes were measured on sediments samples collected in the Lithuanian zone of the Baltic Sea (Figure 1) in the frame of the state monitoring and various projects in 1997-2016.

Plutonium from sediments was first separated by the TOPO/cyclohexane extraction and then purified using UTEVA, TRU and TEVA resins (100 – 150 μm). ^{241}Pu was determined indirectly using alpha spectrometry by measuring of ^{241}Am in-growth. Pu isotopes were re-dissolved from α-counting samples and ^{241}Am was separated using extraction chromatography. The ^{242}Pu and ^{243}Am sources were used as yield tracer during the separation procedure. Accuracy and precision of the analyses were tested using reference materials and information from inter-comparison exercises.

The highest activity concentrations of ^{239,240}Pu and ^{241}Pu were found in samples taken in the Baltic Sea in 2001 at sampling stations 9 and 12A, as well as in samples of suspended particles up to 112 Bq/kg. ^{241}Pu/^{239,240}Pu activity and ^{240}Pu/^{239}Pu atom ratios up to 26 and 0.34, respectively, indicated the presence of the Chernobyl derived hot particles in the samples.

Average ^{239,240}Pu activity concentrations in 2011–2014 ranged from 0.030±0.002 Bq/kg to 3.03±0.19 Bq/kg in the Baltic Sea, whereas in the Curonian Lagoon Pu activities varied from 0.040±0.003 Bq/kg to 1.35±0.09 Bq/kg. The lowest and highest values were measured in the surface sediments of the Baltic Sea at the stations 1B and R7, respectively. The higher ^{238}Pu/^{239,240}Pu and ^{240}Pu/^{239}Pu ratios were found in sediments collected near the coast in the Baltic Sea, in the Curonian Lagoon (e.g., CL10). The Pu isotope ratios were rather low at the open sea sampling stations (e.g., N-6, 64, 64A1 and ChS2) indicating low or no contribution of the Chernobyl-derived plutonium.

HELCOM. 1995. Radioactivity in the Baltic Sea 1984 1991. *Baltic Sea Environment Proceedings*. 61, Helsinki Commission, Helsinki, Finland.

Holm, E., 1995. Plutonium in the Baltic Sea. *Appl. Radiat. Isot.* 46, 1225–1229.

Bergström, St., Carlsson, B. 1994. River runoff to the Baltic Sea – 1950-1990. *Ambio* 23, 280-287.

Skwarzec, B., Jahnz-Bielawska, A., Struminska-Parulska, D.. 2011. The inflow of ^{238}Pu and ^{239,240}Pu from the Vistula River catchment area to the Baltic Sea. *J. Environ. Radioact.* 102, 728–734.

Strumińska-Parulska, D.I., Skwarzec B. 2013. ^{241}Pu in the biggest Polish rivers. *J. Radioanal. Nucl. Chem.* 298, 693-1703.

Rapid analytical method of radionuclide impurities in 99Tc material for quality control

Maoyi Luo[1, 2], Ji Hu[3], Shan Xing[1], Yang Wu[1], Xiongxin Dai[1, 2]

[1]China Institute for Radiation Protection, Taiyuan, 030000, China
[2]Collaborative Innovation Center of Radiation Medicine of Jiangsu Higher Education Institutions, Suzhou, China
[3]Atomic High Technology Co., Ltd, Beijing, China
Keywords: Radionuclide impurity, ^{99}Tc, actinides, rapid method
Presenting author, e-mail: luomaoyi414@gmail.com

With the development of diagnosis and therapy nuclear medical, more and more attention has been paid to the radiopharmaceuticals purity in using radionuclide drug. ^{99}Tc is one of the most important radionuclides used in treatment of autoimmune and bone-destructive diseases. This work aims to develop a rapid analytical method for sequential determination of possible radionuclide impurities including α emitters and β emitters nuclides in ^{99}Tc raw-material. The sequential extraction chromatographic method was developed for simultaneous separation of ^{241}Pu, ^{238}Pu, $^{239+240}$Pu, ^{237}Np, ^{241}Am and $^{243+244}$Cm isotopes and rare earth nuclides (Figure 1). The minimum detectable activity for this method is much lower than the activity concentration limit calculated by GenMOD dosimetry software. A series of ^{99}Tc sample spiked with known quantities of ^{238}Pu, ^{239}Pu, ^{241}Pu, ^{237}Np, ^{241}Am, ^{244}Cm as well as ^{147}Pm in range of 5~7.6×10^4 Bq ^{99}Tc/g were prepared and analysed for method evaluation. The chemical recoveries of all nuclides for the whole procedure is about 80~112%, and the decontamination factor (DF) of ^{99}Tc for β emitters nuclides in the whole procedure is more than 1.5×10^6. The measured results agreed well with the expected values, and the correlation coefficient (r^2) is greater than 0.97. The relative standard deviation of the method is estimated to less than 12%, and the results of same six $K^{99}TcO_4$ raw material samples show good reproducibility for all analytes. These results show that this method would meet the requirement of the quality control according to the limitation of the china pharmacopoeia.

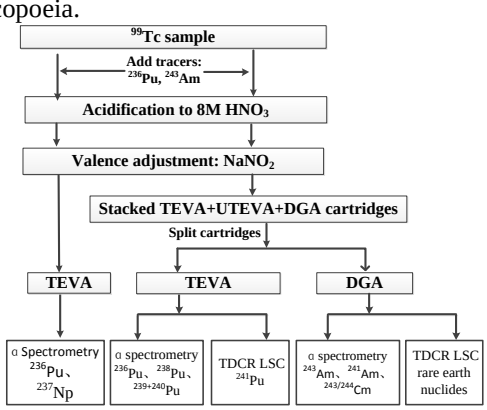

Figure 1. Flow diagram of the sample preparation method for ^{90}Sr/^{90}Y, Pu, Np, Am, Cm and rare earth nuclides in ^{99}Tc sample.

This work was supported by the National Natural Science Foundation of China (No. 11605206 and 11675150), the Ministry of Science and Technology of China (No. 2015FY110800).

A study on relation between the air gamma dose rate increase and radon in the case of rainfall

S. Maeng[1], S.Y. Han[1], S.J. Park[1,] S.Y. Lim[1], S.H. Lee[1, 2,*]

[1] School of Architectural, Civil, Environmental, and Energy Engineering, Kyungpook Nat'l Univ., Daegu, 41566, Korea
[2] Radiation Science Research Institute, Kyungpook Nat'l Univ., Daegu, 41566, Korea
Keywords: Gamma dose rate, Precipitation, Radon
Presenting author (S.J. Park), e-mail: hiyoiris@naver.com

Reflecting the elevated national interest in radiation safety, Korea has established an Integrated Environ-mental Radiation Monitoring Network (IERNet), and has installed about 170 high pressure ion chambers to monitor the air gamma dose rates. A few researchers noticed that the gamma dose rate of these ion chambers increased temporarily during rainfall. In order to explain the increase in the gamma dose rate during rainfall in relation to natural radionuclide radon, 17 cases of rainfall in Daegu area were analyzed.

The air gamma dose rate and precipitation were obtained from each institution. The linear relationship was investigated by fitting using open source data, the gamma dose rate and precipitation. The measurements of 3" x 3" NaI(Tl) gamma spectroscopy at 1 m above ground was conducted 7 times and soil radon exhalation rates were measured using RAD7 radon detector and its surface chamber 13 times for in-depth analysis. NaI(Tl) gamma spectral analysis showed that the net counting rate of ^{214}Bi (0.609 MeV) at the time of rainfall increased to 2.9 times that before rainfall.

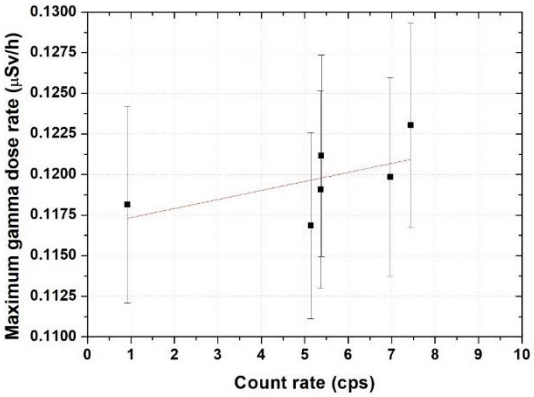

Figure 1. The maximum air gamma dose rate and ^{214}Bi count rates.

The results of RAD7 radon measurements with a surface emission chamber showed that the concentration of radon in the chamber increased again at the time of rainfall and reached a new saturation at higher concentrations. From this, it was possible to deduce the increase of the release rate of soil radon, but the linearity between the integral value of radon and precipitation did not show up.

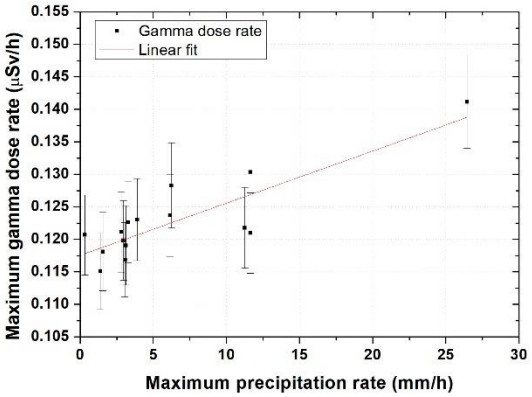

Figure 2. The maximum precipitation rate and the maximum gamma dose rate at rainfall.

The relationship between precipitation and gamma dose rate showed a strong linear relationship between instantaneous maximum precipitation rates and gamma dose rate increases: correlation coefficient: 0.666.

In conclusion, the increase in the gamma dose rate of high pressure ion chamber during rainfall is closely related to the precipitation, and the NaI(Tl) spectrum analysis confirms an increase in the net count rate of the radon progeny (^{214}Bi). Future research on NaI spectra will be conducted to investigate the change in peak net counts of radon and its progeny radionuclides as a function of time.

This work was supported by K-CLOUD project "Measurement and analysis of radon exhalation rates from soil", KOREA HYDRO & NUCLEAR POWER CO., LTD (KCLOUD project 2017-Tech-8).

J.F. Mercier, B.L. Tracy. et. al., 2009, Increased environmental gamma ray dose rate during precipitation: a strong correlation with contributing air mass, *Journal of Environmental Radioactivity*, 100, 527-533.

Nobuyoshi Takeuchi and Akira Katase, 1982, Rainou-Washout model for variation of environmental gamma ray intensity by precipitation, *Journal of nuclear Science and Technology*, 15(5), 393-409.

AMS of ^{90}Sr at the sub-fg-level using laser photodetachment at VERA

Oscar Marchhart[1], Martin Martschini[1], Maki Honda[1], Dag Hanstorp[2], Johannes Lachner[1], Haimei Liang[2], Alfred Priller[1], Peter Steier[1], Alexander Wieser[1], Robin Golser[1]

[1] Faculty of Physics, University of Vienna, 1090 Vienna, Austria
[2] Department of Physics, University of Gothenburg, SE-41296 Gothenburg, Sweden
Keywords: ^{90}Sr, AMS, Laser Photodetachment, ILIAMS
Oscar Marchhart, e-mail: a01263930@unet.univie.ac.at

The fission product ^{90}Sr is one the fragments produced with high yield (≈4%) in the nuclear fuel cycle or in nuclear weapon tests. With a half-life of $T_{1/2}$=28.90 years its incorporation can contribute a relevant dose within a human's lifetime. ^{90}Sr is very mobile in the environment and due to its chemical similarities to Calcium it is easily incorporated in the bones following ingestion or inhalation. ^{90}Sr also has significant potential as an environmental tracer.

The established method to measure ^{90}Sr is decay counting, but as ^{90}Sr is a pure beta emitter this is cumbersome and time consuming. One of the main problems in mass spectrometric detection of this long lived fission product is the interference from the isobars, i.e. ^{90}Zr and ^{90}Y. In accelerator mass spectrometry (AMS) any molecular isobars are dissociated during the stripping process in the accelerator, leaving only the mentioned elemental isobars as a challenge. The problem can be overcome with the new Ion Laser InterAction Mass Spectrometry (ILIAMS) setup at the Vienna Environmental Research Accelerator (VERA). ILIAMS reaches near complete suppression of the negative isobaric ions via selective laser photodetachment, using a gas filled radiofrequency quadrupole (RFQ) ion guide and a cw-laser (Martschini et al., 2017). The technique exploits differences in the electron affinities (EA) of the isobars. Isobars with EAs smaller than the photon energy become neutralized. Additional separation can be reached through chemical reactions and collisional detachment by the buffer gas.

We report on first successful measurements of ^{90}Sr with this technique. Mixing the target material with PbF_2 and extracting SrF_3^- from the ion source gives already some elemental selectivity (Eliades et al., 2013). Using $^{90}SrF_3^-$ with a 352nm cw-laser the isobars YF_3^- and ZrF_3^- are further suppressed by a factor of 10^7. First measurements have been performed on a dilution series from the IAEA-TEL-2016-03 reference solution (Fig. 1), as well as on Zr- and Y-spiked targets to check on the suppression of the interfering isobars. The overall Sr detection efficiency is around 0.4‰ and the blank value $^{90}Sr/Sr<5x10^{-15}$.

Previous LODs of other mass spectrometric or radiometric methods are at the level of ~3 mBq (Bu et al., 2016, S.J. Tumey et al., 2009). Our blank level corresponds to a limit of detection (LOD) of 0.1 mBq or 0.02 fg which is an improvement by more than an order of magnitude.

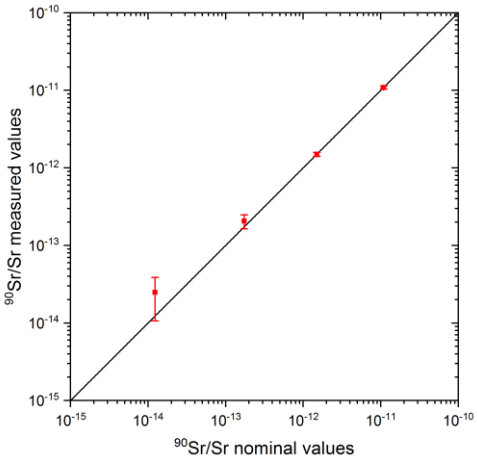

Figure 1. Results of the first dilution series for the in-house reference materials show a good agreement of the measured ^{90}Sr/Sr ratios with the nominal ratios.

J. Eliades et al. 2013, On-line ion chemistry for the AMS analysis of ^{90}Sr and ^{135,137}Cs, *Nucl. Instrum. Meth B* 294, 361-363

M. Martschini et al. 2017, Selective laser photodetachment of intense atomic and molecular negative ion beams with the ILIAS RFQ ion beam cooler, *Int. J. Mass Spect.* 415, 9-17

W. Bu et al. 2016, Mass spectrometry for the determination of fission products ^{135}Cs, ^{137}Cs and ^{90}Sr: A review of methodology and applications, *Spectrochim. Acta Part B* 119, 65-75

S.J. Tumey et al. 2009, Further development of accelerator mass spectrometry for the measurement of ^{90}Sr at Lawrence Livermore, J. Radioanal. Nucl.Chem. 282, 821-824.

Determination of low level tritium concentrations in the Czech Republic for tritium tracing applications

D. Marešová[1], E. Juranová[1,2], B. Sedlářová[1]

[1]Department of Radioecology, T. G. Masaryk Water Research Institute, public research institution, Prague 6, 160 00, Czech Republic
[2] Faculty of Science, Institute for Environmental Studies, Charles University, Prague 2, 128 01, Czech Republic
Keywords: tritium; precipitation; ground water; tracer
Presenting author, e-mail: diana.maresova@vuv.cz

Past tests of nuclear weapons in the atmosphere, nuclear energy facilities and tritium of natural origin are main sources of tritium in the environment. Thanks to its presence in environment and its favourable properties, tritium is used as a radiotracer. Since stopping of atmospheric nuclear tests, tritium in precipitation has been decreasing towards natural levels below 1 Bq/L and precise analyses of low level tritium activities are necessary.

TGM WRI, p.r.i. has been involved in research of very low level tritium volume activities in water for a substantial amount of time. This contribution summarizes the results of tritium monitoring in precipitation and ground water in the Czech Republic. The samples have been pre-treated by electrolytic enrichment from 2010.

Tritium volume activity was monitored in precipitation at sites not influenced by discharges from a nuclear plant. The frequency of sampling was once per month. Precipitation samples were accumulated monthly. The samples were distilled. The measurements were carried out with low background liquid scintillation spectrometer Quantulus 1220 according EN ISO 9698. The relative efficiency was about 26%. A mixture of 8 mL of the sample and 12 mL of ULTIMA GOLD LLT scintillator was measured for 800 min (for samples without electrolytic enrichment until 2010) and for 300 min (for electrolytically enriched samples). The minimum detectable activity at a significance level of 95% was 1.0 and 0.1 Bq/L respectively. Certified material (Czech Metrology Institute) was used for calibration. The initial sample volume was 500 mL for electrolytic enrichment. A sample with added of Na_2O_2 was electrolysed to a volume of 20 – 25 mL. Subsequently, the sample was neutralized with $PbCl_2$ and distilled. A set for electrolytic enrichment allows the simultaneous adjustment of 20 samples; the total elapsed flow is 1400 Ah.

The annual mean concentrations in surface water and precipitation decreased over time all over world since the Nuclear Test Ban Treaty in 1963. This trend of decrease was observed also in the Czech Republic in 1990s. We have not observed any trend in precipitation any more since 2002.

The characteristic seasonality of tritium in precipitation was observed (Fig. 1). Consequently, the weighted averages of tritium were processed for all seasons. The determined average values were maximal for spring and summer, and minimal for winter. This seasonal variation can be assigned to the Spring Leak phenomenon, which leads to tritium release from stratosphere into troposphere due to heating of continents with resulting rise of the tropopause in spring (Zahn et al., 1998).

Monitoring of tritium in boreholes in the surrounding of nuclear power plants is mentioned for example of tritium applications. In the NPPs there is tritium monitoring used for indication if radioactive leakage. Methods with MDA□2 Bq/l are usually used. Some boreholes in the surrounding of Nuclear Power Plant Temelín are monitored with better sensitivity. Results from the period 2015 – 2017 are presented (Fig. 2). It is obvious that tritium activity corresponds to today's tritium background level into the depth 50 m. At depth grater than 50 m there is tritium activity lower which means longer residence time of water. We can conclude that the boreholes are not effected by the nuclear power plant.

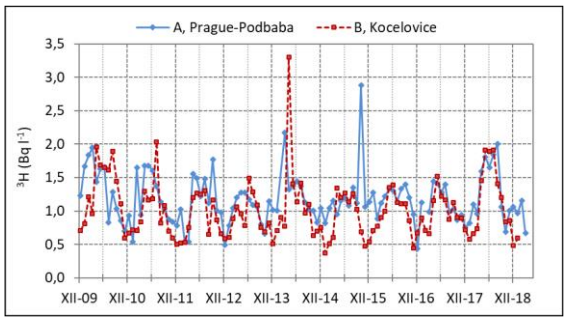

Figure 1. Tritium concentrations in precipitation from selected monitoring sites in the period 2010-2018.

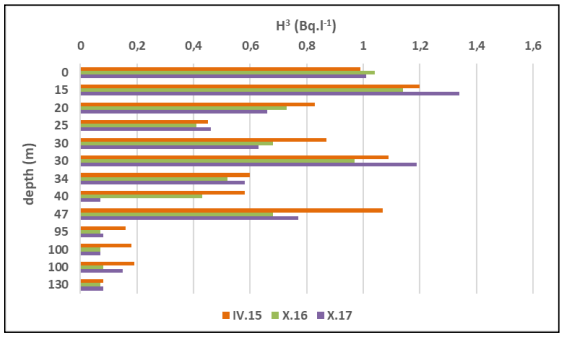

Figure 2. Tritium in boreholes in the surrounding of Nuclear Power Plant Temelín.

Zahn, A., Barth V., Pfeilsticker, K., Platt, U. 1998. Deuterium, oxygen-18, and tritium as a tracers for water vapour transport in the lower stratosphere and tropopause region. *J Atmos Chem* 30(1):25-47.

Cl-36 records in Greenland SE dome ice core

H. Matsuzaki[1], M. Toya[1], K. Horiuchi[2], Y. Iizuka[3], A.T. Bautista[4], L. Wang[1], W. Xiao[1]

[1]Micro Analysis Laboratory, Tandem accelerator, University Museum, University of Tokyo, Tokyo, 113-0033, Japan
[2]Faculy of Science and Technology, Hirosaki University, Hirosaki, 036-8560, Japan
[3]Institute of Low Temperature Science, Hokkaido University, Sapporo, 060-0819, Japan
[4]Department of Science and Technology, Philippine Nuclear Research Institute, 1101, Quezon City, Philippines
Keywords: Cl-36, I-129, Accelerator Mass Spectrometry, Greenland ice core, Nuclear weapons testing
Presenting author, e-mail: hmatsu@um.u-tokyo.ac.jp

Cl-36 (Half life: 3.01E+05 yr) is long lived radio isotope which is produced by the neutron activation of Cl-35. In 1950's and 1960's, vast amount of Cl-36 was produced due to a number of atmospheric nuclear bomb testing. Cl-36 as well as other artificially produced nuclides like I-129, falls with precipitation onto the earth surface and recorded in various natural archives (tree ring, coral, sediments, so on), which in turn provides valuable information of the environmental dynamics of not only the nuclide itself but also atmosphere and seawater. Among various archives ice core is an ideal one which records the time course profile of nuclides most clearly.

In contrast to I-129, Cl-36 is merely released from spent fuel reprocessing plant. The time course profile of Cl-36 recorded in ice core will be totally different from I-129. The objective of this study is to clarify the contrast of time course variation of Cl-36 and I-129 recorded in the same ice core.

The ice core sample used in this work was taken from SE dome located in the southeast Greenland (7.18°N, 36.37°W, 3170 m a.s.l.) in 2015 (Iizuka 2016). It covers from year 2015 to 1955 with high time resolution (Furukawa 2017). Major elemental concentration and oxygen isotope data were already analyzed in details (Iizuka et al 2018). We obtained samples corresponding from 2007 to 1956. We divided into two for each numbering sample, one is for I-129 analysis and the other for Cl-36. I-129 profile from 1976 to 1956 was already analyzed by one of the authors (Bautista 2017). The profile of I-129 from 2007 to 1977 will be presented in this conference by A.T. Bautista VII. This study will present Cl-36 from 1965 to 1956 just covering the "bomb peak". Cl-36 profile for Greenland ice core was previously once analyzed for Dye 3 station (Synal 1990). However it is first time that Cl-36 and I-129 are analyzed from the same ice core.

From previous work of Cl-36 analysis, we estimated the Cl-36 in our samples to be 5E+04 atoms/g to 5E+05 atoms/g from 1965 to 1956. For these levels of Cl-36 concentration, only Accelerator Mass Spectrometry (AMS) can measure. Considering net sample amount (from 200g to 500g), the isotopic ratio ^{36}Cl/Cl of the AMS target (samples ready for set to ion source of the AMS system, AMS = Accelerator Mass Spectrometry) is estimated to be from 3E-13 to 3E-12 with 5mg Cl carrier. For ^{36}Cl-AMS, the most severe interference comes from isobar ^{36}S. To eliminate this, Gas Filled Magnet is used before the final detector at MALT (Micro Analysis Laboratory, Tandem accelerator), The University of Tokyo. The Sulfur reduction during the pre-treatment, especially the washing of AgCl precipitation, is also important. The AMS target is AgCl pressed into a small hole of the cathode. AgCl is known to deliquescent. It absorbs well the moisture from the atmosphere. When it absorbs moisture a severe contamination of Sulfur occurs. We tested several materials for the cathode sample holder and the way how to eliminate the moisture during the pressing. We recently greatly improved the pre-treatment including cathode press procedure, consequently the background of AMS of ^{36}Cl/Cl < 1E-14 was achieved. This performance (back ground) can serve for the determination of isotopic ratio for ice core samples of this study.

The actual ^{36}Cl-AMS measurement of ice core samples is scheduled in August, 2019 and can be reported on the conference.

Prior to the treatment for AMS, we measured the Chlorine concentration in each samples by Ion Chromatogram. It was found that the concentration of all samples were less than 50 ppb which do not affect the measurement of AMS.

Y. Iizuka, S. Matoba, T. Yamasaki, I. Oyabu, M. Kadota, and T. Aoki (2016) Glaciological and meteorological observations at the SE-Dome site, southeastern Greenland Ice Sheet, *Bulletin of Glaciological Research*, 34, 1-10.

R. Furukawa, R. Uemura, K. Fujita, J. Sjolte, K. Yoshimura, S. Matoba, Y. Iizuka (2017) Seasonal-scale dating of a shallow ice core from Greenland using oxygen isotope matching between data and simulation. *J. of Geophysical Research: Atmospheres*, 122, 10873–10887.

Y. Iizuka, R. Uemura, K. Fujita, S. Hattori, O. Seki, C. Miyamoto, T. Suzuki, N. Yoshida, H. Motoyama, S. Matoba (2018) A 60 year record of atmospheric aerosol depositions preserved in a high accumulation dome ice core, Southeast Greenland. *J. of Geophysical Research: Atmospheres*, 123, 574-589.

A.T. Bautista VII, Y. Miyake, H. Matsuzaki, Y. Iizuka, K. Horiuch (2018) High-resolution ^{129}I bomb peak profile in an ice core from SE-Dome site, Greenland, *J. of Environ. Radioactivity*, 184-185, 14-21.

H.-A. Synal, J. Beer, G. Bonani, M. Suter, W. Wolfli (1990) Atmopheric transport of bomb-produced ^{36}Cl, *Nucl. Instr. Meth. In Physics Research B52*, 483-488.

Long-term variation of ^{129}I in *Fucus* from the Swedish west coast

S. Mattsson[1], K. Aquilonius[2], J.M. López-Gutiérrez[3], V. Lerida[3] and R. Garcia-Tenorio[3]

[1]Medical Radiation Physics Malmö, Department of Translational Medicine, Lund University, Malmö, Sweden
[2]Swedish Radiation Safety Authority, Stockholm, Sweden
[3]Centro Nacional de Aceleradores, University of Sevilla, Sevilla, Spain
Keywords: Iodine-129, *Fucus*, AMS
Sören Mattsson, e-mail: soren.mattsson@med.lu.se

The water and thus also the levels of radioactive substances along the Swedish west coast are affected by influx from the North Sea and outflow from the Baltic Sea. In addition, there are run-off from land and supply via sewers and sewage treatment plants. One way to follow changes in the marine environment is to use algae as bio-indicators.

Collection of *Fucus* has from time to time been done at several locations along the Swedish west coast, but this project is concentrated on samples from one station (Särdal; 56.76 ^{o}N, 12.63^{o}E) located between Halmstad and Falkenberg. Here, some of the first analyzes of algae in Nordic coastal waters were made in 1967 (Mattsson 1984, Mattsson and Erlandsson 1991, Lindahl et al, 2003, Bernhardsson et al., 2008) and today there is a very long time series (52 years) of samples of both *Fucus serratus* and *Fucus vesiculosus* taken simultaneously. Since the middle of the 1970s, i.e. during most of the time, samples have been taken every second month and the collections continue.

In coastal areas, marine aerosols are generated at the water–atmosphere interface. It is of interest to investigate whether also radionuclides in the water are spread in this way. The aerosols move inland, but it is not known how far. Therefore, samples of the lichen *Xanthoria parietina* have been collected at various distances from the water-front in 2017 and 2018 to investigate possible contributions in the coastal area beyond what is found at a great distance from the coast.

The long-lived ($T_{1/2}$ = 15.7 × 10^6 year) beta-emitting radionuclide, ^{129}I is produced both naturally and as a result of human activities.

The main releases of ^{129}I to the marine environment are liquid discharges from the two main nuclear fuel reprocessing plants (NFRP) in Europe: Sellafield (United Kingdom) and La Hague (France), of which La Hague has been the dominating one after 1985. ^{129}I remains dissolved in seawater for a long time. The ^{129}I concentration in brown algae (dry) in relation to that in water has been estimated to 10 000 (Gomez-Guzmán et al., 2011 and references therein).

The sample preparation method used for algae and lichen was based on the method published by Schmidt et al. (1998). ^{129}I was measured by Accelerator Mass Spectrometry at CNA-University of Seville (López-Gutiérrez et al., 2000).

The results for the ^{129}I activity concentration in *Fucus* and *Xanthoria parietina* from Särdal analyzed up to now will be presented. For the *Fucus* samples, the plan is to finally cover the entire time period from 1967 and onwards.

The concentration in winter is higher than during summer. This observation is of importance for careful studies of the time variation of ^{129}I. In general, there was a clear trend of increasing concentrations since 2012 up to 2016/2017. This will be discussed in relation to reported releases.

The work was partly funded by the Swedish Radiation Safety Authority (grant SSM2018-905).

Mattsson, S. 1984. ^{137}Cs in algae from the Swedish west coast, 1967-1983. *In: A. Kaul et al. (Eds.): Radiation-risk-protection, Fachverband für Strahlenschutz eV, Jülich, BRD*, pp 901-904.

Mattsson, S., Erlandsson, B. 1991. Variations of the Cs-137 levels in *Fucus* from the Swedish westcoast during a 25-year period. *In: The Chernobyl fallout in Sweden. Ed by L. Moberg. The Swedish Radiation Protection Institute, Stockholm, Sweden,* pp. 143-149.

Bernhardsson, C., Erlandsson, B., Rääf, C.L., Mattsson, S. 2008. Variations in the ^{137}Cs concentration in surface coastal water at the Swedish west coast during 40 years as indicated by *Fucus. In: Strand, P., Brown, J., Jolle, T. (Eds.) Proceedings from the International Conference on Radioecology and Environmental Radioactivity, 15-20 June 2008, Bergen, Norway, (Part 2),* pp 91-94.

Gómez-Guzmán J.M., Holm E., López-Gutiérrez J.M., Niagolova N., Pinto-Gómez A.R. 2011. ^{129}I in macroalgae (*Fucus vesiculosus*) from the Swedish coast. *In: Environmental radiochemical analysis (Ed. by P Warwick), Royal Society of Chemistry Publishing*, pp 95-108.

Lindahl, P., Ellmark, C., Gäfvert, T., Mattsson, S., Roos, P., Holm E., Erlandsson, B. 2003. Long-term study of ^{99}Tc in the marine environment on the Swedish west coast. *J. Environ. Radioactivity*, 67, 145-156.

Schmidt, A., Schnabel, Ch., Handl, J., Jakob, D., Michel, R., Synal, H.-A., Lopez, J.M., Suter, M. 1998. On the analysis of iodine-129 and iodine-127 in environmental materials by accelerator mass spectrometry and ion chromatography, *Sc. Total Env.* 223(2–3), 131-156.

López-Gutiérrez, J.M., García-León, M. García-Tenorio, R., Schnabel, Ch., Suter, M., Synal, H.-A., Szidat, S. 2000.^{129}I/^{127}I ratios and ^{129}I concentrations in a recent sea sediment core and in rainwater from Sevilla (Spain) by AMS, *Nucl. Instr. Meth. B,* 172, 574-578.

Validation of measurement comparability for ^{134}Cs and ^{137}Cs in brown rice sample using interlaboratory comparison

T. Miura[1], M. Hachinohe[2], A. Yunoki[1], S. Hamamatsu[2], Y. Unno[1], R. Furukawa[1], H. Itadzu[3], M. Mizui[3]

[1]National Metrology Institute of Japan, AIST, Tsukuba, 305-8563, Japan
[2]Food Research Institute, NARO, Tsukuba, 305-8517, Japan
[3]SEIKO EG &G Co, Ltd, Chiba, 261-8507, Japan
Keywords: certified reference material, ^{134}Cs, ^{137}Cs, brown rice, interlaboratory comparison
Tsutomu Miura, e-mail: t.miura@aist.go.jp

It is well known that massive amount of radioactive nuclides were spread over eastern Japan resulted from the accident at the Fukushima Daiichi nuclear power plant caused by the earthquake on 11 March 2011. At 1 April 2012, 1 year after the accident, The Ministry of Health, Labor and welfare of Japan established the standard limit of radioactivity in foodstuff. The standard limit for radioactive cesium (^{134}Cs and ^{137}Cs) in general food was announced as 100 Bq kg^{-1}. This requires that a number of foodstuff samples be analyzed against the criteria. Also, it is necessary to control the quality of radioactivity measurement. The application of reference material and participation of interlaboratory comparison in measurement laboratories is useful to establish an inspection system in food market. The aim of this study is validation of measurement quality about measurement laboratory for ^{134}Cs and ^{137}Cs in food. For this purpose, the brown rice grains that contain ^{134}Cs and ^{137}Cs were mixed and homogenized. The certified reference material (CRM) was developed using the homogenized brown rice grain, followed by interlaboratory comparison for Ge semiconductor detector (Ge detector) and NaI scintillation detector (NaI detector). By CRM developing, the certified value of the CRM can be used as the reference value of that of comparisons. Furthermore, it is possible to evaluate the measurement variability of the NaI detector.

Development of NMIJ CRM 7541-b (Miura et al., 2016, Hachinohe et al., 2016) The brown rice grains (180 kg) harvested from northeast region of Japan at 2011 was mixed and homogenized manually using stainless steel scoop. After homogenization, the brown rice grain was packed in units of 81.00 g, each in a polypropylene bottle (U8 type, 300 bottles in total). The bottled samples were sterilized by exposure to 25 kGy γ ray irradiation. The homogeneity of the brown rice grain was estimated based on ISO Guide 35 from the γ ray spectra for 24 bottles recorded using calibrated Ge detector (ORTEC GEM130225). The certified values of ^{134}Cs and ^{137}Cs were determined using above γ ray spectra. The associated uncertainties of the certified values were calculated from standard uncertainties related each component. The certified values are (28.0 ± 1.6) Bq kg^{-1} for ^{134}Cs, (54.2 ± 3.0) Bq kg^{-1} for ^{137}Cs at reference date of May 1, 2013. The measurement capabilities of ^{134}Cs and ^{137}Cs have been confirmed on BIPM.RI(II)-K1 or APMP.RI(II)-S3.

Interlaboratory comparison for Ge detector: The star-type interlaboratory comparison for Ge detector was conducted for the 44 participants. The homogenized brown rice samples (1.88 kg) was packed in ten 2 L Marinelli containers for circulation. The typical measured time of participants was 10800 s.

Interlaboratory comparison of NaI scintillation counter: The star-type interlaboratory comparison for NaI detector was also conducted for 143 laboratories. The participants were used 17 types of NaI detectors. Each of the 17 types of NaI detectors had different geometrical shapes of the detector and the shield, so each NaI detector had used a dedicated measurement container. Therefore, homogenized brown rice (0.38 kg to 1.2 kg) was filled in each dedicated measurement container for each model to prepare a sample for circulation. The typical measurement times and number of repetitions of participants were 1200 s and 5 times.

The results of the comparisons are shown in Table. 1

Table 1 Summarise results of interlaboratory comparisons (Reference date: May 1, 2013.)

Detector	Nuclides	Median, Bq kg^{-1}	*NIQR*, Bq kg^{-1}	*NIQR, relative*
Ge detector	^{134}Cs	26.8	0.64	2.4 %
	^{137}Cs	53.1	1.2	2.2 %
	^{134}Cs^{+137}Cs	80.2	1.5	1.8 %
NaI detector	^{134}Cs	28.0	2.0	7.2 %
	^{137}Cs	53.6	2.6	4.8 %
	^{134}Cs^{+137}Cs	81.8	3.7	4.5 %

Both of medians are good agreement with certified values of NMIJ CRM 7541-b as reference values. The relative *NIQR* of NaI detector's comparison shows large value compared with Ge detector's one. However, the variability of NaI detector is a sufficiently acceptable range as screening use, under considering that the short measurement time and easy maintenance of NaI detector.

T. Miura, A. Yunoki, Y. Unno, S. Hamamatsu, M. Hachinohe, S. Todoriki. 2016. The development of SI traceable brown rice certified reference material for ^{134}Cs and ^{137}Cs measurement. *Radioisotopes*.65, 157-167.

M. Hachinohe, S. Todoriki, Y. Unno, T. Miura, A. Yunoki, S. Hamamatsu. 2016. Preparation of certified reference materials for radioactivity measurement using brown rice. *Radioisotopes*.65, 169-180.

Speciation of radionuclides in seawater and marine organisms

M. Monfort, B. Reeves, C. Moulin - CEA, DAM, DIF, F-91297 Arpajon, France
C. Berthomieu - CEA, DRF, Cadarache, UMR 7265 CNRS CEA Aix-Marseille University, France
C. Den Auwer, M.R. Beccia - University of Nice Sophia Antipolis, Nice Chemistry Institute
UMR CNRS 7272, 06108, Nice, France.

marguerite.monfort@cea.fr

Speciation of radionuclides is mandatory to understand their behavior in the environment such in seawater. The interaction between radionuclides and the marine compartment is therefore essential for better understanding the transfer mechanisms from the hydrosphere to the biosphere. This information allows for the evaluation of the impact on humans via interaction with biotope that is weakly documented up to now.

Two main axes, closely related, are in progress. The first one is to be able to fully characterize the chemical form of the elements of interest in the oceans and simple organism (sponges identified as hyper accumulators of several heavy metals). The second is to study how more complex animals, such a model organism, the sea urchin Paracentrotus lividus can accumulate the elements released in the oceans.

By the use of advanced spectroscopic techniques such as Time-Resolved Laser-Induced Fluorescence (TRLIF), Extended X-ray Absorption Fine Structure (EXAFS) and others (TEM, SEM, STXM, ATR-FTIR…), the speciation of actinides in seawater (SAS) such as americium (europium analogy), uranium and neptunium has been investigated. It was then possible to determine the different structures in seawater that are mainly sodium carbonato complexes such as UO2(CO3)3Ca2, NaAm(CO3)2·nH2O [1, 2]. This molecule is composed of one atom of uranium, two atoms of calcium, and three molecules of carbonates, the two latter species being naturally highly present in oceans. Then interaction with marine species such as sponges [3] as well as sea urchin have been studied in terms of localization and species.

Being less absorbed by living organism, this sodium carbonato complex shows low toxicity [4]. This information on speciation should be taken into account in safety analysis in order to decrease the conservatism used in dose assessment.

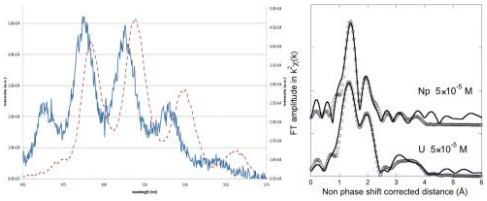

Figure 1. TRLIF and EXAFS spectra of U in seawater, UO2(CO3)3Ca2 (plain curve), UO22+ (dotted line).

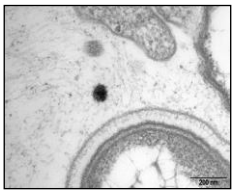

Figure 2. TEM image: Eu particle in the skeleton in containated sponge.

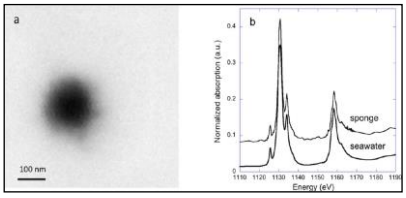

Figure 3. STXM image (a), $M_{IV,V}$ edge XAS (b).

The results we obtained on sea urchins showed that these organisms are slightly able to accumulate uranium. We also managed to quantify the uranium in the sea urchin compartments; test (shell + spikes), gonads and intestinal tract. We were able to determine that a protein, the toposome, is the main ligand of uranium inside gonads and intestinal tract.

Works are in progress concerning the behavior of other radionuclides of interest such as Cs and Co in seawater and sea urchins.

Diffusion of caesium and strontium into concrete under conditions of anaerobic fermentation of contaminated biomass

R. Možnar[1], D. Vopálka[2], J. Škrkal[3], V. Záhorová[3], M. Kajan[4]

[1]Department of Dosimetry and Application of Ionizing Radiation, Czech Technical University in Prague, Prague, 115 19, Czech Republic
[2]Department of Nuclear Chemistry, Czech Technical University in Prague, Prague, 115 19, Czech Republic
[3]National Radiation Protection Institute, Prague, 140 00, Czech Republic
[4]ENKI, o.p.s., Třeboň, 379 01, Czech Republic
Keywords: diffusion, radionuclides, concrete, biogas station
e-mail: radim.moznar@fjfi.cvut.cz

In the case of a serious accident of a nuclear power facility, extensive contamination of crops in agricultural production can be expected. An effective way to deal with the consequences of such an accident can be the fermentation of contaminated biomass in a biogas station. The advantages of this process are the gain of energy in the form of biogas, the biological stabilization of biomass and the reduction of radioactive waste volume.

However, the approach mentioned above is new and unexplored. The risks include, in particular, the exposure of the biogas station personnel and the contamination of the biogas station itself leading to subsequent decontamination costs.

The aim of this work is to quantify possible contamination of structural material of a biogas station (concrete) in such specific conditions. The experiment was designed based on numerical simulations of diffusion and is currently being realized. A numerical study and data from similar experiments (Atkinson, A. et al., 1988), (Albinsson, Y. et al., 1996) show that diffusion should be negligible in terms of radiation protection.

This work was performed within the OPVVV project of the Ministry of Education Youth and Sports (Czech Republic) No. CZ.02.1.01/0.0/0.0/16_019/0000778.

This work was supported by the project of the Ministry of interior of the Czech Republic number VI2VS/507 - Disposal of radiation-contaminated biomass after NPP accident-distribution, logistic of harvesting, exploring in biogas technology.

Atkinson, A., Nickerson, A. K. (1988). Diffusion and Sorption of Cesium, Strontium, and Iodine in Water-Saturated Cement. Nucl. Technol.; (United States). 81:1. 10.13182/NT88-A34082.

Albinsson, Y., Andersson, K., Börjesson, S., Allard, B., Diffusion of radionuclides in concrete and concrete-bentonite systems, *Journal of Contaminant Hydrology*, Volume 21, Issues 1–4, 1996, Pages 189-200, ISSN 0169-7722, https://doi.org/10.1016/0169-7722(95)00046-1.

Concentration of 7Be radionuclide in air of Algeria

M. Nadri[1], M. Alili[2]

[1]Department of Physics, ENS, Algiers, 16050, Algeria
[2]Department of Biology. ENS, Algiers, 16050, Algeria
Keywords: Rain water, Algeria, natural radionuclide ^{7}Be.
Presenting author, e-mail: nadri@ens-kouba.dz

Natural radionuclides such as Beryllium-7 (^{7}Be) is produced in the upper atmosphere by cosmic-ray spallation of nitrogen and oxygen. The rainwater samples were collected from a flat roof at Baba Hassen site Algiers, Algeria (36º 46'N, 3° 03'E) from February to- April 2012. The measurement of ^{7}Be was carried out by using a high resolution HPGe (1.8 keV at 1.33 MeV) with 20% efficiency. For this purpose, all the samples were measured using Marinelli containers, with known - specific geometry for better efficiency, which is the standard method for measuring radioactive liquid samples. (The analysis of the samples performed at the Nuclear Physics Laboratory of the Physics Department of the Aristotle University of Thessaloniki, Greece).

The results demonstrate that ^{7}Be in samples ranged between 0,34 and 3,92 Bq / L.

The rainfall heights were very low and ranged between 0,20 cm and 1,68 cm, expressing a relatively dry climate in the temperate zone. The rate (intensity) of precipitation is also important, and it is defined as the amount of rainfall per unit time (cm / hr), it has been studied and proven that the high Rain Rate (heavy rain) does not imply higher concentrations of ^{7}Be in rainwater sample.

The study of the concentrations of the radioactive isotopes in precipitation samples from the Algerian region is interesting due to the lack of data in the literature. Moreover, the obtained concentrations are in agreement with the values given in the literature, for the region of Thessaloniki, between the period 1987-1990, and UNSCEAR report 1982. (1) (2)

This work was supported by Physics Department, EcoleNormale Supérieure (ENS) de Kouba, Algiers, Algeria.

Ioannidou A., Papastefanou C. 2006. Precipitation scavenging of 7Be and 137Cs radionuclides in air. *J. of Environ. Radioactivity* 85, 121-136.

UNSCEAR 1982. Ionizing radiation: sources and biological effects. *United Nations Scientific Committee on the Effects of Atomic Radiation, UN, New York.*

Secondary cosmic radiation doses during domestic air travel in Japan measured by handy methods

K. Nakamura, M. Furukawa, Y. Shiroma, S. Nakasone, A. Ishimine

Graduate School of Engineering and Science, University of the Ryukyus, Nishihara, Okinawa 903-0213, Japan
Keywords: secondary cosmic rays, ionizing component, commercial aircraft, handy methods
Presenting author, e-mail: k198345@eve.u-ryukyu.ac.jp

The exposure due to secondary cosmic radiation during air travel is a typical case of technologically or artificially enhanced natural radiation, namely aircraft crew and passengers are subject to much higher exposure during air travel than that at ground level. In recent years, particular attention should be paid to the individual dose during air travel, because the long distance flight is going on the growth. Secondary cosmic radiations are produced by the interaction of primary cosmic radiations, mainly high-energy proton from out of the solar system, with atmospheric constituents, and can be classified into a directly ionizing plus photon component and a neutron component. In the atmosphere, absorbed dose rates for both components increase with the increase in altitude. The dose rates reach the maximum at altitude of 10-20 km where corresponds to the cruising altitude for the civilian airliner. Also, the dose rates increase with increase in geomagnetic latitude. In a word, the exposure during air travel depends on the flight path and duration. From these viewpoints, the in-flight measurement is strongly needed to estimate the exposure, but there are particularly few data in and around Japan. In this study, therefore, we tried the in-fright measurements for the domestic airliners in Japan.

Individual doses during air travel have been measured with a pocket-sized dosemeter (Aloka PDM-101) with weight of about 60 g. This PDM has sensitivity to the directly ionizing plus photon component, muon, electron, *etc*. The value of accumulated dose is displayed on LED with the minimum dose resolution in 0.01μSv. Electric power is supplied by a coin-type lithium battery, which continuously works for about one week. Whenever the integrated dose value increased by 0.01μSv during air travel, the value was recorded with time. Also the doses have been measured with a portable dosemeter with GPS function (Fuji Electric PEGASUS PRO) and with weight of about 200 g. The PEGASUS has almost same sensitivity of the PDM and with the minimum dose resolution in 0.001μSv. Electric power is provided by two alkaline AA size batteries, which continuously works for about one day. This device can store the data of integrated dose, dose rate, time and location on the memory at 30 seconds interval.

The measurements with PDM and PEGASUSU were performed about 600 and 10 frights, respectively, from 2000 to 2018. The ranges of integrated doses with PDM for the main measurement routes of Tokyo-Naha, Tokyo-Aomori and Tokyo-Kagoshima (Fig. 1) were about 0.92-2.18 μSv, 7.0-12.0 μSv and 9.0-12.5 μSv, respectively. Figure 2 shows the variation of dose rate with PDM during air travel from Kansai to Naha on 23 April 2019. The data with PEGASUS showed almost same trends for the doses. These results suggest that the convenient measurement keeps the relative variation of the doses due to secondary cosmic rays during air travel, and that the handy equipment are useful to estimate the individual exposure of aircraft crew and passengers.

A part of this study has been performed in cooperation with Fuji Electric Co., Ltd.

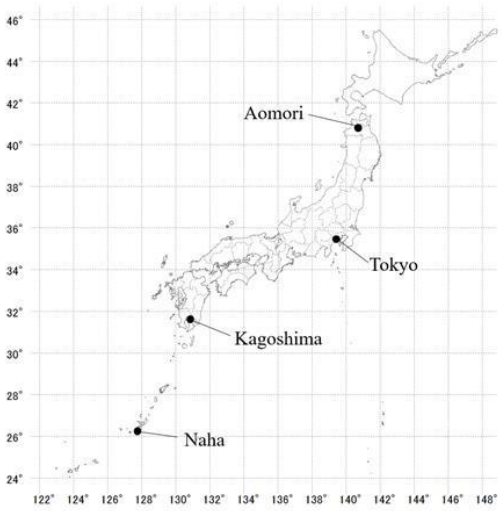

Figure 1. Location of airport rerated the main measurement route in this study.

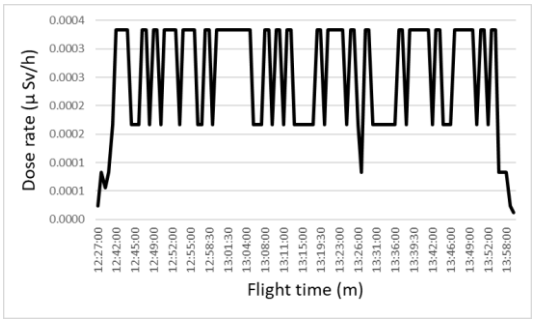

Figure 2. Variation of dose rates due to ionizing component of secondary cosmic rays measured with PDM from Kansai to Naha.

Characteristics of hydrogen and oxygen isotopes and chemical compositions in monthly precipitations collected at Hokkaido, Gifu and Okinawa, Japan

S. Nakasone[1], A. Ishimine[1], Y. Ishizu[1], Y. Shiroma[1], M. Tanaka[2], N. Akata[3], H. Kakiuchi[4], T. Sanada[5], M. Furukawa[1]

[1]University of the Ryukyus, 1 Senbaru, Nishihara, Okinawa 903-0213, Japan
[2]National Institute for Fusion Science, 322-6 Oroshi, Toki, Gifu 509-5292, Japan
[3]Hirosaki University, 66-1 Honcho, Hirosaki, Aomori 036-8564, Japan
[4]Institute for Environmental Sciences, 1-7 Ienomae, Obuchi, Rokkasho, Aomori 039-3212, Japan
[5]Hokkaido University of Science, 15-4-1 Maeda, 7-Jo, Teine, Sapporo, Hokkaido, 006-8585, Japan
Keywords: tritium, stable hydrogen and oxygen isotope, chemical component, precipitation
Presenting author, e-mail: nakashun93@gmail.com

Tritium (^{3}H) is a radioisotope of hydrogen that decays into ^{3}He with a half-life 12.3 years and is a direct tracer of water movement as a part of water molecule. For the Northern Hemisphere, ^{3}H tracer is regaining its popularity with lumped parameter models providing useful metrics of mean transit times and young water fractions (Gusyev *et al*., 2016). On the other hand, stable isotope of hydrogen (δD) and oxygen (δ^{18}O) in atmospheric water vapor and precipitation vary spatially and temporally because of equilibrium and kinetic isotopic fractionations associated with condensation and evaporation. Investigations of isotopic ratios of water have significantly contributed to our understanding of atmospheric circulation (Hoffman *et al*., 2000). In Japan, several studies have been reported on the application of δD and δ^{18}O, for different hydrological researches. However rarely research in Japan reports the combination of ^{3}H and δD and δ^{18}O. The ^{3}H data were partly reported (Nakasone *et al*., 2019). The aim of this study, to obtain a better understanding of trends of ^{3}H concentration to enable application of ^{3}H-tracer for hydrological systems in Japan.

Monthly precipitation samples have been collected at Hokkaido (43°N, 141°E), Gifu (35°N, 137°E) and Okinawa (26°N, 127°E) since June 2014. The samples were distilled and electrolyzed using solid polymer electrolytic enrichment system. The enriched sample was mixed with liquid scintillation cocktail, and the ^{3}H concentration was measured with a low background liquid scintillation counter. A part of the sample waters was filtered and anions (Cl^-, NO_3^-, SO_4^{2-}) and cations (Na^+, Mg^{2+}, Ca^{2+}, K^+, NH_4^+) were analyzed using ion chromatography. After that, δD and δ^{18}O were analyzed using isotope ratio mass spectrometry.

The arithmetic mean (± standard deviation) of ^{3}H concentrations in precipitation samples from Hokkaido, Gifu and Okinawa from June 2014 to June 2016 were estimated to be 0.62 ± 0.29 Bq L^{-1}, 0.33 ± 0.12 Bq L^{-1} and 0.13 ± 0.04 Bq L^{-1}, respectively. These results indicate that the concentrations increase with latitude. In addition, the highest and the lowest concentrations appeared in spring and summer (Fig. 1). The d-excess values in monthly precipitation collected at the three sites were a clear seasonal trend of being high in winter and low in summer (Fig. 1). Moreover, the ^{3}H concentration in monthly precipitation collected at Hokkaido and Okinawa was relatively good correlation with NO_3^- and NH_4^+ concentrations. This result indicated that ^{3}H in precipitation was affected by long-range transported components from Asia continent.

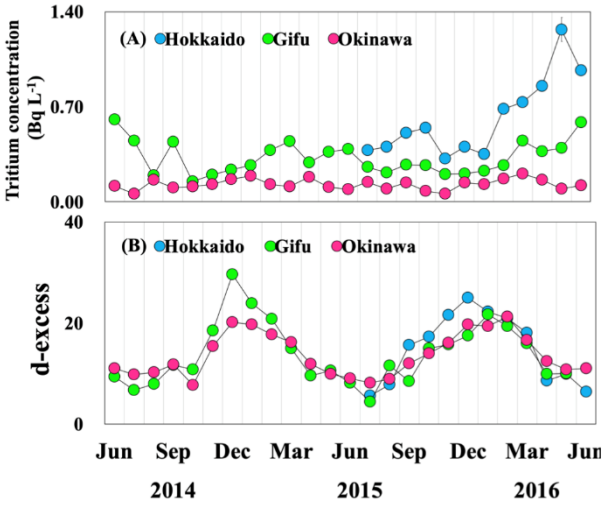

Figure 1. Variations for the ^{3}H concentration (A) and the d-excess value (B) observed in Hokkaido, Gifu and Okinawa.

This work was supported by NIFS Collaborative Research Program [NIFS14KLEA015, NIFS15KNWA001, NIFS18KNWA002].

Gusyev, M. A., Morgenstern, U., Stewart, M K., Yamazaki, Y., Kashiwaya, K., Nishihara, T., Kuribayashi, D., Sawano, H., Iwami, Y. 2016. Application of tritium in precipitation and baseflow in Japan: a case study of groundwater transit times and storage in Hokkaido watersheds. *Hydrol. Earth Syst. Sci*. 20, 1-16.

Hoffman, G., Jouzel, J., Masson, V. 2000. Stable isotopes in atmospheric general circulation models. *Hydrolog. Process*. 14, 1385-1406.

Nakasone., S, Ishimine., A, Ishizu., Y, Shiroma., Y, Tanaka., M, Kakiuchi., H, Sanada., T, Furukawa., M. 2019. Recent tritium concentration of monthly precipitation in Japan. *Radiat. Prot. Dosimetry* (in press).

Radioecology research and education at the University of Tokyo after the Fukushima Nuclear Accident

N. Nihei[1], K. Tanoi[1], and T.M. Nakanishi[1]

[1] Graduate School of Agricultural and Life Sciences, The University of Tokyo, Tokyo, 113-8657, Japan
Keywords: Fukushima, nuclear accident, radiocesium, agriculture
Presenting author email: anaoto@mail.ecc.u-tokyo.ac.jp

Research: Immediately after the Fukushima Nuclear accident, 40-50 academic staff at the Graduate School of Agricultural and Life Sciences, the University of Tokyo, organized several groups to research into the behavior of radioactive materials in the Fukushima prefecture. The targeted items for research ranged widely, including soils, plants, animals, fish, mountains, water, etc. Researchers with expertise in a variety of fields were gathered together to discuss the measures being taken to deal with the contaminated environment. This was the first time our graduate school has undertaken a collaborative project of such size. To measure radioactive Cs, we use pure Ge counters and Na(Tl)I scintillation counters in our radioisotope lab. An enormous number of samples of various types, mainly collected by our colleagues, were brought to this lab, and their radioactivity was measured by professional employees. Over 10,000 samples were measured per year.

One of our research showed that radioactive Cs was found to bind strongly to fine clay particles, weathered biotite, and to organic matters in the soil, therefore, radioactive Cs has not mobilized from mountainous regions, even after heavy rainfall. The downward migration of radioactive Cs in the soil is now estimated at 1–2 mm/year. In the case of farmland, the quantity of radioactive Cs in the soil absorbed by crop plants was small, and this has been confirmed by the real-time imaging experiments in the laboratory. The intake of radioactive Cs by trees occurred via the bark, not from the roots since the active part of the roots is generally deep within the soil where no radioactive materials exist. The distribution profile of radioactive Cs within trees was different among species.

Book: The results we obtained during the first 2 years were summarised and e-published through Springer in a book titled "Agricultural Implications of the Fukushima Nuclear Accident", which has already been downloaded more than 100,000 times. A second book was e-published by Springer in 2016 and the third book in 2019. Using these approaches, our results have been utilized effectively in various ways.

Lecture: For undergraduate and graduate students and for the general public, some parallel lecture series started to learn how the behavior and accumulation pattern of radioactive Cs changes with time. To allow the students to learn about the behavior of the fallout firsthand, several field studies were also carried out at the mountain, agricultural fields, and meadow sites.

Workshop: In the case of the Chernobyl accident, it is well known that the first radioactive measurement of the fallout was performed in Sweden. We found that the study of radioecology is highly advanced in Sweden, whereas before the Fukushima accident, similar research in Japan was limited to some special institutes and was not being done at the universities. Therefore, we planned the Japan–Sweden joint workshop on radioecology not only for our academic staff but also for the students in 2015. Among the Japanese participants, nine of the students selected were actually carrying out their radio-ecological studies of Fukushima at the university. Before visiting Sweden, they were taught how to summarise their data and present at the seminar. As can be seen from their reports, this seminar provided them enormous stimulation and motivation to study radioecology. We all expect that we will continue the radioecological study of Fukushima for a long time, while also working on improvements to our educational techniques.

Seminar: Gradually, our researchers have accumulated data on the movement and accumulation of radioactive fallout in the environment. Our initial purpose, as part of our commitment to contributing to the community, was to show as many people as possible what we have learned about the fallout from the nuclear accident, including how it is distributed and how it moves. Seminars open to the public have been held periodically to report the results obtained from studies in the agricultural environment. The first seminar was held in November 2011.

Information: Ministry of the Environment has collected basic knowledge on radiation and has prepared a booklet to provide basic information since 2012. The English version of the booklet has been publicized so that foreign nationals residing in Japan or visiting Japan or those interested in Japan can obtain basic knowledge on radiation and correctly understand changes in circumstances. The booklet is also available on the website of the Ministry of the Environment, from which you can download the content.

Nakanishi TM, Tanoi K (eds) (2013) Agricultural implications of the Fukushima nuclear accident. Springer, Tokyo
https://www.springer.com/jp/book/9784431543275

Nakanishi TM, Tanoi K (eds) (2016) Agricultural implications of the Fukushima nuclear accident(Ⅱ). The first three years. Springer, Tokyo
https://www.springer.com/gp/book/9784431558262

Nakanishi TM, O'Brien M, Tanoi K (eds) (2019) Agricultural implications of the Fukushima nuclear accident(Ⅲ). After 7 Years. Springer, Tokyo
https://www.springer.com/jp/book/9789811332173

Ministry of the Environment, Booklet to Provide Basic Information Regarding Health Effects of Radiation (2019)
https://www.env.go.jp/en/chemi/rhm/basic-info/

Influence of soil water content, potassium, and "EM-Bokashi" on the soil-to-plant transfer factor of ^{137}Cs for spring wheat and white mustard

A.N. Nikitin[1], O.A. Shurankova[1], S. Okumoto[2], E.V. Mischenko[1], M. Shintani[2], G.A. Leferd[1], T. Higa[3], I. Cheshyk[1], D.V. Sukhareva[1], E.V. Zhukovskaya[1], S.A. Arendar[1]

[1]Institute of Radiobiology, the National Academy of Sciences of Belarus, Gomel, 246007, Belarus
[2]EM Research Organization Inc., 901-2311, Okinawa, Japan
[3]International EM technology center, Meio University, 905-8585, Okinawa, Japan
Keywords: cesium-137, wheat, mustard, soil moisture
Presenting author, e-mail: nikitinale@gmail.com

There is only fragmentary information available concerning the effects of weather and meteorological conditions on changes in the biological availability of radioactive isotopes of cesium and their behavior in the "soil–plant" system. This information is of particular relevance in areas contaminated by artificial radioisotopes as a result of accidents at nuclear power plants. One of the most likely climate change scenarios for the Republic of Belarus implies a decrease in water availability in the soil. Therefore, it is necessary to assess the effect of soil moisture on the transfer of ^{137}Cs to monocotyledons and dicotyledons, as well as the change in the effectiveness of mineral and organic fertilizers with respect to reducing the radioisotope accumulation in plants.

This study aims to investigate the effect of soil moisture on the soil-to-plant transfer of ^{137}Cs in the shoots of spring wheat and white mustard, as well as to analyze the modification of the effect of the soil moisture regime via the application of KCl and the organic soil improver "EM-Bokashi."

The upper 10-cm layer of sandy podzolized soil from the Chernobyl nuclear power plant exclusion zone was used as a plant substrate. The activity concentration of ^{137}Cs in the soil was 7.3 kBq kg^{-1}. The content of mobile potassium in the soil was 41 mg kg^{-1} (in terms of K_2O). The substrate was placed in 1.1-L containers for growing plants. Fertilizers were included in the experimental design: KCl at doses of 200 mg kg^{-1} and 100 mg kg^{-1} of soil (in terms of K) and "EM-Bokashi" at doses of 20 g kg^{-1} and 5 g kg^{-1} of soil. "EM-Bokashi" is wheat bran fermented with effective microorganisms (EM・1®).

Vegetation experiments were performed in a phyto-chamber with controlled conditions. Three soil moisture variants were tested: 40%, 70%, and 85%. The soil moisture was maintained using the gravimetric method.

The soil-to-plant transfer factor of ^{137}Cs for wheat has its maximum value for the minimal soil water content (Table 1). Increasing the soil water content to 70% and 85% reduces the accumulation of the radionuclide by nearly half. A similar pattern is observed for white mustard. The soil-to-plant transfer factor decreases by 22% when increasing the soil moisture from 40% to 70% and by 36% when increasing the soil moisture from 40% to 85%.

Table 1. Soil-to-plant transfer factors of ^{137}Cs for different soil water contents and fertilizers

Water content, %	40	70	85
Spring wheat			
Control	0.78	0.42	0.43
Bokashi, 20 g kg^{-1}	0.26	0.21	0.20
Bokashi, 5 g kg^{-1}	-	0.19	-
KCl, 200 mg kg^{-1}	0.08	0.07	0.06
KCl, 100 mg kg^{-1}	-	0.04	-
White mustard			
Control	2.06	1.61	1.31
Bokashi, 20 g kg^{-1}	0.27	0.13	0.08
Bokashi, 5 g kg^{-1}	-	0.34	-
KCl, 200 mg kg^{-1}	0.17	0.29	0.31
KCl, 100 mg kg^{-1}		0.22	

A decrease in the soil-to-plant transfer factor with increasing soil moisture with the application of "EM-Bokashi" is observed both for wheat and for mustard. "EM-Bokashi" in a dose of 20 g kg^{-1} decreases the accumulation of cesium by mustard by 8–16 times. The most prominent effect of the soil improver was observed in the case with the highest water content. The accumulation of ^{137}Cs in shoots of wheat decreased by 2–3 times after the application of "EM-Bokashi." The highest effectiveness was observed for low soil moisture.

The application of 200 mg kg^{-1} KCl made it possible to significantly reduce the transfer of ^{137}Cs to the aboveground organs of the wheat, and the relationship of this indicator to the soil moisture became significantly weaker. The radionuclide transfer factor into mustard shoots increases with increasing soil moisture content in the case of mineral fertilizer application.

Therefore, a decrease in the soil moisture will lead to an increase in the transfer factors of ^{137}Cs to shoots of monocotyledonous and dicotyledonous plants; however, the effectiveness of potassium fertilizers and the soil improver "EM-Bokashi" with respect to suppressing the transfer of radioisotopes into plants will remain.

Radioactivity measurements of phosphogypsum produced in Serbia

J. Nikolov[1], P. Kuzmanović[1,2], N. Todorović[1], J. Knežević[1], S. Forkapić[1], L. Filipović Petrović[2]

[1]Department of Physics, University of Novi Sad, Novi Sad, 21000, Serbia
[2]Higher medical and business-technological school of applied studies, Sabac, 15000, Serbia
Keywords: phosphogypsum, radioactivity, gamma spectrometry, radium.
Presenting author, e-mail: jovana.nikolov@df.uns.ac.rs

Phosphogypsum is a material occurring as a byproduct of phosphoric acid production (H_3PO_4) in so called "wet process" used for the production of fertilizers (Calin et al., 2015; Cuadri et al., 2014). Phosphogypsum is classified as TENORM (Technologically Enhanced Naturally Occurring Radioactive Material) and contain naturally occurring radioactive elements from series ^{238}U – ^{226}Ra, ^{232}Th, as well as primordial radioisotope ^{40}K (Calin et al., 2015; USEPA, 2002). The activity concentration of ^{226}Ra in the phosphogypsum can range from 200 to 3000 Bq kg^{-1} (USEPA, 1990). In order to use phosphogypsum for the production of building materials, the activity concentration of ^{226}Ra should not be higher than the recommended 370 Bq kg^{-1} (USEPA, 2002). The main goal of this paper is determination of the radioactivity level in phosphogypsum samples for potential re-use in the production of building materials.

Table 1. Activity concentration of ^{226}Ra, ^{232}Th, and ^{40}K in phosphogypsum samples.

Sample ID	Activity concentration (Bq kg^{-1})		
	^{226}Ra	^{232}Th	^{40}K
PG1	488±15	2.8±1.0	< 12
PG2	520±11	3.4±1.0	< 10
PG3	737±8	3.3±1.0	12±6
PG4	512±5	4.5±0.9	< 5
PG5	626±14	2.3±0.9	117±7
PG6	649±9	2.1±0.8	< 17
PG7	609±4	3.9±0.8	105±6
PG8	656±4	3.1±0.9	101±6
Range	488-737	2.1-4.5	5-117
Mean ± Standard Deviation	600±28	3.18±0.26	47±16
World average	50[1]	50[1]	500[1]

[1](UNSCEAR, 1993).

The analyzed samples of phosphogypsum were taken from the chemical industry waste disposal in Elixir Prahovo, located in Eastern Serbia, in the region of Prahovo. This industry is producing about 810000 tons of phosphogypsum as a byproduct in everyday activity of production of fertilizers.

Phosphogypsum samples were measured 40 days after preparation, after a secular radioactive equilibrium between ^{222}Rn and ^{226}Ra was established. The low-background gamma spectrometry method was used to determine the activity concentration of ^{226}Ra, ^{232}Th and ^{40}K in the samples. The measurement time of each sample was around 72000 s. Samples were dried for 24 hours at temperature around 110 °C, then crushed and homogenized to fine powder. Typical sample mass ranged from 250 g to 300 g. The measured activity concentrations of ^{226}Ra, ^{232}Th and ^{40}K are given in Table 1.

Activity concentration of ^{226}Ra in all analyzed samples was higher than value recommended for materials that can be used in building industry and also much higher than world average concentration. The use of the analyzed phosphogypsum is recommended solely as an addition to natural gypsum. In future studies additional analysis will be conducted in order to estimate the potential for the use of those phosphogypsum materials in the production of new building material which is especially interesting from radioecology point of view as the large amount of byproducts would be efficiently reused.

The authors acknowledge the financial support of the Ministry of Education, Science and Technological Development of Serbia, within the projects No. 171002 and 43002.

Calin, M.R., Radulescu, I., Calin, M.A., 2015. Measurement and evaluation of natural radioactivity in phosphogypsum in industrial areas from Romania. *J. Radioanal. Nucl. Chem*. 304, 1303–1312.

Cuadri, A.A., Navarro, F.J., García-Morales, M., Bolívar, J.P. 2014. Valorization of phosphogypsum waste as asphaltic bitumen modifier. *J. Hazard. Mater*. 279, 11–16.

UNSCEAR, 1993. Sources, Effects and risks of ionizing radiation (United Nations Scientific Committee on the Effects of Atomic Radiation, United Nations New York, 1993)

USEPA, 1990. United States Environmental Protection Agency (U.S. EPA), Report to Congress on Special Wastes from Mineral Processing: Summary and Findings, Washington,

USEPA, 2002. U.S. Environmental Protection Agency. National emission standards for hazardous air pollutants subpart R.

Self-absorption effects in the low-energy region in non-destructive nuclear forensics method

J. Nikolov[1], A. Vraničar[1], N. Todorović[1], M. Travar[1], J. Hansman[1], S. Gadžurić[2], D. Mrđa[1]

[1]Department of Physics, Faculty of Sciences, University of Novi Sad, Novi Sad, 21000, Serbia
[2]Department of Chemistry, Biochemistry and Environmental Protection, Faculty of Sciences, University of Novi Sad, Novi Sad, 21000, Serbia
Keywords: gamma spectrometry, self-absorption, uranium ore, nuclear forensics
Presenting author, e-mail: jovana.nikolov@df.uns.ac.rs

Being recognized as one of the main problems in low-energy gamma spectrometry, accurately determining the efficiency of detection in this region proves to be of crucial importance in order to produce precise results for activity concentration of ^{238}U and ^{210}Pb, both of which can be found in either environmental samples or nuclear material (Nikolov et al., 2014). The samples of interest for nuclear forensics may serve as evidence for an ongoing investigation; hence a non-destructive method such as gamma-spectrometry is at all times the preferential choice. In addition to this, being a non-destructive method for sample analysis, laboratory applications of gamma-spectrometry for purposes for nuclear forensics provide means to accurately determine the isotopic composition of gamma-emitting radionuclides in a sample and to quantify the amount of each radioisotope present (Apostol et al., 2016). In case of special nuclear material containing uranium and/or plutonium, gamma spectrometry can also be used for determination of total nuclear material content, the age of the material (time past since last enrichment), the presence of reprocessed uranium and the presence of fission products. The up mentioned information can be of crucial importance in assisting an investigation by providing indicators of the origin of the illicit material. In order to obtain any information about radionuclide such as uranium from gamma spectrum, the main prerequisite must be fulfilled, and that is having an accurate reading for count rate from the lower end part of the spectrum. This can prove to be difficult for mainly two reasons, line positioning in the area which naturally has a substantial background and poorly (inadequately) defined function of detection efficiency for this energy range. One of the reasons for the latter is unquantified self-absorption of the low-energy gammas in the sample and container (Živanović et al., 2012). In the present day, computer software called Multigroup γ-ray Analysis Method for Uranium (MGAU), in combination with gamma-spectroscopy is usually applied for characterization and categorization of samples containing uranium, and full energy peak efficiencies are obtained by Monte Carlo simulations with GESPECOR code (Gunnick et al., 1994). In this work, full energy peak efficiencies were acquired both experimentally (knowing the activity of uranium in our sample) and checked with those derived from software codes Angle and EFFTRAN (Stanić et al., 2019). The self-absorption effect was tested by carrying out multiple measurements of uranium ore samples, on the same Canberra HPGe extended range closed-end coaxial detector with declared relative efficiency of 100%. The samples were prepared from the same uranium ore with different masses, whilst keeping the same beaker radius. The measurements were taken for a period of $7 \cdot 10^4$ s. Therefore, an optimal efficiency to mass ratio was determined, where the self-absorption effect was minimal. In addition to this, the advantages and disadvantages of using Angle and EFFTRAN software codes for improving efficiency determination in low-energy region were discussed. In future studies, different types of beaker geometries will be tested in order to see if a better efficiency to mass ratio can be achieved.

The authors acknowledge the financial support of the International Atomic Energy Agency (IAEA) via IAEA Research Contract No. 23159/R0 and the Provincial Secretariat for higher education and scientific research within the project No. 142-451-2793/2018.

A. Apostol et al. 2016. Isotopic composition analysis and age dating of uranium samples by high resolution gamma ray spectrometry, *Nucl. Instr. and Methods in Phys. Res. B*, 383, 103-108.

R. Gunnick et al. 1994, MGAU: A new analysis code for measuring U-235 enrichments in arbitrary samples, *IAEA-SM-333/88*, IAEA Symposium on International Safeguards, Vienna.

J. Nikolov et al. 2014. Natural radioactivity around former uranium mine, Gabrovnica in Eastern Serbia, *Journal of Radioanalytical and Nuclear Chemistry*, 302, 477-482.

G. Stanić et al. 2019, Angle vs. LabSOCS for HPGe efficiency calibration, *Nucl. Instr. and Methods in Phys. Res.* A, Volume 920, 11 March 2019, Pages 81-87.

M. Živanović et al. 2012. Analysis of interferences from full energy peaks in gamma spectrometry of NORM and TENORM samples, *Nuclear Technology and Radiation protection*, 27, 380-387.

Measurement of radionuclide concentrations in Japanese fish reference materials produced in the aftermath of the Fukushima nuclear power plant accident

S. Nour[1], J. LaRosa[1]

[1]National Institute of Standards and Technology, 100 Bureau Dr. MS 8462, Gaithersburg MD 20899, USA
Keywords: reference material, radionuclide, nuclear accident pollution, fish material, intercomparison, CRM
Presenting author, e-mail: svetlana.nour@nist.gov

As part of an ongoing effort to control the amount of radioactive contamination in foodstuffs, a consortium of Japanese organizations has been preparing and characterizing important foodstuffs with radioactive contamination to serve as key reference materials for the numerous laboratories that are responsible for monitoring the level of radionuclides in commercially available foods. Because the Fukushima accident impact is worldwide, the Japan Society for Analytical Chemistry (JSAC) wished to have their certified reference materials (CRMs) validated through International Intercomparison Exercises (IICE) involving labs recognized worldwide for their accurate radioactivity measurements. NIST's Radioactivity Group recently participated in an IICE whose objective was to ascertain the ^{134}Cs, ^{137}Cs and ^{40}K activity concentrations in JSAC-prepared fish meat and fish bone ash as well as the ^{90}Sr activity concentration in the fish bone ash.

NIST participated in the certification of fish flesh powder and fish bone ash for their ^{134}Cs and ^{137}Cs activity concentrations. Both non-destructive and destructive analyses were carried out using low-level gamma-ray spectrometry for the quantitative measurement of these radionuclides. Comparisons with reference sources containing known amounts of these same radionuclides in very similar matrices and cylindrical geometries permitted the activity concentrations in the CRM samples to be determined. The reference sources where prepared by spiking similar blank material with a calibrated mixture of ^{134}Cs and ^{137}Cs. For destructive assays, the original materials were decomposed (fish meat ignited in an electric furnace to burn off organic matter) and dissolved (fish meat ash residue, fish bone ash) to create homogeneous solutions containing the radionuclides. These solutions were measured on the same HPGe gamma spectrometer and compared with solutions of very similar volume and density that contained well-known amounts of the same radionuclides. The assay of ^{90}Sr concentration in the fish bone ash was based on measurement of Sr-90/Y-90 beta-particle emissions after chemical separation using gas-flow proportional counting.

Semi-empirical efficiency calibration of a $LaBr_3$(Ce) scintillation detector for NORM samples analyses in order to validate in-situ measurements in the field

E. Ntalla[1,3], A. Markopoulos[1], K. Karfopoulos[2], C. Potiriadis[2], A. Clouvas[3] and A. Savidou[1]

[1]Institute of Nuclear and Radiological Sciences & Technology, Energy & Safety, National Center for Scientific Research "Demokritos", Athens, 15310, Greece
[2] Environmental Radioactivity Monitoring Department, Greek Atomic Energy Commission, Athens, 15341, Greece
[3]Department of Electrical and Computer Engineering, Aristotle University of Thessaloniki, Thessaloniki, 54124, Greece
Keywords: $LaBr_3$(Ce), efficiency calibration, NORM
Presenting author e-mail: dalla@ipta.demokritos.gr

The last decade $LaBr_3$(Ce) scintillation detectors have become commercially available and are very promising due to their high light yield (> 65000 photons/MeV) that results in a better energy resolution compared to NaI(Tl) detectors (< 3% FWHM at ^{137}Cs), their decay time of 35 ns and their material density (5.29 g/cm^3) (Knoll, 1999, Quarati et al, 2007). Also, there is no need for nitrogen cooling and it is easier to be simulated comparing to HPGe detectors. Thus, $LaBr_3$(Ce) detectors could be a suitable choice for environmental radiation monitoring (Ciupek et al, 2014) and in-situ measurements of NORM (Mueller et al, 2013).

In this study, a semi-empirical calibration method for NORM samples measurement was developed based on a combination of experimental gamma spectrometry measurements and MCNPX simulations. The aim of this work is to provide us with full energy peak efficiency calibration curves in a wide photon energy range which is of particular importance when selected photon energies of ^{234}Th, ^{214}Pb, ^{214}Bi, ^{228}Ac, ^{208}Tl and ^{226}Ra are to be measured with accuracy. Furthermore, factors that affect NORM samples analysis, such as LaBr3(Ce) internal background and peak interferences, were considered.

A Canberra scintillation detector $LaBr_3$(Ce) (Model LABR-1.5x1.5) and four reference multi-nuclide volume sources made of epoxy material of different densities (0.5, 0.9, 1.5 and 2.0 g/cc) were used. Experimental efficiency calculations for ^{210}Pb, ^{241}Am, ^{137}Cs and ^{60}Co were performed with the volume sources adapted on an acetal holder which was positioned in a vertical direction along the detector axis of symmetry.

MCNPX simulations were performed in an energy range of 46.54 – 1461 keV including the energies used in the experimental calculations. Firstly, simulated and experimentally calculated efficiencies were compared in order to determine the accurate dimensions of the $LaBr_3$(Ce) detector crystal. The maximum acceptable relative deviation for the low energies was 15% (higher statistical error and source uncertainty). Then, the efficiency calibration curves were evaluated by MCNPX simulations for the four different density volume sources. Nominal NORM samples originating from oil and gas industries as well as phosphorite reference samples were analyzed for evaluation of the laboratory technique.

Besides the determination of the $LaBr_3$(Ce) crystal geometry, this work is essential for the accurate NORM samples analysis which is important for validating the in-situ techniques of large volume sources radiological characterization.

This study is supported by the program of Industrial Scholarships of Stavros Niarchos Foundation.

Knoll G. F., John Wiley and Sons, 1999.

Quarati, F., Bos, A.J.J., Brandenburg, S., Dathy, C., Dorenbos, P., Kraft, S., Ostendorf, R.W., Ouspenski, V., Owens, A. 2007. X-ray and gamma-ray response of a 2´´x 2´´ $LaBr_3$:Ce. *Nucl. Instr. Meth. Phys. Res.* A 574, 115-120.

Ciupek, K., Jednoróg, S., Fujak, M., Szewczak, K. 2014. Evaluation of efficiency for in situ gamma spectrometer based upon cerium-doped lanthanum bromide detector dedicated for environmental radiation monitoring. *J. Radioanal. Nucl. Chem.* 299, 1345-1350.

Mueller, W. F., Ilie, G., Lange, H.J., Rotty, M., Russ, W.R. 2013. In-situ measurements and analysis of naturally occurring radioactive materials. *ANIMMA paper #1310*.

Variation of Chlorine-36 deposition flux in precipitation at Tsukuba, Japan

Y. Ochiai[1], K. Sasa[1], Y. Tosaki[2], T. Takahashi[1], M. Matsumura[1], K. Sueki[1]

[1]Acclerator Mass Spectrometry Group, University of Tsukuba, Ibaraki, 305-8577, Japan
[2]Geological survey of Japan, National Institute of Advanced Industrial Science and Technology, Ibaraki, 305-8567, Japan
Keywords: Solar activity, Chlorine-36, Accelerator mass spectrometry, Deposition flux
Y. Ochiai, e-mail: ochiai.yuta.sp@alumni.tsukuba.ac.jp

^{36}Cl (half life = 3.01×10^5 years) is a cosmogenic nuclide, which is produced in the reactions between cosmic rays and elements constituting of the Earth (e.g. ^{40}Ar(n, X)^{36}Cl). ^{36}Cl is rapidly hydrogenated after the production and deposits with rainwater or aerosols. This study focused on ^{36}Cl in precipitation. We measured ^{36}Cl deposition flux based on rainwater samples and evaluated the variability of them.

We have collected monthly rainwater samples since April 2004 at the University of Tsukuba (Tosaki et al., 2012). In this study, ^{36}Cl was analysed during 2010 – 2016. Cl^- in the rainwater samples was extracted by an ion exchange method. Then, Cl^- was precipitated as AgCl with $AgNO_3$ and washed by ultrapure water and ethanol. ^{36}Cl was analysed with accelerator mass spectrometry (AMS) system at the University of Tsukuba (Sasa et al., 2018). Based on the result of AMS, the ^{36}Cl deposition flux was calculated.

Figure 1 shows the variation of the ^{36}Cl deposition flux during 2010 - 2016, which ranged from 6.1 ± 0.4 to (5.6 ± 0.1) × 10^2 atoms m^{-2} s^{-1}. The average of the flux was 50 ± 1 atoms m^{-2} s^{-1}. The average was higher than 2004 – 2009 (32 ± 2 atoms m^{-2} s^{-1}; Tosaki et al., 2012) because ^{36}Cl released from the Fukushima Daiichi Nuclear Power Plant accident was observed on March 2011.

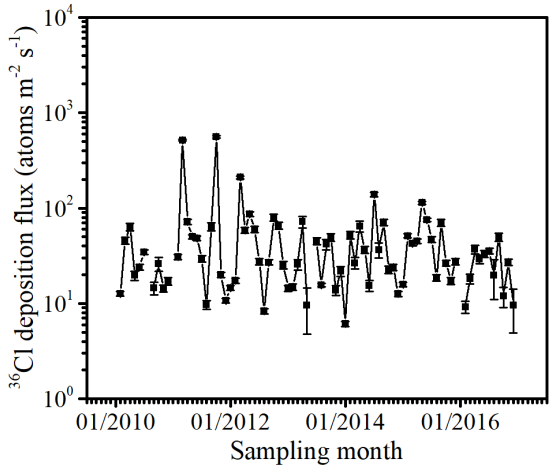

Figure 1. Variation of the ^{36}Cl deposition flux at Tsukuba during 2010 - 2016.

One of the reasons why ^{36}Cl deposition flux varied would be the variation of the solar activity. Previous study reported that when the solar activity is weak, the production rate of ^{36}Cl increase and vice versa (Masarik and Beer, 2009). The 12-months moving average of the ^{36}Cl deposition flux was calculated due to cancelling seasonal variation of ^{36}Cl (Tosaki et al., 2012), and compared with solar modulation potential (Usoskin, I. G. et al., 2017). Based on the comparison, there seemed to be an inverse correlation between the ^{36}Cl deposition flux and solar modulation potential, correlation efficient $r = -0.4$, $p < 0.001$. The solar activity should affect ^{36}Cl deposition flux. However, the correlation was weakened because of meteorological condition like precipitation amount. For further investigation, the ^{36}Cl deposition flux needs to be corrected meteorological effects.

In the presentation, we will report on more details on the correlation between ^{36}Cl deposition flux and solar activity, and the comparison with deposition fluxes of other cosmogenic nuclides that were measured at the University of Tsukuba.

We appreciate staff at the Tandem Accelerator Complex, University of Tsukuba for the ^{36}Cl measurements. This work was supported by JSPS KAKENHI grant numbers of 15H02340 and 19H04252.

Masarik, J. and Beer. 2009. An updated simulation of particle fluxes and cosmogenic nuclide production in the Earch's atmosphere. *J. Geophys Res*. 114, D11103.

Tosaki, Y., Tase, N., Sasa, K., Takahashi, T., Nagashima, Y. 2012. Measuremant of the ^{36}Cl deposition flux in central Japan: natural background levels and seasonal variability. *J. Environ Radioactiv*. 106, 73-80.

Sasa, K., Takahashi, T., Matsunaka, T., Hosoya, S., Matsumura, M., Shen, H., Honda, M., Takano, K., Ohciai, Y., Sakaguchi, A., Sueki, K., Stodola, M., Sundquist, M. 2018. The 6 MV multi-nuclide AMS system at the University of Tsukuba, Japan: First performance report. *Nucl Instrum Meth B*. 437, 98-102.

Usoskin, I.G, Gil, A., Kovaltsov, G.A., Mishev, A.L., Mikhailov, V.V. 2017. Heliospheric modulation of cosmic rays during the neutron monitor era: Calibration using PAMELA data for 2006-2010. *J. Geophys Res*. 122(4), 3875-3887.

Feasibility of a strontium adsorbent to analysis of radiostrontium in seawater

Y. Ogata[1], H. Minowa[2], Y. Kato[3], S. Kojima[4]

[1]Radioisotope Research Center Medical Division, Nagoya University, Showa-ku, Nagoya, 466-8550, Japan
[2]Radioisotope Research Facility, The Jikei University School of Medicine, Minato-ku, Tokyo, 105-8461 Japan
[3]Measuring Systems Design Dept., Hitachi, Ltd. Mitaka-shi, Tokyo, 181-8622, Japan
[4]Aichi Medical University, Aichi, 480-1195, Japan
Keywords: radiostrontium, seawater, monitoring, strontium adsorbent
Presenting author, e-mail: ogata.yoshimune@b.mbox.nagoya-u.ac.jp

Monitoring of environmental radiostrontium, ^{89}Sr and ^{90}Sr, is important because radiostrontium is known to accumulate in bone and to increase a risk of bone cancer and leukemia. Since they emit no γ-rays but solely emit β-rays, isolation from other radionuclides before radioactivity measurement is indispensable. The conventional methods to estimate radiostrontium are time-consuming complicated procedures using lots of deleterious substances. We are investigating simple, quick and safe analytical methods of radiostrontium in environmental samples. There is a new Sr adsorbent; 'Pureceram MAq' (Nippon Chemical Industrial Co. Ltd.), which will selectively adsorb Sr in seawater. The substance is composed of barium silicate and is not water-soluble. The particle size is from several μm to a hundred μm. We applied the Sr Adsorbent to extract Sr from seawater. In this study, the property of the Sr Adsorbent was experimentally analysed and the feasibility of the Sr Adsorbent to use Sr monitoring in seawater was investigated.

Required amount of Sr Adsorbent

The Sr Adsorbent, each amount was 20, 60, and 100 mg, was added to 100-mL artificial seawater spiked with ^{90}Sr. The seawater was stirred with a shaker for 60 min. After that, a fraction of the seawater was sucked into a syringe and was filtered with a filter (pore size 0.45 μm). The ^{90}Sr activity of the filtrate water, i.e.; the liquid phase, was measured with a liquid scintillation counter (LSC-7400, Hitachi Ltd.).

Change-with-time of Sr concentration

The Sr Adsorbent of the amount 100 mg was added to 100-mL artificial seawater spiked with ^{85}Sr. The seawater was stirred. A fraction of the seawater was taken at the time from the start of the stirring, i.e.; 0, 5, 15, 30, 60, 90, and 120 min, respectively. The fraction of the seawater was filtered as the same as above, and the ^{85}Sr activity was measured with a gamma counter (ARC-7001, Hitachi Ltd.).

Change-with-time of concentration of typical cations

The Sr Adsorbent of the amount 100 mg was added to 100-mL artificial seawater of non-radioactive. The seawater was stirred. A fraction was taken at the time from the start of the shake, i.e.; 0, 5, 10, 20, 30, 60, 90, 120, 150, and 210 min, respectively. The fraction of the seawater was filtered, and the concentrations of four main cations in seawater, i.e., Na, K, Mg, and Ca were measured with an ICP-AES, Inductively Coupled Plasma Atomic Emission Spectroscopy (Thermo Jarrel Ash, IRIS/AP).

Required amount of Sr Adsorbent Amount

The percentages of Sr concentration of the liquid phase to that of the initial one were 52%, 34%, 2.5% for 20, 60, and 100 mg of the Sr Adsorbent amounts, respectively. Therefore, it is found that 100 mg of the Sr Adsorbent is needed to adsorb Sr in 100-mL seawater.

Change-with-time of Sr concentration

The Sr concentrations of the liquid phase were exponentially decreased with the stirring time. The concentration after 120 min stirring was 1.6% of that of the initial seawater. It is verified that 120 min stirring is enough to adsorb Sr in seawater to the Sr Adsorbent.

Change-with-time of concentration of typical cations

The concentrations of the four elements, Na, K, Mg, and Ca, in the liquid phase were not changed throughout the stirring time. Thus, it was proved that Sr is selectively adsorbed by the Sr adsorbent.

It is probed that Sr in seawater is selectively adsorbed by the Sr adsorbent, Pureceram MAq, with solely certain time of stirring without any chemical procedure. Thus, the Sr Adsorbent may be applicable to use radiostrontium monitoring of seawater. However, one should notice the self-absorb of beta-rays emitted from ^{90}Sr and/or ^{89}Sr. When the Sr Adsorbent is used for radiostrontium monitoring in seawater, one should pay compensation of the self-absorb or elute Sr from the adsorbent by some method.

The detail of the methods and the results will be presented on the conference.

It was confirmed that the Sr Adsorbent selectively adsorb Sr in seawater. Feasibility of Sr in seawater monitoring using the Sr Adsorbent was shown.

Professor Chisato Takenaka, Graduate School of Bioagricultural Sciences, Nagoya University helped us using an ICP-AES. This study was performed at Radioisotope Research Center Medical Division, Nagoya University.

Extraction efficiency of ^{210}Po and ^{210}Pb in herbal teas

G. Olszewski[1,2,3], A. Moniakowska[1], D. Strumińska-Parulska[1]

[1]Department of Environmental Chemistry and Radiochemistry, Laboratory of Toxicology and Radiation Protection, University of Gdańsk, Gdańsk, 80-308, Poland
[2]Department of Medical and Health Sciences, Division of Radiological Sciences, Linköping University, Linköping, 581 85, Sweden
[3]Swedish Radiation Safety Authority, Stockholm, 171 54, Sweden
Keywords: ^{210}Po, ^{210}Pb, herbal tea, extraction, infusion, effective dose
Presenting author: G. Olszewski; e-mail: grzegorz.olszewski@ug.edu.pl

Air and food are the main sources of many chemical elements, also natural and artificial radionuclides transferred to human organisms. The intensity of radioisotopes intake depends on the place of residence, local radiation quantity, diet habits and food origin. So far, during annual radiation doses evaluations in Poland, the most often consumed food products were taken into account. Among naturally occurring radionuclides, their potential ingestion and internal expose, the most important seems to be ^{210}Po and its parent nuclide ^{210}Pb.

Herbal or medicinal plant products, in different forms known as herbal teas, have been used for hundreds of years in preventing and treating diseases around the world. Currently, in many cultures, especially in developing countries, it is still the main source of medicaments. Estimated at 70-80% of the world's population uses unconventional medicine, and treats it as their primary healthcare.

Presented are results of a study on ^{210}Po and ^{210}Pb extraction efficiency in Polish herbal teas and risk to human consumer due to exposure from highly radiotoxic alpha decay particles emitted by ^{210}Po and beta particles emitted by ^{210}Pb. 12 most popular commercially available Polish herbal teas, and their infusions in tap water and filtered water, were analyzed and ^{210}Po and ^{210}Pb activity concentrations were calculated.

Analysis of ^{210}Po content in analyzed samples was carried out using an alpha spectrometer, while ^{210}Pb determination method was based on its indirect measurement via its daughter ^{210}Po activity measurement. The chemical analysis efficiency of ^{210}Po and ^{210}Pb determination ranged 95-98%.

The results of ^{210}Po activity determination in dried plants were from 2.11±0.09 for milk thistle to 33.7±0.4 Bq·kg^{-1} dry wt. for cistus what equaled 4.21±0.18 for milk thistle and 43.8±0.5 mBq per one teabag. The extraction efficiencies into tap water ranged from 4.93±0.39 for lime to 27.4±1.4 % for elderberry, while for filtered water were between 7.55±0.47 for lime and 20.3±1.1 % for elderberry. There were no statistically significant differences between both extractions and no correlation between ^{210}Po extraction efficiency and ^{210}Po activity in dried herbs.

The highest activity concentration of ^{210}Pb in dried plants was determined in cistus – 35.5 Bq·kg^{-1} dry wt, while the lowest was in milk thistle – 3.25Bq·kg^{-1} dry wt what gives respectively for cistus 46.1±0.7 and 6.50±0.29 mBq for milk thistle per one teabag. The extraction efficiencies in the filtered water oscillated from 5.1±0.5 for milk thistle to 27.3±0.8 % for cistus, while for the tap water they ranged from 7.3±0.6 % for lime to 33.3±2.2 % for white mulberry.

The studies indicated the analyzed herbal teas consumption should not contribute significantly to the annual effective radiation dose in Poland (3.3 mSv) as well as the ICRP international limit given for the public (1 mSv annually). The highest annual effective radiation dose from ^{210}Po ingestion with herbal teas infusions was calculated for white mulberry (3.42±0.09 for tap water and 2.72±0.007 μSv for filtered water), while the lowest in tap water fennel infusion (0.30±0.02 μSv), while in filtered water for milk thistle (0.18±0.02 μSv). The lowest annual effective radiation dose from ^{210}Pb decay ingested with herbal teas infusions (one glass daily) was calculated for milk thistle (0.18±0.01 for tap water and 0.08±0.01 μSv for filtered water), while the highest dose would come with white mulberry tea made in tap water (3.15±0.19 μSv), and for cistus in filtered water (3.17±0.08 μSv).

Measurement of natural radioactivity in a high background radiation area in Palawan, Philippines

L.H. Palad[1], C.O Mendoza[1], K. Iwaoka[2], C.P Feliciano[1], P.F. Cruz[1], F. M Delacruz[1]

[1]Health Physics Research Section, Atomic Research Division,
Department of Science and Technology – Philippine Nuclear Research Institute (DOST-PNRI), Commonwealth Avenue, Diliman, Quezon City, 1101, Philippines.
[2]National Institutes for Quantum and Radiological Sciences and Technology,
4-9-1 Anagawa, Inage, Chiba, 263-8555, Japan.
Keywords: Natural radionuclides, HBNRA, gamma radiation
Lorna H. Palad, e-mail: ljhpalad@pnri.dost.gov.ph

Natural radiation that is present in the earth's crust is due to the presence of primordial radionuclides primarily the ^{238}U series, ^{232}Th series and ^{40}K. Naturally occurring radionuclides in soils are the major contributors of outdoor terrestrial radiation to which humans are exposed to continuously. The associated external exposures due to gamma radiation emitted from these radionuclides vary depending on the geographical and geological conditions in the different regions of the world. High background natural radiation areas (HBNRAs) which are found in some areas in the world are due to enhanced level of natural radionuclides. Many countries have made investigative studies in these HBNRAs due to increasing concern on the adverse health effects of exposure to high natural radiation background. An HBNRA is located along the coastal areas of San Vincente, Palawan, Philippines. With the operation of a newly constructed domestic airport and the plans for establishment of beach resorts, the human health effects of exposure to enhance levels of naturally occurring radionuclides in these areas are deemed necessary for radiation protection of local residents and the tourists alike. In this study, activity concentrations of natural radionuclides will be determined in the HBNRA in San Vicente, Palawan.

Soil samples were collected in Barangay Sto Nino and the beach HBNRA areas of San Vicente. The soils were dried at 105^{0}C in a conventional drying oven and individually placed in 250 ml polyethylene bottles. The tightly sealed containers were allowed to stand for 30 days to reach secular equilibrium between radium-226 and its decay products. The activity concentrations of ^{238}U (^{226}Ra) series, ^{232}Th(^{228}Ra) series and ^{40}K radionuclides were measured using a gamma ray spectrometer coupled with a high purity germanium detector. Gamma lines of ^{214}Bi (609 KeV), ^{228}Ac (911KeV) and ^{40}K (1460KeV) were used to calculate activity concentrations of ^{226}Ra, ^{232}Th and ^{40}K respectively.

Figure 1. An aerial view of the coastal town of San Vicente, Palawan (Google, 2015).

The activity concentrations of natural radionuclides particularly ^{232}Th in soil samples were elevated relative to typical background natural radioactivity values obtained in the Philippines, but lower than the relevant values in the IAEA Safety Standards (IAEA, 2004). The results of this study can serve as reference for radiological impact assessment studies and regulations in the country.

IAEA. 2014. Safety Standards, Radiation Protection and Safety of Radiation Sources: International Basic Safety Standards. General Safety Requirements Part 3. Vienna.

Plutonium-239 and -240 in Lacustrine sediments in an Alpine lake, SW China: distributions and source identification

Shaoming Pan[1], Haiting Guo[1], Yihong Xu[2]

[1]School of Geographic and Oceanographic Sciences, Nanjing University, Nanjing210023, P.R. China. *span@nju.edu.cn*
[2] School of Geography and Tourism, Anhui Normal University, Wuhu 241002, P.R. China. *yhxu@ahnu.edu.cn*

Two sediment cores (30cm and 44cm in length, respectively) collected from an alpine ice-scour lake (Tingming Lake, 3900 ma.s.l.) in south-western China were analysed for plutonium isotopes to elucidate their source terms and deposition history. The average 240Pu/239Pu atomic ratios in the two sediment cores were 0.182±0.029 and 0.183±0.03, respectively, indicating that Pu originated from the global atmospheric fallout. The two 239+240Pu depth profiles showed that plutonium was mainly distributed in the surface layer, indicating that the distribution of Pu isotopes in the two sediment cores were dominated by downward diffusion. An ADE-Peak model was applied to simulate the distribution of Pu isotopes in the two sediment cores and the simulated values fitted by ADE model were coincident very well with the measured values with the Goodness-of-fit coefficient of 0.932. Total Plutonium-239 and -240 inventories of the two sediment cores were calculated to be 56.3 Bq/m2 and 63.9 Bq/m2 respectively, with an average inventory of 60.1Bq/m2, significantly higher than the integrated atmospheric fallout of 36 Bq/m2 for 20-30°N published in UNSCEAR(2000), but comparable with the global fallout Pu inventory (50.7 Bq/m2) obtained in the Lake Hongfeng which located in similar latitude. The sedimentation rate calculated by the 1963/1964 maximum peak was consistent with the one obtained by ADE-Peak model. Our data suggested that the studied Tingming Lake would be an ideal setting for mornitoring atmospheric fallout and environmental changes in SW China.

Radionuclides root uptake of and biometric traits of onion (*Allium cepa* L.) under hydroponic cultivation with ^{137}Cs and ^{243}Am

T.A. Paramonova[1], N.V. Kuzmenkova[2], M.M. Godyaeva[1], and E.O. Slominskaya[1]

[1]Faculty of Soil Science, Lomonosov Moscow State University, Moscow, 199991, Russia
[2]Chemistry Faculty, Lomonosov Moscow State University, Moscow, 199991, Russia
Keywords: long-lived anthropogenic radionuclides, hydroponics, root uptake and translocation, biometric traits
Presenting author, e-mail: kuzmenkova213@gmail.com

Long-lived anthropogenic radionuclides caesium-137 (^{137}Cs) and americium-243 (^{243}Am) are characterized by distinctly different atom structure, chemical properties and geochemical behaviour in environment. It is reasonable to assume quite different features of the radionuclides migration processes in "soil-plant" or "nutrient solution-plant" systems.

A hydroponic experiment with ^{137}Cs- and ^{243}Am-containing solutions (495 kBq l^{-1} and 18.4 kBq l^{-1} correspondently) was conducted for 27 days (until reaching the growth stage of leaves development) to estimate intensity of the radionuclides root uptake by onion (*Allium cepa* L.) and their influence on bioproduction process (through biometric traits of plants). The control plants were cultivated on tap water. Upon the end of growing procedure digital autoradiography, γ-spectrometry, direct measurements of biomass fractions' size and weight, as well as special processing of digital images of the onion's roots in the *Aria* program were used.

Bioavailability of the both radionuclides in conditions of hydroponics was rather small: only 3.5% of ^{137}Cs and 0.7% of ^{243}Am have been incorporated into plant tissues from solutions. The autoradiography and γ-spectrometry data revealed in this case predominant accumulation of the radionuclides in onion roots (table 1) and hence confirmed the barrier function of the underground parts of plants (Shaw et al., 1992; Soudek et al., 2006; Straczek et al., 2010; etc.).

Table 1. Characteristics of ^{137}Cs and ^{243}Am accumulation in onion biomass.

Index	Biomass compartment		
	roots	bulbs	leaves
^{137}Cs activity, kBq g^{-1}	318	8	47
^{137}Cs inventory per 1 plant, kBq	3351	125	843
% of ^{137}Cs inventory	77.6	2.9	19.5
TF_{agg}* for ^{137}Cs	0.321	0.008	0.047
^{243}Am activity, kBq g^{-1}	2.88	0.12	0.002
^{243}Am inventory per 1 plant, kBq	30.61	2.29	0.04
% of ^{243}Am inventory	92.9	6.9	0.1
TF_{agg}* for ^{243}Am	0.078	0.003	<0.01

* TF$_{agg}$ – aggregated transfer factor = kBq g^{-1} in plants / kBq in solution

About 80% of ^{137}Cs and more than 90% of ^{243}Am in plant biomass were deposited in onion's roots. No wonder that the principal effects of radionuclide-plant interaction were fixed in this compartment. The most sensitive indicator seemed to be the root surface area that was significantly reduced by the factor ≈1.5 for ^{137}Cs-containing hydroponic solution and by ≈2.5 times for ^{243}Am-containing solution (table 2). This was due to the suppression in formation of the total number of adventitious roots, the tendencies toward a decrease in general elongation, and a slight decrease in root diameter.

Table 2. Average values and variability of biometric characteristics of onion under ^{137}Cs and ^{243}Am hydroponic cultivation and in control conditions.

Trait	Variant		
	^{137}Cs	^{243}Am	control
Average length of the maximum leaf, mm	237±28*	229±17	276±8
Average length of the maximum root, mm	300±26	312±23	324±56
Average length of roots, mm	260±13	194±15	257±11
Average diameter of roots, mm	1.06±0.04	1.07±0.08	1.21±0.13
Average root surface area, cm^2	150±4	75±4	192±10
Average number of leaves/roots	3.5/28.3	3.3/18.8	3.0/31.2
Total biomass, g**	0.35±0.08	0.35±0.06	0.37±0.09
Root biomass, g	0.08±0.02	0.09±0.02	0.09±0.02
Bulb biomass, g	0.12±0.04	0.14±0.03	0.14±0.05
Leaf biomass, g	0.14±0.03	0.12±0.04	0.13±0.04

* Confidence limits of the mean was calculated as $\pm t_{0.95} \cdot m$ at n=10
** Absolutely dry weight per 1 plant

At the same time, general root bioproduction process, as well as bulbs and shoots growth, apparently was unaffected by the radionuclides – absolutely dry weight of onion plants and biomass structure were nearly the same in all variants of the experiment. In the shoots, only a slight decrease in length was observed under cultivation with ^{137}Cs and ^{243}Am, but the average number of onion leaves even slightly increased.

Thus, even under conditions of extremely high radionuclide activity in hydroponic solutions, their transfer into the onion is significantly limited. Roots of onion successfully act as biological barrier against ecotoxicants, but some biometric traits can be affected.

Shaw, G., Hewamanna, R., Lillywhite, J. et al. 1992. Radiocaesium uptake and translocation in wheat with reference to the transfer factor concept and ion competition effects. *J. Envir. Radioact.* 16, 167–180.

Soudek, P., Valenova, S., Vavrikova, Z. et al. 2006. ^{137}Cs and ^{90}Sr uptake by sunflower cultivated under hydroponic conditions *J. Environ. Radioact.* 88, 236–50.

Straczek, A., Duquene, L., Wegrzynek, D. et al. 2010. Differences in U root-to-shoot translocation between plant species explained by U distribution in roots *J. Environ. Radioact.* 101, 258–66.

Sequential determination of $^{234, 235, 238}$U, $^{228, 230, 232}$Th, $^{238, 239+240}$Pu, and ^{241}Am in sediment

J. Y. Park[1*], J. M. Lim, H.C Kim, Y. G. Ko, W.N. Lee

[1]Environmental Radioactivity Assessment Team, Korea Atomic Energy Research Institute, Korea, 111 Daedeok-daero 989 beon-gil, Yuseong,gu, Daejeon, 34057, Korea
Keywords: Actinide, Plutonim, Uranium, Americium, Thorium, Radiochemisty
Presenting author, e-mail: pjyoung@kaeri.re.kr

There is a growing need to develop rapid actinides analysis methods for emergency response in addition to routine environmental monitoring because actinides (e.g. Pu, Am, U, etc.) have been well known as hazardous elements owing to their toxicity to human health. Therefore, the rapid actinide analysis has been in the limelight not only in the environmental studies for the trace of anthropogenic nuclear activities, the migration of actinide into various environments and the routine environmental monitoring, but also in the radwaste management field that require fast and accurate analysis of a lot of samples.

For accurate identification and quantification of alpha emitting radionuclides in samples, they are required to be separated and purified from each other. The separation and purification are the time-consuming stage in the whole process for the determination of the nuclides. Therefore, a rapid and reliable determination method of the radionuclides is needed to shorten the radiochemical analysis time.

In this study, a procedure for the sequential determination of ^{234,235,238}U, ^{232,230,228}Th, $^{238,239+240}$Pu and ^{241}Am was developed for use of radiological event or routine environmental monitoring. The evaluation of the developed method was carried out using reference materials that include various interesting alpha isotopes in the environmental radioactivity level.

A lithium meta-borate fusion technique was applied to dissolve samples completely within an hour in our developed analysis method. The complete sample dissolution is essential to obtain reliable results for the determination of radionuclide isotopes. Radionuclides in samples were concentrated using a co-precipitation technique and purified by only two extraction chromatography columns packed with TEVA® and TRU® resins (Eichrom) respectively, that were connected in tandem [1,2]. A tandem column system separates Pu/Th and U/Am from the matrix of a sediment sample at TEVA and TRU columns easily and rapidly. Following the elution of radionuclides from the columns, the eluted radionuclides were electrodeposited on the planchet for the determination of their activity using an alpha spectrometer. The potential effect of the transition metals in matrix on alpha spectra was also assessed by the analysis of transition metals in eluted solutions.

This work offers rapid, simple and robust analytical method to determine activities of ^{234,235,238}U, ^{232,230,228}Th, $^{238,239+240}$Pu and ^{241}Am in the sediment sample with high tracer recovery yield and very high peak resolution in alpha spectra.

[1] Maxwell, S.L.mailto:sherrod.maxwell@srs.gov 2006. Rapid column extraction method for actinides and $^{89/90}$Sr in water samples. *J Radioanal Nucl Chem*, 267(3), 537-543.

[2] A. Habibi, B. Boulet, M. Gleizes, D. Larivière, G. Cote. 2015. Rapid determination of actinides and ^{90}Sr in river water. *Anal. Chim. Acta*, 883, 109-116.

Estimation of annual internal exposure to Uranium in foods consumed in Korea

Jaewoo Park, Jung-Seok Chae, Yong-Jae Kim

Korea Institute of Nuclear Safety, 34142, Republic of Korea
Keywords: Internal dose, Uranium, food, ingestion
Presenting author, e-mail: jschae@kins.re.kr

Human beings are exposed to natural radiation in the environment. Dietary intake of naturally occurring radionuclides in food can results in internal exposure in human body. In this study, the annual internal dose from ingestion of Uranium (^{234}U, ^{235}U, ^{238}U) in several foods consumed in Korea is estimated.

300 samples from 7 kinds of food categories were collected in Korea in 1998~2000 by Korea Institute of Nuclear Safety (KINS, 2005). The collected samples were the most frequently consumed foods in Korea, such as rice, pork, etc. The uranium radioactivity measurement was conducted by alpha spectrometry, and the specific activity per samples were determined.

The annual internal dose from radionuclides in foods was calculated using the following equation:

$$D_i = (D_f)_i \times U_i \times C_i$$

Where D is the annual internal dose (μSv yr^{-1}); D_f is the dose conversion coefficient (μSv Bq^{-1}); U is the annual intake amount of food (kg yr^{-1}); C is specific activity of ^{234}U, ^{235}U and ^{238}U. The annual intake amount by food type were determined by the statistical data collected by the Korea Centers for Disease Control & Prevention (KCDC, 2017). The dose conversion coefficients used for ^{234}U, ^{235}U and ^{238}U were 0.049 μSv Bq^{-1}, 0.047 μSv Bq^{-1} and 0.045 μSv Bq^{-1}, respectively (ICRP, 1996).

The average activity concentrations of U isotopes in foods and the estimated annual internal dose are presented in Table 1. The total annual internal dose from intake of U in foods were 0.167 μSv ranged from 0.0002 (Cutlass fish, Red pepper and Garlic) to 0.0450 μSv (Bean sprout).

Table 1. Average specific activities of U in foods and estimated internal dose.

Food Type	Concentration (mBq/kg-fresh)			Internal dose (μSv/y)
	^{234}U	^{235}U	^{238}U	
Milk	6.1	0.39	5.2	0.014
Pork	6.3	0.39	5.3	0.010
Beef	2.4	0.48	2.1	0.002
Chicken	11	0.59	8.8	0.011
Wheat	4.6	0.50	4.2	0.001
Soybean	24	<MDA	23	0.002
Rice	1.0	0.22	0.9	0.005
Cutlass fish	6.1	<MDA	5.8	0.0002
Mackerel	7.9	<MDA	7.0	0.001
Alaska pollock	36	2.0	34	0.005
Squid	60	2.4	53	0.009
Apple	2.4	0.16	2.3	0.004
Persimmon	2.9	<MDA	2.2	0.001
Tangerine	2.2	<MDA	1.9	0.001
Pear	1.6	<MDA	1.6	0.001
Grape	2.2	<MDA	1.8	0.001
Potato	1.0	<MDA	1.1	0.001
Sweet potato	2.4	<MDA	1.9	0.001
Radish	2.2	<MDA	1.9	0.002
Chinese cabbage	2.4	<MDA	2.2	0.006
Red pepper	1.5	0.43	1.3	0.0002
Garlic	1.5	<MDA	1.2	0.0002
Onion	1.1	<MDA	1.0	0.001
Pumpkin	1.4	<MDA	1.3	0.0004
Lettuce	13	<MDA	13	0.003
Spinach	18	<MDA	18	0.004
Bean sprout	150	6.1	143	0.045
Scallion	5.3	<MDA	5.1	0.002
Oyster	404	13	358	0.014
Manila clam	273	9.9	253	0.011
Mussel	231	6.6	202	0.008
Total				0.167

Korea Institute of Nuclear Safety (KINS), 2005. Assessment of Radiation Risk for the Korean Population (KINS/GR-300-2).

Korea Centers for Disease Control & Prevention, 2017. Korea National Health and Nutrition Examination Survey (KNHANES).

International Committee of Radiological Protection (ICRP), 1996. Age dependent doses to members of public from intake of radionuclides: compilation of ingestion and inhalation coefficients. ICRP Publication 72. Elsevier Science.

Assessment of tritium in air humidity, precipitation and surface water using liquid scintillation counting and isotope ratio mass spectrometry

G. Pédehontaa-Hiaa [1], V. Barkauskas [2], C. Nilsson [2] and K. E. Stenström [2]

[1] Medical Radiation Physics Malmö, Department of Translational Medicine, Lund University, Malmö, Sweden
[2] Nuclear Physics Division, Physics Department, Lund University, Lund, Sweden
Keywords: Tritium, European Spallation Source, Liquid Scintillation Counting, Isotope Ratio Mass Spectrometry
Guillaume Pédehontaa-Hiaa, e-mail: guillaume.pedehontaa-hiaa@med.lu.se

Tritium is a naturally occurring beta emitter ($t_{1/2}$ = 12.3 years). Its prevailing form in the environment is tritiated water (HTO). The natural background levels of tritium, resulting from nuclear reactions involving cosmic radiation and atmospheric gases, are between 0.1 and 0.6 $Bq \cdot L^{-1}$ of water (IRSN, 2012). Man-made tritium mainly originates from testing of hydrogen bombs in the 1960's. Tritium levels from the bomb pulse are decreasing globally, however, locally elevated concentrations can be found due to other anthropogenic activities, e.g. neutron activation in nuclear reactors or spallation reactions in accelerator facilities.

The European Spallation Source (ESS), an upcoming most powerful neutron source, is under construction near the centre of Lund, Sweden. The spallation reaction in the ESS tungsten target as well as the activation of materials by its 5 MW linear proton accelerator will generate a wide range of radionuclides including tritium (^3H). Tritium is expected to dominate the source term of continuous radioactive effluents (in $Bq \cdot year^{-1}$). The total tritium activity in the target system has been estimated to reach ~ 10^{15} Bq after 1 year of operation (Ene *et al.*, 2015) and approximately 0.6 TBq is anticipated to be released annually through the main stack (Ene, 2016) mainly as HTO.

The first purpose of this study was to assess the current levels of tritium in Lund area prior the start of operation of the ESS in order to establish local background values. The second aim was to identify possible sources of contamination since several accelerator facilities as well as facilities handling tritium-containing materials are present in the area.

Monthly samples of precipitation (30 d of collection) and air humidity (1 h of collection) were collected at the ESS site. Monthly air humidity urban background as well as tritium-depleted water from a well-characterized aquifer were also sampled.

Regarding surface water, two ponds in a 1 km radius of the ESS target and an urban background pond 5 km away were also sampled monthly.

Samples were analyzed both by liquid scintillation counting (LSC) to measure tritium and $^2H/^1H$ isotope ratio mass spectrometry (IRMS) to measure the hydrogen isotope fractionation in the water (Bernhardsson, 2018).

The activity concentration of tritium measured over a year (from May, 2018 to April, 2019) were only a few $Bq \cdot L^{-1}$. Expected seasonal variations were observed, in particular an increase during the spring (spring leak phenomenon). No significant environmental contamination from the local anthropogenic activities was detected during the sampling campaign.

This work was partly funded by the Swedish Radiation Safety Authority (grant SSM2018-1636-1).

IRSN, 2012, Tritium and the environment.

D. Ene, K. Andersson, M. Jensen, S. Nielsen, and G. Severin, 2015, Management of Tritium in European Spallation Source, *Fusion Sci. Technol.*, 67, 2, 324–327

D. Ene, 2016, Source Term to the Environment from the ESS Target Station, *Proceedings of SATIF13 workshop*, 32–47.

Bernhardsson, C., Eriksson Stenström, K., Jönsson, M., Mattsson, S., Pedehontaa-Hiaa, G., Rääf, C., Sundin, K., et al., 2018, *Assessment of "Zero Point" radiation around the ESS facility.* Report MA RADFYS 2018:01, Report BAR-2018/04. Lund University. Lund.

A new method for the measurement of Ra-isotopes by alpha-particle spectrometry with Si detectors

S. M. Pérez-Moreno[1] M.J. Gázquez[2], M. Casas-Ruiz[2]; E.G. San Miguel[1]and J.P. Bolívar[1]

[1]Departament of Integrated Sciences, University of Huelva, Huelva, Spain.
[2] Department of Applied Physic, University of Cádiz, Cádiz. Spain.
Keywords: *Ra quartet*, *^{225}Ra* tracer, alpha-particle spectrometry, 225Ac removing
Presenting author, e-mail: bolivar@uhu.es

The Ra-isotopes as environmental tracers are recently being widely used, and therefore a rapid and reliable measuring method of these isotopes by alpha-particle spectrometry is needed. The main problem of this technique is the use of an appropriate internal tracer in order to know the chemical yield of the radiochemical process. For the measurement of the radium quartet (^{226,226,223,224}Ra), ^{225}Ra ($T_{1/2}$=14.8 d) in equilibrium at the beginning with ^{229}Th ($T_{1/2}$ = 7.34 10^3 y), is commonly used. ^{225}Ra is a pure beta emitter and the recovery yield must be evaluated by its daughter ^{225}Ac (α-emitter), which shows spectral interferences with other radionuclides, therefore its counts in the α-spectrum is determined through ^{217}At, its short half-life α-emitter daughter. In addition, in a specific radiochemical step it is needed to ensure the total removing of ^{225}Ac from ^{225}Ra to ensure the correct Ra yield evaluation.

Thus, an improved method of Ra isolation was tested (Perez-Moreno et al, 2019). The radiochemical method is based on the method described in Maxwell and Culligan (2012), who used three different resins. In this work several changes in the radiochemical process were carried out for ensuring the total elimination of Ac from the fraction containing radium, only using two resin.

The main novelty of this work is to carry out the aliquot containing Ra coming from Th removing to1.5 M HCl + 1.5 M ascorbic acid medium, to minimize the impact of any Fe^{3+} present. This sample is passed through the AG50X8 resin (Ra and Ac are retained with a high efficiency), and then Ac is eluted by washing the column with NH_4Ac in 0.1M HNO_3 (Perez-Moreno, et al 2019).

Subsequently, the $BaSO_4$ micro-precipitation was performed to obtain the thin source for alpha counting (Pérez-Moreno et al., 2019), showing a high resolution, see Figure 1.

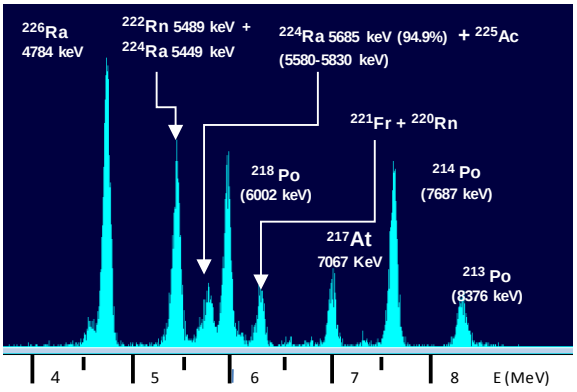

Figure 1. Alpha spectrum from IAEA 447.

The validation of the method was made by the measurement of several certified reference materials (CRM) (see Table 1) and participating in a proficiency test organized by the Spanish Nuclear regulatory Council (CSN). The agreement of our lab measurements with the certified reference materials ones was proved by applying the Z-score methodology.

Table 1. Results obtained (Bq/kg) for certified samples.

		Certified (Bq kg^{-1}) (95% C.I.)	**A(Bq/kg)**	**z-score**
IAEA-RGU-1	^{223}Ra*	228 (226 - 230)	203 ± 14	1.78
	^{226}Ra	4940 (4910 - 4970)	4810 ± 250	0.50
IAEA-375	^{226}Ra	20 (18-22)	22.1 ± 1.8	1.01
	^{228}Ra**	21 (17-25)	27 ± 6	0.95
	^{224}Ra***	20.5 (19.2-21.9)	49 ± 15	1.90
UTS-1	^{228}Ra	680 ± 210	620 ± 50	0.52
	^{224}Ra***	680 ± 210	690 ± 90	0.08
	^{226}Ra	3700 ± 200	3880 ± 230	0.72
IAEA-448	^{226}Ra	19050 ± 260	19160 ± 790	0.14
IAEA-434	^{226}Ra	780 ± 62	740 ± 28	0.02

* secular equilibrium with ^{235}U, ** secular equilibrium with ^{228}Ac, *** secular equilibrium with ^{232}Th

All Z-score values of fractions are lower than 2, showing that it is not possible to reject the null hypothesis with a confidence level of 95 %. Thus, there are no statistically significant differences between the measured concentrations and the certified ones.

This research has been partially supported by the SpanishGovernment Department of Science and Technology (MINECO) (Ref. CTM 2015-68628-R).

Pérez-Moreno S.M., Gázquez M.J., Casas-Ruiz M., San Miguel E.G., Bolívar J.P. 2019. An improved method for radium-isotopes quartet determination by alpha particle spectrometry by using ^{225}Ra (^{229}Th) as isotopic tracer. *J Environ Radioactiv*. 196, 113–124

Maxwell S. L and Culligan B. K., 2012. Rapid determination of ^{226}Ra in environmental samples. *J Radioanal. Nucl. Chem*. 293, 149–156.

Space-time Bayesian analysis of the environmental impact of a dismissing nuclear power plant

A. Petraglia[1], C. Sirignano[1], R. Buompane[1], A. D'Onofrio[1], A. M. Esposito[2], F. Terrasi[1], C. Sabbarese[1],

[1]CIRCE, Dipartimento di Matematica e Fisica, Università degli studi della Campania "L. Vanvitelli" Caserta, Italy
[2]Sogin, Garigliano NPP, Sessa Aurunca (Caserta)
Keywords: NPP, radionuclides, actinides, AMS,
Presenting author, e-mail: carlo.sabbarese@unicampania.it

The decommissioning of a Nuclear Power Plant (NPP) that has completed its productive cycle often presents more societal issues than radiation protection problems. The needed knowledge and techniques to accomplish the series of operations of decontamination of the technological structures and buildings of the plant and their removal under safety conditions are fully acquainted, but the aspect related to the impact on the public opinion needs full attention. Since 2000 a group of physicists of the University of Campania "L. Vanvitelli" (before Second University of Naples) has started a research program in collaboration with the engineers of the Sogin (Society for the management of the Italian nuclear plants) of the Garigliano Nuclear Power Plant (NPP), located in Southern Italy and shut down in 1979. The aims of this collaboration were to verify and update the survey methodology, assess the impact of decommissioning on the environment and communicate the results to the society, in order to improve the awareness on the activities carried out on the site. In particular, the state of the environment radioactivity in the area surrounding the Garigliano NNP has been recorded over the years with different radio-ecological campaigns, aiming to acquire the current situation and to address the sources of both natural and anthropic radioactivity. In this contribution, a reconstruction of the spatial and temporal variations over 30 years, after the NPP stop, is presented using a Bayesian approach. This solves the issues related with the application of frequentist methods to non-normal data distributions, small groups, and the presence of values below the minimum detectable activity. Modelling, calculations and tests were performed using the software R [R] in the framework Rstudio [Rstudio].

Statistical analysis plays a fundamental role in the data analysis of a pollutant in the environment. Among other analyses the comparison between different groups is of particular importance. The groups may refer to different geographical areas, periods of measurement, population groups, and so forth. However, the values corresponding to a given group show a statistical variation from sample to sample, which open a number of possibilities to the experimenter regarding the comparison with other data sets. The commonly used methods are based on qualitative analyses and significance test of the null hypothesis: t-test and analysis of variance, belonging to the frequentist approach.

Spatial variations are studied by collecting samples in several points of the plain of the Garigliano and in some points of the Sele plain, geologically similar to the Garigliano plain, but geographically far away (about 130 km). The temporal analysis was performed based on the results of the three campaigns carried out in the surroundings of the Garigliano NPP in 2001/2002, in 2008/2009 and in 2015/2016 respectively.

In these campaigns, the specific activities of radionuclides in air, groundwater, soil and plant matrices of particular interest have been measured using high energy resolution and low background γ spectrometry (Sabbarese, 2005; Petraglia, 2012) and, in the last campaign, even more sophisticated techniques, AMS and ICPMS, (Petraglia, 2017) were applied to measure isotopes of uranium and plutonium. Superficial unspoiled soils samples were collected in all the environmental campaigns. The Bayesian comparison of their γ specific activities, in particular of the anthropogenic radionuclide ^{137}Cs, makes it possible to frame the environmental situation over time, allowing us to focus on possible sources of pollution.

The analysis shows that the values of γ specific activity in soil are dominated by the natural sources. The anthropogenic contribution, updated for the half-life of the radionuclides, is consistent over the years, with no new contributions in the last decades. The results are consistent with those obtained in the alluvial plain of the Sele river, at a considerable distance from NPP.

These results mainly indicate the fallout from atmospheric nuclear testing during the Cold War years and from the Chernobyl accident as source.

Sabbarese, C., Esposito, A. M., Visciano, L., D'Onofrio, A., Lubritto, C., Terrasi, F., Roca, V., Alfieri, S., Migliore, G. 2005. A Monitoring network of the radioactive releases due to Garigliano nuclear power plant decommissioning. *Radioprotection.* 40, Suppl. 1, 797-802.

A. Petraglia, C. Sabbarese, M. De Cesare, N. De Cesare, F. Quinto, F. Terrasi, A. D'Onofrio, P. Steier, L. K. Fifield, A. M. Esposito. 2012. Assessment of the radiological impact of a decommissioning nuclear power plant in Italy. R*adioprotection.* 47, n.2, 285-297.

A. Petraglia, A., Sirignano, C., Buompane, R., D'Onofrio, A., Sabbarese, C., Esposito, A. M., Terrasi, F. 2017. *A*ctinides measurements on environmental samples of the Garigliano Nuclear Power Plant (Italy) during the decommissioning phase. ISBN 9786099551142. *Proceedings of the 4th International Conference on Environmental Radioactivity - ENVIRA 2017*.

Air radioactivity monitoring in Monaco (1998-2018)

Mai Khanh Pham

1IAEA-Environment Laboratories, Monte Carlo, 98000, Monaco
Keywords: Air monitoring, radionuclides, Monaco, Fukushima, Chernobyl
Presenting author, e-mail: m.pham@iaea.org

Air radioactive quality monitoring in IAEA-Environment Laboratories, Monaco has been carried out from early 1960's. The radionuclides of high interested such as ^{7}Be, ^{137}Cs and ^{210}Pb (of different origin) on aerosol filters and in the wet and dry fallout have been regularly analysed from 1998 to 2018. Investigation of the behaviour of these radionuclides in the atmosphere is an important prerequisite for radioecological assessment studies, especially for possible accidental releases of radionuclides from nuclear installations. For the former case, the maximum ^{7}Be activity concentration was observed in 2009, and the minimum ones in 2000 and 2018, following the influence of the solar modulation of cosmic rays on the production rates of ^{7}Be in the atmosphere by solar activity, respectively (Fig.1). The peaks of ^{137}Cs activity concentration found in May-June 1998 was due to the accident at Algeciras in Spain and the one found in March 2011 was due to Fukushima accident (Pham et al, 2012) (Fig.2). The deposition velocities of ^{7}Be, ^{137}Cs and ^{210}Pb depended on the precipitation rate, and attained maximum values during dry seasons. These ongoing observations confirm our previous studies from 1998 to 2010 (Pham et al., 2011)

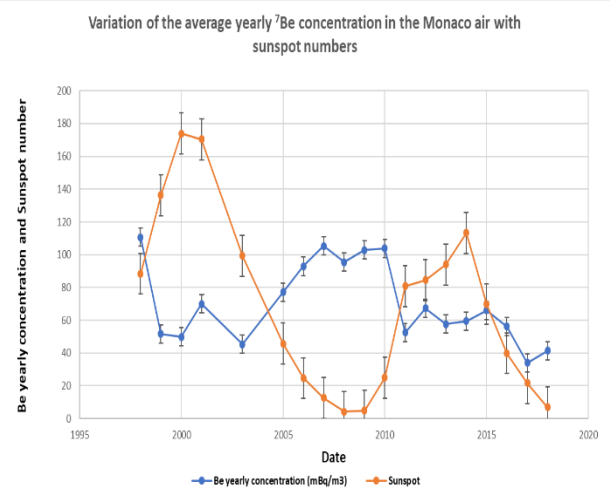

Figure 1. Variation of the average yearly ^{7}Be concentration in the Monaco air (blue) with sunspot numbers (orange; data extracted from SDIC data base http://www.sidc.be).

For the latter case, temporal variations of ^{7}Be, ^{210}Pb and ^{137}Cs activity concentrations in precipitation in Monaco from 1998 to 2018 showed that maxima of ^{7}Be and ^{210}Pb deposition fluxes which coincide with the peaks of precipitation amounts observed in different months of a year. Most of ^{7}Be and ^{210}Pb was washout from the atmosphere by precipitation. The seasonal variations were not uniform from year to year, and the amount of precipitation controlled the deposition fluxes of ^{7}Be and ^{210}Pb, which was not the case for ^{137}Cs. The precipitation-normalized deposition fluxes of ^{7}Be, ^{210}Pb and ^{137}Cs were generally higher during summer time. Activity ratios of ^{7}Be/^{210}Pb observed in winter and fall were generally higher than during summer and spring. Similar seasonal variations of deposition fluxes have been observed in Monaco during 1998-2010 (Pham et al., 2013)

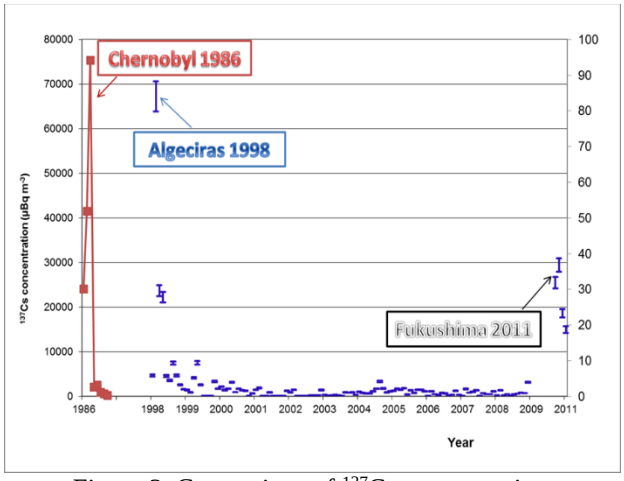

Figure 2. Comparison of ^{137}Cs concentration in the Monaco air from the Fukushima accident with the Chernobyl one (note: ^{137}Cs values of Algeciras and Fukushima events are on the right vertical axis).

Pham, M. K. et al. 2011. Temporal changes of ^{7}Be, ^{137}Cs and ^{210}Pb activity concentrations in surface air at Monaco and their correlation with meteorological parameters. *J. Environ. Radioact.* 102, 1045-1054.

Pham, M. K. et al. 2012. Detection of Fukushima Daiichi nuclear power plant accident radioactive traces in Monaco. *J. Environ. Radioact.* 114, 131-137.

Pham, M. K. et al. 2013. Dry and wet deposition of ^{7}Be, ^{210}Pb and ^{137}Cs in Monaco air during 1998-2010: Seasonal variations of deposition fluxes. *J. Environ. Radioact.* 120, 45-57.

Radionuclide speciation of the transuranic radionuclides in the albic podzols (arenic)

Popova M.[1]

[1]Vernadsky Institute of Geochemistry and Analytical Chemistry of Russian Academy of Sciences
Keywords: radioecology, radionuclide speciation, Kola Peninsula
marbpop@gmail.com

The species of radionuclides in soil determines the intensity and ability of their migration. It indicates the importance of their study because it is the soil that is the main depository of radionuclides in terrestrial ecosystems, showing barrier properties and protecting adjacent environments from anthropogenic contamination (Salbu et. al, 2004). Chemical fractionation of radionuclides in podzols of the background territories remains poorly understood. Currently, such data for transuranic elements are not available in the literature.

Since the ^{237}Np and ^{239,240} Pu activities in the Northern podzols are extremely low, the speciation of these radionuclides studied by setting a model experiment according to the method of sequential extractions of Fanni Pavlotskaya (Pavlotskaya, 1974). Due to this technique, 20 g soil samples were taken from E, B1f and C genetic horizons of albic podzols. Then, 0.3 ml of enriched solution containing 3.3*10-5 g/ml of ^{237}Np and of 0.03 ml enriched solution containing 1500 Bq of ^{239,240}Pu were introduced into the dry soil samples. Within 3 months, these samples were mixed regularly to achieve homogeneity of distribution. Further, 2 g of soil was selected from each sample for sequential processing by extractors according to the methodics. The results are shown in the table 1. Fractions F1-F5 represent water-soluble, exchangeable, acidsoluble (1N and 6N HCl) and fixed forms of radionuclides.

According to the data obtained, ^{237}Np has a high mobility in the albic podzols. More than 60% of this radionuclide is concentrated in a form available for biological uptake.

Plutonium in the podzols have also been much more mobile than in other soils of Russia; its content in water-soluble form 5 times exceeds the same indicator for soils in Central Russia (Goryachenkova et. al, 2005).

Table 1. Speciation of the transuranic radionuclides, %.

Form	^{239}Pu			^{237}Np		
	E	B_1f	C	E	B_1f	C
F1	3	1	3	40	25	44
F2	25	38	22	29	28	18
F3	20	24	36	5	21	9
F4	30	32	27	2	15	22
F5	21	5	12	23	10	7

In conditions of soil poverty with organic matter, exchange cations and clay minerals, transuranic radionuclides exhibit much greater mobility in them than in previously studied soils of Russia (Goryachenkova et. al, 2005). That means an increased risk of biological uptake and food chain migration in Northern taiga ecosystems.

This work was supported by the Russian Science Foundation project №17-17-01212.

Salbu, B., Lind, O.C., Skipperud, L. 2004. Radionuclide speciation and its relevance in environmental impact assessments. *J. of Env. Radioactivity*. 74. 233-242.

Pavlotskaya, F.I. 1974. *Migration of the radioactive product of global fallout in soils*. Moscow: Atomizdat. - 216 p. (Rus.)

Goryachenkova, T.A., Kazinskaya I. E., Clark S. B., Novikov A. P., Myasoedov B. F. 2005. Comparison of Methods for Assessing Plutonium Speciation in Environmental Objects. *Radiochemistry*. 47. 599-604.

Radiocarbon and Cs-137 dating of Slovak wines

P.P. Povinec[1], I. Kontuľ[1], S.-H. Lee[2], I. Sýkora[1], J. Kaizer[1]

[1]Faculty of Mathematics, Physics and Informatics, Comenius University, 84248 Bratislava, Slovakia
Korea Research Institute of Standards and Science, Daejeon, Republic of Korea
Keywords: radiocarbon, Cs-137, gas proportional counting, HPGe gamma-spectrometry, wine
Presenting author e-mail: pavel.povinec@uniba.sk

Radiocarbon (C-14) and Cs-137 have been well known as two important anthropogenic radionuclides which were produced in large quantities during atmospheric tests of nuclear weapons carried out mostly by USA and former Soviet Union during fifties and early sixties. The largest US tests were carried out on the Bikini and Enewetak Atolls in the Pacific Ocean, and the Soviet tests were carried mainly on the Novaya Zemlya island in the Kara Sea (the Arctic Ocean) (Livingston and Povinec, 2002). While C-14 was produced during explosions as a result of nuclear reactions of released neutrons with atmospheric nitrogen and oxygen atoms, Cs-137 was fission product released during the explosions.

After signing moratorium on atmospheric nuclear weapons tests in 1963, the concentrations of anthropogenic radionuclides in the atmosphere, hydrosphere and biosphere were decreasing up to now, although smaller contributions, mainly to their atmospheric concentrations, were also observed after atmospheric tests carried out by France and China (Livingston and Povinec, 2002). Maximum concentrations of anthropogenic radionuclides were therefore observed in 1963 in the atmosphere and in 1964 in the biosphere. The largest activity concentrations in the atmosphere were reached for tritium (about thousand times above the pre-nuclear era), while for example for radiocarbon they were 100% above the background (Burchuladze et al., 1989).

As tritium have a short half-life (12.2 y), its concentrations in the environment were decreasing much faster than in the case of C-14 ($T_{1/2}$ = 5730 y) or Cs-137 ($T_{1/2}$ = 30 y). Radiocarbon atoms produced in the atmosphere were incorporated into $^{14}CO_2$ molecules (Povinec et al., 1968) which were then distributed globally, and became part of the carbon cycle, so all organic matter was labelled with C-14 (Burchuladze et al., 1980, 1986). The Cs-137 atoms were attached on atmospheric aerosols and by dry and wet deposition they contaminated soil and biota. Therefore, even at present we can still find in the atmosphere and biosphere C-14 and Cs-137 produced in atmospheric nuclear weapons tests.

It is therefore natural that wine as a typical biospheric product will be labelled with C-14 and Cs-137 atoms, which will work as time clocks. By measuring concentration of C-14 or Cs-137 in wine we may thus determine its age. This radionuclide dating ability would be therefore very useful, especially when dealing with old (even several hundreds of years) wines as there has been activities (because of possible financial profits of about 100k EUR per bottle of red wine) to declare a recent wine as an old one.

Radiocarbon dating of wine was an old idea realized especially during seventies when C-14 levels in the atmosphere and biosphere were high (Povinec et al., 1968). However, in recent years the C-14 levels decreased to such extent that it has been difficult to fix the wine origin before or after the C-14 peak (1964). Similarly, as C-14, Cs-137 has also been used for dating of wine, and as its levels around 1964 were high, it has been possible to measure its levels non-destructively, without opening the bottles. This has been possible because of registration of gamma-radiation associated with Cs-137 (662 keV), while in the case of C-14 (a pure beta-emitter with maximum energy of beta-electrons of 156 keV) a destructive

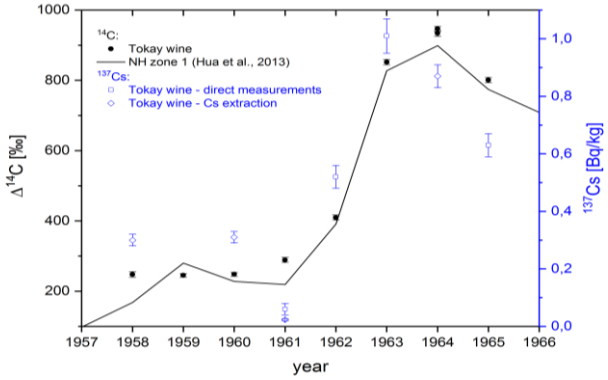

Figure 1. C-14 and Cs-137 levels in Slovak wines.

C-14 analysis is required (at least a mL for accelerator mass spectrometry (AMS), and about 10 mL for gas proportional counting).

Therefore, we came with the idea of a simultaneous C-14 and Cs-137 dating of wine. In the case of C-14 dating, a sample of wine is combusted to produce CO_2, and after its cleaning a CH4 gas was prepared which was analysed in a proportional counter (Povinec et al., 1972, 1978). Another possibility is to prepare graphite targets (Povinec et al., 2015), which can be then analysed by AMS. In the case of Cs-137 dating, the wine can be analysed directly or after radiochemical separation of Cs-137 (Lee et al., 2006) by gamma-spectrometry. Preliminary results of C-14 and Cs-137 dating of Slovak wines are presented in Fig. 1. A reasonable agreement has been obtained for both sets of data which will be discussed in detail.

This work was supported by the EU Research and Development Operational Program funded by the ERDF (project No. 26240220004), and by the International Atomic Energy Agency (TC project SLR-1001).

Burchuladze AA, Pagava S V., Povinec P, Togonidze GI, Usačev S., 1980. *Nature* 287, 320–322.

Burchuladze AA, Chudý M, Eristavi IV, Pagava SV., Povinec P, Šivo A, Togonidze GI, 1989. *Radiocarbon* 31, 771-776.

Hua Q, Barbetti M, Rakowski A (2013). *Radiocarbon*, 55, 2059-2072.

Hubert Ph, Perrot F, Gaye J, Medina B, Pravikoff M., 2009. *S., Comptes Rendus Physique* 10, 622-629.

Lee S-H, Mantura FR, Povinec PP et al., 2006. In (Ed. P.P. Povinec): *Radioactivity in the Environment.* Elsevier, New York, pp. 137-147.

Livingston HD, Povinec PP, 2002. *Health Phys*. 82, 656-668.

Povinec P, 1972. *Radiochem. Radioanal. Lett*. 9, 127-135.

Povinec P, 1978. *Nucl. Instr. Meth*. 156,441-446.

Povinec P, Šáro Š, Chudý M, Šeliga M, 1968. Intern. *J. Appl. Radiat. Isotopes* 19, 877-881.

Povinec P, Chudý M, Šivo A, 1986. *Radiocarbon* 28, 668-672.

Povinec PP et al., 2015. *Nucl. Instr, Meth. Phys. Res. B* 361, 87–94.

Ru-106 variations during 2017 in the atmosphere of Slovakia: monitoring and modelling approaches

P. P. Povinec, I. Sýkora, M. Gera, I. Kontuľ

Faculty of Mathematics, Physics and Informatics, Comenius University, 84248 Bratislava, Slovakia
Keywords: Ru-106, Cs-137, atmospheric aerosols, precipitation, grass, HPGe gamma-spectrometry
Presenting author e-mail: pavel.povinec@uniba.sk

There have been several sources of radionuclides in the atmosphere, primarily consisting of natural (cosmogenic, primordial and radiogenic) and anthropogenic radionuclides. Cosmogenic radionuclides in the ground-level air are represented mainly by Be-7, which is formed prevailingly in the stratosphere (about 70%) by spallation of light atmospheric nuclei such as nitrogen and oxygen. Primordial radionuclides represented mainly by K-40 and decay products from the U-238 and Th-232 chains (e.g. Ra-226, Ra-228 and decay products of gaseous Rn-222 (e.g. Pb-210) and Rn-220 (e.g. Tl-208)), are found in most types of soils, and can be easily resuspended into the lower troposphere (Sýkora et al, 2017). The third group is represented by anthropogenic radionuclides (e.g. H-3, C-14, Sr-90, Cs-137 and plutonium isotopes) which were introduced to the atmosphere mainly during atmospheric nuclear weapons testing (known as global fallout) (Livingston and Povinec, 2002; Povinec et al., 2012a; Hirose and Povinec, 2015), and during nuclear power plant accidents (e.g. Chernobyl and Fukushima) (Povinec et al., 1988, 2012b, 2013). They have been dispersed all over the world and deposited back to the ground by gravitational settling and precipitation washout. The Cs-137 is presently found mainly in soils and vegetation, and it can get back into the atmosphere by soil resuspension (Pham et al., 2011; Povinec et al., 2012a; Sýkora et al., 2012) and by biomass burning (Hirose and Povinec, 2015). Seasonal variations of the Cs-137 concentration in the atmosphere, associated with local meteorological conditions (like winds, air temperature, pressure and precipitations) were observed in post-Chernobyl and post-Fukushima periods by several authors (Povinec et al., 2012b, 2013).

Aerosol radionuclides have regularly been monitored in the Bratislava air since the middle of seventies (Povinec et al., 1988) with the aim to study radionuclide variations in the atmosphere, as well as for assessment of impacts of nuclear power plants in Slovakia. Under normal conditions the air filters were exchanged every week, however, under special circumstances shorter sampling periods were used. The aerosols are collected using a high-volume sampler with flow rate of 80 m^3/h at the height of 2.85 m above the ground. The sampling site is in Bratislava at the Meteorological station of the Faculty of Mathematics, Physics and Informatics of the Comenius University. Nitrocellulose membrane filters (PRAGOPOR 4) with 0.85 mm holes with almost 100% collection efficiency have been used during sampling.

Ruthenium-106 was detected in October 2017 in the atmosphere of several European countries. The observed levels varied from about tens of μBq/m^3 up to several hundreds of μBq/m^3. In Bratislava the main Ru-106 plume was observed in the week of 27th September with maximum activity concentration of 14.7 μBq/m^3 (Table 1). Simulations are going on to trace the plume through European countries with the aim to find its origin. Preliminary results indicate that the plume originated in the Far East Europe.

Table 1. Ru-106 Bratislava results (2017)*.

Aerosols	**mBq/m^3**
27.9.-3.10.	14.68 ± 0.35
3.10.-6.10.	0.155 ± 0.011
6.10.-11.10.	0.013 ± 0.003
Rain water	**mBq/L**
1.8.-31.8.	4.7 ± 0.5
20.9.-27.9.	24 ± 2
3.10.-10.10.	196 ± 12
11.10.-31.10.	6.7 ± 0.6
1.11.-30.11.	4.8 ± 0.5
Grass	**Bq/m^2**
up to 17.10.	± 0.03

*Uncertainties are given at 1 sigma

This work was supported by the EU Research and Development Operational Program funded by the ERDF (project No. 26240220004), and by the International Atomic Energy Agency (TC project SLR-1001).

Hirose, K., Povinec, P.P., 2015. *Sci. Rep*. 5, 15707.

Lee, S.-H., Mantura F.R, Povinec, P.P. et al., 2005. In: *Radioactivity in the Environment* (Edit. P.P. Povinec). Elsevier, New York, pp. 137-147.

Livingston, H.D., Povinec, PP 2002. *Health Phys.* 82, 656-668.

Masson O. et al., 2019. *Proc. Nat. Acad. Sci*. (submitted).

Pham, M.K., Nies, H., Betti, M., Povinec, P.P., 2011. *J. Environ. Radioact*. 102, 1045-1054.

Povinec, P. et al. 1988. *J. Radioanal. Nucl. Chem. Lett.* 126, 467-478.

Povinec, P.P. et all. 2012a. *J. Environ. Radioact.* 108, 33-40.

Povinec, P.P. et al. 2012b. *J. Environ. Radioact*. 114, 81-88.

Povinec, P.P., Hirose, K., Aoyama, M., 2013. *Fukushima Accident: Radioactivity Impact on the Environment.* Elsevier, New York.

Sýkora, I., Holý, K., Ješkovský, M., Müllerova, M., Bulko, M., Povinec, P.P., 2017. *J. Environ. Radioact.* 166, 27-35.

Flexible polysiloxane based scintillators for environmental monitoring

A. Quaranta[1,2], E. Zanazzi[1,2], F. Pino[3], S. Moretto[3], S. Carturan[3,4]

[1]Department of Industrial Engineering, University of Trento, Povo, I-38132, Italy
[2]TIFPA, INFN, Povo (Trento), I-38132, Italy.
[3]Department of Physics and Astronomy, University of Padova, Padova, I-35123, Italy
[4]LNL, INFN, Legnaro (Padova), I-35020, Italy
Keywords: Flexible scintillators, environmental monitoring, neutrons.
Presenting author: A. Quaranta, e-mail: alberto.quaranta@unitn.it

Polysiloxane based scintillators have been deeply studied during last years. Polysiloxanes are characterized by high thermal (up to 200 °C) and chemical stability, and they can be handled without affecting the light yield. Since they are synthesized by mixing precursor resins whose polymerization is induced at 60-100 °C, they can be produced in different shapes, form large cylinders to thin foils with thickness ranging from 1 mm down to few microns. Such flexible and wearable foils are suitable for several applications.

Radiation resistance tests on polysiloxane scintillators shown that they maintain their scintillation yield level after gamma irradiations up to 50 kGy (Quaranta et al. 2010, Quaranta et al. 2013).

By proper doping with boron containing molecules they are able to detect thermal neutrons with an efficiency comparable with commercial systems (Quaranta et al. 2011).

Flexible scintillators mixing ^{6}LiF and ZnS micro-powders have been produced exhibiting quite high efficiency and mechanical stability. The easiness in fabrication allows to prepare mechanically stable systems suitable for outdoor applications (Carturan et al. 2019a).

At present, polysiloxane systems have been doped with luminescent quantum dots in order to obtain hybrid scintillators (Zanazzi et al. 2018).

Recently, the suitability for the detection of fast neutrons through pulse shape discrimination techniques has been demonstrated (Carturan et al. 2019b).

In this work an overview of polysiloxane scintillators properties and capabilities are presented, with specific regards to applications in environmental monitoring.

Quaranta, A., Carturan S.M., Marchi T., Antonaci A., Scian C., Kravchuk V.L., Degerlier M., Gramegna F., Maggioni G. 2010. Radiation hardness of polysiloxane scintillators analyzed by Ion Beam Induced Luminescence. *Nucl. Instr. Meth. B*, 268, 3155-3159.

Quaranta A., Carturan S., Marchi T., Buffa M., Degerlier M., Cinausero M., Guastalla G., Gramegna F., Valotto G., Maggioni G. 2011. Doped polysiloxane scintillators for thermal neutrons detection. *J. Non-Cryst. Solids*, 357, 1921-1925.

Quaranta A., Carturan S., Cinausero M., Marchi T., Gramegna F., Degerlier M., Cemmi A., Baccaro S. 2013. Characterization of polysiloxane organic scintillators produced with different phenyl containing blends. *Mater. Chem. Phys.*, 137, 951-958.

Zanazzi E., Favaro M., Ficorella A., Pancheri L., Dalla Betta G. F., Quaranta A. 2018. Proton Irradiation Effects on Colloidal InGaP/ZnS Core-Shell Quantum Dots Embedded in Polydimethylsiloxane: Discriminating Core from Shell Radiation-Induced Defects Through Time-Resolved Photoluminescence Analysis. *J. Phys. Chem. C*, 122, 22170-22177.

Carturan S.M., Vesco M., Bonesso I., Quaranta A., Maggioni G., Stevanato L., Zanazzi E., Marchi T., Fabris D., Cinausero M., Pino F., Gramegna F. 2019a. Flexible scintillation sensors for the detection of thermal neutrons based on siloxane ^{6}LiF containing composites: Role of ^{6}LiF crystals size and dispersion. *Nucl. Instr. Meth. A*, 925, 109-115.

Carturan S.M. et al. 2019b. Submitted to *Scientific Reports*.

Optimization methods on gross alpha-beta analysis for environmental measurements

I. Radulescu, M.R. Calin, A. Stochioiu

Horia Hulubei National Institute for Physics and Nuclear Engineering - IFIN HH, Magurele, 077125, Romania
Keywords: gross alpha, gross beta, quality assurance, proficiency test
Presenting author, e-mail: I. Radulescu, rileana@nipne.ro

Gross alpha-beta activity measurements are widely applied as a screening technique in many fields, from environmental monitoring to radioecology and industrial applications. One of the most used application is the methodology for monitoring and assessment for dissolved radionuclides for controlling health risks from drinking-water. The process of identifying individual radionuclides in drinking-water and determining their concentration is time-consuming and expensive. A more practical approach is to use a screening procedure, where the total radioactivity present in the form of alpha and beta radiation is first determined, without regard to the identity of specific radionuclides. To have good reliable analytical results laboratories use the proficiency tests as a method to assess the accuracy and precision of the data produced. This paper presents the results obtained by two laboratories in proficiency tests organized by the IAEA in 2016 (IAEA-TEL-2016-03) and 2017 (IAEA-TEL-2017-03) on spiked water in the two years of participation for these actions.

The equipments used for proficiency tests were alpha–beta system PROTEAN ORTEC, MPC-2000-DP from SALMROM laboratory, MPC 9300 windowless detector system (Protean Instrument Corporation) and automatic low background alpha/beta counting system, Model S5 XLB (Canberra Industries) from Laboratory for Personnel and Environment Dosimetry (LDPM). Both laboratories are part of Life and Environmental Physics Department from IFIN-HH.

The evaluation report for each laboratory assesses the result "$Value_{Laboratory}$" and represents an indication of how far is the observed value from the assigned value. This is calculated relative to the assigned value "$Value_{IAEA}$".

To reach the final score *"Acceptable", "Warning"* or *"Not acceptable"* for the laboratory results, various statistics such Z-scores are used (Radulescu and Calin, 2014).

z-Score= $(Value_{Laboratory} - Value_{IAEA})/s^*$.

where: s^*=1.483×median of $|x_i - x^*|$ is the robust standard deviation;

x^*=median of x_i (I = 1,2,…p) is the robust average.

The evaluation of z-Score is such: z <2 Accepted;

$2 \leq z \leq 3$ Warning;

z > 3 Not Accepted

According to this approach, the reported results are evaluated against the acceptance criteria for trueness and for precision.

All results obtained by the both laboratories for the spiked water are presented in Table 1. Most of the results were acceptable, there was only one warning due to high bias of the reported value in respect to true value.

Table 1. Results of SALMROM and LDPM laboratories, gross alpha and gross beta activities ± 1 standard deviation (Bq/L).

Evaluation of the results	IAEA value	SALMROM value	z-Score/ Final evaluation	LDPM value	z-Score/ Final evaluation
Gross Beta (2016)	106 ± 20	102.3 ± 28.5	-0.19/A	114.4 ± 30.5(P), 111 ± 25 (E)	0.47, 0.26/A
Gross Alpha (2016)	58 ± 15	21.5 ± 6.8	-2.43/W	53.0 ± 10 (E)	-0.33/A
Gross Beta (2016-2)	76 ± 20	65.9 ± 17.4	-0.51/A	75.4 ± 15.6 (P), 72 ± 15 (E)	-0.03, -0.20/A
Gross Alpha (2017)	42.3 ± 6.5	38.6 ± 11.0	-0.57/A	39.1 ± 10.4 (P)	-0.49/A
Gross Beta (2017)	38.1 ± 10	22.2 ± 6.5	-1.59/A	51.8 ± 11.2 (P)	1.37/A

(P) - Protean MCP 9300
(E) - Eclipse Canberra

The values of the SALMROM laboratory seem that are always underestimated, resulting in a negative z-Score (Figure 1).

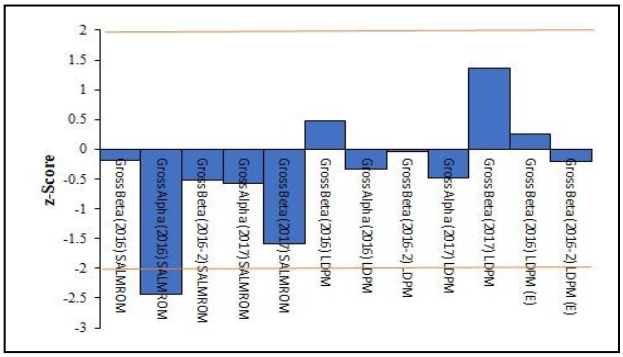

Figure 1. z-Score for spiked water samples results of gross alpha-beta measurements. Yellow line represents the warning limit.

Based on the lessons learned, in order to optimize the accuracy measurements, the quality control records and backgrounds measurements should help, together with more appropriate matrix reference material and appropriate self- attenuation correction.

This work was supported by the Ministry of Research under grant PN 19060203/2019.

Radulescu I. and Calin M.R., 2014. Reliability and performances of a high-purity gamma spectrometry system used for environmental measurements, *J. Radioanal. Nucl. Chem.*, 301, 141-146.

Performances, limitations and comparison of the results of an in-situ spectro-tracer with the laboratory gamma ray spectrometry

I. Radulescu[1], M.R. Calin[1], R. Stochici[2]

Horia Hulubei National Institute for Physics and Nuclear Engineering - IFIN HH, Magurele, 077125, Romania
[2]Institute of Geodynamics of the Romanian Academy, Bucharest, 020032, Romania
Keywords: in-situ spectrometer, soil survey, data reliability, cost effectiveness.
Presenting author, e-mail: I. Radulescu, rileana@nipne.ro

The selection of an appropriate detector for field measurements, in case of natural radioactivity, is an important task taking into account constraints given by data reliability, time and cost effectiveness (Van der Graaf, 2007, Van der Graaf, 2011). This paper provides the necessary data when choosing a portable spectrometer Gamma Surveyor II based on BGO crystal (6.3 in^3). The proven efficiency of the crystal, the weaker energy resolution but still good, and comparable results with HPGe results obtained for ^{238}U, ^{232}Th, ^{40}K, often makes it a good choice. Thus, functional parameters, as energy calibration, energy resolution and background of the system were analyzed. Field data, concentrations of radionuclides ^{238}U, ^{232}Th, ^{40}K (ppm) in surface soil on the Bucharest area are compared with laboratory measurements using HPGe detector for S\soil samples collcted from the same locations where measurements with the Gamma Surveyor II were done. The results for ^{238}U, ^{232}Th and ^{40}K were plotted against HPGe results to show the consistency of the measurements, depicted in Fig. 1. The obtained data are well correlated.

There are many advantages of using this system, such as: - less time-consuming regarding acquisition and time analysis, the reporting of the data being instantaneous, at the elapsed time; -does not require liquid nitrogen, as for the in-situ HPGe detectors; -the BGO crystal contributes to a good response to the presence of radionuclides in the soil; -cost-effective way to obtain concentrations of natural radionuclides in soil.

Among the weaknesses of the system would by the fact that although it has a built-in library of 19 radionuclides (natural and artificial) that are recognized in the spectrum, it does contain an algorithm for their concentrations calculation. From this point of view this represents a loss, because in the samples measured on the HPGe detectors, ^{137}Cs has been measured with activities between few Bq/kg up to more than 100 Bq/kg.

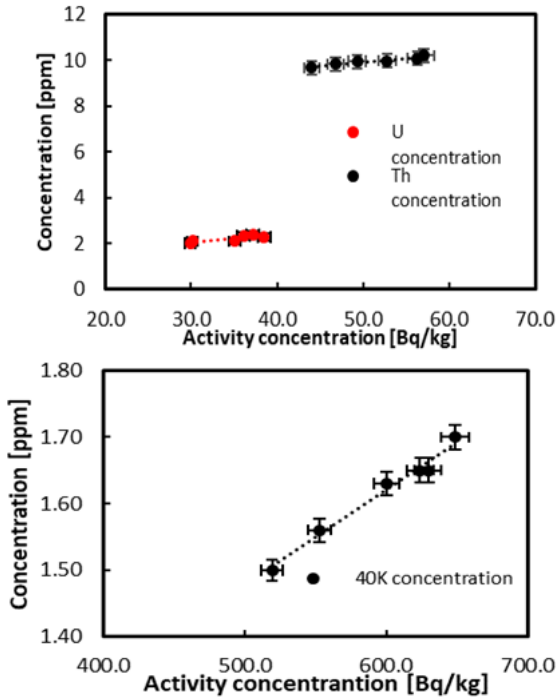

Fig 1. Linear correlation between concentration [ppm] of ^{238}U, ^{232}Th, ^{40}K given by the Surveyor and activity concentration [Bq/kg] obtained from the HPGe detector.

This work was supported by the Ministry of Research under grant PN 19060203/2019.

Van der Graaf E.R, Rigollet C., Maleka P.P., Jones D.G., 2007. Testing and assessment of a large BGO detector for beach monitoring of radioactive particles, *Nuclear Instruments and Methods in Physics Research A* 575, 507–518.

Van der Graaf E.R., Limburg J., Koomans R.L., Tijs M., 2011. Monte Carlo based calibration of scintillation detectors for laboratory and in situ gamma ray measurements, *Journal of Environmental Radioactivity* 102, 270-282.

Radioactivity in North Atlantic deep water corals

D. Ransby[1], P. Lindahl[2], J. Qiao[3], G. Marissens[4], M. Hult[4]

[1]Institute of Environmental Physics, University of Bremen, Bremen, Germany
[2]Swedish Radiation Safety Authority, Stockholm, Sweden
[3]Technical University of Denmark, Roskilde, Denmark
[4]Joint Research Centre – JRC, Geel, Belgium
Keywords: Lophelia pertusa, ^{210}Pb, ^{226}Ra, Coral chronology
Daniela Ransby, e-mail: danaransby@yahoo.com

In a world with a changing climate, deep knowledge of ocean circulation patterns and anomalies as part of ocean – atmosphere interaction, is crucial for understanding its potential impact on the environment and consequently human society. Ocean masses tracer studies are based on the chemistry of water columns. Anthropogenic radionuclides can successfully be used as such tracers. They have been released in the marine environment during atmospheric nuclear weapons testing, by accidents in nuclear installations or as liquid discharges from nuclear reprocessing. Skeletons of corals were proven excellent archives of ocean chemistry, and several previous studies showed prime properties of tropical corals with annual growth bands as archives of ocean chemistry and circulation.

In this study we test the usability of recent deep (or cold) water coral *Lophelia pertusa*, a cosmopolitan species in the Atlantic Ocean, occurring in a wide range of depths, as an archive of dissolved radionuclides in the Northeast Atlantic Ocean. While deep water corals are expected to provide similarly valuable information as tropical corals, dating of their growth increments is more challenging, due to the bush-like growth form of their colonies. We measured samples taken from selected increments of the colonies by non-destructive gamma-ray spectrometry in the HADES 225 m deep underground laboratory, to quantify activities of the natural radionuclides Lead-210 Radium-226, which can be used for radiometric dating. Measurements in HADES enable to achieve the required detection limits at the very low levels of radioactivity in small samples of coral material. Subsequently, we will study artificial radionuclides (Plutonium and Uranium-236) by radiochemical and mass spectrometric methods to provide their first record in NE Atlantic corals and reconstruct their origin and fate.

Table 1. Sampling information.

	Area 1	Area 2
Species	*Lophelia pertusa*	*Lophelia pertusa*
Sampling expedition	POS400 cruise (2010)	RRS James Cook 073 cruise (2012)
Location	SW off Ireland, NE Atlantic, Pollux Mound	Outer Hebrides, NE Atlantic, Mingulay Reef
Water depth	940 m	120 m

Deep water corals colonies for this study were sampled by remote underwater vehicles at two sites (Table 1, Figure 1), located several hundred kilometres down-current and up-current, respectively, from the nuclear reprocessing plant Sellafield at the coast of the Irish Sea. Sellafield represents the most significant emitter of artificial radionuclides in the marine environment of the region.

Samples consisting of individual coral branches were divided into increments equivalent to the single polyps, cleaned mechanically and chemically and then crushed to ensure a well defined geometry. They were sealed into containers and measured in an ultra low background SAGe Well detector. Sample masses ranged from 0.4 to 2.2 g and measurement times were 2-3 weeks/sample.

Preliminary results of the measurement of natural radionuclides in cold water corals (^{226}Ra, ^{210}Pb, ^{234}Th, ^{235}U) from Area 1 will be presented.

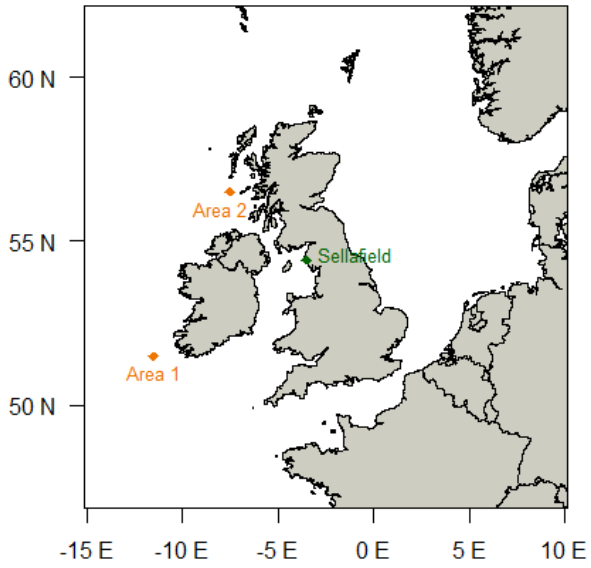

Figure 1. Research areas.

This work was supported by the Joint Research Centre of the European Commission through the Framework of Access to the JRC Physical Research Infrastructure, call Nr 2017-1-RD-EUFRAT-HADES to the Open Access Project DECAROT. The corals samples were kindly provided by A. Freiwald (Senckenberg am Meer, Wilhelmshaven, Germany) and J.M. Roberts (University of Edinburgh, UK).

Radioactive discharges from NPP Bohunice and impact on people living in surrounding area

B. Remenec[1]

[1]Slovenske elektrarne plc., NPP Bohunice, Jaslovske Bohunice, 919 31, Slovakia
Keywords: radioactive discharges, occupational exposure
Presenting author, e-mail: boris.remenec@seas.sk

Bohunice NPP, Slovak republic, consists of two VVER reactors type V213, in operation since 1984, resp. 1985. The last power upgrading in 2012 enhanced the power of each reactor from 440 MW up to 505 MW.

A large attention in Bohunice NPP, as it is in other nuclear plants, is devoted to the radioactive discharges monitoring. Monitoring of radioactive discharges from NPP Bohunice - according to the act No. 87/2018 and decision No. OOZPŽ/6774/2011 of Public Health Authority of the Slovak Republic. Annual regulatory limit for occupational exposure in the NPP Bohunice surrounding area caused by air and water born discharges at NPP Buhunice operation is a total effective dose 50μSv.

This work presents the results of the balances of individual types of radioactive discharges from NPP Bohunice to the atmosphere and hydrosphere. The activities of discharged radioactive noble gases, aerosols, strontium, ^{131}I, transuranic elements ^{241}Am, ^{238,239,240}Pu, tritium and ^{14}C carbon released from ventilation stack are presented. These data are from monitoring instruments in the ventilation stacks (noble gases) and laboratory data evaluations (aerosols filters, ^{131}I - gamma spectrometry, ^{3}H, ^{14}C, ^{90,89}Sr liquid scintillation counting, transuranic elements - alpha spectrometry,). Dominant radionuclides in aerosols were ^{51}Cr, ^{60}Co and ^{110m}Ag. All types of discharges from NPP Bohunice into the atmosphere were below the annual guidance levels.

Control of waterborne discharges was carried out by measuring the volume activity of tritium and the volume activity of corrosion and fission products. From the measured activity and amount of discharged water the balances of liquid effluents were determined. For balance purposes, the radioisotopic composition of the effluent is determined by gamma spectrometry (gamma radionuclides), ^{3}H, ^{14}C, ^{90,89}Sr liquid scintillation counting, transuranic elements - alpha spectrometry.

Discharges from NPP Bohunice into the hydrosphere were below the annual guidance levels except tritium which is dominant radionuclide discharged into hydrosphere.

In order to assess the impact of the NPP Bohunice on the surrounding population, a quarterly analysis of the occupational exposure based on real meteorological measurements and real discharges of radioactive nuclides into the atmosphere and hydrosphere was performed. Calculated effective dose was compared with the annual limit for the population - 50μSv (see Fig. 1. and 2).

The ESTE AI version NPP Bohunice software, author and copyright holder ABmerit ltd., Slovakia, was used to calculate the radiation exposure of the population around NPP Bohunice.

The ESTE AI software allows selectively calculate the impacts for each individual discharge point (ventilation stacks, liquid discharge points into Vah and Dudvah river) and each individual nuclide.

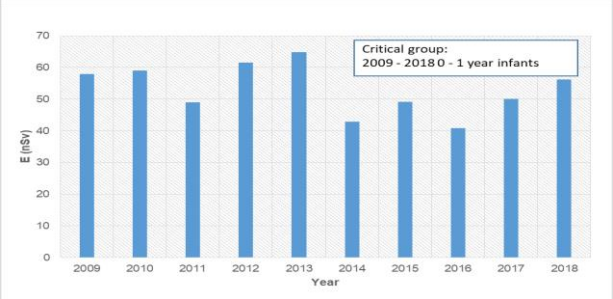

Figure 1. Annual committed effective dose $E_{(70)}$ from Tritium discharges.

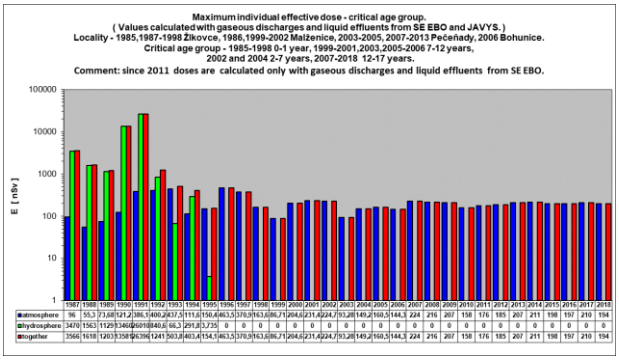

Figure 2. Annual total individual effective dose history for the critical person.

The critical person lives in sector 75 (Pecenady) and is in the age category of 12-17 years. For this category, the total annual effective dose was calculated and has been app. 2.0 E-07 Sv (0.2 μSv) since 1998.

3D printed devices to integrate in flow-through systems for radionuclide measuring: application to uranium and radiostrontium determinations

M. Rodas[1,2], J.M. Estela[3], V. Cerdà[3], L. Ferrer[2], A. Borràs[2]

[1]Environmental Radioactivity Laboratory (LaboRA), University of the Balearic Islands, Palma de Mallorca, 07122, Spain.
[2]Sciware Systems, Spin-Off UIB-004, Bunyola, 07193, Spain.
[3]Chemistry Department, University of the Balearic Islands, Palma de Mallorca, 07122, Spain.
Keywords: 3D printing, uranium extraction, TEVA resin, automatic system
Presenting author, e-mail: toni.borras@uib.es

3D printed devices have been fabricated using stereolithographic (SLA) 3D printing. The device designs were performed using Rhinoceros 5SR11 32 software (MacNeel & Ass., USA), while they were printed with a 3D printer Form +2 (Formlabs Inc., Somerville, USA). This is an upside-down (inverted) SLA, that uses a tank with a transparent bottom and non-stick surface, which serves as a substrate for the liquid resin to cure, allowing the soft detachment of the newly formed layer. One of the advantages of this type of printer is that the volume of construction can substantially exceed the volume of the tank.

A 3D printed device to provide a high surface area in a small volume with a coat of a selective extractant of uranium was designed, constructed and optimized (Figure 1).

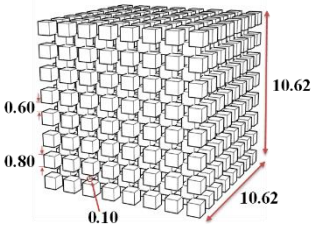

Figure 1. 3D printed device design (dimensions in mm).

A simple process was carried out to immobilize a selective and commercial resin (TEVA resin), in all the surface area of the non-cured SLA 3D printed device, becoming immobilized after UV photocuring. The device was satisfactorily applied to the extraction procedure of uranium from water matrices without doing any previous pretreatment.

Then, the 3D cube-device impregnated with TEVA resin for selective extraction of U(VI) was integrated into a stirred reactor chamber (Figure 2).

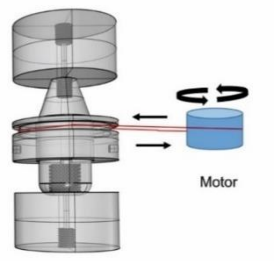

Figure 2. 3D printed reactor chamber with magnetic stirring, by a ring containing neodymium magnets.

This chamber was, in turn, integrated with a magnetic-stirring assisted (in order to improve the extraction efficiency) flow-through system based on Sequential Injection Analysis (SIA).

With the aim to develop a sensor which allows the on-line extraction, treatment, and detection of radiostrontium, a mixer for the eluate and liquid scintillation cocktail (Figure 3) and a dark box to contain the photomultipliers and the flow cell were also designed and 3D printed (Figure 4).

The integration of 3D printed devices in automatic methodologies is a step forward for the extraction of radionuclides in complex matrices

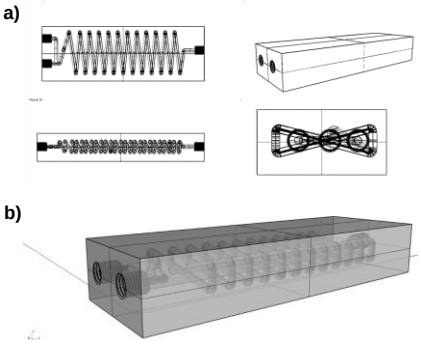

Figure 3. 3D printed mixer a) Four views from Rhinoceros program displays. b) Perspective view.

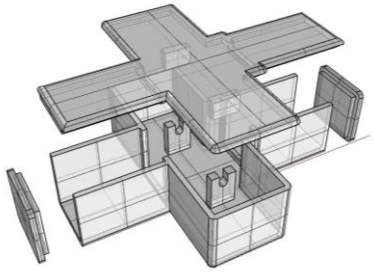

Figure 4. 3D printed dark box.

The use of 3D printing technology allowed the design of customized and low-cost devices, attaining self-manufacturing techniques to design of novel analytical tools for determining radionuclides.

This work was supported by the Government of the Balearic Islands (project PROCOE/7/2017) co-financed by European Regional Development's funds (FEDER).

Comparison of dimension reduction techniques applied to the analysis of airborne radionuclides activity concentration

A. Russo[1], A. Borras[1]

[1]Environmental Radioactivity Laboratory, University of the Balearic Islands, Palma E-07122, Spain.
Keywords: Airborne radionuclides, PCA, t-SNE, UMAP
Presenting author, e-mail: toni.borras@uib.es

Recently introduced dimensional reduction techniques, namely, t-distributed Stochastic Neighbour Embedding (t-SNE) and Uniform Manifold Approximation (UMAP) are tested on a database collected during 10 years (2004-2014) at the University of the Balearic Islands (Spain). The results are compared to those obtained with the more traditional Principal Component Analysis (PCA) technique. The database is composed by ^{7}Be and A_{β} concentration of activity, particulate matter (PM) concentration, wind speed, temperature, precipitation, atmospheric pressure and relative humidity (Rodas et al., 2016).

As a starting point, a PCA is applied to our dataset to obtain a first representation in two dimensions (Fig. 1). Afterwards, t-SNE is applied to the same data. This non-linear transformation technique allows obtaining a reduced dimensional space to map the data while preserving the local structure (van der Maaten and Hinton, 2008). The scale to which the data structure is preserved is controlled by an adjustable parameter, the perplexity (Fig. 2).

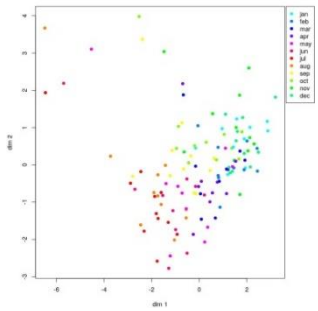

Figure 1. Principal Component Analysis plot.

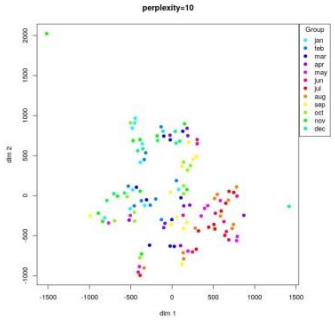

Figure 2. t-SNE plot with perplexity value of 10.

Finally, UMAP is used to obtain an alternative set of lower dimensional spaces. This technique, based on several fuzzy logic principles, preserves the local structure to the desired degree of accuracy without causing an excessive deformation of the global structure (McInnes et al., 2018). UMAP provides the possibility to tune several parameters to control the final output, being the most important the metric of the space and the number of neighbours to consider for each point.

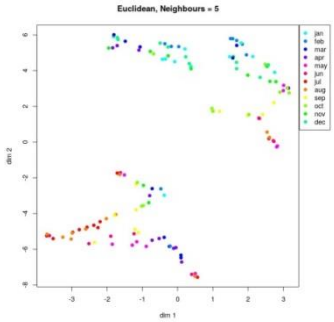

Figure 3. UMAP plot with Euclidean metric and considering 5 neighbours for each point.

Both t-SNE and UMAP perform reduction of dimensionality preserving more detail of the local structure than PCA. UMAP provides the best balance between local and global structure preservation, as well as a wider range of parameters to tune and control the final result. On top of that, UMAP is faster and easier to extend to higher dimensions than t-SNE, and it can be a good starting point to perform a clustering analysis of the database.

Rodas Ceballo, M. et al. 2016. Monitoring of 7Be and gross beta in particulate matter of surface air from Mallorca Island, Spain. *Chemosphere* 152, 481-489.

van der Maaten, L., Hinton, G. 2008. Visualizing Data using t-SNE. *Journal of Machine Learning Research*. 9, 2579-2605.

McInnes, L. et al. J. 2018. UMAP: Uniform Manifold Approximation and Projection for Dimension Reduction. *arXiv*:1802.03436.

Effects of green manuring with hairy vetch (*Vicia villosa*) on rice yield and ^{137}Cs uptake in paddy fields after decontamination

Takashi Saito[1] and Takashi Sato[2]

[1]Hama Agricultural Regeneration Research Centre, Fukushima Agricultural Technology Centre, 45-169 Sukakeba, Kaibama, Haramachi-ku, Minamisoma, Fukushima 9750036, Japan
[2]Faculty of Bioresource Sciences, Akita Prefectural University, 241-438 Kaidobata-Nishi Nakano Shimoshinjo Akita City 010-0195 Japan
Keywords: ^{137}Cs, Hairy vetch, Paddy field
Presenting author, e-mail: saito_takashi_01@pref.fukushima.lg.jp

The accident at the Tokyo Electric Power Company's Fukushima Daiichi Nuclear Power Plant in 2011 released a large amount of radiocesium into the atmosphere, contaminating agricultural and forest land throughout Fukushima Prefecture in Japan. To remove radiocesium deposited on agricultural land in evacuation zones around the plant, fertile surface soil has been removed and replaced with low-fertility sandy soil taken from mountainous areas in Fukushima Prefecture. To restore soil fertility, it is necessary to use green manure crops, since actual manure is in short supply; most animal husbandry in the region has not yet been restarted. However, the effect of incorporating green manure into the soil on the crop uptake of radiocesium has not yet been clarified.

To provide insights into this uptake, we studied two paddy fields after decontamination to estimate the risk of radiocesium uptake in brown rice. We used hairy vetch (*Vicia villosa*) as a green manure. In addition, we examined the recovery of soil fertility after decontamination followed by green manuring.

[Materials and Methods] The test was conducted in 2017 in two paddy fields in Tomioka Town, Fukushima Prefecture. Removal of the surface soil for decontamination was conducted in 2016. The original soil was a gray lowland soil with a ^{137}Cs concentration of about 1500 Bq kg^{-1} dry weight (DW) of soil. The 'Kantaro' cultivar of hairy vetch was sown in November 2017 and plowed into the soil in May 2018. Paddy rice (cv. 'Tenno-tsubu') was transplanted into the paddies in June 2018 and harvested in October of the same year. The study used two 0.3-ha paddy fields: one sown with hairy vetch and treated with reduced nitrogen, and a control. We applied 240 kg ha^{-1} of K_2O equivalent to both paddies in addition to normal fertilization to reduce ^{137}Cs uptake. We used the soil-to-plant transfer factor (*TF*) to quantify plant uptake of a material (here, ^{137}Cs) from the soil. This simple but important parameter can be used to estimate the expected concentrations of radionuclides in plant tissue. To quantify the bioaccumulation of ^{137}Cs in brown rice, we calculated *TF* as the ratio of radiocesium in the brown rice (Bq kg^{-1}) to that in the soil (Bq kg^{-1}), on a dry-weight basis.

The fresh and dry weight of hairy vetch were 10.3 t ha^{-1} and 1.4 t ha^{-1}, respectively (Table 1). The amounts of carbon and nitrogen supplied to the soil by manuring the hairy vetch were 0.59 and 0.054 t ha^{-1}, respectively. Because the plant-available nitrogen provided by hairy vetch is about 50%, we reduced the amount of nitrogen fertilizer (Ammonium sulfate) by approximately 30 kg ha^{-1}.The ^{137}Cs concentrations in the soil and hairy vetch plants were 416 and 1137 Bq kg^{-1}, for a *TF* of 0.379 (Table 2). This value was higher than those of other crops. The brown rice yield per unit area did not differ significantly between the manured and control paddies. In addition, ^{137}Cs concentrations in brown rice in both plots did not differ significantly at 3.9 and 4.1 Bq kg^{-1}, respectively (Table 3). *TF* in the manured and control plots were 0.003 and 0.002, respectively. Because we applied additional potassium fertilizer to reduce ^{137}Cs uptake, this result suggests that the risk of increasing ^{137}Cs uptake by rice after manuring with hairy vetch was small. In future research, we will examine whether this manuring will increase ^{137}Cs uptake under low-potassium conditions.

Table1 The growth of hairy vetch and its supply of carbon and nitrogen to the soil.

Fresh weigh (t ha^{-1})	Dry weight (t ha^{-1})	Carbon (t ha^{-1})[a]	Nitrogen (t ha^{-1})[a]
10.3 ± 2.5	1.4 ± 0.24	0.59	0.054

[a]Total carbon and total nitrogen contents were 44 and 4.4 %, respectively, for hairy vetch biomass.

Table 2. The ^{137}Cs content of hairy vetch, and the transfer factor (TF) and exchangeable K_2O.

^{137}Cs (Bq kg^{-1} DW)			Exchangeable
Plant	Soil	*TF*	K_2O (mg kg^{-1} DW)
416 ± 274	1137 ± 826	0.379 ± 0064	170 ± 24

Table3 Cs-137, transfer factor (*TF*), Exchangeable K_2O in the two rice paddies.

Paddy	^{137}Cs (Bq kg^{-1})			Exchangeable
	Brown Rice	Soil	*TF*	K_2O (mg kg^{-1}DW)
Hairy vetch+ Nitrogen reduction	3.9 ± 0.2	1470 ± 325	0.003 ± 0.001	170 ± 24
Control	4.1 ± 1.9	2187 ± 100	0.002 ± 0.000	300 ± 51

Characteristic of dissolved ^{137}Cs leaching from a forest litter observed from litterbag experiment in Japanese forest affected by the Fukushima nuclear accident

K. Sakuma, K. Yoshimura, T. Nakanishi

Fukushima Environmental Safety Center, Japan Atomic Energy Agency, Fukushima 963-7700, Japan
Keywords: ^{137}Cs leaching, forest litters, Fukushima accident, litterbag experiments
Presenting author, e-mail: sakuma.kazuyuki@jaea.go.jp

Dissolved ^{137}Cs discharge from a forest catchment in upstream of Ohta River in Fukushima, Japan represents approximately 30% of the total ^{137}Cs discharge through river (Tsuji et al., 2016). It is considered that a major source of dissolved ^{137}Cs in river water in forest catchment may be leaching from litter (Sakuma et al., 2018).

We investigated characteristic of dissolved ^{137}Cs leaching from litters collected at a coniferous needle forest (Japanese cedar) and a deciduous broad-leaved forest using litterbags (40 cm × 50 cm, 5 mm mesh size) at upstream area of Ohta River. Each leaf type of litters was collected into 36 litterbags, respectively, and installed each forest floor at riparian zones in June and December, 2017. Triplicate samples were collected at each forest floor and readily transported to laboratory in August and December 2017, March, May, September, and December 2018. Triplicate samples of topsoil (approximately 0–5 cm) just under litterbags were also collected at the same time to compare the characteristic of dissolved ^{137}Cs leaching with forest litters. Samples were put in containers and soaked in distilled water without mixing at room temperature (measured water temperatures of leaching water were 16.3–22.7 °C (mean: 19.9 °C)). Weight ratio of a wet litter sample to distilled water was 1:10. We took leaching water samples from the containers at 20 min, 140 min, and 1 day after soaking. These samples were analysed about ^{137}Cs activity (Bq L^{-1}) after filtering it through 0.45-µm-pore size membrane filters. Total amount of ^{137}Cs (Bq) in litter was also analysed, and leaching ratio is calculated as a proportion of leaching fraction to the total activity in the litter before the soaking. As a results, dissolved ^{137}Cs concentrations in leaching water after soaking litter samples in the water (Japanese cedar: 15.4 Bq L^{-1} (2.26-46.6 Bq L^{-1}), broad-leaved: 40.3 Bq L^{-1} (12.0-102 Bq L^{-1})) were relatively higher than in river water (approximately 0.2 Bq L^{-1} at upstream Ohta River), indicating that dissolved ^{137}Cs leaching from forest litter could be a major source of dissolved ^{137}Cs in river water. The main results were that the deciduous broad-leaved litter showed much higher leaching ratio of ^{137}Cs (mean: 3.2% (0.81–7.3%)) than that of the coniferous needle litter (mean: 0.80% (0.15–2.1%)). Same tendency was observed in the case of topsoil just under litterbags although the ^{137}Cs leaching ratio were obviously lower than in the case of litter. Dissolved ^{137}Cs leaching ratio were sharply increased during 20 min after soaking as shown in Figure 1.

We analysed relationships between dissolved ^{137}Cs leaching ratio from forest litter and environmental factors such as an antecedent precipitation index and an accumulated temperature by using multiple regression analysis. The prediction model can reproduce observed ^{137}Cs leaching ratio within a factor of 2, and the accumulated temperature showed a positive correlation. On the other hand, the antecedent precipitation showed a negative correlation. These relations suggest that easily leachable fraction of ^{137}Cs in forest litter could increase depending on a litter decomposition and the antecedent precipitation could leach ^{137}Cs from forest litter.

Further investigations are needed for hydrologic connectivity between riparian zones and river water about dissolved ^{137}Cs in forest catchment.

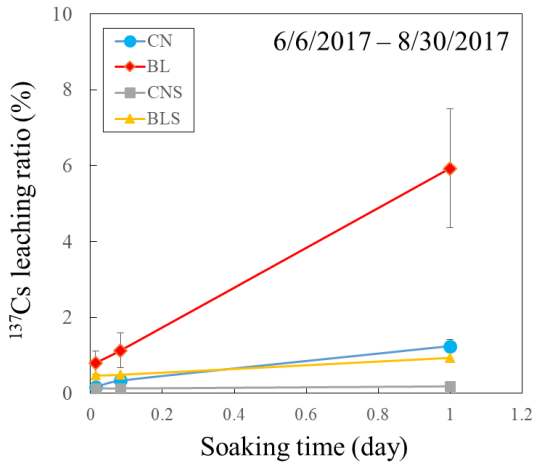

Figure 1. ^{137}Cs leaching ratio from forest litter decomposed from June to August 2017 using litterbags and topsoil under litterbags. CN, BL, CNS, and BLS denote coniferous needle (Japanese cedar), broad-leaved, topsoil under coniferous needle, and topsoil under broad-leaved, respectively. Error bars mean standard deviation (n=3).

H. Tsuji, T. Nishikiori, T. Yasutaka, M. Watanabe, S. Ito, S. Hayashi. 2016. Behavior of dissolved radiocesium in river water in a forested watershed in Fukushima Prefecture. *J. Geophys. Res. Biogeosci.* 121, 2588-2599.

K. Sakuma, H. Tsuji, S. Hayashi, H. Funaki, A. Malins, K. Yoshimura, H. Kurikami, A. Kitamura, K. Iijima, M. Hosomi. 2018. Applicability of K_d for modelling dissolved ^{137}Cs concentrations in Fukushima river water: Case study of the upstream Ota River. *J. Environ. Radioact*. 184-185, 53-62.

Distribution of ^{129}I in the terrestrial environment around the Fukushima Daiichi Nuclear Power Plant before and after the accident

K. Sasa[1], M. Matsumura[1], T. Matsunaka[2], T. Takahashi[1], Y. Satou[3], N. Kinoshita[4], H. Matsuzaki[5] and K. Sueki[1]

[1]AMS Group, Tandem Accelerator Complex, University of Tsukuba, Tsukuba, Ibaraki, 305-8577, Japan
[2]Institute of Nature and Environmental Technology, Kanazawa University, Kanazawa 920-1192, Japan
[3]Japan Atomic Energy Agency, Tomioka Town, Fukushima, 979-1151, Japan
[4]Institute of Technology, Shimizu Corporation, Koto-ku, Tokyo, 135-8530, Japan
[5]The University Museum, The University of Tokyo, Bunkyo-ku, Tokyo, 113-0032, Japan
Keywords: ^{131}I, ^{129}I, FDNPP accident, AMS
Presenting author, e-mail: ksasa@tac.tsukuba.ac.jp

Understanding the distribution and behavior of ^{131}I in the contaminated area by the nuclear accident is important for assessing not only the radiological hazard posed by this radioisotope's high fission yield and gamma-ray energy, but also the radioactive contamination of the terrestrial biosphere. Total amounts of radionuclides discharged into the atmosphere were estimated to be 8.1 GBq for ^{129}I ($T_{1/2} = 1.57 \times 10^7$ y) (Hou et al., 2013) and 120 – 200 PBq for ^{131}I ($T_{1/2}$ = 8.02 d) (Chino et al., 2011, etc.) released from the Fukushima Daiichi Nuclear Power Plant (FDNPP) accident. Radiation monitoring inside the highly contaminated restricted area at Fukushima showed ^{131}I deposition of 2.8 – 55 kBq m^{-2} (decay corrected to 14 June 2011) (MEXT, 2011). Although the accident-derived ^{131}I in soil extinguished in a few months, the long-lived ^{129}I can be used as a tracer to retrospectively infer the level of ^{131}I.

The iodine in the soil samples were chemically purified using a pyrohydrolysis method (Muramatsu et al. 2015). The ^{129}I/^{127}I ratio for the prepared AgI sample including iodine carrier with an ^{129}I/^{127}I ratio of 1.8×10^{-13} was measured using AMS at the MALT, The University of Tokyo. The ^{129}I/^{127}I ratios and ^{129}I concentrations in the soil samples were calculated using the ^{127}I concentration obtained from an inductively coupled plasma-mass spectrometry and the ^{129}I/^{127}I ratio obtained from the AMS, and by subtracting the ^{127}I and ^{129}I contents of the background during the sample preparation. Pre-accident levels of ^{129}I concentration were estimated to be $(2.7 \pm 1.4) \times 10^8$ atoms g^{-1} at Fukushima.

After the accident, there are a few studies of the ^{131}I deposition on the ground released from the FDNPP (Kinoshita et al, 2011; MEXT, 2011). We determinate the ^{129}I/^{131}I atomic ratio in surface soils of Fukushima area for reconstruction of the ^{131}I deposition using the long-lived ^{129}I, which has same behavioural response with ^{131}I in the environment. For this purpose, we investigated the concentrations of ^{129}I among 5-cm-long surface soils in and around Fukushima area, which were measured for ^{131}I immediately after the accident by gamma-ray spectrometry (Kinoshita et al., 2011). Average ratio of ^{129}I/^{131}I was estimated to be 26.0 ± 5.7 as at March 11, 2011. The correlation coefficient (R^2) is 0.98 between concentrations of ^{129}I and ^{131}I in surface soils at Fukushima. We also found the deference of ^{129}I/^{131}I ratios depending on the locations. It is thought to be due to reflect differences related to emission sources from the FDNPP. Previous studies have reported the ^{129}I/^{131}I ratios of 31.6 ± 8.9 (Miyake et al., 2012), 26.1 ± 5.8 (Miyake et al., 2015), and 21 (Muramatsu et al., 2015) in the surface soils of Fukushima. The calculations for ^{129}I/^{131}I ratios by the ORIGEN2 code resulted 31.4 for the Unit 1 reactor, 21.9 for the Unit 2 reactor, and 20.8 for the Unit 3 reactor (Nishihara et al., 2012). Our result of 26.0 ± 5.7 for ^{129}I/^{131}I ratio was consistent with previous studies and the estimates by the ORIGEN2 code.

In this presentation, we summarize the distribution of ^{129}I in the terrestrial environment before and after the accident at Fukushima. We also make a comparative review of previous studies and the ORIGEN2 code calculations with our results. In addition, we try to reconstruct ^{131}I deposition density at Fukushima using the analytical results of ^{129}I/^{131}I ratios in surface soils.

This work was supported by the KAKENHI under grant Nos. of 15H02340 and 19H04252.

Chino, M. et al., 2011. Preliminary estimation of release amounts of ^{131}I and ^{137}Cs accidentally discharged from the Fukushima Daiichi Nuclear Power Plant into the atmosphere. *J. Nucl. Sci. Technol.* 48, 1129–1134.

Hou, X.L. et al., 2013. Iodine-129 in Seawater Offshore Fukushima: Distribution, Inorganic Speciation, Sources, and Budget. *Environ. Sci. Technol*. 47, 3091–3098.

Kinoshita, N. et al., 2011, *PNAS* 108, 19526–19529.

MEXT, 2011. Extension Site of Distribution Map of Radiation Dose, etc. http://ramap.jmc.or.jp/map/eng/

Miyake, Y. et al., 2012, *Geochem. J.*, 46, 327- 333.

Miyake, Y. et al., 2015, *Nucl. Instr. and Meth.* B, 361, 627-631.

Muramatsu, Y. et al., 2015, Analysis of ^{129}I in the soils of Fukushima Prefecture: preliminary reconstruction of ^{131}I deposition related to the accident at FDNPP. *J. Environ. Radioact.* 139, 344–350.

Nishihara, K. et al., 2012. Estimation of Fuel Compositions in Fukushima-Daiichi Nuclear Power Plant. *In: JAEA-Data/Code* 012–018, 1–190.

LSC detection of ^{35}S in low-sulphate water samples avoiding sulphate precipitation

M. Schubert [1], K. Knoeller[2], J. Kopitz[3],

[1] Department Catchment Hydrology, UFZ - Helmholtz Centre for Environmental Research, 04318 Leipzig, Germany
[2] Department Catchment Hydrology, UFZ - Helmholtz Centre for Environmental Research, 06120 Halle, Germany
[3] Institute of Pathology, Heidelberg University, 69120 Heidelberg, Germany
Keywords: ^{35}S measurement, LSC, environmental tracer
Presenting author, e-mail: michael.schubert@ufz.de

A suitable tool for the investigation of groundwater residence times is the application environmental tracers. The resulting data can (e.g.) be used for **(i)** recommending groundwater abstraction rates that allow sustainable aquifer management, **(ii)** assessing groundwater travel times and related matter (contaminant) transport, and **(iii)** evaluating the aquifer vulnerability regarding anthropogenic contamination.

Naturally occurring radioisotopes are powerful environmental tracers. Ideally, their half-lives are in the same time range as the investigated physical and/or chemical processes. Rather long-lived radionuclides, such as ^{3}H, ^{14}C, ^{36}Cl, ^{39}Ar, ^{81}Kr, and ^{85}Kr, have proven as suitable for investigating long term processes. However, radiotracers that are applicable for studying groundwater residence times of less than one year are still scarcely discussed in the literature.

A novel approach for covering this timescale is based on the use of the omnipresent radioactive Sulphur (^{35}S), which is continually produced in the upper atmosphere by cosmic ray spallation of ^{40}Ar. After its production ^{35}S rapidly oxidizes to sulphate, gets dissolved in the meteoric water and is finally transferred with the rain to the groundwater. $^{35}SO_4^{2-}$ activities in precipitation are generally in a range between ca. 5 and 65 mBq/l. Since there are no natural sources of ^{35}S in the subsurface the ^{35}S activity concentration in the groundwater starts to decrease by decay with an 87.4 day half-life as soon as the rainwater enters the ground. This makes ^{35}S a potential tracer for investigating groundwater residence times between about three to nine months (i.e., between one and three ^{35}S half-lives).

^{35}S detection by liquid scintillation counting (LSC) requires pre-concentration of $^{35}SO_4^{2-}$ from large water samples. A related approach entails the precipitation and homogeneous suspensions of fine-grained ^{35}S-containing $BaSO_4$ in Insta-Gel Plus scintillation cocktail. It was developed for water samples that contain high sulphate loads of up to 1500 mg and rather low $^{35}S/^{32}SO_4^{2-}$ ratios typical for groundwater (Urióstegui et al., 2015; Schubert et al., 2019). Our study aimed at optimizing sample preparation for rainwater by avoiding the labour-intensive precipitation step.

Typical for rainwater (compared to groundwater) is a higher $^{35}S/^{32}SO_4^{2-}$ ratio (i.e., higher relative ^{35}S activities). Therefore, a lower SO_4^{2-} sample load is required for attaining a countable ^{35}S sample activity. That allows using a scintillation cocktail that is miscible with aqueous samples of low SO_4^{2-} ionic strength, namely Hionic-Fluor® (PerkinElmer). The cocktail was found to be suitable for total sulphate sample loads of (at least) up to 100 mg and hence for sulphate loads of rainwater volumes (with an assumed SO_4^{2-} concentration of 5 mg/l) of up to 20 litres.

Still, the sulphate has to be pre-concentrated from large (20 litre) rainwater samples. That can be done by extracting the sulphate from the water sample using the anion-exchange resin Amberlite IRA67 (OH-form) (Rohm & Haas). The weak-base exchange resin is previously protonated with acetic acid (CH_3COOH). After extraction the sulphate is eluted off the resin with ammonium hydroxide (NH_4OH). The resulting eluent contains high concentrations of NH_4^+, SO_4^{2-} and CH_3COO^- resulting in a high ionic strength that is not suitable for the Hionic-Fluor cocktail. However, NH_3 and CH_3COOH can easily be evaporated from the eluate. The resulting dry precipitate (ammonium sulphate; $[NH_4]_2SO_4$) is subsequently dissolved in 2 ml H_2O resulting in an aqueous ph neutral solution of an ionic strength that is suitable for the cocktail.

A problem that might occur if the rainwater sample is not "fresh and clean" is the presence of organic materials or algae growth. The resin that is used for extracting the sulphate scavenges also this material out of the rainwater and turns yellow or brown. Thus, the resulting eluent is of brown colour, too. Consequently, the final sample/cocktail mix might show strong colour quench.

Potential solutions of the problem include (1) filtering the water sample or (2) "wet ashing" of the organics in the elutant by adding hydrogen peroxide.

The introduced approach is recommended as alternative to the method that includes $BaSO_4$ precipitation. It is applicable if high $^{35}S/^{32}SO_4^{2-}$ ratios, i.e., low sulfate sample loads can be expected, e.g. in rainwater.

Urióstegui, S.H., Bibby, R.K., Esser, B.K., Clark, J.F. 2015. Analytical Method for Measuring Cosmogenic ^{35}S in Natural Waters. *Anal. Chem.* 87, 6064-6070.

Schubert, M., Kopitz, J., Knöller K. 2019. Improved approach for LSC detection of ^{35}S aiming at its application as tracer for short groundwater residence times. *J. Env. Rad.*, in press.

Radiological risk assessment of stone quarry as a high radon level site (Case Study: Open-pit slate stone mine)

A. Shahrokhi[1], M.E. Adelikhah[1], E. Kocsis[1], T. Kovács[1]

[1]Institute of Radiochemistry and Radioecology, University of Pannonia, 10 Egyetem str., H-8200 Veszprém, Hungary
Keywords: Risk assessment, Radon exhalation, annual effective dose, stone mine
Presenting author, Mohammademad Adelikhah

Radon is the second leading cause of lung cancer and is a major source of naturally occurring radiation human exposures pathway (EPA, 2003). There are various recommended reference level of effective doses of radon radiation for worker included 1.2 $mSvy^{-1}$ as worldwide average value or 2 $mSvy^{-1}$ from natural sources contain ^{238}U by U.S energy department (IAEA, 2004; DOE, 2007; ICRP, 2011).

In this paper, we initially present the concentration of ^{222}Rn in area of three difference sites of an open-pit slate stone mine, near to the Kashan city, Iran. Slate stones are a sedimentary type of stone that have been buildup of volcanic ash and clay. They made from several fine grained layers. A slate stone quarry with total 140000 m^2 in three separate sites with total 35 workers included miners, drivers, engineers and office employees were selected for this study. 3 points from each site were marked to cover all area in order to measure radon exposure concentration in difference height from ground during a period of 30 days.

In related to inhalation of radon by mineworkers, the annual effective does of inhaled radon radiation were measured for 13 of workers included office and open area workers to compare with worldwide average value. To estimate ^{222}Rn concentration exposure to workers and miners, personal CR-39 cap dosimeter detector was used. The concentration and uncertainty of calculated average of Radon concentration activity in sites of slate stone mine are shown in Table 1. In light of results, the cumulative average concentration of ^{222}Rn in all three sites except in three points are bellow than 100 Bqm^{-3} which is significantly lower than recommendation level from EPA, ICRP and European directive.

Table 1. Average ^{222}Rn concentration (Bqm^{-3}) in 3 sites of slate stone quarry.

Site number	Radon Concentration			
	Point 1	Point 2	Point 3	Point 4
1	83±12	193±11	104±10	94±16
2	38±12	49±9	46±13	53±12
3	37±7	39±9	58±10	132±21
Mean	**53±10**	**94±10**	**69±11**	**93±16**

Figure 1 presents the average radon concentration of each site in function of days. 30 days average of ^{222}Rn concentration activity of each site was calculated as 118 Bqm^{-3} for largest site, 1.46 Bqm^{-3} for site 2 and 66 Bqm^{-3} for site 3.

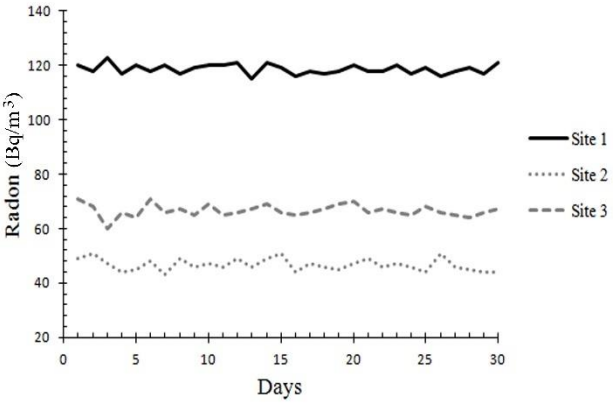

Figure 1. Average radon concentration of each site in function of days.

Annual effective doses of radon inhalation were measured for selected miners and workers individually and based on their average working hours from workers recorder book. Annual working hours was calculated approximately between 1600 to 2010 hours. Table 2 shows the occupational exposure to radon by attention to working place in mine.

Table 2. ^{222}Rn concentration and annual effective dose of inhaled radon exposure to staffs.

Worker	Working Hours	^{222}Rn exposure (Bqm^{-3})	Annual effective dose ($mSvy^{-1}$)
Miner	2010	168	3.8
Office	1960	43	0.9
Driver	2010	55	1
Office	1960	43	0.9
Miner	2010	101	2.3
Miner	2010	106	2.4
Office	1960	53	1.1
Engineer	1670	44	0.8
Engineer	1820	56	1.1
Driver	1600	39	0.7
Miner	2010	98	2.2
Miner	2010	90	2
Miner	2010	148	3.2

Office of Radiation and Indoor Air (2003). EPA assessment of risks from radon in homes. Washington DC, EPA 402-R-03-003.

International Atomic Energy Agency (2003). Radiation, People and the Environment. IAEA/PI/A.75/04-0039.

U.S. Department of Energy (2007). DOE Handbook: Radiological Worker Training. DOE-HDBK-1130-2007.

The International Commission on Radiological Protection (2011). Radiological Protection against Radon Exposure. ICRP ref 4829-9671-6554.

Selection of terrestrial reference organisms for nuclear power plants

Cao Shaofei[1], Chen Ling[2], Li Jianguo[1]

[1]Institute of nuclear environmental science, China Institute for radiation protection, Taiyuan,030006,China

[2]Institute of radiation security, China Institute of atomic energy, Beijing,102413,China

Keywords: reference organism, non-human species, nuclear power plants, radiation protection

Presenting author, e-mail: csf1860@126.com

The research on radiation protection has always been focused on how to protect human beings. At present, this understanding has undergone profound changes. 《Technical guidelines for environmental impact assessment format and content of environmental impact reports for nuclear power plants》(HJ808-2016) proposed a specific requirements for evaluating the effects of ionizing radiation on non-human species in the chapter of "Environmental impact of nuclear power plant operation".

ICRP Publication 91 (ICRP, 2003) pointed out : the objectives of a common approach to the radiological protection of non-human organisms might be to safeguard the environment by preventing or reducing the frequency of effects likely to cause early mortality or reduced reproductive success in individual fauna and flora to a level where they would have a negligible impact on conservation of species, maintenance of biodiversity, or the health and status of natural habitats or communities. Similar to the "Reference Man" used for human radiological protection, the primary task of evaluating the effects of ionizing radiation on non-human species is to develop a set of "Reference animals and plants".

The screening of terrestrial reference organisms for nuclear power plants includes the following steps:（1）Source term characteristic analysis, including the types of radionuclides emitted from airborne effluents in normal operation of nuclear power plants ,its environmental behavior, and the temporal as well as spatial scales;（2）Investigation on the current situation of terrestrial ecological environment near the nuclear power plant site, mainly includes terrestrial plants survey, terrestrial vertebrate（amphibians, reptiles, birds, mammals, and so on）survey and terrestrial invertebrate survey;（3）Selection of terrestrial reference organisms. First of all, based upon knowledge of the distribution of radionuclides within the environment terrestrial ecosystems have been considered as the soil herbaceous layer and canopy compartments. Secondly, analysis of exposure pathways. Namely analysis of the potential of the terrestrial candidate reference organisms through their feeding habits and habitat occupancy to be exposed to significant dose rates from radionuclides in their environment. Finally, selection of terrestrial reference organisms. For each candidate reference organisms, some key criteria used in their selection: legislation relating to wildlife protection, use in toxicity testing, human resource, social and ecological benefits, data on radionuclide accumulation, data on radiation effects, amenable to further study, public resonance, and so on. Terrestrial reference organisms with site characteristics are recommended through comprehensive comparison.

Taking Fuqing Nuclear Power Plant as an example, based on the characteristics of source term radioactivity monitoring data, and the present situation of terrestrial ecological environment near the nuclear power plant site, a 'set' of terrestrial Reference Animals and Plants has therefore been identified: earthworm, peanut, *Rattus losea*, hylarana guentheri, *Marchantia polymorpha L./Funaria hygrometrica*, rice/water spinach *Sageretia theezans/Rhodomyrtus tomentosa*,*Apis cerana*,Gaoshan goat,*Elaphe carinata*，duck egg,egret,*Acacia confusa*，*Pinus massoniana* and *longicorn.*

The authors would like to thank Fan Xiao from FQNPC for the valuable contributions to the paper.

This work was supported by the Youth Research Fund of China Institute for radiation protection.

Species composition and radioactive contamination of mushrooms in the pine forest near Irtysh river

Yu.S. Shevchenko[1], N.V. Larionova[1], V.V. Polevik[2], A.Ш. Aidarkhanov[1]

[1]Branch "Institute of Radiation Safety and Ecology" of the RSE "National Nuclear Center of the Republic of Kazakhstan", Kurchatov, Kazakhstan
[2] Shakarim State University in Semey city, Semey, Kazakhstan
Keywords: Semipalatinsk Test Site (STS), artificial radionuclides, mushrooms
Presenting author, e-mail: Larionova@nnc.kz

In course of nuclear tests in the atmosphere at Semipalatinsk Test Site (the STS), territory of pine forest to the north, northwest from the testing venues, have suffered from radioactive impact several times. The main contribution to radioactive contamination was made by the first nuclear test (29.08.49). Radioactive cloud has passed in direct proximity to Cheremushki, Mostik, Dolon and Kanonerka inhabited localities.

The aim of this research was to find concentrations of ^{241}Am, ^{137}Cs, ^{90}Sr and $^{239+240}$Pu artificial radionuclides in mushrooms art this territory. As the objects of research, russula (*Russula cyanoxantha*), Slippery jack (*Suillus granulatus*), girolle (*Hygrophopsis aurantiaca*), milk mushroom (*Lactarius piperatus*), button mushroom (*Agaricus camprester*), shiitake mushrooms (*Pleurotus ostreatus*), stinking russula (*Russula foetens*), red-capped scaber stalk (*Leccinum aurantiacum),* Milk-white brittlegill *(Russula dilica),* green linnet *(Tricholoma eguestre),* plums and custard *(Tricholomopsis rutilans),* and Birch Bolete *(Leccinium scabrum)* were chosen. In total 45 samples of mushrooms were collected.

Russula cyanoxantha

Lactarius piperatus

All the samples were preliminary treated: they were washed, dried, milled and homogenized. To determine specific activity of ^{137}Cs and ^{241}Am gamma-spectrometric method was used. ^{90}Sr and $^{239+240}$Pu – were measured by means of radiochemical extraction followed by beta- and alpha- spectrometric measurement. Concentrations of radionuclides in the mushrooms was determined in ash, with subsequent conversion to dry matter. Detecting limit for ^{241}Am and ^{137}Cs was <0,1 Bq/kg, ^{90}Sr – <0,4 Bq/kg and $^{239+240}$Pu – <0,02 Bq/kg.

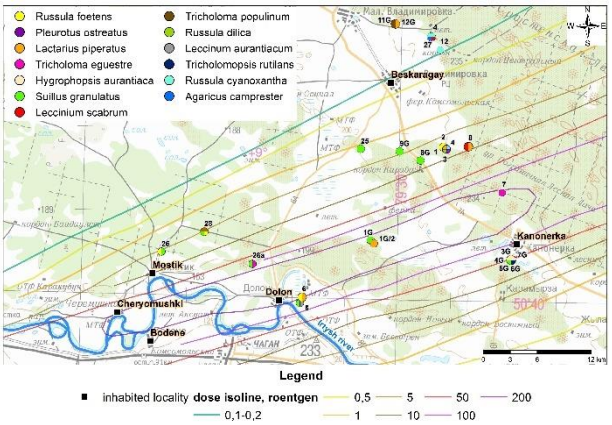

As the result of the research conducted specific activity of ^{137}Cs in mushrooms were found to vary between <0,1 Bq/kg and 150±30 Bq/kg. At that the maximum values belong to the territories in vicinity of Dolon village, where ^{137}Cs concentration in в slippery jacks (*Suillus granulatus*) reaches the value of 260±50 Bq/kg. Concentration of ^{241}Am at the researched territory in most of the cases was below the detecting limit of the equipment used, and in some cases it varied between 0,020±0,004 Bq/kg and 0,7±0,1 Bq/kg. In most cases no quantitative values of ^{90}Sr and $^{239+240}$Pu was registered. However, in some rare cases, concentration of ^{90}Sr in milk mushrooms (*Lactarius piperatus*) was found to be 350±110 Bq/kg and $^{239+240}$Pu concentration in stinking russula (*Russula foetens*) was found to be 2,70±0,12 Bq/kg.

In general, obtained quantitative values of radionuclides specific activity in mushrooms at the territory researched do not exceed permissible level (^{137}Cs – 500 Bq/kg, ^{90}Sr – 50 Bq/kg). Concentration of $^{239+240}$Pu and ^{241}Am in mushrooms is not rated, however, based on the general radiotoxity level иof each of the radionuclides above, it can be assumed, that permissible levels for $^{239+240}$Pu and ^{241}Am will be roughly an order of magnitude lower comparing with ^{90}Sr (approximately 5 Bq/kg each), according to the Health Standards «Sanitary-Epidemiological Requirements for Provision of Radiation Safety». Therefore, consumption of mushrooms poses no hazard for the population of the territories researched.

Inspection and sampling of soil and food after FDNPP accident

T. Shinano[1], M. Hachinohe[2]

[1]Laboratory of Plant Nutrition, Research Faculty of Agriculture, Hokkaido University, Sapporo, 060-8589, Japan
[2]Food Research Institute, National Agriculture and Food Research Organization, Tsukuba, 305-8642, Japan
Keywords: Radioactive caesium, Emergency sampling, Caesium contamination of soil and food
Presenting author, e-mail: shinano@chem.agr.hokudai.ac.jp

Before the Fukushima Dai-ichi Nuclear Power Plant (FDNPP) Accident in 2011, a possibility of large-scale contamination by agricultural lands with artificial radioactive materials had not been considered in Japan and emergency preparedness guidelines were insufficient in coping with this scale of accident. The lack of such guidelines prevented a proper response to the emergency and subsequent lead to additional public concerns. The measurement of radioactivity in food and agricultural land (soil) are essential tasks for keeping the population (not only for the people who had been living there, but all over Japan) safe after a nuclear emergency. This indicates that the need for guidelines for large-scale sampling and monitoring in agriculture in the case of a nuclear emergency such as nuclear power plant accident, affecting food and agricultural land. Emergency monitoring system was introduced in Japan mainly to provide a public reassurance for the food quality produced in the affected areas. We provide the information and generic, non-country specific guidance on approaches for sampling food and soil not only to scientists but it will be useful for policy-makers and decision makers who involved in nuclear emergency preparedness and response and at different stages of the nuclear emergency based on experience learnt from the Tokyo Electric Power Company's FDNPP accident.

Successive change of ^{137}Cs was once increased more than 100 mBq/kg in polishing rice during the global fall era (around 60's) (Fig. 1). The average ^{137}Cs after the FDNPP accident did not reach 100 mBq/kg in average of all Japan.

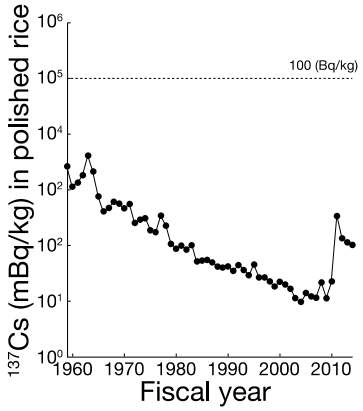

Figure 1. Successive change of ^{137}Cs in polished rice in Japan. (n=10 to 15) (NARO 2019).

The radioactive contamination was mainly observed in Fukushima prefecture and several prefectures surrounding Fukushima prefecture (Fig. 2). While the remediation efforts have been carried out and successfully decreased the radioactivity of food (i.e. brown rice in Table 1).

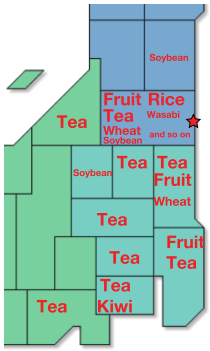

Figure 2. Radioactive caesium concentration (^{134}Cs and ^{137}Cs) in agricultural products more than 100 Bq/kg in 2011 in eastern part of Japan.

Table 1. Results of monitoring (2011) and all bags inspection of brown rice (2012-2018) in Fukushima prefecture, Japan. (Fukushima no megumi, 2019)

		≤ 50 Bq/kg	51–75 Bq/kg	76–100 Bq/kg	100 Bq/kg <	Monitored number
FY 2011	actual no.	20,295	364	219	311	21,189
	(%)	95.78%	1.7179%	1.0336%	1.4677%	100%
FY 2012	actual no.	10,343,548	1678	389	71	10,345,686
	(%)	99.98%	0.0162%	0.0038%	0.0007%	100%
FY 2013	actual no.	10,951,351	492	323	28	10,952,194
	(%)	99.99%	0.0045%	0.0029%	0.0003%	100%
Fy 2014	actual no.	11,014,636	1	1	2	11,014,640
	(%)	100%	0.00001%	0.00001%	0.00002%	100%
Fy 2015	actual no.	10,496,518	4	0	0	10,439,072
	(%)	100%	0.00004%	0	0	100%
Fy 2016	actual no.	10,264,859	0	0	0	10,264,859
	(%)	100%	0%	0%	0%	100%
Fy 2017	actual no.	9,975,884	0	0	0	9,975,884
(2018.11.02)	(%)	100%	0%	0%	0%	100%
Fy 2018	actual no.	9,224,054	0	0	0	9,224,043
(2019.5.22)	(%)	100%	0%	0%	0%	100%

This work was supported by IAEA CRP D1.50.15 and KAKENHI 19H01169.

NARO (National Agriculture and Food Research Organization) 2019. https://vgai.dc.affrc.go.jp/vgai-agrip/samples. (access on 22nd May 2019)

Fukushima no megumi 2019. https://fukumegu.org/ok/contentsV2/kome_summary_2.html. (access on 22nd May 2019)

Determination of ^{137}Cs using non-commercial impregnated fly ash sorbent

V. Silliková[1], S. Dulanská[1], M. Horník[2], Ľ. Mátel[1], J. Jakubčinová[3]

[1]Department of Nuclear Chemistry, Comenius University, Bratislava, 842 15, Slovakia
[2]Department of Ecochemistry and Radioecology, University of SS. Cyril and Methodius in Trnava, Trnava, 917 01, Slovakia
[3]Institute of Chemistry, Slovak Academy of Sciences, Bratislava, 845 38, Slovakia
Keywords: fly ash, ^{137}Cs, impregnation
Veronika Silliková, e-mail: veronikasillik963@gmail.com

A recent accident at Fukushima nuclear power plant drew attention to environmental contamination. After the accident, high contamination of the atmosphere and water by cesium radionuclides was reported (Clearfield, 2010). The distribution of artificial radionuclides such as ^{131}I, ^{134}Cs, ^{137}Cs, ^{239,240}Pu, ^{238}Pu and ^{241}Am in the environment depends on the sources (e.g. nuclear weapon tests, nuclear facility accidents, submarines, aircraft and radioactive waste discharges), release conditions and subsequent transformation processes. Among these artificial radionuclides ^{137}Cs is an important indicator of radioactive pollution in the aquatic environment (Ashraf, 2014). The current annual production of coal ash around the world is estimated at around 600 million tonnes, with fly ash about 500 million tonnes per (75 - 80) % of the total ash produced (Ahmaruzzaman, 2010). The chemical composition of fly ash, as a high percentage of silicon dioxide (60 - 65) %, alumina (25 - 30) % and magnetite, Fe_2O_3 (6 - 15) % allows its use in the synthesis of zeolite, alum and precipitated silica. Other important physical and chemical characteristics of fly ash, such as bulk density, particle size, porosity, water retention capacity and surface area, make it suitable for use as an adsorbent (Kaminski, 2009; Iyer, Scott, 2001). With regard to the use of silicates in the form of a modified sorbent, a lot of papers have been published. Different composite adsorbers were formed by depositing nanoscales of hexacyanoferates on the surface or within the pore of inert solid carriers such as silica gel, zeolite, zirconium hydroxide and titanium hydroxide or various organic ion exchangers (Mimura, Letho, Harjula, 1997).

The objective of this study was to increase the sorption capacity of sorbent prepared from fly ash by modification and to quantify its ability to sorb Cs^+ ions. The fly ash used in this work for the experiments, came from the OFZ production plant in Istebné (Slovak Republic). Its specific surface area 14 m^2/g was measured on the Slovak Academy of Sciences using the BET method. In the first part of the work, the possibility of cesium sorption on the original fly ash (non-modified) was tested. It was found out that the sorption capacity of the non-modified sorbent was low. Because of this, the possibility of modification was tested. The obtained results in this way confirmed the increase of sorption capacity. After applying the Freundlich and Langmuir models, the statistical comparison of models showed, that Langmuir model had lower AIC value, which indicates that this model is more likely to be correct than Freundlich model. The correlation coefficient was 0.966 compared to the Freundlich model. Freundlich assumed that the surface of the adsorbent is heterogeneous and thus the adsorption sites and their energy are exponential and describe the physical adsorption. The test result confirmed that the surface of the modified sorbent is homogeneous and thus the adsorbed cations cannot migrate across the surface or interact. The effect of competitive cations Na^+, K^+, Ca^{2+} and Mg^{2+} on Cs+ ions sorption was evaluated. Na^+ and K^+ cations don't have a significant effect on cesium sorption onto fly ash. Ca^{2+} and Mg^{2+} at a concentration higher than 100 mg/ml lead to decrease the cesium's ability to sorb onto impregnated fly ash with the sorption efficiency only 9 %. It has been proved that chemically modified fly ash is a good alternative for concentrating ^{137}Cs from larger volumes of water. Fly ash seems to be a cheap way to concentrate cesium from different types of wastewater and radioactive liquids.

This work was supported by the grant of Comenius University No. UK/36/2019 and the project of the Slovak Research and Development Agency under the contract No. APVV-17-0150.

Amharuzzaman, M., 2010. A Review on the Utilization of Fly Ash. *Prog. Energ. Combust.* 36, 327-363.

Ashraf, M.A., Akib, S., Maah, M.J., Yusoff, I., Balkhair, K.S., 2014. Cesium-137: Radio-Chemistry, Fate and Transport. Remediation, and Future Concerns. *Cri. Rev. Environ. Sci. Tech*. 44, 1740-1793.

Clearfield, A., 2010. Seizing the Caesium. *Nat. Chem*. 2, 161-162.

Iyer, R.S., Scott, J.A., 2001. Power Station Fly ash – a Review of Value-added Utilization Outside of the Construction Industry. *Resour. Convers. Recycl.* 31, 217-228.

Kaminski, M.D., 2009. Physical Properties of an Alumino-silicate Waste form for Cesium and Strontium. *J. Nucl. Mater.* 392, 510-518.

Mimura, H., Letho, J., Harjula R., 1997. Selective Removal of Cesium from Stimulated High-level Liquid Wastes by Insoluble Ferrocyanides. *J. Nucl. Sci. Tech.* 34(6), 607-609.

Variations of ^{13}C and ^{14}C in carbon dioxide exhaled from the soil

Šivo, K. Holý, M. Műllerová, I. Kontuľ, M. Richtáriková, T. Eckertová, P. P. Povinec

Faculty of Mathematics, Physics and Informatics, Comenius University, Mlynská dolina F-1, 842 48 Bratislava, Slovakia
Keywords: exhalation, carbon dioxide, ^{14}C, ^{13}C, variations.
Terézia Eckertová, e-mail: eckertova@fmph.uniba.sk

Carbon dioxide is produced in soil by the microbial decomposition of the soil organic matter and by the root respiration (Dörr and Münnich, 1986). Part of the carbon dioxide produced is exhaled into the atmosphere and influences, especially in ground-level air, atmospheric CO_2 concentrations, as well as ^{14}C levels in CO_2. The ^{14}C content in the soil CO_2 can be different from the ^{14}C content in the atmospheric CO_2 during the year. The results indicate that $^{14}CO_2$ exhalations from the soil into the atmosphere should be taken into account when accurate results of the ^{14}C content in the atmosphere are required.

In this contribution the results of simultaneous ^{13}C and ^{14}C measurements in the CO_2 exhaled from the soil at Bratislava (Slovakia) are presented. We also focused on the simultaneous measurements of the ^{222}Rn and CO_2 in the soil at depth of 0.8 m. The soil in this area is a type of a sandy clay, middle permeable, uncultivated and with a grass cover.

For carbon isotope determination in CO_2 exhaled from the soil the accumulation method was used. The CO_2 diffusing out of the soil surface was collected under plastic container and absorbed in four glass dishes containing a total of 2 ℓ 3M NaOH. For the carbon isotope measurements in the soil CO_2 the dynamic method of an absorption of CO_2 into NaOH solution has been used. The average sampling time was one month. Subsequently, CH_4 was prepared from the samples to fill a low-level proportional counter, which was used for counting of ^{14}C decays (Povinec et al., 1968). For the determination of $\delta^{13}C$ in samples, a mass spectrometry was used. Simultaneously, the radon concentration in soil air was measured using a scintillation cell of the Lucas type (Müllerová et al., 2014).

$\Delta^{14}C$ in the exhaled CO_2 reaches maximum values in summer months, the same holds true for the $\Delta^{14}C$ in the soil CO_2. However, $\Delta^{14}C$ values in the exhaled CO_2 are often lower than those in the soil CO_2. Unlike the soil, $\delta^{13}C$ in the exhaled CO_2 reaches maximum values in winter months and minimum values in summer months. The $\delta^{13}C$ in the exhaled CO_2 varies predominantly in the range from -17 ‰ to -25 ‰, while the mean value of $\delta^{13}C$ is on the level of -22 ‰.

A mutual relationship of measured data was investigated using correlation analysis. A high correlation coefficient was found between $\Delta^{14}C$ exhaled from the soil and the soil $\Delta^{14}C$ ($R^2 = 0.8$). A similarly high correlation was found between $\delta^{13}C$ in the exhaled CO_2 and the ^{222}Rn concentration in the soil air ($R^2 = 0.72$). This indicates that ^{222}Rn can also be a useful tool for the estimation of exhalation of carbon isotopes from the soil into the atmosphere.

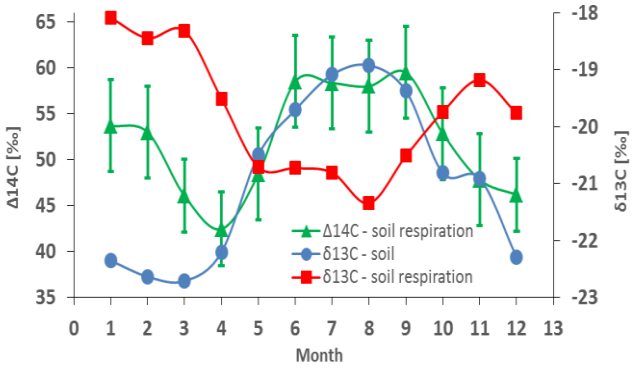

Figure 1. Average seasonal variations of $\Delta^{14}C$ and $\delta^{13}C$ in exhaled and soil carbon dioxide.

This work has been supported by the the Scientific Grant Agency of the Ministry of Education of the Slovak republic under the VEGA projects No. 1/3046/06, 1/0678/09, 1/0143/14 and 1/0213/18.

Dörr, H., Münnich, K. O., 1986. Annual variations of the ^{14}C content of soil CO_2, *Radiocarbon*, 28, 338-345.

Povinec, P., Šáro, Š., Chudý, M., Šeliga, M., 1968. The rapid method of carbon-14 counting in atmospheric carbon dioxide. *Int. J. Appl. Rad. Isotopes*, 19, 877-881.

Müllerová, M., Holý, K., Bulko, M., 2014. Daily and seasonal variations in radon activity concentration in the soil air. *Radiation Protection Dosimetry*, 160, 222-225.

Determination of activity concentration of ^{234}U, ^{235}U, ^{238}U, ^{210}Po, and ^{210}Pb in bottled mineral and spring waters

E. Starościak[1]

[1]Department of Radiation Hygiene, Central Laboratory for Radiological Protection, Warsaw, 03-194, Poland
Keywords: water, uranium, polonium
Presenting author, e-mail: staroscIak@clor.waw.pl

The consumption of water is one of the ways passage of radioactive substances to the human body. Council directive 2013/51/EURATOM of 22 October 2013 "Laying down requirements for the protection of the health of the general public with regard to radioactive substances in water intended for human consumption" and Minister of Health regulation of December 7, 2017 "On the quality of water intended for human consumption" determine the levels of natural and artificial radionuclides permitted in drinking waters. Detailed requirements to be met by mineral and spring waters also regulates Minister of Health regulation of 31.03.2011 "On natural mineral waters, spring waters and table waters".

The aim of the study was to determine the activity concentrations of natural isotopes: uranium-234, uranium-235, uranium-238, polonium-210 and lead-210 in samples of mineral and spring bottled samples from stores in Warsaw, from shots from various regions of Poland.

The following activity concentration were determined: ^{234}U, ^{235}U, ^{238}U, ^{210}Po and ^{210}Pb in 11 samples of water: Aleksandria, Cisowianka, Primavera, Muszynianka, Jurajska, Żywiec Zdrój, Nałęczowianka, Nestle Pure Life, Kryniczanka, Magnesia, Arctic+.

The activity concentration of ^{210}Po ranged from 0,39 ± 0,04 mBq·l^{-1} for water Nałęczowianka to 1,17 ± 0,06 mBq·l^{-1} for Jurajska water (Figure 1).

In the case of ^{210}Pb concentration range is from 2,60 ± 0,18 mBq·l^{-1} for water Cisowianka and Primavera to 6,37 ± 0,23 mBq·l^{-1} for Magnesia water (Figure 1).

In 9 water samples activity concentration of ^{234}U were above the limit of detection (0,5 mBq·l^{-1}) and ranged from 0,50 ± 0,26 mBq·l^{-1} for water Aleksandria to 6,24 ± 0,73 mBq·l^{-1} for Jurajska water. Activity concentration of ^{238}U in 4 samples were above 0,5 mBq·l^{-1} and ranged from 0,50 ± 0,17 mBq·l^{-1} for water Kryniczanka to 1,38 ± 0,35 mBq·l^{-1} for Muszynianka water. For all tested water samples activity concentration of ^{235}U were below 0,5 mBq·l^{-1}. The resulting activity concentrations of uranium isotopes are shown in Figure 2.

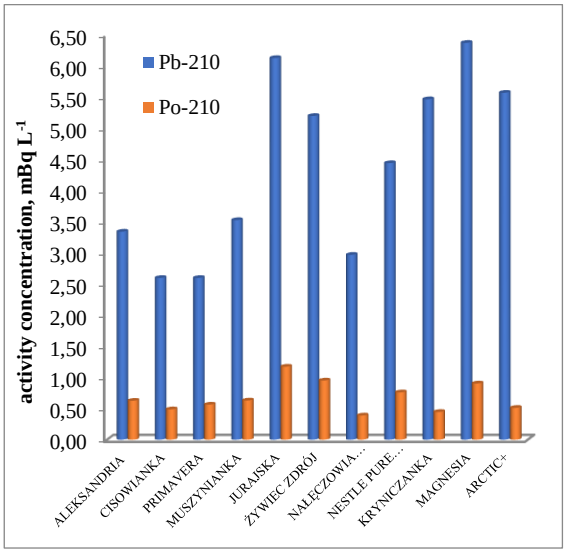

Figure 1. Activity concentration of ^{210}Po and ^{210}Pb in bottled mineral and spring waters.

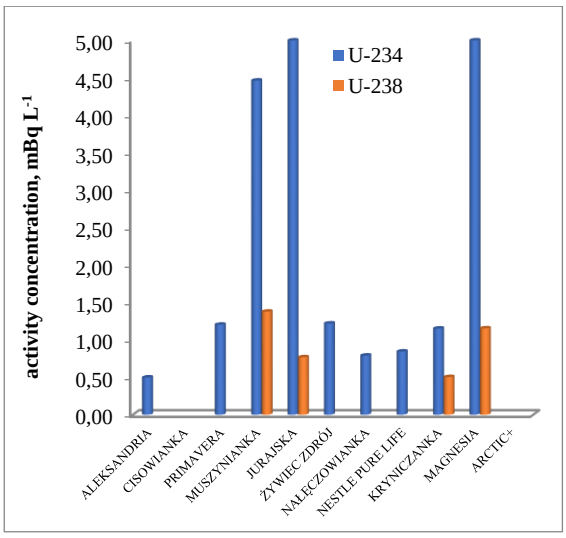

Figure 2. Activity concentrations of ^{234}U and ^{238}U in bottled mineral and spring waters.

All investigated mineral and spring waters meet the requirements stored in the Polish Minister of Health regulation of December 7, 2017 "On the quality of water intended for human consumption".

This work was supported by the Ministry of Science and Higher Education Republic of Poland.

Establishing environmental nuclear forensics with Radiocesium iIsotopes ^{135}Cs and ^{137}Cs using triple quadrupole ICP-MS

G. Steinhauser[1], D. Zok[1], L. Grüger[1], R. Querfeld[1]

[1]Institute of Radioecology and Radiation Protection, Leibniz Universität Hannover, Hannover, 30419, Germany
Keywords: Cesium-135, Cesium-137, Radioecology, Mass Spectrometry
Presenting author, e-mail: zok@irs.uni-hannover.de

Radiocesium, in particular ^{137}Cs ($T_{1/2}$ = 30 y) is one of the most prominent anthropogenic radionuclides in radioecology. It has been released on a multitude of occasions, such as the nuclear weapons fallout of the 20th century and nuclear accidents such as Chernobyl, and Fukushima (only to mention two incidents at a global scale). When mixing of radiocesium from various sources occurs, the distinction of the sources exhibits a true challenge. In some instances, the presence of short-lived ^{134}Cs ($T_{1/2}$ = 2 y) and ratio of ^{134}Cs/^{137}Cs, may help distinguishing two or more sources, but in some cases, most prominently Fukushima, this method faces severe limitations, because the ^{134}Cs/^{137}Cs signatures of reactor units 1, 2, and 3 were quite similar.

As a solution to this challenge, Zheng et al.[1] successfully applied inductively-coupled-plasma triple quadrupole mass spectrometry (ICP-QQQ), which is capable of suppressing isobaric interferences.[2]

In this poster, we present our recent efforts to establish ICP-QQQ in environmental nuclear forensics. Our work focuses on chemical methods for the removal of interfering elements as well as the establishing laser ablation coupled to ICP-QQQ for spatially resolved analyses.

This work was supported by Deutsche Forschungsgemeinschaft (DFG 419819104).

[1] Zheng, J., et al., 2014, *Environ Sci Technol* 48: 5433

[2] Bu, W., et al., 2018, *J. Anal. Atom. Spectrom.* 33:519.

Assessment of radioactivity level in the environment of IFIN-HH area, Romania

Ana Stochioiu[1], Ileana Radulescu[1], Andrei Stochioiu[2]

[1]Horia Hulubei National Institute for R&D in Physics and Nuclear Engineering (IFIN-HH), 30 Reactorului St. PO Box – MG-06, RO-077125 Magurele Ilfov County, Romania; *E-mail: stoc@nipne.ro and rileana@nipne.ro*
[2]National Institute for Laser, Plasma and Radiation Physics (INFPLR) A, Street, No. 409, Magurele city, Ilfov county, Postal code: RO-077125, Romania; *E-mail: andrei.stochioiu@inflpr.ro*

This paper presents representative data on the radioactivity level within the influence zone of the R&D activities carried out in the "Horia Hulubei" National Institute for R&D in Physics and Nuclear Engineering, Bucharest, Romania. The IFIN-HH nuclear activities involve the processing of radioactive materials, as for example: radioactive waste treatment, decommissioning of the VVR-S nuclear reactor research, radioisotope production and the new Extreme Light Infrastructure-Nuclear Physics, ELI-NP, operation. The monitoring of the environmental radioactivity has been carried out continuously for more than fifty years, and the sensitivity and measurement methods, as well as the number of environmental samples to be collected and analysed were much improved during this long period. This duty has been accomplished by the specialized Laboratory for Personal and Environment Dosimetry (LDPM) of IFIN-HH, recognized by the Romanian Nuclear Authority, CNCAN. LDPM elaborated a Programme for the monitoring of environmental radioactivity and the operational procedures to be followed. This paper presents the monitoring of activity in the last two years, 2017 – 2018. The problems regarding: collection of environmental samples, their physical-chemical treatment, measurement, processing of data and interpretation of the results are presented. The accomplishment of the legal requirements regarding the activity concentration derived limits is underlined. The results are the following: : i) drinkable water - the values were much lower than the legally allowed limits, of (0.1 Bq/L-alpha emitters and 1.00 Bq/L- beta emitters); ii) industrial waters : the measured gross beta activity concentration values varied from 0.18 Bq/L to 0.88 Bq/L, inferior to the allowed value 1.85 Bq/L. Atmospheric aerosols were taken twice a month and the filters measured after 3 minutes, 24 hours and 5 days after aspiration. Dry and wet atmospheric depositions were collected weekly or event on a special surface from 0.302 m^2. Soil samples were taken from 9 representative points in the area of influence and a reference point for which global beta values were in the range (668 ± 44) Bq / kg and (1105 ± 58) Bq / kg, and for spontaneous vegetation between (150 ± 14) Bq / kg and (255 ± 20) Bq / kg dry weight. On the other hand, CNCAN imposed an annual dose constraint of 1 00 μSv/y for the representative population of the town Măgurele, where the IFIN-HH is situated. The calculated annual doses due to the environmental radioactivity resulting from IFIN-HH operations were: 15.50 μSv/y in 2017 and 12.25μSv/y respectively in 2018. The general conclusion is that the activities carried out within IFIN-HH have no significant influence over the radiation exposure of Măgurele town residents and environment.

Acknowledgements: This work was supported by the projects: PN 16 42 02 03, PN 18 09 02 02 and PN 19 06 02 03 from Ministry of Research and Inovation of Romania.

SR ISO/IEC-17 025:2018. General Requirements for the Competence of Testing and Calibration Laboratories;

Ana Stochioiu, 2016, Working procedures: PL-UMRM-02,03,04,05 and PL-URPMB-02;

A. Stochioiu, M. Sahagia, S. Bercea, C. Ivan, I. Tudor. 2009, Monitoring of the radioactivity concentration of air in the area of IFIN-HH, Romania. *Romanian Reports in Physics*, Vol. 61, No. 3, P. 581–586,

SR ISO 2889:1998. General principles for sampling of radioactive materials contained in the air.

„Vertebrata fucoides" as a natural sorbent of plutonium isotopes

M. Suplińska[1)], T. Zalewska[2)], M. Saniewski[2)]

[1)] Central Laboratory for Radiological Protection, Warsaw 03-194 Poland
[2)] Institute of Meteorology and Water Management – PIB, Gdynia, 81-342 Poland
Keywords: marine algae, bioaccumulation, plutonium
M. Suplinska, e-mail: suplinska@clor.waw.pl

The aim of the study was to examine the possibility of using a representative of the marine red algae, *Vertebrata* ***fucoides*** as a natural biosorbent of plutonium isotopes. ^{239}Pu – alpha radioactive isotope was used for the study. On the basis of the research, biosorption of plutonium was determined, taking into account the influence of pH and the matrix of eluent.

Algae are a large group of marine macrophytobenthic plants characterized by very good bioaccumulative and biosorbent properties in the case of heavy metals and radioactive isotopes *eg.* ^{137}Cs and ^{90}Sr [1,2,3]. Plutonium isotopes present in the marine environment occur at several degrees of oxidation. The main source of ^{239,240}Pu in the Baltic Sea environment is radioactive fallout after nuclear weapon tests, and radioactive fallout after the Chernobyl accident. Because plutonium isotopes can be released also, although to a small extent, during the routine operation of the Baltic nuclear facilities (omitting hypothetical failures), the concentration of plutonium isotopes should be controlled in the environment due to their documented harmful effects on marine organisms.

The samples of *V. fucoides* for the experiment were collected in the Orlowski Cliff area by the diver in May and September 2018. The algae samples of defined mass were immersed in chromatographic columns, and then the solution of ^{239}Pu are passed through them. Water solutions of ^{239}Pu with different concentrations (40 ÷ 200 mBq dm^{-3}) and with different pH (1 ÷ 10) were used as eluates. Seawater and distilled water was used as the eluate matrix. After the experiment samples of algae were dried and mineralised. The eluate was collected into the bottles.

The determination of ^{239}Pu was performed in algae samples as well as collected eluate to determine the efficiency of the bioaccumulation process. The radiochemical method was applied using ^{242}Pu as a tracer. Measurement of the plutonium isotopes activity after the electro-deposition was performed using alpha spectrometry.

The study has shown that bioaccumulation of plutonium isotopes by a representative of red algae proceeds very efficiently, however it depends on the chemical conditions applied during experiment. Different ^{239}Pu concentrations in the range from 40 to 200 mBq dm^{-3} do not affect bioaccumulation efficiency – this may indicate lack of "saturation" effect. The increase in the pH of solutions based on distilled water reduces the bioaccumulation efficiency of plutonium. The ranges of biosorption efficiencies were: 94.6 ÷ 95.8 % at pH = 1-3, 56.7 ÷ 80.9 % at pH = 7 and 30.8 ÷ 47.4 % at pH = 9 - 10. Bioaccumulation efficiency of ^{239}Pu from the solutions based on seawater, does not depend on the pH of the solution, and it stayed in the range 81.4 ÷ 96.5 %.

The results of our research have shown the possibility of using this species of algae - *Vertebrata* ***fucoides*** - as a natural biosorbent of plutonium isotopes. This selected species of algae is characterized by high prevalence in the marine environment both geographically and the size of biomass which guarantees the availability of material.

Skwarzec B., Bojanowski R. (1992). Distribution of plutonium in selected components of the Baltic ecosystem within the Polish economic zone. *Journal of Environmental Radioactivity*, 15, 249–263

Zalewska T., 2014, Bioaccumulation of gamma emitting radionuclides in *Polysiphonia fucoides*, *Journal of Radioanalytical and Nuclear Chemistry* 299, 1489 – 1497

Zalewska T., 2015. Macrophytobenthic bioindicators in the classification of the marine environment of the Baltic Sea. Monographs of IMGW (in Polish).

Analysis of organically bond tritium in soil samples

I.Světlík[1,2], K. Pachnerová Brabcová[1], L. Tomášková[1], M. Fejgl[2]

[1]Department of Radiation Dosimetry, Nuclear Physics Institute, Prague, CZ18086, Czech Republic
[2]National Radiation Protection Institute, Prague, CZ14000, Czech Republic

In the areas with the tritium activities elevated above background level, the measurements of actual values are requested in the surface and underground water. Likewise, in such localities, the tritium activity is often studied in the biota, in the forms of non-exchangeable organically bound tritium (NE-OBT), or even in tissue-free water form (Boyer et al., 2009; Okada and Momoshima, 1993; Baglan et al., 2011; Pointurier et al., 2004). The OBT analysis in soil samples faces to several unfortunate material properties, resulting from usually low concentration of organic matter and hygroscopic properties of inorganic soil components, which can also contain HTO, in form of crystal water. These unfavourable circumstances are almost completely overcome when using the analysis of tritiogenic ^{3}He (Janovics et al., 2014). A suitable type of instrumentation for the ^{3}He analysis, however, has a relatively high purchase price and is also demanding on the professional skills of laboratory staff.

In contrast, the OBT analysis based on the measurement of the activity of tritium, after conversion to HTO form, is less costly, but requires analytical routine that can effectively suppress unfavourable properties of the soil samples. During the experiments carried out in our laboratory, we developed and pre-tested the combustion apparatus, which allows to remove interfering HTO and exchangeable forms of OBT. This process does not require the opening of the apparatus with sample before combustion.

First, the determination of the basic apparatus parameters and the verification experiments were performed. Then several soil samples were collected in the vicinity of the Mohelno dump, where are released liquid effluents from nuclear power plant Dukovany.

The deep valley of the Mohelno dump and the downstream valley of the Jihlava river are characterized by increased NE-OBT activities even more than the order of magnitude above the background level, as confirmed by our previous research (Svetlik et al. 2013, Kořínková et al. 2015, Simek et al. 2017).

This contribution will discuss both the design and parameters of our apparatus for soil samples processing, as well as the first obtained results.

The work was supported by OP EDE, MEYS, under the project „Ultra-trace isotope research in social and environmental studies using accelerator mass spectrometry“, No. CZ.02.1.01/0.0/0.0/16_019/0000728.

Baglan, N., Alanic, G., Le Meignen, R., Pointurier F. 2011. A follow up of the decrease of non exchangeable organically bound tritium levels in the surroundings of a nuclear research center. *J. Enviro. Radioact.* 102, 695-702.

Boyer, C., Vichot, L., Fromm, M., Losset, Y., Tatin-Froux, F., Guétat, P., Badot, P.M. 2009. Tritium in plants: A review of current knowledge. *Environ. Exp. Bot*. 67, 34–51.

Janovics, R., Bihari, Á., Papp, L., Dezsö, Z., Major, Z., Sárkány K.E., Bujtás, T., Veres, M., Palcsu L. 2014. Monitoring of tritium, 60Co and 137Cs in the vicinity of the warm water outlet of The Paks Nuclear Power Plant, Hungary. *J. Enviro. Radioact.* 128, 20-26.

Kořínková, T., Svetlik, I., Fejgl, M., Povinec, P.P., Simek, P., Tomaskova, L. 2016. Occurrence of organically bound tritium in the Mohelno lake system. *J. Radioanal. and Nucl. Chem*, 307(3), 2295-2299.

Okada, S., Momoshima, N., 1993. Overview of tritium: characteristics, sources and problems. *Health Phys*. 65, 595–608.

Pointurier, F., Baglan, N., Alanic, G. 2004. A method for the determination of low level organic-bound tritium activities in environmental samples. *Appl. Radiat. Isot*. 61, 293-298.

Simek, P., Kořínková, T., Svetlik, I., Povinec. P.P., Fejgl, M., Malátová, I., Tomaskova, L., Stepan, V. 2017. The valley system of the Jihlava river and Mohelno reservoir with enhanced tritium activities. *J. Enviro. Radioact.* 166, 83-90.

Svetlik, I., Fejgl, M., Malátová, I., Tomaskova, L. 2014. Enhanced activities of organically bound tritium in biota samples. *Appl. Rad. and Isot.* 93, 52-56.

Radionuclides in the Bratislava air

I. Sýkora, P.P. Povinec

Department of Nuclear Physics and Biophysics, Comenius University, Bratislava, Mlynská dolina F1, 842 48 Bratislava, Slovakia
Keywords: atmosphere, radioactivity, radionuclide variations
Presenting author, e-mail: Ivan.Sykora@fmph.uniba.sk

From 2003, week periodic measurements of Bratislava air radionuclides have been carried out at the university campus in Mlynská dolina. Aerosol radionuclides have been sampled on nitro-cellulose filters with the average flow rate of about 80 m^3/hour. ^{7}Be, ^{40}K, ^{137}Cs and ^{210}Pb radionuclides on aerosols from the ground-level atmosphere were gamma-spectrometrically analyzed using HPGe detectors situated in low background shields (Sýkora et al. 2008). Wet depositions from year 2009 in month periodic samples have been carried out, too.

The concentrations of ^{210}Pb and ^{7}Be ranged from 0.2 to 2.1 mBq m^{-3} with the mean value of 0.8 ± 0.3 mBq·m^{-3}, and from 0.2 to 5.7 mBqm^{-3} with the mean value of 2.4 ± 1.1 mBq m^{-3}, respectively. Measured concentrations of ^{7}Be and ^{210}Pb are shown in Fig.1 and Fig.2, respectively. Seasonal variations in concentration of both radionuclides have been observed. Concentrations of ^{7}Be show typical trends for inland country of the Northern Hemisphere with maxima in spring and early summer, and minima in winter. Concentrations of ^{210}Pb (a radon decay product) are different, showing minima in summer and maxima in winter. Seasonal variations of activity concentrations of ^{7}Be and ^{210}Pb show thus typical mutually inverse trends.

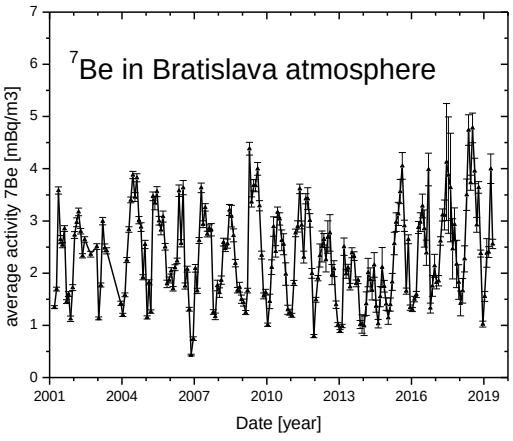

Figure 1. Time variation of ^{7}Be aerosol concentration in the Bratislava atmosphere.

In order to measure low concentrations of ^{137}Cs and ^{40}K in atmospheric aerosols with high precision, monthly samples were accumulated from weekly sampled filters. ^{137}Cs concentration shows decreasing trend (Sýkora et al, 2012, 2017). This radionuclide was introduced to the atmosphere by global fallout and the Chernobyl accident. Higher concentrations in winter months refer to resuspension of soil particles to the atmosphere. The aerosol component of the ground level atmosphere in Bratislava showed typical values of activity concentrations also for ^{137}Cs and ^{40}K, as expected for the Central Europe.

The environmental radioactivity monitoring can be useful to study the transport processes between the troposphere and low-level atmosphere, as well as to assess impact on nuclear power plants on the environment.

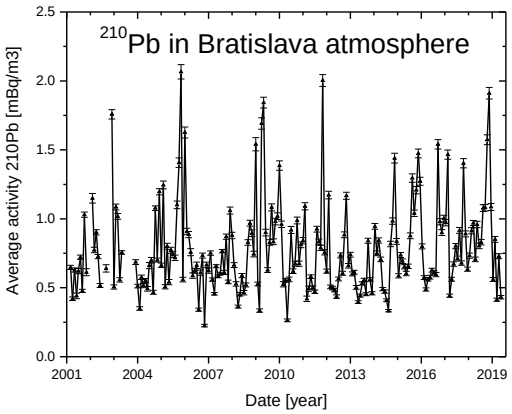

Figure 2. Time variation of ^{210}Pb aerosol concentration in the Bratislava atmosphere.

The authors acknowledge support provided by the EU Research and Development Operational Program funded by the ERDF (project 26240220004), and from the International Atomic Energy Agency (project SLR-1001).

Sýkora, I., Ješkovský, M., Janik, R., Holý, K., Chudý, M., Povinec, P. P. 2008, *J. Radioanal. Nucl. Chem.*, 276, 779-787.

Sýkora, I., Povinec, P. P., Brest'áková, L., Florek, M., Holý, K., Masarik, J. 2012, *J. Environ. Radioact.* 293, 595-599.

Sýkora, I., Holý, K., Ješkovský, M., Müllerová, M., Bulko, M., Povinec, P.P. 2017, *J. Environ. Radioact.*, 166, 27-35.

Transfer of ^{241}Am and $^{238,239+240}$Pu to goat milk from the soil component of the diet

S. A. Tagai[1], A. A. Tsarenok[1], E. K. Nilova[2], V. V. Makarovets[1], N.V. Dudareva[1], A. F. Gvozdik[1]

[1]Institute of Radiobiology of the National Academy of Sciences, Gomel, 246000, Belarus,
[2]Center for Nuclear and Radiation Safety Ministries of Emergency Situations, Minsk, 220012, Belarus
Keywords: ^{241}Am, $^{238,239+240}$Pu, transfer factor, soil component, goat milk
Presenting author, e-mail: lanabuz@tut.by

Long half-lives of α-emitting transuranium elements (TUE) – ^{241}Am and $^{238,239+240}$Pu of the Chernobyl source determine the high radioecological importance of their potential involvement into biological cycle (Konoplia, 2007). The transfer of the radionuclides in the agricultural sphere has an impact on the people ultimately. Among livestock products milk is the "critical" by radiation factor. During the grazing period small and large cattle can consume about 75 and 600 kg of soil with grass, respectively. Due to the small amount of ^{241}Am and Pu isotopes transfer into grass fodder the soil component can determine the main contribution to milk contamination by these radionuclides.

Experiments were carried out on 12 lactating goats receiving ^{241}Am and $^{238,239+240}$Pu of Chernobyl origin in the form of soil component addition (mineral soil – 6 goats and organic soil - 6 goats also) for two terms of feeding – 80 and 160 days. The total daily intake of TUE consumed by experimental animals with mineral and organic soil was about 300 and 1400 Bq·day^{-1} respectively (Averin, 2014). The method of radiochemical purification (IAEA, 1999) was used to determine activity concentrations of TUE in milk samples. The transfer parameters – transfer factor F_m(day·l^{-1}) and concentration ratio CR of americium and plutonium isotopes in goats milk from soil components of the diet were obtained. The parameters are calculated taking into account the international recommendations (IAEA, 2010), (IAEA, 2009).

It is established that the F_m and CR parameters of americium and plutonium for goat milk are not constant values but depend on the duration of the soil component receipt contaminated with these elements. This is due to the fact that the balance of ^{241}Am and $^{238,239+240}$Pu in the body of animals does not occur throughout their all productive life. On 160 days of feeding of organic soil component ^{241}Am and $^{238,239+240}$Pu F_m into milk increased to 4 and 3 times, respectively, compared to F_m of these radionuclides on 80 days. Average values of transfer rates F_m ^{241}Am and $^{239+240}$Pu in the milk of goats from organic soils in each period 80 and 160 days exceed 1.5 times any of the parameters over the same period of the mineral soil (Table 1,2). However, the size of ^{241}Am transfer in the milk of goats for the two types of soil components are comparable and are in the same order of magnitude with the reference data of IAEA TRS-472. The sizes of $^{239+240}$Pu transition to goats milk for the periods of 80 and 160 days are in the same order of magnitude with ^{241}Am–10^{-5}-10^{-6} day·l^{-1} which is a thousandth of a percent of the daily intake of these radionuclides in the diet.

Thus, the results show that the transfer of transuranic elements ^{241}Am and $^{238,239+240}$Pu of Chernobyl origin from the soil component of the diet to goat milk depends more on the duration of receipt than on the type of soil matrix-carrier of TUE

Table 1. Transfer coefficients for ^{241}Am transfer to goat milk from soil components of the diet, F_m, day·l^{-1}, x10^{-5}

Soil component	Feeding period	Animals number	mean	min	max
organic	80 days	6	0,49	0,39	0,58
mineral		6	0,35	0,20	0,70
organic	160 days	3	1,9	0,41	4,7
mineral		3	1,3	0,69	2,0
IAEA TRS-472		2 records	**0,69**	**0,37**	**1,0**

Table 2. Transfer coefficients for $^{239+240}$Pu transfer to goat milk from soil components of the diet, F_m, day·l^{-1}, x10^{-5}

Soil component	Feeding period	Animals number	mean	min	max
organic	80 days	6	0,99	0,69	2,0
mineral		6	0,79	0,45	1,2
organic	160 days	3	2,7	0,39	6,9
mineral		3	1,9	1,2	2,7
IAEA TRS-472		1 record	**10,0**		

This work was supported by the State Program of the Republic of Belarus on Overcoming the Consequences of Disasters at the Chernobyl NPP for 2011-2015 and the period up to 2020 under the grant No. 2/2011.

Konoplia E.F., Kudriashov V.P., Mironov V.P. 2007. Radiation and Chernobyl: Transuranic elements on the Belarus territory. (In Russian).

Averin V.S. et al. 2014. Americium and plutonium in agroecosystems. 1986 Chernobyl disaster. (In Russian).

IAEA. 1999. Generic Procedures for Monitoring in a Nuclear or Radiological Emergency. *TECDOC-1092*.

IAEA. 2010. Handbook of Parameter Values for the Prediction of Radionuclide Transfer in Terrestrial and Freshwater Environments. *TRS-472*.

IAEA. 2009. Quantification of Radionuclide Transfer in Terrestrial and Freshwater Environments for Radiological Assessments. *TECDOC-1616*.

Reconstruction of radiocesium level in bottom sediment off Fukushima

Y. Tateda[1], K. Misumi[1], D. Tsumune[1], M. Aoyama[2], Y. Hamajima[3], T. Aono[4], T. Ishimaru[5], and J. Kanda[5]

[1]Environmental Science Research Laboratory, Central Research Institute of Electric Power Industry, Abiko, Chiba, 270-1194, Japan
[2]Center for Research in Isotopes and Environmental Dynamics, University of Tsukuba, Tsukuba, Ibaraki, 305-8577, Japan
[3]Low Level Radioactivity Laboratory, Institute of Nature and Environmental Technology, Kanazawa University, Nomi, Kanazawa, 923-1224, Japan
[4]National Institute for Quantum and Radiological Science and Technology, Inage, Chiba, 263-8555, Japan
[5]Department of Ocean Science, Tokyo University of Marine Science and Technology, Minato, Tokyo, 108-8477, Japan
Keywords: radiocesium, Fukushima accident, marine demersal fish, dynamic model
Presenting author, e-mail: tateda@criepi.denken.or.jp

The $^{134+137}$Cs were released to the Pacific coast along eastern Japan by the accident of Fukushima Dai-ichi Nuclear Power Plant (1FNPP). The radiocesium level in bottom sediment was remained substantial even after 8 years after the accident (TEPCO 2019). The cesium in sediment was hypothesized to contribute to the delay of decrease rate in radiocesium level in demersal fish by feeding those benthos (Tateda et al., 2016). Therefore, the reconstruction of time series level of cesium in sediment just after the accident to present is important to evaluate the possibility of contribution to food chain. In addition, during 8 years, the fine sediment particle was considered to be resuspended and removed from coastal area by lateral transport (Otosaka et al., 2014). In this study, we reconstruct the ^{137}Cs levels in coastal sediment, especially focusing on fine particle which was commonly ingested by benthic biota.

Using the estimated absorption (0.1 to 0.7 d-1) and desorption (0.01 to 0.02 d^{-1}) rate parameters derived by filed observation of seawater and shore sediment along three coastal study sites (from St. 4 to 6, 30 to 80 km south from 1FNPP, Fig. 1), temporal change of radiocesium concentrations in sediment at seabed surface of 18 field study sites (from TS1 to St.8) off Fukushima were simulated by numerical model (Misumi et al., 2014) associated with seawater level simulation by ROMS (Tsumune et al., 2012). By comparison with measured decrease trend of ^{137}Cs level in coastal study points, the removal rate of fine sediment (particle size < 75 μm) by resuspension/transport was derived.

The simulated levels in fine sediment were well agreed to observed concentrations at bottom fine sediment off Fukushima (Fig. 1). Assuming the resuspension/transport of sediment is primarily by fine sediment, the 8 years decrease trend of ^{137}Cs concentrations at TEPCO monitoring points (T-S1 to T-S8) were reconstructed by fitting the model simulated level to observed concentrations with estimated removal rate by fine particle resuspension/transport. The annual fine particle regeneration rate in bottom sediment was estimated as 4 to 37 % derived by fitting the simulated ^{137}Cs levels to temporal observed concentrations (Fig. 1).

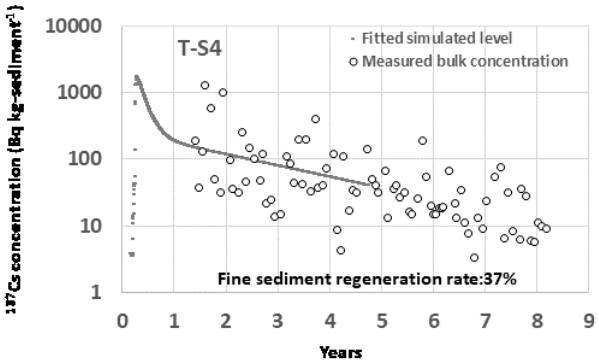

Figure 1. Fitted simulated and measured ^{137}Cs levels in bulk sediment at T-S4 of TEPCO monitoring points. The radiocesium decrease was simulated by initial desorption rate and the conversion rate to refractory fraction with fitting to obsereved level assuming regeneration by fine particle removal from surface bulk sediment.

Part of the data of this work was generated by the Grant-in-Aid for Scientific research on Innovative Areas Grant Number 2411005.

Tateda, Y., Tsumune, D., Tsubono, K., Misumi, K., Yamada, M., Kanda, J., Ishimaru, T. 2016. Status of ^{137}Cs contamination in marine biota along the Pacific coast of eastern Japan derived from a dynamic biological model two years simulation following the Fukushima accident. *J. Environ. Radioact.* 151, 495-501.

Misumi, K., Tsumune, D., Tsubono, K., Tateda, Y., Aoyama, M., Kobayashi, T., Hirose, K. 2014. Factors controlling the spatiotemporal variation of ^{137}Cs in seabed sediment off Fukushima coast: implications from numerical simulations. *J. Environ. Radioact.* 136, 218-228.

Radionuclides in drinking water in Vojvodina and health implication

N. Todorović[1], J. Nikolov[1], I. Stojković[2], B. Tenjović[1], A. Vraničar[1], J. Hansman[1], S. Lučić[3], S. Bjelović[4]

[1]Department of Physics, Faculty of Sciences, University of Novi Sad, Novi Sad, 21000, Serbia
[2]Faculty of Technical Sciences, University of Novi Sad, Novi Sad, 21000, Serbia
[3]Insititute of Oncology of Vojvodina, Sremska Kamenica, 21208, Serbia
[4]Institute of Public Health of Vojvodina, Novi Sad, 21000, Serbia
Keywords: drinking water, gross alpha, LSC, gamma-spectrometry, total dose
Presenting author, e-mail: natasa.todorovic@df.uns.ac.rs

Drinking water may contain radioactive isotopes that pose potential risks to human health. Isotopes from uranium-238 series dominantly contribute to the irradiation risks due to the ingestion of a drinking water. Because of its potential public health hazard, the surveys of radioactivity in water sources are necessary.

According to the World Health Organization (WHO), when activity concentration in drinking water exceeds the recommended level of 0.1 BqL^{-1} for gross-α or 1 BqL^{-1} for gross-β activities, radionuclide-specific concentrations should be brought into compliance with WHO guidance levels (WHO, 2011).

Gross alpha/beta activity concentrations in investigated water samples were determinate by liquid scintillation counter, Quantulus 1220. Ultra-low level liquid scintillation counting coupled to alpha/beta discrimination allows rapid and simple determination of gross alpha and beta activities that are simultaneously measured through alpha/beta discrimination technique.

The radionuclide content of the drinking water samples was determined from a cumulative sample by gamma-spectrometry measurements using the HPGe spectrometer. The nominal efficiency of the detector is 36% and the resolution is 1.9 keV. The detector was operated inside the 12-cm-thick lead shield with a 3-mm Cu inner layer. The sample measurement time was 50 ks. The gamma spectra were acquired and analyzed using the Canberra Genie 2000 software. For the analyzed radionuclides dose calculations were carried out. The total dose is the sum of the dose contributions of the single radionuclides (GD_i), which are calculated from the activity concentrations (C_i) with the legal valid dose conversion factors ($h(g_i)$) for adults respectively and an annual consumption (KM) of 730 l $year^{-1}$(IAEA, 1996).

In this survey, mapping of gross alpha and gross beta activity concentrations in drinking water samples (from water supplies, wells, fountains and from wellsprings) from the territory of Vojvodina province, Serbia, were performed. From totally 820 investigated samples in 73 water samples gross alpha activity exceeded legally established level of 0.1 BqL^{-1}. Additionally, the content of natural radioactive isotopes: ^{226}Ra, ^{232}Th and ^{238}U in the drinking water samples were determined from a cumulative sample by gamma-spectrometry measurements using the HPGe spectrometer. The total dose due to consummation of these waters was estimated. In 38 investigated samples total dose GD from radionuclides in drinking water is higher than 0.1 mSv $year^{-1}$ (EC, 1998).

This work was supported by the Provincial Secretariat for Higher Education and Scientific Research, Republic of Serbia within the project “Radioactivity in drinking water and cancer incidence in Vojvodina”, no. 142-451-2447/2018, the Ministry of Education, Science and Technological Development of the Republic of Serbia within the projects no. OI171002 and III4300.

World Health Organization (WHO), 2011. Guidelines for drinking-water quality, fourth edition. ISBN: 978 92 4 154815 1.

European Commission (EC), 1998. European Drinking Water Directive 98/83/EC of 3 November 1998 on the quality of water intended for human consumption. Official Journal L 330.

International Atomic Energy Agency (IAEA), 1996. International Basic Safety Standards for Protection against Ionizing Radiation and the Safety Radiation Sources. Safety Report Series, No. 115, Vienna.

Simulations of ^{137}Cs in the North Pacific using the atmospheric deposition fluxes from the Fukushima Dai-ichi Nuclear Power Plant accident by two atmospheric chemical transport models

Takaki Tsubono[1], Daisuke Tsumune[1], Kazuhiro Misumi[1], Michio Aoyama[2]

[1]Central Research Institute of Electric Power Industry, Abiko,270-1194, Japan
[2] Center for Research in Isotopes and Environmental Dynamics, University of Tsukuba, Tsukuba, 305-8572, Japan
Keywords: Fukushima Dai-ichi Nuclear Power Plant accident, ^{137}Cs, North Pacific Ocean, Atmospheric deposition
Presenting author, e-mail: tsubono@criepi.denken.or.jp

On 11 March 2011, the cooling facilities of the Fukushima Dai-ichi nuclear power plant (FDNPP) were damaged by the tsunami, resulting in a nuclear accident. Consequently, ^{137}Cs were released to the North Pacific Ocean (NPO) through the pathway of atmospheric deposition and direct release from the FDNPP. The estimation of the atmospheric deposition flux of the ^{137}Cs activity over the NPO, however, were difficult compared to that over the land. We simulated the ^{137}Cs activity in the NPO after the FDNPP accident using two atmospheric deposition fluxes estimated by the different atmospheric chemical transport models and investigated the difference in the ^{137}Cs by comparing the calculations with the observations in the NPO from 2011 to 2014.

Using the Regional Ocean Model System (ROMS) with variable mesh of 1/12º-1/4º in horizontal, we conducted two five-ensemble simulations of the ^{137}Cs activity in the North Pacific Ocean (NPO) from 2011 to 2020 from the direct discharge (Tsumune et al., 2013) and the atmospheric deposition flux following the ensemble simulation of the ^{137}Cs activity derived from global fallout due to the past atmospheric nuclear weapon test from 1945 to 2010. We employed two sets of the atmospheric deposition flux; Model of Aerosol Species IN the Global Atmosphere (MASINGAR MK-II) (Aoyama et al, 2016) and Meteorological Research Institute Passive-tracers Model for radionuclides (MRI-PM/r) (Kajino et al, 2012). The difference between the models is the total deposition amount into the NPO water in March and April 2011; 6.4 PBq for MASINGAR, 5.0 PBq for MPI-PM/r. In addition, The MASINGAR estimated larger (smaller) total deposition in north (south) of Kuroshio Extension than MPI-PM/r.

Since the calculated ^{134}Cs using the original atmospheric deposition fluxes underestimated the observations in the surface water in almost whole area of the NPO from 2011 to 2014, we calculated the magnifications for the fluxes by the regression analysis between the observed and calculated ^{134}Cs. The magnifications provided the total amounts of ^{134}Cs and ^{137}Cs activity in NPO water to reproduce the observations after the accident, which is 16±1.5 PBq for MASINGAR, 21±2 PBq for MPI-PM/r. The comparison between the observed and the calculated ^{137}Cs with the magnified fluxes showed that the correlation coefficient and the root mean square error are 0.86 and 5.7 Bq/m^{-3} for MASINGAR, 0.75 and 7.3 Bq/ m^{-3} for MPI-PM/r.

The models represented similar horizontal distributions of ^{137}Cs activity in surface from 2011 to 2019 in spite of that in Apr. 2011 (Fig. 1) because of the different distribution of atmospheric deposition fluxes. The vertical distributions of the ^{137}Cs for the model with MPI-PM/r flux represented relatively larger in the Subtropical Mode Water (STMW) in 165 ° E in 2012 than that for the model with MASINGAR flux, corresponding to the amount of ^{137}Cs flux in the area where the STMW was formed. The model with MPI-PM/r flux consequentially represented the^{137}Cs activity detected in the area west of Okinawa Islands and Kuroshio area south of Kochi Island until 2014, while MASINGAR until 2012.

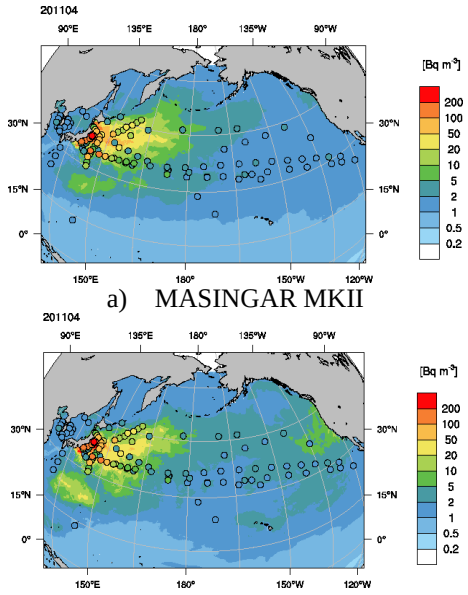

a) MASINGAR MKII

b) MPI-PM/r

Figure 1. ^{137}Cs activity in surface layer of the NPO in Apr. 2011 for MASINGAR MKII (a) and MPI-PM/r (b).

Aoyama M, Kajino M, Tanaka TY, Sekiyama TT, Tsumune D,Tsubono T, Hamajima Y, Inomata Y, Gamo T. 2016 ^{134}Cs and ^{137}Cs in the North Pacific Ocean derived from the March 2011 TEPCO Fukushima Dai-ichi Nuclear Power Plant accident, Japan. Part two: estimation of ^{134}Cs and ^{137}Cs inventories in the North Pacific Ocean. *J Oceanogr* 72:67–76.

Kajino M, Inomata Y, Sato K, Ueda H. 2012 Development of the RAQM2 aerosol chemical transport model and predictions of the Northeast Asian aerosol mass, size, chemistry, and mixing type. *Atmos Chem Phys* 12:11833–11856.

Radioactive cesium and potassium cycle model in Japanese grassland

M. Tsuiki

Department of Animal Science, Faculty of Agriculture, Iwate University, Morioka, 020-8550, Japan
Keywords: grassland, radioactive cesium, potassium, cycle model
Presenting author, e-mail: tsuiki@iwate-u.ac.jp

The damage to the Fukushima Daiichi Nuclear Power Plant following the Great East Japan Earthquake and tsunami on March 11, 2011 resulted in serious radioactive pollution of Eastern Japan. In some grasslands of this area, radioactive cesium (RCs) content of grasses exceeded the provisional safety standard for use as feed for dairy and beef cattle of 100 Bq kg^{-1} fresh weight, and the livestock industry has been seriously affected in numerous ways. The spatial distribution of RCs in grasslands was complex in various scales (Tsuiki and Maeda, 2012a; 2012b). So it is difficult to estimate actual pollution level in grassland ecosystems. Potassium (K) fertilizer application is important for reducing RCs absorption by grasses on polluted grassland (Absalom *et al.*, 2001; Tsuiki *et al.*, 2013). Excessive application of K causes high K concentration of grasses and grass tetany, serious disease of cattle, is developed by fed cattle. Proper fertilization management in important to reduce the risk of radioactive cesium pollution and high K concentration. In this study, RCs and K cycle model in Japanese grassland was constructed to clarify their dynamics and support decision making of grassland management.

System dynamics approach was used for modelling. Dynamic flow of ^{137}Cs in grassland was simulated (Figure 1). Soil unadsorped ^{137}Cs, soil adsorped ^{137}Cs, grass ^{137}Cs and litter ^{137}Cs were selected as level. The flow from soil unadsorped ^{137}Cs to soil adsorped ^{137}Cs was affected by radiocesium interception potential (RIP). RIP was calculated as the product of partition coefficient (K_D) and K in soil solution:

$$RIP = K_D \times K \text{ in soil solution} \quad (1)$$

K_D was defined as the ratio of quantity of ^{137}Cs sorbed per unit mass of frayed edge sites in soil to the equilibrium concentration of contaminant in soil solution.

$$K_D = (^{137}\text{Cs adsorped to frayed edge sites}) / (^{137}\text{Cs in soil solution}) \quad (2)$$

The flow from soil unadsorped ^{137}Cs to vegetation ^{137}Cs was affected by soil exchangeable K content. The flow from litter ^{137}Cs to unadsorped ^{137}Cs was affected by air temperature. The growth of vegetation was decided by observed data with table function. The unit of levels was Bq m^{-2} and the unit of simulation time was day.

Dynamic flow of K in grassland was simulated (Figure 2). Soil exchangeable K, soil unexchangeable K, grass K and litter K were selected as level. Soil exchangeable K was supplied from applied fertilizer K, soil mineral K and litter K. Soil unexchangeable K was supplied from soil mineral K.

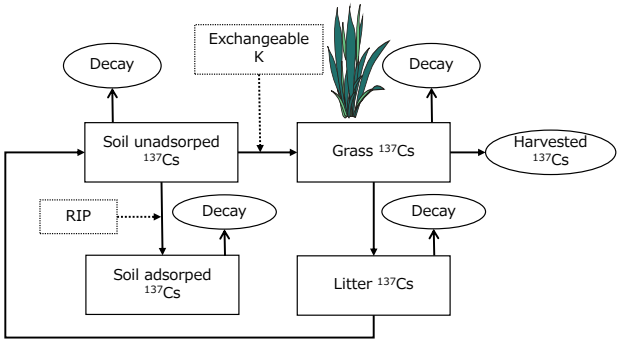

Figure 1. ^{137}Cs flow on grassland. Dotted boxes and lines indicate factors affecting the flow.

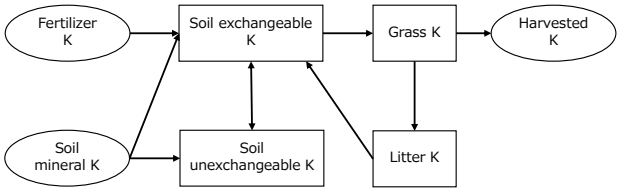

Figure 2. Potassium flow on grassland.

This work was supported by "Elucidation of radionuclide concentration fluctuation and its dynamics in agricultural and forestry production environment" in the radioactivity survey research consignment business 2019.

Absalom, J. P., Young, S. D., Crout, N. M. J., Sanchez, A., Wright, S. M., Smolders, E., Nisbet, A. F., Gillett, A. G. 2001. Predicting the transfer of radiocaesium from organic soils to plants using soil characteristics. *Journal of Environmental Radioactivity* 52: 31–43.

Tsuiki, M., Maeda, T. 2012a. Spatial distribution of radioactive cesium fallout on grasslands from the Fukushima Daiichi Nuclear Power Plant in 2011. *Grassland Science* 58: 153-160.

Tsuiki, M., Maeda, T. 2012b. Spatial variability of radioactive cesium fallout on grasslands in various scales. *Grassland Science* 58: 227-237.

Tsuiki, M., Eguchi, S., Nagata, Y., Maeda, T. 2013. Spatial variability and seasonal change of radioactive cesium concentration in grassland vegetation. Proceedings of the 22nd International Grassland Congress (Sep. 15-19, 2013), Sydney. pp. 899-900.

Effect of biogeochemical process on ^{239,240}Pu distribution in an ocean general circulation model

Daisuke Tsumune[1], Michio Aoyama[2], Katsumi Hirose[3], Takaki Tsubono[1], Kazuhiro Misumi[1]

[1]Central Research Institute of Electric Power Industry, Abiko,270-1194, Japan
[2] Center for Research in Isotopes and Environmental Dynamics, University of Tsukuba, Tsukuba, 305-8572, Japan
[3]Faculty of Science and Technology, Sophia University, Tokyo, 102-0094, Japan
Keywords: Plutonium isotope, ^{137}Cs, Global fallout, Ocean General Circulation Model, Biogeochemical Process
Presenting author, e-mail: tsumune@criepi.denken.or.jp

Before the Fukushima Dai-ichi Nuclear Power Plant (1F NPP) accident, ^{137}Cs and ^{239,240}Pu had been supplied into the ocean mainly by global fallout due to atmospheric weapons tests. The 1F NPP accident has increased total amount of ^{137}Cs by 25-30% in the North Pacific Ocean and did not supply ^{239,240}Pu to the ocean. ^{137}Cs is an inertial tracer that advects and diffuses according to oceanic physical processes. In contract with ^{137}Cs, ^{239,240}Pu is a biogeochemical tracer because it is particle reactive radionuclide. Oceanic ^{239,240}Pu behaviour is governed by scavenging and remineralization processes. ^{239,240}Pu/^{137}Cs ratio is a good proxy of biogeochemical processes. Observed ^{239,240}Pu/^{137}Cs ratio ($R_{Pu/Cs}$) exponentially increased with increasing depth from 100m to 1500m. Hirose et al. (2009) have proposed a half regeneration depth (HRD) of ^{239,240}Pu, which is estimated from the curve fitting the vertical profile of the ratio, to evaluate the biogeochemical process for ^{239,240}Pu.

$$R_{Pu/Cs}(Z) = R_{Pu/Cs}(0)\exp(\lambda Z)$$

$$HRD = 0.692/\lambda$$

Z is a depth. λ is a rate parameter. The HRD is closely related to biogeochemical process in the ocean.

We employed Parallel Ocean Program (POPx3, 3 degree version) with the iron cycle model with different parameters to simulate the ^{239,240}Pu concentration in the ocean. ^{137}Cs behavior in the ocean is caused by physical processes, whereas ^{239,240}Pu behavior is caused by both physical and biogeochemical processes. For example, shallower bias of ^{137}Cs tracer penetration was showed in the model especially in the North Pacific. Models have both physical and biogeochemical biases. Physical bias in the model can be reduced by the comparison of $R_{Pu/Cs}$ and HRD between observation and simulation. In addition, input condition of ^{239,240}Pu to the North Pacific is still unknown due to the close-in fallout from the Pacific Providing Grounds (PPG). Total inventory of ^{239,240}Pu does not affect the HRD because the HRD is determined by the coefficient of the $R_{Pu/Cs}$'s exponential function of depth. It is an advantage to examine the biogeochemical parameters in the model. We employ the data assimilation method using the Green' function to optimize the parameters for ^{239,240}Pu in the biogeochemical model.

We optimized the biogeochemical parameters, ligand concentration, parameter of the Martin curve, scavenging depth, to fit the observed HRD in the North Pacific by the POPx3 with the Green' function method.

The depth of the maximum ^{239,240}Pu concentration deepened and surface ^{239,240}Pu concentration decreased from the 1970s to the 2000s due to biogeochemical processes. Model simulation can represent the vertical profiles and their temporal changes, however the simulated depths of the maximum ^{239,240}Pu concentrations with optimized parameters are shallower than observation (Fig. 1). The simulated vertical distributions of the ^{137}Cs concentration and their temporal change are generally in good agreement with observation. However, simulated penetration depth of ^{137}Cs is shallower than observation by known physical bias (Tsumune et al., 2011).

Simulated HRD by optimized parameters is in a good agreement with observation by optimization of parameters. The HRD is a good observed value to optimize the parameters of the biogeochemical process in the model. The simulated ^{239,240}Pu concentration by optimized biogeochemical parameters in this study still has biases of both physical processes and input conditions. Higher resolution model can reduce the bias of physical processes in the future. Taken into consideration close-in fallout from the PPG, the bias of input conditions can be reduced.

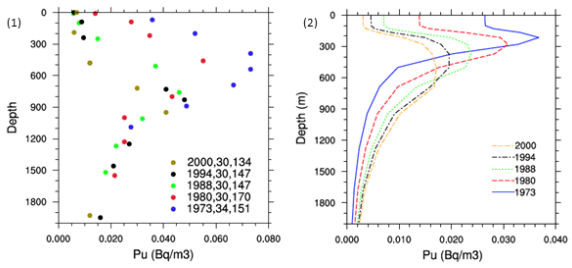

Figure 1. Vertical profiles of ^{239,240}Pu concentration in the North Pacific in 1973, 1980, 1988, 1994 and 2000 (1) Observed data in HAM database (30˚-34˚N, 135˚-170˚E), (2) Simulated results at 33˚N, 147˚E.

Hirose, K., Aoyama, M., Povinec, P. P. 2009. ^{239,240}Pu/^{137}Cs ratios in the water column of the North Pacific: a proxy of biogeochemical processes, *J. Environ. Radioact.*, 100, 258-262.

Tsumune, D., Aoyama, M., Hirose, K., Bryan, F. O., Lindsay, K., and Danabasoglu, G. 2011. Transport of ^{137}Cs to the Southern Hemisphere in an ocean general circulation model, *Progress in Oceanography*, 89, 38-48.

Rapid adsorption of Cu (II), Co (II), Ni (II) and Pb (II) from aqueous solutions using magnetic Prussian blue nanosorbent

I. Uogintė, G. Lujanienė

Center for physical sciences and technology, Savanorių ave. 231, LT-02300 Vilnius, Lithuania
ieva.uoginte@gmailcom

Recently, due to the indiscriminate disposal of wastewater, the great attention has been paid to the removal of heavy metals and radionuclides from liquid media. Wastewater from industries such as mining, chemical manufacturing, metallurgy as well as nuclear power plants accidents contains huge amount of toxic metal ions. Among the current treatment methods to separate pollutants, adsorption is preferred most because of its flexibility, ease of operation, simplicity of design, low cost and minimal sludge production. The main requirements for adsorbent are a large surface area and a lot of active adsorption sites. Most of adsorbents have a major drawback because it is difficult to separate them from the aqueous solution after the adsorption. The magnetic materials have been widely used to solve this problem. However, single magnetic material usually has limited active sites, hence many magnetic composite sorbents has been investigated to improve adsorption capacity.

This study was performed to synthesize and apply magnetic Prussian blue nanosorbent for removal of Cu (II), Co (II), Ni (II) and Pb (II) (as analogues of ^{59}Ni, ^{63}Ni, ^{58}Co, ^{60}Co, ^{64}Cu and ^{210}Pb radionuclides) from aqueous solutions. The sorption isotherms, kinetics and pH analysis were employed to specify the sorption mechanism. The influence of initial concentration of heavy metals, removal time and nanosorbent dosage was analysed by the response surface methodology (RSM). The goodness of fit of the model and the significance of influential variables were tested via the variance analysis (ANOVA).

Results showed that magnetic Prussian blue nano-sorbent posed high sorption capacities (Q_{max} Cu (II) – 138mg/g, Co (II) – 111 mg/g, Ni (II) – 155mg/g, Pb (II) – 778mg/g). The sorption corresponded to the Freundlich isotherm and pseudo-second-order kinetic model, suggesting that the removal mechanism can be chemisorption (H^+ exchange) and/or physisorption (ion trapping). Response surface model and ANOVA results indicated that initial metal concentration and sorbent dosage were the most important factors to the sorption efficiency. The increase of both factors results increasement of the uptake.

Advanced atmospheric ^{14}C monitoring and modelling around the Paks Nuclear Power Plant, Hungary

T. Varga[1], G. Orsovszki[2], I. Major[1], M. Veres[2], T. Bujtás[3], P. Kapás[3], L. Manga[3], M. Molnár[1]

[1]Isotope Climatology and Environmental Research Centre, Institute for Nuclear Research, Hungarian Academy of Sciences, Debrecen Bem tér 18/c, Hungary
[2]Isotoptech Co., Debrecen Bem tér 18/c, Hungary
[3]Paks Nuclear Power Plant, Paks, Hungary
Keywords: atmospheric, radiocarbon, nuclear power plant, AMS, modelling
Presenting author email: varga.tamas@atomki.mta.hu

Atmospheric air samples were collected at 9 monitoring stations (A1 to A9) less than 2 km from the Paks Nuclear Power Plant (Paks NPP) and a background station (B24). The monthly integrated CO_2 and total carbon (CO_2+hydrocarbons (C_nH_m)) samples were collected to determine the excess ^{14}C activity at the vicinity of the NPP. The measurements providing the $^{14}C/^{12}C$ ratio of the monthly integrated samples were carried out on a MICADAS type AMS at HEKAL. Due to the relatively low $^{14}CO_2$ emission of PWR type Paks reactors and the local Suess effect, there was negligible excess ^{14}C activity at the investigated stations in the pure CO_2 fraction during the investigated 2 years period (2015-2016). Contrary, there was a detectable (although minor) excess at every station in the C_nH_m fraction. In case of CO_2, the average $\Delta^{14}C$ excess was 3.8 ‰ and the highest measured value was 91.2 ‰ at the A3 station in February 2015. In case of C_nH_m, the average excess was 31.1 ‰ and the highest measured value was 319.1 ‰ at the A4 station in February 2016. We applied PC-CREAM 08 modelling to investigate the observed excess ^{14}C activity at the environmental sampling stations, which depends on the distance from the NPP and the meteorological conditions, such as wind direction and wind speed. Meteorology data was collected at the operating area of the Paks NPP in a meteorology tower. The direct C-14 emission through the 120 m high stacks was measured in the NPP by liquid scintillation counting. These emission data and our model calculations explain the excess activity in the C_nH_m fraction at the A4 station, which is located only 915 m far from the NPP's stacks in the prevailing wind direction. The excess activity at A3 station (the farthest unit) probably came from the nearby NPP wastewater discharge point. The recently observed average excess and highest excess data is similar to the ones in former studies (Veres et al. 1997, Molnár et al. 2007) on Paks NPP, but the highest $^{14}CO_2$ and $^{14}C_nH_m$ excess are little higher than it was in the former studies, but in these former studies, the A3 station was not equipped with radiocarbon monitoring unit and the level of radiocarbon emission was almost invisible from the wastewater discharge point.

Veres, M., Hertelend, E., Uchrin, G., Csaba, E., Barnabás, I., Ormai, P., Volent, G., Futó, I. 1995. Concentration of radiocarbon and its chemical forms in gaseous effluents, environmental air, nuclear waste and primary water of a pressurized water reactor power plant in Hungary. *Radiocarbon*. 37(2):497–504.

Molnár, M., Bujtás, T., Svingor, É., Futó, I., Světlík, I. 2007. Monitoring of atmospheric excess ^{14}C around Paks Nuclear Power Plant, Hungary. *Radiocarbon*. 49 (2) 1031-1043.

NORM heavy minerals in beach sands: identification, isolation and characterization

I.Vioque[1], C. Bañobre[2], and R. García-Tenorio[1,3]

[1] Grupo Física Nuclear Aplicada. Dept. Física Aplicada II, Universidad de Sevilla, 41012- Sevilla, Spain
[2] Centro Universitario Regional del Este (CURE), Universidad de la República, Rocha, Uruguay
[3] Centro Nacional de Aceleradores, CNA (Universidad Sevilla-J. Andalucía-CSIC), 41092-Sevilla, Spain
Keywords: NORM, heavy minerals, SEM-EDX, XRF, micro-CT,
Presenting author, e-mail: R. García-Tenorio, gtenorio@us.es

Distributed over the world it can be found beach depository areas where naturally heavy minerals, broken off by weathering from the rocks in which they are formed, are concentrated by the effect of gravity on moving particles. In particular, these minerals are formed by wave action on the seashore, are present mixed with the beach sand in the form of grains/nodules and have a quite refractory behaviour.

In these deposits are concentrated minerals with high density such as zircon, ilmenite, monazite, rutile and magnetite, that in some cases constitute a radiological anomaly becaue contain enhanced amounts of radionuclides of the uranium and thorium series. They are well known beach areas in India, China and Brasil recognized as High Background Areas and formed originally in the way described previously, where the radiation doses, due to the presence of natural radionuclides, can be even one order of magnitude higher than the worldwide average,

In this paper, a beach placer deposit located on the east coast of Uruguay and containing a great variety of different heavy minerals has been studied. These minerals can be easily observable forming layers/strata in the beach sand accumulations due to its dark colour (as ii is easily observable in Figure 1)

From representative aliquots of these beach sands, the different heavy minerals grains/nodules have been sequentially isolated by applying gravimetric and magnetic procedures. The isolation of magnetite, ilmenite, monazite, rutile and zircon fractions, between others, have been particularly performed, allowing to submit to the different isolated minerals to different non-destructive characterization analyses.

In particular, the radioactive content in the different minerals was screened by digital autoradiography (an example is shown in Figure 2), being their characterization continued with the determination of their elemental composition by combining the information obtained with SEM-EDX and XRF analysis. In addition, a detailed study about their morphology and internal density distributions was performed by micro-CT.

The main results obtained in the characterization studies of the different minerals will be shown in this presentation together with a discussion of their potential radioecological implications.

Figure 1. Transversal view of beach deposits in Rocha (Uruguay) where well defined black strata formed by heavy minerals can be distinguished.

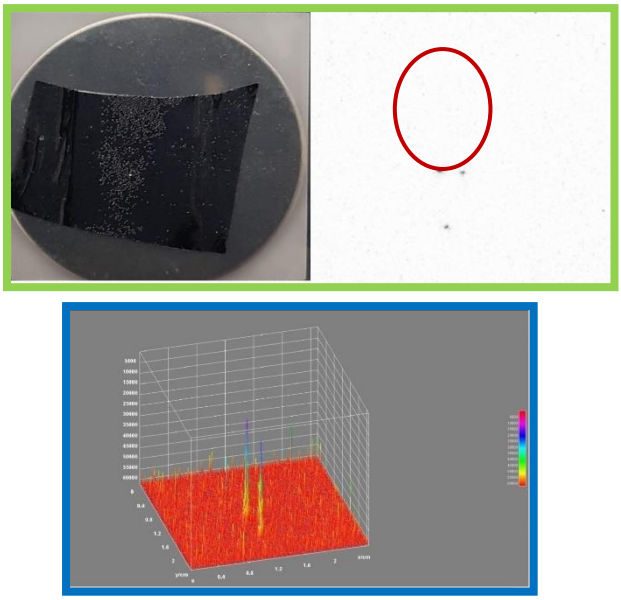

Figure 2. Autoradiography of beach nodules (up), and digital treatment of the autoradiography showing clearly the discrete distribution of the radiation (down).

This work has been supported by the project FIS2015-69673-P of the Spanish government. The collaboration of different research units of the Central Research Services of the University of Seville is deeply acknowledged.

New electrolytic enrichment system for tritium determination in Water Research Institute in Bratislava and it's first results of tritium activity in precipitation

G. Wallova[1], J. Meresova[1], I. Sykora[2]

[1]Water Research Institute, Bratislava, 812 49, Slovakia
[2]Department of nuclear physics and biophysics, Comenius University, Bratislava, 842 48, Slovakia
Keywords: Tritium, seasonal variations, electrolytic enrichment, LSC
Presenting author, e-mail: gabriela.wallova@vuvh.sk

The method of tritium activity measurements by electrolytic enrichment in combination with liquid scintillation counting is well known for many years (Villa and Manjón, 2004). In the Water Research Institute in Bratislava was this system employed since the 60-ties of the 20th century.

In 2018 the laboratory of radiochemistry of Water Research Institute obtained a new electrolytic enrichment system with higher enrichment factor (varying from 9 to 22, depending on the total ampere-hours used). The enrichment factor of the previous system was about 6. Complementary to the new system, also the new LCS counter QUANTULUS GCT 6220 was added. This spectrometer has active background suppression function (Guard Compensation Technology - GCT) and for the tritium measurement the background counts decreased from cca 9 cpm (for TRICARB) to approximately 1 cpm. By combining these two powerful devices the detection limit for the determination of tritium has improved from 0.6 Bq/l (5 TU) to 0.24 Bq/l (2 TU). Further comparison of old and new enrichment systems is in the Table 1. In the article more detailed description of the electrolytic enrichment will be presented.

Table 1. Comparison of the old and the new tritium determination systems.

	Old	New
Number of cells	15	20
Volume of cells	250 ml	500 ml
Enrich. factor	5-7	9-22
Background (cpm)	9	1
Det. Efficiency (%)	27	33
MDA (Bq/l)	0.6	0.24

Moreover, we present results of a 2.5-year study of the tritium concentration in precipitations. During the period from May 2016 to October 2018 was 28 samples collected at the Department of Nuclear Physics and Biophysics, Comenius University in Bratislava. The samples were processed by electrolytic enrichment method and measured by liquid scintillation counting (LSC). First four samples were enriched using the old electrolytic system and the rest with the new one. Two samples were not analysed due to insufficient amount of the sample.

The prime interest of the study at Comenius University is the measurement of different radionuclides (^{7}Be, ^{210}Pb, etc.) in the atmosphere (Sýkora et al., 2017).

The seasonal variations of tritium activities in precipitation are observed, with maximum values in spring season and minimum in winter (Figure 1).

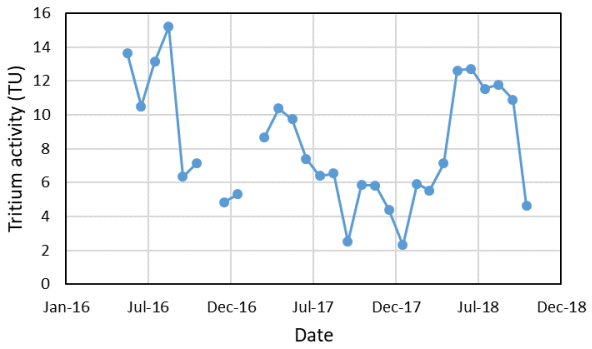

Figure 1. Tritium activities in precipitations in Bratislava.

In the central part of Europe, the maximum tritium concentrations were found in the period from May to July due to the penetration of tritium (of cosmogenic origin) from the stratosphere in to the troposphere. This phenomenon occurs every year causing seasonal variations in the tritium atmospheric concentrations (Rozanski et al., 1991).

Rozanski, K., Gonfiatini, R., Araguas-Araguas, L. 1991. Tritium in the global atmosphere. Distribution patterns and recent trends. *J. Phys. G.* 17, 523-536.

Sýkora, I., Holý, K., Ješkovský, M., Müllerová, M., Bulko, M., Povinec, P.P. 2017 Long-term variations of radionuclides in the Bratislava air. *J. Env. Rad.* 166, 27-35.

Villa, M. and Manjón, G. 2004. Low-level measurements of tritium in water. *Appl. Radiat. Isot.* 61, 319-323.

Developments towards the determination of ^{135}Cs and ^{137}Cs in environmental samples by Accelerator Mass Spectrometry

A. Wieser[1], J. Lachner[1], M. Martschini[1], M. Honda[1], P. Steier[1], A. Priller[1], O. Marchhart[1], R. Golser[1]

[1]Faculty of Physics, University of Vienna, Vienna, Austria
Keywords: Laser-Photo-Detachment, AMS, ^{135}Cs, ^{137}Cs, ILIAMS
Alexander Wieser, e-mail: a1304041@unet.univie.ac.at

The isotopic ratio ^{135}Cs/^{137}Cs can be used to assign sources of anthropogenic cesium input, as a geochemical tracer, or for modifying anthropogenic radionuclide dispersion models (Yang et al. 2016a). The fission product ratio of ^{135}Cs/^{137}Cs varies with the number of thermal neutrons emitted in a reactor by up to a factor 2 (Taylor et al. 2007). Because of the high thermal neutron catching cross-section of ^{135}Xe (σ=2.6·10^6 barn) a "shielding effect" appears for all isobars which are in the decay chain of ^{135}Xe, including ^{135}Cs. Abundances from natural processes (e.g. from spontaneous U fission) are estimated to be in the range of ^{135}Cs/Cs ≈ 10^{-11} (Lachner et al. 2014). ^{135}Cs is a pure beta-emitter with a long, yet not well-known half-life. Recent measurement results (MacDonald et al. 2016) give a range from 0.7 Ma (AMS) to 1.3 Ma (ICPMS), while previous values were as high as 3 Ma (Zeldes et al. 1949). The isotopic ratio ^{135}Cs/Cs in the order of 10^{-9} or below in general environmental samples is hardly detectable via radioactive decay (Lee et al. 1993). Mass spectrometric methods thus are developed for its detection.

The new method of **I**on **L**aser **I**nteraction **A**ccelerator **M**ass **S**pectrometry (**ILIAMS**) at the **V**ienna **E**nvironmental **R**esearch **A**ccelerator (**VERA**) overcomes the problem of isobaric interferences of ^{135}Ba and ^{137}Ba for Cs detection, therefore making it possible to measure the ^{135}Cs/^{137}Cs ratio. CsF_2^- has a higher electron affinity than BaF_2^- (exact values are unknown for both molecules). By overlapping the ion beam with a cw-laser beam with photon energy in between those two electron affinities, an electron of the BaF_2^--ion gets detached, while CsF_2^- remains unaffected.

For this interaction to happen efficiently, the ions get slowed down in a He buffer-gas filled ion guide, so that the time of interaction lengthens. The extraction of F_2-fluorides gives a first suppression of the Ba isobars by a factor of 2·10^3 (Eliades et al. 2013). An additional factor 10 of BaF_2^- suppression is gained by raising the He buffer gas pressure from 0.15 mbar to 0.37 mbar. The Laser suppresses BaF_2^- by 10^4 at high buffer-gas pressure (Figure 1), thus making an overall suppression of > 10^8 achievable with ILIAMS.

A CsF_2^- current in the order of ~100nA from a mixed Cs_2SO_4 and PbF_2 – matrix is extracted from the ion source. The sample material is mobilized by heating the ionizer only and no external sputtering material is used. Our measured samples are in-house reference materials from a 2 Bq/ml ^{137}Cs solution or IAEA reference materials with determined ^{135}Cs/^{137}Cs ratio (Yang et al. 2016b). With 1 mg stable Cs carrier we reach a blank level of ^{137}Cs/^{133}Cs = 2.5·10^{-12}. This corresponds to a limit of detection (LOD) in the range of 13 mBq per sample.

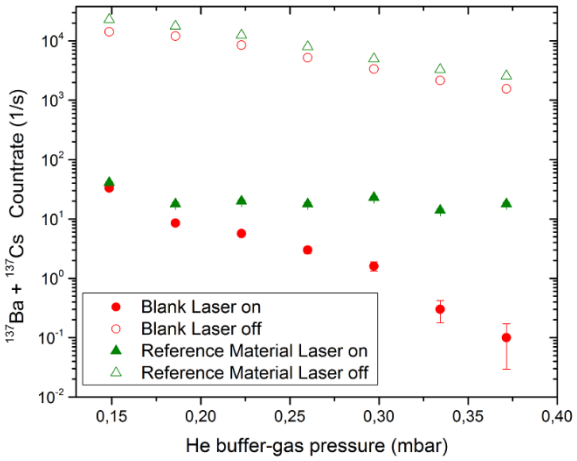

Figure 1. Counting rates for the Ba isobar are reduced with increasing He buffer-gas pressure and by the interaction with the laser. Cs rates in the reference material are not affected.

Yang, G, et al, 2016a. ^{135}Cs activity and ^{135}Cs/^{137}Cs atom ratio in environmental samples before and after the Fukushima Daiichi Nuclear Power Plant accident. *Sci. Rep*. 6, 24119.

Taylor, V.F. et al, 2007. Preliminary evaluation of ^{135}Cs/^{137}Cs as a forensic tool for identifying source of radioactive contamination. *J. Env. Rad.* 99, 109-118.

Lachner, J. et al, 2014. Developments towards detection of ^{135}Cs at VERA. *Nucl. Instrum. Meth. B*. 361, 440-444.

MacDonald, C. et al, 2016. Measurement of the ^{135}Cs half-life with accelerator mass spectrometry and inductively coupled plasma mass spectrometry. *Phys.Rev*. C 93, 014310.

Zeldes, H. et al, 1949. Characterization of ^{135}Cs. *Oak Ridge National Laboratory Progress Report.* 286, 48-52

Lee, T. et al, 1993. First detection of fallout Cs-135 and potential applications of ^{137}Cs/^{135}Cs ratios. *Geochimica et Cosmochimica Acta*. 57, 3493-3497

Eliades, J. et al, 2013. On-line ion chemistry for the AMS analysis of ^{90}Sr and ^{135,137}Cs. *Nucl. Instrum. Meth. B.* 294, 361-363.

Yang, G. et al, 2016b. Rapid determination of ^{135}Cs and precise ^{135}Cs/^{137}Cs atomic ratio in environmental samples by single-column chromatography coupled to triple-quadrupole inductively coupled plasma-mass spectrometry. *Analytica Chimica Acta.* 908, 177-184.

Radioactivity in Saxon Rivers

M. Wendler[1], D. Degering[1], M. Kaden[1], S. Bartel[1]

[1]VKTA – Radiation Protection, Analytics & Disposal Inc., Dresden, 01328, Germany
Keywords: Tritium, River, sampling
Marco Wendler, marco.wendler@vkta.de

In 2018 a campaign of sampling water from river Elbe was started to clarify the origin of earlier mentioned enhanced Tritium levels in that river. Another aim was to verify the concentration of Pb-210, Ra-226 and Ra-228 relating to the new drinking water ordinance.

Tritium is a hydrogen isotope with a half-life of 12.3 years. It decays solely by beta emission (E_{max} = 18 keV). The tritium content in the atmosphere and hydrosphere is both of natural and artificial origin and takes part in the global water cycle. The natural tritium is mainly a result of nuclear reactions of cosmic radiation with air components in the atmosphere. The artificial tritium has its origin both by the nuclear weapons tests in the atmosphere between the 1950s and 1960s and by nuclear facilities. With cooling water tritium can leave facilities and reaches the environment. The most common chemical bounding of tritium is HTO where one hydrogen atom is substituted by tritium. As a result, tritium can also be detected in biological materials like tissues. The largest tritium fraction is concentrated in the hydrosphere, for example in rivers or oceans.

The isotopes Pb-210 and Ra-226 are parts of the uranium-radium decay chain. Ra-228 is part of the thorium decay chain. They all are from natural origin. The mentioned three radionuclides decay with emission of gamma rays.

All samples were analysed with regard to their tritium concentration by liquid scintillation spectrometry (LSC). For activity concentrations < 2 Bq l^{-1} an electrolytic enrichment procedure was applied. Pb-210, Ra-226 and Ra-228 in water were analysed as filter samples by gamma spectrometry after $BaSO_4$ precipitation.

To get an overview over the most important rivers in Saxony it was decided to take samples from Elbe and some selected tributary rivers but also from the rivers Spree and Neisse.

The sampling were taken in June 2018, January 2019 and May 2019. Samples were taken from the riverside, from a boat and from bridges. The best sampling method was chosen during the first stage of investigations. For the lead and radium isotopes 5 liter container made of plastic were used. For the tritium analysis glass bottles were used.

The sampling of river Elbe was started in Schmilka close to the border between the Czech Republic and Germany, Further sampling was performed along the Elbe river in Dresden, Riesa, Torgau and Wittenberg.

It could be proved that the higher tritium activity concentration of about 6 Bq l^{-1} in the Elbe is nearly constant along the river and not caused by contributions from the tributaries.

The activity concentrations of Pb-210, Ra-226 and Ra-228 of the most samples are near the lower limit of detection, meaning the concentrations are below the reference level of the drinking water ordinance.

Rapid determination of uranium isotopes in calcium fluoride sludge by tandem quadrupole ICP-MS/MS

Shan Xing[1], Maoyi Luo[1], Yang Wu[1], Xiongxin Dai[1]

[1]China Institute for Radiation Protection, Taiyuan, 030000, China
Keywords: Uranium, He mode, ICP-MS/MS, Calcium fluoride
Presenting author, e-mail: xingshan@yahoo.com

Uranium has been primarily used to produce fuel for nuclear power plants. To make nuclear fuel from uranium ore, several processes are required including refining, conversion, enrichment and fuel fabrication. In the uranium conversion stage, uranium ore concentrate in the form of uranium oxide (UO_3 or UO_2) is converted to uranium hexafluoride (UF_6), and calcium fluoride (CaF_2) wastes containing small amounts of uranium are generated. Reutilization of the non-radioactive solid waste generated in nuclear industry such as calcium fluoride sludge is one of the most effective ways to minimize radioactive waste. Quantitative analyses of potential radionuclide contaminations in solid wastes are essential for clearance or reutilization of these wastes. In order to measure trace uranium isotopes in calcium fluoride sludge, an analytical procedure was developed utilizing lithium metaborate fusion and anion exchange chromatography method combined with triple quadrupole ICP-MS/MS instrument under the He mode (Figure 1). Based on the focusing effect of He and a negative voltage value of KED, the measurement sensitivity for uranium isotopes can be significantly improved to 750 Mcps ppm^{-1} under the He mode. To validate the performance of the radiochemical separation procedure, samples spiked with known amounts of uranium isotopes were prepared and analysed by ICP-MS/MS employing He as collision gas. The results were in good agreement with the expected values, demonstrating the feasibility of the method for the determination of trace uranium isotopes. The minimal detectable activities of ^{234}U, ^{235}U and ^{238}U were determined to be 0.15 mBq, 0.67 μBq and 0.014 mBq, respectively.

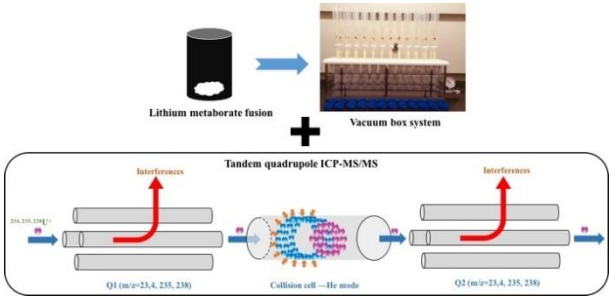

Figure 1. Schematic diagram of the determination of uranium isotopes by ICP-MS/MS.

This work was supported by the National Natural Science Foundation of China (No. 11605206 and 11675150), the Ministry of Science and Technology of China (No. 2015FY110800).

Adaptability evaluation of the food screening without destructive sample preparation to ISO 19581

Takahiro Yamada[1], Akiko Hachisuka[2], Keisuke Soga[2] and Mayumi Hachinohe[3]

[1] Kindai University Atomic Energy Research Institute, Higashiosaka, 5770818, Japan
[2] National Institute of Health Sciences, Kawasaki, 2100821, Japan
[3] National Agriculture and Food Research Organization, Tsukuba, 3058642, Japan
Keywords: food inspection, screening, radioactivity measurement, international standard
Presenting author, e-mail: tyamada@kindai.ac.jp

The radioactivity monitoring for foodstuffs using the sampling inspection procedure has been reinforced since the Fukushima dai-ichi NPP accident. In the conventional radioactivity measurement in foods, the sample preparation procedures involving machining technique are important to homogenize radioactivity in the sample and filling it in the same type of container that is used for the calibration source. Recently voluntary total inspection of the food sample using the instruments for measuring radioactivity in a whole foodstuff sample (hereinafter referred as WSI) without the destructive sample preparation are carried out for all shipping products by producers to ensure the safety of their products. Furthermore, municipal testing stations in Fukushima also use WSIs for the inspection of products collected by residents who refuse destructive machining. In these cases, it might be important to determine the detection efficiency by approximation for various sizes or shapes of samples and also to take into account of variation of detection efficiency due to heterogeneity of radioactivity in each sample. In order to make it clear Yamada et al. conducted the performance evaluation of the several models of WSIs [T. Yamada, 2019] and they revealed that WSIs were evaluated as useful instruments to assess the situation with a bird's-eye view if larger uncertainty caused by detection efficiency evaluation and heterogeneity of samples. However, it is not clear that such types of equipment are also useful for rigorous inspections yet. As one of the standardized approaches, ISO19581[ISO, 2017] is officially available standard to deal with a screening test method to quantify rapidly the activity concentration of gamma-emitting radionuclides in test samples. In the present study, adaptability of the food screening without destructive sample preparation technique to ISO 19581 was studied. A WSI equipped with a CsI (Tl) detector (ϕ110mmx25mm) was employed for the measurement of each the whole sample. Activity of each sample was measured repeatedly after shuffling specimen in each case to check the reproducibility. Various kinds mushrooms of 16 samples having activity concentration below 100 Bq kg^{-1} were used, since the limit for radioactive caesium for general food is 100 Bq kg^{-1} in Japan. After these measurements, individual activity concentrations of the same specimens were determined by the conventional gamma-ray spectrometry technique with sample preparation procedure.

Measurement results obtained from the present study is shown in Fig. 1. According to ISO19581 screening level is the value that are set up by the laboratory taking into account the characteristics of the measuring equipment and the test method to guarantee that the test result and its uncertainty obtained are fit for purpose for comparison with the operational intervention levels (OILs), and screening levels should be set in a range from half of these OILs to close to the OILs in order to reduce false-positives. In addition upper limit of confidence interval of the best estimate of the true value for the screening level $C_{A,\mathrm{SL}}$ shall be below that for the OIL $C_{A,\mathrm{RL}}$ with a 95 % confidence level ($\alpha = 0{,}05$, $k = 2$). The screening level being set above half of the level of the reference value with α=0,02 were required in Japan for the radio-caesium screening test. Dashed lines in Fig. 1 represent upper and lower limits (α=0,02) of $C_{A,\mathrm{SL}}$. As shown in this figure, although the estimated screening level was slightly lower than the limit of screening level of 50 Bq kg^{-1}, the present result was almost satisfied the requirement of ISO19581. However, it should be noted that unexpected large uncertainty for WSI measurements were still found that might due to heterogeneous of radioactivity. More details of uncertainties due to heterogeneous of radioactivity will be represented.

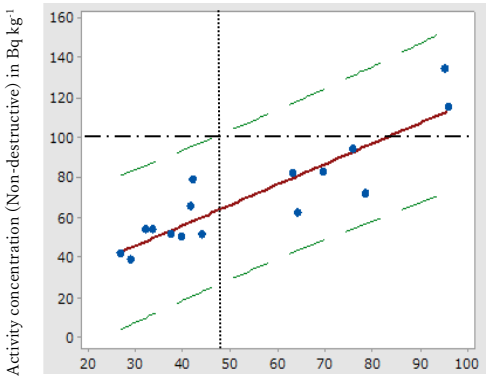

Figure 1. The regression line obtained with the present measurements using the WSI and the Ge detector.

This work was supported by Health Labour Sciences Research Grants.

T. Yamada, et al, Performance Evaluation of the equipment for measuring radioactivity in whole foodstuffs without destructive sample preparation developed after the Fukushima NPP Accident. *Radiation Protection Dosimetry*, ncz112 (2019)

ISO19581 , Measurement of radioactivity -- Gamma emitting radionuclides -- Rapid screening method using scintillation detector gamma-ray spectrometry（2017）

Tritium content variation with fifferent kinds groundwater in Korea

Yoon Yeol Yoon, Kyeong Seok Ko

Korea Institute of Geoscience and Mineral Resources, 124 124 Gwahak-ro Yuseong gu Daejeon 34132 Korea

Tritium content variation in different kinds of groundwater in Korea was studied. Three different types of groundwater such as hot spring water, spring water and well groundwater, was sampled. Tritium content was ranged from 8.16 to below detection limit 0.3 TU in 147 ground water samples. And the average concentration of three different groundwater was; 3.11±1.35 TU for well, 2.58±1.28 for spring water and 1.64±1.55 for hot spring water.

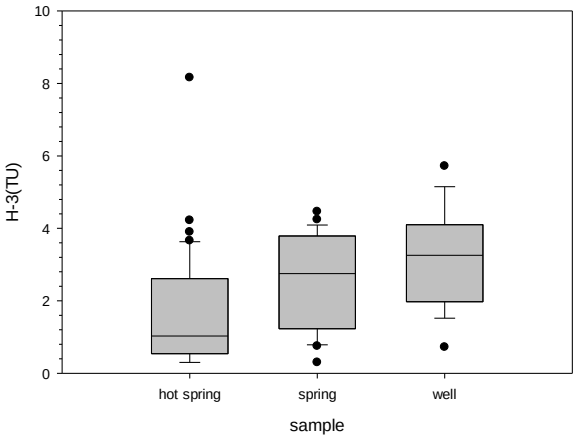

Figure 1. H-3 content distribution with different types of groundwater.

Radiation effects in plant species in Fukushima and Chernobyl

V. Yoschenko[1], K. Nanba[1], S. Geras'kin[2], P. Volkova[2], N. Horemans[3], E. Saenen[3], Y. Watanabe[4], S. Yoshida[4], K. Watanabe[1], H. Nagata[1], T. Takase[1], A. Goto[1] and A. Inada[1]

[1]Institute of Environmental Radioactivity, Fukushima University, Fukushima, 960-1296, Japan
[2]Russian Institute of Radiology and Agroecology, Obninsk, 249032, Russian Federation
[3]Belgian Nuclear Research Centre SCK•CEN, Mol, 2400, Belgium
[4]National Institute of Radiological Sciences, National Institutes for Quantum and Radiological Science and Technology, Chiba, 263-8555, Japan
Keywords: radiation effect, morphological abnormalities, Fukushima, Chernobyl
Presenting author, e-mail: V. Yoschenko, r705@ipc.fukushima-u.ac.jp

Our previous researches in Fukushima and Chernobyl demonstrated high sensitivity of young trees of coniferous plant species to radiation. In particular, under the chronic radiation conditions in the radioactive contaminated areas, we observed increased frequency of morphological abnormalities (cancellation of the apical dominance) in young populations of Scots pine and Japanese red pine (Yoschenko et al., 2011, 2016). Similar abnormalities were also observed in Japanese fir in Fukushima (Watanabe et al., 2015). For the studied pine species we revealed similar temporal patterns of formation of abnormalities and formulated dose rates dependencies of the abnormality frequencies (Figure 1). Also, our studies in Scots pine populations and on other plant species revealed the radiation-induced changes at the molecular and cell levels (Geras'kin et al., 2018; Volkova et al., 2017, 2018; Horemans et al., 2018). Finally, exposing *Arabidopsis thaliana* plants to external γ-radiation under laboratory conditions resulted in morphological abnormalities with signs of fasciation. However, it remains not clear whether and how these changes contribute to formation of the radiation effect at the level of the individual organism.

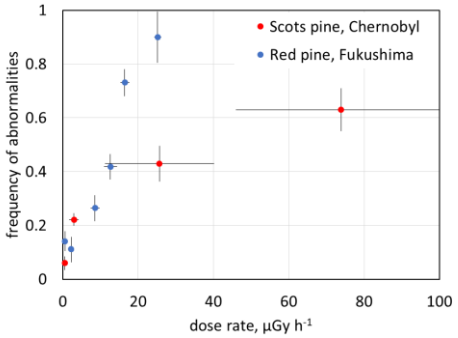

Figure 1. Frequencies of cancellation of the apical dominance in young pine trees versus dose rates on the moment of observation (Chernobyl) and in the first year of exposure (Fukushima).

In 2019, we started the collaborative research project aimed on elucidating the sequence of changes occurring at different levels of biological complexity at the way to abnormal morphological transformation in young Japanese red pine trees and *Capsella bursa-pastoris* plants. Effects will be analysed in normal, abnormal and repaired plants sampled in the field, in plants exposed to low doses of radiation in the lab and on pine trees exposed during 3 months to low doses of radiation at NIRS and are now recovering on the plantation at Fukushima University. Different endpoints will be analysed, including activity of antioxidative enzymes, DNA methylation levels and hormone analyses. Here, we present the current progress of the project.

This work is supported by Japanese Society for the Promotion of Science (JSPS), Russian Foundation for Basic Research (RFBR) and Research Foundation - Flanders (FWO, grant number: VS.017.19N) under the bilateral JSPS-RFBR and JSPS-FWO programs.

Geras'kin, S., Oudalova, A., Kuzmenkov, et al. 2018. Chronic radiation exposure modifies temporal dynamics of cytogenetic but not reproductive indicators in Scots pine populations. *Environ. Pollution*. 239, 399-407.

Horemans, N., Nauts, R., Vives i Batlle, J et al. 2018. Genome-wide DNA methylation changes in two *Brassicaceae* species sampled alongside a radiation gradient in Chernobyl and Fukushima. *J. Environ. Radioact*. 192, 405-416.

Volkova, P.Yu., Geras'kin, S.A., Kazakova, E.A. 2017. Radiation exposure in the remote period after the Chernobyl accident caused oxidative stress and genetic effects in Scots pine populations. *Sci. Reports*. 7:43009.

Volkova, P.Yu., Geras'kin, S.A., Horemans, N.,et al. 2018. Chronic radiation exposure as an ecological factor: Hypermethylation and genetic differentiation in irradiated Scots pine populations. *Environ. Pollution*. 232, 105-112.

Watanabe, Y., Ichikawa, S., Kubota, M., et al.. 2015. Morphological defects in native Japanese fir trees around the Fukushima Daiichi Nuclear Power Plant. *Sci. Reports*. 5:13232.

Yoschenko, V., Kashparov, V., Melnychuk, et al.. 2011. Chronic irradiation of Scots pine trees (*Pinus sylvestris*) in the Chernobyl exclusion zone: dosimetry and radiobiological effects. *Health Phys*. 101, 393–408.

Yoschenko, V., Nanba, K., Yoshida, S et al. 2016. Morphological abnormalities in Japanese red pine (*Pinus densiflora*) at the territories contaminated as a result of the accident at Fukushima Dai-Ichi Nuclear Power Plant. *J. Environ. Radioact*. 165, 60–67.

Vertical and horizontal distributions of caesium-137 on paved surface affected by Fukushima Dai-ichi Nuclear Power Plant accident.

K. Yoshimura[1], T. Watanabe[1], H. Kurikami[1]

[1]Sector of Fukushima Research and Development, Japan Atomic Energy Agency, Fukushima, 975-0036, Japan
Keywords: Fukushima Dai-ichi Nuclear Power Plant accident, Caesium-137, Distribution, Paved surface
e-mail: yoshimura.kazuya@jaea.go.jp

Radiocesium is the major nuclide contributing to ambient dose equivalent rates in the area affected by the Fukushima Dai-ich Nuclear Power Plant (FDNPP) accident. Since urbanized areas are an environment having a large impact on external exposure to residents, the distribution of ^{137}Cs in the urbanized area has been investigated after the Chernobyl Nuclear Power Plant and FDNPP accidents. Yoshimura et al. (2017) reported that ^{137}Cs activity per unit area (Bq m^{-2}) on paved ground accounted for about 20 % of that on unpaved ground (e.g. lawn), and the activities on building surfaces were negligible. The results of these studies demonstrate that the paved and unpaved grounds can be major sources of gamma ray in the fields. The distribution results have also been applied for the simulations of kerma rate and ambient dose equivalent rate in urbanized area. In this way, ^{137}Cs distribution among urban components (i.e. paved and unpaved ground, building surfaces) is an important information for radiation protection. Especially, accurate evaluation of ^{137}Cs distributions on paved and unpaved ground is important when we consider the negligible activity of ^{137}Cs on building surfaces. In-situ Ge spectrometry is an effective method to measure the ^{137}Cs activity for the grounds. Although spectral analysis in this method needs parameter to represent vertical distribution of ^{137}Cs in the object, the vertical distribution has not been evaluated directory for the paved ground. In addition, horizontal variability of ^{137}Cs activity on paved ground has not been investigated, although their horizontal heterogeneity on unpaved ground was evaluated and provides important information for the sampling protocols and spatial resolution of in-situ measurements. To obtain the important information and parameter for the ^{137}Cs activity measurement, this study evaluated vertical and horizontal distributions of ^{137}Cs on the paved ground.

To evaluate vertical distribution, duplicate core sample of asphalt pavement, of which diameter of 103 mm and thickness of around 50 mm, was collected at 5 parking areas located in the evacuation zone around FDNPP on 5 December 2016. Surface layer of the core with thickness less than 1 mm was scrape off by a grinder. The scraped powder was collected using a suction pump and was weighted. The recovery rate of the scraped powder was about 93%. The scraping and collection of the scraped powder were repeated 5 or 6 times. The ^{137}Cs activity of the powder was measured by a germanium gamma-ray detector. The vertical distribution was fitted using the following exponential equation.

$$A_x = A_0 e^{-X/\beta}$$

where A_X and A_0 are the ^{137}Cs concentration (Bq kg^{-1}) at mass depth X (g cm^{-2}) and surface, respectively. Coefficient β is the relaxation mass depth (g cm^{-2}).

The horizontal distribution of ^{137}Cs activity per unit area was evaluated for a parking area located in the evacuation zone from 23 January to 1 March 2017. The area of 20 m square in the parking area was divided into 20×20 grids (i.e. 400 grids with size of 1 m ×1 m). The ^{137}Cs activity were measured for each grid using a portable germanium gamma-ray detector equipped with a cylindrical collimator (30-mm-thick Pb, 60 mm height with 170 mm diameter.) at a height of 0.25 m above the ground. It was simulated that about 80% of the detected gamma-rays were derived from a circular surface with a diameter of 1 m just below the detector under the measurement conditions.

Vertical distribution of ^{137}Cs (Figure 1) showed decrease in activity concentration with increase in mass depth. More than 97% of ^{137}Cs was distributed in the layer with mass depth from 0.35 to 0.51 g cm^{-2}. The averaged β was 0.16 g cm^{-2} with standard deviation of 0.04 g cm^{-2}. But the β was apparent value, because a part of the surface was scraped by every time due to the roughness of the core surface, and fifth or six time of scrape could remove all of the surface. Therefore, the ^{137}Cs was retained in extremely surface layer with mass depth less than 0.51 g cm^{-2}. This study also demonstrated the horizontal variations of ^{137}Cs activity and the relation of the variation with grid size.

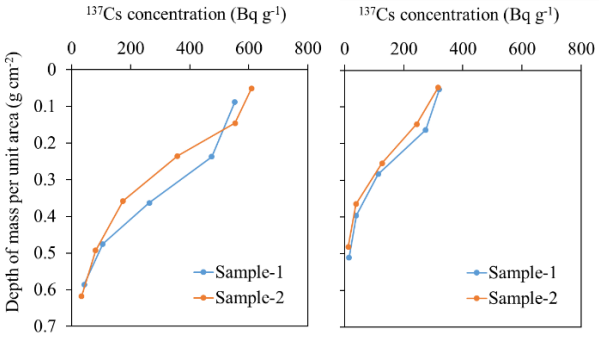

Figure 1. Vertical distributions of ^{137}Cs for core samples collected at site 1 (left) and 2 (right).

Yoshimura, K., Saito, K., Fujiwara, K. 2017. Distribution of ^{137}Cs on components in urban area four years after the Fukushima Dai-ichi Nuclear Power Plant accident. *J. Environ. Radioact.* 178-179, 48-54.